THE ROLE OF PLANT HORMONES IN PLANT-MICROBE SYMBIOSES

EDITED BY: Eloise Foo, Jonathan Michael Plett, Juan Antonio Lopez-Raez and Dugald Reid

PUBLISHED IN: Frontiers in Plant Science and Frontiers in Microbiology

frontiers Research Topics

frontiers

ISSN 1664-8714
ISBN 978-2-88963-275-6
DOI 10.3389/978-2-88963-275-6

About Frontiers

Frontiers is more than just an open-access publisher of scholarly articles: it is a pioneering approach to the world of academia, radically improving the way scholarly research is managed. The grand vision of Frontiers is a world where all people have an equal opportunity to seek, share and generate knowledge. Frontiers provides immediate and permanent online open access to all its publications, but this alone is not enough to realize our grand goals.

Frontiers Journal Series

The Frontiers Journal Series is a multi-tier and interdisciplinary set of open-access, online journals, promising a paradigm shift from the current review, selection and dissemination processes in academic publishing. All Frontiers journals are driven by researchers for researchers; therefore, they constitute a service to the scholarly community. At the same time, the Frontiers Journal Series operates on a revolutionary invention, the tiered publishing system, initially addressing specific communities of scholars, and gradually climbing up to broader public understanding, thus serving the interests of the lay society, too.

Dedication to Quality

Each Frontiers article is a landmark of the highest quality, thanks to genuinely collaborative interactions between authors and review editors, who include some of the world's best academicians. Research must be certified by peers before entering a stream of knowledge that may eventually reach the public - and shape society; therefore, Frontiers only applies the most rigorous and unbiased reviews.
Frontiers revolutionizes research publishing by freely delivering the most outstanding research, evaluated with no bias from both the academic and social point of view. By applying the most advanced information technologies, Frontiers is catapulting scholarly publishing into a new generation.

What are Frontiers Research Topics?

Frontiers Research Topics are very popular trademarks of the Frontiers Journals Series: they are collections of at least ten articles, all centered on a particular subject. With their unique mix of varied contributions from Original Research to Review Articles, Frontiers Research Topics unify the most influential researchers, the latest key findings and historical advances in a hot research area! Find out more on how to host your own Frontiers Research Topic or contribute to one as an author by contacting the Frontiers Editorial Office: researchtopics@frontiersin.org

THE ROLE OF PLANT HORMONES IN PLANT-MICROBE SYMBIOSES

Topic Editors:
Eloise Foo, University of Tasmania, Australia
Jonathan Michael Plett, Western Sydney University, Australia
Juan Antonio Lopez-Raez, Experimental Station of Zaidín (EEZ), Spain
Dugald Reid, Aarhus University, Denmark

Citation: Foo, E., Plett, J. M., Lopez-Raez, J. A., Reid, D., eds. (2019). The Role of Plant Hormones in Plant-Microbe Symbioses. Lausanne: Frontiers Media SA.
doi: 10.3389/978-2-88963-275-6

Table of Contents

frontiers in Plant Science

EDITORIAL
published: 30 October 2019
doi: 10.3389/fpls.2019.01391

Editorial: The Role of Plant Hormones in Plant-Microbe Symbioses

Eloise Foo[1], Jonathan M. Plett[2], Juan Antonio Lopez-Raez[3] and Dugald Reid[4]*

[1] School of Natural Sciences, University of Tasmania, Hobart, Tasmania, Australia, [2] Hawkesbury Institute for the Environment, Western Sydney University, Penrith, NSW, Australia, [3] Department of Soil Microbiology and Symbiotic Systems, Experimental Station of Zaidín (EEZ), Granada, Spain, [4] Department of Molecular Biology and Genetics, Aarhus University, Aarhus, Denmark

Keywords: Mycorrhizae and Rhizobium, Plant hormone, endosymbiont, ectomyccorhizas, plant associated bacteria

Editorial on the Research Topic

The Role of Plant Hormones in Plant-Microbe Symbioses

Plant hormones are regulators of almost all aspects of plant development and plant responses to their environment. Active at very low concentrations, with tight spatial regulation of synthesis and response, many plant hormones have key roles in the interactions between plants and beneficial microbes. In this special issue, "The Role of Plant Hormones in Plant-Microbe Symbioses," new insights are revealed into how hormones derived from both the plant and microbial partner play roles in communication, symbioses establishment, and function. This includes intimate endosymbioses with arbuscular mycorrhizal (AM) fungi formed by the majority of land plants and the more recently evolved nodulation, the symbioses between a limited set of plants in the fabid clade and nitrogen-fixing bacteria. Articles in this special issue also explore the role of hormones in plant interactions with ectomycorrhizae, endophytic bacteria and fungi, as well as beneficial microbes that associate with the root or leaf surfaces. In addition to acting directly, many hormones can interact with each other to control the development of these symbioses, and these complex networks are now emerging.

Two review articles explore the role of hormones in AM symbioses and nodulation. Bedini et al. comprehensively examine the role of nine plant hormone groups (abscisic acid, auxins, brassinosteroids, cytokinins, ethylene, gibberellins, jasmonates, salicylic acid, and strigolactones) in AM symbiosis, including the impact of plant-derived hormones on symbiotic establishment, and their influence on plant metabolism, defense, and phosphorous status. Models are proposed that integrate hormonal signaling with plant and fungal metabolism, and future directions in specific plant priming to promote mycorrhizal performance are discussed. McGuiness et al. take a focused look at the role of gibberellins and brassinosteroids, lately emerging as important regulators of endosymbioses with AM and rhizobial bacteria. These hormones appear to play a complex role in nodulation, with both positive and negative roles proposed, which may be due to different effects of the hormones during infection and nodule organogenesis. A different story emerges for AM symbioses; gibberellins suppress AM symbiosis, while brassinosteroids appear to promote AM formation across species. Future studies examining the spatial and temporal regulation of these hormones during symbioses, including interaction with other hormones are now required.

As outlined above, symbiotic establishment and maintenance require tight regulation. Therefore, sophisticated imaging tools are required to determine the precise spatial and temporal regulation of plant hormone signaling. Nadzieja et al. describe the availability of a "toolbox" of plant imaging tools, when applied with clearing techniques to aid imaging depth, allows for analysis of hormone responses in legume roots.

Edited and Reviewed by:
Pierre-Emmanuel Courty, Institut National de la Recherche Agronomique (INRA), France

****Correspondence:***
Eloise Foo
eloise.foo@utas.edu.au

Specialty section:
This article was submitted to Plant Microbe Interactions, a section of the journal Frontiers in Plant Science

Received: *27 August 2019*
Accepted: *08 October 2019*
Published: *30 October 2019*

Citation:
Foo E, Plett JM, Lopez-Raez JA and Reid D (2019) Editorial: The Role of Plant Hormones in Plant-Microbe Symbioses. Front. Plant Sci. 10:1391. doi: 10.3389/fpls.2019.01391

The essential role for cytokinin in legume nodulation was highlighted by Gauthier-Coles et al. In a striking result, the authors found that application of cytokinin induced pseudonodules in legumes, but not non-legumes that form nodules (e.g. actinorhizal species) or other species that do not nodulate. Cytokinin-induced legume pseudonodules arose from activation of cell division in the cortex and was distinct from cytokinin regulation of other aspects of root development. This legume-specific cytokinin response offers a fascinating perspective on the evolution of nodulation in the fabid clade. As outlined above, cytokinin not only regulates nodule organogenesis but also influence rhizobial infection. Dolgikh et al. use a mutant based approach to examine how DELLA transcription factors, which act as negative regulators of gibberellin signaling, may promote early events in nodulation by influencing the expression of genes encoding cytokinin synthesis and response elements.

In contrast to its central role in nodulation, the influence of cytokinin on AM symbiosis has received considerably less attention. Studies using a pea mutant with low cytokinin level, measurement of cytokinin content, and chemical modification of cytokinin level and response by Goh et al. suggest cytokinin may play a positive role in the development of AM symbiosis. Complex regulation of cytokinin synthesis during AM colonization indicates that spatial regulation of cytokinin that has been observed during nodulation (outlined in Nadzieja et al.) may also occur during AM symbiosis, and may be an important area for future studies.

In addition to roles in uptake and establishment of the symbiotic microbe within the plant tissue, hormones may also play roles in regulating symbiotic function. Using a sophisticated set of pea mutants blocked at specific stages of nodule development, Serova et al. reveal gibberellin promotes bifurcation of the nodule meristem and nodule expansion and suppressed nodule senescence. A model of gibberellin action in nodule development suggests that early in nodule development, high gibberellin levels promotes cell cycle activation, cell division, and persistence of the nodule meristem. Conversely, during nodule aging, downregulation of active gibberellin levels leads to nodule senescence.

To deepen our understanding of the transcriptional network underpinning AM formation, Ho-Plágaro et al. performed RNA seq analysis of AM colonized tomato roots and found that more than 30% of transcription factors from the *GRAS* [acronym of gibberellin-acid insensitive (*GAI*), repressor of GA1 (*RGA*), and scarecrow-like (*SCL*) proteins] family were upregulated by AM symbiosis. Moreover, gene expression, promoter fusion and/or RNA interference analyses of three novel AM-regulated GRAS encoding genes revealed they may act as important players in regulating AM establishment and/or maintenance. The authors speculate that two of these genes, *SlGRAS18* and *SlGRAS38,* could interact with the GA repressor DELLA during arbuscule development and turnover.

In addition to plant-derived hormones outlined above, many plant-associated microbes also produce plant hormones, and this may have an important influence on plant partners. In bacteria, the ability to produce gibberellin appears to be limited to bacteria that associate with plants. Exploring this is more depth, Nagel et al. have recently extended our understanding of this pathway, identifying the responsible operon in a third class of proteobacteria, the beta (β)-rhizobia. Interestingly, in these bacteria the operon has lost the CYP115 enzyme, meaning that only the precursor and not active gibberellin are produced by these bacteria. The authors speculate this may have been due to the fact that gibberellin negatively influences bacterial infection of legume hosts.

Auxin or auxin precursor production by root-associated microbes or modulation of plant auxin production has been suggested as an important mechanism through which microbes regulate plant growth. Meents et al. compared the influence of beneficial and pathogenic root interacting fungi on auxin response (as measured by auxin-inducible promoter system) and hormone content of Arabidopsis. Although several of the fungi produced auxin, only one beneficial fungal endophyte (*Piriformospora indica*) appeared to rapidly and strongly induce auxin response in Arabidopsis, which was correlated with promotion of lateral root development. In contrast, auxin response was attenuated in the other interactions, and in the case of the other beneficial fungal endophyte examined (*Mortierella hyalina*), this may have been due to the production of jasmonic acid. Auxin production and 1-aminocyclopropane-1-carboxylic acid (ACC) deaminase activity, which can lower ethylene levels *in planta,* was also identified in a range of endosymbiotic bacteria isolated from two tea cultivars by Yan et al. Striking variation in the make-up of the endosymbiotic bacteria isolated both from different varieties and across seasons was also observed, suggesting complex regulation of these microbial communities. The authors propose that specific beneficial endophytes with the capacity to produce auxin and/or displaying ACC deaminase activity might assist host plant growth in unfavorable areas.

Microbial-derived hormones can also assist with plant tolerance to biotic and abiotic stress. Wagner et al. found a strong association between mycorrhizal helper bacteria (MHB), able to produce auxin and beneficial effect of ectomycorrhizae on norway spruce growth, and protection from pathogens *Botrytis cinerea* and *Heterobasidion annosum*. Similarly, plant hormone-producing fungal and bacterial endosymbionts assisted soybean to deal with heavy metal stress (Bilal et al.). In addition to promoting growth, co-inoculation with fungi *Paecilomyces formosus* and bacteria *Sphingomonas* sp. lowered Al and Zn uptake, root transport, and related oxidative stress responses in this species.

Our understanding of the role of plant hormones in beneficial plant-microbe interactions has deepened considerably over the past decade. Further research into how these hormones act in distinct cell types and at different stages of development to regulate these associations and the network of plant hormone interactions is now required. Such fundamental knowledge will aid in the implementation of such beneficial microorganisms in sustainable agriculture into the future.

AUTHOR CONTRIBUTIONS

EF wrote the article with contributions from JP, JALR, and DR.

FUNDING

EF was supported by Australian Research Council Future Fellowship and Discovery Grants. JALR was supported by grants AGL2015-64990-C2-1R from the Spanish National R&D Plan of the Ministry of Economy and Competitiveness (MINECO) and the European Regional Development Fund (ERDF), and 201640I040 from the Spanish National Research Council (CSIC). JP would like to acknowledge the Australian Research Council for research funding (DE150100408). DR was supported by Danish National Research Foundation.

Conflict of Interest: The authors declare that the research was conducted in the absence of any commercial or financial relationships that could be construed as a potential conflict of interest.

frontiers in Plant Science

ORIGINAL RESEARCH
published: 04 June 2018
doi: 10.3389/fpls.2018.00750

Jasmonic Acid-Mediated Aliphatic Glucosinolate Metabolism Is Involved in Clubroot Disease Development in *Brassica napus* L.

*Li Xu, Huan Yang, Li Ren, Wang Chen, Lijiang Liu, Fan Liu, Lingyi Zeng, Ruibin Yan, Kunrong Chen and Xiaoping Fang**

Key Laboratory of Biology and Genetic Improvement of Oil Crops, Ministry of Agriculture, Oil Crops Research Institute, Chinese Academy of Agricultural Sciences, Wuhan, China

Glucosinolate (GSL) is associated with clubroot disease, which is caused by the obligate biotrophic protist *Plasmodiophora brassicae*. Due to the complicated composition of GSLs, their exact role in clubroot disease development remains unclear. By investigating clubroot disease resistance in cruciferous plants and characterizing the GSL content in seeds, we can determine if clubroot disease development is related to the components of GSLs. The difference in the infection process between *Matthiola incana* L. (resistant) and *Brassica napus* L. (susceptible) was determined. Root hair infection was definitely observed in both resistant and susceptible hosts, but no infection was observed during the cortical infection stage in resistant roots; this finding was verified by molecular detection of *P. brassicae* via PCR amplification at various times after inoculation. Based on the time course detection of the contents and compositions of GSLs after *P. brassicae* inoculation, susceptible roots exhibited increased accumulation of aliphatic, indolic, and aromatic GSLs in *B. napus*, but only aromatic GSLs were significantly increased in *M. incana*. Gluconapin, which was the main aliphatic GSL in *B. napus* and present only in *B. napus*, was significantly increased during the secondary infection stage. Quantification of the internal jasmonic acid (JA) concentration showed that both resistant and susceptible plants exhibited an enhanced level of JA, particularly in susceptible roots. The exogenous JA treatment induced aliphatic GSLs in *B. napus* and aromatic GSLs in *M. incana*. JA-induced aromatic GSLs may be involved in the defense against *P. brassicae*, whereas aliphatic GSLs induced by JA in *B. napus* likely play a role during the secondary infection stage. Three candidate *MYB28* genes regulate the content of aliphatic GSLs identified in *B. napus*; one such gene was *BnMYB28.1*, which was significantly increased following both the treatment with exogenous JA and *P. brassicae* inoculation. In summary, the increased content of JA during the secondary infection stage may induce the expression of *BnMYB28.1*, which caused the accumulation of aliphatic GSLs in clubroot disease development.

Keywords: *Plasmodiophora brassicae*, clubroot, *Brassica napus*, *Matthiola incana*, glucosinolate, jasmonic acid, MYB28

OPEN ACCESS

Edited by:
Jonathan Michael Plett, Western Sydney University, Australia

Reviewed by:
Shengwu Hu, Northwest A&F University, China
Daolong Dou, Nanjing Agricultural University, China

***Correspondence:**
Xiaoping Fang
xpfang2008@163.com

Specialty section:
This article was submitted to Plant Microbe Interactions, a section of the journal Frontiers in Plant Science

Received: *06 February 2018*
Accepted: *15 May 2018*
Published: *04 June 2018*

Citation:
Xu L, Yang H, Ren L, Chen W, Liu L, Liu F, Zeng L, Yan R, Chen K and Fang X (2018) Jasmonic Acid-Mediated Aliphatic Glucosinolate Metabolism Is Involved in Clubroot Disease Development in Brassica napus L. Front. Plant Sci. 9:750. doi: 10.3389/fpls.2018.00750

INTRODUCTION

Clubroot disease in cruciferous crops, particularly those belonging to the Brassicaceae family, is caused by the obligate biotrophic protist *Plasmodiophora brassicae* (Dixon, 2009). The life cycle of this pathogen contains the following two distinct phases: the primary phase, which occurs in the root hairs, and the secondary phase, which occurs in the cortical cell of the hypocotyls and roots, resulting in serious disruption of the vascular system and gall formation in the roots of susceptible hosts (Kageyama and Asano, 2009). *Brassica napus* L. is one of the most important oilseed crops worldwide; however, clubroot disease has recently emerged as a serious threat to the production of *B. napus* in China (Ren et al., 2016). Due to the lack of a resistant variety in China, the frequent loss of resistance, and the difficulty in chemical protection, elucidation of the molecular mechanism of clubroot disease is urgently needed (Deora et al., 2012).

The glucosinolates (GSLs), which are synthetized from amino acids and sugars, compose one of the largest known groups of secondary metabolites in the Brassicaceae family (Ishida et al., 2014). The GSLs are classified into three groups (aliphatic, aromatic, and indolic GSL) according to their amino acid precursors (Wittstock and Halkier, 2002). The GSL metabolites have recently attracted scientific interest due to their various beneficial activities. The GSLs not only control pests and have various biological activities related to human health but also play roles in plant defense response against microbial pathogens (Brader et al., 2006; Kusnierczyk et al., 2007; Bednarek et al., 2009; Clay et al., 2009; Liu et al., 2016). Aromatic GSLs are generally considered actors in plant defense against pests, whereas aliphatic GSLs are considered defense compounds against plant pathogens (Ludwig-Muller et al., 1999a; Liu et al., 2016). Indolic GSLs directly or indirectly contribute to clubroot disease development; however, these GSLs are also required for the innate immune response in *Arabidopsis thaliana* (Clay et al., 2009; Ludwig-Muller, 2009). In Brassica cultivars and *A. thaliana* mutants, clubroot disease severity is correlated with the content of indole GSLs, which are considered precursors for auxin biosynthesis (Ludwig-Muller et al., 1999b). High auxin levels are involved in gall formation during the late infection stage, and indolic GSLs are in turn precursors for indole-3-acetic acid (IAA) biosynthesis and are correlated with clubroot disease severity (Ludwig-Muller et al., 1999b; Ludwig-Muller, 2009).

Several plant growth regulators, including auxin, cytokinin, abscisic acid, ethylene, salicylic acid (SA), and jasmonic acid (JA), are modulated during clubroot disease (Devos et al., 2005, 2006; Devos and Prinsen, 2006; Siemens et al., 2006; Knaust and Ludwig-Muller, 2013; Ludwig-Muller, 2014; Lemarie et al., 2015; Lovelock et al., 2016). Published results have mostly focused on investigating the role of IAA involved in gall formation during the late infection stage. In our previous study, IAA acted as a signaling molecule that putatively stimulated root hair infection during the early response of *B. napus* to *P. brassicae* infection (Xu et al., 2016). In addition to IAA, increased cytokinin levels were correlated with clubroot disease symptoms and caused increases in cell division during the beginning of club formation (Siemens et al., 2006). Plasmodia synthesize cytokinin, which induces host cell division during clubroot disease development (Devos et al., 2005). The JA and SA signaling pathways are generally considered antagonistic in disease response (Bari and Jones, 2009). However, SA- and JA-triggered defenses result in resistance after *P. brassicae* inoculation in Bur-0 (partially resistant) and Col-0 (susceptible), respectively (Lemarie et al., 2015). In addition, the SA pathway appears to be more efficient than the JA pathway in clubroot resistance. JA accumulation during clubroot infection has been reported in susceptible Chinese cabbage and Arabidopsis Col-0 and Bur-0 during the secondary infection stage (Grsic et al., 1999; Lemarie et al., 2015).

Transcription factors (TFs) function as components of hormone signaling and modulate plant growth, development and the response to stress (Bari and Jones, 2009). During biotic and abiotic stress responses, GSL biosynthesis is regulated by a complex network of TFs belonging to the R2R3-MYB family, including MYB28, MYB29, and MYB76, which are involved in aliphatic GSL biosynthesis, as well as MYB51, MYB122, and MYB34, which are involved in indolic GSL biosynthesis in Arabidopsis (Li et al., 2013; Frerigmann and Gigolashvili, 2014). Of these TFs, MYB28 plays the most important role in aliphatic GSL biosynthesis, followed by MYB29 and MYB76, which have a partial functional redundancy.

Because the hydrolysis products of GSLs are poisonous, the application of rapeseed as feed is greatly limited (Abbadi and Leckband, 2011). Since the 1980s, rapeseed breeders have sought to obtain low-GSL rape varieties, such as double-low rapeseed with low erucic acid and low GSL in seed (Nesi et al., 2008). Recently, double-low rapeseed plantings have suffered from clubroot disease, which poses a serious threat to the production of *B. napus* in China. Evidence regarding the relationship between the poor resistance of the main rape cultivars and double-low rapeseed is lacking. However, more than 200 types of GSLs exist in the Brassicaceae family (Ishida et al., 2014). The exact role of GSLs in clubroot disease remains controversial, and systematic studies are lacking.

Based on a previous study investigating clubroot disease resistance in Brassicaceae, *M. incana* L. (resistant) and *B. napus* L. (susceptible) were chosen for investigation in this study (Ren et al., 2016). The differences in the infection process of *B. napus* and *M. incana* were determined by performing a solution culture technique. By detecting the content and composition of GSLs at various time points after *P. brassicae* inoculation, the role of GSLs was determined during the response of *B. napus* to *P. brassicae*. These data will provide useful information for elucidating the regulatory mechanism of GSL biosynthesis in clubroot disease.

MATERIALS AND METHODS

Plant Materials and Pathogen Isolates

The *P. brassicae* isolates used in this study were collected from clubroot-infested field plots in Zhijiang, Hubei, China. The resting spores of *P. brassicae* were isolated from the galls using a procedure described by Xu et al. (2016). The resting spores were identified as pathotype 4 according to the

differential classification of Williams (1966). The disease status was investigated at 35 days after inoculation (DAI).

The cruciferous plants used in this study were sent for disease resistance identification as previously described (Ren et al., 2016). In total, 14 varieties from seven species were used in this study to detect the GSLs in seeds (**Table 1**). The clubroot-susceptible *B. napus* cultivar 'zhongshuang 11' and clubroot-resistant *M. incana* cultivar 'Francesca' were used for further study. The crops and ornamentals used in this study were obtained from the Oil Crops Research Institute of the Chinese Academy of Agricultural Sciences or purchased from commercial seed companies.

High-Performance Liquid Chromatography (HPLC) Analysis of GSL Content

Desulfo (DS)-GSLs were extracted according to a procedure previously described by Kim and Ishii (2006) and ISO 9167-1 (1992). The seeds or fresh leaves were ground into powder, and 100 mg of freeze-dried sample was extracted twice in 70% methanol. The crude extracts were loaded on Sephadex A25 columns and desulfated overnight using aryl sulfatase. The 1200 series HPLC system (Agilent Technologies, Santa Clara, CA, United States) equipped with an Inertsil ODS-3 column (GL Science, Tokyo, Japan) was used in the analysis of the GSL content. The external standard method was used for quantitative analysis of individual GSLs, and sinigrin was used as an external standard. The values of the total GSLs were obtained by summing the values of the individually identified GSLs (Kim and Ishii, 2006). Three biological duplicates were performed for each treatment.

TABLE 1 | Cruciferous plants tested in this study.

	Common name	Botanical name	Source
R1	English wallflower	*Cheiranthus cheiri*	Takii Seed, Kyoto, Japan
R2	Violet orychophragmus	*Orychophragmus violaceus*	Guomei Horticulture Co., Ltd., Zhejiang
R3	Indigowoad root	*Isatidis Radix*	Guomei Horticulture Co., Ltd., Zhejiang
R4	Violet (hot cakes)	*Matthiola incana*	PanAmerican Seed, West Chicago, IL, United States
R5	Violet (Vintage)	*Matthiola incana*	PanAmerican Seed, West Chicago, IL, United States
R6	Violet (Incana)	*Matthiola incana*	PanAmerican Seed, West Chicago, IL, United States
R7	Violet (Francesca)	*Matthiola incana*	PanAmerican Seed, West Chicago, IL, United States
S1	Chinese cabbage (xin 3)	*Brassica rapa pekinensis*	Jingyan Yinong, Beijing
S2	Radish (Banyeweiqing)	*Raphanus sativus*	Takii Seed, Kyoto, Japan
S3	Radish (Baiyudagen)	*Raphanus sativus*	Takii Seed, Kyoto, Japan
S4	Oilseed (zhongshuang 11)	*Brassica napus*	OCRI, CAAS
S5	Oilseed (zhongyou 821)	*Brassica napus*	OCRI, CAAS
S6	Oilseed (BJ003)	*Brassica napus*	OCRI, CAAS
S7	Oilseed (BJ004)	*Brassica napus*	OCRI, CAAS

OCRI, CAAS: Oil Crops Research Institute of the Chinese Academy of Agricultural Sciences, Wuhan.

Cytological Observation of Clubroot Disease Development

Clubroot disease development in *B. napus* and *M. incana* was determined using an improved solution culture technique and microscopic investigation (Xu et al., 2016).

The development of root hair infection by *P. brassicae* was investigated at 3, 7, 10, and 14 DAI. The roots were washed with tap water, and a segment (0.5 cm long) was cut from the lateral root during each treatment and time point. The segments were stained with FAA Phloxine B, covered with a coverslip, then observed and imaged under an optical microscope (DMLS, Leica) (Donald et al., 2008).

The development of cortex infection by *P. brassicae* was investigated at 14, 21, and 28 DAI. The roots were washed with tap water, and a segment (0.5 cm long) was cut from the top 0 to 1 cm of the taproot during each treatment and time point. The segments were fixed in FAA for 24 h. After routine fixation and dehydration, the samples were embedded in paraffin and sliced into 8-μm-thick sections. Finally, the sections were observed and imaged under an optical microscope (Jin et al., 2014).

Extraction and Determination of JA

The infected and control roots were collected at 3, 7, 14, and 28 DAI. A 0.5-ml aliquot of 1-propanol:H_2O:concentrated HCl (2:1:0.002, v/v/v) was added to 0.1 g of fresh roots, and the mixture was shaken for 30 min at 4°C. After adding 1 ml of dichloromethane, the mixture was shaken for another 30 min and centrifuged at 12,000 × *g* for 5 min. After centrifugation, the bottom organic phase was collected and concentrated with nitrogen. Each sample was redissolved in 1 ml of 80% methanol and extracted using a C18 SPE cartridge (CNWBOND HC-C18, 500 mg, 3 ml). The eluate was evaporated to dryness under vacuum and finally dissolved in 200 μL of methanol: 0.05% formic acid (1:1, v/v). The solution filtered by the filter membrane sterilization was used for quantification of JA. Quantification of JA was performed using our previously published methods (Xu et al., 2016). Three biological duplicates were performed for each treatment.

Treatment With Exogenous JA

The seedlings were treated with 200 μmol/L of JA (Sigma-Aldrich, St Louis, MO, United States) by adding JA to the soil. The roots of the seedlings were collected 48 h after the treatment for RNA extraction. Three biological duplicates were performed for each treatment.

Bioinformatic Analysis of the Involvement of BnMYB28 in GSL Biosynthesis

MYB28 TFs related to the GSL biosynthetic pathway have been previously identified in *B. napus*, *B. rapa*, *B. oleracea,*

and *A. thaliana*, as shown in **Table 2** (Li et al., 2013; Seo et al., 2016; Yin et al., 2017). Multiple alignment analysis of BnMYB28, BrMYB28, BoMYB28 and AtMYB28 was performed using ClustalX2. The phylogenetic relationships of the MYB TFs were analyzed, and a phylogenetic tree was predicted.

DNA Isolation and PCR Amplification

The infected and control *B. napus* and *M. incana* roots sampled at 3, 7, 14, 21, and 35 DAI were used for DNA isolation and PCR amplification. To avoid contamination by spores adhering to the root surface, the roots were rinsed with tap water. At least five plants were randomly selected for the extraction of the genomic DNA using the CTAB method.

The PCR amplifications were conducted using a pathogen specific primer and the plant reference gene primers listed in Supplementary Table S1. All amplifications were conducted as previously described by Ren et al. (2016).

RNA Isolation and Real-Time Quantitative PCR (qPCR)

The total RNA was isolated from the control and used to treat *B. napus* and *M. incana* roots at various time points after the inoculation or JA treatment (3, 7, 14, and 28 DAI) using TRIzol Reagent (Invitrogen, Karlsruhe, Germany) according to the manufacturer's instructions. The Superscript first-strand synthesis system (Invitrogen, Foster City, CA, United States) was used for first-strand cDNA generation. The primers used for the qPCR were designed using Primer Premier 6.0 software and are shown in Supplementary Table S2. The qPCR were performed using our previously published methods (Xu et al., 2016). Three biological duplicates were performed for each treatment.

RESULTS

Disease Development Differences Between Resistant and Susceptible Plants

Disease development was evaluated 35 days after the *P. brassicae* inoculation (DAI) of *B. napus* and *M. incana*. The formation of galls was observed on the roots of the *B. napus,* but not *M. incana,* seedlings (**Figure 1A**). *P. brassicae* was detected via PCR analysis at various time points after inoculation. PCR products were obtained from both resistant and susceptible roots (**Figure 1B**). Increased levels of the pathogen were detected in susceptible roots as the disease developed. However, a relatively low level of the pathogen was detected in resistant roots, and the pathogen level decreased after 21 DAI, suggesting that the infection in *M. incana* was at the root hair infection stage.

An improved solution culture technique was employed to investigate the root hair infection process. Phloxine B-stained root hairs were microscopically examined to detect the presence of *P. brassicae* at 3, 7, 10, and 14 DAI in both resistant and susceptible hosts (**Figure 2**). Root hair infection was observed at 3 DAI in both roots (**Figures 2E–H**). Primary plasmodia were visible in the root hairs at 7 DAI, and swollen cells were observed in the root hairs of the susceptible, but not resistant, hosts (**Figures 2I–L**). The zoosporangia formed clusters in the root hairs at this time point, followed by the release of secondary zoospores. The secondary zoospores penetrated the cortical tissues at 10 DAI in the susceptible hosts (**Figures 2M,N**), and the pathogen developed into secondary plasmodia in the cortical cells of the roots at 14 DAI (**Figures 2Q,R**). The secondary infection was initiated by secondary zoospores, which move into the cortical cells to cause secondary infection.

A histocytological analysis was performed to investigate cross-sections of the inoculated resistant and susceptible roots at 14, 20, and 28 DAI to uncover dynamic changes in the roots during the cortical infection stage (**Figure 3**). A slight difference was observed between resistant and susceptible hosts at 14 DAI, with the exception that susceptible plants showed secondary plasmodia in the inner cortex (**Figures 3A–D**). However, secondary plasmodia were also observed in the root cortex, and compared with the resistant hosts at 20 DAI, the inoculated susceptible roots showed delayed xylem development and decreased lignified xylem bundles, vessels, and interfascicular fibers were observed (**Figures 3E,F**). The secondary plasmodia proliferated, which caused cellular hypertrophy, division and enlargement of the root cells, and gall formation in the root tissues (**Figures 3I,J**). The secondary plasmodia finally developed into resting spores at 28 DAI in the susceptible roots. Moreover, the root cells were disorderly, and the cell wall thickened, resulting in a serious disruption of the vascular system. In contrast, the resistant roots grew normally during this stage.

In summary, the life cycle of *P. brassicae* was complete in *B. napus*, but not *M. incana,* which did not show any secondary infection as confirmed by PCR.

GSL in Cruciferous Plant Seeds

The contents and components of GSL in the seeds were determined by performing an HPLC analysis. The total GSL contents did not show definite tendency among the seven resistant and seven susceptible plants. A high content and percentage of aliphatic GSL and a small percentage of indolic GSL and aromatic GSL were observed in the resistant plants, whereas

TABLE 2 | Ortholog list of transcription factors involved in GSL biosynthesis in *B. napus*.

A. thaliana **(GenBank)**		***B. rapa*** **(Ensembl plants)**		***B. oleracea*** **(Ensembl plants)**		***B. napus*** **(Ensembl plants)**	
AtMYB28	AT5G61420	BrMYB28-1	Bra012961	BoMYB28-1	Bo7g098590	BnMYB28-1	BnaA03g40190D
		BrMYB28-2	Bra035929	BoMYB28-2	Bo2g161590	BnMYB28-2	BnaC09g05300D
		BrMYB28-3	Bra029311	BoMYB28-3	Bo9g014610	BnMYB28-3	BnaCnng43220D

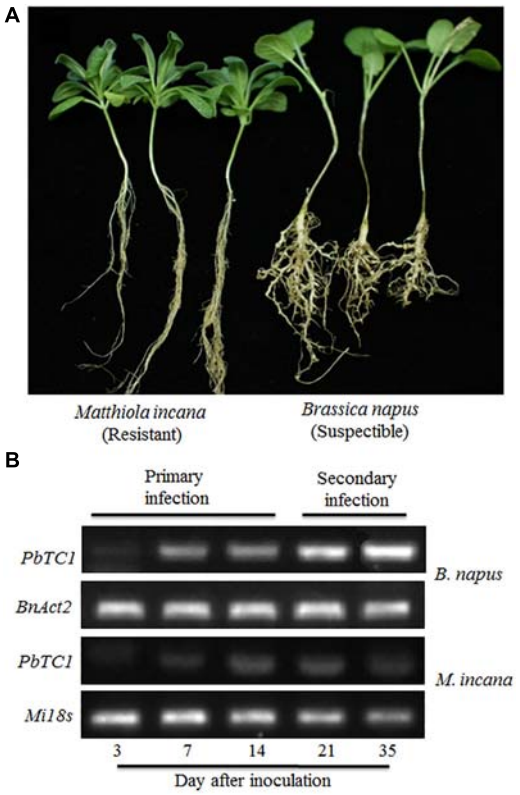

FIGURE 1 | Symptoms of clubroot disease in *Brassica napus* and *Matthiola incana* at 35 days after inoculation (DAI) **(A)** and PCR detection of *P. brassicae* in the roots of *B. napus* and *M. incana* at 3, 7, 14, 21 and 35 DAI **(B)**.

the susceptible plants, such as cabbage and rapeseed, contained comparatively large amounts of indolic GSL and aromatic GSL (**Figure 4A**).

Although both resistant and susceptible plants contained a large amount of aliphatic GSL, the aliphatic GSL components differed. Progoitrin, epi-progoitrin, sinigrin and glucoraphanin greatly accumulated in the seeds of the resistant plants, whereas progoitrin, glucoraphanin, gluconapin and glucobrassicanapin were primarily observed in the susceptible plants (**Figure 4B**). In addition, relatively high levels of gluconasturtiin (aromatic GSL) and 4-hydroxyglucobrassicin (indolic GSL) were observed in the seeds of certain plants that were susceptible to *P. brassicae*.

GSL in Roots During Disease Development

The GSL content in the roots of both resistant and susceptible plants was investigated at each time point after the *P. brassicae* inoculation (**Figure 5**). The content of GSL in the control roots of resistant plants was higher than that in susceptible plants. The pathogen inoculation greatly increased the total content of GSL in susceptible plants except at 3 DAI, whereas the total content of GSL was stable and increased only at 28 DAI in resistant plants (**Figure 3A**). By analyzing the various classes of GSL, distinct patterns of the various GSLs were observed between resistant and susceptible plants. The susceptible roots displayed uninterrupted increases in the synthesis of indolic GSL, and the content of indolic GSL was almost constant in resistant roots. Aliphatic GSL was significantly elevated at 14 and 28 DAI in the susceptible roots but was stable in resistant roots. Aromatic GSL was increased by *P. brassicae* inoculation in susceptible roots at 3 DAI, and an increase was observed only at 28 DAI in resistant roots.

By examining the compositions of GSLs at various time points after inoculation, the compositions of GSLs were observed to greatly vary between resistant and susceptible plants (**Figure 6**). For example, of the two major aromatic GSLs, gluconasturtiin was present only in susceptible plants, whereas glucotropaeolin was mainly present in resistant plants at 28 DAI. The contents of the three major indolic GSLs were very low in resistant plants and did not change after inoculation; furthermore, only 4-methoxyglucobrassicin quickly increased at 3–7 DAI in susceptible plants. In contrast, the content of the aliphatic GSLs was relatively low in susceptible plants, and gluconapin exhibited increased accumulation at 14–28 DAI in susceptible plants, which did not exist in resistant plants. Two other aliphatic GSLs were detected in resistant plants, including glucoalyssin, which displayed increased accumulation during the secondary infection stage, and glucoraphanin, which displayed decreased content.

Detection of JA Content and Induction of GSL by JA

The content of endogenous JA was detected in the roots of *B. napus* and *M. incana,* both of which showed enhanced JA content during the secondary infection stage (**Figure 7A**). However, the JA level in *B. napus* was much higher than that in *M. incana*. After the exogenous treatment with 200 μmol/L JA, the total GSL content increased in both *B. napus* and *M. incana*. The content of aliphatic GSLs was significantly increased in susceptible plants, but only the content of aromatic GSL also increased in resistant plants (**Figure 7B**).

Identification and Expression Pattern of *BnMYB28*

Three candidate *MYB28* genes were identified in *B. napus*, *B. rapa*, and *B. oleracea*. According to a multiple alignment of the 13 MYB28 proteins related to GSL biosynthesis pathways, these proteins are highly conserved, and two typical R2R3 MYB-DNA-binding domains exist in the N-terminal region (Supplementary Figure S1A). In contrast, the C-terminal region is highly polymorphic, resulting in the functional divergence of these genes. A phylogenetic tree was constructed and showed that all proteins could be divided into three subgroups and that BnMYB28.1 is more closely related to AtMYB28 than to BnMYB28.2 and BnMYB28.3 (Supplementary Figure S1B).

The expression patterns of the three *BnMYB28* genes after *P. brassicae* inoculation and exogenous JA treatment were analyzed by performing qPCR. The expression pattern of *BnMYB28.1* showed a significant increase during the secondary infection stage, whereas the expression of *BnMYB28.2* and

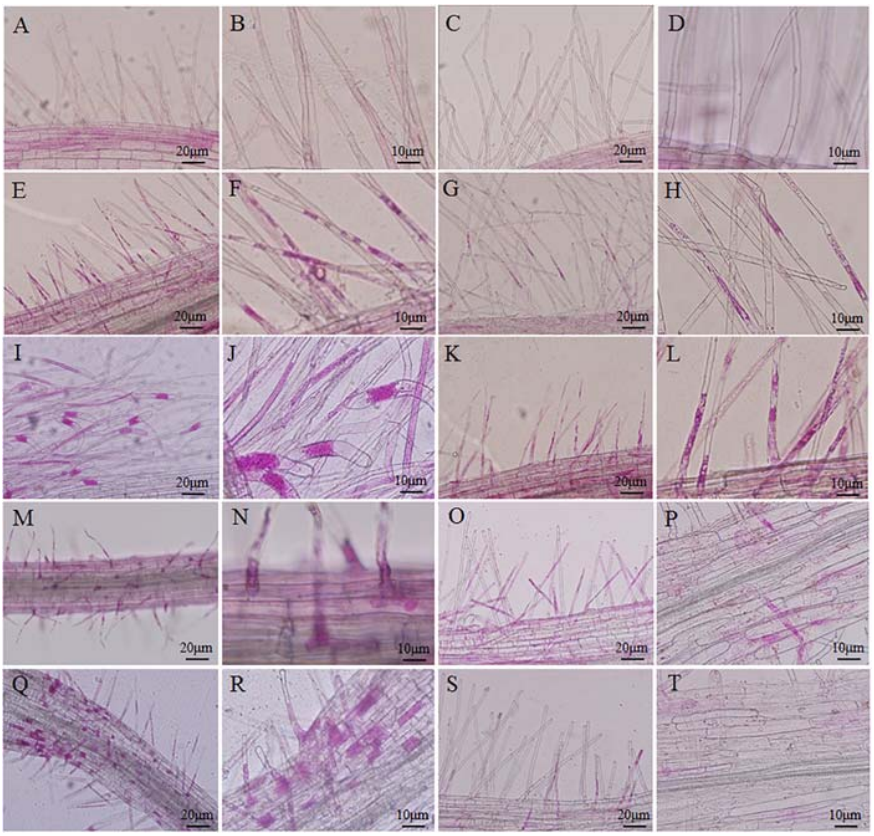

FIGURE 2 | Infection dynamics in the root hairs of resistant and susceptible plants. Root segments were stained with Phloxine B. Staining in the root hairs indicated the presence of root hair infection. **(A,B,E,F,I,J,M,N,Q,R)** Segments of roots of *Brassica napus*. **(C,D,G,H,K,L,O,P,S,T)** Segments of roots of *Matthiola incana*. **(A–D)** Segments of control roots. **(E–H)** Segments of inoculated roots at 3 days after inoculation (DAI). **(I–L)** Segments of inoculated roots at 7 DAI. **(M–P)** Segments of inoculated roots at 10 DAI. **(Q–T)** Segments of inoculated roots at 14 DAI. Adjustments for magnification and illumination were performed to allow optimal viewing of the individual sections.

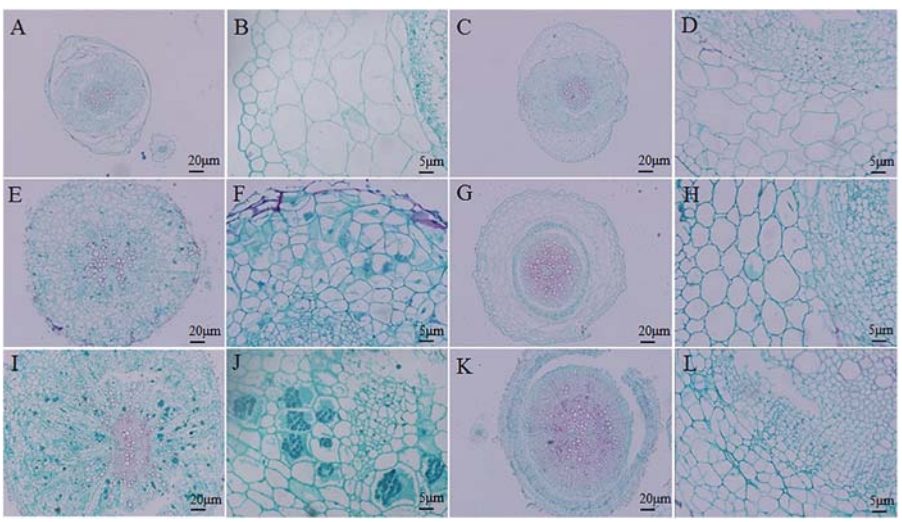

FIGURE 3 | Histocytological analysis of cross-sections of inoculated resistant and susceptible plants. **(A,B,E,F,I,J)** Sections of root of *Brassica napus*. **(C,D,G,H,K,L)** Sections of root of *Matthiola incana.* **(A–D)** Sections of inoculated roots at 14 days after inoculation (DAI). **(E–H)** Sections of inoculated roots at 20 DAI. **(I–L)** Sections of inoculated roots at 28 DAI. Adjustments for magnification and illumination were performed to allow optimal viewing of the individual sections.

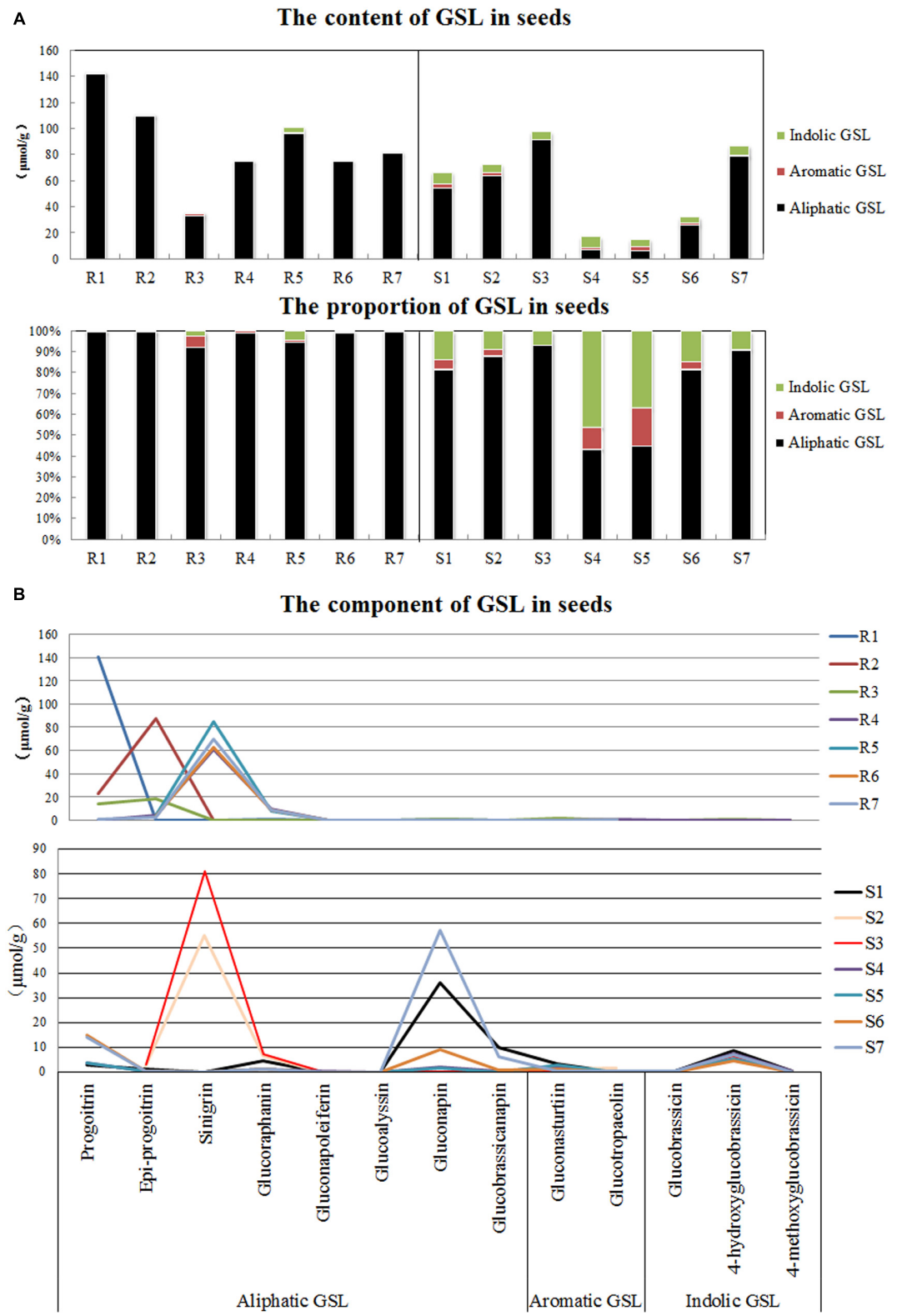

FIGURE 4 | Detection of glucosinolates (GSLs) in seeds of various disease resistance plants. **(A)** Contents of three types of GSLs. **(B)** Proportions of three types of GSLs. R1-R7 refer to the clubroot-resistant plants, and R1-R7 refer to the clubroot-susceptible plants. R1, English wallflower; R2, Violet orychophragmus; R3, Indigowoad Root; R4, Violet (Matthiola hot cakes); R5, Violet (Vintage); R6, Violet (Incana); R7, Violet (Francesca); S1, Chinese cabbage (xin 3); S2, Radish (Banyeweiqing); S3, Radish (Baiyudagen); S4, Oilseed (zhongshuang 11); S5, Oilseed (zhongyou 821); S6, Oilseed (BJ003); S7, Oilseed (BJ004).

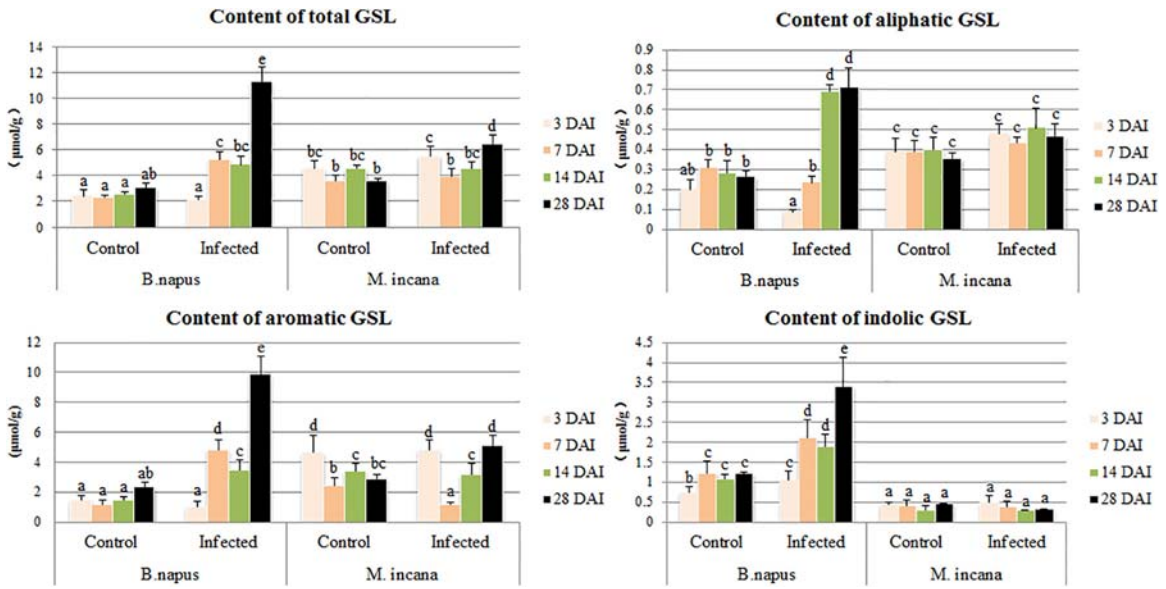

FIGURE 5 | Content of glucosinolates (GSLs) in the roots of *B. napus* and *M. incana* at 3, 7, 14, and 28 days after inoculation (DAI). Error bars represent the standard errors of three independent experiments. Different letters above the bars indicate that the differences are significant ($P < 0.05$).

BnMYB28.3 remained almost constant (**Figure 7C**). Moreover, the treatment with exogenous JA greatly increased the expression of *BnMYB28.1* but not *BnMYB28.2* and *BnMYB28.3* (**Figure 7D**).

DISCUSSION

Clubroot disease has emerged as the main disease in Brassicaceae. Omics and molecular experiments have provided evidence regarding the involvement of GSL metabolites in clubroot disease. However, the exact role played by the metabolic pathway remains unclear. Therefore, an understanding of the regulation of GSL biosynthesis could provide useful information for studies investigating clubroot disease and other improvements in the value of agricultural crops.

Primary Infection Occurred in Both Resistant and Susceptible Plants

First, different infection processes were observed, and the main differences between resistant and susceptible plants were determined. By dynamically monitoring the infection process, we observed that primary infection occurred in the root hairs of both resistant and susceptible plants, and the infection was correlated with the results of the PCR detection of the pathogen contents in the infected roots. Furthermore, even in particular non-host plant species, the germination of *P. brassicae* resting spores was stimulated, and the initial stage of *P. brassicae* pathogenesis was observed. These plant species, including soybean (*Glycine max*), leek (*Allium porrum*), winter rye (*Secale cereale*), and perennial ryegrass (*Lolium perenne*), may be useful in reducing inoculum levels in soil and increasing soil pH and can potentially be used as trap crops to reduce clubroot disease intensity (Ludwig-Muller et al., 1999a; Friberg et al., 2005, 2006; Bhattacharya and Dixon, 2010). Many studies have focused on the life cycle of *P. brassicae*. The present study indicated that both primary and secondary zoospores, which may essentially have the same identity, can cause both primary and secondary infections (Mithen and Magrath, 1992; Feng et al., 2013). Thus, an intriguing question is what is the role of primary infection in clubroot disease? It was still difficult to verify whether the primary infections were necessary during clubroot disease development. In particular, previous studies have focused on whether primary infection affects the initiation of resistance in host species or influences the development of a pathogen at the secondary stage (Kageyama and Asano, 2009; Feng et al., 2013).

The Correlation of Clubroot Disease and GSL Contents in Seeds

Plants belonging to the Brassicaceae family are well known for their high GSL content. The total GSL contents in the seeds did not show definite tendency between resistant and susceptible plants in our study. In a previous report, the total seed GSL contents were suggested to be correlated with the susceptibility of Chinese cabbage varieties, and higher total GSL contents were found in eight different susceptible varieties than in two resistant varieties (Ludwig-Muller et al., 1997). Although our results are discrepant, our conclusion that susceptible plants contain a higher proportion of indolic and aromatic GSL is consistent. To improve the nutritional value of rapeseed oil and the quality of rapeseed meal, reducing the GSL content in the seeds is desirable; thus, double-low rapeseed has recently been bred and popularized (Nesi et al., 2008). In double-low rapeseed, only the content of aliphatic GSL is reduced, which results in enhanced proportions of indolic and aromatic GSLs. However, both the double-low rapeseed and double-high rapeseed strains

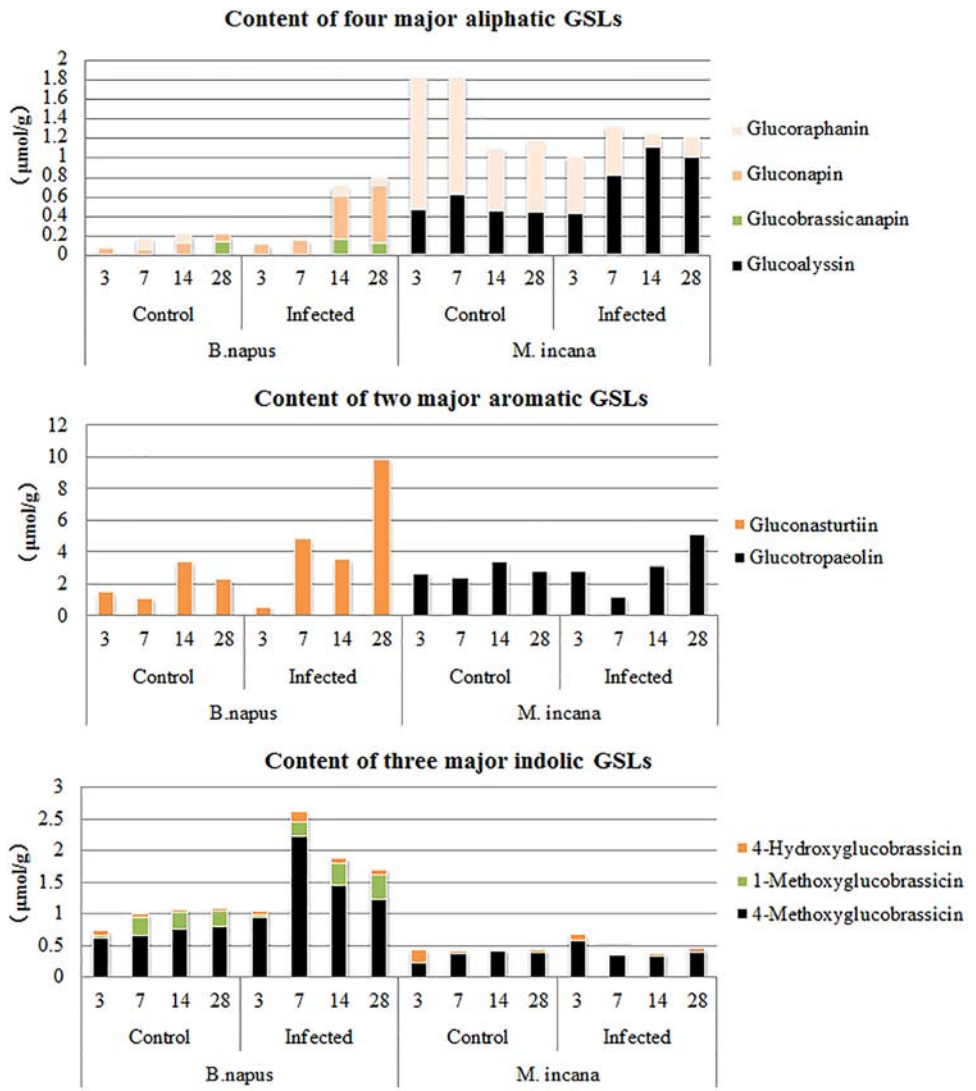

FIGURE 6 | Major components of glucosinolates (GSLs) in the roots of *B. napus* and *M. incana* at 3, 7, 14, and 28 days after inoculation (DAI).

tested in this study were susceptible, and double-low rapeseed had high proportions of indolic and aromatic GSLs. Thus, the higher content and proportion of indolic and aromatic GSLs are unlikely to result in susceptibility to clubroot. Furthermore, no significant difference was observed in the components and contents of GSLs between the roots and seeds in rapeseed, and it remains unknown whether changes in the GSL content in the seeds affect GSL content in other tissues (Kim and Ishii, 2006). Thus, whether the susceptibility of the main varieties to clubroot disease is correlated with low GSL levels in the seeds is unclear due to a lack of direct evidence.

The Contents of GSL in Roots of Susceptible Plants

The contents and components of GSLs differ among plant genera and organs, suggesting that GSLs play diverse roles in metabolism in different organs and during various development stages (Ishida et al., 2014). Although the total contents of GSLs were relatively low in susceptible plants, all classes of GSL responded in susceptible plants at various time points after inoculation, suggesting that other GSLs, in addition to indolic GSL, play a role during disease development. The authors of a previous investigation of GSL content in four Chinese cabbages during clubroot disease development had the same conclusion (Ludwig-Muller et al., 1997).

To date, most studies have focused on the role of indolic GSL rather than aliphatic and aromatic GSLs in clubroot disease. Indolic GSL acts as a precursor for IAA production after *P. brassicae* inoculation, and low levels of root indole GSL may limit pathogen inoculation and development (Ludwig-Muller et al., 1999a; Ludwig-Muller, 2009). In this study, a correlation was observed between low contents of indolic GSL and resistance to clubroot. The content of indolic GSL

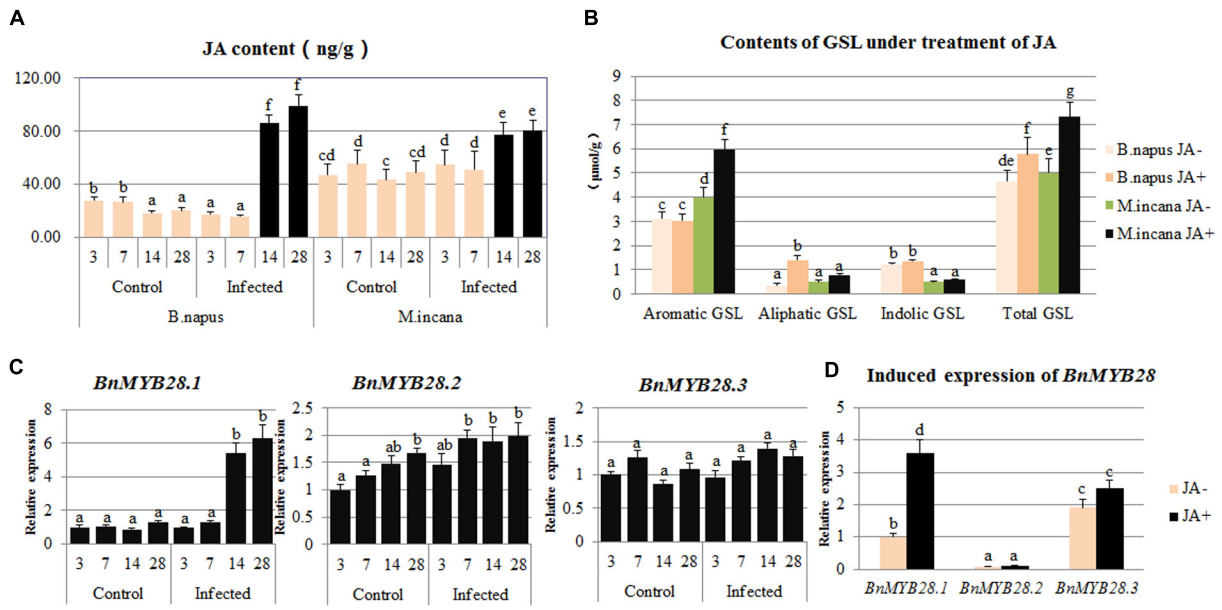

FIGURE 7 | Contents of jasmonic acid (JA) in clubroot disease and induced content of glucosinolates (GSLs) and expression of *BnMYB28* by the exogenous JA treatment. **(A)** Contents of JA in clubroot disease. **(B)** Contents of GSL by exogenous JA treatment. **(C)** Expression of *BnMYB28* in clubroot disease. **(D)** Induced expression of *BnMYB28* by exogenous JA treatment. Error bars represent the standard errors of three independent experiments. Different letters above the bars indicate that the differences are significant ($P < 0.05$).

increased in the *A. thaliana* ecotype Col, which is susceptible to clubroot disease (Ludwig-Muller et al., 1999b). In another study investigating the GSL content differences between resistant and susceptible Chinese cabbage, the two susceptible cultivars exhibited increased indolic GSL content at 14 and 20 DAI, whereas this content did not change in resistant cultivars (Ludwig-Muller et al., 1997). However, contradictory results have been reported. Two Arabidopsis mutants (*tu3* and *tu8*) both showed reduced disease symptoms, but only *tu8* exhibited decreased indolic GSL content compared to that in the wild type. Thus, similar to other disease responses, the disease symptoms caused by *P. brassicae* result from many regulation pathways, in addition to GSL, that interact to participate in the disease response. In our study, susceptible plants exhibited a significant increase in the indolic GSL content throughout the disease course. In addition, the elevation in indolic GSL is largely due to the accumulation of 4-methoxyglucobrassicin. Further study on the exact role of 4-methoxyglucobrassicin will provide useful information on clubroot disease. The earlier induction of indolic GSL may be responsible for the overproduction of IAA during the root hair infection stage. Furthermore, indolic GSL likely acts as a signaling molecule in the response to *P. brassicae*. However, the continuous induction during the secondary infection stage suggests that metabolites meet the needs of the obligate biotrophic pathogen. Thus, indolic GSL likely plays diverse roles in clubroot disease.

Knowledge regarding the aliphatic and aromatic GSLs in clubroot disease is limited. Aromatic GSL generally acts in the plant defense response against pests, whereas aliphatic GSL is a defense compound against plant pathogens. Initially, the induction of aliphatic GSL was hypothesized to be a defense response, but studies did not always support this hypothesis. The Arabidopsis mutant *gsm1-1,* which exhibits a reduced biosynthesis of aliphatic GSL, does not show improved resistance to clubroot disease (Tierens et al., 2001). In contrast, two susceptible Chinese cabbage varieties exhibited increased aliphatic GSL contents after *P. brassicae* inoculation, but no change was observed in the other two resistant varieties; this finding is consistent with our results because only the susceptible roots showed an increased content of aliphatic GSL during the late infection stage (Ludwig-Muller et al., 1997). The content of aliphatic GSL seemed almost unchanged in resistant plants, but not all the components remained constant. It showed the increased content of glucoalyssin, together with the decreased content of glucoraphanin, which made the role of aliphatic GSL more complicated in resistant plants. Gluconapin, which is present only in *B. napus,* was significantly increased during the secondary infection stage. Combined with the result that only seeds of susceptible plants contain gluconapin, gluconapin is likely a key factor in the pathogenesis of clubroot disease. Thus, particular components of GSLs, rather than the total contents of the GSLs, likely contribute to resistance or susceptibility.

The role of aromatic GSLs in clubroot disease is also uncertain, and the possible dual role of aromatic GSL during club formation is presented in non-Brassica species depending on the components of aromatic GSL (Ludwig-Muller, 2009). Both the resistant and susceptible plants showed enhanced content of aromatic GSL during the secondary infection stage, but the component was completely different (glucotropaeolin) in

resistant plants, and gluconasturtiin was found in susceptible plants.

To summarize, these results agreed with the conclusion that disease severity is correlated with particular GSLs in one species, whereas the increase in other GSLs might be regarded as a defense response. Therefore, compared with the total content of GSL, the specific GSL may be more informative. Further studies investigating the exact role of 4-methoxyglucobrassicin and gluconapin should consider investigating hairy roots.

JA May Be Responsible for the Induction of Aliphatic GSL in *B. napus*

Plant growth regulators always participate in clubroot disease as described in the introduction; this finding also suggested that JA plays a role during the secondary infection stage. In this study, both resistant and susceptible plants showed an enhanced accumulation of JA at 14–28 DAI, and this accumulation was even greater in susceptible plants; this finding is similar to previous results reported in Arabidopsis. Both Col-0 and Bur-0 showed increased JA accumulation after inoculation during the secondary infection stage, but the JA level and expression level of the JA-responsive genes were twofold to threefold higher in Col-0, suggesting that the JA response was activated (Lemarie et al., 2015). JA-dependent defenses generally act against necrotrophs, although *P. brassicae* is a biotroph (Bari and Jones, 2009). However, recent evidence has shown that some biotrophic pathogens trigger the defense response mediated by JA (Guerreiro et al., 2016). Interestingly, the JA response was activated during the secondary infection stage but not at the beginning after inoculation, suggesting that the JA-mediated defense response might begin during the cortex infection stage. This conclusion was also demonstrated in a study conducted by Lemarie et al. (2015).

Consistent results were obtained in several reports that showed high JA levels during the secondary infection stage in susceptible plants. The increased accumulation of JA in Col-0 was consistent with the induced expression of JA-responsive genes, suggesting that the JA signaling pathway is activated in clubroot (Siemens et al., 2006; Gravot et al., 2012). The jasmonate resistant 1 (*jar1*) mutant exhibited reduced JA-Ile accumulation and increased susceptibility to clubroot disease (Agarwal et al., 2011). Altogether, the exogenous JA treatment reduced the clubroot symptoms only in Col-0; thus, the JA response also participates in the weak defense in Col-0 (Lemarie et al., 2015). However, JA is upregulated in *B. rapa* roots during gall formation and can induce the content of indolic GSL and the activity of nitrilase (Grsic et al., 1999). This dual role of JA was deduced based on the interaction between susceptible hosts and *P. brassicae*. JA can activate a defense response against biotrophs, but it also participates in pathogenesis by mediating another pathway.

Some have shown the role of JA in GSL metabolism by exogenously applying JA, which increased the content of the indolic and aromatic GSLs in the leaves of *A. thaliana* (Guo et al., 2013), *B. juncea* (Augustine and Bisht, 2015), *B. napus* (Doughty et al., 1995), and various subspecies of *B. oleracea* (Kim and Juvik, 2011; Yi et al., 2016). The total GSL concentration increased up to 20-fold with the treatment of JA in *B. napus*, and the predominant components of the response were indolic GSLs, which together comprised 90% of the total GSLs in treated leaves (Doughty et al., 1995). However, knowledge regarding the role of JA in the modulation of GSL metabolism in roots is still limited. Our finding suggested a completely different result in the roots from that in the leaves, and it showed that exogenous JA treatments greatly increase the content of aliphatic GSL in *B. napus* and enhance the accumulation of aromatic GSL in *M. incana*. This result may be explained by the fact that the effect of JA on the GSL profile may differ among organs. In considering the regulatory role of JA, it can be deduced that JA-induced aromatic GSL may be involved in the defense against *P. brassicae*, whereas aliphatic GSL induced by JA in *B. napus* may participate in pathogenesis.

BnMYB28 May Regulate Clubroot Disease by Modulating JA-Mediated Aliphatic GSL Metabolism

Brassica napus is an allotetraploid derived from the interspecific hybridization of *B. rapa* and *B. oleracea*. Due to the occurrence of polyploidy and genome-wide rearrangements, the regulation of aliphatic GSL biosynthesis in Brassica species is expected to be highly complex compared to that in the closely related diploid Arabidopsis (Qu et al., 2015). *AtMYB28* has been found to positively regulate the synthesis of aliphatic GSLs (Li et al., 2013). Three paralogous *MYB28* genes have been identified in *B. napus*, *B. rapa*, and *B. oleracea*; compared to Arabidopsis, these *MYB28* genes have a high level of sequence homology. A high collinearity has been observed among these genes in *B. napus*, *B. rapa*, and *B. oleracea*. The existence of multiple paralog genes in allopolyploid plants suggests that highly diverse expression patterns and functions exist among the paralogs of the candidate genes (Seo et al., 2016). The overexpression of the three paralogous *BrMYB28* genes in transgenic Chinese cabbage resulted in enhanced content of total GSL in all T_1 and T_2 transgenic plants. Compared to non-transgenic plants, overexpression of *BrMYB28.1* resulted in the highest total GSL contents and increased content of the aliphatic, indolic, and aromatic GSLs (Seo et al., 2016). In studies overexpressing *BoMYB28* in Chinese Kale (*B. oleracea*), aliphatic GSL contents were higher in the overexpression lines than those in non-transgenic plants, and enhanced expression levels of aliphatic GSL biosynthesis-related genes were observed (Yin et al., 2017). Thus, the regulatory mechanism of GSL biosynthesis in Brassica crops differs from that in *A. thaliana*. Although a functional validation of the candidate *MYB28* genes has been performed in *B. rapa* and *B. oleracea*, knowledge regarding the functions of these genes remains limited, particularly in clubroot disease. Among the three *BnMYB28* candidates, the expression level of *BnMYB28.2* was extremely low in the root; this finding is consistent with results showing that *BnMYB28.2* is associated with the seed GSL content *B. napus* (Qu et al., 2015). *BnMYB28.1,* which showed the highest similarity of amino acid sequence with *AtMYB28*, was induced by *P. brassicae* inoculation during the secondary infection stage and exogenous JA treatment. Thus, the increased content of JA during the secondary infection stage

may induce the expression of *BnMYB28.1,* which caused the accumulation of aliphatic GSL in clubroot disease development. However, this assumption requires further investigation.

In summary, GSL metabolites are more likely to play a role during disease development than to act as defense compounds in clubroot. However, the possibility that GSL metabolites participate in the defense response through degradation cannot be eliminated. We hypothesize that a dual role of JA was suggested to participate in clubroot disease via different regulation methods. Further studies exploring the exact role of 4-methoxyglucobrassicin and gluconapin in hairy roots should be performed using *in vitro* culture. The *MYB28* TF, which regulates clubroot disease development by modulating JA-mediated aliphatic GSL metabolism, may play a specific role in clubroot disease development. Future studies investigating the function of *BnMYB28.1* are fundamentally important to better understand the complex mechanisms controlling GSL accumulation during clubroot disease development. Understanding GSL metabolism and the regulatory network in rapeseed clubroot could enable the rational engineering of GSL content to boost plant protection without compromising the crop quality.

AUTHOR CONTRIBUTIONS

LX and XF designed the study. LX, HY, LR, WC, LL, LZ, and RY performed the experiment and analyzed the data. LX wrote the paper. XF revised the paper. All authors read and approved the final manuscript.

FUNDING

The financial support from the National Key Research and Development Program of China (2016YFD0100202) and the National Natural Science Fund (31501617) is greatly appreciated.

SUPPLEMENTARY MATERIAL

The Supplementary Material for this article can be found online at: https://www.frontiersin.org/articles/10.3389/fpls.2018.00750/full#supplementary-material

REFERENCES

Abbadi, A., and Leckband, G. (2011). Rapeseed breeding for oil content, quality, and sustainability. *Eur. J. Lipid Sci. Technol.* 113, 1198–1206. doi: 10.1002/ejlt.201100063

Agarwal, A., Kaul, V., Faggian, R., Rookes, J. E., Ludwig-Muller, J., and Cahill, D. M. (2011). Analysis of global host gene expression during the primary phase of the *Arabidopsis thaliana-Plasmodiophora brassicae* interaction. *Funct. Plant Biol.* 38, 462–478. doi: 10.1071/FP11026

Augustine, R., and Bisht, N. C. (2015). Biotic elicitors and mechanical damage modulate glucosinolate accumulation by co-ordinated interplay of glucosinolate biosynthesis regulators in polyploid *Brassica juncea*. *Phytochemistry* 117, 43–50. doi: 10.1016/j.phytochem.2015.05.015

Bari, R., and Jones, J. D. (2009). Role of plant hormones in plant defence responses. *Plant Mol. Biol.* 69, 473–488. doi: 10.1007/s11103-008-9435-0

Bednarek, P., Pislewska-Bednarek, M., Svatos, A., Schneider, B., Doubsky, J., Mansurova, M., et al. (2009). A glucosinolate metabolism pathway in living plant cells mediates broad-spectrum antifungal defense. *Science* 323, 101–106. doi: 10.1126/science.1163732

Bhattacharya, I., and Dixon, G. R. (2010). "Management of clubroot disease (*Plasmodiophora brassicae*) of brassicas using trap cropping techniques," in *Proceedings of the 5th International Symposium on Brassicas and Xvi International Crucifer Genetics Workshop*, Catania, 157–163. doi: 10.17660/ActaHortic.2010.867.20

Brader, G., Mikkelsen, M. D., Halkier, B. A., and Tapio Palva, E. (2006). Altering glucosinolate profiles modulates disease resistance in plants. *Plant J.* 46, 758–767. doi: 10.1111/j.1365-313X.2006.02743.x

Clay, N. K., Adio, A. M., Denoux, C., Jander, G., and Ausubel, F. M. (2009). Glucosinolate metabolites required for an Arabidopsis innate immune response. *Science* 323, 95–101. doi: 10.1126/science.1164627

Deora, A., Gossen, B. D., and Mcdonald, M. R. (2012). Effect of host resistance on infection by *Plasmodiophora brassicae* in canola. *Can. J. Plant Pathol.* 34, 329–330. doi: 10.1186/1471-2164-15-1166

Devos, S., Laukens, K., Deckers, P., Van Der Straeten, D., Beeckman, T., Inze, D., et al. (2006). A hormone and proteome approach to picturing the initial metabolic events during *Plasmodiophora brassicae* infection on Arabidopsis. *Mol. Plant Microbe Interact.* 19, 1431–1443. doi: 10.1094/MPMI-19-1431

Devos, S., and Prinsen, E. (2006). Plant hormones: a key in clubroot development. *Commun. Agric. Appl. Biol. Sci.* 71(3 Pt B), 869–872.

Devos, S., Vissenberg, K., Verbelen, J. P., and Prinsen, E. (2005). Infection of Chinese cabbage by *Plasmodiophora brassicae* leads to a stimulation of plant growth: impacts on cell wall metabolism and hormone balance. *New Phytol.* 166, 241–250. doi: 10.1111/j.1469-8137.2004.01304.x

Dixon, G. R. (2009). The occurrence and economic impact of *Plasmodiophora brassicae* and clubroot disease. *J. Plant Growth Regul.* 28, 194–202. doi: 10.1007/s00344-009-9090-y

Donald, E. C., Jaudzems, G., and Porter, I. J. (2008). Pathology of cortical invasion by *Plasmodiophora brassicae* in clubroot resistant and susceptible Brassica oleracea hosts. *Plant Pathol.* 57, 201–209. doi: 10.1111/j.1365-3059.2007.01765.x

Doughty, K. J., Kiddle, G. A., Pye, B. J., Wallsgrove, R. M., and Pickett, J. A. (1995). Selective induction of glucosinolates in oilseed rape leaves by methyl jasmonate. *Phytochemistry* 38, 347–350. doi: 10.1016/0031-9422(94)00653-B

Feng, J., Hwang, S. F., and Strelkov, S. E. (2013). Studies into primary and secondary infection processes by *Plasmodiophora brassicae* on canola. *Plant Pathol.* 62, 177–183. doi: 10.1111/j.1365-3059.2012.02612.x

Frerigmann, H., and Gigolashvili, T. (2014). MYB34, MYB51, and MYB122 distinctly regulate indolic glucosinolate biosynthesis in *Arabidopsis thaliana*. *Mol. Plant* 7, 814–828. doi: 10.1093/mp/ssu004

Friberg, H., Lagerlof, J., and Ramert, B. (2005). Germination of *Plasmodiophora brassicae* resting spores stimulated by a non-host plant. *Eur. J. Plant Pathol.* 113, 275–281. doi: 10.1007/s10658-005-2797-0

Friberg, H., Lagerlof, J., and Ramert, B. (2006). Usefulness of nonhost plants in managing *Plasmodiophora brassicae*. *Plant Pathol.* 55, 690–695. doi: 10.1111/j.1365-3059.2006.01408.x

Gravot, A., Deleu, C., Wagner, G., Lariagon, C., Lugan, R., Todd, C., et al. (2012). Arginase induction represses gall development during clubroot infection in Arabidopsis. *Plant Cell Physiol.* 53, 901–911. doi: 10.1093/pcp/pcs037

Grsic, S., Kirchheim, B., Pieper, K., Fritsch, M., Hilgenberg, W., and Ludwig-Muller, J. (1999). Induction of auxin biosynthetic enzymes by jasmonic acid and in clubroot diseased Chinese cabbage plants. *Physiol. Plant.* 105, 521–531. doi: 10.1034/j.1399-3054.1999.105318.x

Guerreiro, A., Figueiredo, J., Sousa Silva, M., and Figueiredo, A. (2016). Linking jasmonic acid to grapevine resistance against the biotrophic oomycete *Plasmopara viticola*. *Front. Plant Sci.* 7:565. doi: 10.3389/fpls.2016.00565

Guo, R., Shen, W., Qian, H., Zhang, M., Liu, L., and Wang, Q. (2013). Jasmonic acid and glucose synergistically modulate the accumulation of glucosinolates in *Arabidopsis thaliana*. *J. Exp. Bot.* 64, 5707–5719. doi: 10.1093/jxb/ert348

Ishida, M., Hara, M., Fukino, N., Kakizaki, T., and Morimitsu, Y. (2014). Glucosinolate metabolism, functionality and breeding for the improvement of Brassicaceae vegetables. *Breed. Sci.* 64, 48–59. doi: 10.1270/jsbbs.64.48

Jin, F. Y., Hu, L. S., Yuan, D. J., Xu, J., Gao, W. H., He, L. R., et al. (2014). Comparative transcriptome analysis between somatic embryos (SEs) and zygotic embryos in cotton: evidence for stress response functions in SE development. *Plant Biotechnol. J.* 12, 161–173. doi: 10.1111/pbi.12123

Kageyama, K., and Asano, T. (2009). Life cycle of *Plasmodiophora brassicae*. *J. Plant Growth Regul.* 28, 203–211. doi: 10.1007/s00344-009-9101-z

Kim, H. S., and Juvik, J. A. (2011). Effect of selenium fertilization and methyl jasmonate treatment on glucosinolate accumulation in broccoli florets. *J. Am. Soc. Hortic. Sci.* 136, 239–246.

Kim, S. J., and Ishii, G. (2006). Glucosinolate profiles in the seeds, leaves and roots of rocket salad (*Eruca sativa* Mill.) and anti-oxidative activities of intact plant powder and purified 4-methoxyglucobrassicin. *Soil Sci. Plant Nutr.* 52, 394–400. doi: 10.1111/j.1747-0765.2006.00049.x

Knaust, A., and Ludwig-Muller, J. (2013). The ethylene signaling pathway is needed to restrict root gall growth in *Arabidopsis* after Infection with the obligate biotrophic protist *Plasmodiophora brassicae*. *J. Plant Growth Regul.* 32, 9–21. doi: 10.1007/s00344-012-9271-y

Kusnierczyk, A., Winge, P., Midelfart, H., Armbruster, W. S., Rossiter, J. T., and Bones, A. M. (2007). Transcriptional responses of *Arabidopsis thaliana* ecotypes with different glucosinolate profiles after attack by polyphagous *Myzus persicae* and oligophagous *Brevicoryne brassicae*. *J. Exp. Bot.* 58, 2537–2552. doi: 10.1093/jxb/erm043

Lemarie, S., Robert-Seilaniantz, A., Lariagon, C., Lemoine, J., Marnet, N., Jubault, M., et al. (2015). Both the jasmonic acid and the salicylic acid pathways contribute to resistance to the biotrophic clubroot agent *Plasmodiophora brassicae* in Arabidopsis. *Plant Cell Physiol.* 56, 2158–2168. doi: 10.1093/pcp/pcv127

Li, Y., Sawada, Y., Hirai, A., Sato, M., Kuwahara, A., Yan, X., et al. (2013). Novel insights into the function of Arabidopsis R2R3-MYB transcription factors regulating aliphatic glucosinolate biosynthesis. *Plant Cell Physiol.* 54, 1335–1344. doi: 10.1093/pcp/pct085

Liu, T., Zhang, X., Yang, H., Agerbirk, N., Qiu, Y., Wang, H., et al. (2016). Aromatic glucosinolate biosynthesis pathway in *Barbarea vulgaris* and its response to *Plutella xylostella* Infestation. *Front. Plant Sci.* 7:83. doi: 10.3389/fpls.2016.00083

Lovelock, D. A., Sola, I., Marschollek, S., Donald, C. E., Rusak, G., van Pee, K. H., et al. (2016). Analysis of salicylic acid-dependent pathways in *Arabidopsis thaliana* following infection with *Plasmodiophora brassicae* and the influence of salicylic acid on disease. *Mol. Plant Pathol.* 17, 1237–1251. doi: 10.1111/mpp.12361

Ludwig-Muller, J. (2009). Glucosinolates and the clubroot disease: defense compounds or auxin precursors? *Phytochem. Rev.* 8, 135–148. doi: 10.1007/s11101-008-9096-2

Ludwig-Muller, J. (2014). Auxin homeostasis, signaling, and interaction with other growth hormones during the clubroot disease of Brassicaceae. *Plant Signal. Behav.* 9:e28593. doi: 10.4161/psb.28593

Ludwig-Muller, J., Bennett, R. N., Kiddle, G., Ihmig, S., Ruppel, M., and Hilgenberg, W. (1999a). The host range of *Plasmodiophora brassicae* and its relationship to endogenous glucosinolate content. *New Phytol.* 141, 443–458. doi: 10.1046/j.1469-8137.1999.00368.x

Ludwig-Muller, J., Pieper, K., Ruppel, M., Cohen, J. D., Epstein, E., Kiddle, G., et al. (1999b). Indole glucosinolate and auxin biosynthesis in *Arabidopsis thaliana* (L.) Heynh. glucosinolate mutants and the development of clubroot disease. *Planta* 208, 409–419.

Ludwig-Muller, J., Schubert, B., Pieper, K., Ihmig, S., and Hilgenberg, W. (1997). Glucosinolate content in susceptible and resistant Chinese cabbage varieties during development of clubroot disease. *Phytochemistry* 44, 407–414. doi: 10.1016/S0031-9422(96)00498-0

Mithen, R., and Magrath, R. (1992). A contribution to the life history of *Plasmodiophora brassicae*: secondary plasmodia development in root galls of *Arabidopsis thaliana*. *Mycol. Res.* 96, 877–885. doi: 10.1016/S0953-7562(09)81035-6

Nesi, N., Delourme, R., Bregeon, M., Falentin, C., and Renard, M. (2008). Genetic and molecular approaches to improve nutritional value of *Brassica napus* L. seed. *C. R. Biol.* 331, 763–771. doi: 10.1016/j.crvi.2008.07.018

Qu, C. M., Li, S. M., Duan, X. J., Fan, J. H., Jia, L. D., Zhao, H. Y., et al. (2015). Identification of candidate genes for seed glucosinolate content using association mapping in *Brassica napus* L. *Genes* 6, 1215–1229. doi: 10.3390/genes6041215

Ren, L., Xu, L., Liu, F., Chen, K. R., Sun, C. C., Li, J., et al. (2016). Host range of *Plasmodiophora brassicae* on cruciferous crops and weeds in China. *Plant Dis.* 100, 933–939. doi: 10.1094/Pdis-09-15-1082-Re

Seo, M. S., Jin, M., Chun, J. H., Kim, S. J., Park, B. S., Shon, S. H., et al. (2016). Functional analysis of three BrMYB28 transcription factors controlling the biosynthesis of glucosinolates in *Brassica* rapa. *Plant Mol. Biol.* 90, 503–516. doi: 10.1007/s11103-016-0437-z

Siemens, J., Keller, I., Sarx, J., Kunz, S., Schuller, A., Nagel, W., et al. (2006). Transcriptome analysis of Arabidopsis clubroots indicate a key role for cytokinins in disease development. *Mol. Plant Microbe Interact.* 19, 480–494. doi: 10.1094/MPMI-19-0480

Tierens, K. F., Thomma, B. P., Brouwer, M., Schmidt, J., Kistner, K., Porzel, A., et al. (2001). Study of the role of antimicrobial glucosinolate-derived isothiocyanates in resistance of Arabidopsis to microbial pathogens. *Plant Physiol.* 125, 1688–1699. doi: 10.1104/pp.125.4.1688

Williams, P. H. (1966). A system for the determination of races of *Plasmodiophora brassicae* that infect cabbage and rutabaga. *Phytopathology* 56, 624–626.

Wittstock, U., and Halkier, B. A. (2002). Glucosinolate research in the *Arabidopsis* era. *Trends Plant Sci.* 7, 263–270. doi: 10.1016/S1360-1385(02)02273-2

Xu, L., Ren, L., Chen, K. R., Liu, F., and Fang, X. P. (2016). Putative role of IAA during the early response of *Brassica napus* L. *to Plasmodiophora brassicae*. *Eur. J. Plant Pathol.* 145, 601–613. doi: 10.1007/s10658-016-0877-y

Yi, G. E., Robin, A. H., Yang, K., Park, J. I., Hwang, B. H., and Nou, I. S. (2016). Exogenous methyl jasmonate and salicylic acid induce subspecies-specific patterns of glucosinolate accumulation and gene expression in *Brassica oleracea* L. *Molecules* 21:E1417. doi: 10.3390/molecules21101417

Yin, L., Chen, H., Cao, B., Lei, J., and Chen, G. (2017). Molecular characterization of MYB28 involved in aliphatic glucosinolate biosynthesis in Chinese Kale (*Brassica oleracea* var. alboglabra Bailey). *Front. Plant Sci.* 8:1083. doi: 10.3389/fpls.2017.01083

Conflict of Interest Statement: The authors declare that the research was conducted in the absence of any commercial or financial relationships that could be construed as a potential conflict of interest.

frontiers in Microbiology

ORIGINAL RESEARCH
published: 21 August 2018
doi: 10.3389/fmicb.2018.01848

Isolation, Diversity, and Growth-Promoting Activities of Endophytic Bacteria From Tea Cultivars of Zijuan and Yunkang-10

Xiaomei Yan, Zhi Wang, Yu Mei, Liqun Wang, Xu Wang, Qingshan Xu, Su Peng, Yu Zhou and Chaoling Wei**

State Key Laboratory of Tea Plant Biology and Utilization, Anhui Agricultural University, Hefei, China

Endophytes are rich in plant tissues and play important roles in plant-microbial interactions and plant-growth regulation. Here, endophytic bacteria from two closely related tea cultivars of Zijuan and Yunkang-10 were isolated, and the diversities were compared. Plant-growth promoting (PGP) activities were determined on the dominant groups or nitrogen-fixing genera from the two cultivars. Endophytic bacteria were isolated by using of different selective media and methods, and the PGP activities were investigated by analytical and molecular technologies. A total of 110 isolates of 18 genera belonging to three phylums (*Proteobacteria*, *Firmicutes,* and *Bacteroidetes*) were obtained from Zijuan, while 164 isolates of 22 genera belonging to two phylums (*Proteobacteria* and *Firmicutes*) were obtained from Yunkang-10. PGP screening indicated that *Herbaspirillum* spp., *Methylobacterium* spp., and *Brevundimonas* spp. showed different PGP abilities. The PGP ability decreased in order of *Herbaspirillum* spp., *Brevundimonas* spp. and *Methylobacterium* spp., and the majority of *Methylobacterium* spp. did not showed PGP activity of nitrogen-fixation, P-solubilization, siderophore, indole-3-acetic acid (IAA) production or 1-aminocyclopropane-1-carboxylate (ACC) deaminase. The study of bacterial community and PGP activities confirmed that endophytes in tea plants are constantly changing in different seasons and tea cultivars, and the PGP bacteria in Zijuan are much abundant than those of Yunkang-10.

Keywords: endophytic bacteria, Zijuan, Yunkang-10, *Camellia sinensis* var. *assamic*, plant growth promoting

OPEN ACCESS

Edited by:
Juan Antonio Lopez Raez, Consejo Superior de Investigaciones Científicas (CSIC), Spain

Reviewed by:
Álvaro López-García, University of Copenhagen, Denmark
Jihong Jiang, Jiangsu Normal University, China

****Correspondence:***
Yu Zhou
microbes@ahau.edu.cn;
zhouyu121121@hotmail.com
Chaoling Wei
weichl@ahau.edu.cn

Specialty section:
This article was submitted to Plant Microbe Interactions, a section of the journal Frontiers in Microbiology

Received: *21 March 2018*
Accepted: *24 July 2018*
Published: *21 August 2018*

Citation:
Yan X, Wang Z, Mei Y, Wang L, Wang X, Xu Q, Peng S, Zhou Y and Wei C (2018) Isolation, Diversity, and Growth-Promoting Activities of Endophytic Bacteria From Tea Cultivars of Zijuan and Yunkang-10. Front. Microbiol. 9:1848. doi: 10.3389/fmicb.2018.01848

INTRODUCTION

Endophytes are a group of microorganisms that reside in healthy plants, but not result in plant disease, and endophytes have attracted increasing attention to microbiologist (Qin et al., 2011). Numerous studies indicated that endophytes play important roles in plant disease resistance, secondary metabolites synthesis, plant growth regulations, and environmental stressors withstand (Coombs and Franco, 2003; Qin et al., 2009, 2011, 2015, 2017; Glick, 2014; Mora et al., 2014; Zhao et al., 2016). Early endophytes studies mainly focused on rice, wheat, cotton, and other staple crops, but endophytes from other plants (including tea and medicinal plants) were rarely considered (Coombs and Franco, 2003; Ji et al., 2014; Hardoim et al., 2015). Recently, endophytes

have become a research hotspot in microbiology field for the abundant secondary metabolites, PGP activities and plant protection roles (Qin et al., 2009, 2015, 2017; Glick, 2014; Mora et al., 2014; Zhao et al., 2016). Hitherto, the interaction patterns between many host plants and endophytes remains unknown (Strobel and Daisy, 2003; Qin et al., 2017). Plenty of studies showed that endophytes can regulate plant growth by means of nitrogen-fixation, phosphate solubilization, siderophore, 1-aminocyclopropane-1-carboxylate (ACC) deaminase activity and indole-3-acetic acid (IAA) synthesis. The study of Zgadzaj et al. (2015) showed that endophytes and symbiotic nitrogen-fixing bacteria in nodules of leguminous plants jointly improved pathogen resistance ability of host plants. Similarly, the endophytic *Klebsiella* sp. and *Enterobacter* sp. in sugarcane significantly promoted the host plant growth by nitrogen-fixation (Zhu et al., 2012; Lin et al., 2015), and the nitrogen-fixation activity of *Klebsiella* sp. assisted the host plant growing on barren dune stubbornly (Chen et al., 2013). *Jatropha curcas* L., a fuel plant prefers to grow on barren sandy soil, contains a rich population of growth-promoting bacteria, and the nitrogen-fixing *Methylobacterium* sp. (L2-4) significantly increased the host plant growth and seed yield (Madhaiyan et al., 2013, 2014, 2015). Endophytic isolates from rice plants (*Oryza sativa*) were the earliest investigated plant endophytes, and the endophytes showed versatile PGP activities of nitrogen-fixation, phosphate solubilization, siderophore and IAA synthesis (Ji et al., 2014). Qin et al. (2014) assessed the PGP functions (i.e., ACC deaminase, IAA synthesis and nitrogen fixation) of 126 endophytic isolates from the medicinal plant *Limonium sinense* (Girard) Kuntze, and found many isolates showed PGP activities, but no further study was made on the PGP mechanisms.

Tea plants (i.e., *Camellia sinensis* var. *assamic* and *C. sinensis*) are evergreen shrub, rich in polyphenols (e.g., flavonoids and catechins), anthocyanins and theanine, and considered as a healthy drink in China and other Asian countries. As we known, catechins and theanine are considered as the most important secondary metabolites in tea plants for their healthy activities of antioxidant, antimicrobial, anticarcinogenic, anti-inflammatory, and antiarteriosclerotic properties (Ito et al., 1992; Wheeler and Wheeler, 2004; Cooper et al., 2005). Anthocyanins are the secondary metabolites extensively distribute in plants that serve as plant pigments for signaling between plants and insects (or microbes); indicating nutrient availability and antioxidant activity; coloring of fruits, vegetables, flowers, and grains; providing defense as feeding deterrents and antimicrobial agents; modulating auxin synthesis and transport (Jia et al., 2015). However, only a few studies have been carried out on tea plant endophytes, and these few studies mainly focused on endophytic fungi and their plant diseases resistance. For example, endophytic fungus *Colletotrichum gloeosporioides* isolated from healthy tea plant tissues showed a strong inhibitory activity on tea plant pathogens of *Pestalotiopsis theae* and *Colletotrichum camelliae*, and the inhibitory mechanism may attribute to the fungus' high efficient chitinase and protease (Rabha et al., 2014). Compared to fungi, endophytic bacteria received less attention to tea plants, and the interaction studies between endophytic bacteria and host tea plant have not yet investigated. Based on the research progress of other plants, the study of diazotrophs and other PGP endophytes on non-legume plant is of great significance on plant growth regulations and agriculture sustainable development. In this study, we aim to isolate and characterize endophytic bacteria from two closest cultivars of Zijuan and Yunkang-10 at different seasons, the PGP activities of nitrogen-fixation, P-solubilization, siderophore, IAA synthesis and ACC deaminase are screened and the PGP mechanisms of nitrogen-fixation and IAA synthesis will further evaluate for the predominant groups.

MATERIALS AND METHODS

Sample Planting and Collection

Tea cultivars of Zijuan and Yunkang-10 (*C. sinensis* var. *assamic*) origin from Yunnan Province of China were transplanted at the same nursery in Shucheng County of Anhui Province (China), and grown under natural environment with the same level of cultivation and management. In this study, 3-year-old clone cuttings of Zijuan and Yunkang-10 from Dechang tea plantation (Shucheng, China) were used as the isolation materials. The samples were obtained on April 15 (spring), August 5 (summer), October 20 (autumn), and December 20 (winter) in 2015. At the time of sampling, 15 branches (one branch from each tree) with the similar growth and no pest injury were selected, and the branches were placed in fully soaked floral foam and transported to the laboratory within 2 h for bacteria isolation.

Determination of Catechine and Anthocyanin in Tea Plant Leaf

Extractions of catechines and anthocyanins from the leaf of Zijuan and Yunkang-10 were performed as previous at room temperature under dark condition (Jiang L. et al., 2013; Jiang X. et al., 2013). Ultra-high performance liquid chromatography (UPLC, Waters ACQUITY) with TUV detector was used for catechines and anthocyanins determination. The chromatographic separation was performed on a phenomenex Kinetex-C_{18} column (2.6 μm, 4.6 mm × 100 mm). The mobile phase A: H_2O/HCOOH (99.5: 0.5, v/v) and mobile phase B: C_2H_3N: 100% were used. The phase B elution gradient was from 10 to 15% in 3 min, 15 to 20% in 2 min, 20 to 25% in 5 min, 25 to 90% in 5 min, and 90% down to 10% in 5 min for anthocyanins determination. The flow rate was 0.4 mL/min, detection wavelength was 520 nm and the injection volume was 2 μL. The phase B elution gradient increased from 5 to 7% in 4 min, remained 7% with 1 min, increased from 7 to 17% in 27 min, 17 to 90% in 8 min, and 90% to 5% in 5 min for catechins determination. The flow rate was 0.8 mL/min, detection wavelength was 280 nm and injection volume was 2 μL. The total catechins in this study are (+)-catechin, (+)-gallocatechin, (−)-epicatechin, (−)-epigallocatechin, (−)-epicatechin-3-gallate and (−)-epigalloccatechin-3-gallate, and the total anthocyanins are scabiolide, delphinidin and pelargonin.

Isolation Procedures and Cultivate Media

Leaf samples were surface-sterilized by the method as described by Qin et al. (2009) with minor modification. The samples were

sterilized in the following order: a 1-min soaking in 70% ethanol, followed by a 6-min soaking in 3.25% NaOCl, a 1-min soaking in 70% ethanol, and a 1-min rinse by sterile water for five times. The sterilized tissues were imprinted onto nutrient agar (NA, Difico) and tryptic soy agar (TSA, Difico), then incubated at 30°C for 1 week to ensure the sterilization effectiveness. After surface-sterilization and drying under aseptic conditions, 5-g surface-sterilized samples from three sampling branches were cut up in a sterile mortar and grinding to homogenate, followed by dilution to 10^{-1}, 10^{-2}, and 10^{-3} with sterile water. An aliquot of 200-μL dilutions were spread over the surface of solid media and incubated at 30°C for 5 days. Three isolation media: NA (Difico), TSA (Difico) and tea-extract agar (Basal content: tryptone 10 g, yeast extract 5 g, NaCl 5 g, agar 18 g, 1 L distilled water, pH 7.3; tea extract: 5.0 mL) were selected for the isolation. The above mentioned NA, TSA and basal content of tea-extract medium were sterilized at 121°C for 15 min. Tea extract was prepared by leaf homogenate and sterilized by 0.22 μm filter, and tea-extract medium was prepared by adding sterilized tea extract to the sterilized and slightly cooled basal medium (∼50°C). After incubation, the bacterial colonies were picked and repeatedly re-streaked onto agar plate until their purity was confirmed for 16S rRNA gene analysis.

DNA Extraction, PCR Amplification, 16S rRNA Gene Analysis

Genomic DNA was extracted by ChargeSwitch® gDNA Mini Bacteria Kit (Invitrogen, Shanghai) following the manufacturer's instruction. The universal primers of 16SF- (AGAGTTTGATCCTGGCTCAG) and 16SR- (GGTTACCTTGTTACGACTT) were used for PCR amplification (Stackebrandt and Goodfellow, 1991). The PCR amplification was performed as described by Qin et al. (2009), and the 16S rRNA gene was sequenced by Life Technologies Inc. (Shanghai, China). The 16S rRNA gene was manually aligned with reference sequences retrieved from GenBank database[1] and EzBioCloud (Yoon et al., 2017) following BLAST searches for fast identification. Phylogenetic tree was constructed by the software package MEGA 6.0 (Tamura et al., 2013) after multiple alignment of sequences data by CLUSTAL_X (Thompson et al., 1997). The corrected evolutionary distance was evaluated according to Kimura's two-parameter model (Kimura, 1980), and the clustering was based on the neighbor-joining method (NJ tree, Saitou and Nei, 1987). Bootstrap analysis was applied to the tree topology by performing 1000 resamplings (Felsenstein, 1985).

Endophytic Bacteria Diversity Analysis

The diversity index (H'), the evenness index (J), the dominance index (D) and the richness index (E) of the endophytic isolates from Zijuan and Yunkang-10 in each season were calculated and compared according to literatures (Shannon, 1948; Simpson, 1949; Menhinick, 1964; Pielou, 1969).

Diversity analysis (Shannon-Wiener index) was calculated as: $H' = -\sum_{i=1}^{n} PiLnPi$, the uniformity analysis (evenness index) was calculated as: $J = -\sum_{i=1}^{n} PiLnPi/LnS$, the dominance index was calculated as: $D = 1 - \sum_{i=1}^{n} Pi^2$and the richness index was calculated as: $E = S - 1/LnN$.

The $Pi = ni/N$, ni is the number of the species i in the sample and N is the number of total isolates in the sample, and S is the number of species in the sample.

PGP Activities Assay

The dominant endophytic bacterial groups from tea cultivars of Zijuan and Yunkang-10, and the recognized PGP bacterial genera obtained in this study were selected for PGP screening and further investigation.

Nitrogen-Fixation Screening and Nitrogenase Activity Determination

The fresh colony was seeded onto the nitrogen-free Ashby's mannitol agar (Sigma-Aldrich) and Nfb agar (Hopebiol, Qingdao, China), respectively. The original isolation medium of NA, TSA or tea-extract agar was set as control, the seeded plates were incubated in 30°C, and the bacterial growth was observed. The isolate displayed growth in Ashby's mannitol agar and made Nfb agar from green to blue was considered as positive strain, positive strain was picked to the second generation test, and the positive isolate from the third generation was recognized as nitrogen-fixing bacteria. Nitrogenase is the most important enzyme involved in nitrogen-fixation and the enzyme contains of two components, commonly called molybdenum ferritin and ferritin, the genes encoding the molybdenum ferritin are *nifD* and *nifK*, and the gene encoding the ferritin is *nifH* (Li et al., 2016; Allen et al., 2017). The *nifH* is a highly conserved 360 base-pairs region which is usually considered as the molecular marker for fast determination of nitrogenase (Allen et al., 2017). The nitrogenase activity was determined by the method of acetylene reduction as described by You et al. (2005) with minor modifications. An aliquot of 200 μL fresh culture was inoculated to 20 mL of nutrient broth and incubated overnight at 30°C. Bacterial growth was collected by centrifugation and was washed twice using sterile water, and resuspended by liquid limited nitrogen culture medium (OD_{600} = 0.2). The 3 mL suspension was transferred to a 25 mL sterilized serum vial and 2.4 mL acetylene gas (99.9999%) was driven into the serum bottle, and then incubated at 30°C for 12 h. The ethylene content and the protein of bacterial suspension were determined as You et al. (2005). DNA from nitrogenase positive isolate was used for *nifH* gene amplification, the primer set and PCR conditions were followed as Poly et al. (2001). The PCR reagents were purchased from TaKaRa (Dalian, China), and the PCR product purification, DNA sequence and phylogenetic analysis were performed as the 16S rRNA gene.

Phytohormone Indole-3-Acetic Acid (IAA) Production Assay

Indole-3-acetic acid production was examined for the dominant endophytic groups of the tea cultivars using the method as

[1] www.ncbi.nlm.nih.gov

Glickmann and Dessaux (1995). The isolate was grown in test tube containing 3 mL of dextrose-minimal salts broth [containing 1.0% Dextrose, 0.1% $(NH_4)_2SO_4$, 0.2% K_2HPO_4, 0.05% $MgSO_4 \cdot 7H_2O$, 0.01% NaCl, 0.05% $CaCO_3$, 0.05% Yeast extract, PH 7.2] supplemented with 0.5 mg/mL tryptophan. The strain was incubated for 2 days at 28°C with 150 rpm, and IAA was determined by spectrophotometry as described by Qin et al. (2014). The positive isolates in preliminary screening were randomly selected for further determination of IAA synthesis dynamics. After incubation, IAA was extracted and determined by UPLC as described by Tien et al. (1979). Chromatographic separation was performed on a reverse-phase column (ACQUITY UPLC® BEH C_{18} 1.7 μm 2.1 × 100 mm) in a Waters Associates liquid chromatograph (ACQUITY UPLC H-Class) equipped with an ultraviolet detector at 280 nm. The injection volume is 5 μL and the mobile phase was acetonitrile: water: acetic acid (85:15:1, v/v/v) at the flow rate of 0.5 mL/min. An Agilent 6500 UPLC-MS system (Q-TOF) was used for LC-MS qualitative analyses. The UPLC-MS separation mobile phase and the chromatographic column were the same as described for UPLC analysis. The flow rate was 0.2 mL/min and the injection volume was 2 μL. The optimum mass spectra, collision energy values and fragmentor energy were obtained by infusion of 20 μg/mL IAA standard directly in positive ionization mode. The ESI conditions were as follow: gas temperature 300°C, gas flow rate 8.0 L/min, sheath gas temperature 300°C, sheath gas flow rate 11.0 L/min, and nebuliser pressure 35 psi. The mass scan range was set as m/z 100–1500.

Other PGP Activities Determination

Isolate screening for ACC deaminase was determined by ACC dworkin-foster minimal salt (ADF) agar (Honma and Shimomura, 1978), in which 3 mM ACC instead of $(NH_4)_2SO_4$ as nitrogen source. The inoculated ADF agar was cultured at 28°C for 7 days, and the observed growth was transferred to the second generation. Positive isolate at the fifth generation indicates the ACC deaminase activity. The quantitative assay of ACC deaminase was determined by the amount of α-ketobutyrate (α-KB) production as described as previous (El-Tarabily, 2008; Qin et al., 2014). Phosphate (P−) solubilization activity was determined by using pikovskayas agar (Sigma-Aldrich). The isolate was inoculated onto the pikovskayas agar, cultured at 28°C for 5 days. After incubation, phosphate-solubilizing isolate would form a clear halo zone around the bacterial colony (Qin et al., 2014). Siderophore production was examined by using chrome azurol S (CAS) agar (Schwyn and Neilands, 1987). Isolate was inoculated onto CAS agar, cultured at 28°C for 2 days, and the positive strain was indicated by an orange halo around the bacterial colony.

Statistical Analysis

Unless otherwise indicated, the experiments of this study were performed in triplicate, and the average value was calculated for the quantitative determinations. GraphPad Prism software was used for data analysis, and data are presented as means ± SD. The difference of bacterial communities between tea cultivars of Zijuan and Yunkang-10 was assessed by PERMANOVA (McArdle and Anderson, 2001), and p-values < 0.05 were considered statistically significant.

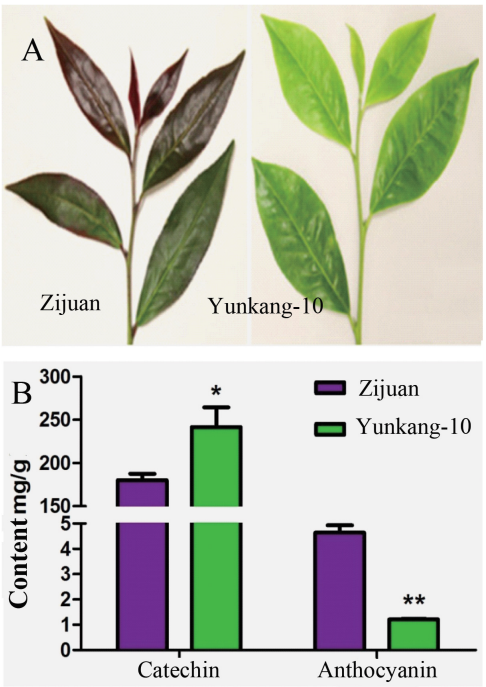

FIGURE 1 | The contents of total catechins and anthocyanins in fresh leaf of Zijuan and Yunkang-10 (*$p < 0.05$, **$p < 0.01$). **(A)** The leaf photographs of Zijuan and Yunkang-10. **(B)** The total contents of catechins and anthocyanins.

RESULTS

The Catechin and Anthocyan Contents in Zijuan and Yunkang-10

The secondary metabolites determination result showed that the catechins content in Zijuan was 180.3 mg/g fresh leaf, and in Yunkang-10 was 241.6 mg/g fresh leaf. In contrast, the anthocyanins content in Zijuan was 4.7 mg/g comparing to 1.2 mg/g in Yunkang-10 fresh leaf, and the high anthocyanins content in cultivar Zijuan is obviously indicated by purple color of the fresh leaf (**Figures 1A,B**). The analysis results showed that the catechins in Zijuan were significantly lower than that of Yunkang-10, while anthocyanins in Zijuan were about 3 ∼ 4 times higher than those of Yunkang-10. The catechins and anthocyans determined in this study were substantial consistent to the previous (Jiang L. et al., 2013), and these secondary metabolites difference might affect microbial colonization (Maximilien et al., 1998).

The Endophytic Bacteria Isolation Results From Tea Plants

The cultivable endophytic bacterial communities from Zijuan and Yunkang-10 were quite different, and the bacterial community in each tea cultivar was always changing from

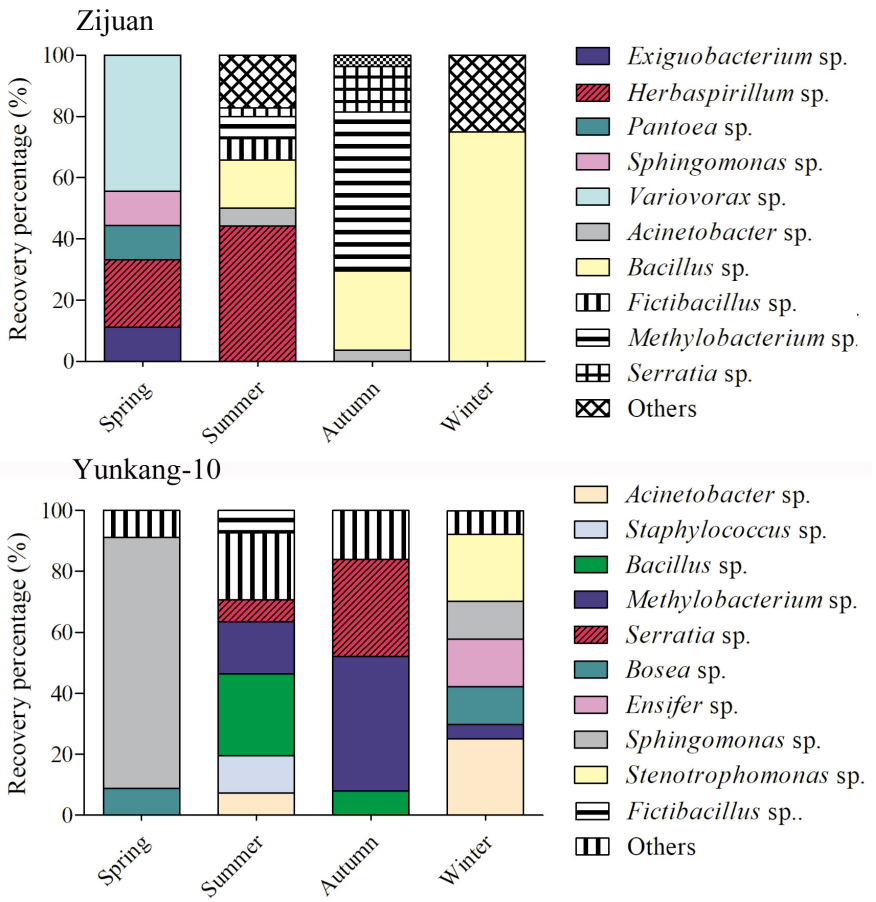

FIGURE 2 | The community dynamics and comparisons for the cultivable endophytic bacteria from Zijuan and Yunkang-10 in four seasons.

one season to another. For the Zijuan results, a total of nine isolates were obtained in spring, and the dominant groups were *Variovorax* spp. (44.4%) and *Herbaspirillum* spp. (22.2%), the other groups were only obtained one isolate for each genus; 70 isolates were obtained in summer, the dominant groups including *Herbaspirillum* spp. (44.29%) and *Bacillus* spp. (15.7%), and the other groups were less than 10% for each genus; 27 isolates were obtained in autumn, and the dominant groups were *Methylobacterium* spp. (51.9%), *Bacillus* spp. (25.9%) and *Serratia* spp. (14.8%), and the other groups were less than 4.0% for each genus; 4 isolates were obtained in winter, the 3 isolates were *Bacillus* spp. and the other was *Brevundimonas* sp. (**Figure 2** and **Supplementary Table S1**). For the Yunkang-10 results, a total of 34 isolates were obtained in spring, and the predominant group was *Sphingomonas* spp. (82.4%), and the other groups were less than 10% for each genus; 41 isolates were obtained in summer, the dominant groups were *Bacillus* spp. (26.8%), *Methylobacterium* spp. (17.1%), *Staphylococcus* spp. (12.2%), and the other groups were less than 10% for each genus; 25 isolates were obtained in autumn, the dominant groups were *Methylobacterium* spp. (44.9%), *Serratia* spp. (32%), and the other groups were less than 10% for each genus; 64 isolates were obtained in winter, the dominant groups were *Acinetobacter* spp. (25%), *Stenotrophomonas* spp. (21.9%), *Ensifer* spp. (15.6%), *Bosea* spp. (12.5%), *Sphingomonas* spp. (12.5%), and the other groups were less than 5% for each genus (**Figure 2** and **Supplementary Table S1**). As indicated above, *Herbaspirillum* spp. were dominant group in Zijuan on spring and summer; *Methylobacterium* spp. were dominant group in Zijuan on autumn, and in Yunkang-10 on summer and autumn; *Bacillus* sp. were dominant group in Zijuan on summer, autumn and winter, and in Yunkang-10 on summer. Hence, the groups of *Herbaspirillum* spp., *Methylobacterium* spp., and *Bacillus* spp. are the most important endophytic bacteria for tea cultivars of Zijuan and Yunkang-10.

Phylogenetic analysis showed that 110 isolates from Zijuan were belonged to three phylums, while the 164 isolates from Yunkang-10 were belonged to two phylums. Specifically, bacterial groups from Zijuan (**Supplementary Figure S1**) included *Proteobacteria* (nine genera: *Sphingomonas*, *Brevundimonas*, *Methylobacterium*, *Variovorax*, *Herbaspirillum*, *Ralstonia*, *Pantoea*, *Acinetobacter*, *Serratia*), *Firmicutes* (eight genera, *Exiguobacterium*, *Bacillus*, *Fictibacillus*, *Bhargavaea*, *Lysinibacillus*, *Sporosarcina*, *Staphylococcus*, *Oceanobacillus*) and *Bacteroidetes* (one genus, *Myroides*). Comparatively, bacterial groups from Yunkang-10 (**Supplementary Figure S2**) were

Proteobacteria (16 genera: *Sphingomonas*, *Bosea*, *Brevundimonas*, *Methylobacterium*, *Sphingobium*, *Bradyrhizobium*, *Ensifer*, *Variovorax*, *Aquincola*, *Burkholderia*, *Massilia*, *Luteibacter*, *Serratia*, *Acinetobacter*, *Pseudomonas*, *Stenotrophomonas*) and *Firmicutes* (6 genera, *Bacillus*, *Fictibacillus*, *Sporosarcina*, *Staphylococcus*, *Oceanobacillus*, *Paenibacillus*). The mutual bacterial genera of the two cultivars were *Sphingomonas*, *Variovorax*, *Acinetobacter*, *Bacillus*, *Fictibacillus*, *Brevundimonas*, *Methylobacterium*, *Serratia*, *Sporosarcina*, *Staphylococcus*, *Oceanobacillus,* and *Brevundimonas*. The genera of *Exiguobacterium*, *Herbaspirillum*, *Pantoea*, *Bhargavaea*, *Lysinibacillus*, *Myroides,* and *Ralstonia* were exclusively obtained from Zijuan, while the genera of *Aquincola*, *Bosea*, *Luteibacter*, *Sphingobium*, *Burkholderia*, *Bradyrhizobium*, *Pseudomonas*, *Ensifer*, *Massilia*, *Paenibacillus,* and *Stenotrophomonas* were only obtained from Yunkang-10. However, no statistical significant difference was observed ($p = 0.1$) for the bacterial communities between Zijuan and Yunkang-10 determined by perMANOVA tests.

The Bacterial Diversity of the Two Tea Cultivars

The diversity index of H' expresses the relative complexity of the community structure. The higher diversity index of H' indicates the more abundant species, whereas the D index expresses dominance or relative concentration of the importance values to few species (Shannon, 1948; Simpson, 1949; Whittaker, 1972). The evenness index of J reflects the uniformity of individual species, and the richness index of E strongly depends on the species number which can reflect the species distribution (Menhinick, 1964; Pielou, 1969; Peet, 1974). Due to the reduced number of species isolated in this study (richness equal to one species in some samples), the statistical tests for the diversity analysis could not be properly carried out, and diversity indexes were calculated for the overall treatments and not for single sample. Diversity index (H'), evenness index (J), dominance index (D) and richness index (E) of the endophytic bacteria from tea cultivars Zijuan and Yunkang-10 were calculated and compared as follow (**Supplementary Figure S3**). The analysis results showed that the endophytic bacterial diversity indexes of H', D, and E from Zijuan in summer were higher than those in autumn and winter, but the evenness index of J showed non-obviously difference. The bacterial diversity indexes of H', J, D, and E from Yunkang-10 in summer and winter were higher than those in autumn and spring, and the diversity indexes of spring were the lowest among four seasons. When compared the two cultivars, the endophytic bacterial diversity indexes of H', J, and D in spring from Zijuan were higher than those of Yunkang-10, and the richness index of E showed no obvious difference from each other. Other than the richness index E in summer, the diversity indexes of H', J, D, and E showed consistently higher values in Yunkang-10 than those of Zijuan in summer, autumn and winter. The diversity results indicated that endophytic bacteria of Zijuan were most abundant in summer, but endophytic bacteria of Yunkang-10 were most abundant in winter; the endophytic bacterial diversities in Yunkang-10 were higher than those of the closest tea cultivar Zijuan in summer, autumn and winter.

PGP Activities of the Endophytic Isolates

Herbaspirillum spp. were the dominant group of Zijuan in spring and summer, *Methylobacterium* spp. were dominant group in Zijuan on autumn, and in Yunkang-10 on summer and autumn, *Bradyrhizobium* spp. were recognized nitrogen-fixing bacterial genus. The isolates of *Herbaspirillum*, *Methylobacterium* and *Bradyrhizobium* were randomly selected and examined for the PGP activities, and the preliminary screening results were summarized in **Table 1**. The screening results showed that 11 selected *Herbaspirillum* isolates showed PGP activities, but only a few *Methylobacterium* isolates displayed PGP activities. Eight *Herbaspirillum* isolates (other than ZXN223, ZXN121, and ZXN122) displayed five tested PGP activities of nitrogen-fixation, P-solubilization, siderophore, IAA production, and ACC deaminase. The *Bradyrhizobium* isolates showed PGP activities of nitrogen-fixation, siderophore and IAA production (or ACC deaminase), but neither of them possessed five PGP activities. IAA biosynthesis was only observed for three *Methylobacterium* isolates, while 10 of 11 *Herbaspirillum* isolates were positive for IAA production. In the phosphate solubilization screening, only *Herbaspirillum* isolates showed appearance of well-developed clearing zones after 5 days incubation, and no isolates from other genera showed the p-solubilization activity.

On the basis of PGP activity screening, three *Herbaspirillum* isolates were further evaluated for IAA production dynamics by UPLC and UPLC-MS. The results showed that IAA produced from *Herbaspirillum* isolates could be quantified by UPLC using the IAA standards, and identified by UPLC-MS using the distinctive m/z value of 176.07 Da (**Figures 3A–D**). As the quantified results, 16 *Herbaspirillum* isolates all produced IAA during the 4-days incubation, but the IAA biosynthesis yields were quite different among these isolates (**Figure 3E**). The production dynamics of the three selected *Herbaspirillum* isolates showed that the yield of isolate ZXN121 was much higher than those of isolates ZXN111 and ZXL111 after 5-days incubation. The maximal IAA concentration (∼20 μg/mL) in ZXN111 or ZXL111 culture supernatant was observed at 5th day, and then the IAA content gradually decreased. While, the IAA content in ZXN121 culture supernatant was steady increased (>30 μg/mL) during 7 days incubation (**Figure 3F**). However, the most efficient *Methylobacterium* and *Bradyrhizobium* isolates for IAA biosynthesis were *Methylobacterium* YFY141, *Methylobacterium* YFY242, and *Methylobacterium* YXN332, but the maximal yield of the three isolates during 7 days was lower than 3.0 μg/mL (data not shown).

The nitrogenase activities of five positive nitrogen-fixing isolates determined by acetylene reduction assay were 34.3, 38.0, 28.5, 42.3, and 29.1 nmol C_2H_4/mg·protein·h (**Figure 4A**), respectively. The nitrogenase activities of this study were higher than *Azotobacter* sp. strain ACCC10006 (19.2 nmol C_2H_4/mg·protein·h), but consistent to *Rhizobium* sp. (30–60 nmol C_2H_4/mg·protein·h; Gibson et al., 1976; Vladimir and Dobereiner, 1988). The PCR products indicated that the five selected nitrogen-fixing isolates contained

an amplifiable expected band (∼360 bp) on agarose gel electrophoresis (**Figure 4B**). The similarities of gene *nifH* from the five isolates were 94 ∼ 99% compared with GenBank database. Twelve *nifH* gene sequences with the highest homology to the five *Herbaspirillum* isolates were selected, and the phylogenetic analysis was performed. The *nifH* gene sequences of the five *Herbaspirillum* isolates were clustered to genera of *Rhizobium* and *Bradyrhizobium*, but were clearly separated from other *Herbaspirillum* spp. and *Paenibacillus* sp. obtained from GenBank database. Specifically, the *nifH* gene sequences of ZXT112, ZXT114, ZXT117, and ZXN111 were closely to genus *Bradyrhizobium*, and the *nifH* gene sequence of ZXT113 showed the highest similarity to genus *Rhizobium*. Phylogenetic analysis indicated that the *nifH* gene of *Herbaspirillum* spp. from Zijuan showed the closest relations to *Bradyrhizobia* sp. and *Rhizobia* sp., but far from the type species of *Herbaspirillum seropedicae* (**Figure 4C**).

DISCUSSION

Tea cultivars of Zijuan and Yunkang-10 are origin from Yunnan Province of China, and two cultivars belong to the same taxonomic species of *C. sinensis* var. *assamic*. The two closest cultivars are the major raw materials for Pu'er tea (dark tea) production. The natural characters and planting environments of the two cultivars are similar, and the leaf anthocyanins content was the major difference (Jiang L. et al., 2013). As indicated in the introduction, tea plants are rich in tea polyphenols, anthocyanins and theanine, and the secondary metabolites have intensive antimicrobial activity to environmental microorganisms (Jiang L. et al., 2013; Jiang X. et al., 2013). Thus, endophytic bacteria of tea plant are relatively scarce, and the endophytes isolation from tea plants is a hard work for microbiologists. This study had tried best to isolate more endophytic bacteria by using different media at different seasons, but only 110 isolates were obtained from Zijuan and 164 isolates were obtained from Yunkang-10 in total. Due to the reduced isolates from two tea cultivars, no significant difference ($p > 0.05$) was observed for the bacterial communities between Zijuan and Yunkang-10 by perMANOVA test. However, the cultivable endophytic bacteria communities of the two cultivars were substantially different. For example, a total of 12 mutual bacteria genera were obtained from the two cultivars, but 18 genera were exclusive for one of the cultivars (i.e., 7 obtained from Zijuan and 11 obtained from Yunkang-10). As the isolation results indicated, *Herbaspirillum* spp. were the dominant and the most important PGP group of tea cultivar Zijuan in spring and summer, but the *Herbaspirillum* sp. was unexpectedly not observed from Yunkang-10 at any season. Similar to *Herbaspirillum* isolates, other dominant groups of the two cultivars were also different. As the results chapter and previous studies indicated (Jiang L. et al., 2013), the difference of the secondary metabolites (especially the of anthocyanins

TABLE 1 | The plant-growth promoting (PGP) activity screening on endophytic bacteria from Zijuan and Yunkang-10.

Isolates	Nitrogen fixation	P-solubilization	Siderophore	IAA production	ACC deaminase
***Herbaspirillum* sp.**					
ZXN223	−	+	+	−	+
ZXN4311	+	+	+	+	+
ZXN111	+	+	+	+	+
ZXT112	+	+	+	+	+
ZXT113	+	+	+	+	+
ZXT114	+	+	+	+	+
ZXT117	+	+	+	+	+
ZXN121	−	+	+	+	+
ZXL111	+	+	+	+	+
ZXL112	+	+	+	+	+
ZXN122	−	+	+	+	+
***Methylobacterium* sp.**					
YFY141	+	−	−	+	+
YFY142	−	−	−	−	−
YFY242	+	−	−	+	+
YXT237	−	−	−	−	−
YXN332	−	−	−	+	−
YXT231	−	−	−	−	−
YXT234	−	−	−	−	−
YXT235	−	−	−	−	−
YXN311	−	−	−	−	+
***Bradyrhizobium* sp.**					
YKFG8152	+	−	+	+	−
YKFT8112	+	−	+	−	+

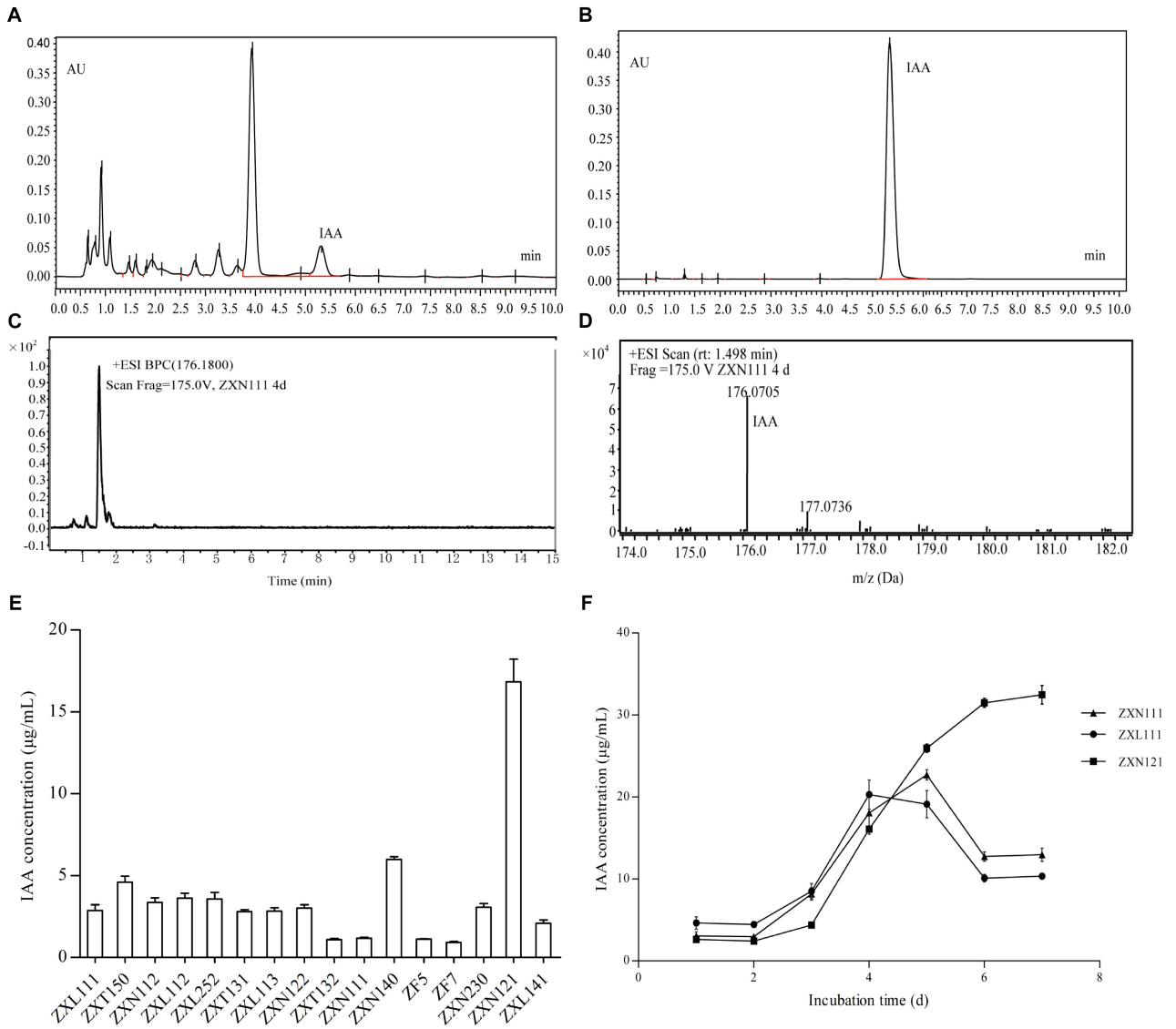

FIGURE 3 | The IAA screening results and accurate determinations on *Herbaspirillum* isolates from Zijuan. **(A)** The IAA extract from isolate ZXN111 by UPLC. **(B)** The IAA standard by UPLC. **(C)** Total ion current chromatogram of IAA extract in UPLC-MS. **(D)** The mass spectra of IAA extract in UPLC-MS. **(E)** The screening results of IAA biosynthesis on endophytic bacteria. **(F)** The IAA biosynthesis dynamics of the three randomly selected *Herbaspirillum* isolates.

content) in the two cultivars might be the intrinsic factor for the difference of endophytic community (Maximilien et al., 1998). Furthermore, the bacterial community in each tea cultivar was always changing from one season to another. This result was similar to previous microbial community studies on other plant endophytes and environmental samples, and the bacterial communities were influenced by temperature and climate changes, nutrition acquisition, and the activities of other living organisms in different seasons (Bulgari et al., 2014; Li et al., 2014; Resende et al., 2016).

As the same plant species, tea cultivar Yunkang-10 grows better than Zijuan (data not shown) at the same transplanted nursery with equal water and fertilizer management. Conversely, the microbial communities between the two cultivars were quite different, and the PGP endophytes of *Herbaspirillum* spp. in Zijuan of the spring and summer were not observed from Yunkang-10. Isolates of *Herbaspirillum* spp. were considered as the most active PGP endophytes among the evaluated isolates from the two cultivars. Although isolates of *Herbaspirillum* spp. were recognized as the dominant endophytic group of Zijuan in spring and summer, they were not observed from Zijuan at autumn and winter. Meanwhile, isolates of *Herbaspirillum* spp. were not obtained from Yunkang-10 at any season of this study. As we known, spring and summer are the most important seasons for tea plants growth and tea-picking, and nitrogen is in great demand in the two seasons; the dominant group of *Herbaspirillum* spp. (PGP endophytes) in the two seasons should be closest

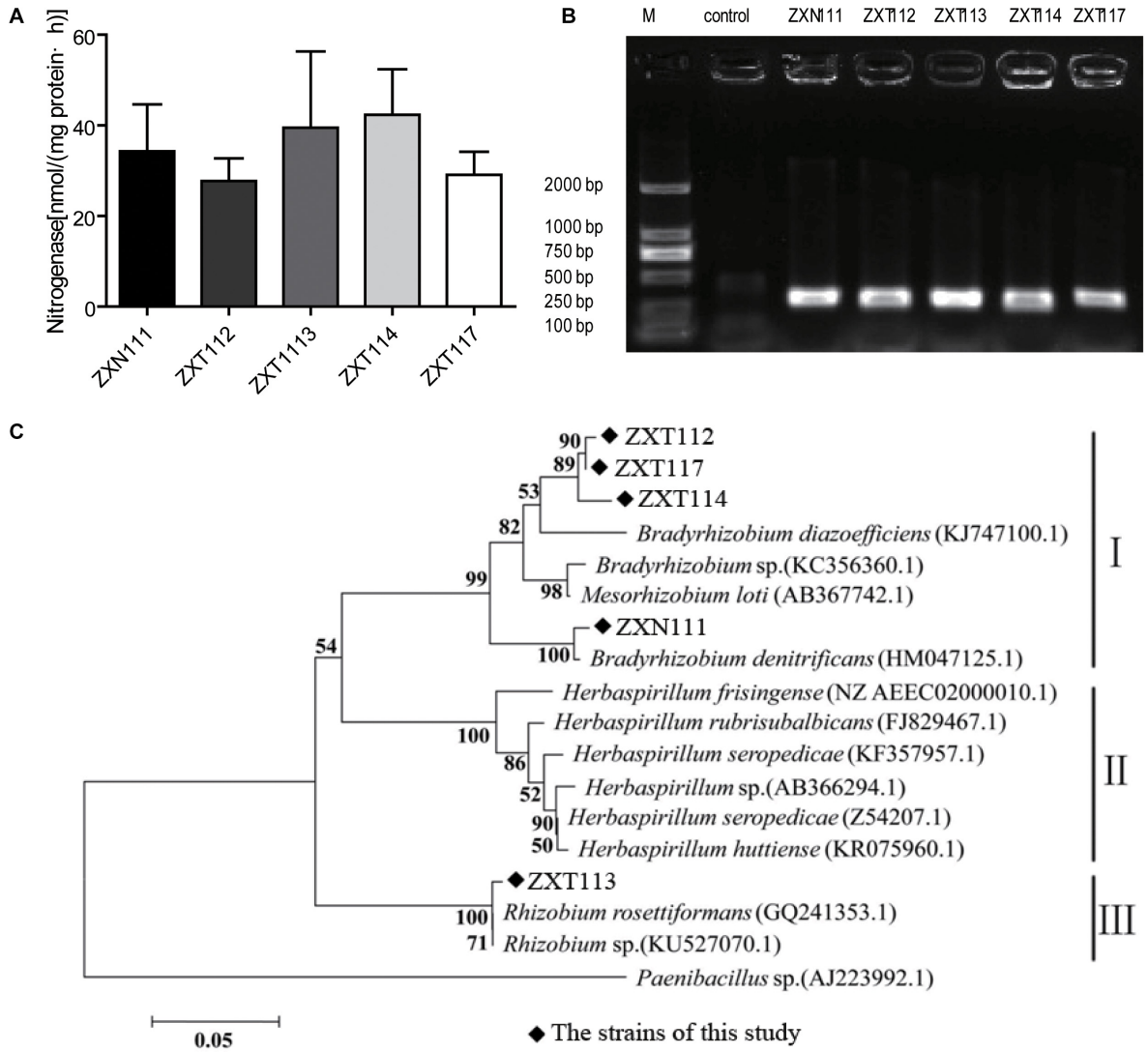

FIGURE 4 | The nitrogen-fixing determination results for the *Herbaspirillum* isolates. **(A)** The result of nitrogenase activity. **(B)** The PCR amplification of *nifH* gene. **(C)** Phylogenetic analysis of the *nifH* gene from *Herbaspirillum* isolates.

related to plant growth regulations of Zijuan. However, the growth of transplanted Yunkang-10 was obviously better that of Zijuan at the same planting conditions. Why the tea plant growths were not consistent to the PGP endophytes investigated results here? Previous studies indicated that the PGP endophytes of *Klebsiella* sp., *Methylobacterium* sp. assisted the host plants (*Psammochloa villosa*, *J. curcas* L.) growing on barren dune stubbornly (Chen et al., 2013; Madhaiyan et al., 2013, 2014, 2015). The study of Qin et al. (2014) found that the endophytic isolates with PGP activity of ACC deaminase, IAA synthesis or nitrogen-fixation enabled the hostplant *L. sinense* (Girard) Kuntze grow better under salt stress (Qin et al., 2014). Tea cultivars of Zijuan and Yunkang-10 (*C. sinensis* var. *assamic*) were transplanted from Yunnan Province of China, and the plateau-climate (∼2000 M of elevation) was the origin growth environment and considered more suitable for the plant growth. Compare to Yunnan province, the growth of Zijuan was weak in Anhui province of China, but the growth of transplanted Yunkang-10 was similar as the origin area. The transplanted environments at Anhui province may not appropriate for Zijuan, and the active PGP endophytes assisted the host plant grow at the flat areas, but these endophytes were not obligatory for Yunkang-10.

The nitrogen-fixation results by phenotype and genotype indicated that the majority isolates of *Herbaspirillum* sp. and *Bradyrhizobium* sp., and a few *Methylobacterium* sp. showed the nitrogenase activities; however, the *nifH* gene of *Herbaspirillum* spp. from Zijuan showed the closest relations to *Bradyrhizobia* sp. and *Rhizobia* sp., but not clustered to the typical nitrogen-fixation *Herbaspirillum* species (*Herbaspirillum seropedicae*) of gramineous plants. The *nifH* gene from *Herbaspirillum* spp. of

this study might originate from *Bradyrhizobia* sp. or *Rhizobia* sp. (**Figure 4C**) by horizontal gene transfer (Yap et al., 1999), but this presume and the specific nitrogen-fixation mechanism still need to be investigated further. Anyway, the special group of *Herbaspirillum* spp. from Zijuan cultivar is the important PGP endophytes and assists the host plants growing on unfavorite environments in Anhui Province.

AUTHOR CONTRIBUTIONS

XY, ZW, YM, LW, and SP performed the experiments. XW and QX analyzed the data and wrote the paper. YZ and CW designed the experiments and reviewed the manuscript. All authors read and approved the final manuscript.

FUNDING

This work was supported by grants from the National Natural Science Foundation of China (31671949), the Natural Science Foundation of Anhui Province (Nos. 1608085J08 and 1608085QC57), and the Project of Talent Team of Nutrition and Quality & Safety of Agricultural Products in Anhui Province—the Special Innovative Province Construction in Anhui Province (15czs08032) and the Special Project for Central Guiding Science and Technology Innovation of Region in Anhui Province (2016080503B024).

SUPPLEMENTARY MATERIAL

The Supplementary Material for this article can be found online at: https://www.frontiersin.org/articles/10.3389/fmicb.2018.01848/full#supplementary-material

FIGURE S1 | Neighbor-joining phylogenetic tree based on 16S rRNA gene showing taxonomic results of endophytic bacteria obtained from Zijuan in different seasons. Percentages at the nodes indicate levels of bootstrap support based on neighbor-joining analyses of 1000 resampled datasets.

FIGURE S2 | Neighbor-joining phylogenetic tree based on 16S rRNA gene showing taxonomic results of endophytic bacteria obtained from Yunkang-10 in different seasons. Percentages at the nodes indicate levels of bootstrap support based on neighbor-joining analyses of 1000 resampled datasets.

FIGURE S3 | The diversity comparisons of endophytic bacteria obtained from tea cultivars of Zijuan and Yunkang-10 in different seasons.

TABLE S1 | The endophytic bacteria list obtained from Zijuan and Yunkang-10 in four seasons.

REFERENCES

Allen, R. S., Tibrook, K., Warden, A. C., Campbell, P. C., Rolland, V., Singh, S. P., et al. (2017). Expression of 16 nitrogenase proteins within the plant mitochondrial matrix. *Front. Plant Sci.* 8:287. doi: 10.3389/fpls.2017.00287

Bulgari, D., Casati, P., Quaglino, F., and Bianco, P. A. (2014). Endophytic bacterial community of grapevine leaves influenced by sampling date and phytoplasma infection process. *BMC Microbiol.* 14:198. doi: 10.1186/1471-2180-14-198

Chen, M., Lin, L., Zhang, Y., Sun, L., and An, Q. (2013). Genome sequence of *Klebsiella oxytoca* SA2, an endophytic nitrogen-fixing bacterium isolated from the pioneer grass *Psammochloa villosa*. *Genome Announc.* 1:e00601-13. doi: 10.1128/genomeA.00601-13

Coombs, J. T., and Franco, C. M. M. (2003). Isolation and identification of actinobacteria from surface-sterilized wheat roots. *Appl. Environ. Microbiol.* 69, 5603–5608. doi: 10.1128/AEM.69.9.5603-5608.2003

Cooper, R., Morre, D. J., and Morre, D. M. (2005). Medicinal benefits of green tea: part I. review of noncancer health benefits. *J. Altern. Complement. Med.* 11, 521–528. doi: 10.1089/acm.2005.11.521

El-Tarabily, K. A. (2008). Promotion of tomato (*Lycopersicon esculentum* Mill.) plant growth by rhizosphere competent 1-aminocyclopropane-1-carboxylic acid deaminase-producing streptomycete actinomycetes. *Plant Soil* 308, 161–174. doi: 10.1007/s11104-008-9616-2

Felsenstein, J. (1985). Confidence limits on phylogenies: an approach using the bootstrap. *Evolution* 39, 783–791. doi: 10.1111/j.1558-5646.1985.tb00420.x

Gibson, A. H., Scowcroft, W. R., Child, J. J., and Pagan, J. D. (1976). Nitrogenase activity in cultured *Rhizobium* sp. strain 32H1: nutritional and physical considerations. *Arch. Microbiol.* 108, 45–54. doi: 10.1007/BF00425092

Glick, B. R. (2014). Bacteria with ACC deaminase can promote plant growth and help to feed the world. *Microbiol. Res.* 169, 30–39. doi: 10.1016/j.micres.2013.09.009

Glickmann, E., and Dessaux, Y. (1995). A critical examination of the specificity of the salkowski reagent for indolic compounds produced by phytopathogenic bacteria. *Appl. Environ. Microbiol.* 61, 793–796.

Hardoim, P. R., van Overbeek, L. S., Berg, G., Pirttilä, A. M., Compant, S., Campisano, A., et al. (2015). The hidden world within plants: ecological and evolutionary considerations for defining functioning of microbial endophytes. *Microbiol. Mol. Biol. Rev.* 79, 293–320. doi: 10.1128/MMBR.00050-14

Honma, M., and Shimomura, T. (1978). Metabolism of l-aminocyclopropane-1-carboxylic acid. *Agric. Biol. Chem.* 42, 1825–1831. doi: 10.1080/00021369.1978.10863261

Ito, N., Hirose, M., and Shirai, T. (1992). "Carcinogenicity and modification of carcinogenic response by plant phenols," in *Proceedings of the ACS Symposium Series Phenolic Compounds in Food and Their Effect on Health II 507*, eds M. T. Huang, C. T. Ho, and C. Y. Lee (Washington, DC: American Chemical Society), 269–281. doi: 10.1021/bk-1992-0507.ch020

Ji, S. H., Gururanib, M. A., and Chun, S. C. (2014). Isolation and characterization of plant growth promoting endophytic diazotrophic bacteria from Korean rice cultivars. *Microbiol. Res.* 169, 83–98. doi: 10.1016/j.micres.2013.06.003

Jia, H., Wang, J. A., Yang, Y., Liu, G., Bao, Y., and Cui, H. (2015). Changes in flavonol content and transcript levels of genes in the flavonoid pathway in tobacco under phosphorus deficiency. *Plant Growth Regul.* 76, 225–231. doi: 10.1007/s10725-014-9990-0

Jiang, X., Liu, Y., Li, W., Zhao, L., Meng, F., Wang, Y., et al. (2013). Tissue-specific, development-dependent phenolic compounds accumulation profile and gene expression pattern in tea plant (*Camellia sinensis*). *PLoS One* 8:e62315. doi: 10.1371/journal.pone.0062315

Jiang, L., Shen, X., Shoji, T., Kanda, T., Zhou, J., and Zhao, L. (2013). Characterization and activity of anthocyanins in zijuan Tea (*Camellia sinensis* var. *kitamura*). *J. Agric. Food Chem.* 61, 3306–3310. doi: 10.1021/jf304860u

Kimura, M. (1980). A simple method for estimating evolutionary rates of base substitutions through comparative studies of nucleotide sequences. *J. Mol. Evol.* 16, 111–120. doi: 10.1007/BF01731581

Li, J., Chen, Q., Long, L. J., Dong, J. D., Yang, J., and Zhang, S. (2014). Bacterial dynamics within the mucus, tissue and skeleton of the coral porites lutea during different seasons. *Sci. Rep.* 4:7320. doi: 10.1038/srep07320

Li, X. X., Liu, Q., Liu, X. M., Shi, H. W., and Chen, S. F. (2016). Using synthetic biology to increase nitrogenase activity. *Microb. Cell Fact.* 15:43. doi: 10.1186/s12934-016-0442-6

Lin, L., Wei, C., Chen, M., Wang, H., Li, Y., Li, Y., et al. (2015). Complete genome sequence of endophytic nitrogen-fixing *Klebsiella variicola* strain DX120E. *Stand Genomic Sci.* 10:22. doi: 10.1186/s40793-015-0004-2

Madhaiyan, M., Alex, T. H., Ngoh, S. T., Prithiviraj, B., and Ji, L. (2015). Leaf-residing *Methylobacterium* species fix nitrogen and promote biomass and seed

production in *Jatropha curcas*. *Biotechnol. Biofuels* 8:222. doi: 10.1186/s13068-015-0404-y

Madhaiyan, M., Chan, K. L., and Ji, L. (2014). Draft genome sequence of *Methylobacterium* sp. strain L2-4, a leaf-associated endophytic N-fixing bacterium isolated from *Jatropha curcas* L. *Genome Announc.* 2:e01306-14. doi: 10.1128/genomeA.01306-14

Madhaiyan, M., Jin, T. Y., Roy, J. J., Kim, S. J., Weon, H. Y., Kwon, S. W., et al. (2013). *Pleomorphomonas diazotrophica* sp. nov., an endophytic N-fixing bacterium isolated from root tissue of *Jatropha curcas* L. *Int. J. Syst. Evol. Microbiol.* 63, 2477–2483. doi: 10.1099/ijs.0.044461-0

Maximilien, R., de Nys, R., Holmström, C., Gram, L., Givskov, M., Crass, K., et al. (1998). Chemical mediation of bacterial surface colonization by secondary metabolites from the red alga *Delisea pulchra*. *Aquat. Microb. Ecol.* 15, 233–246. doi: 10.3354/ame015233

McArdle, B. H., and Anderson, M. J. (2001). Fitting multivariate models to community data: a comment on distance-based redundancy analysis. *Ecology* 82, 290–297. doi: 10.1890/0012-9658(2001)082[0290:FMMTCD]2.0.CO;2

Menhinick, E. F. (1964). A comparison of some species-individuals diversity indices applied to samples of field insects. *Ecology* 45, 859–861. doi: 10.2307/1934933

Mora, Y., Díaz, R., Vargas-Lagunas, C., Peratta, H., Guerrero, G., Aguilar, A., et al. (2014). Nitrogen-fixing rhizobial strains isolated from common bean seeds: phylogeny, physiology, and genome analysis. *Appl. Environ. Microbiol.* 80, 5644–5654. doi: 10.1128/AEM.01491-14

Peet, R. K. (1974). The measurement of species diversity. *Annu. Rev. Ecol. Syst.* 5, 285–307. doi: 10.1146/annurev.es.05.110174.001441

Pielou, E. C. (1969). An introduction to mathematical ecology. *Bioscience* 78, 7–12.

Poly, F., Monrozier, L. J., and Bally, R. (2001). Improvement in the RFLP procedure for studying the diversity of nifH genes in communities of nitrogen fixers in soil. *Res. Microbiol.* 152, 95–103. doi: 10.1016/S0923-2508(00)01172-4

Qin, S., Feng, W. W., Wang, T. T., Ding, P., Xing, K., and Jiang, J. H. (2017). Plant growth-promoting effect and genomics analysis of the beneficial endophyte *Streptomyces* sp. KLBMP 5084 isolated from halophyte *Limonium sinense*. *Plant Soil* 416, 117–132. doi: 10.1007/s11104-017-3192-2

Qin, S., Li, J., Chen, H. H., Zhao, G. Z., Zhu, W. Y., Jiang, C. L., et al. (2009). Isolation, diversity, and antimicrobial activity of rare actinobacteria from medicinal plants of tropical rain forests in Xishuangbanna, China. *Appl. Environ. Microbiol.* 75, 6176–6186. doi: 10.1128/AEM.01034-09

Qin, S., Miao, Q., Feng, W. W., Wang, Y., Zhu, X., Xing, K., et al. (2015). Biodiversity and plant growth promoting traits of culturable endophytic actinobacteria associated with *Jatropha curcas* L. growing in Panxi dry-hot valley soil. *Appl. Soil Ecol.* 93, 47–55. doi: 10.1016/j.apsoil.2015.04.004

Qin, S., Xing, K., Jiang, J. H., Xu, L. H., and Li, W. J. (2011). Biodiversity, bioactive natural products and biotechnological potential of plant-associated endophytic actinobacteria. *Appl. Microbiol. Biotechnol.* 89, 457–473. doi: 10.1007/s00253-010-2923-6

Qin, S., Zhang, Y. J., Yuan, B., Xu, Y. P., Xing, K., Wang, J., et al. (2014). Isolation of ACC deaminase-producing habitat-adapted symbiotic bacteria associated with halophyte *Limonium sinense* (Girard) Kuntze and evaluating their plant growth-promoting activity under salt stress. *Plant Soil* 374, 753–766. doi: 10.1007/s11104-013-1918-3

Rabha, A. J., Naglot, A., Sharma, G. D., Gogoi, H. K., and Veer, V. (2014). In vitro evaluation of antagonism of endophytic *Colletotrichum gloeosporioides* against potent fungal pathogens of *Camellia sinensis*. *Indian J. Microbiol.* 54, 302–309. doi: 10.1007/s12088-014-0458-8

Resende, J. A., Godon, J. J., Bonnafous, A., Arcuri, P. B., Silva, V. L., Otenio, M. H., et al. (2016). Seasonal variation on microbial community and methane production during anaerobic digestion of cattle manure in brazil. *Microb. Ecol.* 71, 735–746. doi: 10.1007/s00248-015-0647-y

Saitou, N., and Nei, M. (1987). The neighbor-joining method: a new method for reconstructing phylogenetic trees. *Mol. Biol. Evol.* 4, 406–425. doi: 10.1093/oxfordjournals.molbev.a040454

Schwyn, B., and Neilands, J. B., (1987). Universal chemical assay for the detection and determination of siderophores. *Anal. Biochem.* 160, 47–56. doi10.1016/0003-2697(87)90612-9

Shannon, C. E. (1948). A mathematical theory of communication. *Bell Syst. Tech. J.* 27, 379–423. doi: 10.1002/j.1538-7305.1948.tb01338.x

Simpson, E. H. (1949). Measurement of diversity. *Nature* 163, 688. doi: 10.1038/163688a0

Stackebrandt, E., and Goodfellow, M. (1991). *Nucleic Acid Techniques in Bacterial Systematics*. Hoboken, NJ: John Wiley & Sons, 115–175.

Strobel, G., and Daisy, B. (2003). Bioprospecting for microbial endophytes and their natural products. *Microbiol. Mol. Biol. Rev.* 67, 491–502. doi: 10.1128/MMBR.67.4.491-502.2003

Tamura, K., Stecher, G., Peterson, D., Filipski, A., and Kumar, S. (2013). MEGA6: molecular evolutionary genetics analysis version 6.0. *Mol. Biol. Evol.* 30, 2725–2729. doi: 10.1093/molbev/mst197

Thompson, J. D., Gibson, T. J., Plewniak, F., Jeanmouqin, F., and Higgins, D. G. (1997). The CLUSTAL_X windows interface: flexible strategies for multiple sequence alignment aided by quality analysis tools. *Nucleic Acids Res.* 25, 4876–4882. doi: 10.1093/nar/25.24.4876

Tien, T. M., Gaskins, M. H., and Hubbell, D. H. (1979). Plant growth substances produced by *Azospirillum brasilense* and their effect on the growth of pearl millet. *Appl. Environ. Microbiol.* 37, 1016–1024.

Vladimir, A. C., and Dobereiner, J. (1988). A new acid-tolerant nitrogen-fixing bacterium associated with sugarcane. *Plant Soil* 108, 23–31. doi: 10.1007/BF02370096

Wheeler, D. S., and Wheeler, W. J. (2004). The medicinal chemistry of tea. *Drug Dev. Res.* 61, 45–65. doi: 10.1002/ddr.10341

Whittaker, R. H. (1972). Evolution and measurement of species diversity. *Int. Assoc. Plant Taxon.* 21, 213–251. doi: 10.2307/1218190

Yap, W. H., Zhang, Z. S., and Wang, Y. (1999). Distinct types of rRNA operons exist in the genome of the actinomycete Thermomonospora chromogena and evidence for horizontal transfer of an entire rRNA operon. *J. Bacteriol.* 181, 5201–5209.

Yoon, S. H., Ha, S. M., Kwon, S., Lim, J., Kim, Y., Seo, H., et al. (2017). Introducing EzBioCloud: a taxonomically united database of 16SrRNA gene sequences and whole-genome assemblies. *Int. J. Syst. Evol. Microbiol.* 67, 1613–1617. doi: 10.1099/ijsem.0.001755

You, M., Nishiguchi, T., Saito, A., Isawa, T., Mitsui, H., and Minamisawa, K. (2005). Expression of the nifH gene of a *Herbaspirillum* endophyte in wild rice species: daily rhythm during the light-dark cycle. *Appl. Environ. Microbiol.* 71, 8183–8190. doi: 10.1128/AEM.71.12.8133-8190.2005

Zgadzaj, R., James, E. K., Kelly, S., Kawaharada, Y., de Jonge, N., Jensen, D. B., et al. (2015). A legume genetic framework controls infection of nodules by symbiotic and endophytic bacteria. *PLoS Genet.* 11:e1005280. doi: 10.1371/journal.pgen.1005280

Zhao, S., Zhou, N., Zhao, Z. Y., Zhang, K., Wu, G. H., and Tian, C. Y. (2016). Isolation of endophytic plant growth-promoting bacteria associated with the halophyte *Salicornia europaea* and evaluation of their promoting activity under salt stress. *Curr. Microbiol.* 73, 574–581. doi: 10.1007/s00284-016-1096-7

Zhu, B., Chen, M., Lin, L., Yang, L., Li, Y., and An, Q. (2012). Genome sequence of *Enterobacter* sp. strain SP1, an endophytic nitrogen-fixing bacterium isolated from sugarcane. *J. Bacteriol.* 194, 6963–6964. doi: 10.1128/JB.01933-12

Conflict of Interest Statement: The authors declare that the research was conducted in the absence of any commercial or financial relationships that could be construed as a potential conflict of interest.

frontiers in Plant Science

ORIGINAL RESEARCH
published: 04 September 2018
doi: 10.3389/fpls.2018.01273

Endophytic Microbial Consortia of Phytohormones-Producing Fungus *Paecilomyces formosus* LHL10 and Bacteria *Sphingomonas* sp. LK11 to *Glycine max* L. Regulates Physio-hormonal Changes to Attenuate Aluminum and Zinc Stresses

*Saqib Bilal[1], Raheem Shahzad[1], Abdul L. Khan[2], Sang-Mo Kang[1], Qari M. Imran[1], Ahmed Al-Harrasi[2], Byung-Wook Yun[1] and In-Jung Lee[1]**

[1] School of Applied Biosciences, Kyungpook National University, Daegu, South Korea, [2] Natural and Medical Sciences Research Center, University of Nizwa, Nizwa, Oman

OPEN ACCESS

Edited by:
Eloise Foo,
University of Tasmania, Australia

Reviewed by:
Mostafa Abdelwahed Abdelrahman,
Tottori University, Japan
Oswaldo Valdes-Lopez,
Universidad Nacional Autónoma de México, Mexico

***Correspondence:**
In-Jung Lee
ijlee@knu.ac.kr

Specialty section:
This article was submitted to Plant Microbe Interactions, a section of the journal Frontiers in Plant Science

Received: 18 May 2018
Accepted: 14 August 2018
Published: 04 September 2018

Citation:
Bilal S, Shahzad R, Khan AL, Kang S-M, Imran QM, Al-Harrasi A, Yun B-W and Lee I-J (2018) Endophytic Microbial Consortia of Phytohormones-Producing Fungus Paecilomyces formosus LHL10 and Bacteria Sphingomonas sp. LK11 to Glycine max L. Regulates Physio-hormonal Changes to Attenuate Aluminum and Zinc Stresses. Front. Plant Sci. 9:1273. doi: 10.3389/fpls.2018.01273

The compatible microbial consortia containing fungal and bacterial symbionts acting synergistically are applied to improve plant growth and eco-physiological responses in extreme crop growth conditions. However, the interactive effects of phytohormones-producing endophytic fungal and bacterial symbionts plant growth and stress tolerance under heavy metal stress have been least known. In the current study, the phytohormones-producing endophytic *Paecilomyces formosus* LHL10 and *Sphingomonas* sp. LK11 revealed potent growth and tolerance during their initial screening against combined Al and Zn (2.5 mM each) stress. This was followed with their co-inoculation in the Al- and Zn-stressed *Glycine max* L. plants, showing significantly higher plant growth attributes (shoot/root length, fresh/dry weight, and chlorophyll content) than the plants solely inoculated with LHL10 or LK11 and the non-inoculated (control) plants under metal stresses. Interestingly, under metal stress, the consortia exhibited lower metal uptake and inhibited metal transport in roots. Metal-induced oxidative stresses were modulated in co-inoculated plants through reduced hydrogen peroxide, lipid peroxidation, and antioxidant enzymes (catalase and superoxide dismutase) in comparison to the non-inoculated plants. In addition, endophytic co-inoculation enhanced plant macronutrient uptake (P, K, S, and N) and modulated soil enzymatic activities under stress conditions. It significantly downregulated the expression of heavy metal ATPase genes *GmHMA13, GmHMA18, GmHMA19*, and *GmPHA1* and upregulated the expression of an ariadne-like ubiquitin ligase gene *GmARI1* under heavy metals stress. Furthermore, the endogenous phytohormonal contents of co-inoculated plants revealed significantly enhanced gibberellins and reduced abscisic acid and jasmonic acid contents, suggesting that this endophytic

interaction mitigated the adverse effect of metal stresses in host plants. In conclusion, the co-inoculation of the endophytic fungus LHL10 and bacteria LK11 actively contributed to the tripartite mutualistic symbiosis in *G. max* under heavy metal stresses; this could be used an excellent strategy for sustainable agriculture in the heavy metal-contaminated fields.

Keywords: soybean, endophytes, macronutrients, soil extracellular enzymes, hormones, reactive oxygen species, antioxidants, heavy metal ATPases

INTRODUCTION

Plants, being sessile in nature, are often exposed to adverse environmental perturbations, which significantly hamper their growth and development, resulting in significant yield loss. Of those environmental stresses, the excessive release of heavy metals and their accumulation in agricultural soils due to continuous technological advancement in industrialization and urbanization has become a serious global concern, which not only impairs crop productivity and soil quality, but also poses serious threats to human health upon accumulation in agricultural products (Khan et al., 2015; Ma et al., 2016a). The serious threats of heavy metal contamination to plant growth and human health necessitate the development of efficient and eco-friendly soil remediating techniques.

Recently, plant–microbe interactions under metal toxicity have gained considerable attention for remediating contaminated soil and improving plant physiology. Various studies have demonstrated the substantial effect of microbial (bacterial and fungal) inoculation on alleviating heavy metal stress as well as on boosting plant growth, development, and nutritive status under metal-contaminated soil conditions. Such synergistic effects of microbes are accredited to the production of siderophores, phytohormones, such as gibberellins, auxin, ethylene, and enzymes, such as ACC-deaminase, which provide an extra arsenal to overcome the adverse effects of metal toxicity. A number of studies have illustrated the impact of the single inoculation of biotic abiotic stress mitigation including metal-resistant and plant growth-promoting microorganisms, including rhizobacteria *Pseudomonas libanensis*, *Pseudomonas reactans, Micrococcus luteus* (Ma et al., 2016b; Pinter et al., 2017) endophytic *Pseudomonas azotoformans, Streptomyces* sp. (Ma et al., 2017; Qin et al., 2017), arbuscular mycorrhizal (AM) fungi *Rhizophagus irregularis, Funneliformis mosseae,* and *F. caledonium* (Mnasri et al., 2017; Zhang et al., 2018), and endophytic *Thermomyces* sp, *Piriformospora indica, Penicillium janthinellum* (Shahabivand et al., 2017; Ali et al., 2018) on alleviating environmental stresses including the metal toxicity-induced stresses and improving soil remediation efficiencies. Conversely, the impact of the co-inoculation of bacterial and fungal interaction on plants under abiotic stresses, including metal toxicity, is rarely studied. The impacts of the synergistic interaction between fungi and bacteria are reported to be beneficial for plant growth promotion by Liu et al. (2012), as the survivability, growth, and development of *Verbascum lychnitis* under Zn and Pb substrates were significantly improved by co-inoculating it with endophytic and AM fungi (Wężowicz et al., 2017). Similarly, the positive effects of reduced excess zinc toxicity and modulated micronutrient uptake in *Glycine max* L. have been observed with the combined inoculation of AM *Gigaspora rosea* and rhizobacterium *Bradyrhizobium diazoefficiens* by Ibiang et al. (2017). The positive outcomes produced by the interaction of bacteria and fungi on plant growth stimulation and regulation of stress tolerance under hostile conditions, including heavy metal stresses, have been extensively reviewed by Martin et al. (2017) and Rozpądek et al. (2017).

In spite of such beneficial consortium, studies investigating the association of bacteria and fungi, particularly the specific interaction between endophytes, in hostile environment are limited. Endophytes (bacteria and fungi) have been extensively reported for their beneficial association with plants for their growth and development, fitness, diversification and mitigation of stresses, including metal-induced toxicity, under harsh environmental conditions (Hardoim et al., 2015). Therefore, their manipulation in the metal-contaminated soil for promoting plant growth and reducing metal toxicity will demonstrate a better knowledge of endophytes synergism and development of appropriate phytoremediation practices. As the persistence of heavy metal toxicity in soil leads to the significant impairment of normal plant functions in a variety of ways, including the impediment of different metabolic processes by the destruction of enzymatic activities, severe disruption of cytoplasmic membrane integrity, excessive production of reactive oxygen species (ROS) (Emamverdian et al., 2015).

Aluminum (Al) is one of the most abundant heavy metals in the earth's crust and is also one of the major inhibitors of crop production and growth. It exhibits toxicity in the acidic soil (pH < 5.0 or 5.5), where it turns into its most phytotoxic form (Al^{3+}) (Saby et al., 2017). No beneficial biological role of Al has been proven in plants; however, it primarily adversely affects the root growth and consequently leads to the deterioration of the aerial plant parts due to early root damage (Xu et al., 2017). Furthermore, it hampers nutritional uptake and impairs cell wall, plasma membrane, cytoskeleton, and nucleus at the cellular level (Emamverdian et al., 2015). Similarly, zinc (Zn) is considered an essential metal, but its excessive levels in the agricultural soil cause stress in plants, leading to the reduced root and shoot growth, curling of young leaves, necrotic spots in mature leaves, leaf chlorosis, reduced photosynthesis, as well as excessive generation of ROS, leading to adverse effects on membrane integrity and permeability, etc. (Shi et al., 2015). Excessive accumulation of metals, including Al and Zn, has also been reported to adversely degrade the activity of metal transporter family members, including H^+-ATPase, low-affinity

cation transporters, and ABC transporters (Singh et al., 2016). In addition, Al and Zn adversely affect the soil extracellular enzymatic activity. Wallenstein and Weintraub (2008) and Ali et al. (2017) have reported the adverse influence of Zn and Al toxicity on soil extracellular enzymatic activity.

Soybean is an important edible crop and a vital source of vegetable oil and proteins worldwide. The growth, yield, and quality of soybean can be significantly damaged by a number of adverse environmental stresses, including metal toxicity. Therefore, the current study was aimed to investigate the co-inoculation effects of the synergistic consortium of the phytohormones Indole-3-acetic acid and gibberellins (IAA and GAs)-producing (Khan et al., 2012, 2014) compatible endophytic bacteria *Sphingomonas* sp. LK11 and fungus *Paecilomyces formosus* LHL10. We aimed to comprehensively assess the metal detoxification, stress alleviation, and growth promotion in *G. max* under Zn- and Al-contaminated soil conditions to investigate the influence of endophytes co-inoculation. Here, we described plant biomass regulation, photosynthesis performance, hormonal regulation and antioxidative system, heavy metal accumulation, heavy metal transporter-mediated translocation, and nutrient acquisition, as well as an improvement in soil extracellular enzymatic activity caused by the co-inoculation of endophytic LK11 and LHL10. The ultimate goal of this study was to develop an ecofriendly phytoremediation strategy for efficiently coping with Al- and Zn-contaminated soil.

MATERIALS AND METHODS

Screening of Endophytic LHL10 and LK11 Tolerance Against Heavy Metals

In the current study, the previously isolated endophytic *Paecilomyces formosus* LHL10 (HQ444388) and *Sphingomonas* sp. LK11 (KF515708) were selected on the basis of their abilities to produce phytohormones, gibberellins (GAs) and Indole-3-acetic acid (IAA) and screened out against different concentrations of Al and Zn (1.5, 2.5, and 3.5 mM each) in potato dextrose broth to assess their metal-tolerating abilities for 7 days and 72 h, respectively. Of all screening concentrations, the media containing 2.5 mM each of Al and Zn showed the best growth of both LHL10 and LK11. Therefore, the fungal mycelia and bacterial cells were harvested via centrifugation from the media containing 2.5 mM of each metal and subjected to the inductively coupled plasma-mass spectrometry (ICP-MS) in order to evaluate their metal-uptake and remediating potential.

Host–Plant and Endophyte Interaction Under Al and Zn Stress

The *G. max* seeds were surface sterilized for 30 s with 70% ethanol followed by a treatment with 5% NaOCl for 15 min and then rinsed with autoclaved double-distilled water. The soybean seeds were sown in autoclaved pots containing 150 g of horticulture soil composed of cocopeat (68%), perlite (11%), zeolite (8%), as well as micronutrients available as NH^{4+} ∼0.09 mg g^{-1}; P_2O_5 ∼0.35 mg g^{-1}; NO_{3-} ∼0.205 mg g^{-1}; and K_2O ∼0.1 mg g^{-1} and kept in a growth chamber (day/night cycle: 14 h; 28°C/10 h; 24°C; relative humidity 60–70%; light intensity 1000 E m^{-2} s^{-1} Natrium lamps). In case of sole inoculation, the metal-resistant endophytic strains LHL10 (1–2 g of mycelia) and LK11 (10^8 CFU mL^{-1}) were separately inoculated in the rhizoshperic area of the 12-day-old soybean seedlings, while in case of dual inoculation, both endophytes LHL10 and LK11 were simultaneously applied to the rhizoshperic area of the seedlings to establish a symbiotic association between endophytes and plants. Subsequently, 80 mL of a solution containing Al and Zn (2.5 mM each) was applied to the 18-day-old seedlings for 12 days. Thereafter, the treated plants were harvested, frozen in liquid nitrogen, and transferred to −80 °C for further biochemical analysis. The growth attributes of the plants under each treatment were recorded and their chlorophyll contents were measured by a chlorophyll meter (SPAD-502 Minolta, Japan). The experiment was replicated three times, and each replicate included 20 plants. The experimental design included the following treatments: (i) control plants treated with only water, (ii) sole endophytic LHL10-treated plants without Al and Zn stress, (iii) sole endophytic LK11-treated plants without Al and Zn stress, (iv) LHL10 and LK11 co-inoculated plants without metal stress, (v) only Al- and Zn-treated plants, (vi) endophytic LHL10-treated plants with Al and Zn stress, (vii) endophytic LK11-treated plants with Al and Zn stress, (viii) LHL10- and LK11-co-inoculated plants with metal stress. The experiment was performed three times, with 20 replicates per treatment.

Analysis of Heavy Metal (Al and Zn) and Macronutrient Uptake in Plant Roots and Shoots via ICP-MS

The freeze-dried powdered samples were used for the quantification of metals (Al and Zn) and nutrient (Potassium, K; Phosphorus, P; Calcium, Ca; and Sulfur, S) uptake in roots and shoots as well as in microbial cells using ICP-MS (Optima 7900DV, Perkin-Elmer, United States), while Nitrogen (N) was quantified with an elemental analyser (Flash2000; ThermoFisher Scientific, Waltham, MA, United States). The translocation efficiency was assessed by measuring the translocation factor (TF), biological concentration factor (BCF), and biological accumulation factor (BAF) as reported by Waqas et al. (2014) and Bilal et al. (2017).

cDNA Synthesis and qRT-PCR

Total RNA was extracted from the soybean roots and leaves by the protocol adopted by Imran et al. (2018). Briefly, the roots and leaves (1.0 g) were grounded to a fine powder in liquid nitrogen using a chilled mortar and pestle and immediately transferred to the RNA-free conical centrifuge tubes (Falcon), followed by the addition of the TRIzol reagent (Invitrogen, Carlsbad, CA, United States) and centrifugation (13000 rpm) for 10 min at 4°C. Thereafter, 200 μL of chloroform was added to the supernatants, vortexed vigorously for 15 s, and incubated on ice for 3 min, followed by centrifugation (13000 rpm) for 15 min at 4°C. Subsequently, the aqueous phase was transferred to a fresh centrifuge tube containing 50 μL of isopropanol

followed by centrifugation (13000 rpm) at 4°C. The supernatant was discarded carefully, and the pellet was washed with 75% ethanol. All samples were dried and resuspended in nuclease-free water, and the RNA concentration was measured using NanoQ (OPTIZEN Korea). The cDNA synthesis and quantitative PCR (qPCR) were performed as described previously by Imran et al. (2018). Briefly, 2 μg of RNA was used to synthesize cDNA using the BioFACT™ RT-Kit (BIOFACT, Korea) according to the manufacturer's standard protocol. The synthesized cDNA was used as a template in a two-step qRT-PCR reaction conducted to quantify transcript accumulation using an Illumina Eco™ system (Illumina, United States). The reaction mixture was prepared by adding 10 μL of 2X Real-Time PCR master mix, including SYBR® Green I (BioFACT, Korea) and 1 μL of each primer (a total of 10 primers) for the respective genes studied. The PCR conditions were initial activation at 95°C for 15 min, followed by 40 cycles of denaturation at 95°C for 20 s and annealing at 60°C for 40 s. The melting curves were analyzed to verify the amplicon specificity of each primer pair. The expression of each gene was measured relative to the expression of the internal control gene *Actin*. **Supplementary Table S1** shows the list of genes and their specific primers.

Soil Extracellular Enzyme Analysis

To quantify the soil extracellular enzymes, the method of Khan et al. (2016) was adopted with some modifications. Briefly, the soil (1 g/50 mL acetate buffer (50 mM; pH 5.5) samples from all treatments were incubated at 26°C and shaken at 150 rpm. Each sample had five replicates. After 24 h, a clear supernatant was obtained by centrifuging (12,000 rpm at 4°C for 10 min) the solution in each flask. The known standard (4-methylumbelliferone) and respective florigenic substrates for each enzyme were prepared according to Khan et al. (2016). The pre-optimized fluorescence spectrophotometer (Shimadzu, Tokyo, Japan) was used to read the absorbance at 360-nm excitation and 460-nm emission at time initial and 30-min intervals for 2 h. The readings were calculated according to the formula: Activity ($\mu mol\ h^{-1}\ L^{-1}$) = slope of concentration versus time in hours.

Quantification of Hydrogen Peroxide, Lipid Peroxidation, and Antioxidants

The measurement of the H_2O_2 concentration in soybean leaves was carried out by the method described by Li et al. (2015). Briefly, 300 mg of plant leaf samples were homogenized with 3 mL of 50 mM phosphate buffer (pH 6.5). The homogenates were centrifuged at 6000 rpm for 25 min. Subsequently, 3 mL of the supernatant was mixed with 1 mL of 0.1% titanium dioxide in 20% H_2SO_4 (w/v) and again centrifuged at 6000 rpm for 15 min. The absorbance of the yellow color of supernatant was read at 410 nm. The H_2O_2 content was calculated by using a standard curve with known concentrations and expressed as $\mu M\ g^{-1}$ FW. The lipid peroxidation levels of soybean leaves were measured spectrophotometrically as described by Bilal et al. (2017). The concentration of lipid peroxidation products was expressed as malondialdehyde (MDA) formed per gram tissue weight.

Similarly, the activities of enzymatic antioxidants, including catalase (CAT) and superoxide dismutase (SOD), in soybean tissues were measured as described by Sirhindi et al. (2016), and their absorbances were measured via spectrophotometer at 240 and 540 nm, respectively and expressed as U/mg protein. One SOD unit is the quantity of enzyme that inhibits 50% photo reduction of nitroblue tetrazolium (NBT).

Extraction and Quantification of Soybean Phytohormones—Gibberellins (GAs), Abscisic Acid (ABA), and Jasmonic Acid (JA)

The extraction and quantification of the soybean GAs were carried out according to Hamayun et al. (2017), and the extract was subjected to chromatography and mass spectroscopy for GA detection, identification, and quantification. The seedlings were crushed in liquid nitrogen to a fine powder. The GAs were extracted and quantified by using 0.5 g of the fine powder, which was supplemented with [$^2H_2$] GA internal standards. The instrument used for the determination of GA was a gas chromatograph (Hewlett-Packard 6890, 5973N mass selective detector). The gas chromatography-mass spectroscopy coupled with selected ion monitor (GC/MS-SIM) conditions used for the analysis and quantification of GAs (GA1, 4, 9, and 24) are listed in **Supplementary Table S2**.

The endogenous ABA was extracted from the plants according to the protocol described by Qi et al. (1998), with slight modifications as reported by Shahzad et al. (2017). Briefly, the freeze-dried plant samples were used for extraction and chromatography with an internal standard Me-[$^2H_6$]-ABA. The resultant extract was dried using the N_2 gas followed by methylation with diazomethane for the detection and quantification of ABA by GC–MS coupled with SIM (5973 Network Mass Selective Detector and 6890 N Network Gas Chromatograph, Agilent Technologies, Santa Clara, CA, United States). The Lab-Base (ThermoQuset, Manchester, United Kingdom) data system software was used to monitor the signal ions at *m*/*z* 162 and 190 for Me-ABA and at *m*/*z* 166 and 194 for Me-[$^2H_6$]-ABA. The experiment was replicated three times. The GC/MS-SIM conditions used for the analysis and quantification of ABA are provided in **Supplementary Table S3**.

To measure the level of JA in soybean, 0.4 g of freeze-dried powder was used as reported by Hamayun et al. (2017). Briefly, the freeze-dried sample was extracted by 50 mM citric acid and acetone (30:70, v/v) having 30 ng of [9, 10-$^2H_2$] Dihydro-JA as an internal standard. The extracts were analyzed by GC-MS (6890 N Network GC System and 5973 Network Mass Selective Detector; Agilent Technologies). We monitored the fragment ion at *m*/*z* 1/4 83 amu, corresponding to the base peaks of JA and [9, 10-$^2H_2$] Dihydro-JA. The GC/MS-SIM conditions used for the analysis and quantification of JA are mentioned in **Supplementary Table S4**.

Statistical Analysis

All experiments were performed independently four to five times. All data were subjected to the analysis of variance (ANOVA)

followed by Duncan's multiple range test using SAS version 9.2 (Cary, NC, United States), and the data displayed are the mean values with standard error (SE).

RESULTS

Effect of Endophytic Co-inoculation on Plant Growth-Promoting Attributes Under Al and Zn Stress

Screening of endophytic LHL10 and LK11 tolerance against heavy metals displayed that LHL10 mycelia and LK11 bacterial cells can approximately accumulate 83 and 79% Zn and 77 and 73% Al, respectively. Thereafter, the application of co-inoculation on soybean growth attributes disclosed the significant effects of the endophytic co-inoculation and sole inoculation on the growth-promoting attributes of the soybean plants compared to the non-inoculated plants (**Figure 1**). In the absence of stress, the endophytic co-inoculation significantly enhanced the shoot length by 71.3, 34.11, and 46.3% and the root length by 90.7, 27.1, and 34.8% when compared with the root and shoot lengths of the non-inoculated, sole LHL10-inoculated, and sole LK11-inoculated plants, respectively (**Table 1**). The fresh and dry weights increased significantly by 71.8 and 130.1% in the co-inoculated plants, followed by 38.9 and 70.5% in the sole LHL10-inoculated plants, and by 10.6 and 52.2% in the sole LK11-inoculated plants, respectively, compared to the fresh and dry weights of the non-inoculated plants under control conditions. However, the metal stress substantially retarded the growth attributes of the non-inoculated plants; nevertheless, the endophytic co-inoculation significantly mitigated the adverse effects of Al and Zn toxicity by displaying significantly higher growth attributes in co-inoculated plants compared to the non-inoculated and sole-inoculated plants. The metal toxicity significantly reduced the shoot and root lengths by 1.8 and 1.7 times in non-inoculated plants, followed by nearly 1.5 and 1.2 times in the LK11-inoculated plants, and by approximately 1.2 and 1.07 times in the LHL10-inoculated plants, respectively, compared to the root and shoot lengths of the co-inoculated plants. On exposure to metals stress, the co-inoculated plants displayed significant restoration of the fresh and dry biomass to the level of control conditions of such plants. The co-inoculated plants displayed significant fresh biomass under stress conditions followed by the LHL10-inoculated, LK11-inoculated, and non-inoculated plants. Same trend line was observed in case of the dry biomass of the co-inoculated plants under stress conditions, but the sole-inoculated plants showed insignificant differences with each other. A significant increase ($p < 0.005$) was detected in the chlorophyll content of the co-inoculated plants under control as well as stress conditions compared to the sole-inoculated as well as non-inoculated plants.

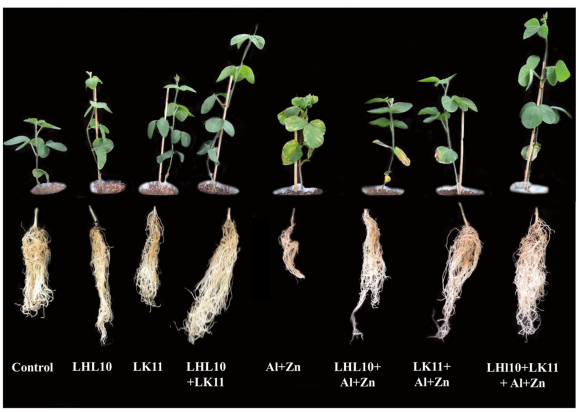

FIGURE 1 | Influence of the co-inoculation of endophytic *Paecilomyces formosus* LHL10 and *Sphingomonas* sp. LK11 on soybean growth under metal (Al/Zn) stress. Each plant represents 20 replicates of eight treatments.

Co-inoculation Influences Al and Zn Uptake in *Glycine max* L. and Availability in Soil

The influence of endophytes co-inoculation on metal uptake and translocation was tested in plant roots and shoots to investigate the plant-endophyte interaction efficiency in remediating the combined toxicity of Al and Zn (**Table 2**). Under control

TABLE 1 | Effect of endophytes inoculation on soybean growth under Al/Zn stress.

Treatment	S.L (Cm)	R.L (Cm)	S.F.W. (g)	S.D.W (Cm)	CC (SPAD)
Without metals stress					
Control	23.4 ± 1.70^{c}	11.2 ± 1.17^{c}	13.7 ± 0.73^{d}	5.7 ± 0.34^{c}	37.6 ± 0.91^{c}
LHL10	29.9 ± 2.38^{b}	14.1 ± 1.28^{b}	19.1 ± 0.57^{b}	9.8 ± 0.59^{b}	44.13 ± 0.81^{b}
LK11	27.4 ± 1.53^{b}	13.3 ± 0.98^{b}	15.2 ± 0.57^{c}	9.0 ± 0.36^{b}	43.51 ± 0.87^{b}
LHL10 + LK11	40.1 ± 2.10^{a}	17.9 ± 0.76^{a}	23.6 ± 0.75^{a}	13.3 ± 0.55^{a}	48.13 ± 0.95^{a}
With metals stress					
Control + Metals	17.0 ± 1.80^{d}	9.7 ± 0.51^{c}	9.4 ± 0.61^{d}	4.8 ± 0.40^{c}	16.53 ± 1.51^{d}
LHL10 + Metals	27.1 ± 1.56^{b}	16.1 ± 0.46^{a}	13.3 ± 0.65^{b}	7.3 ± 0.27^{b}	29.21 ± 0.45^{c}
LK11 + Metals	21.5 ± 1.99^{c}	14.7 ± 0.83^{b}	12.0 ± 0.37^{c}	7.7 ± 0.33^{b}	34.03 ± 1.23^{b}
LHL10 + LK11 + Metals	32.0 ± 2.91^{a}	17.2 ± 0.70^{a}	20.4 ± 0.58^{c}	12.0 ± 0.57^{a}	$41.33.2 \pm 1.02^{d}$

SL, shoot length; RL, root length; SFW, seedlings fresh weight; SDW, seedlings dry weight; CC, chlorophyll content. Each value represents mean ± SD of 20 replicates from three independent experiments. Values with different letters in a column are significantly different at the 5 % level of probability by DMRT.

TABLE 2 | Al and Zn uptake, compartmentalization in *Glycine max* L. and their remediation in soil with or without endophytes interaction.

Treatment	Shoot Al (mgkg^{-1})	Root Al (mgkg^{-1})	Soil Al (mgkg^{-1})	Shoot Zn (mgkg^{-1})	Root Zn (mgkg^{-1})	Soil Zn (mgkg^{-1})	BCF (Al)	BAF (Al)	TF (Al)	BCF (Zn)	BAF (Zn)	TF (Zn)
Without metals stress												
Control	ND	ND	ND	0.015 ± 0.003^{a}	0.019 ± 0.002^{b}	0.33 ± 0.05^{b}	ND	ND	–	0.05	0.04	0.78
LHL10	ND	ND	ND	0.012 ± 0.004^{a}	0.042 ± 0.003^{a}	0.39 ± 0.02^{b}	ND	ND	–	0.10	0.03	0.28
LK11	0.11 ± 0.03^{a}	0.14 ± 0.02^{b}	0.28 ± 0.03^{a}	0.013 ± 0.005^{a}	0.021 ± 0.003	0.52 ± 0.04^{a}	0.51	0.39	0.78	0.04	0.02	0.61
LHL10 + LK11	0.09 ± 0.002^{a}	0.22 ± 0.04^{a}	0.23 ± 0.04^{a}	ND	ND	0.58 ± 0.03^{a}	0.94	0.35	0.40	0.00	0.00	–
With metals stress												
Control + Metals	241.2 ± 14.2^{a}	325.2 ± 18.4^{a}	479.3 ± 24.7^{a}	266.2 ± 17.4^{a}	376.4 ± 27.6^{a}	392.3 ± 2.1^{a}	0.67	0.52	0.74	0.95	0.67	0.70
LHL10 + Metals	125.3 ± 7.83^{c}	201.5 ± 12.6^{c}	359.3 ± 27.4^{b}	82.4 ± 5.2^{c}	102.6 ± 4.5^{c}	168.5 ± 6.3^{b}	0.56	0.34	0.62	0.60	0.48	0.80
LK11 + Metals	148.8 ± 6.58^{b}	276.3 ± 16.5^{b}	302.6 ± 17.6^{c}	96.3 ± 6.7^{b}	138.9 ± 13.7^{b}	155.2 ± 5.7^{b}	0.91	0.49	0.53	0.89	0.62	0.69
LHL10 + LK11 + Metals	92.2 ± 5.75^{d}	170.4 ± 7.6^{d}	243.7 ± 9.74^{d}	66.7 ± 5.8^{d}	88.2 ± 5.2^{d}	118.37 ± 7.9^{c}	0.69	0.37	0.54	0.74	0.56	0.75

BCF, BAF, TF denotes biological concentration factor, biological accumulation factor and translocation factor of Al and Zn respectively. Data of columns indexed by the different letter within each treatment are significantly different at the 5% level ($p < 0.05$) of probability by DMRT.

conditions, the inoculated as well as non-inoculated plants either did not exhibit or posed intangible levels of Al and Zn in their roots and shoots. However, spiking the soil with combined Al and Zn metals under stress treatment significantly enhanced the root and shoot uptake of Al and Zn in all treatments, resulting in poor growth compared to the control conditions. The accumulation of Al ions by the roots and their translocation to the shoots were detected to be substantially higher as compared to the Zn ions. The introduction of endophytes remarkably decreased the uptake and translocation of Al and Zn by several folds in the co-inoculated plants compared to the non-inoculated plants. The endophytic co-inoculation was found to be the most efficient ($p < 0.005$) for lowering Al-ion uptake by roots and translocation to shoots, followed by the sole LK11 inoculation, sole LHL10 inoculation, and no inoculation (control) conditions. Similarly, the co-inoculated plants substantially reduced the levels of Zn uptake and translocation by 299.1%, followed by the LHL10- and LK11-inoculated plants, which showed 223.1 and 176.4% reduction in roots and 326.7, 170.9, and 266.8% reduction in shoots compared to the non-inoculated plants. The influence of the endophytic co-inoculation on plant Al and Zn uptake and translocation was further scrutinized by calculating the BCF, BAF, and TF values (**Table 2**). In the absence of heavy metal stress, the introduction of co-inoculation led to a relatively high BCF in case of Al, whereas in case of Zn, all treatments showed a similar and negligible BCF in the absence of metals stress. Under metals stress, the sole LK11-inoculated plants revealed higher BCF in case of both Al and Zn, while LHl-10 showed the least BCF. The BAF under metals stress remained high in the non-inoculated plants in case of both Al and Zn, i.e., 0.52 and 0.67, respectively. In the absence of heavy metal stress, the sole LK11-inoculated and non-inoculated plants led to an increase in the TF in case of both Al and Zn stress conditions. Under metal stress, the TF was almost similar and ranged between 0.5 to 0.7 in case of Al and 0.7 to 0.8 in case of Zn. Furthermore, we explored the influence of co-inoculation on the availability and remediation of Al and Zn in soil (**Table 2**). The results showed that the sole-inoculated as well as co-inoculated plants markedly immobilized Zn and Al compared to the non-inoculated plants under heavy metal stress. The soil Zn was detected to be markedly immobilized (118.3 ± 5.2 mg kg^{-1} D.WT) by co-inoculation, which was equally followed by the sole inoculation of LHL10 and LK11 under heavy metal stress. Likewise, the application of endophytic co-inoculation led to the significant immobilization of Al (243.7 ± 9.7 mg kg^{-1} D.WT) in soil by displaying approximately 2.0-, 1.5-, and 1.2-fold less availability in comparison with the sole LHL10-inoculation, sole LK11-inoculation, and no inoculation (control) treatments.

Effect of Endophytic Co-inoculation on the Transcript Levels of Different Metal Transporter Genes

In the current study, different key genes (*GmHMA13, GmHMA18, GmHMA19, GmPHA1,* and *GmARI1*) modulating the heavy-metal stress responses and efflux transporters were assessed in the roots and leaves of *G. max* plants co-inoculated

with endophytic LHL10 and LK11 under the combined Al and Zn stress conditions (**Figure 2**). The qPCR data revealed that the relative expressions of *GmHMA13* and *GmHMA19* were significantly upregulated in the co-inoculated roots and leaves under no-stress condition as compared to the sole-inoculated and non-inoculated plants. The expression of *GmHMA18* was significantly upregulated in the roots and leaves of the sole LK11-inoculated plants followed by the LHL10-inoculated, dual-inoculated, and non-inoculated plants. The roots and shoots of the non-inoculated plants showed significantly higher *GmPHA1* expression than those of the co-inoculated and sole inoculated plants under no stress condition. However, under stress conditions, the combined toxicity of Al and Zn significantly up-regulated the transcript levels of *GmHMA13, GmHMA18*, and *GmHMA19* in the non-inoculated plant roots and leaves as compared to the co-inoculated and sole-inoculated plant roots and leaves. The endophytic co-inoculation significantly down-regulated the *GmHMA13*, *GmHMA18*, and *GmHMA19* expression by (12.5, 7.51, and 2.05), (8.48, 1.38, and 3.38) and (56.4, 14.6, and 6.25) fold in roots and (9.54, 5.42, and 1.80), (8.51, 1.77, and 2.51) and (25.4, 10.7, and 2.6) fold in shoots, compared with the non-inoculated, LHL10-inoculated, and LK11-inoculated plants, respectively, under heavy metal stress. Similarly, the relative expression of the plasma membrane H^+-ATPase gene *GmPHA1* and ariadne-like ubiquitin ligase gene *GmARI1* responsible for soybean tolerance to Al toxicity and detoxification showed that co-inoculation significantly upregulated the transcript level of *GmARI1* as compared to the non-inoculated and sole LHL10- and sole LK11-inoculated plant roots and leaves, but did not show significant difference in the relative expression of *GmPHA1* in comparison with sole LHL10- and sole LK11-inoculated plant roots and leaves under no stress condition. Furthermore, co-inoculation under metal stress significantly downregulated the *GmPHA1* expression in soybean roots by (9.4, 1.4, and 1.9) times and (4.9, 1.2, and 1.8) times in shoots as compared to the non-inoculated, sole LHL10-inoculated, and sole LK11-inoculated soybean, respectively. However, the transcript levels of *GmARI1* were significantly upregulated in the roots of the co-inoculated soybean, exhibiting (7.6, 1.6, and 2.0) times and (3.7, 1.5, and 1.7) times escalation in leaves compared to the non-inoculated, sole LHL10-inoculated, and sole LK11-inoculated soybean roots and shoots, respectively.

Effect of Co-inoculation on Soybean Macronutrients

To determine the effects of co-inoculation on the macronutrient status of soybean, four nutrients, including K, P, Ca, and S, were analyzed in their roots and shoots (**Figure 3**). Compared with the non-inoculated and sole-LHL10- and sole LK11-inoculated, the co-inoculated plants significantly ($p < 0.005$) regulated root macronutrients by displaying substantial increase in the concentrations of K, P, Ca, and S under control conditions. The similar trend was observed in the root tissues under metal-induced stress, where the application of co-inoculation remarkably enhanced the K, P, and S contents. However, under stress conditions, the non-inoculated plant roots showed significantly higher Ca content, followed by the sole LK11-inoculated, sole LHL10-inoculated, and co-inoculated plants roots, respectively. Similarly, under control conditions, a significant increase was detected in the macronutrients of the shoots tissues of the co-inoculated plants as compared to the sole inoculated and non-inoculated plant shoots. The shoots of the co-inoculated plants showed an increase in K by 1.54, 1.35, and 1.17 times, in P by 1.26, 1.17, and 1.06 times, in Ca by 1.50, 1.52, and 1.11, and in S by 1.28, 1.17, and 1.10 times as compared to the shoots of the non-inoculated, sole LHL10-inoculated, and sole LK11-inoculated plants, respectively. Under stress conditions, the co-inoculated plants showed differential regulation of macronutrients in shoots, as K and S were detected to be significantly enhanced, whereas Ca was significantly reduced in the co-inoculated plant shoots, followed by the sole LHL10-inoculated, sole LK11-inoculated and non-inoculated plants shoots. However, the sole LHL10-inoculated plants exhibited significantly ($p < 0.005$) higher P contents, whereas the non-inoculated plants presented significantly lower P contents under stress conditions. Furthermore, the effect of endophytes co-inoculation on nitrogen assimilation of soybean under control as well as Al/Zn stress revealed significant ($p < 0.05$) assimilation of nitrogen in both roots and shoots compared to sole LHL10-inoculated, sole LK11-inoculated and non-inoculated plants.

Effect of Co-inoculation on Soil Extra-Cellular Enzymatic Activities Under Al and Zn Stress

The activities of soil enzymes, including glucosidase, phosphatase, glucuronidase, and cellulase, were measured to assess the metal detoxification efficiency of co-inoculation for rehabilitating the quality and efficiency of soil. In the current study, inoculating soil either with sole LHL10 endophyte, sole LK11 endophyte, or with both endophytes significantly regulated soil enzymatic activities both under metal-induced stress and non-stress conditions (**Table 3**). In the absence of metal stress, the phosphatase activity of the endophyte co-inoculated plants significantly increased by 35.42, 23.10, and 85.62% compared to those of the sole LHL10-inoculated, sole LK11-inoculated, and non-inoculated plants, respectively. Likewise, a higher activity trend under no-stress condition was displayed by cellulase in the co-inoculated soil, followed by the sole LK11-inoculated, sole LHL10-inoculated, and non-inoculated soil, respectively. In case of glucuronidase under no-stress condition, the co-inoculated soil exhibited significantly higher activity than the non-inoculated and sole LK11-treated soils, but displayed no significant differences with the LHL10-inoculated soil. The co-inoculated and sole LK11-inoculated soils significantly upregulated the glucosidase activity under no-stress condition compared to the LHL10-inoculated and non-inoculated soils. Under Al and Zn contamination, the co-inoculation treatment significantly ($p < 0.005$) enhanced the phosphatase activity by 1.26, 1.51, and 2.23 times, the cellulase activity by 1.10, 1.51, and 2.02 times, and the glucuronidase activity by 1.23, 1.21, and 1.53 times compared to the sole LHL10-inoculated, sole LK11-inoculated, and non-inoculated plants, respectively.

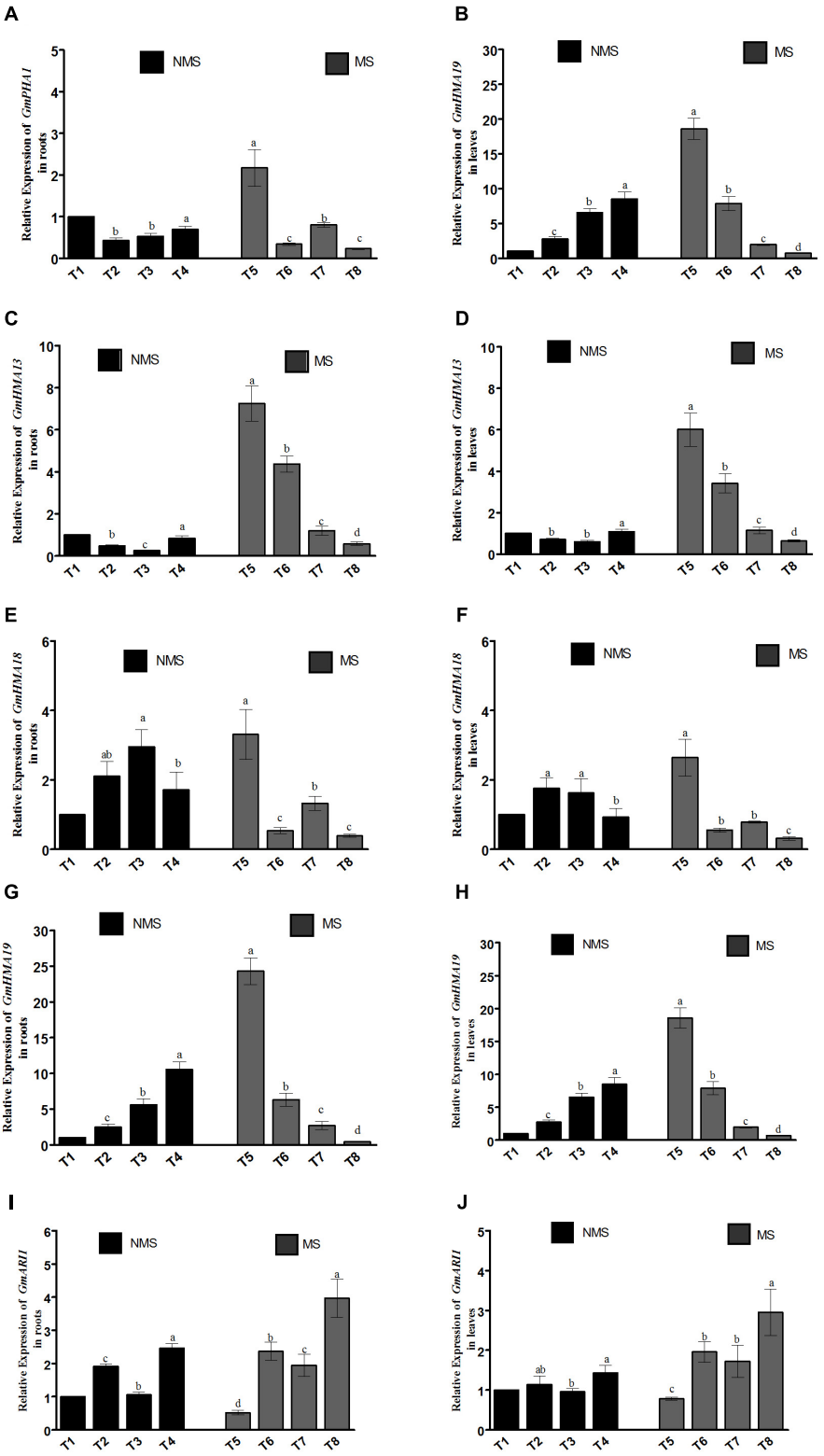

FIGURE 2 | Influence of the endophytic inoculation on the expression patterns of **(A,B)** *GmPHA1* **(C,D)** *GmHMA13,* **(E,F)** *GmHMA18,* **(G,H)**, *GmHMA19,* and **(I,J)** *GmARI1* in soybean roots and leaves under Al and Zn stress. NMS represents "No metal stress" while MS represents "Metal stress." T1 (Control Plants), T2 (LHL10-treated plants), T3 (LK11-treated plants), T4 (LHL10 + LK11-treated plants), T5 (Control + Metals), T6 (LHL10 + Metal-treated plants), T7 (LK11 + Metal-treated plants), T8 (LHL10 + LK11 + Metal-treated plants). Different letters indicate significant differences between means at $p > 0.05$ (DMRT). Values represent means (of four replication) ± standard error.

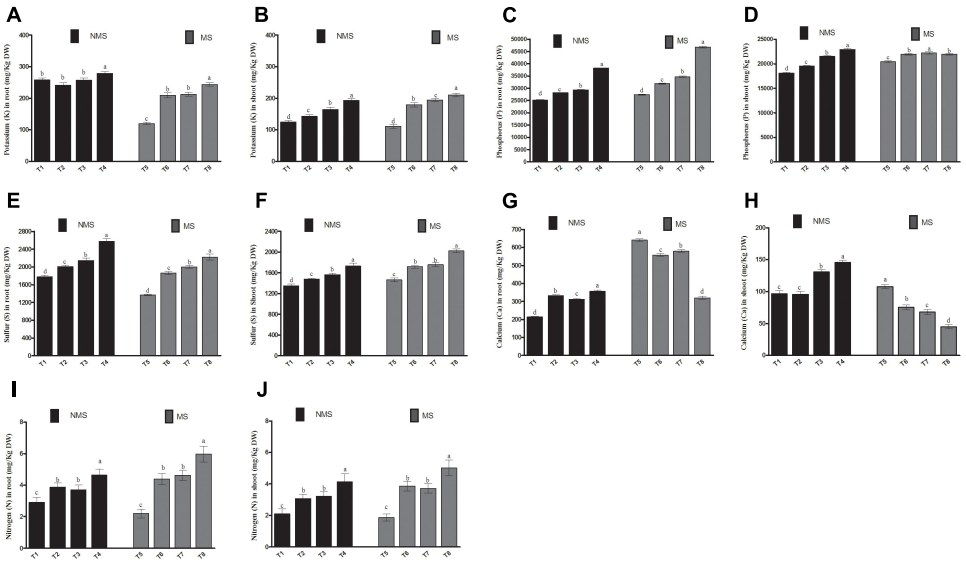

FIGURE 3 | Influence of endophytic LHL10 and LK11 association on soybean root and shoot macronutrient uptake under metals stress. NMS represent "No metal stress" while MS represents "Metal stress." T1 (Control Plants), T2 (LHL10-treated plants), T3 (LK11-treated plants), T4 (LHL10+LK11-treated plants), T5 (Control + Metals), T6 (LHL10 + Metal-treated plants), T7 (LK11 + Metal-treated plants), T8 (LHL10 + LK11 + Metal-treated plants). Different letters indicate significant differences between means at $p > 0.05$ (DMRT). Values represent means (of four replication) ± standard error.

TABLE 3 | Effect of LHL10 and LK11 on soil enzymatic activities in Zn and Al contaminated soil.

Treatment	Phosphatase ($\mu M^{-1}min^{-1}mL$)	Cellulase ($\mu M^{-1}min^{-1}mL$)	Glucuronidase ($\mu M^{-1}min^{-1}mL$)	Glucosidase ($\mu M^{-1}min^{-1}mL$)
Without metals stress				
Control	197.85 ± 6.57^{d}	42.15 ± 2.35^{d}	34.67 ± 2.84^{b}	30.16 ± 1.08^{c}
LHL10	299.74 ± 6.69^{b}	56.02 ± 2.09^{b}	39.33 ± 1.51^{a}	33.05 ± 1.57^{b}
LK11	272.34 ± 6.75^{c}	48.54 ± 2.12^{c}	32.49 ± 1.62^{b}	36.01 ± 1.77^{a}
LHL10 + LK11	368.57 ± 8.37^{a}	68.79 ± 2.77^{a}	42.29 ± 1.58^{a}	35.25 ± 1.21^{ab}
With metals stress				
Control + Metals	221.73 ± 7.39^{d}	27.47 ± 2.58^{d}	25.42 ± 1.05^{c}	14.76 ± 0.91^{c}
LHL10 + Metals	387.38 ± 7.81^{b}	68.39 ± 2.61^{b}	31.84 ± 0.93^{b}	36.861 ± 1.56^{a}
LK11 + Metals	318.94 ± 9.87^{c}	50.54 ± 2.65^{c}	32.68 ± 1.46^{b}	28.292 ± 1.32^{b}
LHL10 + LK11 + Metals	489.86 ± 8.53^{a}	75.49 ± 2.51^{a}	39.65 ± 1.22^{a}	38.79 ± 1.13^{a}

Values in the columns indexed by different letters are significantly different at $P \leq 0.05$ based as evaluated by the DMRT. Values in a column represent the mean ± SD of treatments replicated four times fromthree independent experiments.

The sole LK11-inoculated and co-inoculated soil exhibited almost similar glucosidase activities, followed by the sole LHL10-inoculated and non-inoculated soils under Al and Zn contamination.

Modulation of Soybean Antioxidant System by Co-inoculation Under Al/Zn Exposure

To assess the extent of lipid peroxidation in soybean due to metal-induced oxidative stress, the malondialdehyde (MDA) content was investigated (**Figure 4**). The metal-induced stresses generate MDA, which in turn lead to the induction of lipid peroxidation. In the current study, the MDA content in the co-inoculated plant leaf tissues was comparable with that in the sole LK11-inoculated plant leaf tissues and significantly higher than those of the non-inoculated and sole LHL10-inoculated plant leaf tissues (**Figure 4**). However, the Al and Zn stress exposure substantially increased the MDA levels in the non-inoculated plants compared to the co-inoculated and sole inoculated plants. The MDA content of the co-inoculated plant leaves was significantly reduced by 26.1, 13.3, and 92.3% under metal stress conditions relative to the MDA contents of the sole LK11-inoculated, sole LHL10-inoculated, and non-inoculated plant leaves. Similarly, the co-inoculated or sole inoculated plants revealed insignificant changes in the H_2O_2 content compared to the non-inoculated plants in the absence of stress; this was also validated by the presence of hydrogen peroxide in soybean leaves using the diaminobenzidine (DAB) staining technique (**Supplementary Figure S1**). However, the Al- and Zn-induced stress significantly triggered the generation of H_2O_2 in the non-inoculated plants as compared to the inoculated

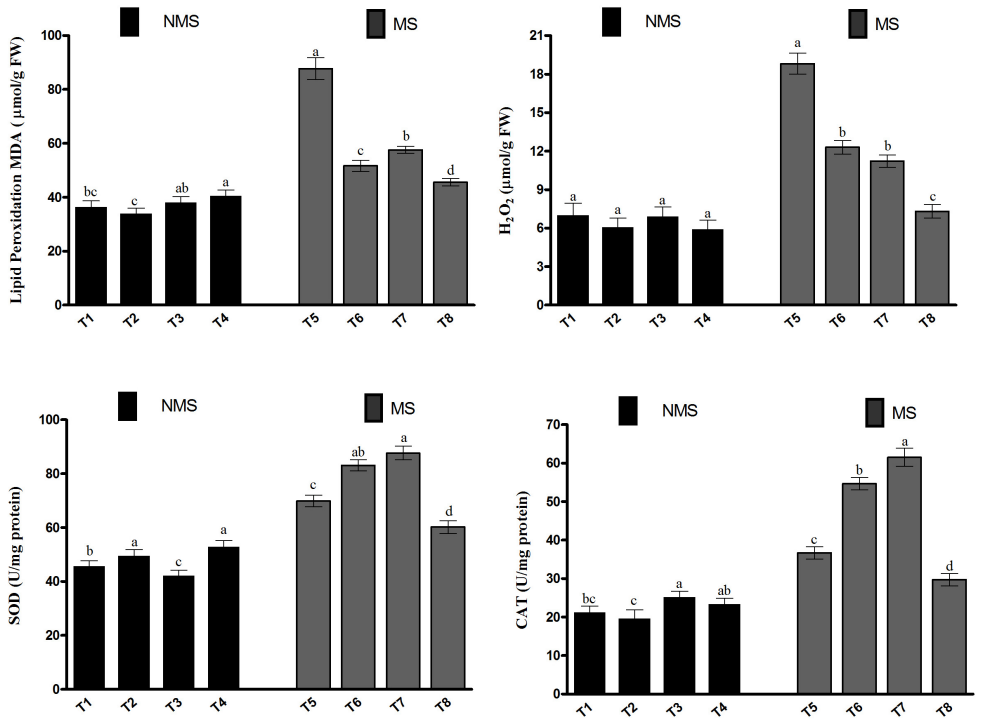

FIGURE 4 | Effects of endophyte inoculation on malondialdehyde (MDA) content, H_2O_2 production, and antioxidant activities of soybean under Al and Zn stress. NMS represent "No metal stress" while MS represents "Metal stress." T1 (Control Plants), T2 (LHL10-treated plants), T3 (LK11-treated plants), T4 (LHL10 + LK11-treated plants), T5 (Control + Metals), T6 (LHL10 + Metal-treated plants), T7 (LK11 + Metal-treated plants), T8 (LHL10 + LK11 + Metal-treated plants). Bars with different letters are significantly different at $p > 0.05$ (DMRT). Values represent means (of four replicates) ± standard error.

plants. The co-inoculated plants demonstrated significantly lower H_2O_2 content than the sole inoculated and non-inoculated plants, suggesting the alleviation of metal-induced stress. To encounter the metal-induced oxidative stress, the activities of the antioxidant enzymes SOD and CAT were investigated (**Figure 4**). The results depicted that the sole inoculation and co-inoculation treatments differentially regulated the SOD and CAT activities under no-stress control conditions, as both co-inoculated and sole LHL10-inoculated plants significantly ($p < 0.005$) enhanced the SOD activity compared to the non-inoculated and sole LK11-inoculated plants. Under no-stress control conditions, the CAT activity was remarkably higher in the sole LK11-inoculated plants, followed by the co-inoculated, non-inoculated, and sole LHL10-inoculated plants. However, under metal-stress conditions, the sole LK11-inoculated plants presented significantly high CAT activity. However, the co-inoculated plants exhibited 2.06-, 1.83-, and 1.23-fold lesser CAT activity compared to the sole LK11-inoculated, sole LHL10-inoculated, and non-inoculated plants, respectively.

Influence of Endophyte Co-inoculation on Soybean Endogenous Gibberellic Acid Content

In the current study, the endogenous GA (GA_1, GA_4, GA_9, GA_{24}) contents of the soybean plant were investigated because of their significance in metal-induced stresses (**Figure 5**). The results depicted that the metal-induced stresses significantly affected the GA contents under metal stresses, particularly in the non-inoculated plants. We found that the co-inoculated plants significantly enhanced the contents of GA_1, GA_4, GA_9, and GA_{24} (5.8, 15.4, 25.3, and 39.7 ng/g DW), followed by the sole LHL10-inoculated, sole LK11-inoculated, and non-inoculated plants under no-stress control conditions. Similarly, the sole LHL10- and sole LK11-inoculated plants displayed higher contents of GA_1, GA_4, GA_9, and GA_{24} as compared to the non-inoculated plants, but exhibited no significant differences with each other in case of GA_1 under the control conditions. However, under Al and Zn stress, the co-inoculated plants displayed 5.5-, 1.3-, and 1.2-fold and 2.5-, 1.5-, and 1.6-fold higher contents of GA_1 and GA_4 as compared to the non-inoculated, sole LHL10-, and sole LK11-inoculated plants, respectively. Similarly, under stress conditions, the co-inoculated and sole LK11-inoculated plants showed no statistical difference in their GA_9 contents, but exhibited approximately 37.44 and 94.7% higher GA_9 production as compared to the sole LHL10-inoculated and non-inoculated plants, respectively. Similarly, the GA_{24} production was recorded significantly higher (35.77 ± 1.8 ng/g DW) in the co-inoculated plants, followed by the sole LHL10inoculated plants (26.4 ± 1.2 ng/g DW), sole LK11-inoculated plants (24.73 ± 1.2 ng/g DW), and non-inoculated plants (12.57 ± 0.72 ng/g DW) under Al and Zn stress.

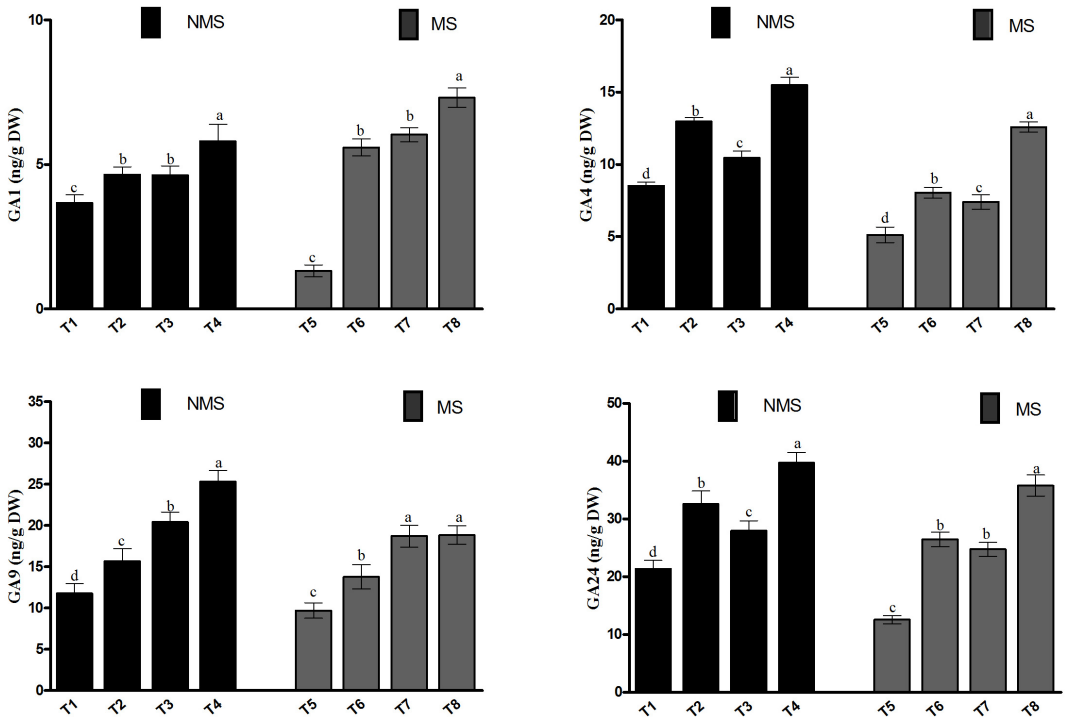

FIGURE 5 | Effect of endophytic LHL10 and LK11 inoculation on the endogenous levels of GAs in soybean under metal stress. NMS represent "No metal stress" while MS represents "Metal stress." T1 (Control Plants), T2 (LHL10-treated plants), T3 (LK11-treated plants), T4 (LHL10 + LK11-treated plants), T5 (Control + Metals), T6 (LHL10 + Metal-treated plants), T7 (LK11 + Metal-treated plants), T8 (LHL10 + LK11 + Metal-treated plants). Different letters show significant differences between means at $p > 0.05$ (DMRT). Values represent means (of four replication) ± standard error.

Effects of Co-inoculation on Endogenous ABA and JA Modulation of Soybean

The current results depicted that in the absence of metal stress, the stress responsive endogenous ABA levels were not significantly different among the non-inoculated, co-inoculated, and sole LK11-inoculated plants. However, the ABA content of the sole LHL10-inoculated plants significantly increased by 18.1, 11.6, and 12.2% compared to the non-inoculated, sole LK11-inoculated, and co-inoculated plants, respectively (**Figure 6**). Under metal stress, the escalation in the ABA production of plants was noticed among all treatments. However, in comparison with the non-inoculated plants, significantly ($p < 0.005$) lower ABA production was detected in the sole inoculated and co-inoculated plants under stress conditions. Co-inoculation under metal stress significantly reduced the ABA levels by 80.27, 16.59, and 24.62% as compared to the non-inoculated, sole LHL10-inoculated, and sole LK11-inoculated plants, respectively. In case of the endogenous JA content, the sole LK11-inoculated plants significantly ($p < 0.005$) enhanced the production of JA, followed by the sole LHL10-inoculated, co-inoculated, and non-inoculated plants, respectively (**Figure 6**). However, the exposure to metal stress markedly alleviated the JA contents of the non-inoculated plants by more than 2- and approximately 1.7-fold as compared to the co-inoculated and sole-inoculated plants, respectively.

DISCUSSION

The phytoremediating techniques based on suitable heavy metal-resisting and -tolerating microbes have gained considerable attention in the modern era. Generally, the interactions of endophytes (bacteria and fungi) with crop plants under harsh environmental conditions, including metals stresses, are acknowledged for boosting plant growth and metabolic processes. The individual applications of endophytic fungi, such as *Lasiodiplodia* sp., *Phialocephala fortinii,* and *Rhizoscyphus* sp., and endophytic bacteria, such as *Pseudomonas* sp., *Methylobacterium oryzae*, and *Sphingomonas* sp., have been reported for increasing plant biomass and ameliorating adverse effects of different heavy metal stresses (Ma et al., 2016a; Yamaji et al., 2016). Some studies have reported the beneficial effects of dual inoculation with arbuscular mycorrhizal fungi, such as *Glomus* sp., *Acaulospora* sp., and *Scutellospora* sp., and plant growth-promoting rhizobacteria, such as *Actinomycetes* sp., *Paenibacillus* sp., *Pseudomonas* sp., and *Azotobacter* sp. on *Pennisetum glaucum,* and *Sorghum bicolor,* which showed a significant increase in plant growth, biomass, and bioremediation of the iron-contaminated soil (Mishra et al., 2016). However, knowledge is lacking on the association of fungal and bacterial endophytes and their interaction with *G. max*, as well as the underlying mechanism for encountering stresses in the metal-contaminated soil. In the current study, a vital growth-benefiting impact

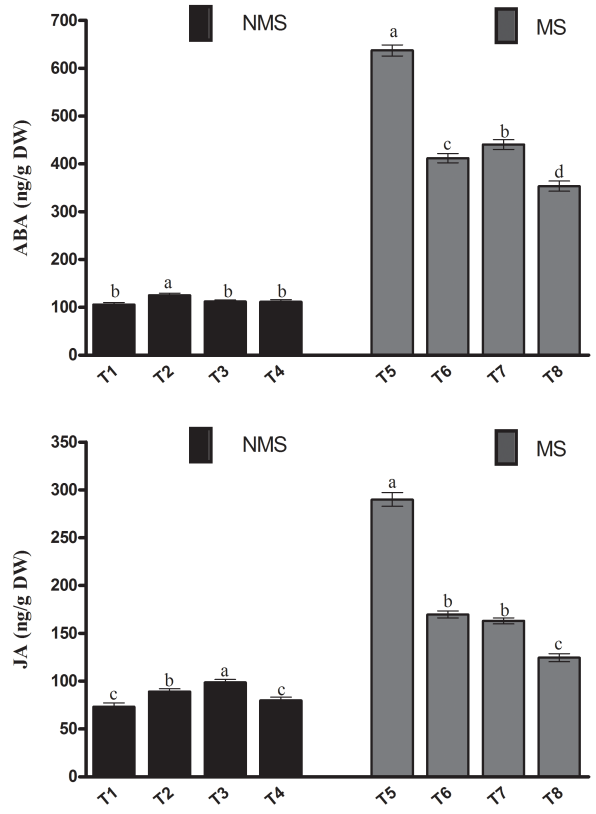

FIGURE 6 | Effect of endophyte inoculation on endogenous abscisic acid (ABA) and jasmonic acid (JA) content of soybean under metal stress. NMS represent "No metal stress" while MS represents "Metal stress." T1 (Control Plants), T2 (LHL10-treated plants), T3 (LK11-treated plants), T4 (LHL10 + LK11-treated plants), T5 (Control + Metals), T6 (LHL10 + Metal-treated plants), T7 (LK11 + Metal-treated plants), T8 (LHL10 + LK11 + Metal-treated plants). Different letters indicate significant differences between means at $p > 0.05$ (DMRT). Values represent means (of four replication) ± standard error.

of the synergistic consortia of endophytic *Sphingomonas* sp. LK11 and endophytic *Paecilomyces formosus* LHL10 was observed on *G. max* plants under the combined toxicity of Al and Zn. On other hand, a decline in plant growth and biomass was detected in non-inoculated plants, likely resulting from the impairment of the Calvin cycle, photosynthetic machinery, and electron transport chain, as well as from the induction of ROS under combined Al and Zn toxicity.

In the current case of dual inoculation, the potential to produce secondary metabolites, e.g., GAs and IAA, of endophytes might be a contributing factor toward tolerating metal toxicity and promoting growth attributes via enhancing nutrient uptake by proliferating roots and mediating roots exudates under normal as well as Al- and Zn-contaminated soil (Velivelli et al., 2014; Singh et al., 2016). As microbial IAA can loosen the roots cells walls and change the properties of root absorption by increasing root, hairs, length and surface as well as enhancing the excretion of root exudates, which subsequently provide additional nutrients to support the growth of microorganism (Etesami, 2018). Such roots exudates are considered vital for dealing with heavy metals toxicity by preventing them from entering the cell symplast by chelating and forming complexation in rhizosphere; thereby decreasing the metal ion toxicity toward the plant and microbes. Both fungi and bacteria with phytohormones (IAA,GA) producing potential and metals remediating capabilities are repeatedly acknowledged for counteracting heavy metals toxicity (Deng and Cao, 2017; Etesami, 2018). Therefore, mitigating metals toxic effects from in co-inoculated soybean could be ascribed to the cumulative effects of endophytes i.e., metals (Al/Zn) remediating ability and phytohormones producing capability of LHL10 and LK11. Our current findings are also in conformity with the findings of Rajkumar et al. (2012), who extensively reviewed the effects of dual inoculation of mycorrhizal fungi with metals remediating bacteria (*P. putida* or *B. cereus*) and reported their positive influence on host plant growth and heavy metals tolerance.

To explore the alleviation mechanism of metal toxicity-induced stress, it is important to scrutinize the distribution, translocation, immobilization, and availability of metals in the roots, shoots and soil. In the current study, the reduced accumulation of Al/Zn in the roots and shoots of the co-inoculated plants was evident when compared with the non-inoculated and sole inoculated plants. The improved growth of co-inoculated *G. max* L. could possibly be related with the reduced accumulation of Al and Zn in the tissues because of a decrease in their bioavailability in the soil through the absorption/desorption mechanism or preventing their entrance into the tissues by the intracellular accumulation of metals or by the sequestrations of metals in the soil via exudation of various metabolites. Moreover, the initial screening of endophytic LHL10 and LK11 survival against combine Al and Zn toxicity revealed a significant reduction of metals in the liquid broth and exhibiting remarkable uptake via intracellular absorption. Therefore, the reduced metals accumulation and uptake in *G. max.* L tissues could probably be due to the locking down of Al and Zn in their biomass, consequently preventing the plants from their toxic effects. The potential of producing extracellular metabolites, i.e., IAA and gibberellins by endophytic LHL10 and LK11 might have facilitated the metal remediation process and alleviated their toxicity-induced stress in plants. As the production of IAA and GAs by microbes has been reported for boosting plant tolerance to heavy metals toxicity (Deng and Cao, 2017). The deployment of both intra and extra cellular mechanisms simultaneously by LHl10 and LK11 could be a possible justification for the reduction of Al and Zn in the tissues of the endophytic LHL10 and LK11-co-inoculated *G. max* plants. Additionally, the genomic analysis of LK11 (unpublished data) revealed that the LK11 plasmid and chromosome harbor a metal-resisting and -degrading operon containing an active efflux system for accumulated metals; this can be correlated with the reduced metal uptake in plants by assisting the Al and Zn detoxification process in soil. The significantly reduced Al and Zn accumulation and their translocation from roots to shoots of the co-inoculated plants

in the current study are in concordance with Fernández-Fuego et al. (2017) and Zahoor et al. (2017), who found relatively low metal uptake in the endophytic *Mucor* sp. MHR-7-inoculated *Brassica campestris* L. and ectomycorrhizal fungus *Paxillus ammoniavirescens*-inoculated *Betula pubescens* Ehr. Contrary to the decrease in metal uptake in the current study, Yihui et al. (2017) found a substantial uptake of Pb in the endophytic *Gaeumannomyces cylindrosporus*-infected *Zea mays* L. Despite the above explanations for reduce metal uptake in *G. max*, the influence of the endophytic fungal LHL10 and endophytic bacterial LK11 co-inoculation on plant Al and Zn cannot be generalized. The uptake and translocation of metals in plants tissues is also reported to be reliant on the interaction between the nature of plants and bacteria/fungi and is also associated with the levels of toxic heavy metals, macro and micronutrients, and soil pH, which eventually critically influence the bioavailability of metals in soil and alter their uptake in plants (Islam et al., 2016; Fernández-Fuego et al., 2017). However, the current findings that indicate the inoculation of the consortia of endophytic bacteria and fungi as a viable strategy for bioremediating the Al- and Zn-contaminated soil and reducing metal uptake in soybean.

In the current study, the plasma membrane H^+-ATPases genes, which are responsible for providing metal resistance, absorption, and transportation in plants, were investigated. Current findings of the study displayed that the heavy metal ATPase gene *GmPHA1*, which is involved in Al accumulation and translocation from the root to shoot of soybean was significantly downregulated in the roots and leaves of the LHL10- and LK11-co-inoculated plants. Such low expression could be correlated with Al accumulation and uptake, which was significantly reduced by the dual inoculation of endophytes in soybean roots and shoots. Similarly, we investigated to explore the gene expression profiles of P_{1B}-ATPases, which are known for transporting diverse range of metals across biological membranes. Therefore, the expression responses of Zn^{2+}-ATPases genes (*GmHMA13, GmHMA18,* and *GmHMA19*), which is a subclass P_{1B}-ATPases, was assessed to analyze the influence of endophyte dual inoculation on Zn uptake and transportation in soybean. Results revealed that the expression levels of *GmHMA13, GmHMA18*, *and GmHMA19* were remarkably downregulated under Zn stress in the dual-inoculated plants root and leaf tissues compared to other treatments. Such downregulation of genes suggest a significant reduction of Zn accumulation and transportation. Interestingly, the ICP-MS findings of the current study evidenced a remarkable decrease of metals in the dual-inoculated soybeans tissues, which might have contributed to the amelioration of adverse effects of excessive metal accumulation in plants tissues. Recent studies have also discovered the vital roles of ariadne-like E3 ubiquitin ligases in plant responses to abiotic stresses, including metal toxicity (Lang-Mladek et al., 2012; Zhang et al., 2014). Therefore, the evaluation of ariadne-like E3 ubiquitin ligase gene *GmARI1* showed that dual inoculation modulated the *GmARI1* gene by revealing significant expression under Al stress conditions. The upregulation of *GmARI1* has been reported for enhancing soybean tolerance and resistance to severe Al toxicity by regulating plant response to Al through suppressing the oxidative stress signals, which could interact with plant hormone signaling pathways to reduce the metal-induced damage or root growth inhibition in plants (Zhang et al., 2014; Gao et al., 2017). The increased transcript accumulation of *GmARI1* in the roots tissues compared to the leaf tissues could be related to the fact that Al stress initially causes damage to plant roots and subsequently leads to uptake of water and nutrient inhibition, thereby affecting plant growth and development. The increased transcript accumulation of *GmARI1* in co-inoculated plants might be attributed to the combined exogenous production of IAA by endophytic LHL10 and LK11 under Al stress, as the exogenous application of IAA significantly upregulated the *GmARI1* expression under Al contamination in soybean roots (Zhang et al., 2014). In current study such decreased plasma membrane H^+-ATPases transporters activity of co-inoculated supports the fact that consortia of endophytic LHL10 and LK11 significantly mitigated Al/Zn toxic effects in soybean by reducing their uptake and accumulation, which could be an effective strategy for reducing metal transfer from the contaminated soil to the food chain.

In addition to adverse impacts on plant growth and biomass, the toxicity of metals, including Al and Zn, negatively influences the availability and uptake of essential elements in plant roots and shoots (Bhattacharya et al., 2010). Conversely, in the current study, the synergistic association of bacterial and fungal endophytes demonstrated a significant increase in the uptake of P, K, and S in plants roots and shoots under metals stress, suggesting that dual inoculation in soybean strictly regulates the uptake and accumulation of both essential and non-essential nutrients. The enhancement in the uptake of P, K, S and N uptake in roots and shoots of the dual-inoculated soybean plants might be due to the nutrient-mobilizing activity and phytohormone (IAA and GAs)-producing potential of the endophytic LK11 and LHL10. The phytohormone production by endophytes associated with the plants under abiotic stresses frequently stimulate the growth and metabolic processes, leading to an extended root system, which effectively contributes to augmented nutrient uptake. As previously endophytic bacteria *Pseudomonas brassicacearum* and endophytic fungi *P. fortinii*, *Rhizodermea veluwensis*, and *Rhizoscyphus* sp. have been reported for enhancing the uptake of host plant macronutrients under diverse metals toxicity conditions (Yamaji et al., 2016; Kong and Glick, 2017). However, in dual inoculated plants, a decrease in Ca uptake was recorded under metal stress compared to other treatments. An increase in the Ca content of the non-inoculated plants compared to the co-inoculated ones could be related to the significant production of H_2O_2 under metal-induced toxicity, triggering the activation of hyperpolarization-activated calcium channels (HACCs) for enhancing Ca^{2+} influx to directly stimulate NADPH oxidase for generating ROS, which might lead to the generation of ABA for regulating plant responses to stress mitigation (Kar, 2011; Leitão and Enguita, 2016). Therefore, in the current study, the considerable decrease in H_2O_2, Ca

accumulation, and ABA production of co-inoculated soybean under metal toxicity could be corroborated with the positive influence of co-inoculation in soybean under combined Al and Zn toxicity.

The sources of soil enzymes have not been fully explored, but the soil microbial community and plants are thought to be the major sources of soil enzymes. Soil extracellular enzymes are considered to be involved in diverse biochemical reactions: reducing metal-induced soil toxicity, maintaining soil texture and structure, conversion and decomposition, cycling and decomposition of organic matter. Numerous studies have demonstrated that heavy metal contamination significantly impairs soil enzymatic potential by interacting with the enzyme-substrate complex and consequently causes the denaturation of enzyme proteins (Ma et al., 2015). The current study revealed that the application of the endophytic LHL10 and LK11 co-inoculation efficiently tackled the lethal effects of combined Al and Zn toxicity by augmenting soil enzymatic activities. Endophyte co-inoculation of plants exponentially improved the phosphatase activity of soil compared to the non-inoculated plants under stress conditions. The enhancement of soil phosphatase activity under metal contamination is the major mechanism recruited for avoiding and detoxifying heavy metal toxicity as well as improving plants tolerance to metal stresses (Wang et al., 2006). Phosphatases are also considered to be involved in the breakdown of various phosphate esters and alternatively enhance phosphorus (P) availability and uptake by plants; this was evidently witnessed in the co-inoculated plants in the current study. Such significant increase demonstrates the positive influence of endophytic co-inoculation in metal detoxification and plant growth enhancement. Curaqueo et al. (2014) and Ali et al. (2017) reported significant enhancement in the phosphatase activity of the soil polluted with various heavy metals by inoculating it with AM fungi and *Streptomyces pactum* (Act12). Similarly, a significant improvement was detected in the cellulase activity of the dual inoculated soil under combined Al and Zn contamination. Jia et al. (2015) and Xian et al. (2015) reported that the heavy metal contamination of soil lead to a reduction in its cellulase activity. An escalation in the cellulase activity of the dual-inoculated soil increases the breakdown of carbohydrates and decomposition of organic matter and is considered crucial for assisting the vertical transmission and colonization of endophytes in plants (Ma et al., 2011; Xian et al., 2015). Likewise, Burges et al. (2015) and Parelho et al. (2016) found that the glucosidase activity of an agricultural soil is highly sensitive to metal toxicity and is significantly reduced. On the contrary, the endophytic dual inoculation under combined Al/Zn toxicity significantly maintained the glucosidase activity similar to that in the control conditions. This suggests that the synergistic inoculation of endophytic LHL10 and LK11 as a potential strategy for supporting soil microbial community and offering a friendly ecosystem for eventual plant growth and yield enhancement under Al- and Zn-contaminated soil conditions.

The current study revealed that the accumulation and translocation of the reducing metals (Al and Zn) in the *G. max* tissues led to a considerable mitigation of the metal-induced oxidative stress compared to the sole inoculation and non-inoculation. The alleviation of Al- and Zn-induced oxidative stress could also be related to the direct impact of dual inoculation on plant biomass, leading to the development of both underground and aboveground plant parts. Excessive accumulations of Al and Zn in plants result in significant inhibition of the photosynthetic electron transport chains, which ultimately lead to the generation of ROS, such as superoxide anion, H_2O_2, and singlet oxygen. Therefore, the dual inoculation of plants considerably influenced their metal uptake in the current study, thereby reducing the level of lipid peroxidation of membranes by exhibiting nearly same amount of MDA as in the absence of metal stress. Similarly, the excessive generation of H_2O_2 due to excessive metal accumulation results in the oxidation of cysteine and methionine residues and tempers the Calvin cycle enzymes and photosynthetic system (Das and Roychoudhury, 2014). However, the inoculation of multiple endophytes under combined Al and Zn toxicity displayed lower production of H_2O_2, suggesting their Al and Zn stress-mitigating effect. The improved chlorophyll content of the co-inoculated plants under metal stress condition could also be attributed to the significantly lower production of H_2O_2 and MDA. The membrane lipids are extremely vulnerable to the oxidation of metal-induced ROS and considered as the first target of metal toxicity. However, plants generally deploy the synergistic activation of antioxidants to counteract the overproduction of metal-induced ROS. Therefore, as major defense enzyme against metal-induced oxidation, SOD acts as the first line of defense for counteracting metal toxicity by dismutating super oxide radicals into H_2O_2 and O_2 via Haber-Weiss reaction. Moreover, the deployment of tetrameric heme-containing CAT further carries out the dismutation of H_2O_2 into H_2O and O_2 (Sharma et al., 2012). However, in the current study, endophyte dual inoculation resulted in the down regulation of the SOD and CAT activities of *G. max* grown under Al- and Zn-contaminated soil. Such low CAT and SOD activities of co inoculated treatment as compared to non-inoculated and sole inoculated treatments could be the consequences of the endophytic LHL10 and LK11 co-inoculation-induced inhibition of metal entrance and subsequent ROS production in plants. Contrary to the dual inoculation, the sole inoculation led to the significant enhancement of the SOD and CAT activities of plants under metal contamination compared to the non-inoculated plants. However, the possible explanation for such variations in the antioxidative activities of the sole- and dual-inoculated plants could be that the combined metal sequestration/immobilization effect of LHL10 and LK11 makes Al and Zn less accessible to plants, lowering down their uptake. Consequently, host plants are successfully escaped from the metal-induced ROS generation, thereby inhibiting the generation of SOD and CAT. The reduced generation of ROS, i.e., MDA (lipid peroxidation), H_2O_2, SOD, and CAT antioxidative enzymes suggests a promising role of endophytic dual inoculation in successfully alleviating metal stress in soybean.

Plant endogenous hormones play a crucial role in plant growth and development, and their interplay is of great significance to

better understand the stress-coping mechanisms of plants. There are strong evidences that phytohormones (ABA, JA and GA) play vital role in the expression of Al and Zn toxicity and the subsequent responses of the plants to their toxicity. Kopittke (2016) extensively reviewed that endogenous hormonal level of plant tissues remarkably change upon exposure to Al stress, which might be either due to direct response of stress responsive hormones to Al stress in order counteract the toxic effects of Al, or due to non-specific change in plant functioning as a result of Al stress. However, the fluctuations of endogenous hormones under hostile conditions including Al/Zn toxicity help to alter plant cellular dynamics and thus play a central role in coordinately regulating growth responses to cope with stresses (Kopittke, 2016; Jalmi et al., 2018). The convergence points among defense responsive hormones signal transduction cascades are referred as crosstalk, and by this way hormones possibly interact together to constitute signal defense networking against environmental stresses.

Limited information is available on the soybean endogenous phytohormone interaction in context to the dual application of endophytes under combined Al and Zn toxicity. The current study revealed the influence of the inoculation of endophytic consortia on endogenous GAs, ABA, and JA production of *G. max* under combined Al and Zn toxicity. GAs are widely recognized for plant growth and development under normal and stress conditions, while their deficiency leads to the susceptibility of plants to various stresses, including metal stress (Asgher et al., 2015). The co-application of endophytic LHL10 and LK11 seems to significantly enhance the production of both bioactive GA_1 and GA_4 under control as well as stress conditions. This suggests that the endophytic consortium triggered both the C-13 hydroxylation and non-C-13 hydroxylation pathways for gibberellin biosynthesis under metal stress. The high amounts of GA_1, GA_4, GA_9, and GA_{24} in endophytic co-inoculation treatment suggest that the endophytic consortium significantly maintained plant growth under stress conditions. Additionally, the relatively higher concentration of the bioactive GA_4 compared to GA_1 suggests non-C-13 hydroxylation as the major GA biosynthetic pathway in dual-inoculated soybean plants. Our results are in the agreement with the previous findings of Kim et al. (2015) and Hamayun et al. (2017), who reported higher production of GA_4 compared to GA_1 and suggested the non-C-13 hydroxylation pathway as the major GA biosynthesis mechanism for growth and development in soybean plant. Endogenous ABA is a multifunctional hormone, whose increased accumulation is considered to be involved in protecting plants against heavy metal stresses including (Al and Zn) via causing stomatal closure for preventing water loss and stress damage. Wani et al. (2016) reported that endogenous level of ABA increase rapidly under environmental stresses including heavy metals stress for activating specific signaling pathways and stress responsible genes expression. As previously Hou et al. (2010) reported significantly accumulation of endogenous ABA level in soybean under aluminum stress. However, in the current study, we detected a significant reduction in the ABA content of co-inoculated soybean under metal stress compared to other treatments and also observed an antagonism between GA and ABA production. As the higher production of ABA in plants is involved in conferring tolerance to various abiotic stresses, but the current reduction in ABA content and enhancement in GAs in metal-affected soybean associated with endophytic dual inoculation demonstrates the alleviation of the combined Al and Zn stress, probably by improving plant growth by the phytohormone (GA, IAA)-producing ability of endophytes and consequently obstructing the accumulation of DELLA proteins. In agreement with this, Al and Zn toxicity also enhanced JA accumulation, showing the possible contribution of JA in stress-mediated signaling. JA has been demonstrated as a critical signaling molecule for boosting plant performance under hostile conditions, including metals stresses (Per et al., 2018). As Huang et al. (2017) reported that transcriptomic analysis of roots and leaves of soybean reveled the significant expression levels of genes involved in jasmonic acid mediated signaling pathway under Al stress. However, it is worth-mentioning that the combined application of endophytes significantly reduced JA levels in soybean under Al/Zn toxicity, suggesting that the application of endophytic consortia has alleviated Al/Zn induced stress in soybean and subsequently lower production of JA was detected. Such reduction of JA in co-inoculated soybean under Al and Zn stress might be ascribed to the enhanced levels of bioactive GAs, leading to the degradation of DELLA proteins and consequently setting the Jasmonate ZIM-domain (JAZs) proteins free to bind with MYC2 and suppressing its activity to attenuate JA signaling (Per et al., 2018). Therefore, a significant increase in the contents GAs and stress-responsive hormones ABA and JA in co-inoculated soybean indicate that the association of LHL10 and LK11 has a beneficial role in mitigating metal stress and promoting plant growth and development.

CONCLUSION

The findings of the current study disclosed that the association of the phytohormone-producing endophytic *Paecilomyces formosus* LHL10 and *Sphingomonas* sp. LK11 are coordinately involved in soybean growth promotion and adaptation to combine Al and Zn induced stress. The endophytic dual inoculation improved plant growth via combined mechanisms of lowering metal toxicity in soybean tissues by inhibiting the uptake and translocation of metals and by enhancing the uptake of essential nutrients and modulation of soil extracellular enzymatic activities. This strategy further resulted in the reduction of metal-induced oxidative stress and tight regulation of stress responsive hormones. These observations indicate the application of a consortium of endophytic bacteria and fungi-as a promising technique for ensuring plant growth and safer food consumption under metal-contaminated soil conditions. However, the comprehensive understanding of the mechanistic aspects of the interaction between endophytic bacteria and fungi for improving plant growth and adaptability to metal contamination requires an in-depth study at the proteomic and transcriptomic levels.

AUTHOR CONTRIBUTIONS

SB designed the experiments. RS and SB performed the experiments. S-MK, B-WY, QMI, and AK analyzed the data. AK, I-JL, and AA-H edited the manuscript.

FUNDING

This work was supported by Korea Institute of Planning and Evaluation for Technology in Food, Agriculture, Forestry and Fisheries (IPET) through Agriculture, Food and Rural Affairs Research Center Support Program, funded by Ministry of Agriculture, Food and Rural Affairs (MAFRA) (Grant No. 716001-7).

SUPPLEMENTARY MATERIAL

The Supplementary Material for this article can be found online at: https://www.frontiersin.org/articles/10.3389/fpls.2018.01273/full#supplementary-material

REFERENCES

Ali, A., Guo, D., Mahar, A., Ma, F., Li, R., Shen, F., et al. (2017). *Streptomyces pactum* assisted phytoremediation in Zn/Pb smelter contaminated soil of Feng County and its impact on enzymatic activities. *Sci. Rep.* 7:46087. doi: 10.1038/srep46087

Ali, A. H., Abdelrahman, M., Radwan, U., El-Zayat, S., and El-Sayed, M. A. (2018). Effect of thermomyces fungal endophyte isolated from extreme hot desert-adapted plant on heat stress tolerance of cucumber. *Appl. Soil Ecol.* 124, 155–162. doi: 10.1016/j.apsoil.2017.11.004

Asgher, M., Khan, M. I. R., Anjum, N. A., and Khan, N. A. (2015). Minimising toxicity of cadmium in plants—role of plant growth regulators. *Protoplasma* 252, 399–413. doi: 10.1007/s00709-014-0710-4

Bhattacharya, T., Chakraborty, S., and Banerjee, D. K. (2010). Heavy metal uptake and its effect on macronutrients, chlorophyll, protein, and peroxidase activity of *Paspalum distichum* grown on sludge-dosed soils. *Environ. Monit. Assess.* 169, 15–26. doi: 10.1007/s10661-009-1146-8

Bilal, S., Khan, A. L., Shahzad, R., Asaf, S., Kang, S.-M., and Lee, I.-J. (2017). Endophytic *Paecilomyces formosus* LHL10 Augments Glycine max L. adaptation to Ni-contamination through affecting endogenous phytohormones and oxidative stress. *Front. Plant Sci.* 8:870. doi: 10.3389/fpls.2017.00870

Burges, A., Epelde, L., and Garbisu, C. (2015). Impact of repeated single-metal and multi-metal pollution events on soil quality. *Chemosphere* 120, 8–15. doi: 10.1016/j.chemosphere.2014.05.037

Curaqueo, G., Schoebitz, M., Borie, F., Caravaca, F., and Roldán, A. (2014). Inoculation with arbuscular mycorrhizal fungi and addition of composted olive-mill waste enhance plant establishment and soil properties in the regeneration of a heavy metal-polluted environment. *Environ. Sci. Pollut. Res.* 21, 7403–7412. doi: 10.1007/s11356-014-2696-z

Das, K., and Roychoudhury, A. (2014). Reactive oxygen species (ROS) and response of antioxidants as ROS-scavengers during environmental stress in plants. *Front. Environ. Sci.* 2:53. doi: 10.3389/fenvs.2014.00053

Deng, Z., and Cao, L. (2017). Fungal endophytes and their interactions with plants in phytoremediation: a review. *Chemosphere* 168, 1100–1106. doi: 10.1016/j.chemosphere.2016.10.097

Emamverdian, A., Ding, Y., Mokhberdoran, F., and Xie, Y. (2015). Heavy metal stress and some mechanisms of plant defense response. *Sci. World J.* 2015:756120. doi: 10.1155/2015/756120

Etesami, H. (2018). Bacterial mediated alleviation of heavy metal stress and decreased accumulation of metals in plant tissues: mechanisms and future prospects. *Ecotoxicol. Environ. Saf.* 147, 175–191. doi: 10.1016/j.ecoenv.2017.08.032

Fernández-Fuego, D., Keunen, E., Cuypers, A., Bertrand, A., and González, A. (2017). Mycorrhization protects *Betula pubescens* Ehr. from metal-induced oxidative stress increasing its tolerance to grow in an industrial polluted soil. *J. Hazard. Mater.* 336, 119–127. doi: 10.1016/j.jhazmat.2017.04.065

Gao, M., Liu, Y., Ma, X., Shuai, Q., Gai, J., and Li, Y. (2017). Evaluation of reference genes for normalization of gene expression using quantitative rt-pcr under aluminum, cadmium, and heat stresses in soybean. *PLoS One* 12:e0168965. doi: 10.1371/journal.pone.0168965

Hamayun, M., Hussain, A., Khan, S. A., Kim, H.-Y., Khan, A. L., Waqas, M., et al. (2017). Gibberellins producing endophytic fungus *Porostereum spadiceum* AGH786 rescues growth of salt affected soybean. *Front. Microbiol.* 8:686. doi: 10.3389/fmicb.2017.00686

Hardoim, P. R., Van Overbeek, L. S., Berg, G., Pirttilä, A. M., Compant, S., Campisano, A., et al. (2015). The hidden world within plants: ecological and evolutionary considerations for defining functioning of microbial endophytes. *Microbiol. Mol. Biol. Rev.* 79, 293–320. doi: 10.1128/MMBR.00050-14

Hou, N., You, J., Pang, J., Xu, M., Chen, G., and Yang, Z. (2010). The accumulation and transport of abscisic acid insoybean (Glycine max L.) under aluminum stress. *Plant soil* 330, 127–137. doi: 10.1007/s11104-009-0184-x

Huang, S.-C., Chu, S.-J., Guo, Y.-M., Ji, Y.-J., Hu, D.-Q., Cheng, J., et al. (2017). Novel mechanisms for organic acid-mediated aluminium tolerance in roots and leaves of two contrasting soybean genotypes. *AoB Plants* 9:plx064. doi: 10.1093/aobpla/plx064

Ibiang, Y. B., Mitsumoto, H., and Sakamoto, K. (2017). *Bradyrhizobia* and arbuscular mycorrhizal fungi modulate manganese, iron, phosphorus, and polyphenols in soybean (Glycine max (L.) Merr.) under excess zinc. *Environ. Exp. Bot.* 137, 1–13. doi: 10.1016/j.envexpbot.2017.01.011

Imran, Q. M., Hussain, A., Mun, B.-G., Lee, S. U., Asaf, S., Ali, M. A., et al. (2018). Transcriptome wide identification and characterization of NO-responsive WRKY transcription factors in *Arabidopsis thaliana* L. *Environ. Exp. Bot.* 148, 128–143. doi: 10.1016/j.envexpbot.2018.01.010

Islam, F., Yasmeen, T., Ali, Q., Mubin, M., Ali, S., Arif, M. S., et al. (2016). Copper-resistant bacteria reduces oxidative stress and uptake of copper in lentil plants: potential for bacterial bioremediation. *Environ. Sci. Pollut. Res.* 23, 220–233. doi: 10.1007/s11356-015-5354-1

Jalmi, S. K., Bhagat, P. K., Verma, D., Noryang, S., Tayyeba, S., Singh, K., et al. (2018). Traversing the links between heavy metal stress and plant signaling. *Front. Plant Sci.* 9:12. doi: 10.3389/fpls.2018.00012

Jia, X., Zhao, Y., Wang, W., and He, Y. (2015). Elevated temperature altered photosynthetic products in wheat seedlings and organic compounds and biological activity in rhizopshere soil under cadmium stress. *Sci. Rep.* 5:14426. doi: 10.1038/srep14426

Kar, R. K. (2011). Plant responses to water stress: role of reactive oxygen species. *Plant Signal. Behav.* 6, 1741–1745. doi: 10.4161/psb.6.11.17729

Khan, A., Khan, S., Khan, M. A., Qamar, Z., and Waqas, M. (2015). The uptake and bioaccumulation of heavy metals by food plants, their effects on plants nutrients, and associated health risk: a review. *Environ. Sci. Pollut. Res.* 22, 13772–13799. doi: 10.1007/s11356-015-4881-0

Khan, A. L., Al-Harrasi, A., Al-Rawahi, A., Al-Farsi, Z., Al-Mamari, A., Waqas, M., et al. (2016). Endophytic fungi from frankincense tree improves host growth and produces extracellular enzymes and indole acetic acid. *PLoS One* 11:e0158207. doi: 10.1371/journal.pone.0158207

Khan, A. L., Hamayun, M., Kang, S.-M., Kim, Y.-H., Jung, H.-Y., Lee, J.-H., et al. (2012). Endophytic fungal association via gibberellins and indole acetic acid can improve plant growth under abiotic stress: an example of Paecilomyces formosus LHL10. *BMC Microbiol.* 12:3. doi: 10.1186/1471-2180-12-3

Khan, A. L., Waqas, M., Kang, S.-M., Al-Harrasi, A., Hussain, J., Al-Rawahi, A., et al. (2014). Bacterial endophyte *Sphingomonas* sp. LK11 produces gibberellins and IAA and promotes tomato plant growth. *J. Microbiol.* 52, 689–695. doi: 10.1007/s12275-014-4002-7

Kim, Y.-H., Hwang, S.-J., Waqas, M., Khan, A. L., Lee, J.-H., Lee, J.-D., et al. (2015). Comparative analysis of endogenous hormones level in two soybean (Glycine max L.) lines differing in waterlogging tolerance. *Front. Plant Sci.* 6:714. doi: 10.3389/fpls.2015.00714

Kong, Z., and Glick, B. R. (2017). *The Role of Plant Growth-Promoting Bacteria in Metal Phytoremediation*, 1st Edn. New York, NY: Elsevier Ltd. doi: 10.1016/bs.ampbs.2017.04.001

Kopittke, P. M. (2016). Role of phytohormones in aluminium rhizotoxicity. *Plant Cell Environ.* 39, 2319–2328. doi: 10.1111/pce.12786

Lang-Mladek, C., Xie, L., Nigam, N., Chumak, N., Binkert, M., Neubert, S., et al. (2012). UV-B signaling pathways and fluence rate dependent transcriptional regulation of ARIADNE12. *Physiol. Plant* 145, 527–539. doi: 10.1111/j.1399-3054.2011.01561.x

Leitão, A. L., and Enguita, F. J. (2016). Gibberellins in *Penicillium* strains: challenges for endophyte-plant host interactions under salinity stress. *Microbiol. Res.* 183, 8–18. doi: 10.1016/j.micres.2015.11.004

Li, X., Cen, H., Peng, L., Li, Y., Sun, L., Cai, S., et al. (2015). Tolerance performance of the cool-season turfgrass species *Festuca ovina, Lolium perenne, Agrostis tenuis*, and *Poa trivialis* to sulfur dioxide stress. *J. Plant Interact.* 10, 75–86. doi: 10.1080/17429145.2015.1019984

Liu, R., Dai, M., Wu, X., Li, M., and Liu, X. (2012). Suppression of the root-knot nematode [Meloidogyne incognita (Kofoid & White) Chitwood] on tomato by dual inoculation with arbuscular mycorrhizal fungi and plant growth-promoting rhizobacteria. *Mycorrhiza* 22, 289–296. doi: 10.1007/s00572-011-0397-8

Ma, S. C., Zhang, H. B., Ma, S. T., Wang, R., Wang, G. X., Shao, Y., et al. (2015). Effects of mine wastewater irrigation on activities of soil enzymes and physiological properties, heavy metal uptake and grain yield in winter wheat. *Ecotoxicol. Environ. Saf.* 113, 483–490. doi: 10.1016/j.ecoenv.2014.12.031

Ma, Y., Rajkumar, M., Luo, Y., and Freitas, H. (2011). Inoculation of endophytic bacteria on host and non-host plants—effects on plant growth and Ni uptake. *J. Hazard. Mater.* 195, 230–237. doi: 10.1016/j.jhazmat.2011.08.034

Ma, Y., Rajkumar, M., Moreno, A., Zhang, C., and Freitas, H. (2017). Serpentine endophytic bacterium *Pseudomonas azotoformans* ASS1 accelerates phytoremediation of soil metals under drought stress. *Chemosphere* 185, 75–85. doi: 10.1016/j.chemosphere.2017.06.135

Ma, Y., Rajkumar, M., Zhang, C., and Freitas, H. (2016a). Beneficial role of bacterial endophytes in heavy metal phytoremediation. *J. Environ. Manage.* 174, 14–25. doi: 10.1016/j.jenvman.2016.02.047

Ma, Y., Rajkumar, M., Zhang, C., and Freitas, H. (2016b). Inoculation of *Brassica oxyrrhina* with plant growth promoting bacteria for the improvement of heavy metal phytoremediation under drought conditions. *J. Hazard. Mater.* 320, 36–44. doi: 10.1016/j.jhazmat.2016.08.009

Martin, F. M., Uroz, S., and Barker, D. G. (2017). Ancestral alliances: plant mutualistic symbioses with fungi and bacteria. *Science* 356:eaad4501. doi: 10.1126/science.aad4501

Mishra, V., Gupta, A., Kaur, P., Singh, S., Singh, N., Gehlot, P., et al. (2016). Synergistic effects of Arbuscular mycorrhizal fungi and plant growth promoting rhizobacteria in bioremediation of iron contaminated soils. *Int. J. Phytoremediation* 18, 697–703. doi: 10.1080/15226514.2015.1131231

Mnasri, M., Janoušková, M., Rydlová, J., Abdelly, C., and Ghnaya, T. (2017). Comparison of arbuscular mycorrhizal fungal effects on the heavy metal uptake of a host and a non-host plant species in contact with extraradical mycelial network. *Chemosphere* 171, 476–484. doi: 10.1016/j.chemosphere.2016.12.093

Parelho, C., Rodrigues, A. S., Barreto, M. C., Ferreira, N. G. C., and Garcia, P. (2016). Assessing microbial activities in metal contaminated agricultural volcanic soils - an integrative approach. *Ecotoxicol. Environ. Saf.* 129, 242–249. doi: 10.1016/j.ecoenv.2016.03.019

Per, T. S., Khan, M. I. R., Anjum, N. A., Masood, A., Hussain, S. J., and Khan, N. A. (2018). Jasmonates in plants under abiotic stresses: crosstalk with other phytohormones matters. *Environ. Exp. Bot.* 145, 104–120. doi: 10.1016/j.envexpbot.2017.11.004

Pinter, I. F., Salomon, M. V., Berli, F., Bottini, R., and Piccoli, P. (2017). Characterization of the As (III) tolerance conferred by plant growth promoting rhizobacteria to in vitro-grown grapevine. *Appl. Soil Ecol.* 109, 60–68. doi: 10.1016/j.apsoil.2016.10.003

Qi, Q., Rose, P. A., Abrams, G. D., Taylor, D. C., Abrams, S. R., and Cutler, A. J. (1998). (+)-Abscisic acid metabolism, 3-ketoacyl-coenzyme a synthase gene expression, and very-long-chain monounsaturated fatty acid biosynthesis in *Brassica napus* embryos. *Plant Physiol.* 117, 979–987. doi: 10.1104/pp.117.3.979

Qin, S., Feng, W.-W., Wang, T.-T., Ding, P., Xing, K., and Jiang, J.-H. (2017). Plant growth-promoting effect and genomic analysis of the beneficial endophyte *Streptomyces* sp. KLBMP 5084 isolated from halophyte *Limonium sinense*. *Plant Soil* 416, 117–132. doi: 10.1007/s11104-017-3192-2

Rajkumar, M., Sandhya, S., Prasad, M. N. V., and Freitas, H. (2012). Perspectives of plant-associated microbes in heavy metal phytoremediation. *Biotechnol. Adv.* 30, 1562–1574. doi: 10.1016/j.biotechadv.2012.04.011

Rozpądek, P., Domka, A., and Turnau, K. (2017). "Mycorrhizal fungi and accompanying microorganisms in improving phytoremediation techniques," in *The Fungal Community: its Organization and Role in the Ecosystem*, 4th Edn, ed. J. F. White (Boca Raton, FL: CRC Press).

Saby, N. P. A., Swiderski, C., Lemercier, B., Walter, C., Louis, B. P., Eveillard, P., et al. (2017). Is pH increasing in the noncalcareous topsoils of France under agricultural management? A statistical framework to overcome the limitations of a soil test database. *Soil Use Manag.* 33, 460–470. doi: 10.1111/sum.12369

Shahabivand, S., Parvaneh, A., and Aliloo, A. A. (2017). Root endophytic fungus *Piriformospora indica* affected growth, cadmium partitioning and chlorophyll fluorescence of sunflower under cadmium toxicity. *Ecotoxicol. Environ. Saf.* 145, 496–502. doi: 10.1016/j.ecoenv.2017.07.064

Shahzad, R., Khan, A. L., Bilal, S., Waqas, M., Kang, S. M., and Lee, I. J. (2017). Inoculation of abscisic acid-producing endophytic bacteria enhances salinity stress tolerance in *Oryza sativa*. *Environ. Exp. Bot.* 136, 68–77. doi: 10.1016/j.envexpbot.2017.01.010

Sharma, P., Jha, A. B., Dubey, R. S., and Pessarakli, M. (2012). Reactive oxygen species, oxidative damage, and antioxidative defense mechanism in plants under stressful conditions. *J. Bot.* 2012, 1–26. doi: 10.1155/2012/217037

Shi, W., Li, H., Liu, T., Polle, A., Peng, C., and Luo, Z. (2015). Exogenous abscisic acid alleviates zinc uptake and accumulation in *Populus* × *canescens* exposed to excess zinc. *Plant Cell Environ.* 38, 207–223. doi: 10.1111/pce.12434

Singh, S., Parihar, P., Singh, R., Singh, V. P., and Prasad, S. M. (2016). Heavy metal tolerance in plants: role of transcriptomics, proteomics, metabolomics, and ionomics. *Front. Plant Sci.* 6:1143. doi: 10.3389/fpls.2015.01143

Sirhindi, G., Mir, M. A., Abd-Allah, E. F., Ahmad, P., and Gucel, S. (2016). Jasmonic acid modulates the physio-biochemical attributes, antioxidant enzyme activity, and gene expression in Glycine max under nickel toxicity. *Front. Plant Sci.* 7:591. doi: 10.3389/fpls.2016.00591

Velivelli, S. L. S., Sessitsch, A., and Prestwich, B. D. (2014). The role of microbial inoculants in integrated crop management systems. *Potato Res.* 57, 291–309. doi: 10.1007/s11540-014-9278-9

Wallenstein, M. D., and Weintraub, M. N. (2008). Emerging tools for measuring and modeling the in situ activity of soil extracellular enzymes. *Soil Biol. Biochem.* 40, 2098–2106. doi: 10.1016/j.soilbio.2008.01.024

Wang, F. Y., Lin, X. G., Yin, R., and Wu, L. H. (2006). Effects of arbuscular mycorrhizal inoculation on the growth of *Elsholtzia splendens* and Zea mays and the activities of phosphatase and urease in a multi-metal-contaminated soil under unsterilized conditions. *Appl. Soil Ecol.* 31, 110–119. doi: 10.1016/j.apsoil.2005.03.002

Wani, S. H., Kumar, V., Shriram, V., and Sah, S. K. (2016). Phytohormones and their metabolic engineering for abiotic stress tolerance in crop plants. *Crop J.* 4, 162–176. doi: 10.1016/j.cj.2016.01.010

Waqas, M., Khan, A. L., Kang, S. M., Kim, Y. H., and Lee, I. J. (2014). Phytohormone-producing fungal endophytes and hardwood-derived biochar interact to ameliorate heavy metal stress in soybeans. *Biol. Fertil. Soils* 50, 1155–1167. doi: 10.1007/s00374-014-0937-4

Wężowicz, K., Rozpądek, P., and Turnau, K. (2017). Interactions of arbuscular mycorrhizal and endophytic fungi improve seedling survival and growth in post-mining waste. *Mycorrhiza* 27, 499–511. doi: 10.1007/s00572-017-0768-x

Xian, Y., Wang, M., and Chen, W. (2015). Quantitative assessment on soil enzyme activities of heavy metal contaminated soils with various soil properties. *Chemosphere* 139, 604–608. doi: 10.1016/j.chemosphere.2014.12.060

Xu, J. M., Fan, W., Jin, J. F., Lou, H. Q., Chen, W. W., Yang, J. L., et al. (2017). Transcriptome analysis of Al-induced genes in buckwheat (*Fagopyrum esculentum* Moench) root apex: new insight into Al toxicity and resistance mechanisms in an Al accumulating species. *Front. Plant Sci.* 8:1141. doi: 10.3389/fpls.2017.01141

Yamaji, K., Watanabe, Y., Masuya, H., Shigeto, A., Yui, H., and Haruma, T. (2016). Root fungal endophytes enhance heavy-metal stress tolerance of *Clethra barbinervis* growing naturally at mining sites via growth enhancement, promotion of nutrient uptake and decrease of heavy-metal concentration. *PLoS One* 11:e0169089. doi: 10.1371/journal.pone.0169089

Yihui, B. A. N., Zhouying, X. U., Yurong, Y., Zhang, H., Hui, C., and Ming, T. (2017). Effect of dark septate endophytic fungus *Gaeumannomyces cylindrosporus* on plant growth, photosynthesis and Pb tolerance of maize (Zea mays L.). *Pedosphere* 27, 283–292. doi: 10.1016/S1002-0160(17)60316-3

Zahoor, M., Irshad, M., Rahman, H., Qasim, M., Afridi, S. G., Qadir, M., et al. (2017). Alleviation of heavy metal toxicity and phytostimulation of *Brassica campestris* L. by endophytic *Mucor* sp. MHR-7. *Ecotoxicol. Environ. Saf.* 142, 139–149. doi: 10.1016/j.ecoenv.2017.04.005

Zhang, X., Wang, N., Chen, P., Gao, M., Liu, J., Wang, Y., et al. (2014). Overexpression of a soybean Ariadne-like ubiquitin ligase gene GmARI1 enhances aluminum tolerance in *Arabidopsis*. *PLoS One* 9:e111120. doi: 10.1371/journal.pone.0111120

Zhang, Y., Hu, J., Bai, J., Wang, J., Yin, R., Wang, J., et al. (2018). Arbuscular mycorrhizal fungi alleviate the heavy metal toxicity on sunflower (*Helianthus annuus* L.) plants cultivated on a heavily contaminated field soil at a WEEE-recycling site. *Sci. Total Environ.* 628, 282–290. doi: 10.1016/j.scitotenv.2018.01.331

Conflict of Interest Statement: The authors declare that the research was conducted in the absence of any commercial or financial relationships that could be construed as a potential conflict of interest.

frontiers in Microbiology

ORIGINAL RESEARCH
published: 27 November 2018
doi: 10.3389/fmicb.2018.02916

A Third Class: Functional Gibberellin Biosynthetic Operon in Beta-Proteobacteria

*Raimund Nagel[1], John E. Bieber[1,2], Mark G. Schmidt-Dannert[1], Ryan S. Nett[1] and Reuben J. Peters[1]**

[1] Roy J. Carver Department of Biochemistry, Biophysics, and Molecular Biology, Iowa State University, Ames, IA, United States, [2] Science Department, Newton Senior High School, Newton, IA, United States

The ability of plant-associated microbes to produce gibberellin A (GA) phytohormones was first described for the fungal rice pathogen *Gibberella fujikuroi* in the 1930s. Recently the capacity to produce GAs was shown for several bacteria, including symbiotic alpha-proteobacteria (α-rhizobia) and gamma-proteobacteria phytopathogens. All necessary enzymes for GA production are encoded by a conserved operon, which appears to have undergone horizontal transfer between and within these two phylogenetic classes of bacteria. Here the operon was shown to be present and functional in a third class, the beta-proteobacteria, where it is found in several symbionts (β-rhizobia). Conservation of function was examined by biochemical characterization of the enzymes encoded by the operon from *Paraburkholderia mimosarum* LMG 23256^T. Despite the in-frame gene fusion between the short-chain alcohol dehydrogenase/reductase and ferredoxin, the encoded enzymes exhibited the expected activity. Intriguingly, together these can only produce GA_9, the immediate precursor to the bioactive GA_4, as the cytochrome P450 (CYP115) that catalyzes the final hydroxylation reaction is missing, similar to most α-rhizobia. However, phylogenetic analysis indicates that the operon from β-rhizobia is more closely related to examples from gamma-proteobacteria, which almost invariably have CYP115 and, hence, can produce bioactive GA_4. This indicates not only that β-rhizobia acquired the operon by horizontal gene transfer from gamma-proteobacteria, rather than α-rhizobia, but also that they independently lost CYP115 in parallel to the α-rhizobia, further hinting at the possibility of detrimental effects for the production of bioactive GA_4 by these symbionts.

Keywords: symbiosis, gibberellin, rhizobia, legume (nodules), evolution

OPEN ACCESS

Edited by:
Eloise Foo,
University of Tasmania, Australia

Reviewed by:
Maria Jose Soto,
Spanish National Research Council (CSIC), Spain
Yuri A. Trotsenko,
Institute of Biochemistry and Physiology of Microorganisms (RAS), Russia

***Correspondence:**
Reuben J. Peters
rjpeters@iastate.edu

Specialty section:
This article was submitted to Plant Microbe Interactions, a section of the journal Frontiers in Microbiology

Received: *14 September 2018*
Accepted: *13 November 2018*
Published: *27 November 2018*

Citation:
Nagel R, Bieber JE, Schmidt-Dannert MG, Nett RS and Peters RJ (2018) A Third Class: Functional Gibberellin Biosynthetic Operon in Beta-Proteobacteria. Front. Microbiol. 9:2916. doi: 10.3389/fmicb.2018.02916

INTRODUCTION

Gibberellin A (GA) was first discovered in the eponymous fungal rice pathogen *Gibberella fujikuroi*, which eventually enabled identification of these diterpenoids in plants where they serve as hormones regulating growth and development (Hedden and Sponsel, 2015). As suggested from their production by *G. fujikuroi*, these phytohormones also affect plant-microbe interactions (De Bruyne et al., 2014). However, in bacteria GA production was first reported from nitrogen-fixing rhizobial symbionts rather than plant pathogens (Bottini et al., 2004).

More recently, bacterial GA biosynthesis has been elucidated (Morrone et al., 2009; Hershey et al., 2014; Lu et al., 2015; Tatsukami and Ueda, 2016; Nagel and Peters, 2017b; Nagel et al., 2017; Nett et al., 2017b), with all the necessary genes generally found in close association within a biosynthetic operon. This operon seems to only be found in plant-associated bacteria (Levy et al., 2017). However, beyond the symbiotic alpha-proteobacteria (α-rhizobia) where the operon was originally reported and characterized (Tully and Keister, 1993; Tully et al., 1998; Keister et al., 1999; Morrone et al., 2009; Hershey et al., 2014; Tatsukami and Ueda, 2016; Nett et al., 2017b), the operon also was found to be functionally present in a diverse group of plant pathogens from the gamma-proteobacteria class (Lu et al., 2015; Nagel and Peters, 2017b; Nagel et al., 2017). Indeed, there is greater phylogenetic diversity of the operon in these phytopathogens than rhizobia (Nagel and Peters, 2017b), suggesting that bacterial GA biosynthesis originally evolved in this distinct class of bacteria.

The GA biosynthetic operon typically contains genes encoding eight enzymes (**Figure 1**). First to be characterized were the pair of diterpene cyclases that produce *ent*-kaurene from the general diterpenoid precursor (*E,E,E*)-geranylgeranyl diphosphate (GGDP). This proceeds via sequential reactions, specifically through initial production of *ent*-copalyl diphosphate (*ent*-CDP) by a CDP synthase (CPS), followed by a subsequently acting *ent*-kaurene synthase (KS) (Morrone et al., 2009; Hershey et al., 2014; Lu et al., 2015). An isoprenyl diphosphate synthase (IDS) that produces GGDP from the common isoprenoid precursors isopentenyl diphosphate (IDP) and dimethylallyl diphosphate (DMADP) is also present (Hershey et al., 2014; Nagel and Peters, 2017b). In addition, there are typically at least three cytochromes P450 (CYPs), CYP112, CYP114 and CYP117, along with a ferredoxin (Fd) and short-chain alcohol dehydrogenase/reductase (SDR). The Fd is required for the ring-contraction reaction catalyzed by CYP114, which generates GA_{12}-aldehyde that is further oxidized to GA_{12} by the SDR (Nagel and Peters, 2017b; Nagel et al., 2017; Nett et al., 2017b). Beyond these common/core genes, many copies of the operon contain an isopentenyl diphosphate isomerase (IDI) that interconverts IDP and DMADP (presumably to optimize production of GGDP), and/or an additional CYP, specifically CYP115 (Nagel and Peters, 2017b; Nagel et al., 2017; Nett et al., 2017a). However, while the core operon enables biosynthesis of GA_9, this has not been shown to have classical hormonal activity, and CYP115 is required to catalyze a subsequent hydroxylation reaction to produce bioactive GA_4 (**Figure 1**).

Intriguingly, while all phytopathogens contain CYP115 in their operons, almost all α-rhizobia only have a non-functional fragment remaining, and of the less than 20% with the GA operon that also contain a full-length CYP115 gene, in every case but one it is not located in the operon (Nett et al., 2017a). Thus, most α-rhizobia can only produce the penultimate intermediate GA_9, as has been demonstrated for *Bradyrhizobium japonicum*, although given that the operon is only expressed in nodules and the inability to otherwise distinguish between plant and bacteria produced GAs, this required isolation of bacteroids from nodules and radio-isotope feeding studies (Mendez et al., 2014). By contrast, phytopathogens can produce the bioactive GA_4. This difference in final GA product presumably reflects their distinct relationships with plant hosts. While it has been noted that a symbiotic beta-proteobacteria (β-rhizobia) also contains the operon (Nagel and Peters, 2017b), this has not otherwise been investigated. The genome of *Paraburkholderia mimosarum* LMG 23256^T contains the core operon necessary for GA biosynthesis. This β-rhizobium was isolated from *Mimosa pigra* and shown to form indeterminate nodules with its host (Chen et al., 2005, 2006). Here the enzymes encoded by the operon from *P. mimosarum* LMG 23256^T were characterized and shown to be functionally conserved, with further phylogenetic analysis indicating not only independent acquisition of the operon from gamma-proteobacteria, but also loss of CYP115, which supports the hypothesis that direct production of bioactive GA_4 may have a deleterious effect in the symbiotic relationship between rhizobia and their leguminous host plants.

MATERIALS AND METHODS

To find copies of the operon from newly sequenced bacterial genomes, BLAST searches were carried out using individual genes from the most divergent copy of the operon, namely that previously characterized from *Erwinia tracheiphila* (Nagel and Peters, 2017b). The results for examples found outside of the α-rhizobia are summarized in **Supplementary Table S2** (along with that for the α-rhizobia used in the phylogenetic analyses reported here). Note that the bacterial genus *Burkholderia* was recently reclassified as *Paraburkholderia* (Sawana et al., 2014; Dobritsa and Samadpour, 2016).

P. mimosarum LMG 23256^T (Willems et al., 2014) was obtained from the German Collection of Microorganisms and Cell Cultures (LMG 23256^T = $DSM21841^T$). Genes from the *P. mimosarum* operon were cloned from genomic DNA with Q5 Hot Start High-Fidelity DNA polymerase (New England Biolabs) according to the product manual with 5 μl of the high-GC-content enhancer and gene specific primers (**Supplementary Table S1**). The IDS, KS, CPS, and CYP112 genes were cloned into pET100/D-TOPO (Invitrogen). CYP117 was cloned into pET101/D-TOPO (Invitrogen) including a stop codon to omit the C-terminal His-Tag of the vector. CYP114 was cloned in tandem with either the Fd-SDR fusion or only the Fd into pET100. For the later construct the amino acid sequence after position 86 was changed from ET to that of the Fd from *Paraburkholderia* sp. JPY251 with the sequence ADDEAT followed by a stop codon. The CPS also was obtained as a synthetic codon optimized gene (Invitrogen) and similarly cloned into pET100. Recombinant expression, protein purification and *in vitro* enzyme assays or recombinant feeding studies, as well as organic extraction and GC-MS analysis were performed as previously described (Nagel and Peters, 2017b). Briefly, all proteins were expressed in *E. coli* BL21(Star). Cells expressing *Pm*IDS were centrifuged to collect cells, which were homogenized in MOPSO buffer pH 7.2 with 10% glycerol and 10 mM $MgCl_2$. The cell lysate was incubated with 1 ml Ni-NTA Agarose (Qiagen) and *Pm*IDS was eluted with imidazole and 20 μg

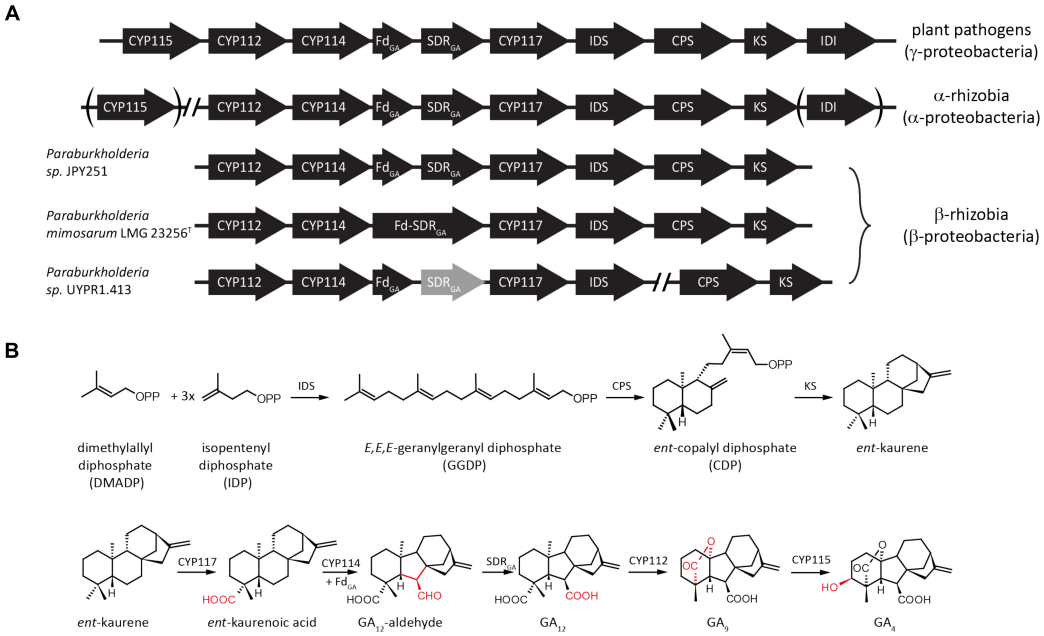

FIGURE 1 | Schematic representation of bacterial gibberellin biosynthetic operon and encoded metabolic pathway. **(A)** Arrows indicate the direction of translation; abbreviations for the genes are CYP, cytochrome P450; Fd, ferredoxin; SDR, short-chain alcohol dehydrogenase/reductase; IDS, isoprenyl diphosphate synthase; CPS, copalyl diphosphate synthase; KS, ent-kaurene synthase; and IDI, isopentenyl diphosphate isomerase. **(B)** Reactions in the pathway catalyzed by the various enzymes encoded by individual genes from the operon.

protein was used in 0.5 ml *in vitro* assays with 50 mM IDP and DMADP each (Sigma-Aldrich). Assays were dephosphorylated using alkaline phosphatase and extracted 3 times with equal volumes of pentane. *Pm*CPS and *Pm*KS were expressed in a 50 ml metabolic engineering setting – i.e., with an IDS from *Abies grandis* that produces GGDP and either *At*KS or *At*CPS, respectively, just as previously described for analysis of other bacterial CPSs and KSs (Morrone et al., 2009; Hershey et al., 2014; Lu et al., 2015) – for 3 days at 18°C together with pIRS, to increase flux to isoprenoids (Morrone et al., 2010). Note that neither CPS or KS alone in this setting produce *ent*-kaurene. *Pm*CYP117, *Pm*CYP114 + Fd, *Pm*CYP114 + Fd-SDR and *Pm*CYP112 were expressed alone and their respective substrates were added to the 25 ml culture and the culture was incubated at 18 °C for 3 days under shaking at 180 rpm. Cultures were extracted with 3 times with equal volumes of hexanes or ethyl acetate in case of *Pm*CYP114 + Fd, *Pm*CYP114 + Fd-SDR and *Pm*CYP112. Extracts were partially purified using silica gel columns developed with hexanes and eluted with increasing concentrations of ethyl acetate. Products of *Pm*CYP117, *Pm*CYP114 + Fd, *Pm*CYP114 + Fd-SDR and *Pm*CYP112 were methylated with diazomethane and quantified by GC-MS using a Varian GC-MS with a HP5-MS column (Agilent). The injector temperature was set at 250 °C with a helium column flow of 1.2 ml/min and 1 µl injections in split-less mode. The initial temperature of the GC oven was 50°C which was held for 3 min and increased by either 15°C/min for products of *Pm*IDS, PmCPS and PmKS or by 10°C/min for all other enzymes, until a temperature of 300 °C was reached, which was held for 3 min.

Phylogenetic analyses focused on a representative set of species and utilized nucleotide sequences spanning the core operon (i.e., from CYP112 to the KS, with CYP115 and IDI not included due to their absence in most rhizobia), including the intergenic regions. This was carried out with the nucleotide sequence of the operon, instead of the previously used concatenated protein sequences of the same region (Nagel and Peters, 2017b), as this allowed inclusion of operons with inactivating mutations (e.g., premature stop codons or frame shift mutations) as well as intergenic regions. Sequences were aligned using the Muscle algorithm in MEGA 7 (Kumar et al., 2016), and phylogenetic trees were then constructed and tested with the Maximum Likelihood Neighbor Joining and Minimum Evolution algorithms. The Tamura 3-parameter model was used with inclusion of a gamma distribution. For the Maximum Likelihood algorithm all sites were used, while for the Neighbor Joining and Minimum Evolution algorithms positions with less than 50% coverage were eliminated. The accuracy of the tree was tested via bootstrap testing with 1000 replicates each.

RESULTS

Beyond the core operon previously reported from *Paraburkholderia sp.* JPY251 (Nagel and Peters, 2017b), BLAST searches found two other copies in β-rhizobia. Another complete copy of the core operon was found in *P. mimosarum* LMG 23256^T, while an incomplete copy is present in *Paraburkholderia sp.* UYPR1.413, where the operon is split between two contigs,

with a transposable element found adjacent to the 3' end of the IDS, and the SDR contains inactivating frame-shift mutations (see **Figure 1A**). As previously reported for *Paraburkholderia sp.* JPY251 (Nagel and Peters, 2017b), CYP115 is not found in the operon, nor elsewhere in the genome, in *P. mimosarum* or *Paraburkholderia sp.* UYPR1.413.

To determine if the operon found in the beta-proteobacteria is fully functional – i.e., enables GA production – that from *P. mimosarum* was biochemically characterized by recombinant expression in *Escherichia coli* and examination of enzymatic activity. *Pm*IDS was assessed via *in vitro* assays, which readily demonstrated the expected production of GGDP from IDP and DMADP (**Figure 2** and **Supplementary Figure S1**). *Pm*CPS was not well-expressed in *E. coli* and no activity was observed with the purified protein *in vitro*. Activity was then assessed via a metabolic engineering approach, involving co-expression with *At*KS, the *ent*-CDP specific KS from *Arabidopsis thaliana*, along with a GGDP producing IDS from *Abies grandis* (*Ag*GGPS), as previously described (Morrone et al., 2009; Hershey et al., 2014; Lu et al., 2015). While the native gene for *Pm*CPS further did not exhibit activity in this setting either, use of a synthetic gene codon-optimized for expression in *E. coli* enabled the expected production of *ent*-kaurene (**Figure 2** and **Supplementary Figure S1**). *Pm*KS also was assessed via a metabolic engineering approach, via co-expression with *Ag*GGPS and *At*CPS, the *ent*-CDP producing CPS from *A. thaliana*, again as previously described (Morrone et al., 2009; Hershey et al., 2014; Lu et al., 2015). These cultures similarly produced the expected *ent*-kaurene (**Figure 2** and **Supplementary Figure S1**).

The remaining oxidative enzymes were investigated by whole-cell feeding studies. Accordingly, *ent*-kaurene was added to *E. coli* expressing *Pm*CYP117, leading to the expected conversion to *ent*-kaurenoic acid, with the intermediates *ent*-kaurenol and *ent*-kaurenal not observed (**Figure 3** and **Supplementary Figure S1**), consistent with the previously investigated mechanism for this reaction (Nagel and Peters, 2017a). Notably, in *P. mimosarum* the genes for the Fd and SDR are fused (in-frame). Given the previously reported requirement for the Fd to enable full activity with CYP114 (Nagel and Peters, 2017b; Nagel et al., 2017; Nett et al., 2017b), two constructs were generated to evaluate the implications of this fusion for activity. First, *Pm*CYP114 was cloned into pET100 together with the fused *Pm*Fd-SDR, including the native intergenic region between CYP114 and the Fd-SDR fusion. The second construct consisted of *Pm*CYP114 and only *Pm*Fd, with introduction of a stop codon based on the sequence of the Fd in *Paraburkholderia sp.* JPY251 where the Fd and SDR are not fused. Both constructs were expressed in *E. coli* and *ent*-kaurenoic acid was added to the resulting cultures. Cultures expressing *Pm*CYP114 + *Pm*Fd (i.e., without the SDR) produced a mixture of GA_{12}-aldehyde and GA_{12}, while the *Pm*CYP114 + *Pm*Fd-SDR construct exclusively produced GA_{12}, with the putative intermediate *ent*-7α-hydroxykaurenoic acid not observed in either case (**Figure 4** and **Supplementary Figure S1**), consistent with previous mechanistic investigation of this reaction (Nett et al., 2016). This demonstrated the ability of

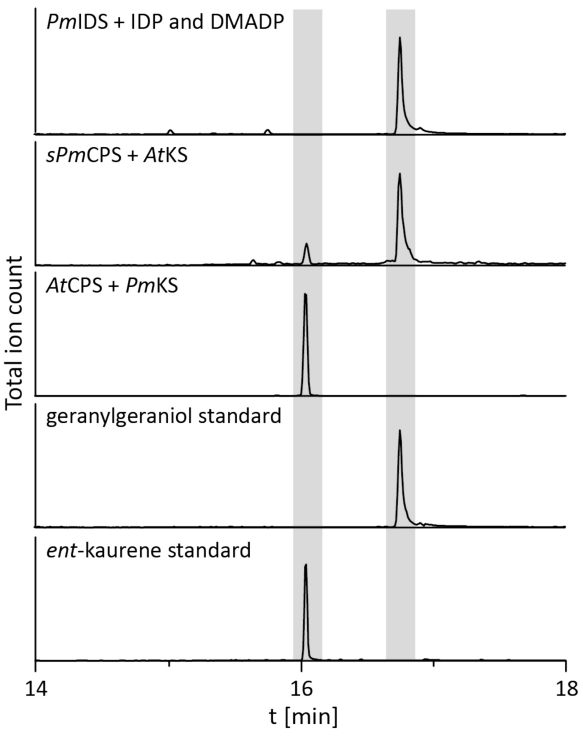

FIGURE 2 | IDS, CPS, and KS enzyme activity. GC-MS chromatogram from an *in vitro* enzyme assay of *Pm*IDS with dimethyl allyl diphosphate (DMADP) and isopentenyl diphosphate (IDP) as substrates, with subsequent dephosphorylation with alkaline calf intestine phosphatase. GC-MS chromatograms of organic extracts from *E. coli* cultures expressing *Pm*KS or synthetic *sPm*CPS along with either *At*CPS or *At*KS, with additional engineering for GGDP production. GC-MS chromatograms of geranylgeraniol (dephosphorylated GGDP) and *ent*-kaurene standards are included for reference.

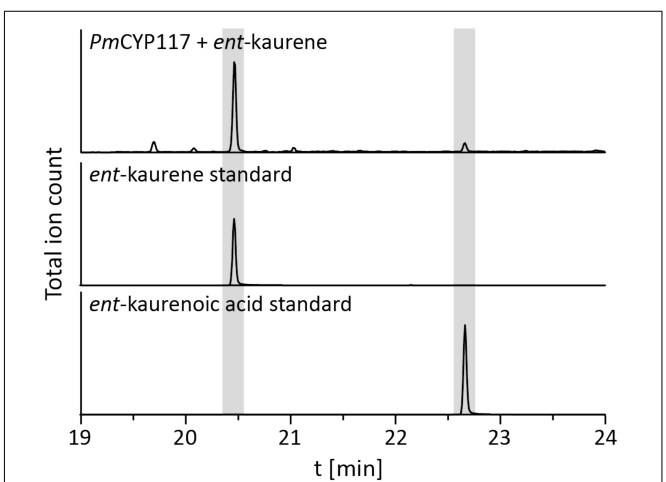

FIGURE 3 | CYP117 enzyme activity. GC-MS chromatogram of the organic extract of an *E. coli* culture expressing *Pm*CYP117 and fed *ent*-kaurene. GC-MS chromatograms of *ent*-kaurene and *ent*-kaurenoic acid standards are included for reference.

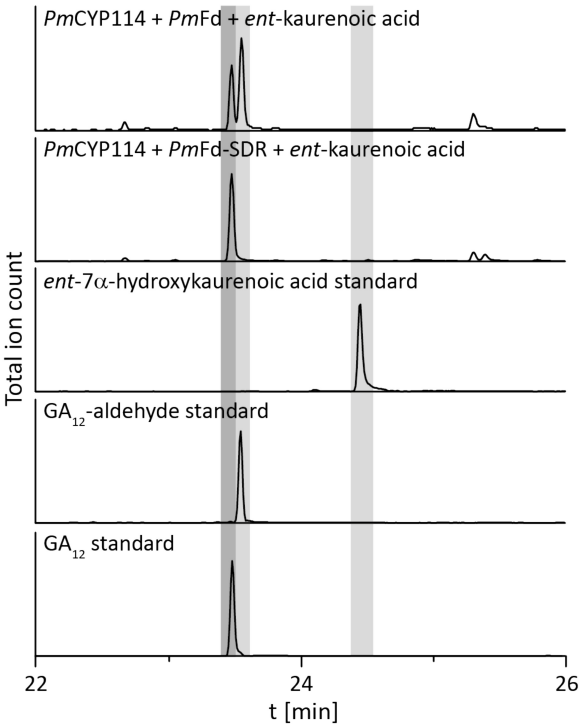

FIGURE 4 | CYP114+Fd and CYP114 + Fd-SDR enzyme activity. GC-MS chromatograms from organic extracts of *E. coli* cultures expressing *Pm*CYP114 either with the artificial *Pm*Fd or the *Pm*Fd-SDR fusion protein found in *P. mimosarum* and fed *ent*-kaurenoic acid. GC-MS chromatograms of *ent*-7a-hydroxykaurenoic acid, GA_{12}-aldehyde and GA_{12} standards are included for reference.

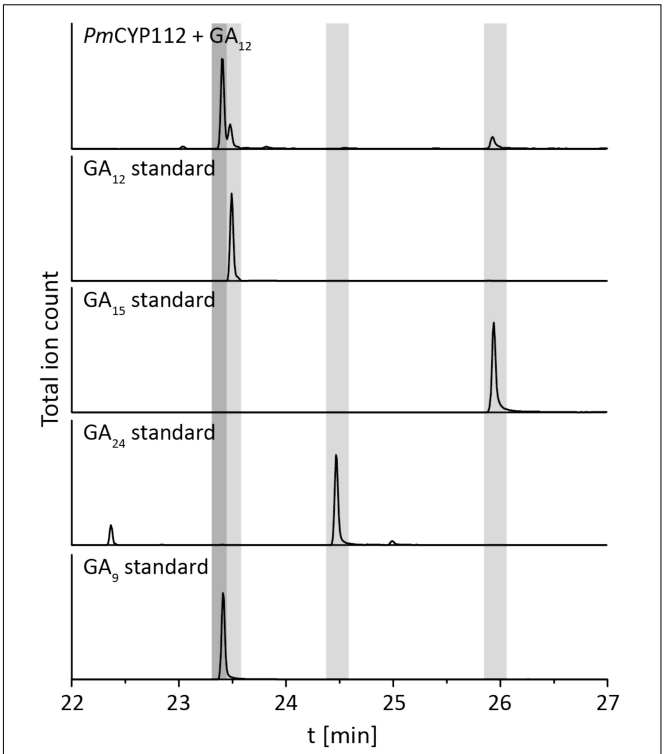

FIGURE 5 | CYP112 enzyme activity. GC-MS chromatograms from organic extract of an *E. coli* culture expressing *Pm*CYP112 and fed GA_{12}. Chromatograms of GA_{12}, GA_{15}, GA_{24}, and GA_9 standards are included for reference.

the Fd to enable full CYP114 activity as a fusion protein with the SDR, as well as the expected more efficient oxidation of GA_{12}-aldehyde to GA_{12} by the SDR. Finally, *E. coli* expressing *Pm*CYP112 and fed GA_{12} efficiently converted this to GA_9, with only small amounts of the intermediate GA_{15} observed and none of the intermediate GA_{24} or the side product GA_{25} (**Figure 5** and **Supplementary Figure S1**), again consistent with the previously investigated mechanism for this reaction (Nagel and Peters, 2018a,b).

Despite the lack of CYP115 in the GA biosynthetic operon from β-rhizobia, which nominally resembles the operons found in α-rhizobia, it has been suggested that β-rhizobia independently obtained the operon via horizontal gene transfer from gamma-proteobacteria (Nagel and Peters, 2017b). However, this hypothesis was proposed by phylogenetic analyses limited by the single examples then available – i.e., that from *Paraburkholderia* JPY251 and the most closely related copy from a gamma-proteobacteria, *Pseudomonas psychrotolerans* (*Ps. psychrotolerans*) NS274, which includes CYP115. Given that increased numbers of species with the operon are now available, including the multiple copies noted above for *Paraburkholderia* and additional strains of *Ps. psychrotolerans*, each of which contain CYP115 (**Supplementary Table S2**), this phylogenetic analysis was repeated here. The results are consistent with the hypothesis that the operon in β-rhizobia is most closely related to that from *Ps. psychrotolerans* (**Figure 6** and **Supplementary Figure S2**).

DISCUSSION

The biochemical results reported here demonstrate that the GA biosynthetic operon is functionally present in β-rhizobia, representing the third class of proteobacteria in which this operon can be found. However, the absence of CYP115 limits the β-rhizobia to production of the penultimate intermediate GA_9 rather than bioactive GA_4. While this nominally resembles previous findings in α-rhizobia, phylogenetic analysis strongly implies that the β-rhizobia independently obtained their copy of the operon from gamma-proteobacteria, as these are most closely related to the operon found in *Ps. psychrotolerans*, where CYP115 is invariably present. This further indicates that β-rhizobia also independently lost CYP115. In α-rhizobia with a full assembled genome the GA operon is invariably located within the symbiotic island or plasmid that also contains the necessary genes for nitrogen fixation (Perret et al., 1999; Gottfert et al., 2001; Sullivan et al., 2002; Gonzalez et al., 2003; Uchiumi et al., 2004; Nett et al., 2017a). However, it is unknown if the operon in beta-proteobacteria also is associated with the symbiotic island as the

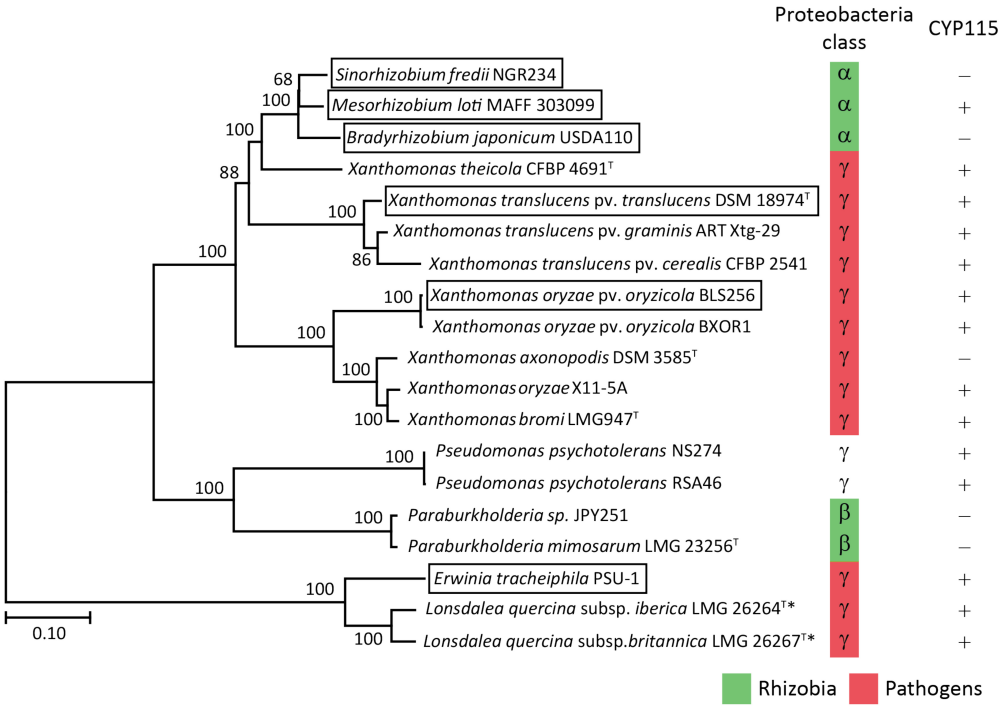

FIGURE 6 | Phylogeny of the GA biosynthetic operon. Unrooted Maximum Likelihood phylogenetic tree of the operon nucleotide sequence spanning CYP112 to KS including intergenic regions. Bootstrap values were determined with 1000 replicates using MEGA 7. The scale bar represents substitutions per site and the asterisk (*) indicates operons with inactivating mutations in at least one gene. The GA operon genes found within boxed species have been functionally characterized. The GeneBank accession numbers of the contig containing the operon for each of the presented bacteria can be found in **Supplementary Table S2**.

genome of all three species are not completely assembled and the contigs with the operon have few adjoining genes.

Beyond such implications for the origin of the operon in β-rhizobia, a number of other observations were derived from the bioinformatic analyses carried out here. For example, copies were found in *Lonsdalea quercina* subsp. *britanica* and *Lonsdalea quercina* subsp. *iberica*, which are close relatives of *Erwinia tracheiphila,* and are pathogens of oak trees (Brady et al., 2012). The *Lonsdalea* operons are also most closely related to that from *E. tracheiphila* (**Figure 6** and **Supplementary Figure S2**), which has already been shown to be fully functional (Nagel and Peters, 2017b). However, the operons from *Lonsdalea* all are disrupted by an inactivating frame-shift mutation in CYP112, with several exhibiting additional inactivating mutations in other genes (**Supplementary Table S2**), suggesting that these are no longer functional, presumably reflecting a loss of selective pressure for GA production in these phytopathogens.

In the *Xanthomonas* genus, consistent with a previous report (Nagel et al., 2017), the operon is selectively present in certain pathovars of *X. oryzae*, namely *Xanthomonas oryzae* pv. *oryzicola* (all 21 sequenced genomes), but not in the other major pathovar *Xanthomonas oryzae* pv. *oryzae*, where it is not found in any of the 380 genomes currently available. By contrast, the operon is widespread in *X. translucens*, where it is present in all 48 sequenced genomes, which cover a range of pathovars, although there appears to be a premature stop codon in CYP115 in 3 of the 5 sequenced strains from *Xanthomonas translucens* pv. *poae* (**Supplementary Table S2**). These form a distinct cluster within the relevant clade from *X. translucens* (Langlois et al., 2017), perhaps indicating some loss of selective pressure for production of bioactive GA_4 relative to the immediate precursor GA_9 in this group of non-cereal phytopathogens. Regardless, it seems clear that *X. translucens* acquired the operon early, with the selective advantage provided by the production of GA_4 leading to its widespread retention (i.e., vertical descent).

In addition, the operon was found in two new *Xanthomonas* species, *X. axonopodis* and *X. theicola*, although the operon in *X. axonopodis* appears to be missing CYP115 (**Supplementary Table S2**). While the division between the operons in *X. translucens* and *X. theicola* relative to *X. oryzae*, *X. bromi* and *X. axonopodis* reflects their broader phylogenic relationship (Merda et al., 2017), the numerous other species within the *Xanthomonas* genus that completely lack the operon indicate that these individually acquired the operon – i.e., via horizontal gene transfer. Consistent with this hypothesis, *X. translucens* and *X. theicola* represent a quite divergent group even within the broader *Xanthomondaceae* family (Naushad et al., 2015). Moreover, although *X. oryzae*, *X. bromi* and *X. axonopodis* all come from the same clade within this genus they do not otherwise group together (Merda et al., 2017), and the selective presence of the operon in *X. oryzae* pv. *oryzicola* versus *X. oryzae* pv. *oryzae*, as well as in *Xanthomonas axonopodis* DSM 3585 versus other strains of *X. axonopodis* (several of which have genome sequences available), suggests that even within this clade

the operon also may be acquired by horizontal gene transfer rather than vertical descent.

Interestingly, the operon from *X. theicola* is more closely related to those from α-rhizobia than even those from *X. translucens* (**Figure 6** and **Supplementary Figure S2**). Accordingly, while the absence of CYP115 in *X. axonopodis* nominally resembles the operon structure in α-rhizobia, this appears to represent an independent gene loss event. In particular, the presence of CYP115 in the much more closely related *X. theicola* operon supports the hypothesis that α-rhizobia originally acquired a full operon with subsequent early loss of CYP115, which contrasts with the complete gene loss observed in β-rhizobia, in that a non-functional fragment remains in almost all α-rhizobia. This further implies that direct production of bioactive GA_4 is generally selected against in the symbiotic relationship between these rhizobia and their leguminous hosts. However, at least one α-rhizobia GA biosynthetic operon retains CYP115 (i.e., in the same position as found in gamma-proteobacteria copies), and this appears to have undergone independent gene transfer into a subset of other α-rhizobia (Nett et al., 2017a), indicating that such direct hormone biosynthesis does provide a selective advantage for at least the α-rhizobia under certain circumstances.

In conclusion, the results reported here extend our understanding of the phylogenetic range for functional acquisition of the GA biosynthetic operon beyond those previously characterized from alpha- and gamma- into beta-proteobacteria as well. Moreover, the phylogenetic analysis not only supports the hypothesis that the operon arose in the gamma-proteobacteria, but also the previously advanced hypothesis that this was acquired by independent horizontal gene transfer by both α- and β-rhizobia (Nagel and Peters, 2017b), as well as suggesting more specific origins. Strikingly, this further supports independent loss of CYP115 in both classes of rhizobia, implying that direct production of bioactive GA_4 relative to the immediate precursor GA_9 generally (although not universally) has deleterious effects in such symbiotic relationships. While this has been suggested to stem from suppression of the host plant defense response against microbial pathogens (Nett et al., 2017a), the actual selective pressure against retention of CYP115 remains unclear, representing an avenue for future investigation.

AUTHOR CONTRIBUTIONS

RN and RP designed the research and wrote the manuscript. RSN, JB, and MS-D revised the manuscript. RN, JB, MS-D, and RSN performed the research and analyzed the data.

FUNDING

This work was supported by grants from the NIH (GM109773) and NSF (CHE-1609917) to RP, along with a postdoctoral fellowship to RN from the Deutsche Forschungsgemeinschaft (DFG) NA 1261/1-2.

SUPPLEMENTARY MATERIAL

The Supplementary Material for this article can be found online at: https://www.frontiersin.org/articles/10.3389/fmicb.2018.02916/full#supplementary-material

REFERENCES

Bottini, R., Cassan, F., and Piccoli, P. (2004). Gibberellin production by bacteria and its involvement in plant growth promotion and yield increase. *Appl. Microbiol. Biotechnol.* 65, 497–503. doi: 10.1007/s00253-004-1696-1

Brady, C. L., Cleenwerck, I., Denman, S., Venter, S. N., Rodríguez-Palenzuela, P., Coutinho, T. A., et al. (2012). Proposal to reclassify *Brenneria quercina* (Hildebrand and Schroth 1967) Hauben et al. 1999 into a new genus, *Lonsdalea* gen. nov., as *Lonsdalea quercina* comb. nov., descriptions of *Lonsdalea quercina* subsp. quercina comb. nov., *Lonsdalea quercina* subsp. *iberica* subsp. nov. and *Lonsdalea quercina* subsp. *britannica* subsp. nov., emendation of the description of the genus *Brenneria*, reclassification of *Dickeya dieffenbachiae* as *Dickeya dadantii* subsp. dieffenbachiae comb. nov., and emendation of the description of *Dickeya dadantii*. *Int. J. Syst. Evol. Microbiol.* 62, 1592–1602. doi: 10.1099/ijs.0.035055-0

Chen, W. M., James, E. K., Chou, J. H., Sheu, S. Y., Yang, S. Z., and Sprent, J. I. (2005). Beta-rhizobia from *Mimosa pigra*, a newly discovered invasive plant in Taiwan. *New Phytol.* 168, 661–675. doi: 10.1111/j.1469-8137.2005.01533.x

Chen, W. M., James, E. K., Coenye, T., Chou, J. H., Barrios, E., De Faria, S. M., et al. (2006). *Burkholderia mimosarum* sp. nov., isolated from root nodules of *Mimosa* spp. from Taiwan and South America. *Int. J. Syst. Evol. Microbiol.* 56, 1847–1851. doi: 10.1099/ijs.0.64325-0

De Bruyne, L., Hofte, M., and De Vleesschauwer, D. (2014). Connecting growth and defense: the emerging roles of brassinosteroids and gibberellins in plant innate immunity. *Mol. Plant* 7, 943–959. doi: 10.1093/mp/ssu050

Dobritsa, A. P., and Samadpour, M. (2016). Transfer of eleven species of the genus *Burkholderia* to the genus *Paraburkholderia* and proposal of *Caballeronia* gen. nov to accommodate twelve species of the genera *Burkholderia* and *Paraburkholderia*. *Int. J. Syst. Evol. Microbiol.* 66, 2836–2846. doi: 10.1099/ijsem.0.001065

Gonzalez, V., Bustos, P., Ramirez-Romero, M. A., Medrano-Soto, A., Salgado, H., Hernandez-Gonzalez, I., et al. (2003). The mosaic structure of the symbiotic plasmid of Rhizobium etli CFN42 and its relation to other symbiotic genome compartments. *Genome Biol.* 4:R36. doi: 10.1186/gb-2003-4-6-r36

Gottfert, M., Rothlisberger, S., Kundig, C., Beck, C., Marty, R., and Hennecke, H. (2001). Potential symbiosis-specific genes uncovered by sequencing a 410-kilobase DNA region of the *Bradyrhizobium japonicum* chromosome. *J. Bacteriol.* 183, 1405–1412. doi: 10.1128/JB.183.4.1405-1412.2001

Hedden, P., and Sponsel, V. (2015). A century of gibberellin research. *J. Plant Growth Regul.* 34, 740–760. doi: 10.1007/s00344-015-9546-1

Hershey, D. M., Lu, X., Zi, J., and Peters, R. J. (2014). Functional conservation of the capacity for ent-kaurene biosynthesis and an associated operon in certain rhizobia. *J. Bact.* 196, 100–106. doi: 10.1128/JB.01031-13

Keister, D. L., Tully, R. E., and Van Berkum, P. (1999). A cytochrome P450 gene cluster in the Rhizobiaceae. *J. Gen. Appl. Microbiol.* 45, 301–303. doi: 10.2323/jgam.45.301

Kumar, S., Stecher, G., and Tamura, K. (2016). MEGA7: molecular evolutionary genetics analysis version 7.0 for bigger datasets. *Mol. Biol. Evol.* 33, 1870–1874. doi: 10.1093/molbev/msw054

Langlois, P. A., Snelling, J., Hamilton, J. P., Bragard, C., Koebnik, R., Verdier, V., et al. (2017). Characterization of the *Xanthomonas translucens* complex using draft genomes, comparative genomics, phylogenetic analysis, and diagnostic lamp assays. *Phytopathology* 107, 519–527. doi: 10.1094/PHYTO-08-16-0286-R

Levy, A., Salas Gonzalez, I., Mittelviefhaus, M., Clingenpeel, S., Herrera Paredes, S., Miao, J., et al. (2017). Genomic features of bacterial adaptation to plants. *Nat. Genet.* 50, 138–150. doi: 10.1038/s41588-017-0012-9

Lu, X., Hershey, D. M., Wang, L., Bogdanove, A. J., and Peters, R. J. (2015). An ent-kaurene derived diterpenoid virulence factor from *Xanthomonas oryzae* pv. *oryzicola*. *New Phytol.*406, 295–302. doi: 10.1111/nph.13187

Mendez, C., Baginsky, C., Hedden, P., Gong, F., Caru, M., and Rojas, M. C. (2014). Gibberellin oxidase activities in *Bradyrhizobium japonicum* bacteroids. *Phytochemistry* 98, 101–109. doi: 10.1016/j.phytochem.2013.11.013

Merda, D., Briand, M., Bosis, E., Rousseau, C., Portier, P., Barret, M., et al. (2017). Ancestral acquisitions, gene flow and multiple evolutionary trajectories of the type three secretion system and effectors in Xanthomonas plant pathogens. *Mol. Ecol.* 26, 5939–5952. doi: 10.1111/mec.14343

Morrone, D., Chambers, J., Lowry, L., Kim, G., Anterola, A., Bender, K., et al. (2009). Gibberellin biosynthesis in bacteria: Separate ent-copalyl diphosphate and ent-kaurene synthases in *Bradyrhizobium japonicum*. *FEBS Lett.* 583, 475–480. doi: 10.1016/j.febslet.2008.12.052

Morrone, D., Lowry, L., Determan, M. K., Hershey, D. M., Xu, M., and Peters, R. J. (2010). Increasing diterpene yield with a modular metabolic engineering system in *E. coli*: comparison of MEV and MEP isoprenoid precursor pathway engineering. *Appl. Microbiol. Biotechnol.* 85, 1893–1906. doi: 10.1007/s00253-009-2219-x

Nagel, R., and Peters, R. J. (2017a). 18O2 labeling experiments illuminate the oxidation of ent-kaurene in bacterial gibberellin biosynthesis. *Org. Biomol. Chem.* 15, 7566–7571. doi: 10.1039/c7ob01819c

Nagel, R., and Peters, R. J. (2017b). Investigating the phylogenetic range of Gibberellin biosynthesis in bacteria. *Mol. Plant Microbe Interact.* 30, 343–349. doi: 10.1094/MPMI-01-17-0001-R

Nagel, R., and Peters, R. J. (2018a). Diverging mechanisms: cytochrome-P450-catalyzed demethylation and gamma-lactone formation in bacterial gibberellin biosynthesis. *Angew. Chem. Int. Ed. Engl.* 57, 6082–6085. doi: 10.1002/anie.201713403

Nagel, R., and Peters, R. J. (2018b). Probing the specificity of CYP112 in bacterial gibberellin biosynthesis. *Biochem. J.* 475, 2167–2177. doi: 10.1042/BCJ20180317

Nagel, R., Turrini, P. C. G., Nett, R. S., Leach, J. E., Verdier, V., Van Sluys, M. A., et al. (2017). An operon for production of bioactive gibberellin A4 phytohormone with wide distribution in the bacterial rice leaf streak pathogen *Xanthomonas oryzae* pv. *oryzicola*. *New Phytol.* 214, 1260–1266. doi: 10.1111/nph.14441

Naushad, S., Adeolu, M., Wong, S., Sohail, M., Schellhorn, H. E., and Gupta, R. S. (2015). A phylogenomic and molecular marker based taxonomic framework for the order *Xanthomonadales*: proposal to transfer the families *Algiphilaceae* and *Solimonadaceae* to the order *Nevskiales* ord. nov. and to create a new family within the order *Xanthomonadales,* the family *Rhodanobacteraceae* fam. nov., containing the genus *Rhodanobacter* and its closest relatives. *Antonie Van Leeuwenhoek* 107, 467–485. doi: 10.1007/s10482-014-0344-8

Nett, R. S., Contreras, T., and Peters, R. J. (2017a). Characterization of CYP115, a gibberellin 3-oxidase, demonstrates that certain rhizobia produce bioactive gibberellin A4. *ACS Chem. Biol.* 12, 912–917. doi: 10.1021/acschembio.6b01038

Nett, R. S., Montanares, M., Marcassa, A., Lu, X., Nagel, R., Charles, T. C., et al. (2017b). Elucidation of gibberellin biosynthesis in bacteria reveals convergent evolution. *Nat. Chem. Biol.* 13, 69–74. doi: 10.1038/nchembio.2232

Nett, R. S., Dickschat, J. S., and Peters, R. J. (2016). Labeling studies clarify the committed step in bacterial Gibberellin biosynthesis. *Org. Lett.* 18, 5974–5977. doi: 10.1021/acs.orglett.6b02569

Perret, X., Freiberg, C., Rosenthal, A., Broughton, W. J., and Fellay, R. (1999). High-resolution transcriptional analysis of the symbiotic plasmid of Rhizobium sp. NGR234. *Mol. Microbiol.* 32, 415–425. doi: 10.1046/j.1365-2958.1999.01361.x

Sawana, A., Adeolu, M., and Gupta, R. S. (2014). Molecular signatures and phylogenomic analysis of the genus *Burkholderia*: proposal for division of this genus into the emended genus *Burkholderia* containing pathogenic organisms and a new genus *Paraburkholderi*a gen. nov. harboring environmental species. *Front. Genet.* 5:429. doi: 10.3389/fgene.2014.00429

Sullivan, J. T., Trzebiatowski, J. R., Cruickshank, R. W., Gouzy, J., Brown, S. D., Elliot, R. M., et al. (2002). Comparative sequence analysis of the symbiosis island of *Mesorhizobium loti* strain R7A. *J. Bacteriol.* 184, 3086–3095. doi: 10.1128/JB.184.11.3086-3095.2002

Tatsukami, Y., and Ueda, M. (2016). Rhizobial gibberellin negatively regulates host nodule number. *Sci. Rep.* 6:27998. doi: 10.1038/srep27998

Tully, R. E., and Keister, D. L. (1993). Cloning and mutagenesis of a Cytochrome P-450 Locus from *Bradyrhizobium japonicum* that is expressed anaerobically and symbiotically. *Appl. Environ. Microbiol.* 59, 4136–4142.

Tully, R. E., Van Berkum, P., Lovins, K. W., and Keister, D. L. (1998). Identifcation and sequencing of a cytochrome P450 gene cluster from *Bradyrhizobium japonicum*. *Biochim. Biophys. Acta* 1398, 243–255. doi: 10.1016/S0167-4781(98)00069-4

Uchiumi, T., Ohwada, T., Itakura, M., Mitsui, H., Nukui, N., Dawadi, P., et al. (2004). Expression islands clustered on the symbiosis island of the *Mesorhizobium loti* genome. *J. Bacteriol.* 186, 2439–2448. doi: 10.1128/JB.186.8.2439-2448.2004

Willems, A., Tian, R., Bräu, L., Goodwin, L., Han, J., Liolios, K., et al. (2014). Genome sequence of Burkholderia mimosarum strain LMG 23256(T), a *Mimosa pigra* microsymbiont from Anso. *Taiwan. Standards in Genomic Sciences* 9, 484–494. doi: 10.4056/sigs.4848627

Conflict of Interest Statement: The authors declare that the research was conducted in the absence of any commercial or financial relationships that could be construed as a potential conflict of interest.

frontiers in Plant Science

REVIEW
published: 17 December 2018
doi: 10.3389/fpls.2018.01800

Unraveling the Initial Plant Hormone Signaling, Metabolic Mechanisms and Plant Defense Triggering the Endomycorrhizal Symbiosis Behavior

Alberico Bedini[1†], Louis Mercy[1†], Carolin Schneider[1], Philipp Franken[2,3] and Eva Lucic-Mercy[1]*

[1] INOQ GmbH, Schnega, Germany, [2] Department of Plant Physiology, Humboldt-Universität zu Berlin, Berlin, Germany, [3] Leibniz-Institut für Gemüse- und Zierpflanzenbau Großbeeren/Erfurt, Großbeeren, Germany

Arbuscular mycorrhizal (AM) fungi establish probably one of the oldest mutualistic relationships with the roots of most plants on earth. The wide distribution of these fungi in almost all soil ecotypes and the broad range of host plant species demonstrate their strong plasticity to cope with various environmental conditions. AM fungi elaborate fine-tuned molecular interactions with plants that determine their spread within root cortical tissues. Interactions with endomycorrhizal fungi can bring various benefits to plants, such as improved nutritional status, higher photosynthesis, protection against biotic and abiotic stresses based on regulation of many physiological processes which participate in promoting plant performances. In turn, host plants provide a specific habitat as physical support and a favorable metabolic frame, allowing uptake and assimilation of compounds required for the life cycle completion of these obligate biotrophic fungi. The search for formal and direct evidences of fungal energetic needs raised strong motivated projects since decades, but the impossibility to produce AM fungi under axenic conditions remains a deep enigma and still feeds numerous debates. Here, we review and discuss the initial favorable and non-favorable metabolic plant context that may fate the mycorrhizal behavior, with a focus on hormone interplays and their links with mitochondrial respiration, carbon partitioning and plant defense system, structured according to the action of phosphorus as a main limiting factor for mycorrhizal symbiosis. Then, we provide with models and discuss their significances to propose metabolic targets that could allow to develop innovations for the production and application of AM fungal inocula.

Keywords: carbon partitioning, mycorrhizal fungi, phosphorus, physiology, phytohormones, plant defense, plant priming, signaling

OPEN ACCESS

Edited by:
Eloise Foo,
University of Tasmania, Australia

Reviewed by:
Jose M. Garcia-Mina,
Universidad de Navarra, Spain
Erik Limpens,
Wageningen University & Research, Netherlands

***Correspondence:**
Eva Lucic-Mercy
lucic@inoq.de

† These authors have contributed equally to this work

Specialty section:
This article was submitted to Plant Microbe Interactions, a section of the journal Frontiers in Plant Science

Received: *31 August 2018*
Accepted: *19 November 2018*
Published: *17 December 2018*

Citation:
Bedini A, Mercy L, Schneider C, Franken P and Lucic-Mercy E (2018) Unraveling the Initial Plant Hormone Signaling, Metabolic Mechanisms and Plant Defense Triggering the Endomycorrhizal Symbiosis Behavior. Front. Plant Sci. 9:1800. doi: 10.3389/fpls.2018.01800

INTRODUCTION

Plant hormones, also called phytohormones, are organic compounds other than nutrients that are naturally produced by plant tissues in response to specific stimuli. They act spatially and temporally as endogenous signals able to organize all plant developmental stages (seed dormancy, seed germination, plant growth, flowering, etc.) by regulating at a very low dose various physiological functions. Plant hormones belong to the class of plant growth regulators,

which group both natural and synthetic compounds that can regulate plant development (Sajjad et al., 2017). In addition to developmental regulation, they also play important roles in abiotic and biotic stress responses and in mutualistic interactions between plants and other organisms. Each of the plant hormones or plant growth regulators possesses specific functions, but they interact with each other antagonistically or cooperatively by complex crosstalks.

One of the most ancient and widespread mutualistic association concerns the endomycorrhizal symbiosis, in which particular soil fungi, called arbuscular mycorrhizal (AM) fungi, colonize the root of most (74%) plant families on earth (van der Heijden et al., 2015). These fungi belong to the Glomeromycotina (among the phylum Mucoromycota), regrouping at least 313 characterized species[1]. They were extensively studied for more than 60 years, as it was shown that they are key components of soil fertility. Many examples suggest to exploit AM fungi for promoting plant performances (growth, survival, and tolerance) as they can enhance nutrition (water and minerals), photosynthesis, protection against biotic and abiotic stresses, regulation of developmental processes (flowering, fruit and seed formation, rooting, etc.) and take part in soil structuration (Smith and Read, 2008). However, the wider use of mycorrhizal *inocula* in agricultural fields remains challenging, due to their cost, variability in term of quality and responses on plants as well as incompatibility with high available phosphorus (P) levels in soils (Vosátka et al., 2008; Ijdo et al., 2011; Berruti et al., 2016).

Arbuscular mycorrhizal fungi are obligate biotrophs, the completion of their life cycle requires the absolute presence of host plants that provide a specific habitat (as a physical support and a favorable metabolic frame) allowing fungal uptake and assimilation of likely several energy sources (sugars, probably lipids and maybe other unknown compounds) (Pfeffer et al., 1999; Helber et al., 2011; Rich et al., 2017). This definition remains vague because a formal demonstration of AM fungi development and production under axenic conditions is still lacking, feeding numerous debates within the mycorrhizologist community but illustrating a gap of knowledge in plant and fungal physiology. Consequently, the biology of AM fungi is probably among the most complex and difficult field of research in plant science and clues obtained are mostly indirect due to the presence of the host plant. Nevertheless, it can be confidently stated that P concentration as well as plant hormones, as signals targeting numerous biochemical reactions and gene regulation, can finally generate or not a favorable root tissue environment, driving the completion of the AM life cycle. Therefore, most approaches that create a range of conditions concerning P and phytohormones can represent valuable tools for understanding the regulation of AM fungi development *in planta* or *in vitro*.

Negatively correlated responses between P concentration in soil and mycorrhizal phenotype and function are well investigated (Smith and Read, 2008). However, the comprehensive action of P through plant metabolism beyond hormonal interplays is still not well understood. In recent years, there have been more studies published about the AM fungi responses to hormones. Evidence has shown that AM fungi are sensitive to plant hormones (*in planta* but also *in vitro*, in presence or not of plant, respectively, monoxenic and axenic conditions) and that they are able to produce at least some of them (see section "Phytohormones Influence the Mycorrhizal Symbiosis"). However, phytohormones represent only part of the signaling in AM symbioses and their concret translations on plant metabolic pathways, especially those involved in energetic partitioning (glycolysis, fermentation, REDOX potentials, lipid metabolism, TCA or mitochondrial respiration), remain poorly discussed. To fill in the knowledge gap of the definition of favorable or non-favorable plant metabolic framework for AM fungi is a major step toward understanding fungal needs, and can then provide insights about the mode of action of some elements such as phosphorus, as well as clues to artificially promote mycorrhizal performances (root colonization and AM responses on plants).

The use of mutant plants or hormonal plant pretreatments (discussed in sections below) suggests that the AM behavior within roots is consequently driven by the metabolic interplay initially set in the plant. The aim of this review is to provide a detailed theoretical picture, based on available knowledge, connecting plant hormones, plant metabolic pathways involved in cell energy, plant defense and AM development and growth. The key point is to define the physiological basis of the plant susceptibility to mycorrhiza prior to inoculation with AM fungi or AM root contact.

The first section reviews the impact of 9 plant hormones, strigolactones (SL), abscisic acid (ABA), ethylene (ET), gibberellins (GA), salicylic acid (SA), jasmonate (JA), auxins (AUX), cytokinins (CK), and brassinosteroids (BR), on mycorrhizal behavior (root colonization, arbuscule formation and functionality). In the second section, we debate about the links between plant defense systems, compounds that induce a primed state (elicitors), plant hormone interplay, and AM fungal development. In the third section, we illustrate the impact of hormone interplay on plant energetic system [including photosynthesis, glycolysis, fermentation, lipid metabolism, tricarboxylic acid cycle (TCA), mitochondrial respiration, and REDOX potential]. As P represents a crucial criterion for the development and functionality of AM fungi, we describe here metabolic interplays under two hypothetic contrasting situations, low and high P, and we discuss whether the role of hormones and regulations within cells can be driven by P concentrations. Then, in a last section, we propose models that integrate signaling and plant energetic systems in mycorrhizal development, and strategies in which specific plant priming could be exploited as a tool to promote mycorrhizal performances (**Figure 1**).

PHYTOHORMONES INFLUENCE THE MYCORRHIZAL SYMBIOSIS

The knowledge of hormonal interplay in AM symbiosis is progressing for the past decade, but some phytohormones have been investigated more extensively than others. Up to now, SL and ET seem to be the most studied phytohormones,

[1]http://glomeromycota.wixsite.com/lbmicorrizas/copia-informacoes-gerais-lista

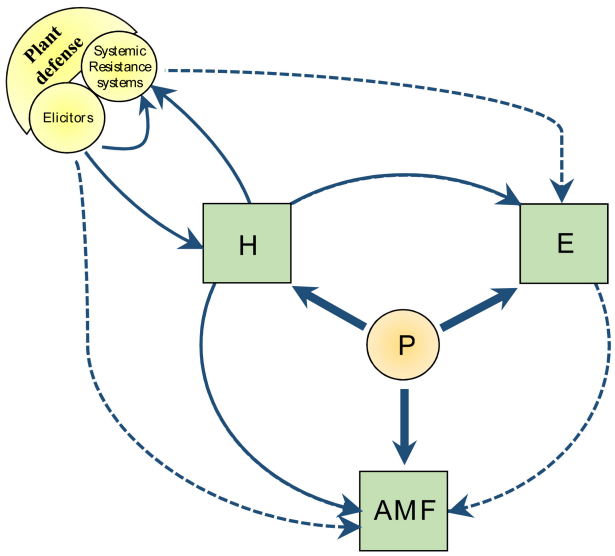

FIGURE 1 | Overview of the metabolic crosstalk directions discussed in this review. Solid lines indicate state of the art according to the bibliographic survey. Dashed lines indicate perspectives based on interpretation of the metabolic crosstalk. P, phosphorus; H, plant hormone; E, energetic system (carbon partitioning, respiration, and REDOX potential); AMF, arbuscular mycorrhizal fungi.

while SA and BR are the least investigated (**Figure 2A**). Overall most experiments use *ex vitro* (greenhouse/growth chambers) conditions (**Figure 2B**), and few trials were done in presence of various phosphorus concentrations (**Figure 2C**). Three main methodological approaches are classically used (**Figures 2D,E**): (i) exogenous application of hormones, (ii) use of mutant plants (deficient, overproducing, insensitive and hypersensitive), and (iii) application of hormone inhibitors. A list of a hundred references (non-exhaustive) surveyed for this review is available in a table (see **Supplementary Material**), in which we considered most AM fungal phenotypic parameters at different stages of the AM symbiosis development: (i) asymbiosis: propagule germination, but considering only AM spores and not mycorrhizal root fragments used as inoculum (studied in Gryndler et al., 1998), (ii) presymbiosis: hyphal growth and branching, and (iii) symbiotic stages: hyphopodium formation, root colonization, sporulation, arbuscule abundance and morphology (**Figure 2F**). The effects of phytohormones and their interplays on AM fungi and symbiosis were already described in several reviews (Foo et al., 2013a; Bucher et al., 2014; Fusconi, 2014; Gutjahr, 2014; Miransari et al., 2014; Pozo et al., 2015). Moreover, the regulation of the signaling between the symbionts and the molecular mechanisms beyond were detailed in a recent review (Liao et al., 2018). Therefore, we only briefly summarize actions of each hormone in the sub-sections below.

Abscisic Acid (ABA)

Abscisic acid is a stress phytohormone belonging to the class of sesquiterpenes. It regulates negatively plant growth and controls stomatal closure, limiting water loss by transpiration (Świątek et al., 2004; Cutler et al., 2010). ABA also plays a role in interactions with phytopathogens by modulating tissue invasion depending on type of microorganism, site and time of infection (Ton et al., 2009).

Abscisic acid can play a role in all phases of AM symbiosis: exogenous ABA application promotes root colonization and arbuscule formation during the early symbiotic stage, but is also able to maintain spore dormancy during the asymbiotic phase (Herrera-Medina et al., 2007; Martín-Rodríguez et al., 2010, 2011, 2016; Mercy et al., 2017). Effects of soil applications of ABA seem dose dependent: in *Medicago truncatula*, low ABA concentration (5×10^{-5} M) promotes AM fungi development, arbuscule branching and abundance, while higher concentration (5×10^{-4} M) reduces the level of colonization (Charpentier et al., 2014). *In vitro* plant pre-treatment with ABA (applied in the culture medium) resulted in higher root colonization and arbuscule abundance (Mercy et al., 2017), which indicates that ABA creates a favorable metabolic context before contact with and colonization by AM fungi.

Majority of studies on ABA were conducted by using deficient or insensitive mutant plants. ABA-deficient *sitiens* tomato mutant harbored a reduced mycorrhizal susceptibility, with lower percentage of vesicules, arbuscules and fungal alkaline phosphatase activity compared to the corresponding wild type (Herrera-Medina et al., 2007; Aroca et al., 2008; García-Garrido et al., 2010; Martín-Rodríguez et al., 2010, 2011, 2016; Fracetto et al., 2017). The arbuscules were also not completely formed and fewer branches were counted (Herrera-Medina et al., 2007; Fracetto et al., 2017). Another ABA-deficient tomato mutant (*notabilis*) was also used, but except for one study in which mycorrhizal development and arbuscule intensity was reduced (Xu et al., 2018), no particular response on mycorrhizal colonization was noticed (Zsögön et al., 2008; Martín-Rodríguez et al., 2010; Fracetto et al., 2017) probably because ABA levels in the roots remained similar to the wild type (Martín-Rodríguez et al., 2010). AM fungi are able to produce ABA (Esch et al., 1994), and it was shown that AM fungi can increase endogenous ABA content in plant during colonization (Ludwig-Müller, 2010).

Abscisic acid signaling establishes complex crosstalks with other phytohormones, especially ET, SA, GA, and SL. Higher ET levels were found in roots of the tomato mutant *sitiens* (Herrera-Medina et al., 2007). Several studies described a negative effect of ET on AM fungal colonization (see below), but ABA can act independently of ET (Herrera-Medina et al., 2007; Martín-Rodríguez et al., 2010), confirming a direct role of ABA in AM fungi development. Furthermore, ABA levels in plants are interconnected with GA that negatively regulate later stages of AM fungi development in roots (see GA sub-chapter below; Foo et al., 2013a; Martín-Rodríguez et al., 2016). ABA downregulates gene expression involved in GA biosynthesis and increases GA catabolism (Martín-Rodríguez et al., 2016), but also represses biosynthesis and metabolic responses to ET and SA (Vlot et al., 2009). It is well accepted that the antagonistic signaling between ABA and GA targets specifically DELLA proteins, which belong to the GRAS family of plant regulatory proteins. DELLA proteins act as transcriptional suppressors in GAs signaling (Harberd, 2003) and are destabilized by GA (Silverstone et al., 2001)

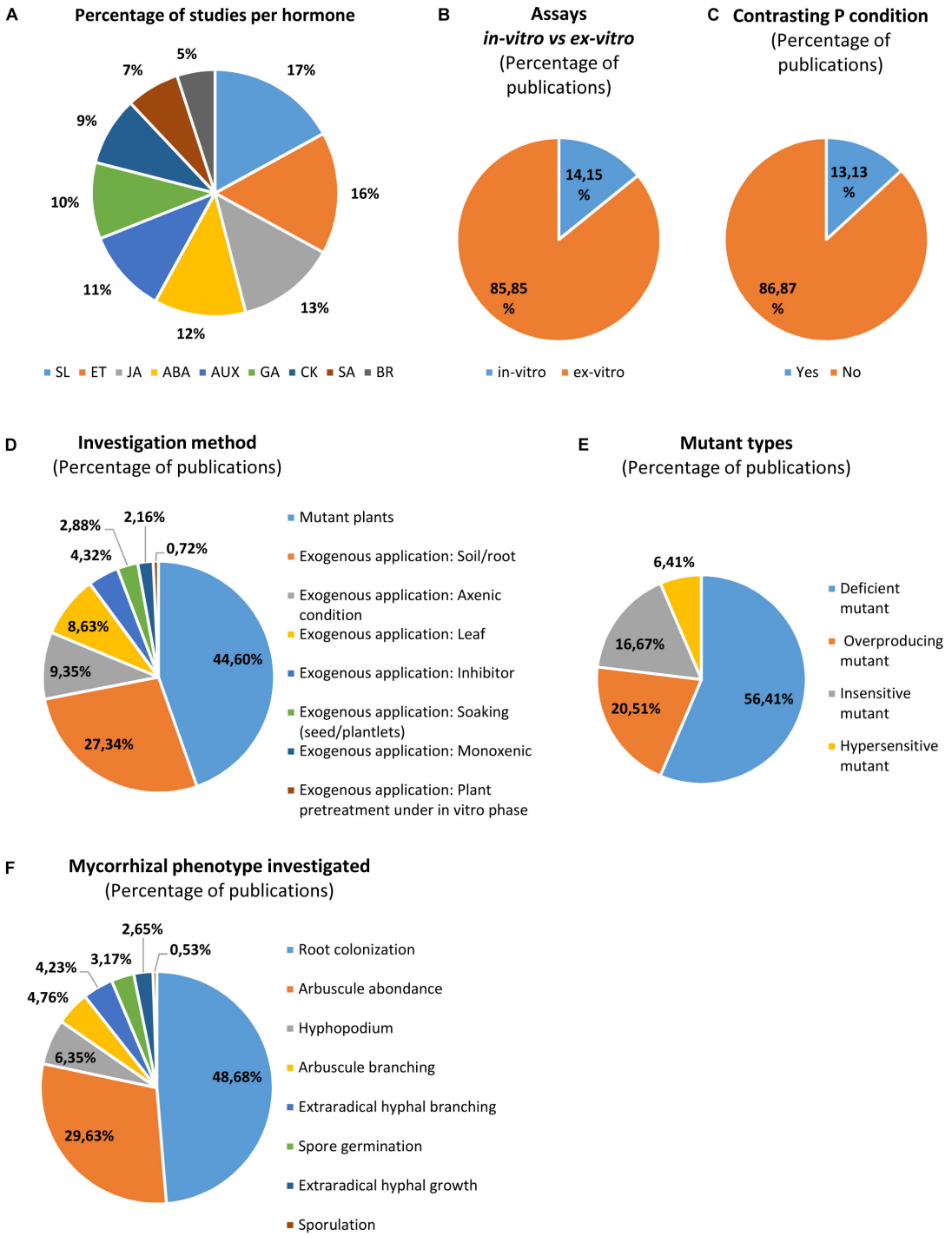

FIGURE 2 | Overview of the methodologies used and the fungal phenotypic parameters analyzed to investigate hormone response in endomycorrhizal symbiosis. The percentage of publication studying each hormone **(A)** indicates that SL and ET are likely the most studied while SA and BR are the least investigated. Most of assays were conducted *in planta* (in greenhouse or growth chambers), **(B)** but few works were conducted under contrasting P levels **(C)**. The use of mutant plants is the most common method, but pharmacological approaches were also done with hormones (mostly by application on soil/root, in presence of mycorrhizal propagules) and inhibitors **(D)**. Less studies were conducted under monoxenic conditions or by hormonal plant pretreatment (which allow to limit direct interaction between hormones and AM inoculum) **(D)**. Hormone deficient mutants are most often used while hypersensitive mutant plants are less exploited **(E)**. Then, several AM phenotypic parameters were investigated, mostly root colonization and arbuscule abundance, but less data are available regarding other structures, in particular spore germination, extraradical hyphal growth and sporulation **(F)**. ABA, abscisic acid; JA, jasmonate; GA, gibberellins; SA, salicylic acid; SL, strigolactones; ET, ethylene; CK, cytokinins; IAA, auxins; BR, brassinosteroids. Note that more than one phytohormone was studied in some publications, creating redundancies which were counted to calculate the percentages presented in the figures (see **Supplementary Material**).

while ABA maintains DELLA integrity (Silverstone et al., 2001; Achard et al., 2006). DELLA was demonstrated as a central node connecting various signaling pathways activated during AM formation and positively regulating arbuscule formation (Floss et al., 2013; Foo et al., 2013a; Yu et al., 2014; Pimprikar et al., 2016). ABA and SL biosynthesis and/or signaling are probably connected because root contents of both hormones were positively correlated when comparing wild type with ABA-deficient mutant plants (*sitiens*, *flacca,* and to a lesser extent *notabilis*, López-Ráez et al., 2010).

In summary, it is consensus that ABA plays an enhancing role in the AM symbiosis, but we noticed that all the trials were conducted under low P concentrations (less than 50 ppm P) and no report evaluated the response of AM fungi to ABA under higher P level. Moreover, no study was conducted in order to connect natural endogenous ABA levels and mycorrhizal susceptibility from various plant species and/or cultivars. It is therefore not clear, if a dose dependence of ABA responses exists.

Jasmonate (JA)

Jasmonate and its derivatives belong to a diverse class of lipid metabolites known as oxylipins (Wasternack, 2007; Mosblech et al., 2009) and are mainly involved in plant responses to biotic and abiotic stresses (Creelman and Mullet, 1997; Wasternack and Hause, 2002). JA is part of a signal transduction pathway activated by plant interaction with microorganisms (Pozo et al., 2004), leaf wounding (Schilmiller and Howe, 2005), and generally by abiotic stress conditions (Pedranzani et al., 2015). JA mediates higher transport rates of photosynthates to the roots (Babst et al., 2005; Schwachtje and Baldwin, 2008; Kaplan, 2012), and this might explain some of the positive effects on AM fungal colonization described below.

Exogenous application of JA has been shown to enhance AM fungal colonization (Regvar et al., 1996; Tejeda-Sartorius et al., 2008; Kiers et al., 2010; León-Morcillo et al., 2012) or to reduce it (Ludwig-Müller et al., 2002; Vierheilig, 2004; Herrera-Medina et al., 2008; Gutjahr et al., 2015). Repeated wounding or various abiotic stresses induce endogenous JA accumulation, and this was associated with higher AM fungal development (Landgraf et al., 2012; Pedranzani et al., 2015). Tests with various JA concentrations under contrasting P showed a strong dose dependence of the AM fungal response: mycorrhizal colonization is enhanced preferentially at 0.5 mM JA under high P (75 kg P Ha^{-1} $year^{-1}$) but decreased at 5 mM JA under low P (25 kg P Ha^{-1} $year^{-1}$; Kiers et al., 2010). However, no fungal phenotype response from P levels was obtained in JA-deficient rice line *cpm2* (Gutjahr et al., 2015). Presence of AM fungi was associated with up-regulation of oxylipins biosynthesis, and JA-deficient tomato lines *spr-2* and *def-1* showed reduced AM fungal colonization (Tejeda-Sartorius et al., 2008; León-Morcillo et al., 2012; Song et al., 2013, 2014, 2015). In particular, the genes encoding 9-lipoxygenases (9-LOXs) involved in JA biosynthesis seem to have a role in regulation of AM fungal development and in restriction of pathogen spreading (Blée, 2002; Vellosillo et al., 2007; Mosblech et al., 2009). A reduction of root colonization and arbuscule abundance of *Rhizoglomus irregulare* in *M. truncatula* was observed when a gene that encodes for allene oxidase cyclase (AOC), which is involved in JA biosynthesis, was suppressed by a root application of a *MtAOC1antisense* construct (Isayenkov et al., 2005). Repeating this experiment in *M. truncatula* with an *AOC1* RNAi and an overexpression construct did not show any impact on AM fungal colonization or on mycorrhiza-induced resistance (Hilou et al., 2014). Moreover, a JA-signaling perception mutant *jai-1* (jasmonic acid insensitive 1) was shown to be associated with higher AM fungal colonization and arbuscule formation (Herrera-Medina et al., 2008), but this response was not reproductible (Song et al., 2013).

Increased JA levels in roots of mycorrhizal plants were observed several times in different species (Vierheilig and Piché, 2002; Meixner et al., 2005; Stumpe et al., 2005; Hause et al., 2007). JA is also known to be linked with other phytohormones. It especially induces ABA biosynthesis, but ABA as well as SL are also required for JA production (Adie et al., 2007; Torres-Vera et al., 2014; de Ollas et al., 2015; de Ollas and Dodd, 2016; Haq et al., 2017). It is, moreover, well known that JA and SA are antagonists (see sections "Relationship Between Plant Defense Components and Mycorrhizal Symbiosis" and "Hormonal and Energetic Regulation of Plant Metabolism Under Contrasting P Conditions" below).

To conclude, JA effects are less clear but observations favor the hypothesis that JA is a promoting regulator of the AM symbiosis. Nevertheless, the contrasting data suggest that JA response is strongly sensitive to its endogenous concentrations, which can also modulate responses to exogenous JA application. Moreover, environmental factors (such as P) can interfere with JA perception, making interpretations quite delicate. This is well illustrated by the lack of mycorrhizal responses when JA is applied at low P, probably because endogenous JA levels are already high (Khan et al., 2016), but plant performance improvement can be observed at high P (Kiers et al., 2010). The effect of JA on AM fungi has not been studied *in vitro,* and if AM fungi are able to produce this phytohormone remains to be investigated.

Auxin (AUX)

Auxins are mainly formed from tryptophan and indole-3-acetic acid (IAA) is the most abundant auxin. AUX regulate various aspects of plant growth and development, such as phototropism, geotropism and cell elongation and polarity (Benková et al., 2003). IAA regulates the development of lateral and secondary roots, which represent the preferential sites for AM fungal colonization (Kaldorf and Ludwig-Müller, 2000; Yao et al., 2005).

Observation *in planta* indicated that applications of various auxins (IAA, indole-3-butyric acid, 2,4-dichlorophenoxyacetic acid and 1-naphthaleneacetic acid) are able to promote AM fungal spread and arbuscule abundance (Dutra et al., 1996; Niranjan et al., 2007; Etemadi et al., 2014; Liu et al., 2016). In axenic conditions, it was also shown that IAA decreased both spore germination and subsequent hyphal germ tube growth (Fernández Suárez et al., 2015). The use of P-chlorophenoxyisobutyric acid, an IAA inhibitor, negatively affects the number of fungal entry points and further intraradical AM fungal development (Liu et al., 2014). AUX effects were also studied under monoxenic conditions. Mohan Raj et al. (2016) tested various indole-3-butyric acid and IAA concentrations

(alone and combined) with *Daucus carota* transformed roots (*in vitro*) inoculated with *R. irregulare*, and shown a slight decrease in both root colonization and spore numbers.

Studies with the auxin (IAA)-deficient *bushy* mutant (Symons et al., 1999, 2002) is associated with a reduction in the AM fungal colonization but without further alteration of AM fungal structures inside the roots (Foo, 2013). Moreover, tomato auxin-resistant *diageotropica* (*dgt*) mutant shows lower AM fungal development in both monoxenic and *ex vitro* conditions (Hanlon and Coenen, 2011), although this was not always reproducible (Zsögön et al., 2008). The AM fungal response to auxin appears even more complex, as the auxin hyper-transporting *polycotyledon* (*pct*) mutant fails to generate an AM symbiosis monoxenically with root organ culture, but shows increased colonization in *ex vitro* plants, and authors suggested the existence of shoot-derived factors that modulate auxin action (Hanlon and Coenen, 2011). In another approach, microRNAs were used, which are non-coding RNAs that target particular genes and impair their expression. In this way, suppression of auxin-related signaling was achieved by overexpression of microRNA393, known to post-transcriptionally modulate the expression of the auxin receptors TIR1 and several AFBs (Navarro et al., 2006, 2008; Parry et al., 2009; Vidal et al., 2010). This strongly inhibited AM fungal colonization and arbuscule abundance and morphology in several plant species (Etemadi et al., 2014).

Regarding the interaction with other hormones, it has been proposed that auxins regulate positively SL biosynthesis genes (Foo et al., 2005; Johnson et al., 2006; Agusti et al., 2011), thereby participating in mycorrhizal development (Foo et al., 2013b). Moreover, auxin/cytokinins antagonism in root is very well known (Moubayidin et al., 2009), and a recent publication demonstrated that CK produced in roots are detrimental for AM fungi development (Cosme et al., 2016).

Several authors described increased IAA levels in mycorrhizal roots (Meixner et al., 2005; Ludwig-Müller and Güther, 2007; Fiorilli et al., 2009; Hanlon and Coenen, 2011; Liu et al., 2018) suggesting an involvement of IAA signaling in the first stages of colonization. Moreover, auxin-like molecules or IAA were found in small quantities in AM fungal spores (Barea and Azcón-Aguilar, 1982; Barea, 1986; Ludwig-Müller et al., 1997), but AUX were not detected in hyphae (Jentschel et al., 2007). Recent survey of the *R. irregularis* genome indicates that typical auxin biosynthesis genes are lacking (Tisserant et al., 2013), which may interrogate the (plant?) origin of AUX found in mycorrhizal structures, shown in previous publications.

To conclude, a positive effect of AUX seems to dominate, and is therefore classified as an AM-promoting hormone.

Strigolactone (SL)

Strigolactones are terpenoid lactones derived from carotenoids which were originally discovered in root exudates, as they stimulate seed germination of parasitic plants like *Striga* (Mangnus and Zwanenburg, 1992). It turned later out that they also induce hyphal branching of AM fungal hyphae by affecting different molecular and cellular processes (Akiyama et al., 2005; Besserer et al., 2006). Despite SL being a recently discovered phytohormone, it is probably the most studied one in endomycorrhiza (**Figure 2**).

In planta, exogenous application of GR24 (a synthetic analog of SL) promotes mycorrhizal development in wild-type but also in SL-deficient plant mutants (Gomez-Roldan et al., 2007; Breuillin et al., 2010; Balzergue et al., 2011; Illana et al., 2011; Yoshida et al., 2012; Foo et al., 2013b). However, this induction appears to occur only under low P concentrations (Breuillin et al., 2010; Balzergue et al., 2011). SL application is unable to trigger mycorrhizal development in non-host plants such as *Arabidopsis thaliana*, *Spinacia oleracea*, *Lupinus polyphyllus*, or *Fagopyrum esculentum* (Illana et al., 2011). *In vitro* studies showed that SLs increase fungal metabolism, as application of synthetic analogs (GR24 and GR7) under axenic conditions was shown to activate mitochondrial differentiation, number and activity toward fungal cytochrome oxidase (COX) pathway with an increase in NADH and ATP during the pre-symbiotic phase in hyphea, and goes concomitantly with higher hyphal branching (Akiyama et al., 2005, 2010; Besserer et al., 2006, 2008; Balzergue et al., 2011; Kretzschmar et al., 2012). Moreover, spores in contact with SLs harbor higher germination rates in a shorter time (Besserer et al., 2006, 2008). In another work, Genre et al. (2013) demonstrated that GR24 is also able to stimulate production and release of Myc factors from spore exudates, which in turn induce Ca^{2+}-spiking in the plant.

Strigolactone-deficient mutants or transgenic lines harboring constructs for RNAi-mediated silencing of genes participating in SL biosynthesis or signaling showed lower mycorrhizal colonization levels than the corresponding controls in tomato, rice, pea and petunia (Gomez-Roldan et al., 2008; Breuillin et al., 2010; Koltai et al., 2010; López-Ráez et al., 2010; Vogel et al., 2010; Illana et al., 2011; Kohlen et al., 2012; Kretzschmar et al., 2012; Yoshida et al., 2012; Foo et al., 2013b; Guillotin et al., 2017; Kobae et al., 2018). SL-insensitive mutant plants possess reduced to neutral responses on mycorrhizal rate, depending of the mutant type and plant variety (Yoshida et al., 2012).

Strigolactone interplays displayed positive crosstalk with ABA and AUX (see section above), and both of them have been recognized to stimulate mycorrhizal growth. The consensus for the role of SLs in mycorrhiza is clear, and can be confidently classified as promoter. However, the production of SL by AM fungi is not known.

Brassinosteroid (BR)

Brassinosteroids represent a class of phytohormones defined as growth promoters (Kosová et al., 2012). They modulate plant development through important processes like cell elongation, cell division and cell differentiation. Furthermore, they are involved in defense against pathogens and abiotic stresses (Zhu et al., 2013).

Foliar application of epibrassinolid was shown to enhance slightly mycorrhizal colonization (Tofighi et al., 2017). Inoculation of the brassinosteroid-deficient pea mutant *lk* (Reid and Potts, 1986; Ross et al., 1989), which shows a strong reduction in BR content (Nomura et al., 2004), resulted in a strongly reduced total root colonization and a lower amount of arbuscules compared to the wild type (Foo et al., 2016). Tomato

mutants defective in BR biosynthesis were analyzed with respect to mycorrhizal symbiosis and showed decreased mycorrhization (Bitterlich et al., 2014a,b). However, the leaky brassinosteroid-deficient *lkb* mutant pea did not induce a similar depressed fungal spread within roots (Foo et al., 2013a) suggesting that the reduction of BR levels must be severe to impact the AM symbiosis.

It is known that BRs can antagonize the plant innate immune response (Bajguz and Hayat, 2009; De Vleesschauwer et al., 2012; Nahar et al., 2013), and act together with other phytohormones in the case of interactions with biotrophs/necrotrophs (Saini et al., 2015). The later seems to be true also in the case of mycorrhizal interactions. The model proposed by Foo et al. (2016) suggested indeed that BR interacts negatively with ET in regulation of mycorrhizal behavior. However, how BR can interact with other hormones within mycorrhizal symbiosis remains to be elucidated. BRs also interact with the carbohydrate metabolism, and it was supposed that improvement of mycorrhizal development by BRs is based on a physical interaction between proteins involved in BR biosynthesis and signaling and a sucrose transporter (Bitterlich et al., 2014a,b).

In conclusion, BR is still poorly studied with respect to the AM symbiosis, but first data suggest that it acts as a promoter of mycorrhizal colonization. Nevertheless, more investigations are needed like, e.g., the impact of exogenous application of BR on the mycorrhizal symbiosis under *in vitro* and *ex vitro* conditions and the ability of AM fungi to synthetize BRs.

Ethylene (ET)

Ethylene is a gaseous plant hormone; it plays an important role in plant signaling with fundamental effects on plant growth and development (fruit ripening, stem and root elongation inhibition, flowering, seed germination and leave senescence) as well as defense (van Loon et al., 2006a; Lei et al., 2011).

Exogenous soil and foliar treatments with ET or its commercial analogous ethephon have been shown to impair mycorrhizal colonization (Azcón-Aguilar et al., 1981; Morandi, 1989; Geil et al., 2001; Geil and Guinel, 2002; Foo et al., 2016) and to reduce arbuscule abundance (Geil et al., 2001; Geil and Guinel, 2002; Foo et al., 2016) with effects on arbuscule branching (Geil et al., 2001; Geil and Guinel, 2002). Interestingly, ET applied in specific amounts is able to promote mycorrhizal development under high P (Torres de Los Santos et al., 2016). Dose dependency was also shown under axenic conditions, where ET promoted hyphal growth and spore germination at low dosage, but inhibited it at a dosage higher than 0.2 ppm (Ishii et al., 1996).

Several studies using mutants have been conducted to determine the ET effect on AM symbiosis, but results were contradictive. In ET-overproducing tomato plants (*epinastic*), mycorrhizal colonization and arbuscule abundance were impaired at low P (Zsögön et al., 2008; Torres de Los Santos et al., 2011, 2016; Fracetto et al., 2013, 2017), but increased at higher P (Torres de Los Santos et al., 2016). In ET-insensitive mutant plants (tomato *never ripe*, tobacco *etr1* and pea *ein2* mutants), mycorrhizal colonization was found to be repressed (Zsögön et al., 2008), improved (Penmetsa et al., 2008; Martín-Rodríguez et al., 2011) or remained constant (Riedel et al., 2008; Fracetto et al., 2013; Foo et al., 2016; Torres de Los Santos et al., 2016). Similar inconsistent observations were found with ET-deficient tomato plants, with inhibited (Martín-Rodríguez et al., 2011), enhanced (Torres de Los Santos et al., 2011, 2016) or without effect on mycorrhizal root growth compared to wild-type plants (Riedel et al., 2008). No changes were recorded in the mycorrhizal development within an ET-hypersensitive tomato line (Martín-Rodríguez et al., 2011). Conflicting observations were also found for effects on biomass. In ET-deficient tomato, plant root growth was reduced (Martín-Rodríguez et al., 2011), enhanced (Torres de Los Santos et al., 2011, 2016) or remained unaffected by mycorrhization. Mycorrhizal development remained unaffected in ET-deficient (silencing of *coi1*) and ET-insensitive (*etr1*) tobacco plants, but mycorrhizal growth responses were strongly enhanced in both mutants (Riedel et al., 2008).

The relationship between endogenous ET level in roots and the mycorrhizal behavior is also not always clear: (i) negative correlation was observed within pea E107 (brz) (Resendes et al., 2001; Morales Vela et al., 2007) or in ABA-deficient *notabilis* and *sitiens* tomato mutant plants (Herrera-Medina et al., 2007; Martín-Rodríguez et al., 2010); and (ii) even more confusing, a positive correlation between endogenous ET root content and mycorrhization was noticed in both, ET-overproducing (*epinastic*) and ET-deficient (*rin*) tomato mutants, while harboring curiously, respectively, lower and higher ET content compared to the wild type (Torres de Los Santos et al., 2016).

Interactions between ET and other phytohormones was demonstrated. ABA-deficient *notabilis* and *sitiens* mutant plants harbor elevated ET levels in roots and an impaired mycorrhizal development, while exogenous ABA application reduced ET concentrations (Sharp et al., 2000; Herrera-Medina et al., 2007; Martín-Rodríguez et al., 2011; Fracetto et al., 2017). This suggests an antagonistic interaction between ABA and ET. ET was also shown to be negatively regulated by BR (Morales Vela et al., 2007), and ET-insensitive *ein2* mutant harbored reduced GA but elevated IAA levels (Foo et al., 2016). This corresponds with another study showing that application of 1-aminocyclopropane carboxylic acid (ACC), a precursor of ET, decreases free IAA content in roots (Negi et al., 2010).

Ethylene is likely the most problematic hormone to study as illustrated by the conflicting reports. Discrepancies with the use of mutant plants are likely due to the plant species or to the experimental conditions, which consequently limit formal interpretation. It was also suggested that ET has to reach a threshold before it influences AM fungal colonization and might explain why the mutants did not always show the same outcomes (Foo et al., 2016). The difficulties to interprete ET responses may also be due to the gaseous nature of ET. Its synthesis is stoichiometrically correlated with HCN by-production in plants (Peiser et al., 1984; Grossmann, 2003) and exogenous ET application stimulates endogenous ET biosynthesis. Versatile responses may be therefore attributed to the action of both, ET and HCN and the fine-tuning of their concentrations. Even though HCN is usually detoxified rapidly by plants (Miller and Conn, 1980), high local concentrations (up to 350 μM) can occur

(Mizutani et al., 1988), with known impact on mitochondrial respiration (Siegień and Bogatek, 2006). Considering the aerobic nature of AM fungi, it is possible that high HCN concentrations are detrimental for fungal spread in roots but may promote locally arbuscule formation and functionality as it was observed with KCN application (Mercy et al., 2017). Moreover, HCN can elicit responses similar to ET when applied at low concentrations (McMahon Smith and Arteca, 2000). ET production by AM fungi remains unknown. Therefore, to understand the role of ET in the mycorrhizal symbiosis appears very challenging. In summary, we here state (with a risk) that ET negatively affects the mycorrhizal symbiosis.

Cytokinin (CK)

Cytokinins are a class of diverse phytohormones formed by N^6-substituted purine derivatives. CKs regulate several aspects of plant development such as shoot cell division and development and mineral uptake of roots (Werner and Schmülling, 2009; Kieber and Schaller, 2014).

Few studies investigated the response of AM to CK application: kinetin/kinetin riboside did not impact mycorrhizal development (Xie et al., 1998; Rabie, 2005) while 6-benzylaminopurine decreased it (Bompadre et al., 2015). Application of kinetin riboside on *Glomus clarum* spores (axenic conditions) promoted spore germination and germ tube growth (Fernández Suárez et al., 2015). AM fungi seems able to produce CK or CK-like hormones (Barea and Azcón-Aguilar, 1982). Many publications reported changes of endogenous CK content (ranging most often from increase to sometimes decrease) following AM fungi inoculation (Cosme et al., 2016).

Experiments with the CK-insensitive *bushy root* (Zsögön et al., 2008) or the CK receptor mutant *cre1* (Laffont et al., 2015) showed no impact on AM fungal colonization patterns. Laffont et al. (2015), however, stated that this is consistent with the limited transcriptional response of CK-regulated genes in roots. A tobacco transgenic line with low CK production showed increased AM colonization (Cosme and Wurst, 2013), but this effect was not reproducible. Indeed, when those plants were inoculated with two other AM fungal strains, the lower CK content was associated with impaired mycorrhizal colonization (Cosme et al., 2016). This was supported by another study, where increased colonization has been observed in a CK-overproducing pea mutant *E151* (Jones et al., 2015).

There exist antagonistic interplays between CK and ABA, as exogenous application of ABA can reduce CK content and perception (Werner et al., 2006; Tran et al., 2007; Großkinsky et al., 2014) and vise-versa (El-Showk et al., 2013; Guan et al., 2014). CKs also act synergetically with SA and GA, with consequences for the systemic acquired resistance (SAR, Großkinsky et al., 2014). CK perception and content is also regulated by P, and was shown to be repressed under P starvation (Salama and Wareing, 1979; Horgan and Wareing, 1980; Franco-Zorrilla et al., 2002, 2005; Rouached et al., 2010). Moreover, CKs act antagonistically to auxins in control of lateral root development (Moubayidin et al., 2009). Taking these findings into account, cytokinin biosynthesis seems not to be part of favorable condition frame (P level) and physical support (lateral roots) for possessing a positive influence on mycorrhizal development.

Formal interpretation of CK impact on mycorrhizal symbioses from existing literature remains delicate due to the low number of trials, different plant species and P concentration used in these tests, and the ability of AM fungi to produce this hormone (**Supplementary Material**). To conclude, the consensus of this phytohormone is not obvious but data suggest that CK does not play a major role in endomycorrhizal symbiosis but may act negatively mostly indirectly, *via* its impact on root system, its crosstalks with other hormones and its interplay with carbohydrate metabolism.

Gibberellin (GA)

Gibberellins are a class of phytohormones synthesized from geranylgeranyl diphosphate. They move relatively free from shoots to roots promoting plant growth including stem elongation, flowering and inhibit leaf and fruit senescence (Swain et al., 2005; Wang and Irving, 2011; Claeys et al., 2014).

Many studies show that soil or leaf applications of GA reduce colonization and/or arbuscule abundance in several plant species (El Ghachtouli et al., 1996; Floss et al., 2013; Foo et al., 2013a; Yu et al., 2014; Martín-Rodríguez et al., 2015, 2016; Takeda et al., 2015; Khalloufi et al., 2017). In accordance, application of the GA biosynthesis inhibitor prohexadione calcium promotes mycorrhizal development (Martín-Rodríguez et al., 2015, 2016). GA seems able to promote spore germination under axenic conditions (Mercy et al., 2017) and AM fungi can produce this phytohormone (Barea and Azcón-Aguilar, 1982; Strzelczyk and Pokojska-Burdziej, 1984).

Several studies with overexpressing or deficient mutant plants for GA-biosynthesis and GA-signaling indicated a negative role of GA for arbuscule formation and development, emphasizing a negative impact on late stage of development (Floss et al., 2013; Foo et al., 2013a; Martín-Rodríguez et al., 2015, 2016). Growth regulator interconnection converges toward the stabilization status of DELLA proteins, which are integrated in abiotic and biotic stress (Zentella et al., 2007; Davière and Achard, 2013; Yu et al., 2014). GA was demonstrated as reciprocal antagonist with ABA and JA (Brenner et al., 2005; Greenboim-Wainberg et al., 2005; Razem et al., 2006; Yang et al., 2012; Heinrich et al., 2013; Shu et al., 2018) in almost all plant physiology aspects (plant defense reaction, seed dormancy and germination, growth, etc.). It appears that DELLA proteins negatively control all GA responses, and the degree of its stability in cell depends on the GA/ABA-JA ratio. Thus, ABA (Achard et al., 2006) and JA (Yang et al., 2012; Wild and Achard, 2013) stabilize or promote the DELLA complex, positively associated with arbuscule formation, while GA induces its ubiquitin-proteasome degradation associated with collapsed arbuscules (Floss et al., 2013; Bucher et al., 2014; Yu et al., 2014; Martín-Rodríguez et al., 2015). Moreover, GA-induced degradation of DELLA proteins enhances SA signaling, increasing plant resistance to biotrophic microorganisms (Navarro et al., 2008; Wasternack and Hause, 2013) like AM fungi. The consensus for GA is therefore well defined as a negative regulator of the mycorrhizal symbiosis.

Salicylic Acid (SA)

Salicylic acid is a phenolic compound classified as plant hormone a decade ago (Eraslan et al., 2008; Shi et al., 2009). It regulates many aspects of plant physiology, such as growth, ion uptake and chlorophyll content (Singh and Usha, 2003; Eraslan et al., 2008; Belkhadi et al., 2010). Furthermore, SA has long been known to play a major role in reducing plant stress, increasing the antioxidant activity (Shi et al., 2009) and promoting activation and modulation of plant defense responses, especially in interaction with biotrophic pathogens (Beckers and Spoel, 2006; Lu, 2009).

Exogenous applications of SA was shown to reduce mycorrhizal development, at least during the first weeks (Blilou et al., 2000; Costa et al., 2000; Özgönen et al., 2001; de Román et al., 2011), but neutral responses were also observed (Ludwig-Müller et al., 2002; Ansari et al., 2016). AM colonization can also increase following soaking seeds with SA (Garg and Bharti, 2018). Moreover, tobacco SA-overproducing mutant *CSA* and SA-deficient *nahG* showed, respectively, reduced and enhanced root colonization in the first days following fungal penetration (Herrera-Medina et al., 2003). Similarly, the Myc^- pea mutant P2 was found to accumulate higher SA concentration in roots (Blilou et al., 1999).

Salicylic acid seems to affect mycorrhizal development mainly at early stages. This effect seems transitory, probably due to the ability of the fungus to modulate the plant defense response further (Dumas-Gaudot et al., 2000; Campos-Soriano et al., 2010; de Román et al., 2011). Regulation of SA on other hormones within mycorrhizal symbiosis remains to be elucidated, but some connections can be found in relation with plant defense system (discussed in sections below). However, it can be stated as consensus that SA act as inhibitor of the mycorrhizal symbiosis. It is not yet known if AM fungi can synthetize this hormone, and effect of SA on mycorrhizal behavior under axenic conditions remains to be investigated.

RELATIONSHIP BETWEEN PLANT DEFENSE COMPONENTS AND MYCORRHIZAL SYMBIOSIS

Hormone signaling is tightly linked with defense pathway activation *in planta* (Bonneau et al., 2013). Contact with pathogens, beneficial microorganisms, natural and synthetic compounds or presence of abiotic stress trigger at various physiological, transcriptional, metabolic and epigenetic levels an unique plant state called "priming," resulting in establishment of induced defense mechanisms (Conrath et al., 2006; Mauch-Mani et al., 2017). Usually, but non-exclusively, two main antagonistic induced responses are engaged in plants, depending on the priming signal (named elicitor): systemic acquired resistance (SAR) and induced systemic resistance (ISR). The SAR response is induced by biotrophic pathogens (Ton et al., 2009; Thakur and Sohal, 2013) and involves SA accumulation, which mediates the activation of pathogenesis-related (PR) genes (Durrant and Dong, 2004). PR proteins are known especially for their antifungal activity based mainly on the hydrolytic capacity toward fungal cell wall components (Edreva, 2005). The ISR response, instead, is induced by necrotrophs or plant growth-promoting rhizobacteria (PGPRs) and involves JA and ET signaling without modification of defense gene expression (Pieterse et al., 1996, 2002). Specifically, ISR is based more on enhanced sensitivity to these plant hormones rather than to an increase in their production (Pieterse et al., 1998; Pieterse and van Loon, 2004; De Vleesschauwer et al., 2006). The role of ET remains somewhat difficult to define as a strict ISR component: it was shown originally to be required in ISR (Pieterse et al., 1998), but it contributes also to SAR by the induction of PR genes during the hypersensitive response against tobacco mosaic virus as one of the mobile signals, that SA is not in this case (Kuć, 2006; van Loon et al., 2006b). The mode of action of ET largely depends on the moment when it is produced, and ET treatment of plants can lead to opposite effects (i.e., before or after pathogen infections, van Loon et al., 2006b). Finally, many studies showed that almost all the plant hormones could participate to different extent in induced plant resistance (Pieterse et al., 2012). For example, additionally to abiotic stresses, ABA has a role in plant pathogen interactions (Fan et al., 2009; Cao et al., 2011). Emerging evidences state importance of ABA in plant defense system, with suppression of SAR induction and involvement in SA-SAR-mediated signaling (Yasuda et al., 2008; Jiang et al., 2010; Kusajima et al., 2010) but its potential role in ISR establishment is less clear as it can also counteract JA/ET defense related pathways (Cao et al., 2011).

Although the knowledge on plant pathogen interactions made important progress in the last years, classification of many important hormones involved as part of either ISR or SAR system remains incomplete (Pieterse et al., 2012). Moreover, interactions between plants and beneficial microorganisms partially exploit the same defense related pathways. Firstly, as shown by Güimil et al., 2005, there is a 40% overlap between genes responding to AM fungi and pathogen agents in rice. Although these responses are temporally and spatially limited in mycorrhizal symbiosis compared to phytopathosystems, this suggests that the plant defense system may play a role in the establishment and control of the endomycorrhizal symbiosis (Dumas-Gaudot et al., 1996; García-Garrido and Ocampo, 2002). Secondly, several authors suggested that AM fungi implement ISR in plant, during the first colonization stages (Pozo et al., 2002; Hause and Fester, 2005; Hause et al., 2007; Pozo and Azcón-Aguilar, 2007; Kapoor et al., 2008; Pieterse et al., 2014) but also that PGPRs, known to elicit ISR, can increase the mycorrhizal development (Alizadeh et al., 2013). By contrast, SAR system seems to generate a non-favorable metabolic context for AM fungi, since the use of SAR elicitors can lead to inhibition of mycorrhizal development (Faessel et al., 2010; de Román et al., 2011; Bedini et al., 2017) sharing therefore similarities with biotrophic pathogens (Delaney et al., 1994). As a point, while glycerol-3-phosphate is converted into glycerol and phosphate under P-deficient conditions (Hammond et al., 2004), it probably accumulates under P-sufficient plants increasing SAR stimulation potentials via SA (Chanda et al., 2011; Shah and Zeier, 2013).

HORMONAL AND ENERGETIC REGULATION OF PLANT METABOLISM UNDER CONTRASTING P CONDITIONS

Phytohormones act as messengers within the plant, which syntheses are usually regulated by various stimuli. However, their actions on mycorrhizal behavior should be connected to a specific metabolic plant state, favoring or not mycorrhizal development beyond their energetic needs. In this section, we discuss the connection between the metabolic context and hormone interplay under two contrasting situations of P level, supporting (low P) and inhibiting (high P) mycorrhizal colonization.

Plants acquire P by two different pathways. The first one, common for all plants, is called the direct pathway by which P is collected directly *via* the surface plant roots. The second one, called mycorrhizal pathway, is builded by the presence of mycorrhizal fungi which are able to uptake and transfer the P from soil to the root *via* the mycelium. In both cases, P uptake and transfer involves an active translocation mediated by H^+-ATPases which create a proton motive force allowing P entering the cell *via* Pi/H^+ symporters localized in the rhizodermis or the root hairs (direct pathway) or in the periarbuscular membrane at the arbuscule branch domain (mycorrhizal pathway, Smith and Smith, 2011b; Młodzińska and Zboińska, 2016).

Mycorrhizal Fungal Growth Has a Preference for a Metabolic Context Related to P Stressed Plants

Plant Respiration Under Low P

In this review, low available P is defined as a concentration belonging or being close to plant P starvation, which favors mycorrhizal development within roots (Smith and Read, 2008). Frequently, natural soils have P concentrations below 1 μM. Furthermore, P absorption by the roots results in a rapid depletion zone due to the low mobility of this ion (Marschner, 1995). This consequently engenders plant P starvation. Plant primary metabolism is then altered, as P stress induces a shift in plant respiration with reduced plant capacity to produce ATP (Theodorou and Plaxton, 1993; Plaxton and Tran, 2011) and is associated with deficient photosynthesis (Fredeen et al., 1990; Ghannoum and Conroy, 2007). Thus, plants undertake a series of metabolic adaptations in order to conserve the use of P, such as reduction of cell energetic potentials associated with plant growth depression, increased efficiency in P utilization, and remobilization of internal P and mitochondrial bypass P-requiring steps (Schachtman et al., 1998; Plaxton and Carswell, 1999; Raghothama, 1999; Uhde-Stone et al., 2003a,b; Plaxton and Tran, 2011).

One of the first adjustments at P deficiency is the re-organization of the electron chain transport within plant mitochondria. In the last steps of respiration, electrons provided by the TCA cycle are typically transported along the mitochondrial complexes I, II, III, and complex IV, the cytochrome oxidase pathway (COX). Complexes I, III, and IV constitute proton pumps during the electron transport, leading to the formation of a proton gradient between the mitochondrial matrix and the intermembrane space (Alberts et al., 2008). The gradient generated by the complexes is then used by ATP-synthases to produce ATP (Nakamoto et al., 2008). In cases of stress like P starvation, electrons are redirected to another terminal oxidase that is part of the alternative oxidase pathway (AOX). This pathway, present in plants and fungi, is sited between complexes II and III and catalyzes the reduction of oxygen into water, resulting in a lower intermembrane proton gradient and reduced ATP yield (Sluse and Jarmuszkiewicz, 1998). AOX pathway has been described as a pivotal element able to maintain the cell metabolic homeostasis, participating to the carbon metabolism flexibility (Gomez-Casanovas et al., 2007; Gandin et al., 2009; Leakey et al., 2009; Vanlerberghe, 2013). For this reason, it has been proposed as an important marker for plant acclimatization to stress conditions (Arnholdt-Schmitt et al., 2006; Clifton et al., 2006). Finally, AOX pathway was also proposed to play a role in AM spore dormancy and germination, as well as, AM fungal behavior *in planta*, influencing both colonization and arbuscules functionality (Besserer et al., 2009; Campos et al., 2015; Mercy et al., 2017).

P starvation directly inhibits both COX activity and the ATP synthase, resulting in low ATP/ADP ratios, while it promotes AOX activity, associated with higher $NADH^+H^+/NAD^+$ ratios. This was demonstrated in *Phaseolus vulgaris* (Rychter and Mikulska, 1990; Rychter et al., 1992), *Catharanthus roseus* (Hoefnagels et al., 1993), *Chlamydomonas reinhardtii* (Weger and Dasgupta, 1993), *Lupinus albus* (Florez-Sarasa et al., 2014), and tobacco cell cultures (Parsons et al., 1999). The electron flow directed to the AOX pathway allows conserving the intercellular P pool (Theodorou et al., 1991; Parsons et al., 1999; Juszczuk et al., 2001; Juszczuk and Rychter, 2003; Day et al., 2004) but also allows NADH oxidation, produced during citrate synthesis, to maintain continuation of TCA cycle reactions (Vanlerberghe and McIntosh, 1996; Shane et al., 2004; Gupta et al., 2012; Florez-Sarasa et al., 2014). Moreover, under P limitation, AOX activity in roots seems positively correlated with synthesis and release of carboxylates (citrate and malate, López-Bucio et al., 2000; Veneklaas et al., 2003; Del-Saz et al., 2018).

The metabolic role of AOX remains unclear given the non-conserving energy of this pathway (Vanlerberghe, 2013). Other metabolic functions could be involved to sustain the basal metabolic process mainly based on a specific redox status ($NAD(P)^+/NAD(P)H^+H^+$ cell pool). It has been also proposed that, concomitantly with AOX pathway, energy demand for plant metabolism is provided by fermentative activity (Mercy et al., 2017). AOX activity is promoted by accumulation of pyruvate, $NADH^+H^+$ and CO_2 (Gonzàlez-Meler et al., 1996; Siedow and Umbach, 2000; Vanlerberghe, 2013), whose contents in roots are higher under low P (Juszczuk and Rychter, 2003). These three molecules can also favor fermentation activity (both lactic and alcoholic) while CO_2 inhibites the COX pathway (Gonzàlez-Meler et al., 1996). Furthermore, malic enzyme converts malate to pyruvate, $NADH^+H^+$ and CO_2, supplying fermentation pathway with suited substrates. It was shown that up-regulation of malic enzyme activity is associated with fermentation (Sakano, 2001), and is part of the alternative glycolytic pathway that is enhanced in P-deficient conditions (Schachtman et al., 1998;

Plaxton and Carswell, 1999; Raghothama, 1999; Uhde-Stone et al., 2003a,b; Plaxton and Tran, 2011). Under P-deficient conditions, significant induction of fermentative related genes as alcohol dehydrogenase (Massonneau et al., 2001; Wu and Yang, 2003; Manan, 2012) and formate dehydrogenase (Herbik et al., 1996; Suzuki et al., 1998; Uhde-Stone et al., 2003b) has been shown, allowing the regeneration of NAD^+ pool which avoids glycolysis inhibition (Tadege et al., 1999). Finally, increased ethanol concentration is observed with the application of COX inhibitors (Solomos and Laties, 1976; Kato-Noguchi, 2000), or antisense-induction of AOX genes in *Arabidopsis* under aerobic conditions (Potter et al., 2001). In mycorrhizal symbioses, the role of plant fermentation is not known but may contribute to fungal fitness as part of the favorable plant metabolism driven under low P.

Carbon Fluxes and Root Exudation Under Low P

Low P sensing *in planta* drives changes in carbon partitioning between shoots and roots. Sucrose is reallocated to the root where it participates to a rise in glucose concentration (Hammond and White, 2011; Lemoine et al., 2013), increasing availability of carbon sources for AM fungal uptake. Contents in many sugars, organic acids and several aminoacids are increased within roots and are released in the rhizosphere under P starvation, derived from blocked glycolysis and TCA cycle (Hoffland et al., 1992; Dakora and Phillips, 2002; Hernández et al., 2007; Yamakawa and Hakata, 2010; Carvalhais et al., 2011; Gupta et al., 2012). Such compounds can modulate AM spores germination and can mediate plant-AM fungi interactions at presymbiotic phases (Ratnayake et al., 1978; Graham et al., 1981; Hepper and Jakobsen, 1983; Gachomo et al., 2009). Many other compounds synthetized and released by plants under abiotic stress (notably low P) have known stimulatory impacts on mycorrhizal development: it is the case for H_2O_2 (Liu et al., 2012), for polyamines (El Ghachtouli et al., 1995; Wu et al., 2012), for certain flavonoids (Nair et al., 1997; Davies et al., 1999; Davies et al., 2005; Scervino et al., 2005) and other phenolic compounds (Fries et al., 1997) and probably most importantly strigolactones (Sun et al., 2014). Such molecules can also stimulate the release of diffusible factors from spore exudates, among which lipochitooligosaccharides and chitooligosaccharides (LCOs and COs), were characterized as so-called "Myc factors" (Nadal and Paszkowski, 2013; Schmitz and Harrison, 2014).

Plant-derived ET and diffusible factors present in germinating spore exudate (GSE) act antagonistically: compounds isolated from GSE (such as Myc factors) can stimulate mycorrhizal plant susceptibility, while ET inhibits GSE-induced symbiotic gene expression (Maillet et al., 2011; Mukherjee and Ané, 2011). Interestingly, pure LCO compounds extracted from *Bradyrhizobium japonicum* (similar to Myc factor found in GSE) applied to soybean leaves were shown to induce host stress response, activating AOX and repressing hormone-related components belong to GA signaling (Wang et al., 2012). Moreover, although composition of root exudates can vary depending on soil pH, plant species and plant age (Vierheilig et al., 2003; Badri and Vivanco, 2009; Tahat and Sijam, 2012; Balzergue et al., 2013), many of them released under low P (plant hormones as in particular SL, phenolic compounds, hydroxy fatty acids, glucosamine, specific aminoacids and sugars) were shown to act at pre-symbiotic stages (promoting spore germination, hyphal growth, hyphal branching), thus supporting the mycorrhizal symbiosis (Tamasloukht et al., 2003; Besserer et al., 2006, 2008; Nagahashi et al., 2010; Tawaraya et al., 2013; Nadal et al., 2017).

Hormone Interplay and Action Under Low P

Recognition and adaptation of plants to external metabolic stimuli is often mediated by phytohormone signaling. In particular, P starvation is associated with ABA accumulation (Mizrahi and Richmond, 1972; Vysotskaya et al., 2008), but also BRs (Nibau et al., 2008; Wang et al., 2014), IAA (Nacry et al., 2005), SL (Akiyama et al., 2005; Besserer et al., 2006, 2008; Foo et al., 2013b), and JA (Khan et al., 2016). As first well described hormonal regulation, plant mineral nutrition sensing is considered as the main driver modulating SL production (Umehara et al., 2010; Yoneyama et al., 2012) which is consistently promoted at P and nitrogen starvation (Bonneau et al., 2013; Foo et al., 2013b). For this reason, SL production at low P is considered as a plant strategy to recruit AM fungi for improving P uptake (Gu et al., 2011). P deficiency is also well correlated with low ET and reduced bioactive GA levels in roots, linked with an accumulation of DELLA proteins (Drew et al., 1989; Borch et al., 1999; Wu et al., 2003; Jiang et al., 2007; Kim et al., 2008; Devaiah et al., 2009; Hammond and White, 2011), although ET contributes to primary and adventitious root elongation (Nagarajan and Smith, 2012). The involvement of ABA signaling is linked with a positive cross-talk with JA and SL (López-Ráez et al., 2010; Lackman et al., 2011). JA and ABA can antagonize GA signaling *via* stabilization of DELLA proteins (Fu and Harberd, 2003; Yang et al., 2012) and can also negatively regulate SA signaling (Proietti et al., 2013; Manohar et al., 2017). Moreover, P starvation is known to decrease the synthesis of bioactive CKs, and some reports suggested that ABA participates to this inhibition (Pieterse and van Loon, 2004; Rouached et al., 2010; Nishiyama et al., 2011; Ha and Tran, 2014). It is well recognized that ABA regulates AOX gene expression and activity in plants (Finkelstein et al., 1998; Choi et al., 2000; Rook et al., 2006; Giraud et al., 2009; Lynch et al., 2012; Wind et al., 2012). In the work of Shen et al. (2003), abiotic stress and ABA were proposed to increase cytosolic levels of $NADH^+H^+$, which stimulate ROS production but also participate in the conversion of dihydroxyacetone phosphate to glycerol-3-phosphate, which then converts FAD to $FADH_2$, providing electron flow toward the AOX pathway. Compelling evidence also demonstrates the role of ROS as a signal occurring in most abiotic and biotic stresses but also in symbiosis (Puppo et al., 2013; Ghosh and Xu, 2014) and in potentiating the ABA pathway (Kwak et al., 2003). Nutrient starvation (as low P) is usually associated with overproduction of H_2O_2 in roots (Shin and Schachtman, 2004; Shin et al., 2005; Cheeseman, 2007) able to upregulate AOX gene expression, protein content and activity (Juszczuk and Rychter, 2003; Yamaguchi-Shinozaki and Shinozaki, 2005; Ho et al., 2008; Wang et al., 2010). H_2O_2 originates mainly from NADPH oxidase and polyamine oxidase activities, both of which are induced

by ABA (Wang, 2008; Liu et al., 2012). In particular, H_2O_2 is produced in arbuscules (Fester and Hause, 2005) and the use of scavengers (ascorbic acid or salicylhydroxamic acid) reduce both H_2O_2 and mycorrhizal development (Liu et al., 2012). Both ABA and ROS induce the production of JA (Howe, 2004; Yang et al., 2012) which plays an important role in plant defense.

The Existential Problem of Mycorrhizal Fungi Under High Available P

The second condition that we describe is the situation of high available P, which is defined as concentrations known to inhibit mycorrhizal colonization in plants (Graham et al., 1981; Thomson et al., 1986; Balzergue et al., 2011) but also create the optimal state for plant growth in absence of AM fungi. Excluding the mycorrhizal context, several studies regarding plant physiology have been conducted under high (or optimal for the plant partner) P availability, and the metabolic frame is therefore relatively well known. In absence of stress, plant metabolism, especially photosynthesis, flows optimally, maximizing the energy yield (Nátr, 1992), associated with COX activity resulting in a high ATP/ADP ratio (Sluse and Jarmuszkiewicz, 1998; Day et al., 2004). This constant energy flux enables a steady state of metabolism (Kouchi and Yoneyama, 1984; Rontein et al., 2002). This steady state is an approximation that is always subjected to the so called "carbon economy" (Poorter et al., 1990) where the carbon accumulation, redistribution and utilization is continuously adjusted. However, a situation close to the steady state allows the plant to optimize many pathways involved in primary metabolism, providing important intermediates for other reactions (Krebs and Johnson, 1937). Part of the fixed carbon pass through the respiration while a fraction is then stored in lipid form in oil bodies (Napier et al., 1996).

Under high P, content and perception of some hormones is increased in roots such as ET, CK, GA, and SA (Drew et al., 1989; McArthur and Knowles, 1992; Jiang et al., 2007; Devaiah et al., 2009) and all can regulate positively photosynthetic pathways (Khan, 2004, 2006; Yaronskaya et al., 2006; Tholen et al., 2008; Rivas-San Vicente and Plasencia, 2011; Xie et al., 2016). GA controls sucrose synthesis by positively regulating fructose-1,6-bisphosphatase and sucrose phosphate synthase (Zamski and Schaffer, 1996) while SA promotes rubisco activity, chloroplastic structure (reviewed by Rivas-San Vicente and Plasencia, 2011) and net increase of CO_2 assimilation (Fariduddin et al., 2003). GA and SA are known to have a reciprocal stimulation and it seems that both are involved in DELLA loss-of-function (Alonso-Ramírez et al., 2009a,b). A recent study indicated that GA signaling downregulates endogenous SL levels (Ito et al., 2017). High levels of GA, SA and ET repress synthesis and signaling of ABA and JA (Vlot et al., 2009). SL content in non-mycorrhizal roots is reduced under high P, and decreases also when P concentration increases locally (in arbuscocytes) after colonization is established (Foo et al., 2013b; Fusconi, 2014). GA biosynthesis and signaling is coupled with active COX pathway and both are key components to promote plant growth. *Arabidopsis* CYTc deficient mutant plant contains less bioactive GA, less ATP but elevated DELLA protein levels and similar observation was noticed when mitochondrial (COX pathway) inhibitors is applied in wild type (Racca et al., 2018). GA can upregulate cytochrome C gene expression involved in the COX pathway (Yang and Komatsu, 2004) and GA biosynthesis inhibitor mimicks the effect of CYTc deficiency (Racca et al., 2018). GA promotes respiration in *Amaranthus* while this effect is prevented by KCN (Loo et al., 1960). Robinson and Wellburn (1981) found that GA application increased the rate of NADH-dependant ATP formation, which is highly inhibited by cyanide (Cunningham, 1963) and can promote growth and lipogenesis (Yu et al., 2016). Then, SA was reported in many papers as promotor of AOX expression associated with increased protein levels, but it has actually no influence on its activity (Lennon et al., 1997; Simons et al., 1999). Instead, whole-cell tobacco respiration rate is enhanced when SA is applied at less than 1 mM (Norman et al., 2004). Finally, CKs may also act in mitochondria, by blocking the AOX pathway (Musgrave, 1994).

The negative influence of high P on mycorrhizal fungi is systematic and systemic as it was shown that foliar application of P can lead to the same depression phenomena (Breuillin et al., 2010). Knowledge of mechanisms involved in P inhibition on mycorrhiza remains fragmented, but deserves attention. Indeed, this element limits mycorrhizal inoculum performances under field conditions, where soils usually contain high amounts of available P (due to high application of P fertilization – Tóth et al., 2014). The statement that plants that are able to uptake P *via* the direct pathway do not need to establish mycorrhizal symbiosis appears simplistic, but underestimates the complex regulations that lead to AM inhibition. Actually, the hormonal composition (SA, GA and ET), enhanced under high P, creates an inhibitory context for mycorrhizal development, as detailed in section Phytohormones Influence the Mycorrhizal Symbiosis. From another point of view, the lack of mycorrhizal colonization was generally described as an economic determinism, so called "cost-benefit" trade between P uptake for plant and carbon delivery for AM fungi (Smith et al., 2011). From this perspective, it is recognized that plants usually adapt resource allocation to organ involved in mineral acquisition in order to stimulate their growth, where more energy is translocated from shoot to root under mineral shortage (such as sucrose, polyols such as mannitol and sorbitol and other oligosaccharides from raffinose family), but is linked with an impaired photosynthesis (Lemoine et al., 2013). By opposition, the source (shoot)-sink (root) balance is modified under high P: carbon sources become less available surrounding the mycorrhizal structures in roots, which may participate to reduce AM fungal growth and interface formation (arbuscules), thus repressing fungal P delivery to the plant. This goes also along with lower release of various molecules (sugars, amino acids, as well as some hormones such as SL) which can be recognized by mycorrhizal hyphae. Such lower release would limit root-fungus interactions. In addition to plant physiology, high P was also shown to inhibit directly spore germination and mycelium development *in vitro* (de Miranda and Harris, 1994; Olsson et al., 2002), limiting soil exploration and contact to the plant roots. However, it is not yet known, at the best of our knowledge, if AM fungi exudation of Myc factors is directly

negatively affected under high P, like it is described for plant exudates. Importantly, AM fungi are partly aerobic organisms: this would mean that the processing of fungal energy from carbon sources must go concomitantly with higher O_2 consumption to allow formation of ATP orientated by higher flow of electron toward the COX pathway. As a result, the inhibition of the COX pathway induced by application of KCN is associated with reduced mycorrhizal development under low P (Mercy et al., 2017). It can be questioned whether high P may induce a stronger source-sink (or competition) for oxygen, favoring plant cell energy which consequently becomes less accessible for the fungus.

P affects also the functionality of the symbiosis as mycorrhizal responses have been shown to be negatively correlated with increased P concentration (Smith and Smith, 2011a). This phenomena is not necessarily due to a decrease of carbon delivery to the fungus but more to a shift of P uptake between the direct and the mycorrhizal pathway. The current hypothesis states that AM fungi impair the direct pathway while the mycorrhizal P pathway does not compensate, probably due to a lower functional P transfer under high P (Smith and Smith, 2011b). To support part of this hypothesis, the down-regulation of the mycorrhiza-inducible P transporter genes PT4 have been described in several works for different plant species following application of high P concentration (Drissner et al., 2007; Breuillin et al., 2010). Moreover, it is possible that AM fungi try to prime a specific propitious plant metabolism (notably ISR based plant context, see section "Relationship Between Plant Defense Components and Mycorrhizal Symbiosis" above) but the full completion of this system permanently fails (leading therefore to persistent plant growth depression) due to the continuous and paradoxical responses from plant sensing and signaling under high available P.

CONCLUSION AND PERSPECTIVES

Drawing Links Between AM Fungi, Plant Respiration, Phytohormones, Carbon Partitioning, and Plant Defense Upon Available P Concentration

Physiological Models of Plant Susceptibility to Mycorrhiza

Studying phytohormone interrelationships is always delicate, since there exist fine and complex regulations which depend on tissues and the plant physiological stage. Nevertheless, we propose two models (**Figures 3**, **4**) that sum up two antagonistic metabolic situations according to P levels. This allows to distinguish two groups of acting hormones: (i) a first group (JA, ABA, IAA, SL, and BR) is involved in signaling under low P (**Figure 3**), has known overall promoting activities toward AM fungi development and seems to be linked potentially to the ISR system. The metabolic state comprises higher fermentation activities, increased free cytosolic amounts and root release of sugars, aminoacids and carboxylate acids, promotion of lipid catabolism, higher cytosolic reductive potential and the involvement of AOX pathway; (ii) a second group of hormones (GA, SA, ET, and potentially CK) is active under high P (**Figure 4**), has inhibitory impacts on AM fungi development and seems to be linked to the SAR system. It involves repression of fermentation, implementation of lipid anabolism, a higher cytosolic oxidative potential and the involvement of the COX pathway.

Consequently, the processing (uptake and metabolic assimilation) by AM fungi of the energy sources provided by the plant (sugars, lipids and maybe other compounds as products of fermentation) may depend on the presence of a surrounding metabolic context that integrates favorable signaling (partly mediated by hormones and reductive potential, upon likely available oxygen fluxes). Our literature survey suggests that plant AOX pathway may play one central role in the implementation of a specific metabolism, which occurs consequently to environmental stimuli (stress). Obviously, phytohormone regulations and electron flow partitioning between AOX and COX is dynamic in time and space and this must be taken into account during mycorrhizal development under normal conditions. The AOX pathway coupled with fermentative processes is probably a main component during the first stages of mycorrhizal development, explaining perhaps the well known stunt phenomenon which follows plant inoculation. Successively, electron route to AOX pathway and the related plant metabolism is very likely shifted toward the COX pathway (Del-Saz et al., 2017), as a consequence of increasing level of P delivered by the mycorrhizal pathway. Therefore, the metabolic context occurring at later stages of the mycorrhizal symbiosis may shift partly toward the model described in the **Figure 4**. This would fit with the known increased photosynthetic activity, reduced root exudation of compounds and electron partitioning through the COX pathway, as responses that AM fungi trigger in plant. This shift might also participate in the autoregulation of mycorrhization, a mechanism which prevents subsequent mycorrhizal development following a first plant inoculation with AM fungi (Vierheilig et al., 2000). ABA and JA seem not to take part in this phenomenon, while AUX and CK might be involved (Meixner et al., 2005; Wang et al., 2018), but the role of other AM-inhibiting hormones remain to be studied.

Gaps and Limits of Hormonal Studies in Mycorrhiza

We attempted to link pieces of the puzzle that shows fragments of the final picture but does not allow yet full understanding of the whole composition. Many efforts are still needed to deeply investigate the role of phytohormones with respect to AM fungi and plant metabolic adaptation. To date, the use of different plant species, their related mutants, and the different application ways of phytohormones create sometime discrepancies in the final outcomes. It is not trivial to interprete phenotypic and molecular data only related to the specific mutation which requires several internal controls. When mutant plants are able to survive, general metabolic and/or signaling pathways are likely differentially adapted surrounding the deleted or overexpressed targeted gene(s), thus participating at a whole on the responses on the mycorrhizal behavior. It appears also that some methods might create biases. For example, soil hormone application can

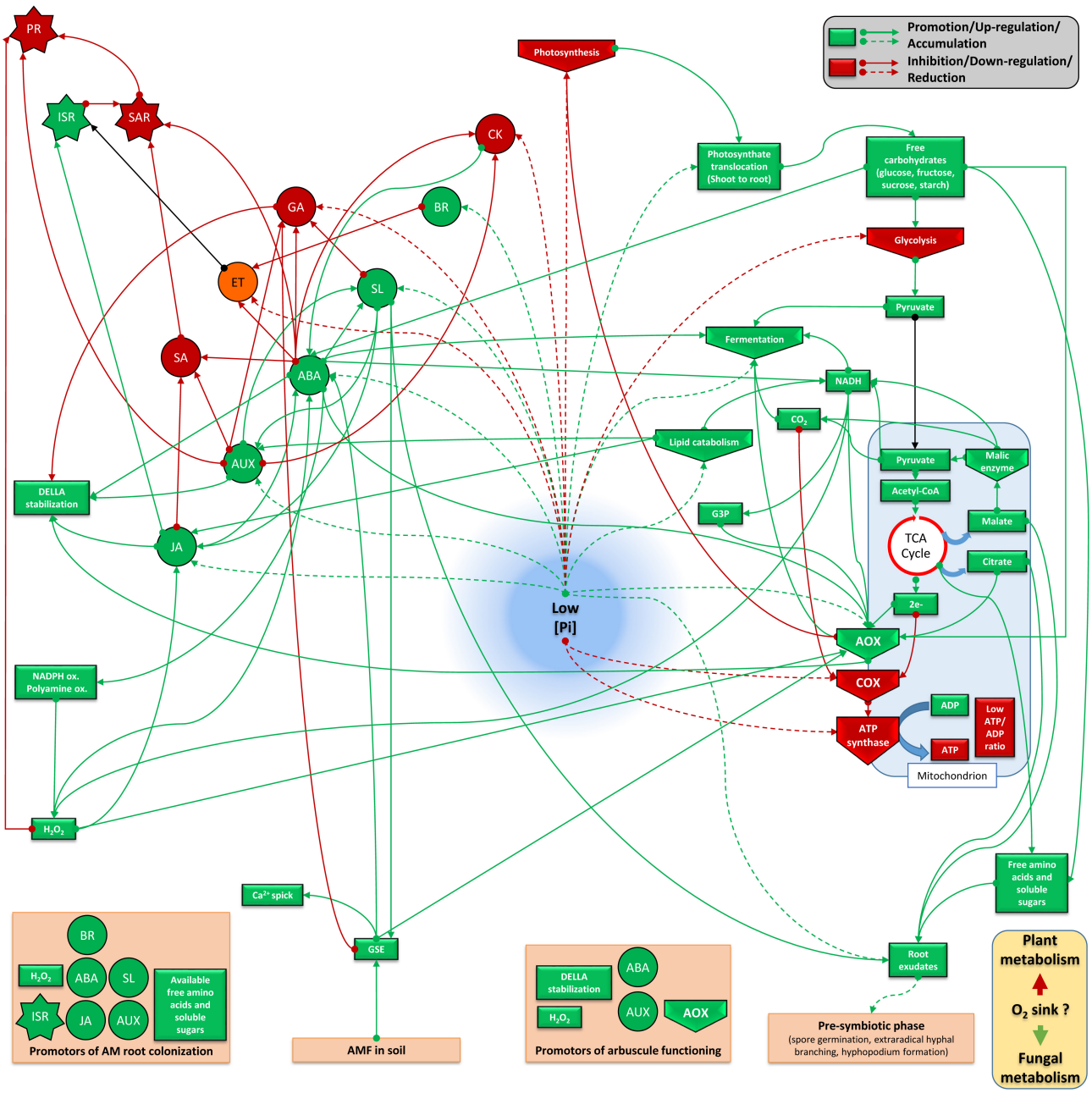

FIGURE 3 | Plant metabolic orientation of hormone interplay, carbon partitioning and responses on mycorrhizal development under low available P. Box and arrow color indicate repression (red), or promotion (green). Orange boxes and black arrows are used for uncertain conditions. Based on the literature survey, mycorrhizal colonization is enhanced under low available P which goes together with the action of AM-promoting hormones (such as ABA, SL, and JA). This hormonal interplay is connected to a favorable metabolic frame which involves lower phytosynthetic activity, higher translocation of photosynthetats from shoots to roots, accumulation of sugars (reduced glycolysis flow and enhanced lipid oxidation), enhanced plant fermentation activity, cytosolic reductive potential (elevated NADH pool), electron partitioning which is orientated toward the alternative oxidase pathway, reduced ATP formation and ISR implementation. Root exudation of several sugars, aminoacids, some carboxylic acids and hormones (such as SL) participate to the molecular dialog with mycorrhizal fungi present in the rhizosphere. This can support physical contact with the root by stimulating hyphal branching and to induce plant responses by promoting Myc factor release from germative spore exudates. It is questioned if this metabolic flux is accompanied by lower oxygen consumption by plant cells, which may become more available for the fungus (as aerobic organism) under low P. ABA, abscisic acid; JA, jasmonate; GA, gibberellins; SA, salicylic acid; SL, strigolactones; ET, ethylene; CK, cytokinins; IAA, auxins; BR, brassinosteroids; PR, pathogenesis related protein; ISR, induced systemic response; SAR, systemic acquired resistance; AOX, alternative oxidase; COX, cytochrome oxidase; CytC, cytochrome C; TCA, Krebs cycle; NADPH ox., NADPH oxydase; polyamine ox., polyamine oxydase; GSE, germinative spore exudate; G3P, Glycerol 3-phosphate.

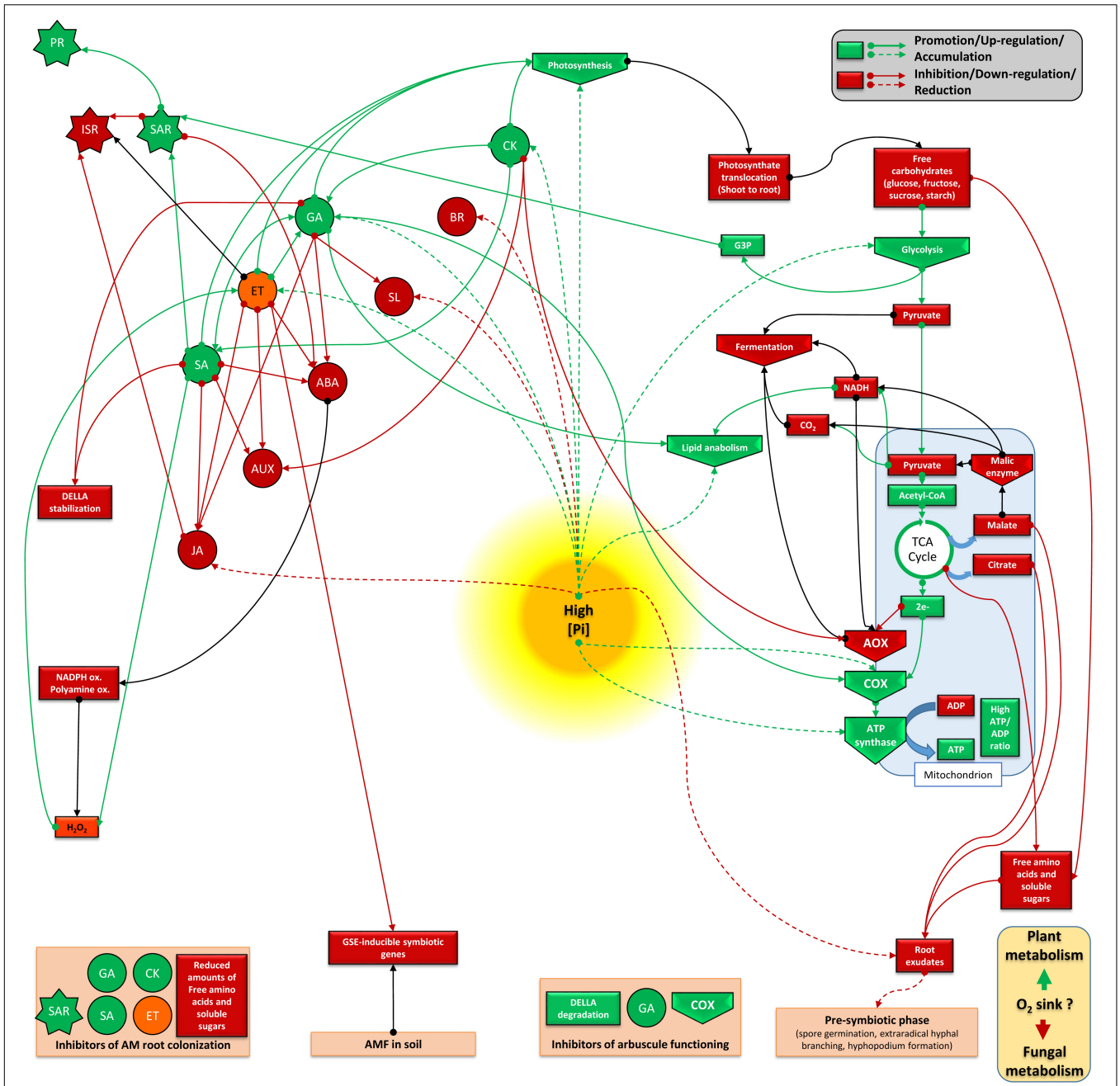

FIGURE 4 | Plant metabolic orientation of hormone interplay, carbon partitioning and responses on mycorrhizal development under high available P. Box and arrow color indicate repression (red), or promotion (green). Orange boxes and black arrows are used for uncertain conditions. Based on the literature survey, high available P affects mycorrhizal performances mainly due to the activity of mycorrhiza-inhibiting hormones (such as GA, SA, and ET), and in which SAR is potentialized. This goes together with a non-favorable metabolic frame which seems connected to an enhanced photosynthesis activity, lower translocation of photosynthetats from shoots to roots, a continuous flow of sugars processed via glycolysis, lipogenesis, and TCA, but also reduced fermentation activity and higher oxidative potential (reduced $NADH^+H^+$ cytosolic pool). In this system, lower free amounts of compounds (sugars, aminoacids, SL, and carboxylate acids) are released in the root exudate, thus reducing possible molecular dialog between AM fungi and plant root. In addition, high P favors electron partitioning toward the plant COX pathway, thus participating to ATP formation. It is questioned if this metabolic flux is accompanied by higher oxygen consumption by plant cells, which may become less available for the fungus (as aerobic organism) under high P. ABA, abscisic acid; JA, jasmonate; GA, gibberellins; SA, salicylic acid; SL, strigolactones; ET, ethylene; CK, cytokinins; IAA, auxins; BR, brassinosteroids; PR, pathogenesis related protein; ISR, induced systemic response; SAR, systemic acquired resistance; AOX, alternative oxidase; COX, cytochrome oxidase; CytC, cytochrome C; TCA, Krebs cycle; NADPH ox., NADPH oxydase; polyamine ox., polyamine oxydase; GSE, germinative spore exudate; G3P, Glycerol 3-phosphate.

already affect the mycorrhizal propagules during pre-symbiotic phase, and the eventual release of hormones by AM fungi could interfer with phenotypic responses of mutant plants. Production of several hormones (as SL, ET, JA, SA, and BR) by AM fungi remains unknown, while they may potentially participate in fungal spread within roots like pathogenic fungi (Chanclud and Morel, 2016). For example (but not exclusively), although SL biosynthesis seemed never investigated in any other organism than plants, it would be interesting to check the eventual ability of AM fungi to secrete this hormone. This might explain why arbuscules are still well formed within different SL deficient mutant plants (Kobae et al., 2018). In addition, data are sparse regarding influence of hormones on mycorrhizal behavior (pre-symbiotic and symbiotic stages) under *in vitro* conditions, and reports seem lacking for some of them (such as JA, SA, or BR). Moreover, most of the studies conducted with phytohormones within endomycorrhizal systems were set under low P, as it represents suitable conditions to investigate fungal phenotypes. Nonetheless, we recommand to perform more assays with different P concentrations (but also with other elements), in order to better define the mode of action of each hormone. Then, it could be interesting to report mycorrhizal phenotype traits under axenic and monoxenic systems that combine a given hormone in presence of various carbon sources. Despite several sugar transporters were localized in arbuscules but also in hyphae of the extraradical mycelium (Helber et al., 2011), assimilation and processing of carbon sources could require specific signals for generating efficiently fungal energetic fluxes, thus supporting growth and sporulation. In the future, the creation of a shared study platform would be useful, where application of all phytohormones are standardized under common conditions, taking care to evaluate not only the mycorrhizal phenotypic traits, but also metabolic plant adaptation.

Some aspects were not addressed in this review. This concerns the sporulation process, because the metabolic context that drives this specific fungal developmental step belongs to physiological changes that take place following root colonization at late stage. Moreover, the relationship between hormone interplay and mycorrhizal spore formation is only poorly investigated, despite this structure could reflect the energy status of the fungus (**Supplementary Material**). Information about the importance of fatty acid transfer as source of energy from plant to AM fungi did not find much space in our scheme, despite recent findings about its potential role (Keymer et al., 2017; Luginbuehl et al., 2017; Roth and Paszkowski, 2017). This field of research can represent a breakthrough in the understanding of AM symbiosis, but to date, almost no information is available regarding AM fungal phenotypes related to regulations between plant lipid energetic metabolism, hormone interplays and P levels, at the best of our knowledge. Plant *RAM1*, *RAM2*, *FatM,* and *STR/STR2* were proposed to act as operational unit to synthetize and deliver fatty acid to AM fungi (Keymer et al., 2017). In particular, reduced mycorrhizal development was demonstrated in *ram1/2* deficient mutant plants (Gobbato et al., 2012; Keymer et al., 2017). To illustrate first links toward lipid pathway in relation with fungal energetic needs, it was shown that application of Myc factors can upregulate *RAM1/2* expressions (Jiang et al., 2018), while GA (inhibiting mycorrhizal development) can downregulate *RAM2* expression (Takeda et al., 2015). However, a question raises whether the reduced mycorrhizal colonization in *ram2* mutant plants is due to the specific mutation, or due to a side effect from mycorrhizal inhibiting hormones (such as GA), that might be overexpressed as part of a signaling adaptation.

We are aware that hormonal interplays and regulations at different environmental conditions and in various plant species are much more complex than our models suggest, which remain largely incomplete. Therefore, next steps should attempt to validate or reject some of the hypotheses deduced from the models with further investigations. The effort that we made was an attempt to define a consensus, but also to propose several research topics aiming to elucidate some fundamental aspects of the endosymbiotic relationship which are still not fully understood and exploited.

Perspectives for Application: The Induction Methods for Mycorrhiza

According to our model, AM fungi development *in planta* seems to be promoted by the occurrence of ISR and its related signaling, prior to AM fungi contact. The induction of ISR or SAR system can be primed by application of specific elicitors for one or the other system. The use of specific molecules able to generate a favorable metabolic context to promote an effective colonization can therefore be proposed to master mycorrhizal inoculum applications under practical field condition or other research area as degraded land restauration. In this view and among those stimulatory molecules, potential affordable strategies exist from the application at low doses (seen as signal) of oligosaccharides on plants. Interestingly, oligosaccharides were shown since some decades to act as elicitors and therefore implement specific plant defense responses against biotic but also abiotic stress (Trouvelot et al., 2014). Oligosaccharides possess several advantages, such as being cheap and available, non-toxic, biodegradable, easy to use and not classified as phytohormones (whose field application is

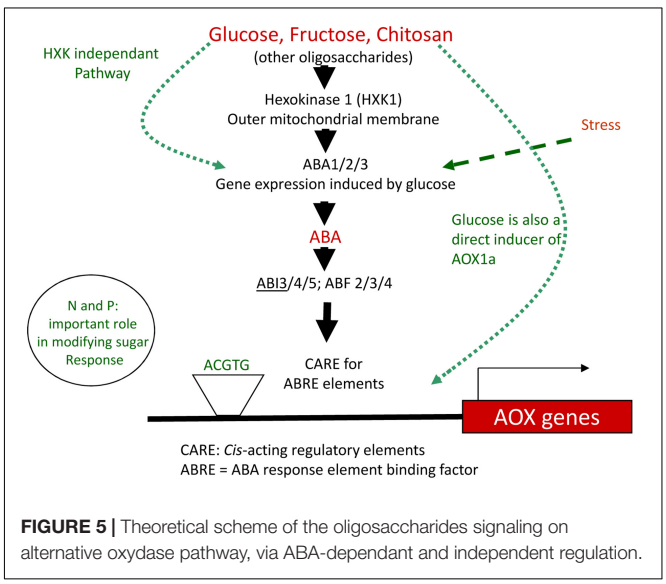

FIGURE 5 | Theoretical scheme of the oligosaccharides signaling on alternative oxydase pathway, via ABA-dependant and independent regulation.

highly restricted in Europe). Linking plant respiration and plant priming, the idea consists to induce a specific transient plant stress, by targeting the AOX pathway and its related metabolism, as it was shown to play a crucial role in arbuscule formation and positive mycorrhizal response (Mercy et al., 2017). Sugar signaling can promote AOX pathway directly (Li et al., 2006) or indirectly via the ABA signaling. In this last case, sugar recognition by the hexokinase 1 (Ramon et al., 2008), present on the outer mitochondrial membrane, initiates ABA synthesis (Cheng et al., 2002) and then stimulates the AOX gene expression *via* transcription factors (Finkelstein et al., 1998; Rook et al., 2006; Ho et al., 2008; Giraud et al., 2009; Millar et al., 2011). Although this signaling scheme (illustrated **Figure 5**) remains hypothetical, first trials using application (soil or on leaves) of low dose of oligosaccharides (such as glucose, fructose, and xylose) show possibilities to improve mycorrhizal development and responses under various P concentrations and in several plant and AM fungal species (Lucic and Mercy, 2014 – Patent application EP2982241A1; Bedini et al., 2017; Lucic-Mercy et al., 2017). Since the same compounds were termed initially as elicitors, related to the implementation of plant defense upon pathosystems but can also promote mycorrhizal performances, we propose to use rather the appellation "inducer" (or Mycorrhizal Helper Signaling Molecules), which defines signaling molecules that are intended to act specifically as stimulants in endomycorrhizal systems. In the same way, it would be also interesting to check if the mycorrhizal susceptibility is connected with plant species and cultivars that harbor naturally preferential mitochondrial electron partitioning toward the AOX pathway (as one metabolic selection trait). Such an approach may allow then to define interesting strategies for breeders, in order to orientate the plant selection in view to optimize mycorrhizal interactions in crops.

AUTHOR CONTRIBUTIONS

LM took the lead in writing the manuscript and conceived the main subject of this review. AB and LM drafted the manuscript. CS, PF, and EL-M supervised the writing, critically revised the manuscript, and contributed to its final version. All authors approved the final version of the manuscript.

FUNDING

This project has received funding from the European Union's Horizon 2020 research and innovation program under the Marie Skłodowska-Curie grant agreement no. 676480.

SUPPLEMENTARY MATERIAL

The Supplementary Material for this article can be found online at: https://www.frontiersin.org/articles/10.3389/fpls.2018.01800/full#supplementary-material

TABLE S1 | List of references and overview of hormone on AM symbiosis.

REFERENCES

Achard, P., Cheng, H., De Grauwe, L., Decat, J., Schoutteten, H., Moritz, T., et al. (2006). Integration of plant responses to environmentally activated phytohormonal signals. *Science* 311, 91–94. doi: 10.1126/science.1118642

Adie, B. A., Pérez-Pérez, J., Pérez-Pérez, M. M., Godoy, M., Sánchez-Serrano, J. J., Schmelz, E. A., et al. (2007). ABA is an essential signal for plant resistance to pathogens affecting JA biosynthesis and the activation of defenses in Arabidopsis. *Plant Cell* 19, 1665–1681. doi: 10.1105/tpc.106.048041

Agusti, J., Herold, S., Schwartz, M., Sanchez, P., Ljung, K., Dun, E. A., et al. (2011). Strigolactone signaling is required for auxin-dependent stimulation of secondary growth in plants. *Proc. Natl. Acad. Sci. U.S.A.* 108, 20242–20247. doi: 10.1073/pnas.1111902108

Akiyama, K., Matsuzaki, K. I., and Hayashi, H. (2005). Plant sesquiterpenes induce hyphal branching in arbuscular mycorrhizal fungi. *Nature* 435, 824–827. doi: 10.1038/nature03608

Akiyama, K., Ogasawara, S., Ito, S., and Hayashi, H. (2010). Structural requirements of strigolactones for hyphal branching in AM fungi. *Plant Cell Physiol.* 51, 1104–1117. doi: 10.1093/pcp/pcq058

Alberts, B., Johnson, A., Lewis, J., Raff, M., Roberts, K., and Walter, P. (2008). *Molecular Biology of the Cell*, 5th Edn. New York, NY: Garland Publishing, 815–827.

Alizadeh, O., Azarpanah, A., and Ariana, L. (2013). Induction and modulation of resistance in crop plants against disease by bioagent fungi (arbuscular mycorrhiza) and hormonal elicitors and plant growth promoting bacteria. *Int. J. Farm. Allied Sci.* 2, 982–998.

Alonso-Ramírez, A., Rodríguez, D., Reyes, D., Jiménez, J. A., Nicolás, G., López-Climent, M., et al. (2009a). Cross-talk between gibberellins and salicylic acid in early stress responses in: *Arabidopsis thaliana* seeds. *Plant Signal. Behav.* 4, 750–751. doi: 10.4161/psb.4.8.9175

Alonso-Ramírez, A., Rodríguez, D., Reyes, D., Jiménez, J. A., Nicolás, G., López-Climent, M., et al. (2009b). Evidence for a role of gibberellins in salicylic acid-modulated early plant responses to abiotic stress in Arabidopsis seeds. *Plant Physiol.* 150, 1335–1344. doi: 10.1104/pp.109.139352

Ansari, A., Razmjoo, J., and Karimmojeni, H. (2016). Mycorrhizal colonization and seed treatment with salicylic acid to improve physiological traits and tolerance of flaxseed (*Linum usitatissimum* L.) plants grown under drought stress. *Acta Physiol. Plant.* 38:34. doi: 10.1007/s11738-015-2054-x

Arnholdt-Schmitt, B., Costa, J. H., and de Melo, D. F. (2006). AOX–a functional marker for efficient cell reprogramming under stress? *Trends Plant Sci.* 11, 281–287. doi: 10.1016/j.tplants.2006.05.001

Aroca, R., Del Mar, A. M., Vernieri, P., and Ruíz-Lozano, J. M. (2008). Plant responses to drought stress and exogenous ABA application are modulated differently by mycorrhization in tomato and an ABA-deficient mutant (sitiens). *Microb. Ecol.* 56, 704–719. doi: 10.1007/s00248-008-9390-y

Azcón-Aguilar, C., Rodríguez-Navarro, D. N., and Barea, J. M. (1981). Effects of ethrel on the formation and responses to VA mycorrhiza in Medicago and Triticum. *Plant Soil* 60, 461–468. doi: 10.1007/BF02149642

Babst, B. A., Ferrieri, R. A., Gray, D. W., Lerdau, M., Schlyer, D. J., Schueller, M., et al. (2005). Jasmonic acid induces rapid changes in carbon transport and partitioning in Populus. *New Phytol.* 167, 63–72. doi: 10.1111/j.1469-8137.2005.01388.x

Badri, D. V., and Vivanco, J. M. (2009). Regulation and function of root exudates. *Plant Cell Environ.* 32, 666–681. doi: 10.1111/j.1365-3040.2009.01926.x

Bajguz, A., and Hayat, S. (2009). Effects of brassinosteroids on the plant responses to environmental stresses. *Plant Physiol. Biochem.* 47, 1–8. doi: 10.1016/j.plaphy.2008.10.002

Balzergue, C., Chabaud, M., Barker, D. G., Bécard, G., and Rochange, S. F. (2013). High phosphate reduces host ability to develop arbuscular mycorrhizal symbiosis without affecting root calcium spiking responses to the fungus. *Front. Plant. Sci.* 4:426. doi: 10.3389/fpls.2013.00426

Balzergue, C., Puech-Pagès, V., Bécard, G., and Rochange, S. F. (2011). The regulation of arbuscular mycorrhizal symbiosis by phosphate in pea involves early and systemic signalling events. *J. Exp. Bot.* 62, 1049–1060. doi: 10.1093/jxb/erq335

Barea, J. M. (1986). "Importance of hormones and root exudates in mycorrhizal phenomena," in *Physiological and Genetical Aspects of Mycorrhizae*, eds V. Gianinazzi-Pearson and S. Gianinazzi (Paris: INRA), 177–187.

Barea, J. M., and Azcón-Aguilar, C. (1982). Production of plant growth-regulating substances by the vesicular-arbuscular mycorrhizal fungus *Glomus mosseae*. *Appl. Environ. Microbiol.* 43, 810–813.

Beckers, G. J. M., and Spoel, S. H. (2006). Fine-tuning plant defence signalling: salicylate versus jasmonate. *Plant Biol.* 8, 1–10. doi: 10.1055/s-2005-872705

Bedini, A., Mercy, L., Schneider, C., Franken, P., and Lucic-Mercy, E. (2017). *How Hormone Interplay, Carbon Partitionning and Plant Priming Affect the Endomycorrhizal Symbiosis: A Theory*. Dr. Dissertation, ICOM, Prague.

Belkhadi, A., Hediji, H., Abbes, Z., Nouairi, I., Barhoumi, Z., Zarrouk, M., et al. (2010). Effects of exogenous salicylic acid pre-treatment on cadmium toxicity and leaf lipid content in *Linum usitatissimum* L. *Ecotoxicol. Environ. Saf.* 73, 1004–1011. doi: 10.1016/j.ecoenv.2010.03.009

Benková, E., Michniewicz, M., Sauer, M., Teichmann, T., Seifertová, D., Jürgens, G., et al. (2003). Local, efflux-dependent auxin gradients as a common module for plant organ formation. *Cell* 115, 591–602. doi: 10.1016/S0092-8674(03)00924-3

Berruti, A., Lumini, E., Balestrini, R., and Bianciotto, V. (2016). Arbuscular mycorrhizal fungi as natural biofertlizers: let's benefit from past successes. *Front. Microbiol.* 6:1559. doi: 10.3389/fmicb.2015.01559

Besserer, A., Bécard, G., Jauneau, A., Roux, C., and Séjalon-Delmas, N. (2008). GR24, a synthetic analog of strigolactones, stimulates the mitosis and growth of the arbuscular mycorrhizal fungus *Gigaspora rosea* by boosting its energy metabolism. *Plant Physiol.* 148, 402–413. doi: 10.1104/pp.108.121400

Besserer, A., Bécard, G., Roux, C., and Séjalon-Delmas, N. (2009). Role of mitochondria in the response of arbuscular mycorrhizal fungi to strigolactones. *Plant Signal. Behav.* 4, 75–77. doi: 10.4161/psb.4.1.7419

Besserer, A., Puech-Pagès, V., Kiefer, P., Gomez-Roldan, V., Jauneau, A., Roy, S., et al. (2006). Strigolactones stimulate arbuscular mycorrhizal fungi by activating mitochondria. *PLoS Biol.* 4:e226. doi: 10.1371/journal.pbio.0040226

Bitterlich, M., Krügel, U., Boldt-Burisch, K., Franken, P., and Kühn, C. (2014a). Interaction of brassinosteroid functions and sucrose transporter SlSUT2 regulate the formation of arbuscular mycorrhiza. *Plant Signal. Behav.* 9:e970426. doi: 10.4161/15592316.2014.970426

Bitterlich, M., Krügel, U., Boldt-Burisch, K., Franken, P., and Kühn, C. (2014b). The sucrose transporter SlSUT2 from tomato interacts with brassinosteroid functioning and affects arbuscular mycorrhiza formation. *Plant J.* 78, 877–889. doi: 10.1111/tpj.12515

Blée, E. (2002). Impact of phyto-oxylipins in plant defense. *Trends Plant Sci.* 7, 315–322. doi: 10.1016/S1360-1385(02)02290-2

Blilou, I., Ocampo, J. A., and García-Garrido, J. M. (1999). Resistance of pea roots to endomycorrhizal fungus or Rhizobium correlates with enhanced levels of endogenous salicylic acid. *J. Exp. Bot.* 50, 1663–1668. doi: 10.1093/jxb/50.340.1663

Blilou, I., Ocampo, J. A., and García-Garrido, J. M. (2000). Induction of Ltp (lipid transfer protein) and Pal (phenylalanine ammonia-lyase) gene expression in rice roots colonized by the arbuscular mycorrhizal fungus Glomus mosseae. *J. Exp. Bot.* 51, 1969–1977. doi: 10.1093/jexbot/51.353.1969

Bompadre, M. J., Fernandez Bidondo, L., Silvani, V. A., Colombo, R., Pérgola, M., Pardo, A. G., et al. (2015). Combined effects of arbuscular mycorrhizal fungi and exogenous cytokinins on pomegranate (*Punica granatum*) under two contrasting water availability conditions. *Symbiosis* 65, 55–63. doi: 10.1007/s13199-015-0318-2

Bonneau, L., Huguet, S., Wipf, D., Pauly, N., and Truong, H. N. (2013). Combined phosphate and nitrogen limitation generates a nutrient stress transcriptome favorable for arbuscular mycorrhizal symbiosis in Medicago truncatula. *New Phytol.* 199, 188–202. doi: 10.1111/nph.12234

Borch, K., Bouma, T. J., Lynch, J. P., and Brown, K. M. (1999). Ethylene: a regulator of root architectural responses to soil phosphorus availability. *Plant Cell Environ.* 22, 425–431. doi: 10.1046/j.1365-3040.1999.00405.x

Brenner, W. G., Romanov, G. A., Kollmer, I., Burkle, L., and Schmulling, T. (2005). Immediate-early and delayed cytokinin response genes of *Arabidopsis thaliana* identified by genome-wide expression profiling reveal novel cytokinin-sensitive processes and suggest cytokinin action through transcriptional cascades. *Plant J.* 44, 314–333. doi: 10.1111/j.1365-313X.2005.02530.x

Breuillin, F., Schramm, J., Hajirezaei, M., Ahkami, A., Favre, P., Druege, U., et al. (2010). Phosphate systemically inhibits development of arbuscular mycorrhiza in *Petunia hybrida* and represses genes involved in mycorrhizal functioning. *Plant J.* 64, 1002–1017. doi: 10.1111/j.1365-313X.2010.04385.x

Bucher, M., Hause, B., Krajinski, F., and Küster, H. (2014). Through the doors of perception to function in arbuscular mycorrhizal symbioses. *New Phytol.* 204, 833–840. doi: 10.1111/nph.12862

Campos, C., Cardoso, H., Nogales, A., Svensson, J., López-Ráez, J. A., Pozo, M. J., et al. (2015). Intra and Inter-spore variability in *Rhizophagus irregularis* AOX Gene. *PLoS One* 10:e0142339. doi: 10.1371/journal.pone.0142339

Campos-Soriano, L., García-Garrido, J. M., and Segundo, B. S. (2010). Activation of basal defense mechanisms of rice plants by *Glomus intraradices* does not affect the arbuscular mycorrhizal symbiosis. *New Phytol.* 188, 597–614. doi: 10.1111/j.1469-8137.2010.03386.x

Cao, F. Y., Yoshioka, K., and Desveaux, D. (2011). The roles of ABA in plant–pathogen interactions. *J. Plant Res.* 124, 489–499. doi: 10.1007/s10265-011-0409-y

Carvalhais, L. C., Dennis, P. G., Fedoseyenko, D., Hajirezaei, M. R., Borriss, R., and von Wirén, N. (2011). Root exudation of sugars, amino acids, and organic acids by maize as affected by nitrogen, phosphorus, potassium, and iron deficiency. *J. Plant Nutr. Soil Sci.* 174, 3–11. doi: 10.1002/jpln.201000085

Chanclud, E., and Morel, J. B. (2016). Plant hormones: a fungal point of view. *Mol. Plant Pathol.* 17, 1289–1297. doi: 10.1111/mpp.12393

Chanda, B., Xia, Y., Mandal, M. K., Yu, K., Sekine, K. T., Gao, Q. M., et al. (2011). Glycerol-3-phosphate is a critical mobile inducer of systemic immunity in plants. *Nat. Genet.* 43, 421–427. doi: 10.1038/ng.798

Charpentier, M., Sun, J., Wen, J., Mysore, K. S., and Oldroyd, G. E. (2014). Abscisic acid promotion of arbuscular mycorrhizal colonization requires a component of the protein phosphatase 2A complex. *Plant Physiol.* 166, 2077–2090. doi: 10.1104/pp.114.246371

Cheeseman, J. M. (2007). Hydrogen peroxide and plant stress: a challenging relationship. *Plant Stress* 1, 4–15. doi: 10.1371/journal.pone.0023776

Cheng, W. H., Endo, A., Zhou, L., Penney, J., Chen, H. C., Arroyo, A., et al. (2002). A unique short-chain dehydrogenase/reductase in Arabidopsis glucose signaling and abscisic acid biosynthesis and functions. *Plant Cell* 14, 2723–2743. doi: 10.1105/tpc.006494

Choi, H., Hong, J., Ha, J., Kang, J., and Kim, S. Y. (2000). ABFs, a family of ABA–responsive element binding factors. *J. Biol. Chem.* 275, 1723–1730. doi: 10.1074/jbc.275.3.1723

Claeys, H., De Bodt, S., and Inzé, D. (2014). Gibberellins and DELLAs: central nodes in growth regulatory networks. *Trends Plant Sci.* 19, 231–239. doi: 10.1016/j.tplants.2013.10.001

Clifton, R., Millar, A. H., and Whelan, J. (2006). Alternative oxidases in Arabidopsis: a comparative analysis of differential expression in the gene family provides new insights into function of non-phosphorylating bypasses. *Biochim. Biophys. Acta Bioenerg.* 1757, 730–741. doi: 10.1016/j.bbabio.2006.03.009

Conrath, U., Beckers, G. J., Flors, V., García-Agustín, P., Jakab, G., Mauch, F., et al. (2006). Priming: getting ready for battle. *Mol. Plant Microbe Interact.* 19, 1062–1071. doi: 10.1094/MPMI-19-1062

Cosme, M., Ramireddy, E., Franken, P., Schmülling, T., and Wurst, S. (2016). Shoot-and root-borne cytokinin influences arbuscular mycorrhizal symbiosis. *Mycorrhiza* 26, 709–720. doi: 10.1007/s00572-016-0706-3

Cosme, M., and Wurst, S. (2013). Interactions between arbuscular mycorrhizal fungi, rhizobacteria, soil phosphorus and plant cytokinin deficiency change the root morphology, yield and quality of tobacco. *Soil Biol. Biochem.* 57, 436–443. doi: 10.1016/j.soilbio.2012.09.024

Costa, H. S., Ríos-Ruiz, W. F., and Lambais, M. R. (2000). Salicylic acid inhibits arbuscular mycorrhyzae formation and changes chitinase and b-1, 3-glucanase expression in bean roots. *Sci. Agricola* 57, 19–25. doi: 10.1590/S0103-90162000000100005

Creelman, R. A., and Mullet, J. E. (1997). Biosynthesis and action of jasmonates in plants. *Annu. Rev. Plant Biol.* 48, 355–381. doi: 10.1146/annurev.arplant.48.1.355

Cunningham, D. J. C. (1963). Some quantitative aspects of the regulation of human respiration in exercise. *Br. Med. Bull.* 19, 25–30. doi: 10.1093/oxfordjournals.bmb.a070000

Cutler, S. R., Rodriguez, P. L., Finkelstein, R. R., and Abrams, S. R. (2010). Abscisic acid: emergence of a core signalling network. *Ann. Rev. Plant Biol.* 61, 651–679. doi: 10.1146/annurev-arplant-042809-112122

Dakora, F. D., and Phillips, D. A. (2002). Root exudates as mediators of mineral acquisition in low-nutrient environments. *Plant Soil* 245, 35–47. doi: 10.1023/A:1020809400075

Davière, J. M., and Achard, P. (2013). Gibberellin signaling in plants. *Development* 140, 1147–1151. doi: 10.1242/dev.087650

Davies, F. T. Jr., Calderón, C. M., Huaman, Z., and Gómez, R. (2005). Influence of a flavoinoid (formononetin) on mycorrhizal activity and potato crop productivity in the highlands of Peru. *Sci. Hortic.* 106, 318–329. doi: 10.1016/j.scienta.2005.04.013

Davies, F. T., Egilla, J. N., Miller, J. C. Jr., and Saraiva Grossi, J. A. (1999). Influence of mycorrhiza and an isoflavonoid on plant growth and gas exchange of potatoes started from minitubers. *Hortscience* 34:498.

Day, D., Millar, A. H., and Whelan, J. (2004). *Advances in Photosynthesis and Respiration, vol 17: Plant mitochondria: From Genome to Function*. Dordrecht: Kluwer Academic Publishers. doi: 10.1007/978-1-4020-2400-9

de Miranda, J. C. C., and Harris, P. J. (1994). The effect of soil phosphorus on the external mycelium growth of arbuscular mycorrhizal fungi during the early stages of mycorrhiza formation. *Plant Soil* 166, 271–280. doi: 10.1007/BF00008340

de Ollas, C., Arbona, V., and Gómez-Cadenas, A. (2015). Jasmonoyl isoleucine accumulation is needed for abscisic acid build-up in roots of Arabidopsis under water stress conditions. *Plant Cell Environ.* 38, 2157–2170. doi: 10.1111/pce.12536

de Ollas, C., and Dodd, I. C. (2016). Physiological impacts of ABA-JA interactions under water-limitation. *Plant Mol. Biol.* 91, 641–650. doi: 10.1007/s11103-016-0503-6

de Román, M., Fernández, I., Wyatt, T., Sahrawy, M., Heil, M., and Pozo, M. J. (2011). Elicitation of foliar resistance mechanisms transiently impairs root association with arbuscular mycorrhizal fungi. *J. Ecol.* 99, 36–45. doi: 10.1111/j.1365-2745.2010.01752.x

De Vleesschauwer, D., Cornelis, P., and Höfte, M. (2006). Redox-Active pyocyanin secreted by *Pseudomonas aeruginosa* 7NSK2 triggers systemic resistance to *Magnaporthe grisea* but enhances *Rhizoctonia solani* susceptibility in rice. *Mol. Plant Microbe Interact.* 19, 1406–1419. doi: 10.1094/MPMI-19-1406

De Vleesschauwer, D., Van Buyten, E., Satoh, K., Balidion, J., Mauleon, R., Choi, I. R., et al. (2012). Brassinosteroids antagonize gibberellin- and salicylate-mediated root immunity in rice. *Plant Physiol.* 158, 1833–1846. doi: 10.1104/pp.112.193672

Delaney, T. P., Uknes, S., Vernooij, B., Friedrich, L., Weymann, K., Negrotto, D., et al. (1994). A central role of salicylic acid in plant disease resistance. *Science* 266, 1247–1250. doi: 10.1126/science.266.5188.1247

Del-Saz, N. F., Romero-Munar, A., Alonso, D., Aroca, R., Baraza, E., Flexas, J., et al. (2017). Respiratory ATP cost and benefit of arbuscular mycorrhizal symbiosis with *Nicotiana tabacum* at different growth stages and under salinity. *J. Plant Physiol.* 218, 243–248. doi: 10.1016/j.jplph.2017.08.012

Del-Saz, N. F., Romero-Munar, A., Cawthray, G. R., Palma, F., Aroca, R., Baraza, E., et al. (2018). Phosphorus concentration coordinates a respiratory bypass, synthesis and exudation of citrate, and the expression of high-affinity phosphorus transporters in Solanum lycopersicum. *Plant Cell Environ.* 41, 865–875. doi: 10.1111/pce.13155

Devaiah, B. N., Madhuvanthi, R., Karthikeyan, A. S., and Raghothama, K. G. (2009). Phosphate starvation responses and gibberellic acid biosynthesis are regulated by the MYB62 transcription factor in Arabidopsis. *Mol. Plant* 2, 43–58. doi: 10.1093/mp/ssn081

Drew, M. C., He, C. J., and Morgan, P. W. (1989). Decreased ethylene biosynthesis, and induction of aerenchyma, by nitrogen- or phosphate-starvation in adventitious roots of *Zea mays* L. *Plant Physiol.* 91, 266–271. doi: 10.1007/s11104-009-0150-7

Drissner, D., Kunze, G., Callewaert, N., Gehrig, P., Tamasloukht, M. B., Boller, T., et al. (2007). Lyso-phosphatidylcholine is a signal in the arbuscular mycorrhizal symbiosis. *Science* 318, 265–268. doi: 10.1126/science.1146487

Dumas-Gaudot, E., Gollotte, A., Cordier, C., Gianinazzil, S., and Gianinazzi-Pearson, V. (2000). "Modulation of host defence systems," in *Arbuscular mycorrhizas: Physiology and Function*, eds Y. Kapulnik and D. D. Douds (Dordrecht: Springer Science+Business Media), 173–200. doi: 10.1007/BF02257526

Dumas-Gaudot, E., Slezack, S., Dassi, B., Pozo, M. J., Gianinazzi-Pearson, V., and Gianinazzi, S. (1996). Plant hydrolytic enzymes (chitinases and β-1, 3-glucanases) in root reactions to pathogenic and symbiotic microorganisms. *Plant Soil* 185, 211–221. doi: 10.1007/BF02257526

Durrant, W. E., and Dong, X. (2004). Systemic acquired resistance. *Annu. Rev. Phytopathol.* 42, 185–209. doi: 10.1146/annurev.phyto.42.040803.140421

Dutra, P. V., Abad, M., Almela, V., and Agusti, M. (1996). Auxin interaction with the vesicular-arbuscular mycorrhizal fungus *Glomus intraradices* Schenck & Smith improves vegetative growth of two citrus rootstocks. *Sci. Hortic.* 66, 77–83. doi: 10.1016/0304-4238(96)00887-4

Edreva, A. (2005). Pathogenesis-related proteins: research progress in the last 15 years. *Gen. Appl. Plant Physiol.* 31, 105–124.

El Ghachtouli, N., Martin-Tanguy, J., Paynot, M., and Gianinazzi, S. (1996). First report of the inhibition of arbuscular mycorrhizal infection of *Pisum sativum* by specific and irreversible inhibition of polyamine biosynthesis or by gibberellic acid treatment. *FEBS Lett.* 385, 189–192. doi: 10.1016/0014-5793(96)00379-1

El Ghachtouli, N., Paynot, M., Morandi, D., Martin-Tanguy, J., and Gianinazzi, S. (1995). The effect of polyamines on endomycorrhizal infection of wild-type *Pisum sativum*, cv. Frisson (nod^+myc^+) and two mutants (nod^-myc^+ and nod^-myc^-). *Mycorrhiza* 5, 189–192. doi: 10.1007/s005720050058

El-Showk, S., Ruonala, R., and Helariutta, Y. (2013). Crossing paths: cytokinin signalling and crosstalk. *Development* 140, 1373–1383. doi: 10.1242/dev.086371

Eraslan, F., Inal, A., Pilbeam, D. J., and Gunes, A. (2008). Interactive effects of salicylic acid and silicon on oxidative damage and antioxidant activity in spinach (*Spinacia oleracea* L. cv. Matador) grown under boron toxicity and salinity. *Plant Growth Regul.* 55:207. doi: 10.1007/s10725-008-9277-4

Esch, H., Hundeshagen, B., Schneider-Poetsch, H. J., and Bothe, H. (1994). Demonstration of abscisic acid in spores and hyphae of the arbuscular-mycorrhizal fungus Glomus and in the N2-fixing cyanobacterium *Anabaena variabilis*. *Plant Sci.* 99, 9–16. doi: 10.1016/0168-9452(94)90115-5

Etemadi, M., Gutjahr, C., Couzigou, J.-M., Zouine, M., Lauressergues, D., Timmers, A., et al. (2014). Auxin perception is required for arbuscule development in arbuscular mycorrhizal symbiosis. *Plant Physiol.* 166, 281–292. doi: 10.1104/pp.114.246595

Faessel, L., Nassr, N., Lebeau, T., and Walter, B. (2010). Chemically-induced resistance on soybean inhibits nodulation and mycorrhization. *Plant Soil* 329, 259–268. doi: 10.1007/s11104-009-0150-7

Fan, X. W., Li, F. M., Song, L., Xiong, Y. C., An, L. Z., Jia, Y., et al. (2009). Defense strategy of old and modern spring wheat varieties during soil drying. *Physiol. Plant.* 136, 310–323. doi: 10.1111/j.1399-3054.2009.01225.x

Fariduddin, Q., Hayat, S., and Ahmad, A. (2003). Salicylic acid influences net photosynthetic rate, carboxylation efficiency, nitrate reductase activity, and seed yield in *Brassica juncea*. *Photosynthetica* 41, 281–284. doi: 10.1023/B:PHOT.0000011962.05991.6c

Fernández Suárez, K., Pérez Ortega, E., and Medina García, L. R. (2015). La kinetina ribósido como estimulador de la germinación In Vitro de esporas de *Glomus clarum*. *Cultivos Trop.* 36, 45–49.

Fester, T., and Hause, G. (2005). Accumulation of reactive oxygen species in arbuscular mycorrhizal roots. *Mycorrhiza* 15, 373–379. doi: 10.1007/s00572-005-0363-4

Finkelstein, R. R., Wang, M. L., Lynch, T. J., Rao, S., and Goodman, H. M. (1998). The Arabidopsis abscisic acid response locus ABI4 encodes an APETALA 2 domain protein. *Plant Cell* 10, 1043–1054. doi: 10.1105/tpc.10.6.1043

Fiorilli, V., Catoni, M., Miozzi, L., Novero, M., Accotto, G. P., and Lanfranco, L. (2009). Global and cell-type gene expression profiles in tomato plants colonized by an arbuscular mycorrhizal fungus. *New Phytol.* 184, 975–987. doi: 10.1111/j.1469-8137.2009.03031.x

Florez-Sarasa, I., Lambers, H., Wang, X., Finnegan, P. M., and Ribas-Carbó, M. (2014). The alternative respiratory pathway mediates carboxylate synthesis in white lupin cluster roots under phosphorus deprivation. *Plant Cell Environ.* 37, 922–928. doi: 10.1111/pce.12208

Floss, D. S., Levy, J. G., Lévesque-Tremblay, V., Pumplin, N., and Harrison, M. J. (2013). DELLA proteins regulate arbuscule formation in arbuscular mycorrhizal symbiosis. *Proc. Natl. Acad. Sci. U.S.A.* 110, E5025–E5034. doi: 10.1073/pnas.1308973110

Foo, E. (2013). Auxin influences strigolactones in pea mycorrhizal symbiosis. *J. Plant Physiol.* 170, 523–528. doi: 10.1016/j.jplph.2012.11.002

Foo, E., Bullier, E., Goussot, M., Foucher, F., Rameau, C., and Beveridge, C. A. (2005). The branching gene RAMOSUS1 mediates interactions among two novel signals and auxin in pea. *Plant Cell* 17, 464–474. doi: 10.1105/tpc.104.026716

Foo, E., McAdam, E. L., Weller, J. L., and Reid, J. B. (2016). Interactions between ethylene, gibberellins, and brassinosteroids in the development of rhizobial and mycorrhizal symbioses of pea. *J. Exp. Bot.* 67, 2413–2424. doi: 10.1093/jxb/erw047

Foo, E., Ross, J. J., Jones, W. T., and Reid, J. B. (2013a). Plant hormones in arbuscular mycorrhizal symbioses: an emerging role for gibberellins. *Ann. Bot.* 111, 767–779. doi: 10.1093/aob/mct041

Foo, E., Yoneyama, K., Hugill, C. J., Quittenden, L. J., and Reid, J. B. (2013b). Strigolactones and the regulation of pea symbioses in response to nitrate and phosphate deficiency. *Mol. Plant* 6, 76–87. doi: 10.1093/mp/sss115

Fracetto, G. G., Peres, L. E., Mehdy, M. C., and Lambais, M. R. (2013). Tomato ethylene mutants exhibit differences in arbuscular mycorrhiza development and levels of plant defense-related transcripts. *Symbiosis* 60, 155–167. doi: 10.1007/s13199-013-0251-1

Fracetto, G. G. M., Peres, L. E. P., and Lambais, M. R. (2017). Gene expression analyses in tomato near isogenic lines provide evidence for ethylene and abscisic acid biosynthesis fine-tuning during arbuscular mycorrhiza development. *Arch. Microbiol.* 199, 787–798. doi: 10.1007/s00203-017-1354-5

Franco-Zorrilla, J. M., Martín, A. C., Leyva, A., and Paz-Ares, J. (2005). Interaction between phosphate-starvation, sugar, and cytokinin signaling in Arabidopsis and the roles of cytokinin receptors CRE1/AHK4 and AHK31. *Plant Physiol.* 138, 847–857. doi: 10.1104/pp.105.060517

Franco-Zorrilla, J. M., Martín, A. C., Solano, R., Rubio, V., Leyva, A., and Paz-Ares, J. (2002). Mutations at CRE1 impair cytokinin-induced repression of phosphate starvation responses in Arabidopsis. *Plant J.* 32, 353–360.

Fredeen, A. L., Raab, T. K., Rao, I. M., and Terry, N. (1990). Effects of phosphorus nutrition on photosynthesis in *Glycine max* (L.) Merr. *Planta* 181, 399–405. doi: 10.1007/BF00195894

Fries, L. L. M., Pacovsky, R. S., Safir, G. R., and Siqueira, J. O. (1997). Plant growth and arbuscular mycorrhizal fungal colonization affected by exogenously applied phenolic compounds. *J. Chem. Ecol.* 23, 1755–1767. doi: 10.1023/B:JOEC.0000006449.09141.cd

Fu, X., and Harberd, N. P. (2003). Auxin promotes Arabidopsis root growth by modulating gibberellin response. *Nature* 421, 740–743. doi: 10.1038/nature01387

Fusconi, A. (2014). Regulation of root morphogenesis in arbuscular mycorrhizae: what role do fungal exudates, phosphate, sugars and hormones play in lateral root formation? *Ann. Bot.* 113, 19–33. doi: 10.1093/aob/mct258

Gachomo, E., Allen, J. W., Pfeffer, P. E., Govindarajulu, M., Douds, D. D., Jin, H. R., et al. (2009). Germinating spores of Glomus intraradices can use internal and exogenous nitrogen sources for de novo biosynthesis of amino acids. *New Phytol.* 184, 399–411. doi: 10.1111/j.1469-8137.2009.02968.x

Gandin, A., Lapointe, L., and Dizengremel, P. (2009). The alternative respiratory pathway allows sink to cope with changes in carbon availability in the sink-limited plant Erythronium americanum. *J. Exp. Bot.* 60, 4235–4248. doi: 10.1093/jxb/erp255

García-Garrido, J. M., León-Morcillo, R. J., Martín-Rodríguez, J. Á, and Ocampo, J. A. (2010). Variations in the mycorrhization characteristics in roots of wild-type and ABA-deficient tomato are accompanied by specific transcriptomic alterations. *Mol. Plant Microbe Interact.* 23, 651–664. doi: 10.1094/MPMI-23-5-0651

García-Garrido, J. M., and Ocampo, J. A. (2002). Regulation of the plant defence response in arbuscular mycorrhizal symbiosis. *J. Exp. Bot.* 53, 1377–1386. doi: 10.1093/jexbot/53.373.1377

Garg, N., and Bharti, A. (2018). Salicylic acid improves arbuscular mycorrhizal symbiosis, and chickpea growth and yield by modulating carbohydrate metabolism under salt stress. *Mycorrhiza* 28, 1–20. doi: 10.1007/s00572-018-0856-6

Geil, R. D., and Guinel, F. C. (2002). Effects of elevated substrate ethylene on colonization of leek (*Allium porrum*) by the arbuscular mycorrhizal fungus *Glomus aggregatum*. *Rev. Can. Bot.* 80, 114–119. doi: 10.1139/b01-135

Geil, R. D., Peterson, L. R., and Guinel, F. C. (2001). Morphological alterations of pea (*Pisum sativum* cv. Sparkle) arbuscular mycorrhizas as a result of exogenous ethylene treatment. *Mycorrhiza* 11, 137–143. doi: 10.1007/s005720100120

Genre, A., Chabaud, M., Balzergue, C., Puech-Pagès, V., Novero, M., Rey, T., et al. (2013). Short-chain chitin oligomers from arbuscular mycorrhizal fungi trigger nuclear Ca^{2+} spiking in *Medicago truncatula* roots and their production is enhanced by strigolactone. *New Phytol.* 198, 190–202. doi: 10.1111/nph.12146

Ghannoum, O., and Conroy, J. P. (2007). Phosphorus deficiency inhibits growth in parallel with photosynthesis in a C3 (*Panicum laxum*) but not two C4 (*P. coloratum* and *Cenchrus ciliaris*) grasses. *Funct. Plant Biol.* 34, 72–81. doi: 10.1071/FP06253

Ghosh, D., and Xu, J. (2014). Abiotic stress responses in plant roots: a proteomics perspective. *Front. Plant Sci.* 5:6. doi: 10.3389/fpls.2014.00006

Giraud, E., Van Aken, O., Ho, L. H., and Whelan, J. (2009). The transcription factor ABI4 is a regulator of mitochondrial retrograde expression of alternative oxidase1a. *Plant Physiol.* 150, 1286–1296. doi: 10.1104/pp.109.139782

Gobbato, E., Marsh, J. F., Vernié, T., Wang, E., Maillet, F., Kim, J., et al. (2012). A GRAS-type transcription factor with a specific function in mycorrhizal signaling. *Curr. Biol.* 22, 2236–2241. doi: 10.1016/j.cub.2012.09.044

Gomez-Casanovas, N., Blanc-Betes, E., Gonzàlez-Meler, M. A., and Azcon-Bieto, J. (2007). Changes in respiratory mitochondrial machinery and cytochrome and alternative pathway activities in response to energy demand underlie the acclimation of respiration to elevated CO_2 in the invasive *Opuntia ficus-indica*. *Plant Physiol.* 145, 49–61. doi: 10.1104/pp.107.103911

Gomez-Roldan, V., Fermas, S., Brewer, P. B., Puech-Pagès, V., Dun, E. A., Pillot, J. P., et al. (2008). Strigolactone inhibition of shoot branching. *Nature* 455, 189–194. doi: 10.1038/nature07271

Gomez-Roldan, V., Roux, C., Girard, D., Bécard, G., and Puech-Pagès, V. (2007). Strigolactones: promising plant signals. *Plant Signal. Behav.* 2, 163–164. doi: 10.4161/psb.2.3.3689

Gonzàlez-Meler, M. A., Ribas-Carbó, M., Siedow, J. N., and Drake, B. G. (1996). Direct inhibition of plant mitochondrial respiration by elevated CO_2. *Plant Physiol.* 112, 1349–1355. doi: 10.1104/pp.112.3.1349

Graham, J. H., Leonard, R. T., and Menge, J. A. (1981). Membrane-mediated decrease in root exudation responsible for phorphorus inhibition of vesicular-arbuscular mycorrhiza formation. *Plant Physiol.* 68, 548–552. doi: 10.1104/pp.68.3.548

Greenboim-Wainberg, Y., Maymon, I., Borochov, R., Alvarez, J., Olszewski, N., Ori, N., et al. (2005). Cross talk between gibberellin and cytokinin: the Arabidopsis GA response inhibitor SPINDLY plays a positive role in cytokinin signalling. *Plant Cell* 17, 92–102. doi: 10.1105/tpc.104.028472

Grossmann, K. (2003). Mediation of herbicide effects by hormone interaction. *J. Plant Growth Regul.* 22, 109–122. doi: 10.1007/s00344-003-0020-0

Großkinsky, D. K., van der Graaff, E., and Roitsch, T. (2014). Abscisic acid-cytokinin antagonism modulates resistance against *Pseudomonas syringae* in tobacco. *Phytopathology* 104, 1283–1288. doi: 10.1094/PHYTO-03-14-0076-R

Gryndler, M., Hršelová, H., Chvátalová, I., and Jansa, J. (1998). The effect of selected plant hormones on in vitro proliferation of hyphae of *Glomus fistulosum*. *Biol. Plant.* 41, 255–263. doi: 10.1023/A:1001874832669

Gu, M., Chen, A., Dai, X., Liu, W., and Xu, G. (2011). How does phosphate status influence the development of the arbuscular mycorrhizal symbiosis? *Plant Signal. Behav.* 6, 1300–1304. doi: 10.4161/psb.6.9.16365

Guan, C. M., Wang, X. C., Feng, J., Hong, S. L., Liang, Y., Ren, B., et al. (2014). Cytokinin antagonizes abscisic acid-mediated inhibition of cotyledon greening by promoting the degradation of abscisic acid insensitive5 protein in Arabidopsis. *Plant Physiol.* 164, 1515–1526. doi: 10.1104/pp.113.234740

Guillotin, B., Etemadi, M., Audran, C., Bouzayen, M., Bécard, G., and Combier, J. P. (2017). Sl-IAA27 regulates strigolactone biosynthesis and mycorrhization in tomato (var. *MicroTom*). *New Phytol.* 213, 1124–1132. doi: 10.1111/nph.14246

Güimil, S., Chang, H. S., Zhu, T., Sesma, A., Osbourn, A., Roux, C., et al. (2005). Comparative transcriptomics of rice reveals an ancient pattern of response to microbial colonization. *Proc. Natl. Acad. Sci. U.S.A.* 102, 8066–8070. doi: 10.1073/pnas.0502999102

Gupta, K. J., Shah, J. K., Brotman, Y., Jahnke, K., Willmitzer, L., Kaiser, W. M., et al. (2012). Inhibition of aconitase by nitric oxide leads to induction of the alternative oxidase and to a shift of metabolism towards biosynthesis of amino acids. *J. Exp. Bot.* 63, 1773–1784. doi: 10.1093/jxb/ers053

Gutjahr, C. (2014). Phytohormone signalling in arbuscular mycorrhiza development. *Curr. Opin. Plant Biol.* 20, 26–34. doi: 10.1016/j.pbi.2014.04.003

Gutjahr, C., Siegler, H., Haga, K., Iino, M., and Paszkowski, U. (2015). Full establishment of arbuscular mycorrhizal symbiosis in rice occurs independently of enzymatic jasmonate biosynthesis. *PLoS One* 10:e0123422. doi: 10.1371/journal.pone.0123422

Ha, S., and Tran, L. S. (2014). Understanding plant responses to phosphorus starvation for improvement of plant tolerance to phosphorus deficiency by biotechnological approaches. *Crit. Rev. Biotechnol.* 34, 16–30. doi: 10.3109/07388551.2013.783549

Hammond, J. P., Broadley, M. R., and White, P. J. (2004). Genetic responses to phosphorus deficiency. *Ann. Bot.* 94, 323–332. doi: 10.1093/aob/mch156

Hammond, J. P., and White, P. J. (2011). Sugar signaling in root responses to low phosphorus availability. *Plant Physiol.* 156, 1033–1040. doi: 10.1104/pp.111.175380

Hanlon, M. T., and Coenen, C. (2011). Genetic evidence for auxin involvement in arbuscular mycorrhiza initiation. *New Phytol.* 189, 701–709. doi: 10.1111/j.1469-8137.2010.03567.x

Haq, B. U. I., Ahmad, M. Z., ur Rehman, N., Wang, J., Li, P., Li, D., et al. (2017). Functional characterization of soybean strigolactone biosynthesis and signaling genes in Arabidopsis MAX mutants and GmMAX3 in soybean nodulation. *BMC Plant Biol.* 17:259. doi: 10.1186/s12870-017-1182-4

Harberd, N. P. (2003). Relieving DELLA restraint. *Science* 299, 1853–1854. doi: 10.1126/science.1083217

Hause, B., and Fester, T. (2005). Molecular and cell biology of arbuscular mycorrhizal symbiosis. *Planta* 221, 184–196. doi: 10.1007/s00425-004-1436-x

Hause, B., Mrosk, C., Isayenkov, S., and Strack, D. (2007). Jasmonates in arbuscular mycorrhizal interactions. *Phytochemistry* 68, 101–110. doi: 10.1016/j.phytochem.2006.09.025

Heinrich, M., Hettenhausen, C., Lange, T., Wünsche, H., Fang, J., Baldwin, I. T., et al. (2013). High levels of jasmonic acid antagonize the biosynthesis of gibberellins and inhibit the growth of *Nicotiana attenuata* stems. *Plant J.* 73, 591–606. doi: 10.1111/tpj.12058

Helber, N., Wippel, K., Sauer, N., Schaarschmidt, S., Hause, B., and Requena, N. (2011). A versatile monosaccharide transporter that operates in the arbuscular mycorrhizal fungus Glomus sp is crucial for the symbiotic relationship with plants. *Plant Cell* 23, 3812–3823. doi: 10.1105/tpc.111.089813

Hepper, C. M., and Jakobsen, I. (1983). Hyphal growth from spores of the mycorrhizal fungus *Glomus caledonius*: effect of amino acids. *Soil Biol. Biochem.* 15, 55–58. doi: 10.1016/0038-0717(83)90119-0

Herbik, A., Giritch, A., Horstmann, C., Becker, R., Balzer, H. J., Baumlein, H., et al. (1996). Iron and copper nutrition-dependent changes in protein expression in a tomato wild type and the nicotianamine-free mutant chloronerva. *Plant Physiol.* 111, 533–540. doi: 10.1104/pp.111.2.533

Hernández, G., Ramírez, M., Valdés-López, O., Tesfaye, M., Graham, M. A., Czechowski, T., et al. (2007). Phosphorus stress in common bean: root transcript and metabolic responses. *Plant Physiol.* 144, 752–767. doi: 10.1104/pp.107.096958

Herrera-Medina, M. J., Gagnon, H., Piché, Y., Ocampo, J. A., García-Garrido, J. M., and Vierheilig, H. (2003). Root colonization by arbuscular mycorrhizal fungi is affected by the salicylic acid content of the plant. *Plant Sci.* 164, 993–998. doi: 10.1016/S0168-9452(03)00083-9

Herrera-Medina, M. J., Steinkellner, S., Vierheilig, H., Ocampo, J. A., and García-Garrido, J. M. (2007). Abscisic acid determines arbuscule development and functionality in the tomato arbuscular mycorrhiza. *New Phytol.* 175, 554–564. doi: 10.1111/j.1469-8137.2007.02107.x

Herrera-Medina, M. J., Tamayo, M. I., Vierheilig, H., Ocampo, J. A., and García-Garrido, J. M. (2008). The jasmonic acid signalling pathway restricts the development of the arbuscular mycorrhizal association in tomato. *J. Plant Growth Regul.* 27, 221–230. doi: 10.1007/s00344-008-9049-4

Hilou, A., Zhang, H., Franken, P., and Hause, B. (2014). Do jasmonates play a role in arbuscular mycorrhiza-induced local bioprotection of *Medicago truncatula* against root disease caused by *Aphanomyces euteiches*? *Mycorrhiza* 24, 45–54. doi: 10.1007/s00572-013-0513-z

Ho, L. H., Giraud, E., Uggalla, V., Lister, R., Clifton, R., Glen, A., et al. (2008). Identification of regulatory pathways controlling gene expression of stress-responsive mitochondrial proteins in Arabidopsis. *Plant Physiol.* 147, 1858–1873. doi: 10.1104/pp.108.121384

Hoefnagels, M. H., Broome, S. W., and Shafer, S. R. (1993). Vesicular-arbuscular mycorrhizae in salt marshes in North Carolina. *Estuaries* 16, 851–858. doi: 10.2307/1352444

Hoffland, E., Boogaard, R., Nelemans, J. A. A. P., and Findenegg, G. (1992). Biosynthesis and root exudation of citric and malic acids in phosphate-starved rape plants. *New Phytol.* 122, 675–680. doi: 10.1111/j.1469-8137.1992.tb00096.x

Horgan, J. M., and Wareing, P. F. (1980). Cytokinins and the growth responses of seedlings of *Betula pendula* Roth. And *Acer pseudoplatanus* L. to nitrogen and phosphorus deficiency. *J. Exp. Bot.* 31, 525–532. doi: 10.1093/jxb/31.2.525

Howe, G. A. (2004). Jasmonates as signals in the wound response. *J. Plant Growth Regul.* 23, 223–237. doi: 10.1007/s00344-004-0030-6

Ijdo, M., Cranenbrouck, S., and Declerck, S. (2011). Methods for large-scale production of AM fungi: past, present, and future. *Mycorrhiza* 21, 1–16. doi: 10.1007/s00572-010-0337-z

Illana, A., García-Garrido, J. M., Sampedro, I., Ocampo, J. A., and Vierheilig, H. (2011). Strigolactones seem not to be involved in the nonsusceptibilty of arbuscular mycorrhizal (AM) nonhost plants to AM fungi. *Botanique* 89, 285–288. doi: 10.1139/b11-014

Isayenkov, S., Mrosk, C., Stenzel, I., Strack, D., and Hause, B. (2005). Suppression of allene oxide cyclase in hairy roots of *Medicago truncatula* reduces jasmonate levels and the degree of mycorrhization with *Glomus intraradices*. *Plant Physiol.* 139, 1401–1410. doi: 10.1104/pp.105.069054

Ishii, T., Shrestha, Y. H., Matsumoto, I., and Kadoya, K. (1996). Effect of ethylene on the growth of vesicular-arbuscular mycorrhizal fungi and on the mycorrhizal formation of trifoliate orange roots. *J. Jpn. Soc. Hortic. Sci.* 65, 525–529. doi: 10.2503/jjshs.65.525

Ito, S., Yamagami, D., Umehara, M., Hanada, A., Yoshida, S., Sasaki, Y., et al. (2017). Regulation of strigolactone biosynthesis by gibberellin signaling. *Plant Physiol.* 174, 1250–1259. doi: 10.1104/pp.17.0030

Jentschel, K., Thiel, D., Rehn, D., and Ludwig-Müller, J. (2007). Arbuscular mycorrhiza enhances auxin levels and alters auxin biosynthesis in *Tropaeolum majus* during early stages of colonization. *Physiol. Plant.* 129, 320–333. doi: 10.1111/j.1399-3054.2006.00812.x

Jiang, C., Gao, X., Liao, L., Harberd, N. P., and Fu, X. (2007). Phosphate starvation root architecture and anthocyanin accumulation responses are modulated by the gibberellin-DELLA signalling pathway in Arabidopsis. *Plant Physiol.* 145, 1460–1470. doi: 10.1104/pp.107.103788

Jiang, C. J., Shimono, M., Sugano, S., Kojima, M., Yazawa, K., Yoshida, R., et al. (2010). Abscisic acid interacts antagonistically with salicylic acid signalling pathway in rice–*Magnaporthe grisea* interaction. *Mol. Plant Microbe Interact.* 23, 791–798. doi: 10.1094/MPMI-23-6-0791

Jiang, Y., Xie, Q., Wang, W., Yang, J., Zhang, X., Yu, N., et al. (2018). Medicago AP2-domain transcription factor WRI5a is a master regulator of lipid biosynthesis and transfer during mycorrhizal symbiosis. *Mol. Plant* 10, 1–16. doi: 10.1016/j.molp.2018.09.006

Johnson, X., Brcich, T., Dun, E. A., Goussot, M., Haurogné, K., Beveridge, C. A., et al. (2006). Branching genes are conserved across species. Genes controlling a novel signal in pea are coregulated by other long-distance signals. *Plant Physiol.* 142, 1014–1026. doi: 10.1104/pp.106.087676

Jones, J. M., Clairmont, L., Macdonald, E. S., Weiner, C. A., Emery, R. N., and Guinel, F. C. (2015). E151 (sym15), a pleiotropic mutant of pea (*Pisum sativum* L.), displays low nodule number, enhanced mycorrhizae, delayed lateral root emergence, and high root cytokinin levels. *J. Exp. Bot.* 66, 4047–4059. doi: 10.1093/jxb/erv201

Juszczuk, I., Malusà, E., and Rychter, A. M. (2001). Oxidative stress during phosphate deficiency in roots of bean plants (*Phaseolus vulgaris* L.). *J. Plant Physiol.* 158, 1299–1305. doi: 10.1078/0176-1617-00541

Juszczuk, I. M., and Rychter, A. M. (2003). Alternative oxidase in higher plants. *Acta Biochim. Polon. English Edn.* 50, 1257–1272.

Kaldorf, M., and Ludwig-Müller, J. (2000). AM fungi might affect the root morphology of maize by increasing indole-3-butyric acid biosynthesis. *Physiol. Plant.* 109, 58–67. doi: 10.1034/j.1399-3054.2000.100109.x

Kaplan, I. (2012). Attracting carnivorous arthropods with plant volatiles: the future of biocontrol or playing with fire. *Biol. Control* 60, 77–89. doi: 10.1016/j.biocontrol.2011.10.017

Kapoor, R., Sharma, D., and Bhatnagar, A. K. (2008). Arbuscular mycorrhizae in micropropagation systems and their potential applications. *Sci. Hortic.* 116, 227–239. doi: 10.1016/j.scienta.2008.02.002

Kato-Noguchi, H. (2000). Abscisic acid and hypoxic induction of anoxia tolerance in roots of lettuce seedlings. *J. Exp. Bot.* 51, 1939–1944. doi: 10.1093/jexbot/51.352.1939

Keymer, A., Pimprikar, P., Wewer, V., Huber, C., Brands, M., Bucerius, S. L., et al. (2017). Lipid transfer from plants to arbuscular mycorrhiza fungi. *eLife* 6:e29107. doi: 10.7554/eLife.29107

Khalloufi, M., Martínez-Andújar, C., Lachaâl, M., Karray-Bouraoui, N., Pérez-Alfocea, F., and Albacete, A. (2017). The interaction between foliar GA3 application and arbuscular mycorrhizal fungi inoculation improves growth in salinized tomato (Solanum lycopersicum L.) plants by modifying the hormonal balance. *J. Plant Physiol.* 214, 134–144. doi: 10.1016/j.jplph.2017.04.012

Khan, G. A., Vogiatzaki, E., Glauser, G., and Poirier, Y. (2016). Phosphate deficiency induces the jasmonate pathway and enhances resistance to insect herbivory. *Plant Physiol.* 171, 632–644. doi: 10.1104/pp.16.00278

Khan, N. A. (2004). An evaluation of the effects of exogenous ethephon, an ethylene releasing compound, on photosynthesis of mustard (*Brassica juncea*) cultivars that differ in photosynthetic capacity. *BMC Plant Biol.* 4:21. doi: 10.1186/1471-2229-4-21

Khan, N. A. (2006). *Ethylene Action in Plants*. Berlin: Springer. doi: 10.1007/978-3-540-32846-9

Kieber, J. J., and Schaller, G. E. (2014). Cytokinins. *Arabidopsis Book* 12, e0168. doi: 10.1199/tab.0168

Kiers, E. T., Adler, L. S., Grman, E. L., and Van Der Heijden, M. G. A. (2010). Manipulating the jasmonate response: how do methyl jasmonate additions mediate characteristics of aboveground and belowground mutualisms? *Funct. Ecol.* 24, 434–443. doi: 10.1111/j.1365-2435.2009.01625.x

Kim, H. J., Lynch, J. P., and Brown, K. M. (2008). Ethylene insensitivity impedes a subset of responses to phosphorus deficiency in tomato and petunia. *Plant Cell Environ.* 31, 1744–1755. doi: 10.1111/j.1365-3040.2008.01886.x

Kobae, Y., Kameoka, H., Sugimura, Y., Saito, K., Ohtomo, R., Fujiwara, T., et al. (2018). Strigolactone biosynthesis genes of rice are required for the punctual entry of arbuscular mycorrhizal fungi into the roots. *Plant Cell Physiol.* 59, 544–553. doi: 10.1093/pcp/pcy001

Kohlen, W., Charnikhova, T., Lammers, M., Pollina, T., Tóth, P., Haider, I., et al. (2012). The tomato carotenoid cleavage dioxygenase8 (SlCCD8) regulates rhizosphere signaling, plant architecture and affects reproductive development through strigolactone biosynthesis. *New Phytol.* 196, 535–547. doi: 10.1111/j.1469-8137.2012.04265.x

Koltai, H., Dor, E., Hershenhorn, J., Joel, D. M., Weininger, S., Lekalla, S., et al. (2010). Strigolactones' effect on root growth and root-hair elongation may be mediated by auxin-efflux carriers. *J. Plant Growth Regul.* 29, 129–136. doi: 10.1007/s00344-009-9122-7

Kosová, K., Prášil, I. T., Vítámvás, P., Dobrev, P., Motyka, V., Floková, K., et al. (2012). Complex phytohormone responses during the cold acclimation of two wheat cultivars differing in cold tolerance, winter Samanta and spring Sandra. *J. Plant Physiol.* 169, 567–576. doi: 10.1016/j.jplph.2011.12.013

Kouchi, H., and Yoneyama, T. (1984). Dynamics of carbon photosynthetically assimilated in nodulated soya bean plants under steady-state conditions 1. Development and application of 13CO2 assimilation system at a constant 13C abundance. *Ann. Bot.* 53, 875–882. doi: 10.1093/oxfordjournals.aob.a086757

Krebs, H. A., and Johnson, W. A. (1937). Metabolism of ketonic acids in animal tissues. *Biochem. J.* 31, 645–660. doi: 10.1042/bj0310645

Kretzschmar, T., Kohlen, W., Sasse, J., Borghi, L., Schlegel, M., Bachelier, J. B., et al. (2012). A petunia ABC protein controls strigolactone- dependent symbiotic signalling and branching. *Nature* 483, 341–344. doi: 10.1038/nature10873

Kuć, J. (2006). "What's old and what; new in concepts of induced systemic resistance in plants, and its applications," in *Multigenic and Induced Resistance in Plants*, eds S. Tuzun and E. Bent (Boston, MA: Springer Science+Business Media), 9–20.

Kusajima, M., Yasuda, M., Kawashima, A., Nojiri, H., Yamane, H., Nakajima, M., et al. (2010). Suppressive effect of abscisic acid on systemic acquired resistance in tobacco plants. *J. Gen. Plant Pathol.* 76, 161–167. doi: 10.1007/s10327-010-0218-5

Kwak, J. M., Mori, I. C., Pei, Z. M., Leonhardt, N., Torres, M. A., Dangl, J. L., et al. (2003). NADPH oxidase AtrbohD and AtrbohF genes function in ROS-dependent ABA signaling in Arabidopsis. *EMBO J.* 22, 2623–2633. doi: 10.1093/emboj/cdg277

Lackman, P., González-Guzmán, M., Tilleman, S., Carqueijeiro, I., Pérez, A. C., Moses, T., et al. (2011). Jasmonate signalling involves the abscisic acid receptor PYL4 to regulate metabolic reprogramming in Arabidopsis and tobacco. *Proc. Natl. Acad. Sci. U.S.A.* 108, 5891–5896. doi: 10.1073/pnas.1103010108

Laffont, C., Rey, T., André, O., Novero, M., Kazmierczak, T., Debellé, F., et al. (2015). The CRE1 cytokinin pathway is differentially recruited depending on *Medicago truncatula* root environments and negatively regulates resistance to a pathogen. *PLoS One* 10:e0116819. doi: 10.1371/journal.pone.0116819

Landgraf, R., Schaarschmidt, S., and Hause, B. (2012). Repeated leaf wounding alters the colonization of Medicago truncatula roots by beneficial and pathogenic microorganisms. *Plant Cell Environ.* 35, 1344–1357. doi: 10.1111/j.1365-3040.2012.02495.x

Leakey, A. D., Ainsworth, E. A., Bernacchi, C. J., Rogers, A., Long, S. P., and Ort, D. R. (2009). Elevated CO2 effects on plant carbon, nitrogen, and water relations: six important lessons from FACE. *J. Exp. Bot.* 60, 2859–2876. doi: 10.1093/jxb/erp096

Lei, M., Zhu, C., Liu, Y., Karthikeyan, A. S., Bressan, R. A., Raghothama, K. G., et al. (2011). Ethylene signalling is involved in regulation of phosphate starvation-induced gene expression and production of acid phosphatases and anthocyanin in Arabidopsis. *New Phytol.* 189, 1084–1095. doi: 10.1111/j.1469-8137.2010.03555.x

Lemoine, R., La Camera, S., Atanassova, R., Dédaldéchamp, F., Allario, T., Pourtau, N., et al. (2013). Source-to-sink transport of sugar and regulation by environmental factors. *Front. Plant Sci.* 4:272. doi: 10.3389/fpls.2013.00272

Lennon, A. M., Neuenschwander, U. H., Ribas-Carbó, M., Giles, L., Ryals, J. A., and Siedow, J. N. (1997). The effects of salicylic acid and tobacco mosaic virus infection on the alternative oxidase of tobacco. *Plant Physiol.* 115, 783–791. doi: 10.1104/pp.115.2.783

León-Morcillo, R. J., Martín-Rodríguez, J. Á, Vierheilig, H., Ocampo, J. A., and García-Garrido, J. M. (2012). Late activation of the 9-oxylipin pathway during arbuscular mycorrhiza formation in tomato and its regulation by jasmonate signalling. *J. Exp. Bot.* 63, 3545–3558. doi: 10.1093/jxb/ers010

Li, Y., Lee, K. K., Walsh, S., Smith, C., Hadingham, S., Sorefan, K., et al. (2006). Establishing glucose- and ABA-regulated transcription networks in Arabidopsis by microarray analysis and promoter classification using a relevance vector machine. *Genome Res.* 16, 414–427. doi: 10.1101/gr.4237406

Liao, D., Wang, S., Cui, M., Liu, J., Chen, A., and Xu, G. (2018). Phytohormones regulate the development of arbuscular mycorrhizal symbiosis. *Int. J. Mol. Sci.* 19:3146. doi: 10.3390/ijms19103146

Liu, C. Y., Srivastava, A. K., and Wu, Q. S. (2014). Effect of auxin inhibitor and AMF inoculation on growth and root morphology of trifoliate orange (*Poncirus trifoliata*) seedlings. *Indian J. Agric. Sci.* 84, 1342–1346.

Liu, C. Y., Zhang, F., Zhang, D. J., Srivastava, A. K., Wu, Q. S., and Zou, Y. N. (2018). Mycorrhiza stimulates root-hair growth and IAA synthesis and transport in trifoliate orange under drought stress. *Sci. Rep.* 8:1978. doi: 10.1038/s41598-018-20456-4

Liu, J., Guo, C., Chen, Z. L., He, J. D., and Zou, Y. N. (2016). Mycorrhizal inoculation modulates root morphology and root phytohormone responses in trifoliate orange under drought stress. *Emir. J. Food Agric.* 28, 251–256. doi: 10.9755/ejfa.2015-11-1044

Liu, Z. Q., Yan, L., Wu, Z., Mei, C., Lu, K., Yu, Y. T., et al. (2012). Cooperation of three WRKY-domain transcription factors WRKY18, WRKY40, and WRKY60 in repressing two ABA-responsive genes ABI4 and ABI5 in Arabidopsis. *J. Exp. Bot.* 63, 6371–6392. doi: 10.1093/jxb/ers293

Loo, S. W., Lie, S. H., and Liu, K. Y. (1960). Studies on the physiological actions of the gibberellins. III. The effect of gibberellin on the respiration of plants. *Acta Biol. Exp. Sin. Z* 1, 109–122.

López-Bucio, J., Martínez de la Vega, O., Guevara-García, A., and Herrera-Estrella, L. (2000). Enhanced phosphorus uptake in transgenic tobacco plants that overproduce citrate. *Nat. Biotechnol.* 18, 450–453. doi: 10.1038/74531

López-Ráez, J. A., Verhage, A., Fernández, I., García, J. M., Azcón-Aguilar, C., Flors, V., et al. (2010). Hormonal and transcriptional profiles highlight common and differential host responses to arbuscular mycorrhizal fungi and the regulation of the oxylipin pathway. *J. Exp. Bot.* 61, 2589–2601. doi: 10.1093/jxb/erq089

Lu, H. (2009). Dissection of salicylic acid-mediated defense signalling networks. *Plant Signal. Behav.* 4, 713–717. doi: 10.4161/psb.4.8.9173

Lucic, E., and Mercy, L. (2014). A method of mycorrhization of plants and use of saccharides in mycorrhization. Eurpean Patent EP2982241A1.

Lucic-Mercy, E., Mercy, L., Lartigue, J., Thongo, A., Mercy, L., Hutter, I., et al. (2017). *Oligosaccharides as Signals: A New Opportunity for Promoting Mycorrhizal Development and Effectiveness in Revegetation Programs?* Dr. Dissertation, ICOM, Prague.

Ludwig-Müller, J. (2010). "Hormonal responses in host plants triggered by arbuscular mycorrhizal fungi," in *Arbuscular Mycorrhizas: Physiology and Function*, eds H. Koltai and Y. Kapulnik (Dordrecht: Springer Science + Business Media B.V), 169–190. doi: 10.1007/978-90-481-9489-6_8

Ludwig-Müller, J., Bennett, R. N., García-Garrido, J. M., Piché, Y., and Vierheilig, H. (2002). Reduced arbuscular mycorrhizal root colonization in *Tropaeolum majus* and *Carica papaya* after jasmonic acid application can not be attributed to increased glucosinolate levels. *J. Plant Physiol.* 159, 517–523. doi: 10.1078/0176-1617-00731

Ludwig-Müller, J., and Güther, M. (2007). Auxins as signals in arbuscular mycorrhiza formation. *Plant Signal. Behav.* 2, 194–196. doi: 10.4161/psb.2.3.4152

Ludwig-Müller, J., Kaldorf, M., Sutter, E. G., and Epsteind, E. (1997). Indole-3-butyric acid (IBA) is enhanced in young maize (*Zea mays* L.) roots colonized with the arbuscular mycorrhizal fungus *Glomus intraradices*. *Plant Sci.* 125, 153–162. doi: 10.1016/S0168-9452(97)00064-2

Luginbuehl, L. H., Menard, G. N., Kurup, S., Van Erp, H., Radhakrishnan, G. V., Breakspear, A., et al. (2017). Fatty acids in arbuscular mycorrhizal fungi are synthesized by the host plant. *Science* 356, 1175–1178. doi: 10.1126/science.aan0081

Lynch, T., Erikson, B. J., and Finkelstein, R. R. (2012). Direct interactions of ABA–insensitive (ABI) clade protein phosphatase (PP)2Cs with calcium–dependent protein kinases and ABA response element–binding bZIPs may contribute to turning off ABA response. *Plant Mol. Biol.* 80, 647–658. doi: 10.1007/s11103-012-9973-3

Maillet, F., Poinsot, V., André, O., Puech-Pagès, V., Haouy, A., Gueunier, M., et al. (2011). Fungal lipochitooligosaccharide symbiotic signals in arbuscular mycorrhiza. *Nature* 469, 58–63. doi: 10.1038/nature09622

Manan, F. A. (2012). *Arabidopsis thaliana Cell Suspension Culture as a Model System to Understand Plant responses Under Phosphate Stress*. Ph.D. Thesis, Faculty of natural and agricultural sciences, the University of Western Australia, Perth.

Mangnus, E. M., and Zwanenburg, B. (1992). Tentative molecular mechanism for germination stimulation of Striga and Orobanche seeds by strigol and its synthetic analogs. *J. Agric. Food Chem.* 40, 1066–1070. doi: 10.1021/jf00018a032

Manohar, M., Wang, D., Manosalva, P. M., Choi, H. W., Kombrink, E., and Klessig, D. F. (2017). Members of the abscisic acid co-receptor PP2C protein family mediate salicylic acid–abscisic acid crosstalk. *Plant Direct* 1:e00020. doi: 10.1002/pld3.20

Marschner, H. (1995). *Mineral Nutrition of Higher Plants*, 2nd Edn. London: Academic Press.

Martín-Rodríguez, J. A., Huertas, R., Ho-Plágaro, T., Ocampo, J. A., Tureèková, V., Tarkowská, D., et al. (2016). Gibberellin–abscisic acid balances during arbuscular mycorrhiza formation in tomato. *Front. Plant Sci.* 7:1273. doi: 10.3389/fpls.2016.01273

Martín-Rodríguez, J. Á, León-Morcillo, R. J., Vierheilig, H., Ocampo, J. A., Ludwig-Müller, J., and García-Garrido, J. M. (2010). Mycorrhization of the notabilis and sitiens tomato mutants in relation to abscisic acid and ethylene contents. *J. Plant Physiol.* 167, 606–613. doi: 10.1016/j.jplph.2009.11.014

Martín-Rodríguez, J. Á, León-Morcillo, R. J., Vierheilig, H., Ocampo, J. A., Ludwig-Müller, J., and García-Garrido, J. M. (2011). Ethylene-dependent/ethylene-independent ABA regulation of tomato plants colonized by arbuscular mycorrhiza fungi. *New Phytol.* 190, 193–205. doi: 10.1111/j.1469-8137.2010.03610.x

Martín-Rodríguez, J. Á, Ocampo, J. A., Molinero-Rosales, N., Tarkowská, D., Ruíz-Rivero, O., and García-Garrido, J. M. (2015). Role of gibberellins during arbuscular mycorrhizal formation in tomato: new insights revealed by endogenous quantification and genetic analysis of their metabolism in mycorrhizal roots. *Physiol. Plant.* 154, 66–81. doi: 10.1111/ppl.12274

Massonneau, A., Langlade, N., Léon, S., Smutny, J., Vogt, E., Neumann, G., et al. (2001). Metabolic changes associated with cluster root development in white lupin (*Lupinus albus* L.): relationship between organic acid excretion, sucrose metabolism and energy status. *Planta* 213, 534–542. doi: 10.1007/s004250100529

Mauch-Mani, B., Baccelli, I., Luna, E., and Flors, V. (2017). Defense priming: an adaptive part of induced resistance. *Annu. Rev. Plant. Biol.* 68, 485–512. doi: 10.1146/annurev-arplant-042916-041132

McArthur, D. A., and Knowles, N. R. (1992). Resistance responses of potato to vesicular–arbuscular mycorrhizal fungi under varying abiotic phosphorus levels. *Plant Physiol.* 100, 341–351. doi: 10.1104/pp.100.1.341

McMahon Smith, J., and Arteca, R. N. (2000). Molecular control of ethylene production by cyanide in Arabidopsis thaliana. *Physiol. Plant.* 109, 180–187. doi: 10.1034/j.1399-3054.2000.100210.x

Meixner, C., Ludwig-Müller, J., Miersch, O., Gresshoff, P., Staehelin, C., and Vierheilig, H. (2005). Lack of mycorrhizal autoregulation and phytohormonal changes in the supernodulating soybean mutant nts1007. *Planta* 222, 709–715. doi: 10.1007/s00425-005-0003-4

Mercy, L., Lucic-Mercy, E., Nogales, A., Poghosyan, A., Schneider, C., and Arnholdt-Schmitt, B. (2017). A functional approach towards understanding the role of the mitochondrial respiratory chain in an endomycorrhizal symbiosis. *Front. Plant Sci.* 8:417. doi: 10.3389/fpls.2017.00417

Millar, A. H., Whelan, J., Soole, K. L., and Day, D. A. (2011). Organization and regulation of mitochondrial respiration in plants. *Annu. Rev. Plant Biol.* 62, 79–104. doi: 10.1146/annurev-arplant-042110-103857

Miller, J. M., and Conn, E. E. (1980). Metabolism of hydrogen cyanide by higher plants. *Plant Physiol.* 65, 1199–1202. doi: 10.1104/pp.65.6.1199

Miransari, M., Abrishamchi, A., Khosbakht, K., and Niknam, V. (2014). Plant hormones as signals in arbuscular mycorrhizal symbiosis. *Crit. Rev. Biotechnol.* 34, 123–133. doi: 10.3109/07388551.2012.731684

Mizrahi, Y., and Richmond, A. E. (1972). Abscisic acid in relation to mineral deprivation. *Plant Physiol.* 50, 667–670. doi: 10.1104/pp.50.6.667

Mizutani, F., Sakita, Y., Hino, A., and Kadoya, K. (1988). Cyanide metabolism linked with ethylene biosynthesis in ripening processes of climacteric and non-climacteric fruits. *Sci. Hortic.* 35, 199–205. doi: 10.1016/0304-4238(88)90113-6

Młodzińska, E., and Zboińska, M. (2016). Phosphate uptake and allocation – a closer look at *Arabidopsis thaliana* L. and *Oryza sativa* L. *Front. Plant Sci.* 7:1198. doi: 10.3389/fpls.2016.01198

Mohan Raj, B., Bharath Kumar, R., Venkata Rao, G., and Sri Rama Murthy, K. (2016). Impact of different carbon sources, tri-calcium phosphate and auxins on in vitro multiplication of rhizophagus irregularis. *Int. J. Curr. Res. Biosci. Plant Biol.* 3, 162–166. doi: 10.20546/ijcrbp.2016.307.022

Morales Vela, G., Molinero-Rosales, N., Ocampo, J. A., and García-Garrido, J. M. (2007). Endocellulase activity is associated with arbuscular mycorrhizal spread in pea symbiotic mutants but not with ethylene content in root. *Soil Biol. Biochem.* 39, 786–792. doi: 10.1016/j.soilbio.2006.09.028

Morandi, D. (1989). Effect of xenobiotics on endomycorrhizal infection and isoflavonoid accumulation in soybean roots. *Plant Physiol. Biochem.* 27, 697–701.

Mosblech, A., Feussner, I., and Heilmann, I. (2009). Oxylipins: structurally diverse metabolites from fatty acid oxidation. *Plant Physiol. Biochem.* 47, 511–517. doi: 10.1016/j.plaphy.2008.12.011

Moubayidin, L., Di Mambro, R., and Sabatini, S. (2009). Cytokinin–auxin crosstalk. *Trends Plant Sci.* 14, 557–562. doi: 10.1016/j.tplants.2009.06.010

Mukherjee, A., and Ané, J. M. (2011). Germinating spore exudates from arbuscular mycorrhizal fungi: molecular and developmental responses in plants and their regulation by ethylene. *Mol. Plant Microbe Interact.* 24, 260–270. doi: 10.1094/MPMI-06-10-0146

Musgrave, M. E. (1994). "Cytokinins and oxidative processes," in *Cytokinins: Chemistry, Activity, and Function*, eds D. W. S. Mok and M. C. Mok (Boca Raton, FL: CRC), 167–178.

Nacry, P., Canivenc, G., Müller, B., Azmi, A., Van Onckelen, H., Rossignol, M., et al. (2005). A role for auxin redistribution in the responses of the root system architecture to phosphate starvation in Arabidopsis. *Plant Physiol.* 138, 2061–2074. doi: 10.1104/pp.105.060061

Nadal, M., and Paszkowski, U. (2013). Polyphony in the rhizosphere: presymbiotic communication in arbuscular mycorrhizal symbiosis. *Curr. Opin. Plant Biol.* 16, 473–479. doi: 10.1016/j.pbi.2013.06.005

Nadal, M., Sawers, R., Naseem, S., Bassin, B., Kulicke, C., Sharman, A., et al. (2017). An N-acetylglucosamine transporter required for arbuscular mycorrhizal symbioses in rice and maize. *Nat. Plants* 3:17073. doi: 10.1038/nplants.2017.73

Nagahashi, G., Douds, D. D., and Ferhatoglu, Y. (2010). "Functional categories of root exudate compounds and their relevance to AM fungal growth," in *Arbuscular Mycorrhizas: Physiology and Function*, eds H. Koltai and Y. Kapulnik (Dordrecht: Springer), 33–56.

Nagarajan, V. K., and Smith, A. P. (2012). Ethylene's role in phosphate starvation signaling: more than just a root growth regulator. *Plant Cell Physiol.* 53, 277–286. doi: 10.1093/pcp/pcr186

Nahar, K., Kyndt, T., Hause, B., Hofte, M., and Gheysen, G. (2013). Brassinosteroids suppress rice defense against root-knot nematodes through antagonism with the jasmonate pathway. *Mol. Plant Microbe Interact.* 26, 106–115. doi: 10.1094/MPMI-05-12-0108-FI

Nair, M. G., Safir, G. R., Schutzki, R. E., and Niemira, B. A. (1997). Alkali metal formononetin and method of mycorrhizal stimulation. U.S. Patent No 5,691,275,

Nakamoto, R. K., Scanlon, J. A. B., and Al-Shawi, M. K. (2008). The rotary mechanism of the ATP synthase. *Arch. Biochem. Biophys.* 476, 43–50. doi: 10.1016/j.abb.2008.05.004

Napier, J. A., Stobart, A. K., and Shewry, P. R. (1996). The structure and biogenesis of plant oil bodies: the role of the ER membrane and the oleosin class of proteins. *Plant Mol. Biol.* 31, 945–956. doi: 10.1007/BF00040714

Nátr, L. (1992). Mineral nutrients – a ubiquitous stress factor for photosynthesis. *Photosynthetica* 27, 271–294.

Navarro, L., Bari, R., Achard, P., Lisón, P., Nemri, A., Harberd, N. P., et al. (2008). DELLAs control plant immune responses by modulating the balance of jasmonic acid and salicylic acid signalling. *Curr. Biol.* 18, 650–655. doi: 10.1016/j.cub.2008.03.060

Navarro, L., Dunoyer, P., Jay, F., Arnold, B., Dharmasiri, N., Estelle, M., et al. (2006). A plant miRNA contributes to antibacterial resistance by repressing auxin signalling. *Science* 312, 436–439. doi: 10.1126/science.1126088

Negi, S., Sukumar, P., Liu, X., Cohen, J. D., and Munday, G. K. (2010). Genetic dissection oft he role of ethylene in regulating auxin-dependant lateral and adventitious root formation in tomato. *Plant J.* 61, 3–15. doi: 10.1111/j.1365-313X.2009.04027.x

Nibau, C., Gibbs, D. J., and Coates, J. C. (2008). Branching out in new directions: the control of root architecture by lateral root formation. *New Phytol.* 179, 595–614. doi: 10.1111/j.1469-8137.2008.02472.x

Niranjan, R., Mohan, V., and Rao, V. M. (2007). Effect of indole acetic acid on the synergistic interactions of bradyrhizobium and *Glomus fasciculatum* on growth, nodulation, and nitrogen fixation of *Dalbergia sissoo* Roxb. *Arid Land Res. Manage.* 21, 329–342. doi: 10.1080/15324980701603573

Nishiyama, R., Watanabe, Y., Fujita, Y., Le, D. T., Kojima, M., Werner, T., et al. (2011). Analysis of cytokinin mutants and regulation of cytokinin metabolic genes reveals important regulatory roles of cytokinins in drought, salt and abscisic acid responses, and abscisic acid biosynthesis. *Plant Cell* 23, 2169–2183. doi: 10.1105/tpc.111.087395

Nomura, T., Jager, C. E., Kitasaka, Y., Takeuchi, K., Fukami, M., Yoneyama, K., et al. (2004). Brassinosteroid deficiency due to truncated steroid 5α-reductase causes dwarfism in the lk mutant of pea. *Plant Physiol.* 135, 2220–2229. doi: 10.1104/pp.104.043786

Norman, C., Howell, K. A., Millar, A. H., Whelan, J. M., and Day, D. A. (2004). Salicylic acid is an uncoupler and inhibitor of mitochondrial electron transport. *Plant Physiol.* 134, 492–501. doi: 10.1104/pp.103.031039

Olsson, P. A., van Aarle, I. M., Allaway, W. G., Ashford, A. E., and Rouhier, H. (2002). Phosphorus effects on metabolic processes in monoxenic arbuscular mycorrhiza cultures. *Plant Physiol.* 130, 1162–1171. doi: 10.1104/pp.009639

Özgönen, H., Biçici, M., and Erkłłç, A. (2001). The effect of salicylic acid and endomycorrhizal fungus Glomus etunicatum on plant development of tomatoes and Fusarium wilt caused by *Fusarium oxysporum* f. sp *lycopersici*. *Turk. J. Agric. For.* 25, 25–29.

Parry, G., Calderon-Villalobos, L. I., Prigge, M., Peret, B., Dharmasiri, S., Itoh, H., et al. (2009). Complex regulation of the TIR1/AFB family of auxin receptors. *Proc. Natl. Acad. Sci. U.S.A.* 106, 22540–22545. doi: 10.1073/pnas.0911967106

Parsons, H. L., Yip, J. Y., and Vanlerberghe, G. C. (1999). Increased respiratory restriction during phosphate-limited growth in transgenic tobacco cells lacking alternative oxidase. *Plant Physiol.* 121, 1309–1320. doi: 10.1104/pp.121.4.1309

Pedranzani, H., Tavecchio, N., Gutiérrez, M., Garbero, M., Porcel, R., and Ruiz-Lozano, J. M. (2015). Differential effects of cold stress on the antioxidant response of mycorrhizal and non-mycorrhizal *Jatropha curcas* (L.) plants. *J. Agric. Sci.* 7, 35–43. doi: 10.5539/jas.v7n8p35

Peiser, G. D., Wang, T. T., Hoffman, N. E., Yang, S. F., Liu, H. W., and Walsh, C. T. (1984). Formation of cyanide from carbon 1 of 1-aminocyclopropane-1-carboxylic acid during its conversion to ethylene. *Proc. Natl. Acad. Sci. U.S.A.* 81, 3059–3063. doi: 10.1073/pnas.81.10.3059

Penmetsa, R. V., Uribe, P., Anderson, J., Lichtenzveig, J., Gish, J. C., Nam, Y. W., et al. (2008). The Medicago truncatula ortholog of Arabidopsis EIN2, sickle, is a negative regulator of symbiotic and pathogenic microbial associations. *Plant J.* 55, 580–595. doi: 10.1111/j.1365-313X.2008.03531.x

Pfeffer, P. E., Douds, D. D., Bécard, G., and Shachar-Hill, Y. (1999). Carbon uptake and the metabolism and transport of lipids in an arbuscular mycorrhiza. *Plant Physiol.* 120, 587–598. doi: 10.1104/pp.120.2.587

Pieterse, C. M., Van der Does, D., Zamioudis, C., Leon-Reyes, A., and Van Wees, S. C. (2012). Hormonal modulation of plant immunity. *Annu. Rev. Cell Dev. Biol.* 28, 489–521. doi: 10.1146/annurev-cellbio-092910-154055

Pieterse, C. M., Van Wees, S. C., Van Pelt, J. A., Knoester, M., Laan, R., Gerrits, H., et al. (1998). A novel signalling pathway controlling induced systemic resistance in Arabidopsis. *Plant Cell* 10, 1571–1580. doi: 10.1105/tpc.10.9.1571

Pieterse, C. M., Zamioudis, C., Berendsen, R. L., Weller, D. M., Van Wees, S. C., and Bakker, P. A. (2014). Induced systemic resistance by beneficial microbes. *Annu. Rev. Phytopathol.* 52, 347–375. doi: 10.1146/annurev-phyto-082712-102340

Pieterse, C. M. J., and van Loon, L. C. (2004). NPR1: the spider in the web of induced resistance signaling pathways. *Curr. Opin. Plant Biol.* 7, 456–464. doi: 10.1016/j.pbi.2004.05.006

Pieterse, C. M. J., Van Wees, S. C. M., Ton, J., Van Pelt, J. A., and van Loon, L. C. (2002). Signalling in rhizobacteria-induced systemic resistance in *Arabidopsis thaliana*. *Plant Biol.* 4, 535–544. doi: 10.1111/j.1438-8677.2011.00549.x

Pieterse, C. M. L., Van Wees, S. C., Hoffland, E., Van Pelt, J. A., and van Loon, L. C. (1996). Systemic resistance in Arabidopsis induced by biocontrol bacteria is independent of salicylic acid accumulation and pathogenesis-related gene expression. *Plant Cell* 8, 1225–1237. doi: 10.1105/tpc.8.8.1225

Pimprikar, P., Carbonnel, S., Paries, M., Katzer, K., Klingl, V., Bohmer, M. J., et al. (2016). A CCaMK-CYCLOPS-DELLA complex activates transcription of ram1 to regulate arbuscule branching. *Curr. Biol.* 26, 987–998. doi: 10.1016/j.cub.2016.01.069

Plaxton, W. C., and Carswell, M. C. (1999). "Metabolic aspects of the phosphate starvation response in plants," in *Plant Responses to Environmental Stresses: From Phytohormones to Genome Reorganization*, ed. H. R. Lerner (New York, NY: Marcel Dekker), 349–372.

Plaxton, W. C., and Tran, H. T. (2011). Metabolic adaptations of phosphate-starved plants. *Plant Physiol.* 156, 1006–1015. doi: 10.1104/pp.111.175281

Poorter, H., Remkes, C., and Lambers, H. (1990). Carbon and nitrogen economy of 24 wild species differing in relative growth rate. *Plant Physiol.* 94, 621–627. doi: 10.1104/pp.94.2.621

Potter, F. J., Wiskich, J. T., and Dry, I. B. (2001). The production of an inducible antisense alternative oxidase (Aox1a) plant. *Planta* 212, 215–221. doi: 10.1007/s004250000369

Pozo, M. J., and Azcón-Aguilar, C. (2007). Unraveling mycorrhiza-induced resistance. *Curr. Opin. Plant Bio.* 10, 393–398.

Pozo, M. J., López-Ráez, J. A., Azcón-Aguilar, C., and García-Garrido, J. M. (2015). Phytohormones as integrators of environmental signals in the regulation of mycorrhizal symbioses. *New Phytol.* 205, 1431–1436.

Pozo, M. J., Slezack-Deschaumes, S., Dumas-Gaudot, E., Gianinazzi, S., and Azcón-Aguilar, C. (2002). "Plant defense responses induced by arbuscular mycorrhizal fungi," in *Mycorrhizal Technology in Agriculture*, eds S. Gianinazzi, H. Schüepp, J. M. Barea, and K. Haselwandter (Basel: Birkhäuser Verlag), 103–111.

Pozo, M. J., van Loon, L. C., and Pieterse, C. M. (2004). Jasmonates-signals in plant-microbe interactions. *J. Plant Growth Regul.* 23, 211–222.

Proietti, S., Bertini, L., Timperio, A. M., Zolla, L., Caporale, C., and Caruso, C. (2013). Crosstalk between salicylic acid and jasmonate in Arabidopsis investigated by an integrated proteomic and transcriptomic approach. *Mol. Biosyst.* 9, 1169–1187. doi: 10.1039/c3mb25569g

Puppo, A., Pauly, N., Boscari, A., Mandon, K., and Brouquisse, R. (2013). Hydrogen peroxide and nitric oxide: key regulators of the legume-rhizobium

and mycorrhizal symbioses. *Antioxid. Redox Signal.* 18, 2202–2219. doi: 10.1089/ars.2012.5136

Rabie, G. H. (2005). Influence of arbuscular mycorrhizal fungi and kinetin on the response of mungbean plants to irrigation with seawater. *Mycorrhiza* 15, 225–230. doi: 10.1007/s00572-004-0345-y

Racca, S., Welchen, E., Gras, D. E., Tarkowská, D., Tureèková, V., Maurino, V. G., et al. (2018). Interplay between cytochrome c and gibberellins during Arabidopsis vegetative development. *Plant J.* 94, 105–121. doi: 10.1111/tpj.13845

Raghothama, K. G. (1999). Phosphate acquisition. *Annu. Rev. Plant Biol.* 50, 665–693. doi: 10.1146/annurev.arplant.50.1.665

Ramon, M., Rolland, F., and Sheen, J. (2008). Sugar sensing and signaling. *Arabidopsis Book* 6, e0117. doi: 10.1199/tab.0117

Ratnayake, M., Leonard, R. T., and Menge, J. A. (1978). Root exudation in relation to supply of phosphorus and its possible relevance to mycorrhizal formation. *New Phytol.* 81, 543–552. doi: 10.1111/j.1469-8137.1978.tb01627.x

Razem, F. A., Baron, K., and Hill, R. D. (2006). Turning on gibberellin and abscisic acid signaling. *Curr. Opin. Plant Biol.* 9, 454–459. doi: 10.1016/j.pbi.2006.07.007

Regvar, M., Gogala, N., and Zalar, P. (1996). Effects of jasmonic acid on mycorrhizal *Allium sativum*. *New Phytol.* 134, 703–707. doi: 10.1111/j.1469-8137.1996.tb04936.x

Reid, J. B., and Potts, W. C. (1986). Internode length in Pisum. Two further mutants, lh and ls, with reduced gibberellin synthesis, and a gibberellin insensitive mutant, lk. *Physiol. Plant.* 66, 417–426. doi: 10.1111/j.1399-3054.1986.tb05945.x

Resendes, C. M., Geil, R., and Guinel, F. (2001). Mycorrhizal development in a low nodulating pea mutant. *New Phytol.* 150, 563–572. doi: 10.1046/j.1469-8137.2001.00131.x

Rich, M. K., Nouri, E., Courty, P. E., and Reinhardt, D. (2017). Diet of arbuscular mycorrhizal fungi: bread and butter? *Trends Plant Sci.* 22, 652–660. doi: 10.1016/j.tplants.2017.05.008

Riedel, T., Groten, K., and Baldwin, I. T. (2008). Symbiosis between *Nicotiana attenuata* and *Glomus intraradices*: ethylene plays a role, jasmonic acid does not. *Plant Cell Environ.* 31, 1203–1213. doi: 10.1111/j.1365-3040.2008.01827.x

Rivas-San Vicente, M., and Plasencia, J. (2011). Salicylic acid beyond defence: its role in plant growth and development. *J. Exp. Bot.* 62, 3321–3338. doi: 10.1093/jxb/err031

Robinson, D. C., and Wellburn, A. R. (1981). Light quality and hormonal influences upon the rate of ATP formation by mitochondria during greening. *Biochem. Physiol. Pflanzen* 176, 54–59. doi: 10.1016/S0015-3796(81)80008-X

Rontein, D., Dieuaide-Noubhani, M., Dufourc, E. J., Raymond, P., and Rolin, D. (2002). The metabolic architecture of plant cells stability of central metabolism and flexibility of anabolic pathways during the growth cycle of tomato cells. *J. Biol. Chem.* 277, 43948–43960. doi: 10.1074/jbc.M206366200

Rook, F., Hadingham, S. A., Li, Y., and Bevan, M. W. (2006). Sugar and ABA response pathways and the control of gene expression. *Plant Cell Environ.* 29, 426–434. doi: 10.1111/j.1365-3040.2005.01477.x

Ross, J. J., Reid, J. B., Gaskin, P., and MacMillan, J. (1989). Internode length in Pisum. Estimation of GA1 levels in genotypes Le, le and led. *Physiol. Plant.* 76, 173–176. doi: 10.1111/j.1399-3054.1989.tb05627.x

Roth, R., and Paszkowski, U. (2017). Plant carbon nourishment of arbuscular mycorrhizal fungi. *Curr. Opin. Plant Biol.* 39, 50–56. doi: 10.1016/j.pbi.2017.05.008

Rouached, H., Arpat, A. B., and Poirier, Y. (2010). Regulation of phosphate starvation responses in plants: signaling players and cross-talks. *Mol. Plant.* 3, 288–299. doi: 10.1093/mp/ssp120

Rychter, A. M., Chauveau, M., Bomsel, J. L., and Lance, C. (1992). The effect of phosphate deficiency on mitochondrial activity and adenylate levels in bean roots. *Physiol. Plant.* 84, 80–86. doi: 10.1111/j.1399-3054.1992.tb08768.x

Rychter, A. M., and Mikulska, M. (1990). The relationship between phosphate status and cyanide-resistant respiration in bean roots. *Physiol. Plant.* 79, 663–667. doi: 10.1111/j.1399-3054.1990.tb00041.x

Saini, S., Sharma, I., and Pati, P. K. (2015). Versatile roles of brassinosteroid in plant in the context of its homeostasis, signalling and crosstalks. *Front. Plant Sci.* 6:950. doi: 10.3389/fpls.2015.00950

Sajjad, Y., Jaskani, M. J., Asif, M., and Qasim, M. (2017). Application of plant growth regulators in ornamental plants: a review. *Pak. J. Agric. Sci.* 54, 327–333. doi: 10.21162/PAKJAS/17.3659

Sakano, K. (2001). Metabolic regulation of pH in plant cells: role of cytoplasmic pH in defense reaction and secondary metabolism. *Int. Rev. Cytol.* 206, 1–44. doi: 10.1016/S0074-7696(01)06018-1

Salama, A. M., and Wareing, P. F. (1979). Effects of mineral nutrition on endogenous cytokinins in plants of sunflower. *J. Exp. Bot.* 30, 971–981. doi: 10.1093/jxb/30.5.971

Scervino, J. M., Ponce, M. A., Erra-Bassells, R., Vierheilig, H., Ocampo, J. A., and Godeas, A. (2005). Flavonoids exhibit fungal species and genus specific effects on the presymbiotic growth of Gigaspora and Glomus. *Mycol. Res.* 109, 789–794. doi: 10.1017/S0953756205002881

Schachtman, D. P., Reid, R. J., and Ayling, S. M. (1998). Phosphorus uptake by plants: from soil to cell. *Plant Physiol.* 116, 447–453. doi: 10.1104/pp.116.2.447

Schilmiller, A. L., and Howe, G. A. (2005). Systemic signalling in the wound response. *Curr. Opin. Plant Biol.* 8, 369–377. doi: 10.1016/j.pbi.2005.05.008

Schmitz, A. M., and Harrison, M. J. (2014). Signaling events during initiation of arbuscular mycorrhizal symbiosis. *J. Integr. Plant Biol.* 56, 250–261. doi: 10.1111/jipb.12155

Schwachtje, J., and Baldwin, I. T. (2008). Why does herbivore attack reconfigure primary metabolism? *Plant Physiol.* 146, 845–851. doi: 10.1104/pp.107.112490

Shah, J., and Zeier, J. (2013). Long-distance communication and signal amplification in systemic acquired resistance. *Front. Plant Sci.* 4:30. doi: 10.3389/fpls.2013.00030

Shane, M. W., Cramer, M. D., Funayama-Noguchi, S., Cawthray, G. R., Millar, A. H., Day, D. A., et al. (2004). Developmental physiology of cluster-root carboxylate synthesis and exudation in harsh hakea. Expression of phosphoenolpyruvate carboxylase and the alternative oxidase. *Plant Physiol.* 135, 549–560. doi: 10.1104/pp.103.035659

Sharp, R. E., LeNoble, M. E., Else, M. A., Thorne, E. T., and Gherardi, F. (2000). Endogenous ABA maintains shoot growth in tomato independently of effects on plant water balance: evidence for an interaction with ethylene. *J. Exp. Bot.* 51, 1575–1584. doi: 10.1093/jexbot/51.350.1575

Shen, Y. G., Zhang, W. K., He, S. J., Zhang, J. S., Liu, Q., and Chen, S. Y. (2003). An EREBP/AP2-type protein in *Triticum aestivum* was a DRE-binding transcription factor induced by cold, dehydration and ABA stress. *Theor. Appl. Genet.* 106, 923–930. doi: 10.1007/s00122-002-1131-x

Shi, G. R., Cai, Q. S., Liu, Q. Q., and Wu, L. (2009). Salicylic acid-mediated alleviation of cadmium toxicity in hemp plants in relation to cadmium uptake, photosynthesis, and antioxidant enzymes. *Acta Physiol. Plant.* 31, 969–977. doi: 10.1007/s11738-009-0312-5

Shin, R., Berg, R. H., and Schachtman, D. P. (2005). Reactive oxygen species and root hairs in Arabidopsis root response to nitrogen, phosphorus and potassium deficiency. *Plant Cell Physiol.* 46, 1350–1357. doi: 10.1093/pcp/pci145

Shin, R., and Schachtman, D. P. (2004). Hydrogen peroxide mediates plant root cell response to nutrient deprivation. *Proc. Natl. Acad. Sci. U.S.A.* 101, 8827–8832. doi: 10.1073/pnas.0401707101

Shu, K., Zhou, W., Chen, F., Luo, X., and Yang, W. (2018). Abscisic acid and gibberellins antagonistically mediate plant development and abiotic stress responses. *Front. Plant Sci.* 9:416. doi: 10.3389/fpls.2018.00416

Siedow, J. N., and Umbach, A. L. (2000). The mitochondrial cyanide-resistant oxidase: structural conservation amid regulatory diversity. *Biochim. Biophys. Acta Bioenerg.* 1459, 432–439. doi: 10.1016/S0005-2728(00)00181-X

Siegień, I., and Bogatek, R. (2006). Cyanide action in plants – from toxic to regulatory. *Acta Physiol. Plant.* 28, 483–497. doi: 10.1007/BF02706632

Silverstone, A., Jung, H.-S., Dill, A., Kawaide, H., Kamiya, Y., and Sun, T. (2001). Repressing a repressor: gibberellin-induced rapid reduction of the RGA protein in Arabidopsis. *Plant Cell* 13, 1555–1565. doi: 10.1105/TPC.010047

Simons, B. H., Millenaar, F. F., Mulder, L., van Loon, L. C., and Lambers, H. (1999). Enhanced expression and activation of the alternative oxidase during infection of Arabidopsis with *Pseudomonas* syringae pv tomato. *Plant Physiol.* 120, 529–538. doi: 10.1104/pp.120.2.529

Singh, B., and Usha, K. (2003). Salicylic acid induced physiological and biochemical changes in wheat seedlings under water stress. *Plant Growth Regul.* 39, 137–141. doi: 10.1023/A:1022556103536

Sluse, F. E., and Jarmuszkiewicz, W. (1998). Alternative oxidase in the branched mitochondrial respiratory network: an overview on structure, function, regulation, and role. *Braz. J. Med. Biol. Res.* 31, 733–747. doi: 10.1590/S0100-879X1998000600003

Smith, F. A., and Smith, S. E. (2011a). What is the significance of the arbuscular mycorrhizal colonization of many economically important crop plants? *Plant Soil* 348, 63–79. doi: 10.1007/s11104-011-0865-0

Smith, S. E., Jakobsen, I., Grønlund, M., and Smith, F. A. (2011). Roles of arbuscular mycorrhizas in plant phosphorus nutrition: interactions between pathways of phosphorus uptake in arbuscular mycorrhizal roots have important implications for understanding and manipulating plant phosphorus acquisition. *Plant Physiol.* 156, 1050–1057. doi: 10.1104/pp.111.174581

Smith, S. E., and Read, D. J. (2008). *Mycorrhizal Symbiosis*, 3rd Edn. New York, NY: Academic Press, 605.

Smith, S. E., and Smith, F. A. (2011b). Roles of arbuscular mycorrhizas in plant nutrition and growth: new paradigms from cellular to ecosystem scales. *Annu. Rev. Plant Biol.* 62, 227–250. doi: 10.1146/annurev-arplant-042110-103846

Solomos, T., and Laties, G. G. (1976). Induction by ethylene of cyanide-resistant respiration. *Biochem. Biophys. Res. Commun.* 70, 663–671. doi: 10.1016/0006-291X(76)91098-6

Song, Y., Chen, D., Lu, K., Sun, Z., and Zeng, R. (2015). Enhanced tomato disease resistance primed by arbuscular mycorrhizal fungus. *Front. Plant Sci.* 6:786. doi: 10.3389/fpls.2015.00786

Song, Y. Y., Ye, M., Li, C., He, X., Zhu-Salzman, K., Wang, R. L., et al. (2014). Hijacking common mycorrhizal networks for herbivore-induced defence signal transfer between tomato plants. *Sci. Rep.* 4:3915. doi: 10.1038/srep03915

Song, Y. Y., Ye, M., Li, C. Y., Wang, R. L., Wei, X. C., Luo, S. M., et al. (2013). Priming of anti-herbivore defense in tomato by arbuscular mycorrhizal fungus and involvement of the jasmonate pathway. *J. Chem. Ecol.* 39, 1036–1044. doi: 10.1007/s10886-013-0312-1

Strzelczyk, E., and Pokojska-Burdziej, A. (1984). Production of auxins and gibberellin-like substances by mycorrhizal fungi, bacteria and actinomycetes isolated from soil and the mycorrhizosphere of pine (*Pinus silvestris* L.). *Plant Soil* 81, 85–194. doi: 10.1007/BF02197150

Stumpe, M., Carsjens, J. G., Stenzel, I., Göbel, C., Lang, I., Pawlowski, K., et al. (2005). Lipid metabolism in arbuscular mycorrhizal roots of *Medicago truncatula*. *Phytochemistry* 66, 781–791. doi: 10.1016/j.phytochem.2005.01.020

Sun, H., Tao, J., Liu, S., Huang, S., Chen, S., Xie, X., et al. (2014). Strigolactones are involved in phosphate- and nitrate-deficiency-induced root development and auxin transport in rice. *J. Exp. Bot.* 65, 6735–6746. doi: 10.1093/jxb/eru029

Suzuki, K., Itai, R., Suzuki, K., Nakanishi, H., Nishizawa, N. K., Yoshimura, E., et al. (1998). Formate dehydrogenase, an enzyme of anaerobic metabolism, is induced by iron deficiency in barley roots. *Plant Physiol.* 116, 725–732. doi: 10.1104/pp.116.2.725

Swain, S. M., Singh, D. P., Helliwell, C. A., and Poole, A. T. (2005). Plants with increased expression of ent-kaurene oxidase are resistant to chemical inhibitors of this gibberellin biosynthesis enzyme. *Plant Cell Physiol.* 46, 284–291. doi: 10.1093/pcp/pci027

Świątek, A., Van Dongen, W., Esmans, E. L., and Van Onckelen, H. (2004). Metabolic fate of jasmonates in tobacco bright yellow-2 cells. *Plant Physiol.* 135, 161–172. doi: 10.1104/pp.104.040501

Symons, G. M., Murfet, I. C., Ross, J. J., Sherriff, L. J., and Warkentin, T. D. (1999). bushy, a dominant pea mutant characterised by short, thin stems, tiny leaves and a major reduction in apical dominance. *Physiol. Plant.* 107, 346–352. doi: 10.1034/j.1399-3054.1999.100312.x

Symons, G. M., Ross, J. J., and Murfet, I. C. (2002). The bushy pea mutant is IAA-deficient. *Physiol. Plant.* 116, 389–397. doi: 10.1111/ppl.12246

Tadege, M., Dupuis, I., and Kuhlemeier, C. (1999). Ethanolic fermentation: new functions for an old pathway. *Trends Plant Sci.* 4, 320–325. doi: 10.1016/S1360-1385(99)01450-8

Tahat, M. M., and Sijam, K. (2012). Arbuscular mycorrhizal fungi and plant root exudates bio-communications in the rhizosphere. *Afr. J. Microbiol. Res.* 6, 7295–7301. doi: 10.5897/AJMR12.2250

Takeda, N., Handa, Y., Tsuzuki, S., Kojima, M., Sakakibara, H., and Kawaguchi, M. (2015). Gibberellins interfere with symbiosis signalling and gene expression and alter colonization by arbuscular mycorrhizal fungi in *Lotus japonicus*. *Plant Physiol.* 167, 545–557. doi: 10.1104/pp.114.247700

Tamasloukht, M. B., Séjalon-Delmas, N., Kluever, A., Jauneau, A., Roux, C., Bécard, G., et al. (2003). Root factors induce mitochondrial-related gene expression and fungal respiration during the developmental switch from asymbiosis to presymbiosis in the arbuscular mycorrhizal fungus Gigaspora rosea. *Plant Physiol.* 131, 1468–1478. doi: 10.1104/pp.012898

Tawaraya, K., Horie, R., Saito, A., Shinano, T., Wagatsuma, T., Saito, K., et al. (2013). Metabolite profiling of shoot extracts, root extracts, and root exudates of rice plant under phosphorus deficiency. *J. Plant Nutr.* 36, 1138–1159. doi: 10.1080/01904167.2013.780613

Tejeda-Sartorius, M., Martínez de la Vega, O., and Délano-Frier, J. P. (2008). Jasmonic acid influences mycorrhizal colonization in tomato plants by modifying the expression of genes involved in carbohydrate partitioning. *Physiol. Plant.* 133, 339–353. doi: 10.1111/j.1399-3054.2008.01081.x

Thakur, M., and Sohal, B. S. (2013). Role of elicitors in inducing resistance in plants against pathogen infection: a review. *ISRN Biochem.* 2013:762412. doi: 10.1155/2013/762412

Theodorou, M. E., Elrifi, I. R., Turpin, D. H., and Plaxton, W. C. (1991). Effects of phosphorus limitation on respiratory metabolism in the green alga *Selenastrum minutum*. *Plant Physiol.* 95, 1089–1095. doi: 10.1104/pp.95.4.1089

Theodorou, M. E., and Plaxton, W. C. (1993). Metabolic adaptations of plant respiration to nutritional phosphate deprivation. *Plant Physiol.* 101, 339–344. doi: 10.1104/pp.101.2.339

Tholen, D., Pons, T. L., Voesenek, L. A., and Poorter, H. (2008). The role of ethylene perception in the control of the photosynthesis. *Plant Signal. Behav.* 3, 108–109. doi: 10.4161/psb.3.2.4968

Thomson, B. D., Robson, A. D., and Abbott, L. K. (1986). Effects of phosphorus on the formation of mycorrhizas by *Gigaspora calospora* and *Glomus fasciculatum* in relation to root carbohydrates. *New Phytol.* 103, 751–765. doi: 10.1111/j.1469-8137.1986.tb00850.x

Tisserant, E., Malbreil, M., Kuo, A., Kohler, A., Symeonidi, A., Balestrini, R., et al. (2013). Genome of an arbuscular mycorrhizal fungus provides insight into the oldest plant symbiosis. *Proc. Natl. Acad. Sci. U.S.A.* 110, 20117–20122. doi: 10.1073/pnas.1313452110

Tofighi, C., Khavari-Nejad, R. A., Najafi, F., Razavi, K., and Rejali, F. (2017). Brassinosteroid (BR) and arbuscular mycorrhizal (AM) fungi alleviate salinity in wheat. *J. Plant Nutr.* 40, 1091–1098. doi: 10.1080/01904167.2016.1263332

Ton, J., Flors, V., and Mauch-Mani, B. (2009). The multifaceted role of ABA in disease resistance. *Trends Plant Sci.* 14, 310–317. doi: 10.1016/j.tplants.2009.03.006

Torres de Los Santos, R., Molinero-Rosales, N., Ocampo, J. A., and García-Garrido, J. M. (2016). Ethylene alleviates the suppressive effect of phosphate on arbuscular mycorrhiza formation. *J. Plant Growth Regul.* 35, 11–617. doi: 10.1007/s00344-015-9570-1

Torres de Los Santos, R., Vierheilig, H., Ocampo, J. A., and García Garrido, J. M. (2011). Altered pattern of arbuscular mycorrhizal formation in tomato ethylene mutants. *Plant Signal. Behav.* 6, 755–758. doi: 10.4161/psb.6.5.15415

Torres-Vera, R., García, J. M., Pozo, M. J., and López-Ráez, J. A. (2014). Do strigolactones contribute to plant defence? *Mol. Plant Pathol.* 15, 211–216. doi: 10.1111/mpp.12074

Tóth, G., Guicharnaud, R. A., Tóth, B., and Hermann, T. (2014). Phosphorus levels in croplands of the European Union with implications for P fertilizer use. *Eur. J. Agron.* 55, 42–52. doi: 10.1016/j.eja.2013.12.008

Tran, L. S. P., Urao, T., Qin, F., Maruyama, K., Kakimito, T., Shinozaki, K., et al. (2007). Functional analysis of AHK1/ATHK1 and cytokinin receptor histidine kinases in response to abscisic acid, drought, and salt stress in Arabidopsis. *Proc. Natl. Acad. Sci. U.S.A.* 104, 20623–20628. doi: 10.1073/pnas.0706547105

Trouvelot, S., Héloir, M. C., Poinssot, B., Gauthier, A., Paris, F., Guillier, C., et al. (2014). Carbohydrates in plant immunity and plant protection: roles and potential application as foliar sprays. *Front. Plant Sci.* 5:592. doi: 10.3389/fpls.2014.00592

Uhde-Stone, C., Gilbert, G., Johnson, J. M., Litjens, R., Zinn, K. E., Temple, S. J., et al. (2003a). Acclimation of white lupin to phosphorus deficiency involves enhanced expression of genes related to organic acid metabolism. *Plant Soil* 248, 99–116. doi: 10.1023/A:1022335519879

Uhde-Stone, C., Zinn, K. E., Ramirez-Yáñez, M., Li, A., Vance, C. P., and Allan, D. L. (2003b). Nylon filter arrays reveal differential gene expression in proteoid roots of white lupin in response to phosphorus deficiency. *Plant Physiol.* 131, 1064–1079.

Umehara, M., Hanada, A., Magome, H., Takeda-Kamiya, N., and Yamaguchi, S. (2010). Contribution of strigolactones to the inhibition of tiller bud outgrowth under phosphate deficiency in rice. *Plant Cell Physiol.* 51, 1118–1126. doi: 10.1093/pcp/pcq084

van der Heijden, M. G., Martin, F. M., Selosse, M. A., and Sanders, I. R. (2015). Mycorrhizal ecology and evolution: the past, the present, and the future. *New Phytol.* 205, 1406–1423. doi: 10.1111/nph.13288

van Loon, L. C., Geraats, B. P., and Linthorst, H. J. (2006a). Ethylene as a modulator of disease resistance in plants. *Trends Plant Sci.* 11, 184–191.

van Loon, L. C., Rep, M., and Pieterse, C. M. (2006b). Significance of inducible defense-related proteins in infected plants. *Annu. Rev. Phytopathol.* 44, 135–162.

Vanlerberghe, G. C. (2013). Alternative oxidase: a mitochondrial respiratory pathway to maintain metabolic and signalling homeostasis during abiotic and biotic stress in plants. *Int. J. Mol. Sci.* 14, 6805–6847. doi: 10.3390/ijms14046805

Vanlerberghe, G. C., and McIntosh, L. (1996). Signals regulating the expression of the nuclear gene encoding alternative oxidase of plant mitochondria. *Plant Physiol.* 111, 589–595. doi: 10.1104/pp.111.2.589

Vellosillo, T., Martínez, M., López, M. A., Vicente, J., Cascón, T., Dolan, L., et al. (2007). Oxylipins produced by the 9-lipoxygenase pathway in Arabidopsis regulate lateral root development and defense responses through a specific signalling cascade. *Plant Cell* 19, 831–846. doi: 10.1105/tpc.106.046052

Veneklaas, E. J., Stevens, J., Cawthray, G. R., Turner, S., Grigg, A. M., and Lambers, H. (2003). Chickpea and white lupin rhizosphere carboxylates vary with soil properties and enhance phosphorus uptake. *Plant Soil* 248, 187–197. doi: 10.1023/A:1022367312851

Vidal, E. A., Araus, V., Lu, C., Parry, G., Green, P. J., Coruzzi, G. M., et al. (2010). Nitrate-responsive miR393/AFB3 regulatory module controls root system architecture in *Arabidopsis thaliana*. *Proc. Natl. Acad. Sci. U.S.A.* 107, 4477–4482. doi: 10.1073/pnas.0909571107

Vierheilig, H. (2004). Regulatory mechanisms during the plant-arbuscular mycorrhizal fungus interaction. *Can. J. Bot.* 82, 1166–1176. doi: 10.1139/b04-015

Vierheilig, H., Garcia-Garrido, J. M., Wyss, U., and Piché, Y. (2000). Systemic suppression of mycorrhizal colonization of barley roots already colonized by AM fungi. *Soil Biol Biochem.* 32, 589–595. doi: 10.1016/S0038-0717(99)00155-8

Vierheilig, H., Lerat, S., and Piché, Y. (2003). Systemic inhibition of arbuscular mycorrhiza development by root exudates of cucumber plants colonized by *Glomus mosseae*. *Mycorrhiza* 13, 167–170. doi: 10.1007/s00572-002-0219-0

Vierheilig, H., and Piché, Y. (2002). "Signalling in arbuscular mycorrhiza: facts and hypotheses"," in *Flavonoids in Cell Function*, eds B. S. Buslig and J. A. Manthey (Boston, MA: Springer-Verlag US), 23–39. doi: 10.1007/978-1-4757-5235-9_3

Vlot, A. C., Dempsey, D. M. A., and Klessig, D. F. (2009). Salicylic acid, a multifaceted hormone to combat disease. *Annu. Rev. Phytopathol.* 47, 177–206. doi: 10.1146/annurev.phyto.050908.135202

Vogel, J. T., Walter, M. H., Giavalisco, P., Lytovchenko, A., Kohlen, W., Charnikhova, T., et al. (2010). SlCCD7 controls strigolactone biosynthesis, shoot branching and mycorrhiza-induced apocarotenoid formation in tomato. *Plant J.* 61, 300–311. doi: 10.1111/j.1365-313X.2009.04056.x

Vosátka, M., Albrechtová, J., and Patten, R. (2008). "The international market development for mycorrhizal technology"," in *Mycorrhiza,* 3rd Edn, ed. A. Varma (Berlin: Springer Verlag), 419–438.

Vysotskaya, L. B., Korobova, A. V., and Kudoyarova, G. R. (2008). Abscisic acid accumulation in the roots of nutrient-limited plants: its impact on the differential growth of roots and shoots. *J. Plant Physiol.* 165, 1274–1279. doi: 10.1016/j.jplph.2007.08.014

Wang, C., Reid, J. B., and Foo, E. (2018). The art of self-control - autoregulation of plant-microbe symbioses. *Front. Plant Sci.* 9:988. doi: 10.3389/fpls.2018.00988

Wang, E., Schornack, S., Marsh, J. F., Gobbato, E., Schwessinger, B., Eastmond, P., et al. (2012). A common signalling process that promotes mycorrhizal and oomycete colonization of plants. *Curr. Biol.* 22, 2242–2246. doi: 10.1016/j.cub.2012.09.043

Wang, H., Huang, J., and Bi, Y. (2010). Induction of alternative respiratory pathway involves nitric oxide, hydrogen peroxide and ethylene under salt stress. *Plant Signal. Behav.* 5, 1636–1637. doi: 10.4161/psb.5.12.13775

Wang, W., Bai, M. Y., and Wang, Z. Y. (2014). The brassinosteroid signalling network – a paradigm of signal integration. *Curr. Opin. Plant Biol* 21, 147–153. doi: 10.1016/j.pbi.2014.07.012

Wang, X. (2008). Effects of polyamines on nutrient element absorption in the leaves of nymphoides peltatum under Zn stress. *J. Anhui Agric. Sci.* 2, 404–416.

Wang, Y. H., and Irving, H. R. (2011). Developing a model of plant hormone interactions. *Plant Signal. Behav.* 6, 494–500. doi: 10.4161/psb.6.4.14558

Wasternack, C. (2007). Jasmonates: an update on biosynthesis, signal transduction and action in plant stress response, growth and development. *Ann. Bot.* 100, 681–697. doi: 10.1093/aob/mcm079

Wasternack, C., and Hause, B. (2002). Jasmonates and octadecanoids: signals in plant stress responses and development. *Prog. Nucleic Acid Res. Mol. Biol.* 72, 165–221. doi: 10.1016/S0079-6603(02)72070-9

Wasternack, C., and Hause, B. (2013). Jasmonates: biosynthesis, perception, signal transduction and action in plant stress response, growth and development. An update to the 2007 review in Annals of Botany. *Ann. Bot.* 111, 1021–1058. doi: 10.1093/aob/mct067

Weger, H. G., and Dasgupta, R. (1993). Regulation of alternative pathway respiration in *Chlamydomonas reinhardtii* (Chlorophyceae). *J. Phycol.* 29, 300–308. doi: 10.1111/j.0022-3646.1993.00300.x

Werner, T., Köllmer, I., Batrina, I., Holst, K., and Schmülling, T. (2006). New insights into the biology of cytokinin degradation. *Plant Biol.* 8, 371–381. doi: 10.1055/s-2006-923928

Werner, T., and Schmülling, T. (2009). Cytokinin action in plant development. *Curr. Opin. Plant Biol* 12, 527–538. doi: 10.1016/j.pbi.2009.07.002

Wild, M., and Achard, P. (2013). The DELLA protein RGL3 positively contributes to jasmonate/ethylene defense responses. *Plant Signal. Behav.* 8:e23891. doi: 10.4161/psb.23891

Wind, J. J., Peviani, A., Snel, B., Hanson, J., and Smeekens, S. C. (2012). ABI4: versatile activator and repressor. *Trends Plant Sci.* 19, 1360–1385.

Wu, Q. S., He, X. H., Zou, Y. N., Liu, C. Y., Xiao, J., and Li, Y. (2012). Arbuscular mycorrhizas alter root system architecture of *Citrus tangerine* through regulating metabolism of endogenous polyamines. *Plant Growth Regul.* 68, 27–35. doi: 10.1007/s10725-012-9690-6

Wu, Y., Sanchez, J. P., Lopez-Molina, L., Himmelbach, A., Grill, E., and Chua, N. H. (2003). The abi1-1 mutation blocks ABA signaling downstream of cADPR action. *Plant J.* 34, 307–315. doi: 10.1046/j.1365-313X.2003.01721.x

Wu, Z., and Yang, S. T. (2003). Extractive fermentation for butyric acid production from glucose by Clostridium tyrobutyricum. *Biotechnol. Bioeng.* 82, 93–102. doi: 10.1002/bit.10542

Xie, J., Tian, J., Du, Q., Chen, J., Li, Y., Yang, X., et al. (2016). Association genetics and transcriptome analysis reveal a gibberellin-responsive pathway involved in regulating photosynthesis. *J. Exp. Bot.* 67, 3325–3338. doi: 10.1093/jxb/erw151

Xie, Z. P., Müller, J., Wiemken, A., Broughton, W. J., and Boller, T. (1998). Nod factors and tri-iodobenzoic acid stimulate mycorrhizal colonization and affect carbohydrate partitioning in mycorrhizal roots of Lablab purpureus. *New Phytol.* 139, 361–366. doi: 10.1046/j.1469-8137.1998.00186.x

Xu, L., Li, T., Wu, Z., Feng, H., Yu, M., Zhang, X., et al. (2018). Arbuscular mycorrhiza enhances drought tolerance of tomato plants by regulating the 14-3-3 genes in the ABA signaling pathway. *Appl. Soil Ecol.* 125, 213–221. doi: 10.1016/j.apsoil.2018.01.012

Yamaguchi-Shinozaki, K., and Shinozaki, K. (2005). Organization of cis-acting regulatory elements in osmotic-and cold-stress-responsive promoters. *Trends Plant Sci.* 10, 88–94. doi: 10.1016/j.tplants.2004.12.012

Yamakawa, H., and Hakata, M. (2010). Atlas of rice grain filling-related metabolism under high temperature: joint analysis of metabolome and transcriptome demonstrated inhibition of starch accumulation and induction of amino acid accumulation. *Plant Cell Physiol.* 51, 795–809. doi: 10.1093/pcp/pcq034

Yang, D. L., Yao, J., Mei, C. S., Tong, X. H., Zeng, L. J., Li, Q., et al. (2012). Plant hormone jasmonate prioritizes defense over growth by interfering with gibberellin signalling cascade. *Proc. Natl. Acad. Sci. U.S.A.* 109, E1192–E1200. doi: 10.1073/pnas.1201616109

Yang, G., and Komatsu, S. (2004). Microarray and proteomic analysis of brassinosteroid-and gibberellin-regulated gene and protein expression in rice. *Genomics Proteomics Bioinform.* 2, 77–83. doi: 10.1016/S1672-0229(04)02013-3

Yao, Q., Zhu, H., and Chen, J. (2005). Growth responses and endogenous IAA and iPAs changes of litchi (*Litchi chinensis* Sonn.) seedlings induced by arbuscular mycorrhizal fungal inoculation. *Sci. Hort.* 105, 145–151. doi: 10.1016/j.scienta.2005.01.003

Yaronskaya, E., Vershilovskaya, I., Poers, Y., Alawady, A. E., Averina, N., and Grimm, B. (2006). Cytokinin effects on tetrapyrrole biosynthesis and photosynthetic activity in barley seedlings. *Planta* 224, 700–709. doi: 10.1007/s00425-006-0249-5

Yasuda, M., Ishikawa, A., Jikumaru, Y., Seki, M., Umezawa, T., Asami, T., et al. (2008). Antagonistic interaction between systemic acquired resistance and the

abscisic acid–mediated abiotic stress response in Arabidopsis. *Plant Cell* 20, 1678–1692. doi: 10.1105/tpc.107.054296

Yoneyama, K., Xie, X., Kim, H. I., Kisugi, T., Nomura, T., Sekimoto, H., et al. (2012). How do nitrogen and phosphorus deficiencies affect strigolactone production and exudation? *Planta* 235, 1197–1207. doi: 10.1007/s00425-011-1568-8

Yoshida, S., Kameoka, H., Tempo, M., Akiyama, K., Umehara, M., Yamaguchi, S., et al. (2012). The D3 F-box protein is a key component in host strigolactone responses essential for arbuscular mycorrhizal symbiosis. *New Phytol.* 196, 1208–1216. doi: 10.1111/j.1469-8137.2012.04339.x

Yu, N., Luo, D., Zhang, X., Liu, J., Wang, W., Jin, Y., et al. (2014). A DELLA protein complex controls the arbuscular mycorrhizal symbiosis in plants. *Cell Res.* 24, 130–133. doi: 10.1038/cr.2013.167

Yu, X. J., Sun, J., Zheng, J. Y., Sun, Y. Q., and Wang, Z. (2016). Metabolomics analysis reveals 6-benzylaminopurine as a stimulator for improving lipid and DHA accumulation of *Aurantiochytrium* sp. *J. Chem. Technol. Biotechnol.* 91, 1199–1207. doi: 10.1002/jctb.4869

Zamski, E., and Schaffer, A. A. (1996). *Photoassimilate Distribution in Plants and Crops: Source-Sink Relationships*. New York, NY: Marcel Dekker Inc.

Zentella, R., Zhang, Z. L., Park, M., Thomas, S. G., Endo, A., Murase, K., et al. (2007). Global analysis of DELLA direct targets in early gibberellin signalling in Arabidopsis. *Plant Cell* 19, 3037–3057. doi: 10.1105/tpc.107.054999

Zhu, J. Y., Sae-Seaw, J., and Wang, Z. Y. (2013). Brassinosteroid signalling. *Development* 140, 1615–1620. doi: 10.1242/dev.060590

Zsögön, A., Lambais, M. R., Benedito, V. A., Figueira, A. V. O., and Peres, L. E. P. (2008). Reduced arbuscular mycorrhizal colonization in tomato ethylene mutants. *Sci. Agricola* 65, 259–267. doi: 10.1590/S0103-90162008000300006

Conflict of Interest Statement: The authors declare that the research was conducted in the absence of any commercial or financial relationships that could be construed as a potential conflict of interest.

frontiers in Plant Science

ORIGINAL RESEARCH
published: 08 January 2019
doi: 10.3389/fpls.2018.01901

Nodulating Legumes Are Distinguished by a Sensitivity to Cytokinin in the Root Cortex Leading to Pseudonodule Development

*Christopher Gauthier-Coles[1], Rosemary G. White[2] and Ulrike Mathesius[1]**

[1] Division of Plant Sciences, Research School of Biology, Australian National University, Canberra, ACT, Australia, [2] CSIRO Agriculture, Canberra, ACT, Australia

Root nodule symbiosis (RNS) is a feature confined to a single clade of plants, the Fabids. Among Fabids capable of RNS, legumes form root cortex-based nodules in symbioses with rhizobia, while actinorhizal species form lateral root-based nodules with actinomycetes. Cytokinin has previously been shown to be sufficient for "pseudonodule" initiation in model legumes. Here, we tested whether this response correlates with the ability to nodulate across a range of plant species. We analyzed the formation of pseudonodules in 17 nodulating and non-nodulating legume species, and 11 non-legumes, including nodulating actinorhizal species, using light and fluorescence microscopy. Cytokinin-induced pseudonodules arising from cortical cell divisions occurred in all nodulating legume species, but not in any of the other species, including non-nodulating legumes. Pseudonodule formation was dependent on the CRE1 cytokinin receptor in *Medicago truncatula*. Inhibition of root growth by cytokinin occurred across plant groups, indicating that pseudonodule development is the result of a specific cortical cytokinin response unique to nodulating legumes. Lack of a cortical cytokinin response from the *Arabidopsis thaliana* cytokinin reporter *TCSn::GFP* supported this hypothesis. Our results suggest that the ability to form cortical cell-derived nodules was gained in nodulating legumes, and likely lost in non-nodulating legumes, due to a specific root cortical response to cytokinin.

Keywords: actinorhizal symbiosis, root cortex, cytokinin, evolution of nodulation, legumes, root growth

OPEN ACCESS

Edited by:
Dugald Reid,
Aarhus University, Denmark

Reviewed by:
Arjan Van Zeijl,
Wageningen University and Research, Netherlands
Katharina Schiessl,
University of Cambridge, United Kingdom

***Correspondence:**
Ulrike Mathesius
Ulrike.mathesius@anu.edu.au

Specialty section:
This article was submitted to Plant Microbe Interactions, a section of the journal Frontiers in Plant Science

Received: *12 October 2018*
Accepted: *07 December 2018*
Published: *08 January 2019*

Citation:
Gauthier-Coles C, White RG and Mathesius U (2019) Nodulating Legumes Are Distinguished by a Sensitivity to Cytokinin in the Root Cortex Leading to Pseudonodule Development. Front. Plant Sci. 9:1901. doi: 10.3389/fpls.2018.01901

INTRODUCTION

Root nodule symbiosis (RNS) is a key innovation allowing certain plants to associate with bacteria capable of converting atmospheric nitrogen into ammonia, a process known as nitrogen fixation (Sprent and Sprent, 1990). In exchange for this nitrogen, the plant provides the bacteria with a specialized habitat, a root-derived organ known as a nodule. The plant also provides the bacteria with a source of carbon in the form of sugars and organic acids (Udvardi and Poole, 2013). Due to the cost associated with this symbiotic relationship, RNS plants have evolved the ability to down-regulate nodule formation when sufficient nitrogen is present in the soil (Streeter, 1988). The ability to form RNS is likely dependent on a single predisposition event, the nature of which remains unknown, and is limited to a single clade, the Fabids (Soltis et al., 1995;

Werner et al., 2014). This clade includes four orders, all of which contain species capable of RNS. The greatest diversity of RNS plants is found in the order Fabales (Sprent, 2009), which contains the legume family, Fabaceae. Within the Fabaceae the subfamily Papilionoideae contains the greatest number of RNS species and the majority of agriculturally significant species (Sprent, 2007). A characteristic phylogenetic trait of Papilionoids is a 50-kb inversion in their genome, which occurred early in their diversification, and this is theorized to have played a part in their rapid radiation, although the mechanisms for this are not clear (Cannon et al., 2014). Interestingly, a number of species within each legume subfamily are incapable of forming RNS, and phylogenetic studies have suggested that these species have likely lost this ability (Werner et al., 2014; Griesmann et al., 2018; van Velsen et al., 2018). An alternative hypothesis is that nodulation has evolved several times independently within the Fabid clade following the predisposition event (Soltis et al., 1995). The nature of the selection pressures as well as the specific genetic components that have led to this gain or loss of function remain unknown (Doyle, 2016).

Among RNS plants, nodule morphology is highly diverse. Nodulating legumes produce nodules originating predominately from the root cortex (e.g., Xiao et al., 2014). There is diversity in nodule morphology even among legumes, with some species forming "indeterminate nodules" which originate from the inner cortex, the layer of cells closest to the endodermis, and these nodules maintain an active meristem. Other legume species form "determinate nodules" and these originate from the outer and middle cortex and their growth terminates after nodule maturation (Hirsch, 1992). In the early stages of development, indeterminate as well as determinate nodules also involve some cell divisions originating from the pericycle (Hirsch, 1992). In contrast to legumes, other RNS plants produce nodules that originate predominantly from the root pericycle. These nodules are described as modified lateral roots. For example, plant species nodulating with filamentous actinorhizal bacteria (mainly *Frankia* spp.) form nodules that are initiated as lateral roots and later modified by *Frankia* to form nodules (Pawlowski and Sprent, 2007; Svistoonoff et al., 2014). These so-called "actinorhizal" symbioses are formed in some members of eight families of the Rosids, but not in legumes. It has been suggested that the cortical origin of legume nodules allowed nodulation "*sui generis*," i.e., independent of lateral root formation (Hirsch and LaRue, 1997), but the nature of the predisposition for cortical-based nodules is not known.

Legume nodule development is a complex and tightly regulated process starting with the recognition between symbionts and the activation of rhizobia in the soil by root exudates, including flavonoids, followed by perception of Nod factors by the plant root by Nod factor receptors (Radutoiu et al., 2003). A signaling cascade is then initiated by the plant leading to nodule development; this involves the initiation of calcium spiking, followed by activation of a number of transcription factors including Nodule INception (NIN) and Nodulation Signaling Pathway1/2 (NSP1/2) (Oldroyd, 2013).

The term "Cytokinin" refers to a class of plant hormones ubiquitous across plants that are involved in many aspects of plant development (Werner and Schmülling, 2009; Hwang et al., 2012). In the root apical meristem, cytokinin inhibits meristematic activity by activating a repressor of auxin signaling, leading to changes in auxin transport proteins and subsequent auxin redistribution (Dello-Ioio et al., 2008; Rùžička et al., 2009). Similarly, in the pericycle, cytokinin inhibits lateral root emergence by acting on auxin transport proteins (Laplaze et al., 2007; Marhavý et al., 2014). In contrast to its inhibiting role on root growth, in nodulating legumes, cytokinin appears to play a role in activating meristematic activity in the normally non-meristematic cortex, which is necessary for nodule organogenesis (Gamas et al., 2017).

Cytokinin responses following infection by rhizobia are activated in the root cortex in both *M. truncatula* and *L. japonicus* (Plet et al., 2011; Held et al., 2014). Increased cytokinin concentrations have been measured in response to rhizobia in *M. truncatula* (van Zeijl et al., 2015) and *L. japonicus* (Reid et al., 2017) and the activation of genes involved in cytokinin synthesis are expressed in the cortex during nodulation in both species (Mortier et al., 2014; Reid et al., 2017). Additionally, using a cytokinin-responsive *TCSn::GUS* reporter line it was shown that the cortical cells of *M. truncatula* respond to exogenous cytokinin, suggesting that cytokinin signaling is active at the site of nodule organogenesis (Fonouni-Farde et al., 2017). CRE1 (CYTOKININ RESPONSE1), homologous to the Arabidopsis cytokinin receptor AHK4, is a membrane-bound cytokinin receptor necessary for nodulation in *M. truncatula* (Gonzalez-Rizzo et al., 2006; Plet et al., 2011). Cytokinin responses mediated by CRE1 during nodule organogenesis include the activation of *NIN* and *NSP2* expression (Plet et al., 2011; Ariel et al., 2012), as well as induction regulation of auxin transport (Plet et al., 2011; Suzaki et al., 2012), which is mediated by the induction of flavonoids, at least in *M. truncatula* (Ng et al., 2015).

Cytokinin is not only necessary but also sufficient for legume nodule initiation. An *L. japonicus* mutant expressing a constitutively active cytokinin receptor forms spontaneous nodules (Tirichine et al., 2007). Furthermore, exogenous application of cytokinin has been shown to lead to the formation of nodule-like, but uninfected, cortical cell-derived structures also known as "pseudonodules" in *M. sativa*, *L. japonicus*, *Trifolium repens*, and *Macroptilium atropurpureum* (Joshi et al., 1991; Relić et al., 1993; Hirsch et al., 1997; Mathesius et al., 2000a; Heckmann et al., 2011). In some cases, these pseudonodules expressed early nodulation genes and developed peripheral vasculature, suggesting that they closely resemble rhizobia-induced nodules (Hirsch et al., 1997; Fang and Hirsch, 1998; Mathesius et al., 2000a; Heckmann et al., 2011). There appears to be some variation in this response, with some ecotypes of *L. japonicus*, for example, showing little or no ability to form pseudonodules in response to exogenous cytokinin (Heckmann et al., 2011). Interestingly, cytokinin-induced pseudonodules have also been reported in the non-Fabid *Nicotiana tabacum* (Arora et al., 1959) and the non-legume actinorhizal RNS species *Alnus glutinosa* (Rodriguez-Barrueco and Bermudez De Castro, 1973). However, the role of cytokinin during actinorhizal nodulation is currently largely unknown.

Although these findings provide convincing evidence of the important role that cytokinin plays in cortical dedifferentiation and subsequent nodule development, to date, only a few nodulating legume species have been examined. Therefore, we investigated the actions of cytokinin across a broad phylogenetic and functional range of nodulating and non-nodulating legumes as well as non-legumes to find out whether the ability of plants to form pseudonodules in response to cytokinin correlates with their ability to nodulate with rhizobia or actinorhizal bacteria.

MATERIALS AND METHODS

Species Selection

A total of 28 plant species were selected to represent the broad diversity of nodulating and non-nodulating Fabids as well as non-Fabids. These species can be placed into the following five categories: nodulating legumes (13 spp.); non-nodulating legumes (4 spp.); nodulating non-legume Fabids (3 spp.); non-nodulating non-legume Fabids (3 spp.); and non-Fabids (5 spp.) (**Figure 1**).

All species were propagated via seed germination. Seeds were acquired from Austrahort (Cleveland, QLD, Australia) for *Adenanthera pavonina*, *Castanospermum australe*, *M. atropurpureum*, *Mimosa pudica*, *Trema tomentosa*; Cleanseeds (Bungendore, NSW, Australia) for *Medicago sativa*, *T. repens*, *Trifolium subterraneum*; Royston Petrie Seeds (Mudgee, NSW, Australia) for *Acacia longifolia*, *Begonia semperflorens*, *Cassia eremophila*, *Cassia nodosa*, *Casuarina glauca*, *Glycine max*, *Solanum lycopersicum*, *Pisum sativum*; Mr Fothergill's seeds (South Windsor, NSW, Australia) for *Cucurbita pepo*, *Helianthus annuus*, and *Zea mays*; Queensland Agricultural Seeds (Towoomba, QLD, Australia) for *Chamaecrista rotundifolia*; and the South Australian Research and Development Institute (Adelaide, SA, Australia) for *Medicago truncatula* cv. Jemalong A17. *Alnus glutinosa* seeds were harvested from a local park in Canberra. *Arabidopsis thaliana* Col-0 seeds were sourced from the Arabidopsis Biological Resource Centre (Ohio State University, United States). *Datisca glomerata* was supplied by Katharina Pawlowski (Stockholm University), *Sesbania rostrata* by Barry Rolfe (formerly Australian National University), *Cicer arietinum* by Angela Pattison (University of Sydney), *Lotus japonicus* by Brett Ferguson (University of Queensland), *N. tabacum* Wis. #381 by Spencer Whitney (Australian National University), the *cre1-1* mutant by Florian Frugier (Institute of Plant Sciences Paris-Saclay, France), and *A. thaliana TCSn::GFP* seeds by Bruno Müller (University of Zürich).

Plant Propagation

Seeds were surface-sterilized in sodium hypochlorite solution 6% (w/v) [except 1% (w/v) for *A. thaliana*, *B. semperflorens*, *D. glomerata*, and *N. tabacum*]. Some species required pre-germination seed treatments (see **Supplementary Table 1** for corresponding treatments per species) which included (1) acid treatment: soaking in 2 M sulfuric acid for 30 s prior to sterilization (except for *A. pavonina* and *C. nodosa*, which were soaked for 45 min); (2) stratification: dark storage at 4°C for 48 h after sterilization; (3) heat treatment: soaking in freshly boiled water for 1 h prior to sterilization; (4) soaking: soaking in water at 21°C overnight prior to sterilization. Most species were grown on sterile agar plates (16 h day, 8 h night with a light intensity of approximately 120 μmole photons m^{-2} s^{-1}; 23°C). Plates contained Fåhraeus medium (Fåhraeus, 1957) for most plants, except for *D. glomerata*, which was grown on Hoagland's nutrient agar (Hoagland and Arnon, 1950) (**Supplementary Table 1**); media was free of nitrogen with the exception of very small-seeded species which were supplemented with 0.5 mM KNO_3 (**Supplementary Table 1**). Larger-seeded species were grown in pots (600 mL volume) containing autoclaved grade 3 vermiculite and kept in a glasshouse at 15/25°C (min/max for night/day) and supplemented with liquid N-free Fåhraeus medium once a week. To determine the effect of nitrogen on pseudonodule formation, 10 mM KNO_3 was added to their respective media where indicated.

Rhizobia Inoculation

Mesorhizobium ciceri strain CC1192, *Mesorhizobium loti* strain MAFF303099, *Sinorhizobium meliloti* strain 1021, and *Sinorhizobium fredii* NGR234 strain ANU280 were cultured on Bergersen's Modified Medium (BMM) (Gresshoff et al., 1977) agar plates for 48 h at 28°C. Before inoculation, single colonies of rhizobia were grown overnight in liquid BMM on a shaking incubator at 28°C. Seeds of *L. japonicus*, *C. arietinum*, *M. atropurpureum*, *M. sativa*, and *M. truncatula* were germinated as described above and inoculated either when the main root was approximately 5 cm long, or in the case of *C. arietinum*, which was grown in pots, when seedlings were 5 days old. Plants grown on plates were inoculated either by flooding treatment, whereby seedlings were immersed in an aqueous solution containing liquid rhizobia culture for 60 s, which was then decanted, or in the case of *C. arietinum* by pipetting 1 mL of culture onto the soil surface. The optical density at 600 nm (OD600) of each culture was adjusted to 0.05, or 0.1 in the case of *M. ciceri*, just before inoculation.

To confirm that pseudonodules contained no rhizobia, 10 individual *C. arietinum* pseudonodules from different plants were surface-sterilized in aqueous sodium hypochlorite solution 1% (w/v) for 5 min and then thoroughly rinsed with sterile water. Pseudonodules were then crushed in an Eppendorf tube using a sterile glass rod and the resulting mixture was cultured on BMM agar plates for 48 h at 28°C. Single colonies of bacteria were grown overnight in liquid BMM on a shaking incubator at 28°C and re-inoculated onto untreated *C. arietinum* plants to test whether they induced nodules, or whether they were other contaminants. *C. arietinum* pseudonodules were chosen as they most closely resembled rhizobia-induced nodules. In addition, solvent-treated plants of each species were included to ensure that nodules did not result from rhizobial contamination in the glasshouse.

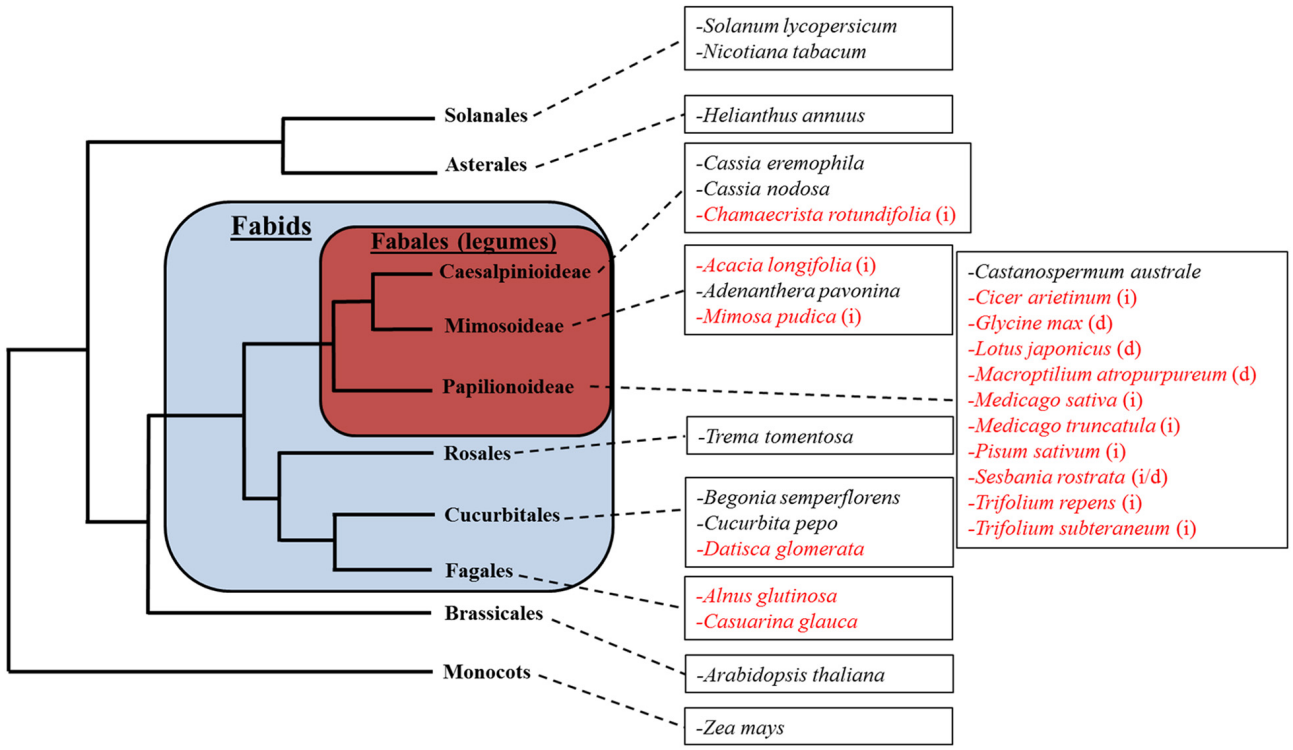

FIGURE 1 | The relative phylogenetic relationship between subject species. Species in red indicate nodulating plant species. Legumes forming indeterminate nodules are marked with (i); legumes forming determinate nodules are marked with (d). Note that this tree does not reflect the exact phylogenetic relationship between the species shown, but merely illustrates their relative classification into different orders.

Cytokinin Treatments

Five different types of cytokinins were used in this study: the synthetic cytokinin BAP (benzylaminopurine) as well as four endogenous cytokinins, *cis*-zeatin, *trans*-zeatin, dihydro-zeatin, and kinetin (all form Sigma Chemicals). For plate-grown plants, cytokinin was administered once via flooding, whereby seedlings were immersed in 20 mL of cytokinin solution for 20 s on the plate before decanting the solution. Cytokinin was applied to plate-grown plants once the main root measured more than 3 cm. For species grown in vermiculite, plants were watered with 50 mL cytokinin solution 1 week after germination and a second time 1 week later. Cytokinin concentrations varied across experiments from 10 nM to 40 μM. We initially treated all plant species with 1 and 10 μM BAP, but if no obvious signs of root growth inhibition were observed at those concentrations, we varied the concentrations of BAP to concentrations that resulted in visible changes in root growth. In nodulating legumes, we also tested additional concentrations of BAP to gain a more detailed picture of active concentrations. Therefore, not all species were treated with the same BAP concentrations in the presented experiments. Stock solutions of 10 mM of the various cytokinins were made in dimethyl sulfoxide (DMSO, Sigma Chemicals) and treatment solutions were made up with sterile distilled water, all solutions were filter sterilized. Appropriately diluted and filter-sterilized DMSO was used as a negative control treatment.

Quantifying Pseudonodules

Plate-grown plants were harvested 4 weeks following treatments; plants grown in vermiculite were harvested 3 weeks after the first treatment and gently rinsed in tap water. Pseudonodules were counted with the aid of a magnifying glass or stereo microscope. Pseudonodules were identified by their bulbous shape, which contrasted with emerging lateral roots identified by their clearly recognizable conical shape.

A Chi-square analysis was performed between each cytokinin treatment and control to determine the statistical significance of the number of replicates producing pseudonodules using Prism from GraphPad (La Jolla, CA, United States). A non-parametric Kruskal–Wallis test with a Dunn *post hoc* test was performed between treatments producing pseudonodules in order to determine cytokinin concentration-dependent frequency of pseudonodulation.

Root Growth Assays

Following harvesting and nodule counting, plants grown in agar, as well as some grown in vermiculite were scanned on a flat-bed scanner (Epson Perfection V700 Photo). A ruler was scanned next to the roots for calibration. Main root length, lateral root length, and total root numbers were determined using ImageJ[1]. For vermiculite-grown plants with highly complex root

[1]https://imagej.nih.gov/ij/

architecture, fresh root weight was measured as a proxy for the overall length of the root system. Analysis of variance (ANOVA) with Tukey *post hoc* test was performed between treatments for each species using Prism.

Anatomical Analysis of Roots

Transverse cross-sections of cytokinin-treated roots and control roots were examined in all species. At least five 1 cm-long root segments from different plants were serially cross-sectioned per species and treatment. This was done in order to qualitatively identify the cellular origin of pseudonodules. Small root segments were embedded in 3% (w/v) DNA-grade agarose (Amresco). Transverse cross-sections of 100 μm were made using a vibratome (1000plus, Vibratome Company). Cross-sections were transferred to glass slides and visualized using a compound microscope (Leica DM5500B) using brightfield or fluorescence illumination (excitation 360 ± 40 nm, emission 470 ± 40 nm) with a Leica DFC7000T color digital camera. Fluorescence microscopy allowed clear identification of the endodermis to assess any cell division in the cortex. To ensure that pseudonodules contained no infected cells, *C. arietinum* pseudonodules and rhizobia-infected nodules were sectioned and stained with Toluidine Blue (0.05%, pH 4.4) to identify infected nodules (Maunoury et al., 2010).

Assessing Cytokinin Response in *A. thaliana TCSn::GFP* Reporter Line Using Confocal Microscopy

Following sterilization and cold-treatment, *A. thaliana TCSn::GFP* seeds (Zürcher et al., 2013) were grown on the surface of glass slides coated with a thin film of N-free Fåhraeus agar, on which roots could be directly visualized through a microscope. These slides were placed in sterile magenta jars containing a layer of dental wax on the base to secure the slides. The magenta jars were placed in a temperature-controlled growth chamber at 20°C, with a 16 h light period at 120 μmole photons m^{-2} s^{-1} light intensity. After germination, seedlings were grown for four more days.

Prior to BAP treatment, the GFP fluorescence in roots of five seedlings was recorded by imaging 1 mm from the main root tip using a Leica SP8 laser scanning confocal microscope (488 nm excitation, 500–550 nm emission) with corresponding transmitted brightfield image. In order to obtain a vertical profile of fluorescence through each root, a series of optical sections was collected using the confocal Z-stack software.

Seedlings were then incubated in a 1 μM BAP solution for 20 h in the dark, as described by Zürcher et al. (2013). Following cytokinin incubation, the fluorescence from the same part of each root was recorded using the same confocal imaging settings. Pre-cytokinin and post-cytokinin images were then compared using the Leica LasX image analysis software in order to quantify the GFP signal in separate cell layers. To statistically compare the change in fluorescence, the pre-cytokinin and post-cytokinin signal intensity values were analyzed using a two-tailed Student's *t*-test for each cell layer using Prism.

TCSn::GFP expression in whole seedling roots was visualized using a fluorescence stereomicroscope (Leica M205FA) after excitation with a ET Blue LP filter system (excitation 470 nm, emission 515 nm long pass filter). Photos were taken with a Leica DFC550 digital camera.

RESULTS

Morphological and Anatomical Effects of Cytokinin on Root Development

The synthetic cytokinin BAP has been used previously to induce pseudonodules in legumes (e.g., Mathesius et al., 2000a; Heckmann et al., 2011) and was therefore used to screen all 28 species. BAP-induced nodule-like structures ("pseudonodules") formed on roots of all nodulating legume species examined, with some morphological variation between species (**Figure 2**). The ability to form pseudonodules did not seem to be more frequent or efficient in legumes forming either determinate or indeterminate nodules (as indicated in **Figure 1**), but varied even within a genus (see below). Across species, pseudonodules were fully developed between 2 and 4 weeks post-BAP treatment and formed in species grown in plates as well as in pots containing vermiculite. *Mimosa pudica* was grown in both plates and vermiculite and both growth media resulted in pseudonodulation after BAP treatment. No pseudonodules were observed in any of the non-nodulating legumes, or in any of the non-legume species, irrespective of their growth on plates or in vermiculite (**Supplementary Table 2**). No pseudonodules or cortical cell divisions were seen after application of 1 μM BAP to roots of the Medicago *cre-1* mutant (0/20 roots), which is defective in the cytokinin receptor gene *CRE-1* (**Supplementary Figure 1e**), compared to successful pseudonodules found in wild-type roots (9/20 roots). None of the solvent-treated plants showed any nodulation except the legume *M. sativa*, which showed some degree of spontaneous nodulation as previously reported (**Figure 2h**; Joshi et al., 1991).

We also tested whether endogenous cytokinins were able to induce pseudonodules. For this experiment, we chose one legume species that readily formed pseudonodules with BAP, *M. atropurpureum*, and two non-legumes. For the non-legumes, we chose *A. glutinosa* and *N. tabacum*, because in these species pseudonodules had been reported in previous studies (Arora et al., 1959; Rodriguez-Barrueco and Bermudez De Castro, 1973). In addition, *A. glutinosa* represented a nodulating actinorhizal species and *N. tabacum* represented a non-nodulating non-fabid. These hormones were tested at concentrations of 10, 20, 50, 60, and 100 μM. Application of *cis*-zeatin, *trans*-zeatin, dihydrozeatin, or kinetin all induced pseudonodules in the nodulating legume *M. atropurpureum* (**Figure 3**), showing that all applied cytokinins could induce pseudonodules on a nodulating legume, although with some differences in resulting morphology and effective concentrations. The photos in **Figure 3** show the lowest tested cytokinin concentrations that led to the formation of pseudonodules, although pseudonodules were also formed at higher concentrations. However, no pseudonodules were found

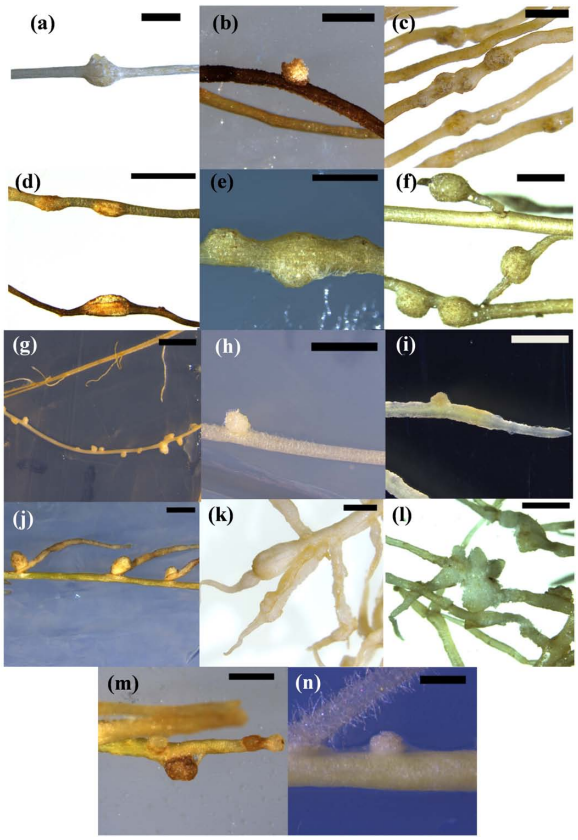

FIGURE 2 | *Pseudonodules in nodulating legume species*. **(a)** *Acacia longifolia* 5 μM BAP; **(b)** *Chamaecrista rotundifolia* 10 μM BAP; **(c)** *Cicer arietinum* 10 μM BAP; **(d)** *Glycine max* 1 μM BAP; **(e)** *Lotus japonicus* 1 μM BAP; **(f)** *Macroptilium atropurpureum* 10 μM BAP; **(g)** *Medicago sativa* 10 nM BAP; **(h)** *Medicago sativa* untreated spontaneous nodule; **(i)** *Medicago truncatula* 1 μM BAP; **(j)** *Mimosa pudica* 10 μM BAP; **(k)** *Pisum sativum* 10 μM BAP; **(l)** *Sesbania rostrata* 1 μM BAP, **(m)** *Trifolium repens* 10 μM BAP; **(n)** *Trifolium subterraneum* 10 μM BAP. Bars **(a,c,d,g,j,k)** 2 mm; **(b,e,f,h,i,l,m,n)** 1 mm.

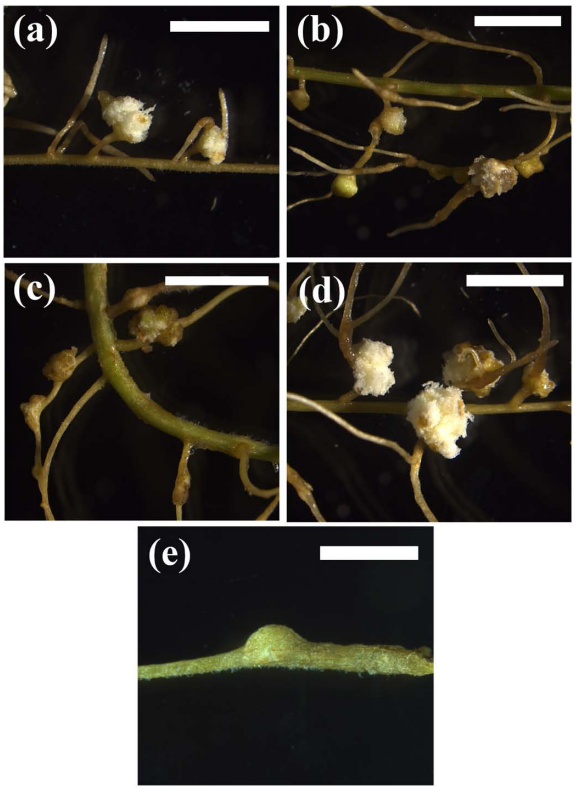

FIGURE 3 | Phenotypic response of different cytokinins on *M. atropurpureum*. **(a)** 10 μM BAP. **(b)** 50 μM *cis*-zeatin. **(c)** 10 μM dihydrozeatin. **(d)** 50 μM kinetin. **(e)** 60 μM *trans*-zeatin. Pseudonodules are shown 4 weeks after treatment. Bars **(a–d)** 500 μm; **(e)** 200 mm.

after application of these endogenous cytokinins at any of the concentrations in the actinorhizal species *A. glutinosa* or the non-fabid *N. tabacum*, although some cortical cell-swelling was observed in *A. glutinosa* (**Supplementary Figure 1**).

Across nodulating legume species, pseudonodules emerged from both main roots and lateral roots. A notable exception was *M. pudica*, where pseudonodules emerged exclusively from the junction between the main root and lateral roots (**Figure 2j**). In *P. sativum*, significant root swelling due to expanded cortical cells (**Figure 2k**) resulting from BAP treatment made it difficult to enumerate pseudonodules without sectioning the root. However, cross sections clearly showed the formation of pseudonodule primordia (**Supplementary Figure 2**).

The frequency of pseudonodulation was species- and concentration-dependent, but there was no interspecific trend in the frequency of pseudonodulation as there was significant variation between species in the optimum BAP concentration. In some species (*M. truncatula* and *L. japonicus*), higher BAP concentrations lead to lower pseudonodulation frequency (**Supplementary Table 2**) possibly due to the concomitant inhibition of root growth by BAP.

Cross sections through BAP-treated roots revealed that pseudonodules (and spontaneous nodules of *M. sativa*) appeared to originate from cell divisions in the root cortex (outside the autofluorescent endodermis) (**Figure 4** and **Supplementary Figure 2**). In certain species, however, such as *A. longifolia* (**Figure 4**) the endodermis was no longer clearly discernible, making it difficult to identify the cellular origins of the structure.

In *C. arietinum*, pseudonodules consistently contained a pink pigment in the center, which made them appear similar to leghemoglobin-containing rhizobia-induced nodules (**Figure 5**). Control-treated plants showed no pink pigmentation. To test whether these pink pseudonodules contained rhizobia or not, bacteria isolated from surface-sterilized pseudonodules were re-inoculated onto sterile-grown chickpea plants. None of these plants developed nodules. In addition, sections of rhizobia-induced nodules displayed characteristic staining indicative of infected nodule cells after Toluidine Blue staining, whereas pseudonodules did not appear to contain any infected cells (**Figure 5**).

Non-nodulating legumes, nodulating non-legume Fabids, non-nodulating non-legume Fabids, and non-Fabids, none of which developed visible pseudonodules, also showed no cortical

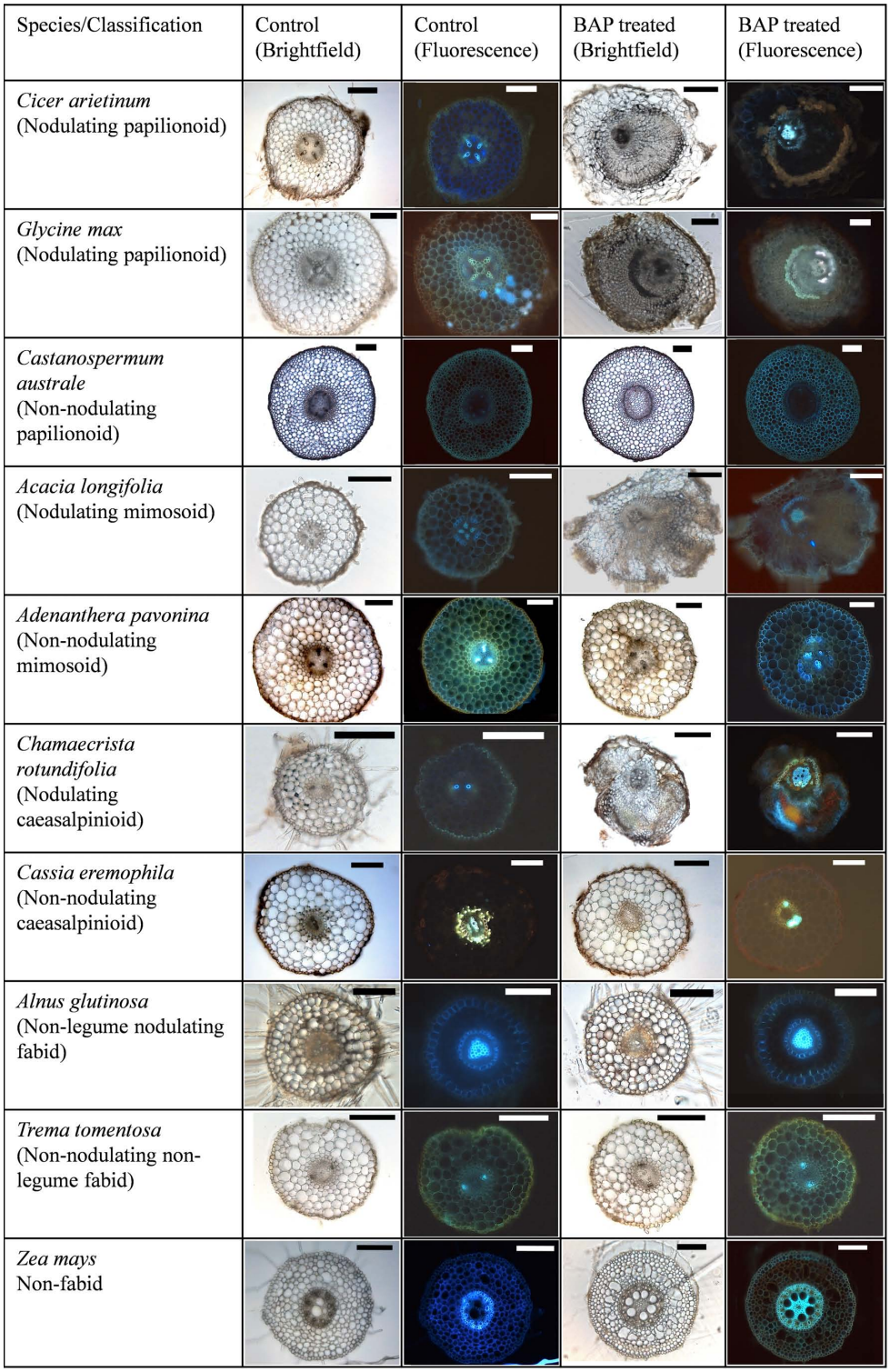

FIGURE 4 | Cytokinin-induced organogenesis is a conserved feature of nodulating legumes. A range of examples of nodulating and non-nodulating legumes from the three legume subfamilies are shown along with actinorhizal plants, non-nodulating Fabids, and non-nodulating non-Fabids. *Cicer arietinum* 1 μM BAP; *Glycine max* 10 μM BAP; *Castanospermum australe* 10 μM BAP; *A. longifolia* 10 μM BAP; *Adenanthera pavonina* 20 μM BAP; *C. rotundifolia* 10 μM BAP; *Cassia eremophila* 20 μM; *Alnus glutinosa* 10 μM BAP; *Trema tomentosa* 20 μM BAP; *Zea mays* 20 μM BAP. All bars = 200 μm, except BAP-treated *C. arietinum*, *A. longifolia* (500 μm), and control and treated *A. glutinosa* (100 μm).

cell divisions in response to BAP, confirmed in serial sections of several roots for each species (**Figure 4** and **Supplementary Figures 2**, **3**). One exception was that in the non-Fabid *H. annuus* (sunflower), BAP induced limited cortical cell division; however, this never advanced to the stage of organogenesis (**Supplementary Figure 1d**). Cell swelling, mainly of cortical cells, was another cytokinin-induced phenotype observed across several plant species irrespective of their ability to nodulate or form pseudonodules (**Supplementary Figure 1**). However, cell swelling was also observed to some extent in the *cre1* mutant of *M. truncatula* (**Supplementary Figure 1e**), and is therefore likely an unrelated effect.

To test if the ability of BAP to form pseudonodules was correlated with the species' ability to respond to BAP with other known cytokinin-induced root phenotypes, we determined root length and lateral root numbers; in pot-grown species with complex root systems, root weight was measured as a proxy for root length and root numbers. Both assays revealed a consistent and usually dose-dependent reduction in either root length or lateral root number or both, following BAP treatment, irrespective of a species' ability to form pseudonodules (**Supplementary Figures 4**, **5**), except for *S. lycopersicum*, *C. nodosa*, and *A. pavonina*, which did not respond to any applied BAP concentration. This suggests that pseudonodulation is the result of a specific response to BAP in nodulating legumes.

Comparison of BAP-Induced Pseudonodules and Infected Nodules

The developmental stages of nodules and pseudonodules were compared by examining cross-sections over a time course of 2–4 weeks in two species forming indeterminate nodules (*M. sativa*, *C. arietinum*) and two species forming determinate nodules (*L. japonicus*, *M. atropurpureum*), which were treated either with BAP or their respective symbionts. These species were chosen because they formed well-synchronized and well-differentiated pseudonodules at high frequencies. In *M. sativa* and *C. arietinum*, both BAP and rhizobia led to initiation of cell divisions mainly in the inner cortex that later developed into mature structures derived mainly from the root cortex (**Figure 6** and **Supplementary Figure 6**). However, the final nodule shapes were somewhat different, with pseudonodules often either multi-lobed or broader than rhizobia-induced nodules (**Figure 6** and **Supplementary Figure 6**). In both *M. sativa* and *M. truncatula*, roots containing pseudonodules often showed extensive differentiation of the vascular tissue (**Supplementary Figure 6**), although this was likely a result of natural root differentiation in older parts of the roots as it also occurred in untreated roots forming spontaneous nodules (**Supplementary Figure 2**).

In *L. japonicus* and *M. atropurpureum*, both BAP and rhizobia treatment lead to initiation of cell divisions in the outer as well as inner root cortex (**Figure 7** and **Supplementary Figure 7**). Mature *M. atropurpureum* pseudonodules often contained multiple central vascular strands and nodule lobes compared to single lobed rhizobia-induced nodules with peripheral vasculature (**Figures 7e,f,k,l**). Chickpea pseudonodules were often broad-shaped and typically formed peripheral vasculature (**Figure 6e**). Infected nodules as well as pseudonodules often contained fluorescent flavonoids, which appear to be markers of cortical cell division across legumes (Mathesius et al., 1998; **Figures 6**, **7** and **Supplementary Figures 6**, **7**). The effects of external nitrogen on the inhibition of pseudonodulation and nodulation were also assayed in four legume species (*C. arietinum*, *M. sativa*, *T. repens*, *M. atropurpureum*). *T. repens* was included in this experiment because a previous study had shown that nitrate addition only partially prevented *ENOD40* induction by BAP (Mathesius et al., 2000a), while nitrate inhibition of pseudonodules in *L. japonicus* had been demonstrated previously (Heckmann et al., 2011). All four species displayed significant reduction of nodule and pseudonodule numbers following addition of 10 mM KNO_3 to the growth media (**Supplementary Figure 8**).

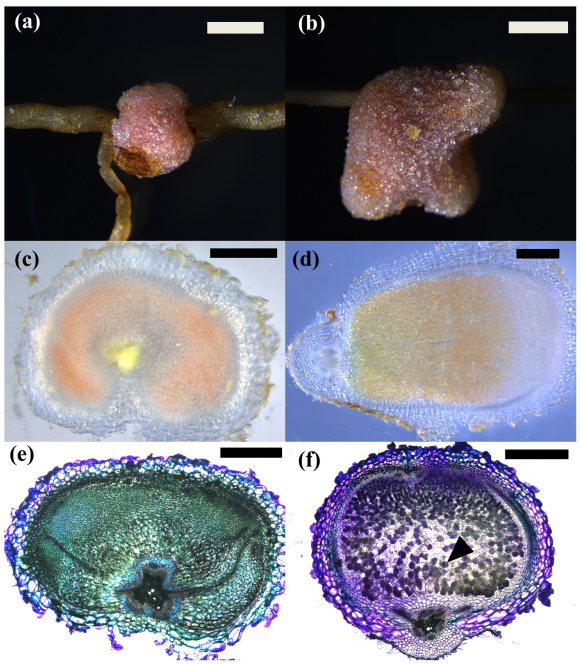

FIGURE 5 | Phenotypes of 4-week-old pseudonodules and infected nodules in *C. arietinum*. **(a,c,e)** *C. arietinum* treated with 5 μM BAP; **(b,d,f)** *C. arietinum* infected with *Mesorhizobium ciceri*. **(a,b)** Stereo microscope image of mature (pseudo)nodules showing pink coloration from the outside. Bar = 500 μm. **(c,d)** Cross sections through mature (pseudono)nodules. While pseudonodules form in a wide area around the root, infected nodules are more elongated. **(e,f)** Toluidine Blue-stained cross sections of (pseudo)nodules showing dark purple, large infected cells in infected nodules (black arrow) **(f)** and smaller cells without intracellular staining inside the pseudonodule, suggesting that these cells are not infected **(e)**.

Localizing Tissue Responses to Cytokinin in *A. thaliana TCSn::GFP* Reporter Plants

The fluorescence of *A. thaliana* seedlings expressing the cytokinin reporter *TCSn::GFP* was recorded before and after 20 h incubation in 1 or 10 μM BAP. Visualization of whole seedling

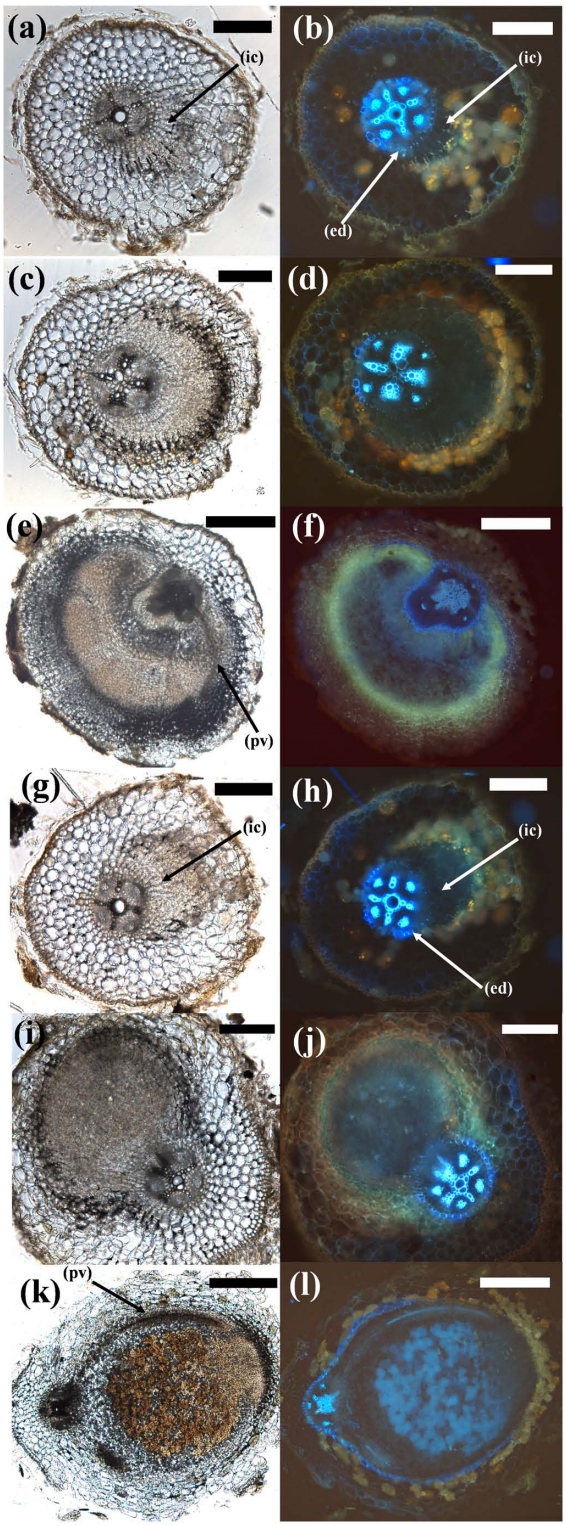

FIGURE 6 | Comparison of different stages of pseudonodule and nodule development in *C. arietinum*. **(a–f)** *C. arietinum* roots treated with 10 μM BAP; **(g–l)** *C. arietinum* inoculated with *M. ciceri*. Sections on the left show the brightfield images, photos on the right side show the respective images under UV exposure to visualize flavonoids (yellow–orange or blue autofluorescent cell (*Continued*)

FIGURE 6 | Continued
content mainly in cortical cells surrounding nodules/primordia) and the endodermis (strongly blue auto-fluorescent cell walls). (**a,b**; 5d post-BAP) and (**g,h**; 5d post-inoculation) Early-stage primordia showing first cell divisions in the inner cortex (ic) which can be distinguished from the vascular tissue and the pericycle by the fluorescent endodermis (ed). (**c,d**; 7d post-BAP) and (**i,j**; 7d post-inoculation) Medium-stage primordia. Note the more clearly defined structure of the inoculated phenotype. (**e,f**; 14d post-BAP) Mature pseudonodule displaying peripheral vasculature (pv). (**k,l**; 14d post-inoculation) Mature nodule displaying peripheral vasculature (pv). Bars **(a–d)**, **(g,h)** 200 μm; **(e,f)**, **(k,l)** 500 μm.

roots under a fluorescent stereomicroscope showed expression in the root apical meristem and the vascular tissue, which was enhanced in the same tissues after BAP application, as described in other studies (Zürcher et al., 2013; **Supplementary Figure 9**). A more detailed analysis was carried out using confocal microscopy. Six *A. thaliana* seedlings expressing the cytokinin reporter *TCSn::GFP* were analyzed at 1 mm from the root tip, the root–hair elongation zone where pseudonodules and nodules are typically initiated in legumes, before and after 20 h incubation in 1 μM BAP. Untreated roots showed GFP expression in vascular and epidermal cells, but not in cortical cells (**Figure 8**). The GFP expression was significantly increased in the vascular tissue following BAP application, but remained unchanged in the epidermis and was not induced in cortical cells (**Figure 8**).

DISCUSSION

Cytokinin-Induced Pseudonodulation Is a Conserved Response Among Nodulating Legumes

Prior to this study, BAP-induced pseudonodulation had only been described in detail in three nodulating legume species; *M. sativa* (Hirsch et al., 1997), *T. repens* (Mathesius et al., 2000a), and *L. japonicus* (Heckmann et al., 2011). This study has shown that BAP-induced pseudonodulation is a conserved feature among nodulating legumes, and was observed in species from all three legume subfamilies. Pseudonodulation was also induced by the exogenous application of four endogenous cytokinins in *M. atropurpureum*, suggesting that this is not a BAP-specific response. A characteristic phylogenetic trait of Papilionoids is a 50-kb inversion in their genome, which occurred early in the diversification of Papilionoids (Cannon et al., 2014) and may have led to the diversification of nodulation-related genes, including cytokinin response regulators (Op den Camp et al., 2011). The functional consequences of this inversion are still not fully known. On account of the conserved response observed between species of each legume subfamily, it appears that cytokinin-induced phenotypes are not contingent upon the inheritance of the 50-kb inversion.

Cross-sectional analysis revealed that pseudonodules in all species display anatomical similarities with infected nodules, namely cortical cell divisions. In the two species forming determinate nodules, *L. japonicus* and *M. atropurpureum*, BAP

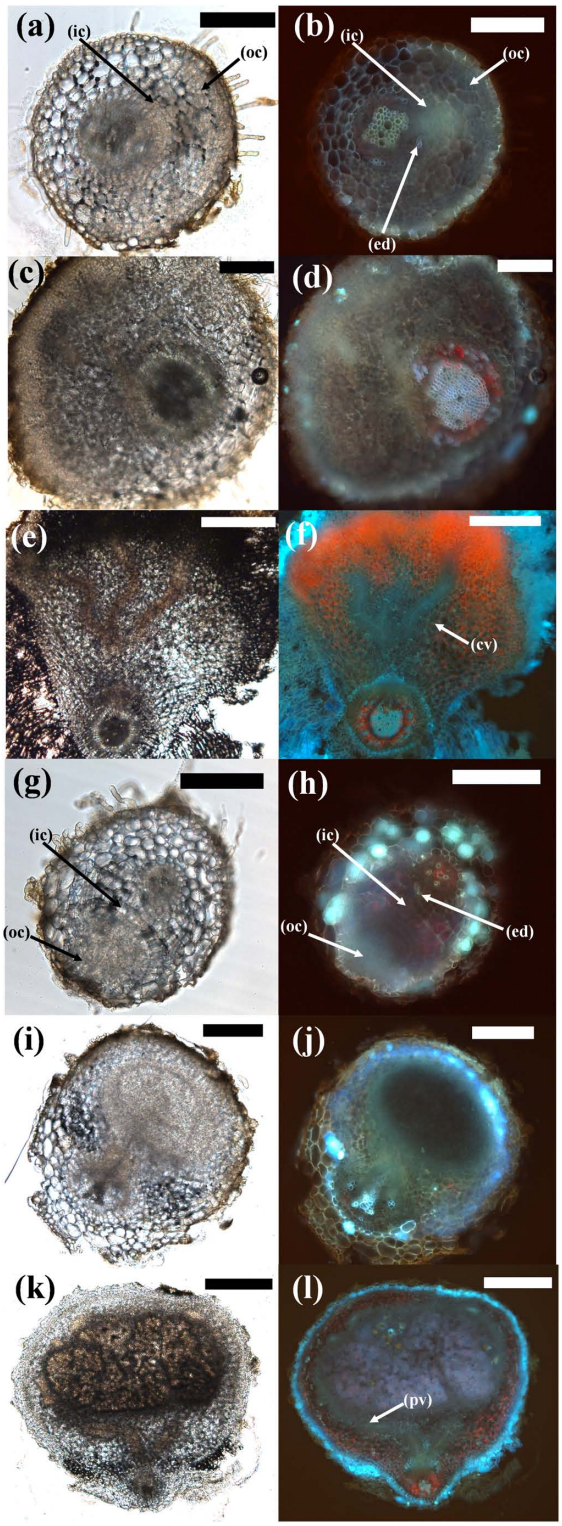

FIGURE 7 | Comparison of different stages of pseudonodule and nodule development in *M. atropurpureum*. **(a–f)** *Macroptilium atropurpureum* roots treated with 10 μM BAP; **(g–l)** inoculated with *Sinorhizobium fredii* NGR234 strain ANU280. Sections on the left show the brightfield images, photos on the right side show the respective images under UV exposure to visualize the (*Continued*)

FIGURE 7 | Continued
endodermis (light blue auto-fluorescent cell walls). (**a,b**; 7d post-BAP) and (**g,h**; 5d post-BAP) Early-stage primordia showing first cell divisions in the outer (oc) and inner cortex (ic) which can be distinguished from the vascular tissue and the pericycle by the fluorescent endodermis (ed). (**c,d**; 14d post-BAP) and (**i,j**; 10d post-inoculation) Medium-stage primordia showing divisions predominately originating from the outer cortex in both treatments. (**e,f**; 21d post-BAP) Mature pseudonodule displaying central vasculature (cv). (**k,l**; 14d post-inoculation) Mature nodule displaying peripheral vasculature (pv). Bars **(a–j)** 200 μm; **(k,l)** 500 μm. Red pigment is most likely due to chlorophyll autofluorescence, especially in the mature pseudonodule and vascular tissue.

treatment induced initial cell divisions in the outer and inner cortex, whereas in two species forming indeterminate nodules, *C. arietinum* and *M. sativa*, initial cell divisions were seen mainly in the inner cortex. These similarities in phenotypic response between pseudonodules and rhizobia-induced nodules suggest that the origin of nodule primordia is determined by a cell-specific cytokinin response.

In *M. pudica*, pseudonodules originated only from the junction of the main root with lateral roots and may reflect a "crack-entry" infection strategy common among Mimosoids (Sprent, 2009). Interestingly, peripheral vascularization and even pink pigmentation were prominent in pseudonodules of *C. arietinum*, which only appeared during late stages of development. The presence of vascular tissue in *C. arietinum* and *M. atropurpureum* pseudonodules contrasted with the noted absence of vascular tissue in *L. japonicus* pseudonodules reported here and by Heckmann et al. (2011). Another indication that pseudonodules share developmental similarities with infected nodules is that nitrogen in the growth media inhibited their development, consistent with previous observations (Heckmann et al., 2011).

In addition, the *M. truncatula cre1-1* mutant defective in the transduction of Nod factor-induced cytokinin signaling (Plet et al., 2011) did not form pseudonodules or cortical cell divisions. This indicates that the cytokinin-induced phenotype is dependent on the same cytokinin receptor involved in nodule development. Similarly, the *L. japonicus lhk1* cytokinin receptor mutant was shown not to form pseudonodules in response to BAP (Heckmann et al., 2011).

One role of cytokinin in plant development is as a negative regulator of root growth by inhibiting lateral root initiation in the pericycle (e.g., Laplaze et al., 2007) and inhibition of the root apical meristem (e.g., Růžička et al., 2009). In view of the conserved pseudonodulation observed in nodulating legumes, it is important to consider whether this response is the result of a heightened general sensitivity to cytokinin, or rather a specific sensitivity. Cytokinin treatments resulted in a consistent reduction in root growth and lateral root formation across most species, irrespective of their propensity to form pseudonodules. This indicates that pseudonodulation is dependent on a positive effect of cytokinin in the root cortex, which is independent of inhibition of cell proliferation in the pericycle and root apical meristem.

Apart from differences in the observed cytokinin responses between nodulating and non-nodulating species, significant

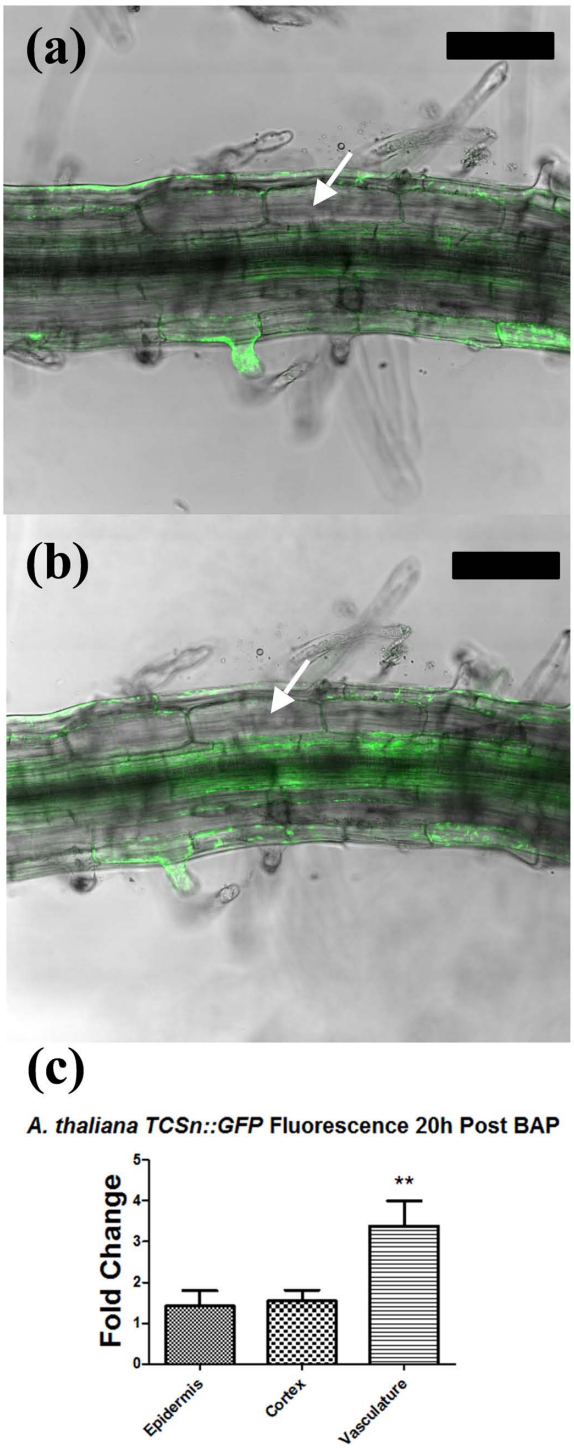

FIGURE 8 | Tissue-specific response in *Arabidopsis thaliana* TCSn::GFP following cytokinin treatment. **(a,b)** Confocal laser scanning microscope images of *A. thaliana TCSn::GFP* root 1 cm behind the root tip. GFP fluorescence (green) is overlaid on the brightfield image. **(a)** Root before treatment. **(b)** Root after incubation in 1 μM BAP solution for 20 h. **(c)** Fold change increase in GFP fluorescence intensity in three different tissue types. Fold changes reflect the ratio of fluorescence intensity values before and after BAP treatment. Values were statistically compared using a two-tailed *t*-test. $n = 6$. ** indicates $p < 0.01$. White arrows, cortical cells. Bars, 100 μm.

variation in cytokinin-induced pseudonodulation has been observed in different ecotypes of *L. japonicus* (Heckmann et al., 2011). A stark difference in response to cytokinin was also noted here between two closely related species: *M. sativa* and *M. truncatula*. Only *M. sativa* produced pseudonodules spontaneously, as previously reported by Joshi et al. (1991). Furthermore, pseudonodules produced by *M. sativa* displayed a more advanced degree of development compared to those produced in *M. truncatula*. This difference between closely related plants may be due to differential expression of cytokinin oxidases, which have been shown to play important roles in coordinating cytokinin responses during nodule development, and which could confer feedback inhibition to external cytokinin application (Reid et al., 2016). Additionally, different members of type-A response regulators in different species may differentially regulate cytokinin responses during nodulation (Gamas et al., 2017).

Pseudonodules Were Not Observed in Plant Species Unable to Form Cortical-Based Nodules

RNS is not a unique feature of legumes, as it is found in numerous species belonging to the other three orders that make up the Fabid clade. These non-legume RNS plants recruit actinorhizal bacteria as their nitrogen-fixing symbiont, as opposed to legumes which recruit rhizobia. In this study, we have shown that nodulating non-legume Fabids (*A. glutinosa*, *C. glauca*, and *D. glomerata*) produced neither pseudonodules nor cortical cell divisions following exogenous cytokinin treatment. This differential response may indicate key anatomical differences between rhizobial and actinorhizal nodules (**Figure 9**). Actinorhizal nodules originate from the pericycle and are morphologically akin to lateral roots (Pawlowski and Sprent, 2007) and as such may implement a different signaling pathway to initiate nodule organogenesis, even though some of the early symbiotic signaling pathway is shared with legumes (Svistoonoff et al., 2014).

We note that our results contradict previously published findings which reported the development of pseudonodules in *A. glutinosa* (Rodriguez-Barrueco and Bermudez De Castro, 1973) and *N. tabacum* (Arora et al., 1959) following treatment with kinetin. In our study, exogenous treatment with BAP did not result in organogenesis despite root growth being significantly inhibited in both species. Treatment with four endogenous cytokinins including kinetin also did not result in organogenesis, although cell-swelling resulted in *A. glutinosa* following treatment with *cis*-zeatin. This discrepancy may be due to differences in experimental design. Rodriguez-Barrueco and Bermudez De Castro (1973) grew plants in hydroponics with roots exposed to a constant concentration of cytokinin for several weeks. Arora et al. (1959) propagated plants via tissue culture and also grew them in hydroponics with roots exposed to a constant source of kinetin. Propagation via tissue culture can induce genetic changes in plants (e.g., Phillips et al., 1994) and it is possible

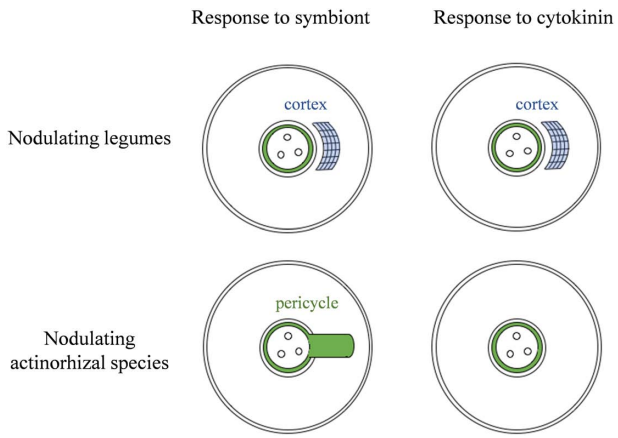

FIGURE 9 | Model for the observed correlation between the site of nodule organogenesis and cortical response to cytokinin. Nodulating legumes typically form nodules originating predominantly in the cortex, and this correlates with the ability to proliferate cortical cells in response to cytokinin, which then leads to pseudonodule formation. Actinorhizal species that nodulate with *Frankia* spp. typically form nodules from modified lateral roots. These species lack cortical cytokinin responses and pseudonodule formation.

that the growth conditions induced a phenotypic response not generally observed under natural growth conditions. Arora and colleagues also noted that the structures displayed considerable morphological differences compared to legume nodules in that they were largely undifferentiated and always associated with the induction of lateral roots. We cannot rule out the possibility that lack of pseudonodule formation observed in many species in our study was due to our specific growth conditions, nevertheless, we conclude that the non-nodulating species we examined are either unable to form pseudonodules, or differ significantly from nodulating legumes in their sensitivity to the action of cytokinin in the cortex.

A surprising result was the observation that *H. annuus* (sunflower) responded to cytokinin with limited cortical cell divisions, although these did not proceed to give rise to primordia, as was observed in all nodulating legume species. It is possible that the cytokinin response in *H. annuus* is rapidly downregulated after cytokinin addition or that cytokinin addition activates its degradation, similar to observations in *L. japonicus* (Reid et al., 2016). Alternatively, the cytokinin response observed in *H. annuus* may be lacking elements necessary for transition of cortical cell divisions to primordium formation (Tirichine et al., 2007; Heckmann et al., 2011). Other non-legume species are capable of activating cortical cell divisions, for example during lateral root development, but these do not proceed to form nodule primordia (McCully, 1975). This includes members of the Rosids related to actinorhizal species, e.g., *C. pepo* (Ilina et al., 2018) as well as legumes (Mathesius et al., 2000b; Herrbach et al., 2014).

Evidence from phylogenetic studies suggests that non-nodulating legume species have lost the ability to form RNS (Sprent, 2009), in one of many possible ways. With environmental changes leading to increased soil nitrogen, the carbon-cost associated with RNS may have outweighed the benefits. Many plant pathogens exploit the cytokinin pathway of plants either through direct synthesis of cytokinin or by altering the plant host's cytokinin pathway (Giron et al., 2013) and therefore the costs associated with pathogenicity may have played a part in driving the loss of a specific cytokinin sensitivity. Comparative phylogenomics studies have so far not identified any genes specific to nodulating plants (Griesmann et al., 2018) and of the few that could explain loss of nodulation in non-nodulators, the main candidates are *NIN* and *Rhizobium-directed Polar Growth* (*RPG*). *RPG* is required for infection and thus unlikely to be associated with pseudonodule formation. NIN is essential for infection and cortical cell division in legumes, and for pseudonodule formation in *L. japonicus* (Heckmann et al., 2011), and it interacts with cytokinin signaling in the cortex through a positive feedback loop (Gamas et al., 2017). *NIN* has been lost in several non-nodulating species, including *C. australe* (Griesmann et al., 2018), which was included in this study. However, *NIN* is unlikely to predict the ability for pseudonodule formation because it was shown to be necessary for the formation of nodules in actinorhizal species, which did not form pseudonodules in our study, and do not show cortical-based nodule development (Svistoonoff et al., 2014). To our knowledge, no other candidate genes are currently known that could explain the differential ability of nodulating legumes to form pseudonodules.

A. thaliana Lacks a Cortical Cytokinin Response Following BAP Treatment

Since *A. thaliana* was shown in prior assays to not respond to cytokinin with induction of cortical-cell divisions it was hypothesized that the cortex cannot perceive cytokinin. To investigate this possibility, the spatial profile of cytokinin perception was analyzed in *A. thaliana TCSn::GFP* reporter plants, which revealed that cytokinin elicited a response in the vascular tissue, but not in the cortical cell layer. In contrast, the *TCSn::GUS* reporter was induced in the cortex of *M. truncatula* (Fonouni-Farde et al., 2017) and *L. japonicus* (Reid et al., 2017) in response to cytokinin. One possible explanation for why some plants are able to respond to cytokinin with the initiation of pseudonodules, while others cannot, is that cytokinin is either not perceived or not translated into the required downstream responses by the cortex in non-responders. Differences in expression or localization of cytokinin response genes may account for the lack of cortical response in non-nodulating plants. An expansion of the cytokinin response pathway is a noted feature of land plant evolution (Pils and Heyl, 2009), and this might extend to a novel cytokinin perception module in the cortex of nodulating legumes, correlating with their unique ability to initiate nodules *de novo* from cortical cells. Future studies will have to identify the nature of such a proposed cortex-specific cytokinin response in

nodulating legumes, and its suggested loss in non-nodulating legumes.

AUTHOR CONTRIBUTIONS

All authors contributed to the conception of the study and writing of the manuscript. CG-C carried out experimental work with contributions from RW and UM.

FUNDING

This work was supported by the Australian Research Council (DP150102002 to UM).

ACKNOWLEDGMENTS

We thank Florian Frugier for the *cre1-1* mutant, Bruno Müller for the Arabidopsis *TCSn::GFP* line, Brett Ferguson for the *L. japonicus* seeds, Katharina Pawlowski for the *D. glomerata* seeds, Barry Rolfe for the *S. rostrata* seeds, Angela Pattison for the *C. arietinum* seeds, and Spencer Whitney for the *N. tabacum* seeds.

SUPPLEMENTARY MATERIAL

The Supplementary Material for this article can be found online at: https://www.frontiersin.org/articles/10.3389/fpls.2018.01901/full#supplementary-material

REFERENCES

Ariel, F., Brault-Hernandez, M., Laffont, C., Huault, E., Brault, M., Plet, J., et al. (2012). Two direct targets of cytokinin signaling regulate symbiotic nodulation in *Medicago truncatula*. *Plant Cell* 24, 3838–3852. doi: 10.1105/tpc.112.103267

Arora, N., Skoog, F., and Allen, O. N. (1959). Kinetin-induced pseudonodules on tobacco roots. *Am. J. Bot.* 46, 610–613. doi: 10.1002/j.1537-2197.1959.tb07060.x

Cannon, S. B., McKain, M. R., Harkess, A., Nelson, M. N., Dash, S., Deyholos, M. K., et al. (2014). Multiple polyploidy events in the early radiation of nodulating and nonnodulating legumes. *Mol. Biol. Evol.* 32, 193–210. doi: 10.1093/molbev/msu296

Dello-Ioio, R. D., Nakamura, K., Moubayidin, L., Perilli, S., Taniguchi, M., Morita, M. T., et al. (2008). A genetic framework for the control of cell division and differentiation in the root meristem. *Science* 322, 1380–1384. doi: 10.1126/science.1164147

Doyle, J. J. (2016). Chasing unicorns: nodulation origins and the paradox of novelty. *Am. J. Bot.* 103, 1865–1868. doi: 10.3732/ajb.1600260

Fåhraeus, G. (1957). The infection of clover root hairs by nodule bacteria studied by a simple glass slide technique. *J. Gen. Microbiol.* 16, 374–381. doi: 10.1099/00221287-16-2-374

Fang, Y., and Hirsch, A. M. (1998). Studying early nodulin gene ENOD40 expression and induction by nodulation factor and cytokinin in transgenic alfalfa. *Plant Physiol.* 116, 53–68. doi: 10.1104/pp.116.1.53

Fonouni-Farde, C., Kisiala, A., Brault, M., Emery, R. J. N., Diet, A., and Frugier, F. (2017). DELLA1-mediated gibberellin signaling regulates cytokinin-dependent symbiotic nodulation. *Plant Physiol.* 175, 1795–1806. doi: 10.1104/pp.17.00919

Gamas, P., Brault, M., Jardinaud, M.-F., and Frugier, F. (2017). Cytokinin in symbiotic nodulation: when, where, what for? *Trends Plant Sci.* 22, 792–802. doi: 10.1016/j.tplants.2017.06.012

Giron, D., Frago, E., Glevarec, G., Pieterse, C. M., and Dicke, M. (2013). Cytokinins as key regulators in plant–microbe–insect interactions: connecting plant growth and defence. *Funct. Ecol.* 27, 599–609. doi: 10.1111/1365-2435.12042

Gonzalez-Rizzo, S., Crespi, M., and Frugier, F. (2006). The *Medicago truncatula* CRE1 cytokinin receptor regulates lateral root development and early symbiotic interaction with *Sinorhizobium meliloti*. *Plant Cell* 18, 2680–2693. doi: 10.1105/tpc.106.043778

Gresshoff, P. M., Skotnicki, M. L., Eadie, J. F., and Rolfe, B. G. (1977). Viability of *Rhizobium trifolii* bacteroids from clover root nodules. *Plant Sci. Lett.* 10, 299–304. doi: 10.1016/0304-4211(77)90142-0

Griesmann, M., Chang, Y., Liu, X., Song, Y., Haberer, G., Crook, M. B., et al. (2018). Phylogenomics reveals multiple losses of nitrogen-fixing root nodule symbiosis. *Science* 361:eaat1743. doi: 10.1126/science.aat1743

Heckmann, A. B., Sandal, N., Bek, A. S., Madsen, L. H., Jurkiewicz, A., Nielsen, M. W., et al. (2011). Cytokinin induction of root nodule primordia in *Lotus japonicus* is regulated by a mechanism operating in the root cortex. *Mol. Plant Microbe Interact.* 24, 1385–1395. doi: 10.1094/MPMI-05-11-0142

Held, M., Hou, H., Miri, M., Huynh, C., Ross, L., Hossain, M. S., et al. (2014). *Lotus japonicus* cytokinin receptors work partially redundantly to mediate nodule formation. *Plant Cell* 26, 678–694. doi: 10.1105/tpc.113.119362

Herrbach, V., Rembliére, C., Gough, C., and Bensmihen, S. (2014). Lateral root formation and patterning in *Medicago truncatula*. *J. Plant Physiol.* 171, 301–310. doi: 10.1016/j.jplph.2013.09.006

Hirsch, A. (1992). Developmental biology of legume nodulation. *New Phytol.* 122, 211–237. doi: 10.1111/j.1469-8137.1992.tb04227.x

Hirsch, A. M., Fang, Y., Asad, A., and Kapulnik, Y. (1997). The role of phytohormones in plant-microbe symbioses. *Plant Soil* 194, 171–184. doi: 10.1023/A:1004292020902

Hirsch, A. M., and LaRue, T. A. (1997). Is the legume nodule a modified root or stem or an organ sui generis? *Crit. Rev. Plant Sci.* 16, 361–392. doi: 10.1080/07352689709701954

Hoagland, D. R., and Arnon, D. I. (1950). The water-culture method for growing plants without soil. *Calif. Agric. Exp. Station Circ.* 347:32.

Hwang, I., Sheen, J., and Müller, B. (2012). Cytokinin signaling networks. *Annu. Rev. Plant Biol.* 63, 353–380. doi: 10.1146/annurev-arplant-042811-105503

Ilina, E. L., Kiryushkin, A. S., Semenova, V. A., Demchenko, N. P., Pawlowski, K., and Demchenko, K. N. (2018). Lateral root initiation and formation within the parental root meristem of *Cucurbita pepo*: is auxin a key player? *Ann. Bot.* 122, 873–888. doi: 10.1093/aob/mcy052

Joshi, P. A., Caetano-Anolles, G., Graham, E. T., and Gresshoff, P. M. (1991). Ontogeny and ultrastructure of spontaneous nodules in alfalfa (*Medicago sativa*). *Protoplasma* 162, 1–11. doi: 10.1007/BF01403895

Laplaze, L., Benková, E., Casimiro, I., Maes, L., Vanneste, S., Swarup, R., et al. (2007). Cytokinins act directly on lateral root founder cells to inhibit root initiation. *Plant Cell* 19, 3889–3900. doi: 10.1105/tpc.107.055863

Marhavý, P., Duclercq, J., Weller, B., Feraru, E., Bielach, A., Offringa, R., et al. (2014). Cytokinin controls polarity of PIN1-dependent auxin transport during lateral root organogenesis. *Curr. Biol.* 24, 1031–1037. doi: 10.1016/j.cub.2014.04.002

Mathesius, U., Bayliss, C., Weinman, J. J., Schlaman, H. R. M., Spaink, H. P., Rolfe, B. G., et al. (1998). Flavonoids synthesized in cortical cells during nodule initiation are early developmental markers in white clover. *Mol. Plant Microbe Interact.* 11, 1223–1232. doi: 10.1094/MPMI.1998.11.12.1223

Mathesius, U., Charon, C., Rolfe, B. G., Kondorosi, A., and Crespi, M. (2000a). Temporal and spatial order of events during the induction of cortical cell divisions in white clover by Rhizobium inoculation or localised cytokinin addition. *Mol. Plant Microbe Interact.* 13, 617–628.

Mathesius, U., Weinman, J. J., Rolfe, B. G., and Djordjevic, M. A. (2000b). Rhizobia can induce nodules in white clover by "hijacking" mature cortical cells activated during lateral root development. *Mol. Plant Microbe Interact.* 13, 170–182.

Maunoury, N., Redondo-Nieto, M., Bourcy, M., Van de Velde, W., Alunni, B., Laporte, P., et al. (2010). Differentiation of symbiotic cells and endosymbionts in *Medicago truncatula* nodulation are coupled to two transcriptome-switches. *PLoS One* 5:e9519. doi: 10.1371/journal.pone.0009519

McCully, M. E. (1975). "The development of lateral roots," in *The Development and Function of Roots*, eds J. G. Torrey and D. T. Clarkson (London: Academic Press), 105–124.

Mortier, V., Wasson, A., Jaworek, P., De Keyser, A., Decroos, M., Holsters, M., et al. (2014). Role of LONELY GUY genes in indeterminate nodulation on *Medicago truncatula*. *New Phytol.* 202, 582–593. doi: 10.1111/nph.12681

Ng, J. L. P., Hassan, S., Truong, T. T., Hocart, C. H., Laffont, C., Frugier, F., et al. (2015). Flavonoids and auxin transport inhibitors rescue symbiotic nodulation in the *Medicago truncatula* cytokinin perception mutant cre1. *Plant Cell* 27, 2210–2226. doi: 10.1105/tpc.15.00231

Oldroyd, G. E. (2013). Speak, friend, and enter: signalling systems that promote beneficial symbiotic associations in plants. *Nat. Rev. Microbiol.* 11, 252–263. doi: 10.1038/nrmicro2990

Op den Camp, R. H. M., De Mita, S., Lillo, A., Cao, Q., Limpens, E., Bisseling, T., et al. (2011). A phylogenetic strategy based on a legume-specific whole genome duplication yields symbiotic cytokinin type-A response regulators. *Plant Physiol.* 157, 2013–2022. doi: 10.1104/pp.111.187526

Pawlowski, K., and Sprent, J. I. (2007). "Comparison between actinorhizal and legume symbioses," in *Actinorhizal Symbiosis*, eds K. Pawlowski and W. E. Newton (Dordrecht: Springer), 261–288.

Phillips, R. L., Kaeppler, S. M., and Olhoft, P. (1994). Genetic instability of plant tissue cultures: breakdown of normal controls. *Proc. Natl. Acad. Sci. U.S.A.* 91, 5222–5226. doi: 10.1073/pnas.91.12.5222

Pils, B., and Heyl, A. (2009). Unraveling the evolution of cytokinin signaling. *Plant Physiol.* 151, 782–791. doi: 10.1104/pp.109.139188

Plet, J., Wasson, A., Ariel, F., Le Signor, C., Baker, D., Mathesius, U., et al. (2011). MtCRE1-dependent cytokinin signaling integrates bacterial and plant cues to coordinate symbiotic nodule organogenesis in *Medicago truncatula*. *Plant J.* 65, 622–633. doi: 10.1111/j.1365-313X.2010.04447.x

Radutoiu, S., Madsen, L. H., Madsen, E. B., Felle, H. H., Umehara, Y., Grønlund, M., et al. (2003). Plant recognition of symbiotic bacteria requires two LysM receptor-like kinases. *Nature* 425, 585–592. doi: 10.1038/nature02039

Reid, D., Nadzieja, M., Novák, O., Heckmann, A. B., Sandal, N., and Stougaard, J. (2017). Cytokinin biosynthesis promotes cortical cell responses during nodule development. *Plant Physiol.* 175, 361–375. doi: 10.1104/pp.17.00832

Reid, D. E., Heckmann, A. B., Novak, O., Kelly, S., and Stougaard, J. (2016). CYTOKININ OXIDASE/DEHYDROGENASE3 maintains cytokinin homeostasis during root and nodule development in *Lotus japonicus*. *Plant Physiol.* 170, 1060–1074. doi: 10.1104/pp.15.00650

Relić, B., Talmont, F., Kopcinska, J., Golinowski, W., Promé, J., and Broughton, W. J. (1993). Biological activity of *Rhizobium* sp. *NGR*234 Nod-factors on *Macroptilium atropurpureum*. *Mol. Plant Microbe Interact.* 6, 764–774. doi: 10.1094/MPMI-6-764

Rodriguez-Barrueco, C., and Bermudez De Castro, F. (1973). Cytokinin-induced pseudonodules on *Alnus glutinosa*. *Physiol. Plant.* 29, 277–280. doi: 10.1111/j.1399-3054.1973.tb03107.x

Rùžièka, K., Šimášková, M., Duclerq, J., Petrásek, J., Zažimalová, E., Simon, S., et al. (2009). Cytokinin regulates root meristem activity via modulation of the polar auxin transport. *Proc. Natl. Acad. Sci. U.S.A.* 106, 4284–4289. doi: 10.1073/pnas.0900060106

Soltis, D. E., Soltis, P. S., Morgan, D. R., Swensen, S. M., Mullin, B. C., Dowd, J. M., et al. (1995). Chloroplast gene sequence data suggest a single origin of the predisposition for symbiotic nitrogen fixation in angiosperms. *Proc. Natl. Acad. Sci. U.S.A.* 92, 2647–2651. doi: 10.1073/pnas.92.7.2647

Sprent, J. I. (2007). Evolving ideas of legume evolution and diversity: a taxonomic perspective on the occurrence of nodulation. *New Phytol.* 174, 11–25. doi: 10.1111/j.1469-8137.2007.02015.x

Sprent, J. I. (2009). *Legume Nodulation – A Global Perspective*. Oxford: Wiley-Blackwell. doi: 10.1002/9781444316384

Sprent, J. I., and Sprent, P. (1990). *Nitrogen Fixing Organisms: Pure and Applied Aspects*. London: Chapman and Hall.

Streeter, J. (1988). Inhibition of legume nodule formation and N2 fixation by nitrate. *Crit. Rev. Plant Sci.* 7, 1–23. doi: 10.1080/07352688809382257

Suzaki, T., Yano, K., Ito, M., Umehara, Y., Suganuma, N., and Kawaguchi, M. (2012). Positive and negative regulation of cortical cell division during root nodule development in *Lotus japonicus* is accompanied by auxin response. *Development* 139, 3997–4006. doi: 10.1242/dev.084079

Svistoonoff, S., Hocher, V., and Gherbi, H. (2014). Actinorhizal and nodule symbioses: what is the signaling telling on the origins of nodulation? *Curr. Opin. Plant Biol.* 20, 11–18. doi: 10.1016/j.pbi.2014.03.001

Tirichine, L., Sandal, N., Madsen, L. H., Radutoiu, S., Albrektsen, A. S., Sato, S., et al. (2007). A gain-of-function mutation in a cytokinin receptor triggers spontaneous root nodule organogenesis. *Science* 315, 104–107. doi: 10.1126/science.1132397

Udvardi, M., and Poole, P. S. (2013). Transport and metabolism in legume-rhizobia symbioses. *Annu. Rev. Plant Biol.* 64, 781–805. doi: 10.1146/annurev-arplant-050312-120235

van Velsen, R., Holmer, R., Bu, F., Rutten, L., van Zeijl, A., Liu, W., et al. (2018). Comparative genomics of the nonlegume *Parasponia* reveals insights into the evolution of nitrogen-fixing rhizobium symbioses. *Proc. Natl. Acad. Sci. U.S.A.* 115, E4700–E4709. doi: 10.1073/pnas.1721395115

van Zeijl, A., Op den Camp, R. H. M., Deinum, E. E., Charnikhova, T., Franssen, H., den Camp, H. J. O., et al. (2015). Rhizobium lipo-chitooligosaccharide signaling triggers accumulation of cytokinins in *Medicago truncatula* roots. *Mol. Plant* 8, 1213–1226. doi: 10.1016/j.molp.2015.03.010

Werner, G. D. A., Cornwell, W. K., Sprent, J. I., Kattge, J., and Kiers, E. T. (2014). A single evolutionary innovation drives the deep evolution of symbiotic N2-fixation in angiosperms. *Nat. Commun.* 5:4087. doi: 10.1038/ncomms5087

Werner, T., and Schmülling, T. (2009). Cytokinin action in plant development. *Curr. Opin. Plant Biol.* 12, 527–538. doi: 10.1016/j.pbi.2009.07.002

Xiao, T. T., Schilderink, S., Moling, S., Deinum, E. E., Kondorosi, E., Franssen, H., et al. (2014). Fate map of *Medicago truncatula* root nodules. *Development* 141, 3517–3528. doi: 10.1242/dev.110775

Zürcher, E., Tavor-Deslex, D., Lituiev, D., Enkeli, K., Tarr, P. T., and Müller, B. (2013). A robust and sensitive synthetic sensor to monitor the transcriptional output of the cytokinin signaling network in planta. *Plant Physiol.* 161, 1066–1075. doi: 10.1104/pp.112.211763

Conflict of Interest Statement: The authors declare that the research was conducted in the absence of any commercial or financial relationships that could be construed as a potential conflict of interest.

frontiers in Microbiology

ORIGINAL RESEARCH
published: 20 February 2019
doi: 10.3389/fmicb.2019.00307

The Ectomycorrhizospheric Habitat of Norway Spruce and *Tricholoma vaccinum*: Promotion of Plant Growth and Fitness by a Rich Microorganismic Community

Katharina Wagner[1†‡], Katrin Krause[1*‡], Ramses Gallegos-Monterrosa[2], Dominik Sammer[1†], Ákos T. Kovács[2†] and Erika Kothe[1]

[1] Microbial Communication, Institute of Microbiology, Friedrich Schiller University Jena, Jena, Germany, [2] Terrestrial Biofilms Group, Institute of Microbiology, Friedrich Schiller University Jena, Jena, Germany

The contribution of the mycorrhizospheric microbes in a stand of ectomycorrhizal Norway spruce (*Picea abies*) featuring mycorrhiza with the basidiomycete *Tricholoma vaccinum* was addressed by microbiome analysis and *in vitro* reconstruction of microbial as well as plant-microbe interactions. The protective role of the mycorrhizal fungus with respect to pathogen attack could be validated against *Botrytis cinerea* and *Heterobasidion annosum* in co-cultures revealing reduced pathogen growth, higher survival rate of the spruce trees and reduced symptoms on needles upon symbiosis with *T. vaccinum.* The community structure was shown to yield a high diversity in ECM forming basidiomycetes of *Thelephorales* and *Agaricales* associated with a rich bacterial diversity dominated by *Rhizobiales* with the most abundant *Nitrobacter winogradski* (3.9%). Isolated bacteria were then used to address plant growth promoting abilities, which included production of the phytohormone indole-3-acetic acid (performed by 74% of the bacterial isolates), siderophores (22%), and phosphate mobilization (23%). Among the isolates, mycorrhiza helper bacteria (MHB) were identified, with *Bacillus cereus* MRZ-1 inducing hyperbranching in *T. vaccinum*, supporting tree germination, shoot elongation, and root formation as well as higher mycorrhization rates. Thus, a huge pool of potential MHB and fungal community with widely distributed auxin-production potential extended the ability of *T. vaccinum* to form ectomycorrhiza. The forest community profited from the mycorrhizal fungus *T. vaccinum,* with spruce survival enhanced by 33% in microcosms using soil from the native habitat. A higher fungal abundance and diversity in cases where the tree had died during the experiment, showing that decomposition of plant litter from a dead tree supported a different community. *T. vaccinum* thus actively structured the community of microorganisms in its habitat.

Keywords: ectomycorrhiza, community, microcosm, indole-3-acetic acid, *Tricholoma*, plant growth promoting bacteria

OPEN ACCESS

Edited by:
Jonathan Michael Plett, Western Sydney University, Australia

Reviewed by:
Jessie Karen Uehling, University of California, Berkeley, United States
François Noêl Le Tacon, INRA Université de Lorraine and INRA, France
Sabine Dagmar Zimmermann, Centre National de la Recherche Scientifique (CNRS), France

****Correspondence:***
Katrin Krause
Katrin.Krause@uni-jena.de

†Present address:
Katharina Wagner, Food GmbH Jena, Analytik & Consulting, Jena, Germany
Dominik Sammer, Wacker Biotech GmbH, Jena, Germany
Ákos T. Kovács, Technical University of Denmark, Department of Biotechnology and Biomedicine, Lyngby, Denmark

‡These authors have contributed equally to this work

Specialty section:
This article was submitted to Plant Microbe Interactions, a section of the journal Frontiers in Microbiology

Received: *27 September 2018*
Accepted: *05 February 2019*
Published: *20 February 2019*

Citation:
Wagner K, Krause K, Gallegos-Monterrosa R, Sammer D, Kovács ÁT and Kothe E (2019) The Ectomycorrhizospheric Habitat of Norway Spruce and Tricholoma vaccinum: Promotion of Plant Growth and Fitness by a Rich Microorganismic Community. Front. Microbiol. 10:307. doi: 10.3389/fmicb.2019.00307

INTRODUCTION

Forest ecosystems are stabilized by the mutual symbiosis between tree roots and mainly basidiomycete fungi forming the ectomycorrhizal symbiosis with nutrient and water supply to the roots in exchange for photosynthesis products from the tree. In the specific mutualistic symbiosis between mainly basidiomycete fungi and trees, the ectomycorrhiza (ECM), the fungal partner forms a mantle around the short roots of its host, which has been suggested to protect the tree from pathogen attack (Smith and Read, 1987). In addition, hyphae grow between the rhizosphere cells forming the Hartig' net which is the interface for nutrient and signal exchange (for review, see Raudaskoski and Kothe, 2015). Since mycorrhiza is known to increase tree fitness, the late stage basidiomycete *Tricholoma vaccinum* was chosen for investigation. It forms host specific spruce ectomycorrhiza (Asiimwe et al., 2012). *T. vaccinum* produces the auxin phytohormone indole-3-acetic acid (IAA), which promotes higher branching and increases hyphal lengths of the mycelium, combined with an increased Hartig' net formation during symbiosis (Krause et al., 2015).

However, additional functions may be supplied by the rich microbiota present in the surrounding soil. To address interactions in the ectomycorrhizosphere, the microbiome of this habitat needs to be addressed with specific regard to the ectomycorrhiza. Here, *Tricholoma vaccinum* and Norway spruce (*Picea abies*) were investigated and the community assessed in a natural stand of spruce/*T. vaccinum*.

Spruce is the most common tree in Europe, making up over 30% of German and Switzerland forests, and 10% of the total land area are covered by *P. abies* owing to forestry management (Klimo et al., 2000). Spruce pathogens include *Botrytis cinerea* leading to blight especially in seedlings, and *Heterobasidion annosum* leading to root and butt rot. The gray mold *B. cinerea* is a virulent and common plant pathogen. It shows low host selectivity and mainly infects the needles of conifers (Williamson et al., 2007). Counter-acting induction of systemic acquired resistance involves up-regulation of salicylic acid, shown to be produced by, e.g., the fungus *T. vaccinum* in pure culture (Wagner, 2016). Therefore, an effect of mycorrhiza on protecting young seedlings in a systemic manner can be tested. On contrast, *H. annosum* is a typical forest root pathogen (Lundén et al., 2015). Two types, one more prevalent on pine (P type on *Pinus* species) and one on fir or spruce (S/F on species of *Abies*/*Picea*; see Asiegbu et al., 2005) have been assigned. The second type thus can be used to study root pathogenic fungi for a protective effect of mycorrhiza. The different strategies employed by these two pathogens lend themselves for investigation of beneficial interactions protecting the tree.

In addition, other saprophytic and parasitic fungi, as well as bacteria, archaea, protists, nematodes or viruses are present in forest soil (Bais et al., 2004). This microbial community structure and diversity is considered an important factor in responding to anthropogenic or other ecosystem disturbances (Baldrian et al., 2012). In coniferous forest soils, fungi are dominant in plant litter decomposition in the upper horizon (Buee et al., 2009), and competition within the diverse fungal community would affect fungal pathogens (Alabouvette, 1990). Bacteria more often are involved in the biogeochemical cycles in lower horizons (Bååth and Anderson, 2003). The habitat around the mycorrhized roots with its microbiota is defined as mycorrhizosphere (Johansson et al., 2004). The chemical communication in the mycorrhizosphere represents a complex process and includes diverse phytohormones, pheromones and various allelochemicals with different structures, e.g., steroids and proteins (Raudaskoski and Kothe, 2015, and citations therein).

Mycorrhiza helper bacteria (MHB) can enhance mycorrhiza establishment or increase mycorrhization strength on an individual plant (Deveau et al., 2012; Wu et al., 2012). MHBs can impact phosphate and iron nutrition (Ahmad et al., 2008), and they can mediate plant defense by signals supporting mycorrhiza formation (Wang et al., 1993). Other plant growth promoting bacteria are also present in the rhizosphere and can supply traits like nitrogen fixation, phosphate mobilization, antifungal or antibacterial properties, as well as cyanide, phytohormone, or siderophore synthesis (Saharan and Nehra, 2011). The phytohormone indole-3-acetic acid (IAA) is required for cell growth and differentiation in the plant and stimulates Hartig' net development (Gea et al., 1994). Therefore, microorganisms that are able to produce IAA (or IAA inhibiting compounds) are able to modulate ectomycorrhization (Tsavkelova et al., 2006; Hause and Schaarschmidt, 2009).

Here, we aimed to characterize the natural mycorrhizosphere community of soil below *T. vaccinum* fruiting bodies found with their host *P. abies.* The influence of the community was investigated in microcosm experiments, and the response of the community to tree death from an ectomycorrhizosphere to a forest soil community was evaluated. Isolated community members were checked for their influence on either symbiotic partner *in vitro,* and plant growth promoting as well as specific mycorrhiza helper functions were verified. In co-cultivation, the protection of spruce against two known pathogens was shown for inoculation with *T. vaccinum*. With this combined approach, we could show the impact of *T. vaccinum* on the community structure, identify potential functions of the mycorrhizosphere community and link both to spruce health.

MATERIALS AND METHODS

Soil Sampling and Characterization

Soil was sampled in the rhizosphere of two spruce trees in a forest dominated by spruce and pine trees near Jena, Germany at a marked point with the coordinates 50°55′10.8"N 11°31′30.4"E at different time points over 3 years to validate the general mycorrhizosphere community stability and response to seasonal changes. The samples were taken, where *T. vaccinum* fruiting bodies had been found and morphotyping had validated occurrence of *T. vaccinum* (**Supplementary Figure S1**). Sampling dates for sequential extraction were in October 2012, for the investigation of fungal community in March 2014 and for the investigation of bacterial community at six time points in October 2012, April 2013, October 2013, April 2014, October 2014, and April 2015. Soil was taken from the organic horizon (O) with

litter and humus rich zones (L and H horizon) in 1–10 cm depth. The soil was transferred immediately to the laboratory at 4°C and sieved with a 3–4 mm mesh to eliminate bigger plant material.

The pH was measured as described by Minasny et al. (2011). For sequential extraction, soil was air-dried and sieved to <2 mm. Extraction was performed in triplicates for the mobile (F1) and specifically absorbed (F2) fraction for the biomobile and bioavailable element contents (**Supplementary Table S1**, Schütze et al., 2014). Sequential extraction and analysis of the carbon (C), sulfur (S), and nitrogen (N) contents in the soil samples were performed as described earlier (Schütze et al., 2013).

DNA Extraction, Pyrosequencing, and Bioinformatics Community Evaluation

Total DNA of the microbial community was isolated using the MoBio Soil DNA Extraction Kit (MoBio Laboratories, Carlsbad, CA, United States) with four extractions of 0.3 g soil each to gain a representative result. DNA was stored at −20°C, and samples sent to GATC Biotech (Konstanz, Germany) for pyrosequencing after amplification of bacterial 16S rRNA (using primers 27F: AGA GTT TGA TCC TGG CTC AG and 534R: ATT ACC GCG GCT GCT GG) or fungal ITS1 (primers ITS1F: CTT GGT CAT TTA GAG GAA GTA A and ITS2: GCT GCG TTC TTC ATC GAT GC; Gardes and Bruns, 1993). The reason for using ITS2 was to show broader coverage of fungal lineages as compared to using the ITS4 primer (Ihrmark et al., 2012). FLX titanium and paired-end Illumina sequencing was used. Non-chimeric unique clusters (see **Supplementary Table S2** for read statistics and OTU assignment) were used for BLASTn analysis with an *E*-value cutoff of 1e-06 by non-redundant ITS references from UNITE database (updated on February, 2014) for fungi and 16S rDNA sequences from Ribosomal Database Project (RDP release 11, updated on March 2014; Cole et al., 2009). Sequences were deposited at GenBank MG255224-MG255268 (fungal ITS) and at GenBank MG282098-MG282149 (bacterial16S rRNA). Sequences for all representative species were retrieved from the mentioned databases and aligned using MAFFT online (version 7)[1]. The alignment was corrected manually, a neighbor-joining tree constructed and data bootstrapped using MrBayes (Bayesian Inference of Phylogeny, version 3.2)[2] with 6 Mio generations for bacteria and 1 Mio generations for fungi. Rarefaction was controlled (see **Supplementary Figure S2**).

Isolation of Bacteria and Identification

A dilution series in 0.9% NaCl was plated on Standard I medium (StdI; Merck, Darmstadt, Germany). After incubation at 28°C for 2 days, colony forming units (CFU/g soil) were determined. Morphologically different isolates were selected as operational taxonomic units (OTUs) for further analyses. From the total OTUs, 94 were randomly selected for further identification. Fast DNA isolation was achieved by boiling a loop of biomass in 50 µl distillated water for 5 min. DNA was isolated using CTAB preparation (Ausubel et al., 1992). 16S rDNA sequence was amplified with the primers A1 (GAG TTT GAT CAT GGC TCA) and B6 (TTG CGG GAC TTA ACC CAA CAT) using PCR (program: 95°C for 3 min, 35 cycles of 95°C 30 sec, annealing at 52°C for 45 s, elongation at 72°C for 1 min 30 s, and final extension at 72°C for 10 min). Fragments were eluted from agarose gel and directly used for sequencing at GATC (Konstanz, Germany) or cloned into pGEM-TEasyTM vector (Promega, Madison, United States) followed by transformation into competent *Escherichia coli* DH5α cells. Plasmids were isolated using the GeneJetTM Plasmid Miniprep Kit after manufacturers' instructions (Fermentas, Heidelberg, Germany). BlastN search was used to identify the isolates on genus level at www.ncbi.nlm.nih.gov.

Screening of Bacteria for Plant Growth Promotion Abilities

Selected bacteria were incubated for 2–3 days in liquid StdI at room temperature. Optical densities (OD_{600}) of the cultures were measured and their supernatant used for Salkowski assay to determine IAA concentrations (Gordon and Weber, 1951). The ability to produce siderophores or mobilize phosphate were assessed on CAS (Schwyn and Neilands, 1987) or Pikovskaya agar medium (Mehta and Nautiyal, 2001) after 1 week of incubation at room temperature. The production of antibiotics was tested using the gram negative bacterium *Escherichia coli* and the gram positive *Micrococcus luteus*. They were grown by shaking in 30 ml liquid StdI medium for 12 h. Hundred microliter of both liquid cultures were transferred in 7 ml StdI with 7% agar, and transferred on plates with bacterial cultures to check their ability to produce antibiotics. All experiments were performed in triplicates and controls with non-inoculated plates were used. We additionally selected four bacteria (MRZ-1 through MRZ-4) based on their characteristics and investigated growth on nitrogen-free medium (5 g glucose, 5 g mannitol, 0.1 g $CaCl_2 \times 2H_2O$, 5 mg $Na_2MoO_4 \times 2H_2O$, 0.9 g K_2HPO_4, 0.1 g KH_2PO_4, 0.01 g $FeSO_4 \times H_2O$) for potential nitrogen fixation. These isolates (*Bacillus cereus* MRZ-1 (JMRC:ST:036355), *Lysinibacillus* sp. MRZ-2 (JMRC:ST:036356), *Bacillus pumilus* MRZ-3 (JMRC:ST:036358), and *Bacillus zhangzhouensis* MRZ-4 (JMRC:ST:036357) were deposited at Jena Microbial Resource Collection (JMRC), Jena, Germany.

Effect of Selected Bacterial Isolates on *T. vaccinum* and/or *P. abies*

To evaluate the effects of isolated bacteria on *T. vaccinum* GK6514 (JMRC:FSU:4731, JMRC, Jena, Germany), 100 µl supernatant of bacterial overnight cultures (isolates MRZ-1 through MRZ-4, and pure StdI medium for control) grown in StdI (Merck, Darmstadt, Germany) were obtained and plated on modified Melin Norkrans b (MMNb) medium (Kottke et al., 1987), followed by *T. vaccinum* inoculation and cultivation over 4 weeks. The mycelial diameter and hyphal branching were recorded counting 100 hyphal tips selected randomly for branching within 500 µm distance from the tip. The influence of volatiles was examined using divided plates, where one half was inoculated with bacteria (four isolates: MRZ-1 through MRZ-4, and without inoculation for control) on StdI medium, while

[1] http://mafft.cbrc.jp/alignment/server/

[2] http://mrbayes.sourceforge.net/

the other half contained 2 weeks old colonies of *T. vaccinum* on MMNb medium. After 20 days the evaluation of growth properties was performed using the software Spot version 4.6 (Diagnostic Instruments, Munich, Germany). Every treatment was performed in triplicates. The impact of the bacteria on germination of *Picea abies* seedlings (Landesforst Mecklenburg-Vorpommern, Germany) was investigated on germination medium (Krause and Kothe, 2006) using bacterial overnight cultures (set to OD_{600} = 0.1 after washing in 0.9% NaCl) and surface sterilized seeds, mixed for 1 min, and transferred to germination medium (ten seeds per plate). For control, treatment without bacteria was performed. All experiments were performed in triplicates. Data were recorded after 20 days.

For the investigation of the mycorrhization rate with selected bacteria, *P. abies* and *T. vaccinum* were cultivated in hydroponic cultures (Henke et al., 2015a) after axenic *P. abies* pre-cultivation on germination medium over 4 weeks and in the hydroponic system over 3 weeks before *T. vaccinum* was inoculated. After 3 more weeks, 100 µl of the selected bacteria with an OD_{600} of 0.1 washed in 0.9% NaCl were inoculated. After 3 months, the hydroponic cultures were evaluated for spruce vitality, root and shoot biomass, root architecture, fungal biomass and the mycorrhization rate of the root system in percentage of total roots with obvious mantle formation or mycorrhiza-typical thickened and coiled short root morphology.

Isolation of Fungi With Selective Media

A soil dilution series (1 g soil 1:10 w/v in 0.9% NaCl) was plated on MMNb, well suited for ectomycorrhizal basidiomycetes, or supplemented minimal medium (SUP), optimal for the growth of mucoromycetes (Wöstemeyer, 1985). Spectinomycin or cycloheximide were added to prevent bacterial growth or inhibit most fungi to provide access to some resistant but less competitive genera like *Absidia*. Incubation at 22 or 28°C for 3–4 days or 4 weeks to select slow growing fungi was followed by selection of different OTUs and the total number of fungal colony forming units (cfu) was calculated. DNA was isolated from all OTUs with three freeze/thaw cycles of the mycelium in liquid nitrogen followed by heating for 1 min at 50°C followed by ITS PCR (primers ITS1: TCC GTA GGT GAA CCT GCG G and ITS 4: TCC TCC GCT TAT TGA TAT GC; see Innis et al., 1990) and identification was performed through sequencing (GATC Biotech, Germany).

Microcosm Experiments

Microcosm tubes of 50 ml contained 20 ml sieved (<2 mm) soil with its natural microbial community. After treatment with 30% hydrogen peroxide for 1.5 h and rinsing with sterilized water *P. abies* seeds were placed on germination medium (Kottke et al., 1987). A 2 months sterily pre-grown *P. abies* seedling was planted using a sterile spatula and watered with sterile tap water. The microcosms were inoculated with *T. vaccinum* GK6514 and/or plus and minus mating types of the ubiquitous soil fungus *Mucor mucedo* (SF:JMRC:000620 or SF:JMRC:000621, JMRC, Jena, Germany). Strains of *Mucor* were chosen, because they may affect phytohormone signaling of fungi and trees and modulate their morphology (Wagner et al., 2016). Using a sterile stamp 7 mm diameter inocula of *T. vaccinum* were transferred from MMNb cultivation plates and for *M. mucedo* the same procedure was performed from SUP cultivation plates. The microcosms were incubated in a climate chamber (12 h light/23°C; 12 h dark/17°C; 80% humidity) and watered with 1 ml sterile tap water weekly (n = 12). After 8 weeks, vitality of trees (living or dead), microorganisms plated on SUP and MMNb for OTUs, and fungal CFU were checked.

Effect of *T. vaccinum* on Spruce Pathogens

To analyze the role of *T. vaccinum* to protect the tree from pathogen attack *Botrytis cinerea* (SF:JMRC:001099) and *Heterobasidion annosum* S/F type (SF:JMRC:008560; both JRMC, Jena, Germany) were used. Well-overgrown agar blocks (5 mm × 5 mm) of both fungi were inoculated on MMNb plates with pre-grown (2 weeks) *T. vaccinum,* (see **Supplementary Figure S3**). After 2 weeks, pathogen growth was evaluated in comparison with pure cultures of the fungi using Image J 1.46[3]. The effect of volatiles of *T. vaccinum* on the phytopathogens was scored using divided plates with pure and co-cultures (see **Supplementary Figure S3B**). The disease symptoms of pathogens were checked with plate cultures (see **Supplementary Figure S3C**), where an axenic 8 weeks old spruce seedling was placed between two sterile cellophane membranes with fungal inocula on MMN agar media with 2% glucose and without malt extract (modified after Kottke et al., 1987). For quantitative data on pathogen protection, hydroponic cultures (Henke et al., 2015a) were used with the more aggressive and faster pathogen, *B. cinerea* (see **Supplementary Figure S3D**). Three 8 weeks old spruce seedlings were inoculated with two well-overgrown agar blocks of *T. vaccinum.* After 3 weeks *B. cinerea* was added (n = 4). Cultures containing either *T. vaccinum* or the pathogen were used as control. After 1 month, living trees were counted, root and shoot dried and biomass examined.

In silico Analyses

The genome of *T. vaccinum* GK6514 was screened for genes involved in the biosynthesis of the pigment melanin, extending both to DHN melanin (Tsai et al., 1999) and L-DOPA melanin (Eisenman and Casadevall, 2012). The genome is available on request via JGI IMG[4] under the submission ID59348. BLASTN search was performed with software sequenceserver[5] and with NCBI database[6].

Statistical Analyses

Every treatment was performed in triplicates if not mentioned otherwise. The statistical analyses for comparison of two treatments was performed with unpaired Student's *t*-test, and for more than two treatments with one-way analysis of variance (ANOVA) after Levene's test. Tukey test was used for *post hoc* analyses. Significance levels are indicated with small letters

[3]http://rsb.info.nih.gov/ij/download.html

[4]http://img.jgi.doe.gov/

[5]http://www.sequenceserver.com

[6]http://blast.ncbi.nlm.nih.gov

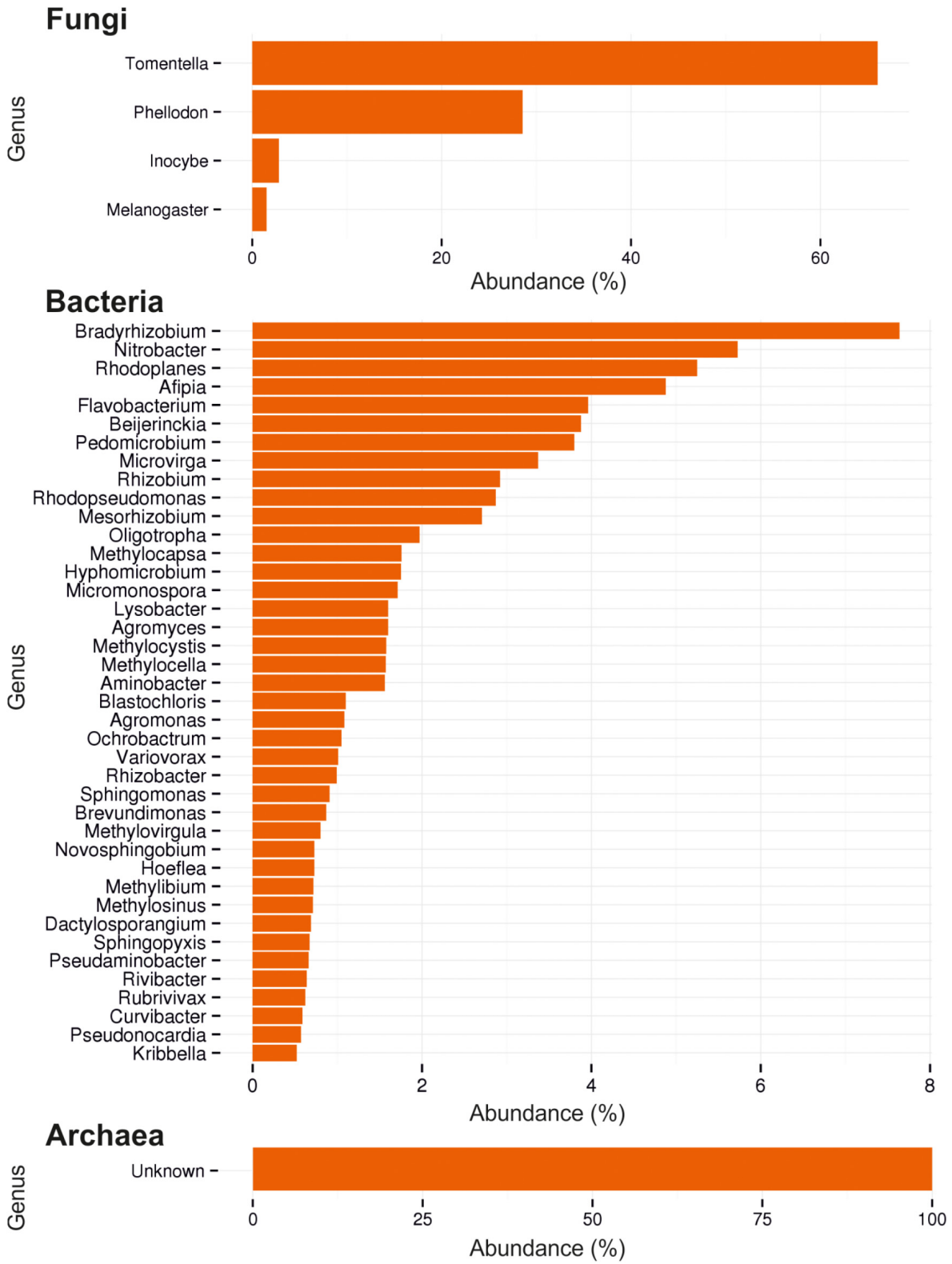

FIGURE 1 | Ectomycorrhizosphere community assessment by ITS and 16S rDNA sequencing. Composition of fungi, bacteria and archaea by most abundant reads (%) are shown.

TABLE 1 | Identified OTUs by pyrosequencing (90% sequence similarity level) and their different lifestyles.

Clade	Life style*
ASCOMYCOTA	
Sordariomycetes	
Hypocreales	
Hypocrea_stellata	MPAR
*Trichoderma*_sp.	MPAR
Hypocrea_cremea	MPAR
Hypocrea_chlorospora	MPAR
BASIDIOMYCOTA	
Agaricomycetes	
Agaricales	
*Alnicola*_sp.	ECM
Cortinarius_infractus	ECM
Cortinarius_cinnamomeus	ECM
Cortinarius_cedretorum	ECM
Cortinarius_cupreorufus	ECM
*Cortinarius*_sp.	ECM
*Cortinarius*_sp.	ECM
Cortinarius_langeorum	ECM
Cortinarius_aurora	ECM
Cortinarius_caesibulga	ECM
Cortinarius_cinereoroseolus	ECM
Cortinarius_argyronius	ECM
Cortinarius_eutactus	ECM
Inocybe_dulcamara	ECM
Inocybe_substraminipes	ECM
Inocybe_substraminipes	ECM
Inocybe_terrigena	ECM
Inocybe_leucoblema	ECM
Inocybe_leucoloma	ECM
Inocybe_myriadophylla	ECM
Inocybe_cf_dulcamara	ECM
Hebeloma_testaceum	ECM
Hebeloma_syrjense	ECM
Hymenogaster_luteus_var._luteus	ECM
Lepiota_acutesquamosa	SAP
Lyophyllum_shimeji	ECM
Stropharia_inuncta	SAP
Stropharia_hornemannii	SAP
Tricholoma_ustale	ECM
Tricholoma_psammopus	ECM
*Tricholoma*_sp.	ECM
Boletales	
Melanogaster_broomeianus	ECM
Melanogaster_variegatus	ECM
Polyporales	
Perenniporia_pyricola	MPAR
Perenniporia_truncatospora	PPATH
Russulales	
Russula_aquosa	ECM
Lactarius_blennius	ECM
Thelephorales	
Tomentella_lateritia	ECM
Tomentella_cinerascens	ECM
*Tomentella*_sp.	ECM
*Pseudotomentella*_sp.	ECM
*Phellodon*_sp.	ECM

* *ECM, ectomycorrhizal; PPATH, phytopathogenic; MPAR, mycoparasitic; SAP, saprophytic.*

and were set to $P < 0.05$. Data are shown as average values ± standard deviation.

RESULTS

The Mycorrhizosphere Habitat

In order to establish potential interactions of fungi or bacteria present in the mycorrhizosphere surrounding *T. vaccinum* ectomycorrhiza, soil from the natural habitat was characterized. The soil samples were slightly acidic at pH 6.5 and featured high concentrations of bioavailable lanthanides, Pb and Mn (see **Supplementary Table S1**). A high C (26.92% ± 0.012) to N (0.84% ± 0.008) ratio of 32:1 and raised S contents (0.11% ± 0.009) were observed.

In soil from O, L, and H horizon of this forest habitat, the fungal community composition was determined (**Figure 1**). For fungi it revealed 53 OTUs consisting mainly of Basidiomycota (99.95%), with almost 95% of the basidiomycetes being ectomycorrhizal members of *Thelephorales* and 3.5% *Agaricales* (**Table 1**). Among the most abundant genera, 16 basidiomycetes, 12 with an ectomycorrhizal lifestyle, were identified. At species level, the dominant species clearly was *Tomentella lateritia*.

The bacterial community showed a high diversity with 1517 different bacterial OTUs detected (**Supplementary Table S3**). The five most abundant genera were *Rhodoplanes* (19.5%), *Pedomicrobium* (8.16%), *Afipia* (6.93%), *Methylibium* (5.02%), and *Dongia* (4.67%), the three dominant ones being *Rhizobiales* (compare **Figure 1**). On species level, the mycorrhizosphere was dominated by the *Rhizobiales* member *Nitrobacter winogradskyi* with 3.9% of reads, with another 0.5% being other *Rhizobiales* with potential function in nitrogen cycling (**Figure 2**).

Of the detected OTUs, 505 represented less than 0.01% of the total community (<18 reads), containing mainly Gram-positives with high species heterogeneity (44% Actinobacteria). Among the archaea, low abundance and low diversity, again hinting at nitrogen cycling, was detected.

Physiological Traits of Isolated Fungi and Bacteria

To assess the physiological potential of strains present in the mycorrhizosphere, fungal and bacterial isolates were obtained. On complex media the conidiospore forming genus *Penicillium* dominated. At lower temperature and with increased incubation time, fungi with different life styles were isolated (**Table 2**). Using antibiotics, different

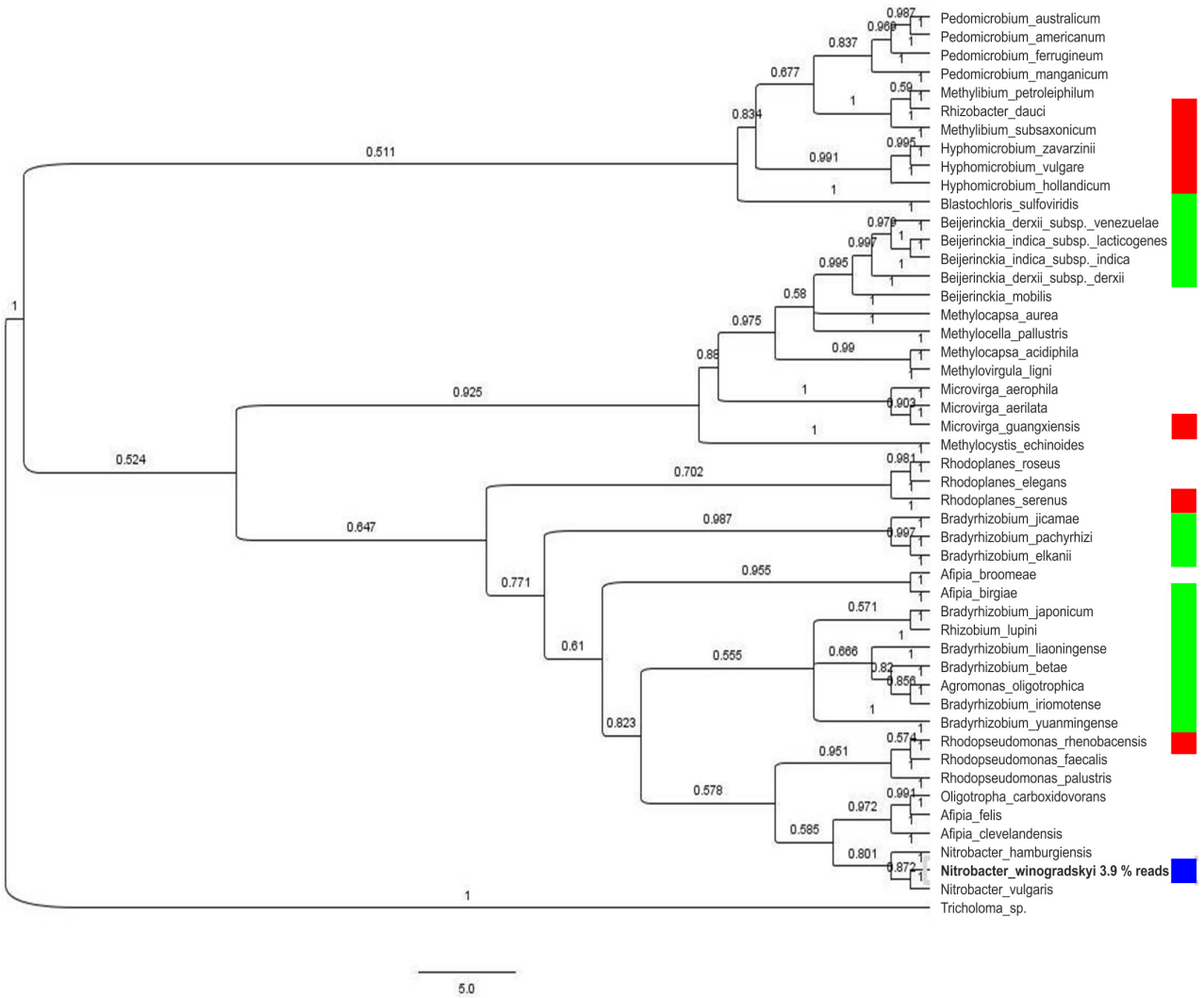

FIGURE 2 | Phylogenetic tree of the 16S rDNA fragments of the most abundant species (over 0.5% composition reads) on 93% sequence similarity level. Relevance in nitrogen cycling is indicated for nitrogen fixation (green), nitrification (blue), and denitrification (red).

taxa were enriched with cycloheximide selecting for *Absidia* mucoromycetes and ascomycetous *Hypocreales*, namely *Lecanicillum*, *Acremonium*, *Beauveria*, and *Penicillium* (see **Table 2**), while spectinomycin led to *Penicillium* and *Beauveria* isolation, with the Hypocreales fungus *Pochonia* and the Mucoromycota *Mortierella* and *Umbelopsis* being enriched. Of all fungal isolates, only 6.3% produced IAA without tryptophan addition, and 7.4% with the addition of 0.5 mM tryptophan to the medium.

To detect seasonal changes in the mycorrhizosphere community and the related changes in ecological functions relating to the formation of mycorrhiza and tree growth, bacteria were isolated in three different years from the same site during spring and autumn (**Figure 3**). The average bacterial abundance was found to be around 10^7 with 111 isolated strains belonging to *Bacillus* (n = 29), *Pseudomonas* (n = 27), *Micrococcus* (n = 11), *Streptomyces* (n = 6), *Bacteroides* and α- and ß-proteobacteria including *Burkholderia* (n = 2). The selected isolates could be shown to provide a range of plant growth promoting abilities with changes visible specifically for siderophore production between different time points and seasons (**Supplementary Figure S4**). Around 23% of the isolates produced siderophores, 22% mobilized phosphate, and around 74% excreted the phytohormone IAA. Streptomycetes, *Micrococcus* and *Pseudomonas* showed the highest potential to mobilize phosphate, and all of the dominant phyla produced IAA (**Supplementary Table S3**).

T. vaccinum Alters the Fungal Community Structure in Microcosms

To see the influence of *T. vaccinum* on fungal community and spruce health, we used microcosms with soil obtained from the habitat. After 8 weeks of cultivation, the transplanted

TABLE 2 | Isolated fungi and their different life styles.

Clade	Lifestyle*	Isolation from soil
BASIDIOMYCOTA		
Tricholoma	ECM	+
Hypholoma	SAP	+
Kuehneromyces	SAP	+ (2 strains)
Psathyrella	SAP	+ (3 strains)
ASCOMYCOTA		
Hypocrea/Hypocreales	MPAR	+
Penicillium	SAP, PATH	+ (24 strains)
Beauveria	EPATH	+ (4 strains)
Acremonium	SAP, PATH	+
Lecanicillium	EPATH	+ (2 strains)
Cryptosporiopsis	PPATH	+
Microdochium	PPATH	+ (2 strains)
Helotiales	PPATH, MYC, SAP, MPAR	+ (2 strains)
Cladosporium	SAP	+
Mycosphearella	PPATH	+
MUCOROMYCOTA		
Umbelopsis		+ (5 strains)
Mortierella	SAP	+ (4 strains)
Absidia	PATH	+ (3 strains)

** ECM, ectomycorrhizal; PPATH, phytopathogenic; MPAR, mycoparasitic; EPATH, entomopathogenic; PATH, pathogenic for mammals; SAP, saprophytic.*

spruce seedlings showed a high mortality. A tendency to a higher vitality with *T. vaccinum* (58% alive compared to 25% in control) was visible. Inoculation with the non-wood degrading mucoromycete *M. mucedo* slightly increased spruce health (42% alive). No significant difference of shoot, primary and lateral root growth, or needle development was obtained at the seedling stage (data not shown).

An effect of *T. vaccinum* on the mycorrhizosphere was obtained in the microcosms containing dead trees. There, *T. vaccinum* significantly increased the number of fungal colonies and OTUs indicating a higher prevalence of plant decomposers, if *T. vaccinum* was present (**Figure 4**).

To show the ability of *T. vaccinum* to degrade plant material, it was grown on MMNb where the only C source was replaced by cellulose, the main component of plant cell walls, which supported growth (**Supplementary Figure S5**).

Mycorrhiza Helper Bacteria

Four isolates were selected based on their ability to produce IAA, siderophores, or to grow on nitrogen-free medium suggesting nitrogen fixation (**Supplementary Tables S3, S4**). *Bacillus cereus* MRZ-1, *Lysinibacillus* sp. MRZ-2, *Bacillus pumilus* MRZ-3 and *Bacillus zhangzhouensis* MRZ-4 all synthesized IAA, but did not solubilize phosphate; *B. cereus* MRZ-1 produced IAA only in the presence of an additional tryptophan source. All, with the exception of *Lysinibacillus* sp. MRZ-2, grew on nitrogen-free medium. These were tested for their effect on *Tricholoma* and mycorrhiza.

Volatile compounds produced by bacteria *B. cereus* MRZ-1, *Lysinibacillus* sp. MRZ-2, and *B. zhangzhouensis* MRZ-4 affected fungal growth and significantly reduced the colony diameter of axenically grown *T. vaccinum* (**Figure 5**), when co-cultivated on divided plates that allow for volatile transmission, but not for diffusion of compounds. Volatiles, especially of *B. cereus* MRZ-1, strongly induced the formation of a brownish pigment by *T. vaccinum* which was not observed using bacterial supernatant (**Supplementary Figure S6**). To see whether this pigment might be melanin, the genome of *T. vaccinum* was checked for genes involved in melanin biosynthesis. Genes *alb1* (ID: g2107.t1), *arp1* (g3608.t1), *arp2* (g10130.t1), *abr1* (g4688.t1), and *abr2* (g3608.t1), known to be involved in the biosynthesis of DHN melanin, as well as the laccase *lac1* (g4688.t1) of L-DOPA melanin biosynthesis could be identified.

In addition to volatiles, supernatants were checked for morphological effects. *B. cereus* MRZ-1 sterile culture filtrate increased primary and secondary hyphal branching

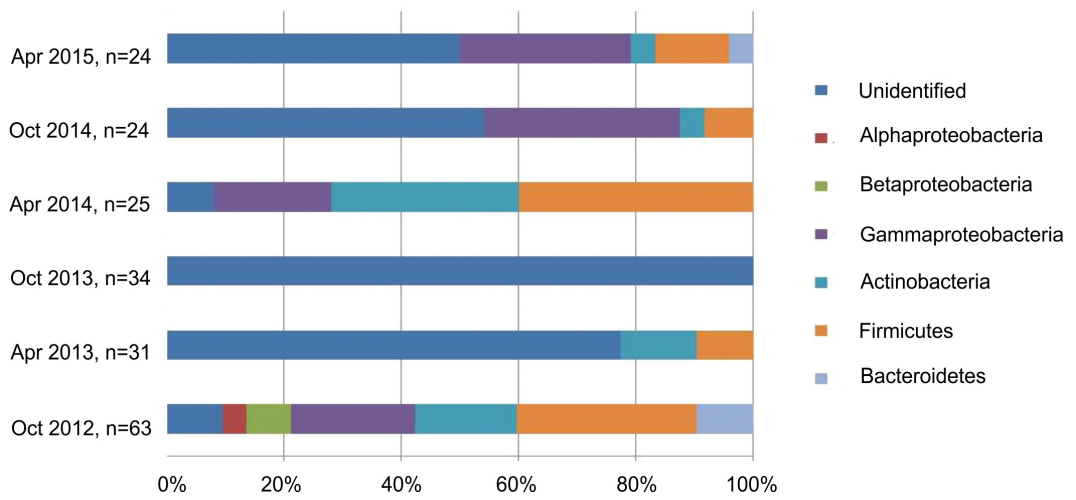

FIGURE 3 | Composition of the isolated bacteria (%) at different sampling times.

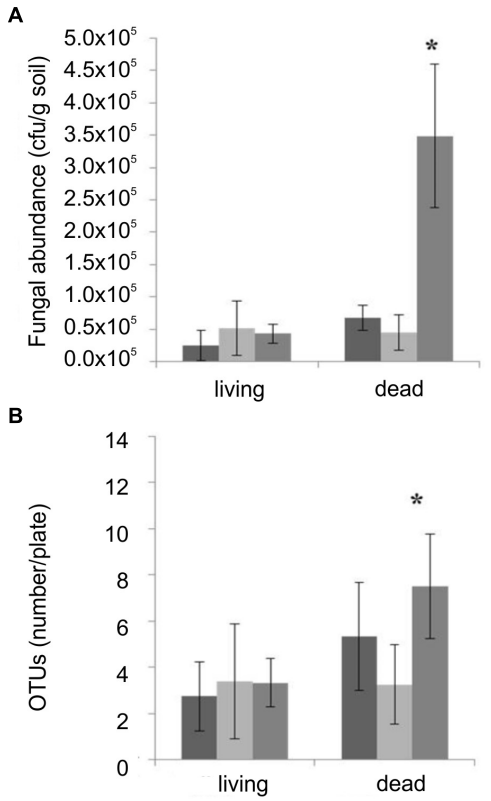

FIGURE 4 | Fungal CFU **(A)** and OTUs **(B)** compared between microcosms non-inoculated (black), inoculated with *M. mucedo* (light gray) or *T. vaccinum* (dark gray) of living or dead spruce trees. *Significance level, $p < 0.05$, error bars indicate standard deviation; $n = 12$.

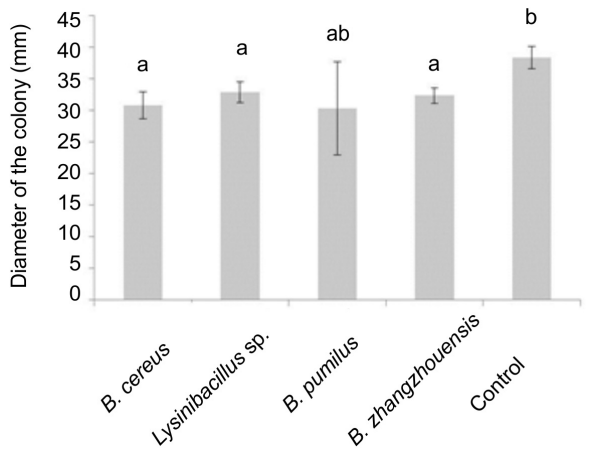

FIGURE 5 | Influence of bacterial volatiles in divided plates on the diameter of the colony of *T. vaccinum*, significance level $p < 0.05$, $n = 3$.

of *T. vaccinum* (number of 1st order branches increased from 1.76 to 2.95 and 2nd order branches from 1.01 to 2.83), which was not the case with the other bacteria tested.

As for an impact on tree development, germination rate of spruce seedlings inoculated with the bacterial suspension showed a slight increase (**Figure 6**). A significantly higher number of germinated seeds had an elongated germination tube after 20 days (not shown). Moreover, the length of the germination tubes that sometimes already developed into a shoot was significantly enhanced when treated with *B. cereus* MRZ-1, *B. pumilus* MRZ-3, and *B. zhangzhouensis* MRZ-4 (see **Figure 6B**).

Suspension of the two isolates with best effects were then screened for their impact on mycorrhization. After 3 months, mycorrhiza formation was slightly improved by *B. cereus* MRZ-1 with increased number of lateral branches in the root system (see **Figure 6C**) and mycorrhization rates (see **Figure 6D**).

T. vaccinum Reduced Pathogen Growth

The protection of mycorrhiza against pathogen attack was shown using *T. vaccinum,* which significantly reduced the growth of both pathogens tested *in vitro* (**Supplementary Figure S7**).

The reduced growth of the root pathogen *H. annosum* already allows for some protection of the host tree. In this case, volatiles emitted by *T. vaccinum* had no effect on *H. annosum* in divided plates.

For the more severe and faster growing needle pathogen *B. cinerea,* a slight effect of volatiles was seen in addition to growth reduction in co-culture indicating the potential to work at a distance (see **Supplementary Figure S7**).

In hydroponic mycorrhizal co-cultures, *T. vaccinum* redirected the growth of *B. cinerea* to the medium-air interface, away from the *T. vaccinum* inoculant. From 12 incubated spruces, all survived when inoculated with *T. vaccinum* or in the co-inoculation of *T. vaccinum* and *B. cinerea*. All spruces of both treatments appeared healthy, whereas only 9 of 12 spruces that were incubated with the pathogen alone were alive. The pathogen stayed at the root and caused typical disease symptoms like needle discoloration, needle death or black points at needles (**Figure 7**).

DISCUSSION

Here, we analyzed the composition of the microbial community in a spruce mycorrhizosphere and the effect of the ectomycorrhizal fungus *T. vaccinum* on community structure in a microcosm experiment. Pyrosequencing revealed a high diversity in Basidiomycota, whereas Ascomycota were underrepresented, and other phyla did not appear. Ten most abundant OTUs featured an ECM lifestyle, and clearly reflected the fact that forest trees are colonized by different ECM fungi simultaneously (Smith and Read, 1987). We also could show a much higher diversity at the sampling site than had been reported earlier for the ECM community of Norway spruce with 34 different taxa, which is known to change between tree species, geographical as well as climatic conditions, soil composition and seasons (Dighton et al., 2005; Korkama et al., 2006). Thus, a saturated diversity sampling seems to be highly important, which was checked in this study by rarefaction analysis (compare **Supplementary Figure S2**). Remarkably, the 10 most abundant

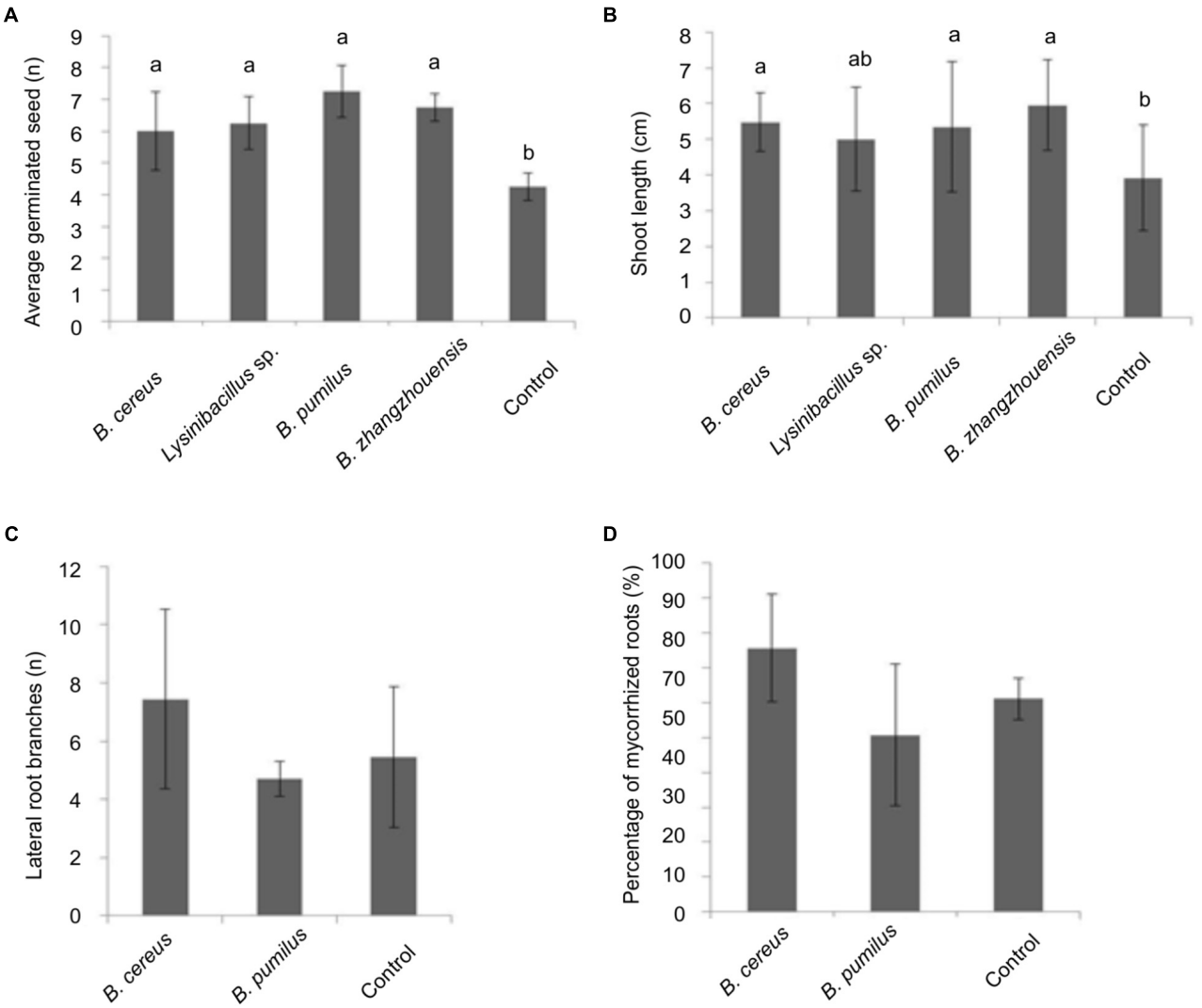

FIGURE 6 | Effect of suspension of the selected bacterial isolates on *P. abies* **(A)** germination and **(B)** germination tube or shoot length, significance level $p < 0.05$. Effect of bacterial suspension on mycorrhized trees after 3 months of incubation with total number of lateral branches per root system **(C)** or percentage of total mycorrhized roots **(D)**, error bars indicate standard deviations, $n = 3$.

OTUs from this work were not represented in the *P. abies* ECM study performed by Korkama et al. (2006) indicating the high variability between habitats.

We isolated common soil colonizing and fast growing fungi, which might have outcompeted in culture other slower growing fungi detected in amplicon sequencing. The isolates belong to the genera *Umbelopsis*, *Penicillium*, *Mortierella*, *Absidia* (Warcup, 1951), insect or nematode parasites *Beauveria* (Meyling and Eilenberg, 2006) and *Pochonia* (Atkins et al., 2003). *Umbelopsis ramanniana*, different *Penicillium* species, *Beauveria bassiana* and *Pochonia bulbillosa* were frequently found in free soil, the rhizosphere, mycorrhizosphere and hyphosphere of spruce trees (Voronina, 2011). Additionally, *Penicillium* and *Umbelopsis* species have been described as endophytes in spruce roots (Kernaghan and Patriquin, 2011). Species of *Lecanicillium* (Goettel et al., 2008) and *Acremonium* (Latch, 1994) can colonize grasses as endophytes, but were also found in the rhizosphere of healthy black spruce trees (Vujanovic et al., 2007) and *Lecanicillium* sp. in the hyphosphere (Voronina, 2011).

Voronina (2011) showed increased mycomycete diversity in *T. fulvum* mycorrhizosphere compared to the hyphosphere alone, which was not the case for most of the other studied ECM fungi. These experiments fit well with the microcosm studies, where a higher abundance and diversity of fungi was observed with dead spruce trees that might provide a saprotrophic food source. Since *T. vaccinum* is able to use cellulose as sole C source, its degradative capacity could possibly have supported the growth of other fungi through decomposition of dead spruce trees. The ability of ECM fungi to live as saprotrophs which can decompose plant litter is intensively discussed (Baldrian, 2009). The sequenced genome of *T. vaccinum* covers multiple

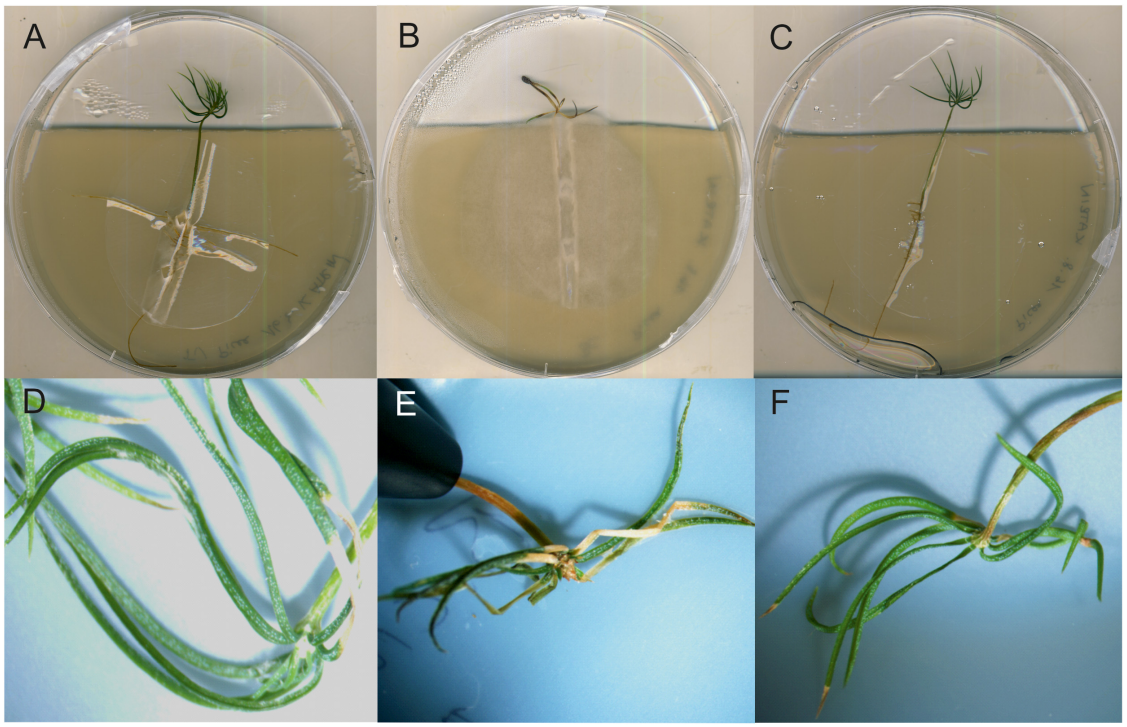

FIGURE 7 | Spruce seedlings inoculated with *T. vaccinum* **(A,D)**, with *B. cinerea* displaying typical symptoms in needle development **(B,E)**, co-inoculated, healthy seedlings **(F)**, and without fungal inoculation **(C)**.

gene copies coding for cellulolytic enzymes and laccases – more than the ECM average (Wagner et al., 2015). Interestingly, its activity decreased in the presence of spruce root exudates, functioning as early signaling molecules (Wagner et al., 2015). For other ECM fungi, decomposition of proteins, cellulose, hemicellulose and other organic carbons was shown, as well as the colonization of soil organic matter patches (Haselwandter et al., 1990; Bending and Read, 1995).

The high C:N ratio detected at the test site suggests that the studied mycorrhizosphere is a nitrogen limited habitat with a potentially reduced microbial activity (Paul, 2014). Research pointed out that nitrogen fixation is essential in mycorrhizal interactions and raised the question if the symbiotic fungal partners can perform this task, or if this function is delegated to MHB (Mikola, 1986). This hypothesis was strengthened by detection of nitrogen fixing *Bradyrhizobium japonicum* on non-legumes, as is seen with the present study (Lian et al., 2002). Further, three of four proposed MHB showed growth on nitrogen-free medium suggesting nitrogen fixation (compare **Supplementary Table S4**).

ECM microbial communities are diverse, but share structural similarities not present with the surrounding bulk soil. Uroz et al. (2012) identified Proteobacteria with 56%; the 10 dominant genera were *Acidobacteria* (19%), *Burkholderia* (6%; with a function in mineral weathering), *Rhodoplanes* (5%), *Chitinophage* (4%), and *Bradyrhizobium* (4%) in the mycorrhizosphere of oak with *Scleroderma citrinum* and *Xerocomus pruinatus*. Here Alphaproteobacteria dominated the mycorrhizophere, including two *Bradyrhizobium* species (together 2.27%) and *Rhodoplanes* (together 4.24%).

A largely dissimilar microbial diversity was observed by analysis of cultivated microbial isolates, showing the bias of cultivation versus different recovery rates during DNA isolation, amplification and sequencing. Our isolation supported fast growers and omitted obligate symbionts and other bacteria with special growth requirements (compare Bakken, 1997). We isolated mostly streptomycetes, pseudomonads, and *Bacillus* or *Micrococcus* species, indicating the higher abundance of Gram-positives and pseudomonads compared to the pyrosequencing result. Sixty *Pseudomonas fluorescens* strains had been isolated from a mycorrhizosphere including 81% inorganic phosphate mobilizers, 80% IAA and 74% siderophore producers (Frey-Klett et al., 2005). These values are higher compared to our results, which might be attributed to our broader selection for all bacterial phyla with, e.g., actinobacteria that have been shown to impact the symbiosis positively, like the positive effect reported for *Streptomyces orientalis* on spore germination of *Glomus mosseae* (Mugnier and Mosse, 1987).

The majority of the isolated bacteria showed plant growth promoting abilities; especially auxin biosynthesis was found with most strains. IAA is able to increase branching of *T. vaccinum* and increases mycorrhization with *P. abies* (Krause et al., 2015). Thus, hyperbranching in the presence of *B. cereus* MRZ-1 might be related to IAA produced only when tryptophan from root exudates induces IAA synthesis (Frey-Klett et al., 2005). Changes in the IAA flux, induced by morphogenic compounds

in the mycorrhizosphere like the fungal intermediate D'orenone, also may alter the physiology of the symbiotic partners and ECM formation (Wagner et al., 2015). Moreover, all four MHB produced IAA and stimulated the germination and shoot growth in *P. abies*. Siderophores produced by three of the selected bacteria (*B. cereus* MRZ-1, *B. pumilus* MRZ-3, *B. zhangzhouensis* MRZ-4) may be involved in shoot elongation seen with MHB through enhanced iron bioavailability in addition to siderophores from ECM and AM fungi reported to increase iron uptake in host plants (Haselwandter, 1995). The siderophore production and phosphate mobilization ability varied between our samples, possibly caused by a seasonal effect, abiotic factors like water availability, or heterogeneity in the sampling microhabitat.

B. cereus MRZ-1 showed the highest potential as MHB because it positively affected spruce germination and shoot growth, enhanced lateral branching and the rate of mycorrhization and spruce health. Moreover, volatiles changed *T. vaccinum* morphology by increasing its pigment production and reducing the mycelia diameter. We interpret this feature of a somewhat decreased extraradical growth not detrimental to advancing mycorrhization, since an earlier and more pronounced formation of intraradical symbiotic structures might be the result of this interaction. This warrants further research into signaling via volatile compounds. The pigment production might be linked to melanin, reported to mediate fungal stress resistance toward radiation, drought or reactive oxygen species, as well as being a virulence factor for plant and human pathogens (Pagano and Dhar, 2015). The initiation of pigment production in *T. vaccinum* thus could be a stress response induced through bacterial volatiles, and subsequently increase fungal vitality and thus mycorrhization.

T. vaccinum enhanced the survival rate of spruce trees during 8 weeks of incubation, which is impressive because mycorrhization evolves over several months. The positive effect on the plant partner in early mycorrhization has been discussed to involve stimulation of defense mechanisms with phytohormone signaling, because *T. vaccinum* is able to produce jasmonic acid, ethylene and salicylic acid (Wagner, 2016), with jasmonic and salicylic acids known to increase spruce defense against the stem and butt rot causing fungus *H. parviporum* (Arnerup et al., 2013). While the related *H. annosum* that infects spruce *via* the root (Stenlid and Johansson, 1987) did not respond to volatiles produced by *T. vaccinum*, the pathogen *B. cinerea* was impaired in growth. The induction of systemic acquired resistance through salicylic acid production by *T. vaccinum* can confer protection even against a needle pathogen such as *B. cinerea*. In addition, volatiles of *T. vaccinum* included potential antimicrobial compounds, like the typical fungal volatiles octen3-ol and 3-octanone, the terpenoid plant metabolites limonene and β- barbatene, as well as geosmin (Wagner, 2016). The mycorrhization with *T. vaccinum*, at the same time, changed the VOC pattern of spruce. Increased limonene production with antimicrobial activity (Henke et al., 2015b) may also have contributed to resistance against *B. cinerea* root infection. Thus, further research on the precise identification of the chemical components of the volatiles involved in the specific interaction is needed.

With the holistic approach on the entire mycorrhizosphere, we could show complex interactions involving more than two partners. *T. vaccinum*, as ectomycorrhizal fungus, enhances survival of its host, spruce. At the same time, *T. vaccinum* can suppress pathogen attack likely by induction of plant defense and antimicrobial activity of *T. vaccinum* compounds. A third function of *T. vaccinum* is correlated with its saprotrophic growth, where it decomposed dead host material and, thus, changed the fungal community present in the mycorrhizosphere. Bacteria isolated from mycorrhizspheric soil were shown to act as MHB through the production of phytohormones and volatiles, which might be true as well for other, non-cultivable members of the bacterial community.

AUTHOR CONTRIBUTIONS

KW designed and conducted experiments, analyzed, and wrote the first draft of the manuscript. DS, RG-M, and KK conducted experiments, analyzed, and contributed to the manuscript preparation. AK, KK, and EK designed experiments, interpreted results, and contributed to the manuscript preparation.

FUNDING

This research was funded and supported by the Max Planck Society, Germany via the International Max Planck Research School, by the Excellence Graduate School GSC 214, by the Friedrich Schiller University Jena and the Research Training Group GRK 1257 funded by the German Science foundation. RG-M was supported by Consejo Nacional de Ciencia y Tecnología-German Academic Exchange Service (CONACyT-DAAD).

ACKNOWLEDGMENTS

We would like to thank David Heil for the characterization and identification of fungal strains, Johannes Gmeiner for the characterization of bacterial strains and plant pathogen experiments, and the numerous practical course students between 2013 and 2015 for their contribution in isolating bacterial strains. Further, we thank Dirk Merten for sequential extraction and we acknowledge Ines Hilke from the Max Planck Institute of Biogeochemistry in Jena for CNS analyzes, Matthias Gube for *T. vaccinum* fruiting bodies and Jennifer Stoiber-Lipp for support in rarefaction analysis.

SUPPLEMENTARY MATERIAL

The Supplementary Material for this article can be found online at: https://www.frontiersin.org/articles/10.3389/fmicb.2019.00307/full#supplementary-material

REFERENCES

Ahmad, F., Ahmad, I., and Khan, M. (2008). Screening of free-living rhizospheric bacteria for their multiple plant growth promoting activities. *Microbiol. Res.* 163, 173–181. doi: 10.1016/j.micres.2006.04.001

Alabouvette, C. (1990). "Biological control of *Fusarium* wilt pathogens in suppressive soils" in *Biological Control of Soil-Borne Plant Pathogens*, ed. D. Hornby (Wallingford, CAB International), 27–43.

Arnerup, J., Nemesio-Gorriz, M., Lunden, K., Asiegbu, F. O., Stenlid, J., and Elfstrand, M. (2013). The primary module in norway spruce defence signalling against *H. annosum* s.l. seems to be jasmonate-mediated signalling without antagonism of salicylate-mediated signalling. *Planta* 237, 1037–1045. doi: 10.1007/s00425-012-1822-8

Asiegbu, F. O., Adomas, A., and Stenlid, J. (2005). Conifer root and butt rot caused by *Heterobasidion annosum* (Fr.) Bref. s.l. *Mol. Plant Pathol.* 6, 395–409. doi: 10.1111/j.1364-3703.2005.00295.x

Asiimwe, T., Krause, K., Schlunk, I., and Kothe, E. (2012). Modulation of ethanol stress tolerance by aldehyde dehydrogenase in the mycorrhizal fungus *Tricholoma vaccinum*. *Mycorrhiza* 22, 471–484. doi: 10.1007/s00572-011-0424-9

Atkins, S. D., Hidalgo-Diaz, L., Clark, I. M., Morton, C. O., Montes de Oca, N., Gray, P. A., et al. (2003). Approaches for monitoring the release of *Pochonia chlamydosporia* var. catenulata, a biocontrol agent of root-knot nematodes. *Mycol. Res.* 107, 206–212. doi: 10.1017/S095375620300724X

Ausubel, F. M., Brent, R., Kingston, R. E., Moore, D. D., Seidman, J., Smith, J. A., et al. (1992). *Short Protocols in Molecular Biology*. New York, NY: John Wiley and Sons.

Bååth, E., and Anderson, T.-H. (2003). Comparison of soil fungal/bacterial ratios in a pH gradient using physiological and PLFA-based techniques. *Soil Biol. Biochem.* 35, 955–963. doi: 10.1016/S0038-0717(03)00154-8

Bais, H. P., Park, S.-W., Weir, T. L., Callaway, R. M., and Vivanco, J. M. (2004). How plants communicate using the underground information superhighway. *Trends Plant Sci.* 9, 26–32. doi: 10.1016/j.tplants.2003.11.008

Bakken, L. R. (1997). "Culturable and nonculturable bacteria in soil", in *Modern Soil Microbiology,* eds J. D. van Elsas, J. T. Trevors and E. M. H. Wellington (New York, NY: Marcel Dekker Inc), 47–61.

Baldrian, P. (2009). Ectomycorrhizal fungi and their enzymes in soils: is there enough evidence for their role as facultative soil saprotrophs? *Oecologia* 161, 657–660.

Baldrian, P., Kolařík, M., Štursová, M., Kopecký, J., Valášková, V., Větrovský, T. et al. (2012). Active and total microbial communities in forest soil are largely different and highly stratified during decomposition. *ISME J.* 6, 248–258. doi: 10.1038/ismej.2011.95

Bending, G. D., and Read, D. J. (1995). The structure and function of the vegetative mycelium of ectomycorrhizal plants. VI. Activities of nutrient mobilizing enzymes in birch litter colonized by *Paxillus involutus* (Fr.) Fr. *New Phytol.* 130, 411–417. doi: 10.1111/j.1469-8137.1995.tb01835.x

Buee, M., Reich, M., Murat, C., Morin, E., Nilsson, R. H., Uroz, S., et al. (2009). 454 Pyrosequencing analyses of forest soils reveal an unexpectedly high fungal diversity. *New Phytol.* 184, 449–456. doi: 10.1111/j.1469-8137.2009.03003.x

Cole, J. R., Wang, Q., Cardenas, E., Fish, J., Chai, B., Farris, R. J., et al. (2009). The Ribosomal Database Project: improved alignments and new tools for rRNA analysis. *Nucleic Acids Res.* 37, D141–D145. doi: 10.1093/nar/gkn879

Deveau, A., Plett, J. M., Legué, V., Frey-Klett, P., and Martin, F. (2012). "Communication between plant, ectomycorrhizal fungi and helper bacteria", in *Biocommunication of Fungi*, ed. G. Witzany (Haarlem: Springer), 229–247.

Dighton, J., White, J. F. Jr., White, J., and Oudemans, P. (2005). *The Fungal Community: Its Organization and Role in the Ecosystem*. Boca Raton, FL: CRC Press. doi: 10.1201/9781420027891

Eisenman, H. C., and Casadevall, A. (2012). Synthesis and assembly of fungal melanin. *Appl. Microbiol. Biotechnol.* 93, 931–940. doi: 10.1007/s00253-011-3777-2

Frey-Klett, P., Chavatte, M., Clausse, M. L., Courrier, S., Le Roux, C., Raaijmakers, J., et al. (2005). Ectomycorrhizal symbiosis affects functional diversity of rhizosphere fluorescent pseudomonads. *New Phytol.* 165, 317–328. doi: 10.1111/j.1469-8137.2004.01212.x

Gardes, M., and Bruns, T. D. (1993). ITS primers with enhanced specificity for basidiomycetes-application to the identification of mycorrhizae and rusts. *Mol. Ecol.* 2, 113–118. doi: 10.1111/j.1365-294X.1993.tb00005.x

Gea, L., Normand, L., Vian, B., and Gay, G. (1994). Structural aspects of ectomycorrhiza of *Pinus pinaster* (Ait.) Sol. formed by an IAA-overproducer mutant of *Hebeloma cylindrosporum* romagnési. *New Phytol.* 128, 659–670. doi: 10.1111/j.1469-8137.1994.tb04030.x

Goettel, M. S., Koike, M., Kim, J. J., Aiuchi, D., Shinya, R., and Brodeur, J. (2008). Potential of *Lecanicillium* spp. for management of insects, nematodes and plant diseases. *J. Invertebr. Pathol.* 98, 256–261. doi: 10.1016/j.jip.2008.01.009

Gordon, S. A., and Weber, R. P. (1951). Colorimetric estimation of indoleacetic acid. *Plant Physiol.* 26, 192–195. doi: 10.1104/pp.26.1.192

Haselwandter, K. (1995). Mycorrhizal fungi: siderophore production. *Crit. Rev. Biotechnol.* 15, 287–291. doi: 10.3109/07388559509147414

Haselwandter, K., Bobleter, O., and Read, D. (1990). Degradation of 14C-labelled lignin and dehydropolymer of coniferyl alcohol by ericoid and ectomycorrhizal fungi. *Arch. Microbiol.* 153, 352–354. doi: 10.1007/BF00249004

Hause, B., and Schaarschmidt, S. (2009). The role of jasmonates in mutualistic symbioses between plants and soil-born microorganisms. *Phytochemistry* 70, 1589–1599. doi: 10.1016/j.phytochem.2009.07.003

Henke, C., Jung, E.-M., and Kothe, E. (2015a). Hartig'net formation of *Tricholoma vaccinum*-spruce ectomycorrhiza in hydroponic cultures. *Environ. Sci. Pollut. Res.* 22, 19394–19399. doi: 10.1007/s11356-015-4354-5

Henke, C., Kunert, M., Veit, D., Kunert, G., Krause, K., Kothe, E., et al. (2015b). Analysis of volatiles from *Picea abies* triggered by below-ground interactions. *Environ. Exp. Bot.* 110, 56–61.

Ihrmark, K., Bödeker, I. T., Cruz-Martinez, K., Friberg, H., Kubartova, A., Schenck, J., et al. (2012). New primers to amplify the fungal ITS2 region–evaluation by 454-sequencing of artificial and natural communities. *FEMS Microbiol. Ecol.* 82, 666–677. doi: 10.1111/j.1574-6941.2012.01437.x

Innis, M., Gelfand, D., Sninsky, J., and White, T. (1990). *PCR Protocols: A Guide to Methods and Applications*. San Diego, CA: Academic Press.

Johansson, J. F., Paul, L. R., and Finlay, R. D. (2004). Microbial interactions in the mycorrhizosphere and their significance for sustainable agriculture. *FEMS Microbiol. Ecol.* 48, 1–13. doi: 10.1016/j.femsec.2003.11.012

Kernaghan, G., and Patriquin, G. (2011). Host associations between fungal root endophytes and boreal trees. *Microb. Ecol.* 62, 460–473. doi: 10.1007/s00248-011-9851-6

Klimo, E., Hager, H., and Kulhavý, J. (2000). Spruce monocultures in central Europe: problems and prospects. *Eur. Forest Inst. Portal* 33, 1–208.

Korkama, T., Pakkanen, A., and Pennanen, T. (2006). Ectomycorrhizal community structure varies among Norway spruce (*Picea abies*) clones. *New Phytol.* 171, 815–824. doi: 10.1111/j.1469-8137.2006.01786.x

Kottke, I., Guttenberger, M., Hampp, R., and Oberwinkler, F. (1987). An in vitro method for establishing mycorrhizae on coniferous tree seedlings. *Trees* 1, 191–194. doi: 10.1007/BF00193562

Krause, K., Henke, C., Asiimwe, T., Ulbricht, A., Klemmer, S., Schachtschabel, D., et al. (2015). Indole-3-acetic acid biosynthesis, secretion, and its morphological effects on *Tricholoma vaccinum*-spruce ectomycorrhiza. *Appl. Environ. Microbiol.* 81, 7003–7011. doi: 10.1128/AEM.01991-15

Krause, K., and Kothe, E. (2006). Use of RNA fingerprinting to identify fungal genes specifically expressed during ectomycorrhizal interaction. *J. Basic Microbiol.* 46, 387–399. doi: 10.1002/jobm.200610153

Latch, G. (1994.) Influence of *Acremonium* endophytes on perennial grass improvement. *N. Z. J. Agric. Res.* 37, 311–318. doi: 10.1080/00288233.1994.9513069

Lian, B., Souleimanov, A., Zhou, X., Smith, D. L. (2002). *In vitro* induction of lipo-chitooligosaccharide production in *Bradyrhizobium japonicum* cultures by root extracts from non-leguminous plants. *Microbiol. Res.* 157, 157–160. doi: 10.1078/0944-5013-00145

Lundén, K., Danielsson, M., Durling, M. B., Ihrmark, K., Nemesio Gorriz, M., Stenlid, J., et al. (2015). Transcriptional responses associated with virulence and defence in the interaction between *Heterobasidion annosum* s.s. and Norway spruce. *PLoS One* 10:e0131182. doi: 10.1371/journal.pone.0131182

Mehta, S., and Nautiyal, C. S. (2001). An efficient method for qualitative screening of phosphate-solubilizing bacteria. *Curr. Microbiol.* 43, 51–56. doi: 10.1007/s002840010259

Meyling, N. V., and Eilenberg, J. (2006). Occurrence and distribution of soil borne entomopathogenic fungi within a single organic agroecosystem. *Agric. Ecosyst. Environ.* 113, 336–341. doi: 10.1016/j.agee.2005.10.011

Mikola, P. U. (1986). Relationship between nitrogen fixation and mycorrhiza. *MIRCEN J. Appl. Microbiol. Biotechnol.* 2, 275–282. doi: 10.1007/BF00933493

Minasny, B., McBratney, A. B., Brough, D. M., and Jacquier, D. (2011). Models relating soil pH measurements in water and calcium chloride that incorporate electrolyte concentration. *Eur. J. Soil Sci.* 62, 728–732. doi: 10.1111/j.1365-2389.2011.01386.x

Mugnier, J., and Mosse, B. (1987). Spore germination and viability of a vesicular arbuscular mycorrhizal fungus, *Glomus mosseae*. *Transact. Br. Mycol. Soc.* 88, 411–413. doi: 10.1016/S0007-1536(87)80018-9

Pagano, M. C., and Dhar, P. P. (2015). "Fungal pigments: an overview," in *Fungal Biomolecules: Sources, Applications and Recent Developments*. eds V. K. Gupta, R. L. Mach, and S. Sreenivasaprasad (Oxford: Wiley-Blackwell), 173.

Paul, E. A. (2014). *Soil Microbiology, Ecology and Biochemistry*. Amsterdam: Academic press.

Raudaskoski, M., and Kothe, E. (2015). Novel findings on the role of signal exchange in arbuscular and ectomycorrhizal symbioses. *Mycorrhiza* 25, 243–252. doi: 10.1007/s00572-014-0607-2

Saharan, B., and Nehra, V. (2011). Plant growth promoting rhizobacteria: a critical review. *LSMR* 21, 1–30.

Schütze, E., Klose, M., Merten, D., Nietzsche, S., Senftleben, D., Roth, M., et al. (2014). Growth of streptomycetes in soil and their impact on bioremediation. *J. Hazard. Mater.* 267, 128–135. doi: 10.1016/j.jhazmat.2013.12.055

Schütze, E., Weist, A., Klose, M., Wach, T., Schumann, M., Nietzsche, S., et al. (2013). Taking nature into lab: biomineralization by heavy metal-resistant streptomycetes in soil. *Biogeosciences* 10, 3605–3614. doi: 10.5194/bg-10-3605-2013

Schwyn, B., and Neilands, J. B. (1987). Universal chemical assay for the detection and determination of siderophores. *Anal. Biochem.* 160, 47–56. doi: 10.1016/0003-2697(87)90612-9

Smith, S. E., and Read, D. J. (1987). *Mycorrhizal Symbiosis*, 2nd Edn. San Diego, CA: Academic press.

Stenlid, J., and Johansson, M. (1987). Infection of roots of Norway spruce (*Picea abies*) by *Heterobasidion annosum*. *Eur. J. For. Pathol.* 17, 217–226. doi: 10.1111/j.1439-0329.1987.tb01019.x

Tsai, H. F., Wheeler, M. H., Chang, Y. C., and Kwon-Chung, K. J. (1999). A developmentally regulated gene cluster involved in conidial pigment biosynthesis in *Aspergillus fumigatus*. *J. Bacteriol.* 181, 6469–6477.

Tsavkelova, E. A., Klimova, S. Y., Cherdyntseva, T. A., and Netrusov, A. I. (2006). Hormones and hormone-like substances of microorganisms: a review. *Appl. Biochem. Microbiol.* 42, 229–235. doi: 10.1134/S000368380603001X

Uroz, S., Oger, P., Morin, E., and Frey-Klett, P. (2012). Distinct ectomycorrhizospheres share similar bacterial communities as revealed by pyrosequencing-based analysis of 16S rRNA genes. *Appl. Environ. Microbiol.* 78, 3020–3024. doi: 10.1128/AEM.06742-11

Voronina, E. Y. (2011). Effect of the mycorrhizosphere on soil micromycete biodiversity and community structure and its relation to the rhizosphere and hyphosphere effects. *Microbiology* 80, 584–590. doi: 10.1134/S0026261711040217

Vujanovic, V., Hamelin, R., Bernier, L., Vujanovic, G., and St-Arnaud, M. (2007). Fungal diversity, dominance, and community structure in the rhizosphere of clonal *Picea mariana* plants throughout nursery production chronosequences. *Microb. Ecol.* 54, 672–684. doi: 10.1007/s00248-007-9226-1

Wagner, K. (2016). *Chemical Communication Between Soil Microorganisms, Basidiomycetes and Their Tree Host*. Dissertation, University of Jena, Jena.

Wagner, K., Krause, K., David, A., Kai, M., Jung, E.-M., Sammer, D. et al. (2016). Influence of zygomycete-derived D'orenone on IAA signaling in *Tricholoma*-spruce ectomycorrhiza. *Environ. Microbiol.* 18, 2470–2480. doi: 10.1111/1462-2920.13160

Wagner, K., Linde, J., Krause, K., Gube, M., Koestler, T., Sammer, D. et al. (2015). *Tricholoma vaccinum* host communication during ectomycorrhiza formation. *FEMS Microbiol. Ecol.* 91:fiv120. doi: 10.1093/femsec/fiv120

Wang, Y., Brown, H., Crowley, D., and Szaniszlo, P. (1993). Evidence for direct utilization of a siderophore, ferrioxamine B, in axenically grown cucumber. *Plant Cell Environ.* 16, 579–585. doi: 10.1111/j.1365-3040.1993.tb00906.x

Warcup, J. (1951). The ecology of soil fungi. *Trans. Br. Mycol. Soc.* 34, 376–399. doi: 10.1016/S0007-1536(51)80065-2

Williamson, B., Tudzynski, B., Tudzynski, P., and van Kan, J. A. L. (2007). *Botrytis cinerea*: the cause of grey mould disease. *Mol. Plant Pathol.* 8, 561–580. doi: 10.1111/j.1364-3703.2007.00417.x

Wöstemeyer, J. (1985). Strain-dependent variation in ribosomal DNA arrangement in *Absidia glauca*. *Eur. J. Biochem.* 146, 443–448. doi: 10.1111/j.1432-1033.1985.tb08671.x

Wu, X.-Q., Hou, L.-L., Sheng, J.-M., Ren, J.-H., Zheng, L., Chen, D., et al. (2012). Effects of ectomycorrhizal fungus *Boletus edulis* and mycorrhiza helper *Bacillus cereus* on the growth and nutrient uptake by *Pinus thunbergii*. *Biol. Fertil. Soils* 48, 385–391. doi: 10.1007/s00374-011-0638-1

Conflict of Interest Statement: The authors declare that the research was conducted in the absence of any commercial or financial relationships that could be construed as a potential conflict of interest.

frontiers in Plant Science

ORIGINAL RESEARCH
published: 12 March 2019
doi: 10.3389/fpls.2019.00262

A Stimulatory Role for Cytokinin in the Arbuscular Mycorrhizal Symbiosis of Pea

*Dane M. Goh[1†], Marco Cosme[2†], Anna B. Kisiala[3†], Samantha Mulholland[1], Zakaria M. F. Said[1], Lukáš Spíchal[4], R. J. Neil Emery[3], Stéphane Declerck[2] and Frédérique C. Guinel[1]**

[1] Biology, Wilfrid Laurier University, Waterloo, ON, Canada, [2] Mycology, Applied Microbiology, Earth and Life Institute, Université catholique de Louvain, Louvain-la-Neuve, Belgium, [3] Biology, Trent University, Peterborough, ON, Canada, [4] Centre of the Region Haná for Biotechnological and Agricultural Research, Palacký University Olomouc, Olomouc, Czechia

OPEN ACCESS

Edited by:
Eloise Foo, University of Tasmania, Australia

Reviewed by:
Juan Antonio Lopez Raez, Experimental Station of Zaidín (EEZ), Spain
Jonathan Michael Plett, Western Sydney University, Australia
Jutta Ludwig-Müller, Technische Universität Dresden, Germany
Bettina Hause, Leibniz-Institut für Pflanzenbiochemie (IPB), Germany

***Correspondence:**
Frédérique C. Guinel
fguinel@wlu.ca

† These authors have contributed equally to this work

Specialty section:
This article was submitted to Plant Microbe Interactions, a section of the journal Frontiers in Plant Science

Received: *30 October 2018*
Accepted: *19 February 2019*
Published: *12 March 2019*

Citation:
Goh DM, Cosme M, Kisiala AB, Mulholland S, Said ZMF, Spíchal L, Emery RJN, Declerck S and Guinel FC (2019) A Stimulatory Role for Cytokinin in the Arbuscular Mycorrhizal Symbiosis of Pea. Front. Plant Sci. 10:262. doi: 10.3389/fpls.2019.00262

The arbuscular mycorrhizal (AM) symbiosis between terrestrial plants and AM fungi is regulated by plant hormones. For most of these, a role has been clearly assigned in this mutualistic interaction; however, there are still contradictory reports for cytokinin (CK). Here, pea plants, the wild type (WT) cv. Sparkle and its mutant E151 (*Pssym15*), were inoculated with the AM fungus *Rhizophagus irregularis*. E151 has previously been characterized as possessing high CK levels in non-mycorrhizal (myc^-) roots and exhibiting high number of fungal structures in mycorrhizal (myc^+) roots. Myc^- and myc^+ plants were treated 7, 9, and 11 days after inoculation (DAI) with synthetic compounds known to alter CK status. WT plants were treated with a synthetic CK [6-benzylaminopurine (BAP)] or the CK degradation inhibitor INCYDE, whereas E151 plants were treated with the CK receptor antagonist PI-55. At 13 DAI, plant CK content was analyzed by mass spectrometry. The effects of the synthetic compounds on AM colonization were assessed at 28 (WT) or 35 (E151) DAI via a modified magnified intersections method. The only noticeable difference seen between myc^- and myc^+ plants in terms of CK content was in the levels of nucleotides (NTs). Whereas WT plants responded to fungi by lowering their NT levels, E151 plants did not. Since NTs are thought to be converted into active CK forms, this result suggests that active CKs were synthesized more effectively in WT than in E151. In general, myc^+ and myc^- WT plants responded similarly to INCYDE by lowering significantly their NT levels and increasing slightly their active CK levels; these responses were less obvious in BAP-treated WT plants. In contrast, the response of E151 plants to PI-55 depended on the plant mycorrhizal status. Whereas treated myc^- plants exhibited high NT and low active CK levels, treated myc^+ plants displayed low levels of both NTs and active CKs. Moreover, treated WT plants were more colonized than treated E151 plants. We concluded that CKs have a stimulatory role in AM colonization because increased active CK levels were paralleled with increased AM colonization while decreased CK levels corresponded to reduced AM colonization.

Keywords: AM symbiosis, cytokinin, INCYDE, legume, PI-55, *Pisum sativum* L., plant hormone, *Rhizophagus irregularis*

INTRODUCTION

The biological association between land plants and AM fungi is one of the most ancient, widespread, and functionally important symbioses on Earth. Its development can be dissected into several steps reflecting the progression of the fungus during colonization of the host roots (Smith and Read, 2008). In the pre-contact step, the hyphae growing from a propagule (i.e., spores, vesicles, colonized roots) often start branching to increase the number of potential entry points into the roots (Akiyama et al., 2005). Once in contact with the root surface, the hyphae differentiate into hyphopodia to facilitate fungal penetration into the plant epidermis. In the *Arum*-type of AM colonization, which is the most studied type, the fungal hyphae proliferate intercellularly within the root cortex and eventually invade cortical cells to develop into arbuscules (Dickson et al., 2007), which are the main interfaces in the bi-directional exchange of nutrients between the two partners. While the fungus provides phosphorus, nitrogen, and other mineral elements to the plant (Rausch et al., 2001; Harrison et al., 2002; Guether et al., 2009; Gaude et al., 2012), the plant delivers sugars and lipids to the fungus (Helber et al., 2011; Bravo et al., 2017). Newly acquired carbon is translocated through the hyphae mostly in lipid forms, which are either used in fungal metabolism or stored in spores and other fungal structures, such as vesicles and auxiliary cells depending on the genus.

The development of AM symbiosis involves a complex molecular dialogue between partners and is partially regulated by the host plant through the highly specific action of several hormones. Regulatory aspects of most of the hormones in this process have been discussed in several reviews (Foo et al., 2013; Bucher et al., 2014; Fusconi, 2014; Gutjahr, 2014; Pozo et al., 2015; Lace and Ott, 2018; Liao et al., 2018; Das and Gutjahr, 2019), wherein the role of CKs appears noticeably obscure.

CKs can exist in various forms that differ in their structure and activity, and their homeostasis is fine-tuned through biosynthesis and degradation (**Figure 1**; Spíchal, 2012). They are perceived by receptors which consist of an extracellular CHASE domain and an intracellular portion made up of a His kinase domain and two receiver domains (Kieber and Schaller, 2010). Upon CK perception, a signal is transduced and decrypted, and a biological response ensues (**Figure 1**). It still remains controversial whether CKs have a role in the establishment and maintenance of AM colonization. A regulatory role for CKs is either considered not well understood (Pozo et al., 2015; Liao et al., 2018), continues to cast doubts (Foo et al., 2013; Lace and Ott, 2018; Das and Gutjahr, 2019), or is just overlooked (Bucher et al., 2014; Gutjahr, 2014), possibly because of the contradictory conclusions documented in the literature. For instance, mycorrhizal colonization did not appear to alter gene expression in the CK signaling of the legume species *Medicago truncatula* (Laffont et al., 2015). Yet, recent studies employing powerful biochemical tools (Adolfsson et al., 2017; Schmidt et al., 2017; Yurkov et al., 2017) confirmed what earlier studies had documented (e.g., Allen et al., 1980; Shaul-Keinan et al., 2002), i.e., that mycorrhizal (myc^+) plants exhibit altered CK levels compared to non-mycorrhizal (myc^-) plants. The intensity of these mycorrhizal effects on CK accumulation in plants depends on the fungal species, P availability in soil, as well as on plant tissue and development stage.

Several hypotheses have been proposed to explain the AM-mediated changes in CK content of the host plants. First, the AM fungus may produce and deliver CKs to the host roots (Allen et al., 1980; Shaul-Keinan et al., 2002). Second, the AM fungus may stimulate host plant CK biosynthesis (Drüge and Schönbeck, 1992). Third, either a plant or a fungal compound may inhibit CK degradation (Allen et al., 1980; Shaul-Keinan et al., 2002). Finally, the AM-mediated increase in P uptake may indirectly affect the plant CK homeostasis (Drüge and Schönbeck, 1992; Shaul-Keinan et al., 2002). Regardless of the mechanism, considering the strong impact of CKs on plant development (e.g., Werner and Schmülling, 2009), it is likely that alteration of CK levels in the host plant affects AM symbiosis. Yet, the effects that CKs have on AM development appear inconsistent in the few existing reports. For example, the exogenous application of synthetic CK to myc^+ plants suggests an inhibitory effect of CKs on AM development (Gryndler et al., 1998; Bompadre et al., 2015; Schmidt et al., 2017), whereas both endogenous CK deficiency (Cosme and Wurst, 2013) and elevated CK levels (Jones et al., 2015) in the host plant hint at a stimulatory role. Some of these inconsistencies might be explained by the fact that CKs, depending on their location (shoots or roots), may have distinct roles in the AM symbiosis (Cosme et al., 2016).

Here, we investigated (1) whether the presence of an AM fungus (*Rhizophagus irregularis*) affects the CK levels in the shoots and roots of a legume host plant and (2) whether altering the CK homeostasis of this legume influences AM development. To tackle these two objectives, we used pea (*Pisum sativum* L.) cv. Sparkle (WT) and its pleiotropic mutant E151 (*Pssym15*) as host plants. This mutant was characterized as sparsely forming nodules when grown in the presence of rhizobia (Kneen et al., 1994). Early in its development, i.e., 6 days after planting, E151 is known to accumulate a larger amount of CKs than its WT. Furthermore, later in life, E151 exhibits enhanced mycorrhizal colonization under the control of its shoot as determined by grafting experiments (Jones et al., 2015). In this work, we studied AM development in both these plant lines along several time points and analyzed the CK content of myc^+ and myc^- plants 13 DAI, when pea is known to have entered its vegetative phase (Knott, 1987). To manipulate CK homeostasis, we undertook pharmacological treatments using

Abbreviations: 2MeSiP, 2-methylthio-isopentenyladenine; 2MeSiPR, 2-methylthio-isopentenyladenosine; 2MeSZ, 2-methylthio-zeatin; 2MeSZR, 2-methylthio-zeatin riboside; AM, Arbuscular mycorrhiza; ANOVA, one-way analysis of variance; BAP, 6-benzylaminopurine; BAPR, 6-benzylaminopurine riboside; CK, cytokinin; DAI, day after inoculation; DHZ, dihydrozeatin; DHZOG, dihydrozeatin-O-glucoside; DHZR, dihydrozeatin-riboside; DHZRMP, dihydrozeatin riboside-5′-monophosphate; DHZROG, dihydrozeatin riboside-O-glucoside; DMSO, dimethyl sulfoxide; FB, free base; HC, hyphal compartment; HPLC-(+ESI)-MS/MS), high-performance liquid chromatography-positive electrospray ionization tandem mass spectrometry; INCYDE, 2-chloro-6-(3-methoxyphenyl)-aminopurine; iP, isopentenyladenine; iP7G, isopentenyladenine-7-glucoside; iPR, isopentenyladenosine; iPRMP, isopentenyladenosine-5′-monophosphate; MSR, Modified Strullu-Romand; NT, nucleotide; PACK, putatively active cytokinin; PI-55, 6-(2-hydroxy-3-methylbenzyl)-aminopurine; RB, riboside; TDZ, thidiazuron; WT, wild type; Z, zeatin; Z9G, zeatin-9-glucoside; ZOG, zeatin O-glucoside; ZR, zeatin riboside; ZRMP, zeatin riboside-5′-monophosphate; ZROG, zeatin riboside-O-glucoside.

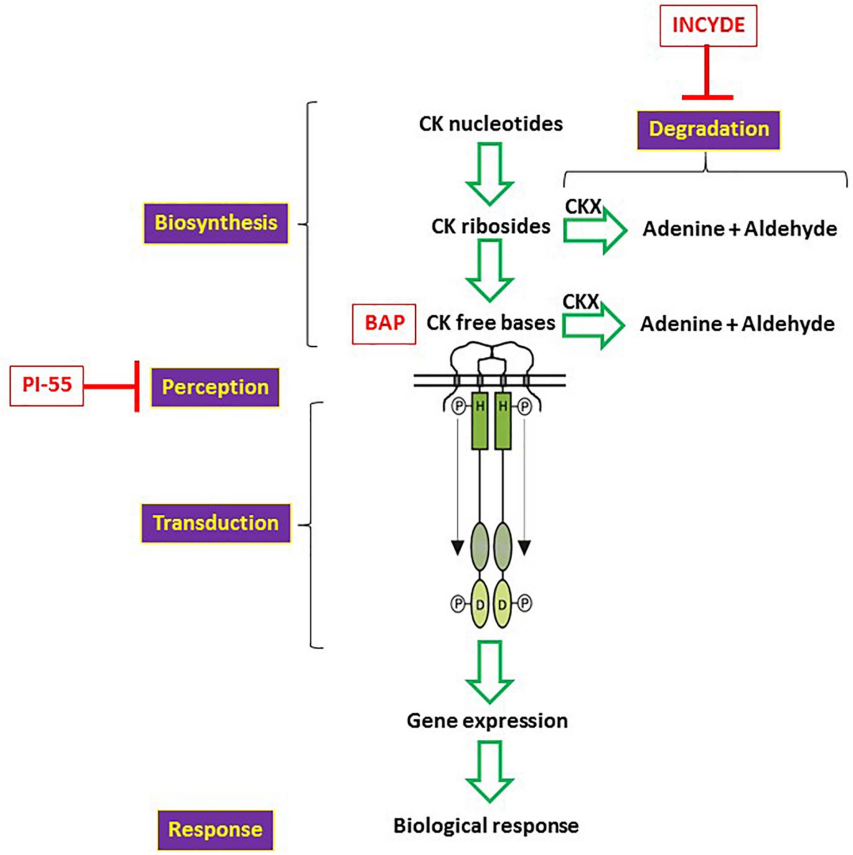

FIGURE 1 | Schematic representation of CK homeostasis in a plant cell. CK nucleotides are the precursors of the CK ribosides and CK free bases (e.g., BAP). Both types of CKs are substrates of the enzyme CK oxidase (CKX) and they will be degraded upon enzymatic activity. When active free bases are perceived by CK receptors, a signal is transduced to the nucleus triggering the expression of response regulators, which ultimately will lead to a biological response. INCYDE, an inhibitor of CK degradation, and PI-55, a competitive inhibitor of CK action, are capable of regulating CK homeostasis.

synthetic compounds modifying the CK status of the plant. Finally, we used bi-compartmented *in vitro* root organ cultures to test if these CK status-modifying compounds have direct effects on the AM fungus development. Overall, our results suggest that fluctuations in CK homeostasis affect significantly AM development in pea. At an early stage of the interaction, a decrease in plant CK NTs, reflecting a fast turnover rate of these precursor molecules into active CKs, facilitated the fungal entry into the roots, while at a later stage high levels of active CKs in the shoot stimulated intraradicular fungal progression.

MATERIALS AND METHODS

Fungal and Plant Growth Conditions

The AM fungal strain used in this study was *R. irregularis* [(Blaszk, Wubet, Renker, and Buscot) C. Walker and Schuessler 2010 as ("irregulare")] DAOM 197918 originally obtained from the Agriculture and Agri-Food Canada Glomeromycota *in vitro* collection (AAFC, Ottawa, ON, Canada) and propagated in our lab using leek (*Allium ampeloprasum*) as a host. The leek plant cultures with the AM fungus were grown in peat and Turface® [1:1, v:v; ASB Greenworld Ltd. (Mount Elgin, ON, Canada) and Plant Products Company Ltd. (Brampton, ON, Canada), respectively]. They were kept in a growth chamber (16/8 h, 23/18°C, light/dark cycle) and watered weekly. Every 3 weeks, they received a low phosphorus Long-Ashton nutrient solution (Audet and Charest, 2010) instead of water. Roots of leek plants containing hyphae, vesicles and spores of the AM fungus were cut in small fragments. These fragments were mixed with the soil in which the leeks had been grown and together were used as an inoculum source for the growth-room experiments described below. For the *in vitro* experiment, spores and mycelium of *R. irregularis* MUCL 41833 as well as the Ri T-DNA transformed carrot (*Daucus carota*) roots were obtained from the Glomeromycota *in vitro* collection (GINCO[1]), where starting inocula are maintained and distributed, under *in vitro* conditions, in modified Strullu-Romand (MSR) medium.

Seeds of *P. sativum* L. cv. Sparkle and of its mutant E151 were surface-sterilized with 8% bleach, and left imbibing in water overnight in the dark. They were then sown in black Cone-tainers™ (600 mL, Stuewe and Sons, Inc., Tangent, OR,

[1]http://www.mycorrhiza.be/ginco-bel

United States) filled with a substrate mixture [1:1:1, v:v:v] of peat: Turface®: vermiculite (Therm-O-Rock East Inc., New Eagle, PA, United States). The substrate mixture was autoclaved to eliminate any potential microbial contaminants. For the myc^+ plants, the fungal inoculum was added at a ratio of 1:5 (v:v) to the sterile substrate mixture before planting. All plants were kept in a growth room (16/8 h, 23/18°C, light/dark regime). For the first 10 days, seedlings were watered when needed. Once established, except when noted otherwise, all plants were subjected to a cycle of water, water, and low phosphorus Hoagland nutrient solution (Resendes et al., 2001), until they were harvested. Harvest time was variable depending on the experiments. Plants used for CK analysis were harvested 13 DAI while plants in the AM development study were harvested 5, 10, 15, 20, and 25 DAI. An initial delay of fungal entry was observed into E151 roots compared to the WT roots (see below section E151 Delays Fungal Entry but Accelerates Intraradical Fungal Development); therefore, WT and E151 myc^+ plants treated with the synthetic CK status-modifying compounds were harvested at 28 and 35 DAI, respectively. This was considered acceptable because the size of the root systems of 35 day-old E151 plants was similar to that of 28 day-old WT plants. Both treated myc^+ plant lines were analyzed in comparison to either their respective myc^- controls or their respective non-treated myc^+ controls. For a better visualization of the chronology of events, the timeline of the CK and AM experiments is included as **Supplementary Figures 1A,B**, respectively.

Assessment of AM Colonization in Plants

To evaluate the colonization of roots by the AM fungi, root systems were cleaned at harvest, and lateral roots from each plant were randomly selected. They were then cut into 3 cm-segments, and stained for AM structures with Indian ink (Vierheilig et al., 1998). Root segments were mounted onto microscope slides using 60% aqueous glycerol. The magnified intersections method (McGonigle et al., 1990) modified by MacColl (2017) was used to assess AM colonization, yielding estimates of the percentage of root length colonized by hyphae, arbuscules, and vesicles. Briefly, the modification consisted of assessing 105 intersections per slide (15 passes were made over seven roots). Each time an arbuscule or a vesicle was scored, a hypha was scored as well. Root sections were observed under a Zeiss Axiovision light microscope at a 200× magnification (20× objective; 10× ocular).

Treatment of Plants With Synthetic Compounds Modifying CK Status

To alter plant endogenous CK status, 7, 9, and 11 DAI, myc^+ and myc^- seedlings received several synthetic compounds (**Supplementary Table 1**). Because 6-day-old WT plants had reduced CK levels compared to the E151 mutant (Jones et al., 2015), the WT plants were treated with 0.1 μM 6-benzylaminopurine (BAP) or with 1 μM 2-chloro-6-(3-methoxyphenyl)-aminopurine (INCYDE; Zatloukal et al., 2008) to increase their CK levels. As well, E151 plants were treated with 10 μM 6-(2-hydroxy-3-methylbenzyl)-aminopurine (PI-55; Spíchal et al., 2009) to reduce their endogenous CK sensing and mimic the effect of CK deficiency. In addition, to confirm the role of PI-55 as a competitor for plant CK receptors, the E151 mutant was treated with either 1 μM BAP or with a mixture of PI-55 (5 mL of 10 μM) and BAP (5 mL of 1 μM). On each day of treatment, plants received at their crown 10 mL of the chemical aqueous solution [with a minimal concentration of the solvent DMSO for INCYDE and PI-55 (0.002 and 0.1%, respectively)].

CK Extraction, Purification, and Quantification by HPLC-(+ESI)-MS/MS

To assess whether the CK levels were altered by the synthetic compounds modifying the plant CK status, both myc^- and myc^+ plants were harvested 13 DAI. Throughout their life, these plants were provided only with water, i.e., they were never exposed to mineral nutrient fertilization. The roots were immediately separated from the shoots and carefully cleaned. For the aboveground plant tissue sampling, the entire leaf positioned on the fourth node was collected from each plant and approximately 0.1 g of fresh leaf tissue was freeze-dried. For the belowground plant tissue sampling, a total fresh weight of 0.2 g of root tissue per plant was sampled. For this, the fourth lateral root was detached and weighed; in the case when more root tissue was required, the lateral root positioned just below (in terms of vascular pole positioning) was also sampled.

Freeze-dried samples were homogenized in cold (−20°C) modified Bieleski No. 2 extraction buffer [$CH_3OH : H_2O : HCO_2H$ (15:4:1, v:v:v)] using a ball mill grinder and ZnO_2 beads (25 Hz, 2 min, 4°C, Retsch MM300, Haan, Germany). Internal standards were added to each sample to enable endogenous hormone quantification through isotope dilution. The following standards were added (10 ng of each): [$^2H_7$]BAP, [$^2H_7$]BAPR, [$^2H_5$]ZOG, [$^2H_7$]DHZOG, [$^2H_5$]ZROG, [$^2H_7$]DHZROG, [$^2H_6$]iP7G, [$^2H_5$]Z9G, [$^2H_5$]2MeSZ, [$^2H_6$]2MeSiP, [$^2H_5$]2MeSZR, [$^2H_6$]2MeSiPR, [$^2H_6$]iPR, [$^2H_5$]ZR, [$^2H_3$]DHZR, [$^2H_6$]iP, [$^2H_3$]DHZ, [$^2H_5$]Z, [$^2H_6$]iPRMP, [$^2H_6$]ZRMP, [$^2H_3$]DHZRMP (OlChemIm Ltd., Olomouc, Czechia). CK extraction and purification were carried out as described in Quesnelle and Emery (2007) and modified by Farrow and Emery (2012).

High-performance liquid chromatography-positive electrospray ionization tandem mass spectrometry [HPLC-(+ESI)-MS/MS] was conducted according to Farrow and Emery (2012). Briefly, samples were analyzed using a Shimadzu LC (Kyoto, Japan) connected to a 5500 QTrap triple quadrupole mass spectrometer (Sciex Applied Biosystem, Concord, ON, Canada) with a turbo V-spray ionization source. A 20 μL sample was injected onto a reverse phase C18 column (Kinetex 2.6u C18 100 A, 2.1 × 50 mm; Phenomenex, Torrance, CA, United States). The samples were analyzed in a positive-ion mode. All hormone fractions were eluted with component A: H_2O with 0.08% CH_3CO_2H and component B: CH_3CN with 0.08% CH_3CO_2H, at a flow rate of 0.4 mL min^{-1}. The CK fractions were eluted with a multistep gradient. Starting conditions were 5% B increasing linearly to 10% B over 2 min followed by an increase to 95% B over 6.5 min; 95% B was held constant for 1.5 min before returning to starting conditions for 5 min.

All data were analyzed with Analyst 1.5.1 software (AB SCIEX, Concord, ON, Canada). CK types were identified based on their multiple reaction monitoring channels and retention times. CK levels were determined according to isotope dilution analysis via direct comparison of the endogenous analyte peak area to that of the recovered internal standard. The analysis of *cis*Z types was done relative to both the recovery of labeled *trans*Z types and the retention time of unlabeled *cis*Z CKs (Farrow and Emery, 2012).

Treatment of the AM Fungus With Synthetic CK-Related Compounds Using *in vitro* Root Organ Culture

To understand whether the synthetic CK status-modifying compounds can have direct effects on the growth of the AM fungus, we used *in vitro* bi-compartmented Petri plates containing root organ cultures in one of the compartments (referred to hereafter as the root compartment). The root compartment was filled with MSR medium (Declerck et al., 1998; using Phytagel™ instead of Bacto™ agar as gelling agent). The opposite compartment (hereafter referred to as the HC) was filled with a modified MSR medium, which did not contain sucrose and vitamins (the absence of sucrose and vitamins minimizes potential invasion of HC by roots). Fresh fragments of host roots, i.e., transformed carrot roots, were placed into each root compartment, and inoculated with approximately 400 spores accompanied by hyphal fragments of *R. irregularis* MUCL 41833. All plates were incubated in the dark at 27°C. The plates were checked regularly, and any root tips attempting to cross the compartment barrier were trimmed and removed. In contrast, the AM fungus was allowed to migrate and grow into the HC. Because of the variability between plates of the initial time at which hyphae would invade the HC, the fungus was first left to proliferate in this compartment. Then, the medium in the HC of each plate was removed with a sterile spatula, and the HC was re-filled with the modified MSR medium, this time enriched with 10 μM of either INCYDE, PI-55, or BAP in DMSO solution (0.1%), or with a DMSO solution as a negative control. Each solution had been previously sterilized through a syringe filter (0.2 μm). Afterward, the AM fungus was allowed to regrow into the HC in the presence of the synthetic CK status-modifying compounds or DMSO. We focused on the fungal regrowth to assure that the hyphae in the HC had a similar starting point between plates, and importantly, were exposed to the different synthetic compounds for a similar period. After 35 days of fungal regrowth, the hyphal length density in the HC was determined using the grid-line intersect method (Giovannetti and Mosse, 1980) adapted to determine hyphal length.

Statistical Analysis

Mean values and standard errors were generated for all data sets and were subjected to different statistical tests depending on the data. Student's *t*-test (or Mann-Whitney *U*-test in the event of non-normally distributed data) was used to compare: (1) the fungal colonization of WT and E151 roots at different developmental stages; and (2) the CK levels of myc^+ and myc^- pea lines treated with the same synthetic CK status-modifying compound. A one-way analysis of variance (ANOVA) test was used to compare: (a) the *in vitro* hyphal length density treated or not with CK status-modifying compounds; (b) the CK levels measured in both WT and E151 plants with a similar mycorrhizal status; and (c) E151 plants treated or not with CK status-modifying compounds. Each ANOVA was followed by Duncan's *post hoc* test for (a and b), and a Tukey's HSD *post hoc* test for (c). To compare the fungal colonization of WT plants treated or not with CK status-modifying compounds, a Kruskal–Wallis test was used followed by a multiple comparison test. Finally, a linear regression was performed to determine whether the levels of putatively active CKs (PACKs; equaled to the sum of the RB and FB levels) is a significant predictor of fungal colonization. All tests were conducted using R Studio (R Core Team, 2017).

RESULTS

E151 Delays Fungal Entry but Accelerates Intraradical Fungal Development

There were obvious qualitative (**Figure 2**) and quantitative (**Figure 3**) differences between the two pea lines throughout the development of the AM association. Five DAI, there were no clear signs of fungal presence on the roots of either pea line. The earliest visible interaction between *R. irregularis* and the pea plants occurred 10 DAI (**Figures 2A,B**). At this time, extraradical hyphae ran along the root surface, but did not appear to penetrate the roots. Quantitatively, only half of the sampled WT roots were colonized at 10 DAI, and each colonization unit [i.e., infection unit as per Franson and Bethlenfalvay (1989)] had on average two hyphopodia. There were neither visible hyphopodia nor colonization units on the roots of the E151 mutant line at that time. At 15 DAI, hyphopodia had formed on both pea lines (**Figures 2C,D**); there were 3.6 ± 0.83 and 2.88 ± 0.73 hyphopodia per colonization unit on the WT and E151 plants, respectively. Although this difference in hyphopodia numbers between lines was not significant, it was associated with a significant increase (Student's *t*-test; $P \leq 0.05$) in the percentage of root length colonized by the AM fungus in the WT plants, compared with that of the E151 plants (**Figures 3A,C,E**). At 20 DAI and later, an obvious shift in AM fungal colonization was observed, with the root cortex of E151 plants being more colonized than that of WT plants (**Figures 2E–H**). This qualitative increase in fungal colonization of the root cortex at 20 DAI in E151, compared with that of its WT, was quantitatively significant (Student's *t*-test; $P \leq 0.05$) for all measured fungal structures (**Figures 3B,D,F**). In a later stage of fungal colonization, i.e., at 25 DAI, mycorrhizal levels tended to be higher in E151 than in WT, but the difference was not significant (data not shown). Overall, fungal entry into the roots appeared to be delayed in E151. However, once the fungus was established in the cortex of E151, its intraradical proliferation was accelerated in terms of hyphal growth as well as of fungal differentiation into arbuscules and vesicles, when compared with that of the WT.

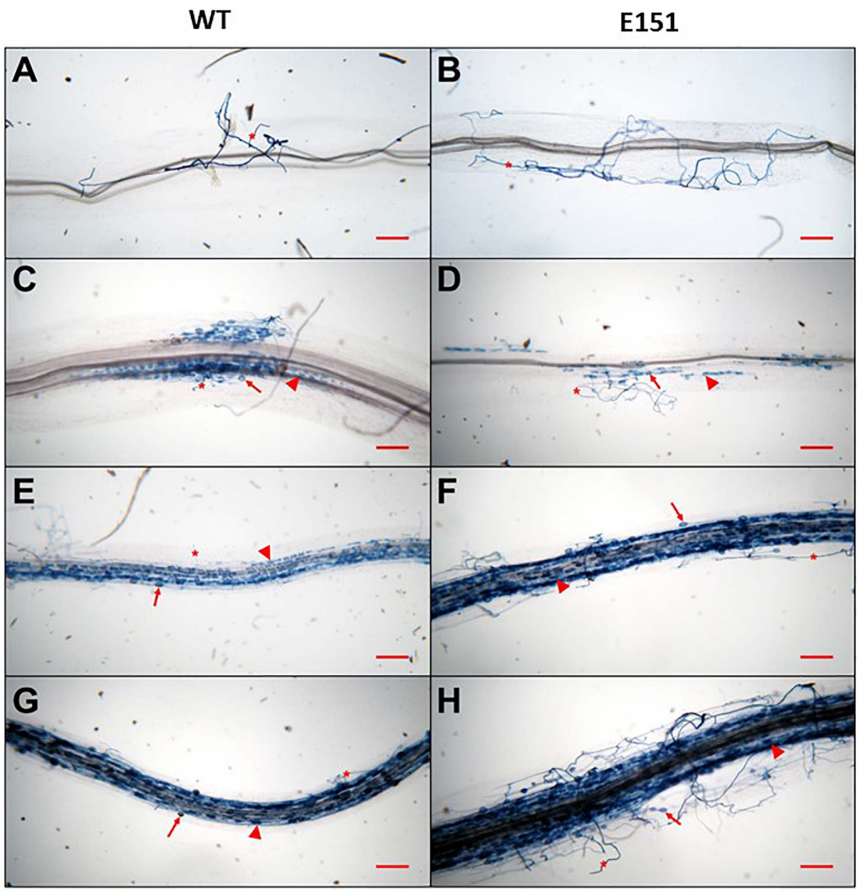

FIGURE 2 | Development of arbuscular mycorrhizae resulting from the association formed between *Rhizophagus irregularis* and pea plants. WT **(A,C,E,G)** and the mutant E151 **(B,D,F,H)** were compared at different time points. At 10 DAI **(A,B)**, extra-radicular hyphae (asterisks) were seen on the root surface of both pea lines. Root entry and subsequent internal colonization of the fungus were first observed at 15 DAI **(C,D)**, at which point fungal colonization in WT appears to be more extensive than in E151. At 15 DAI, arbuscules (arrowheads) and vesicles (arrows) were already formed. At 20 DAI **(E,F)** and 25 DAI **(G,H)**, E151 roots exhibited many more fungal structures than WT roots. Bars = 250 μm.

Mycorrhizal WT Plants Exhibit Reduced Endogenous CK Nucleotide Levels at 13 DAI While E151 Plants Do Not

To understand how the AM fungus affected the CK profiles of WT and E151 pea plants, we measured the CK levels in shoots and roots of both myc$^-$ and myc$^+$ plants at 13 DAI. The mycorrhizal status (myc$^-$ and myc$^+$) of the plants was confirmed at harvest by assessing fungal colonization (absence/presence, respectively).

Although no obvious differences were detectable in the total CK levels between myc$^-$ WT and myc$^-$ E151 plants in either shoots or roots (**Table 1**), the response of E151 differed markedly from its WT counterpart in terms of the fluctuations observed in the NT levels following AM colonization (**Figure 4**). Whereas the levels of the NT fraction in WT plants were reduced significantly (Student's *t*-test; $P \leq 0.05$) in both shoots (**Figure 4A**) and roots (**Figure 4B**) in response to the AM fungus, the levels of the NT fraction in both shoots and roots of E151 plants remained mostly unaltered. Among all NT compounds detected, i.e., *trans*ZNT, *cis*ZNT and iPNT, the most abundant form in the shoots of WT and E151 plants was iPNT (**Table 2**). In WT shoots, iPNT levels were significantly reduced (Student's *t*-test; $P \leq 0.05$) following AM colonization, while the levels of *trans*ZNT and *cis*ZNT were moderately reduced (**Table 2**). In contrast, in the roots of WT and E151, the levels of iPNT were below the detection limit, while the most abundant NT compound was *cis*ZNT (**Table 3**). After colonization, the levels of *cis*ZNT were significantly reduced (Student's *t*-test; $P \leq 0.05$) in WT roots, while the levels of *trans*ZNT remained almost unaltered (**Table 3**). The levels of NT in roots of E151 decreased slightly following colonization; however, the observed changes were not significant.

The AM fungus did not significantly affect the other CK fractions in either the WT or the E151 mutant (**Tables 2**, **3**), except for the O-glucosides in the roots of E151. Among the O-glucosides measured in the roots (**Table 3**), the levels of *trans*ZROG were below detection limit, while those of *cis*ZROG were detected in low amounts and revealed a significant reduction (Student's *t*-test; $P \leq 0.05$) in myc$^+$ E151 roots,

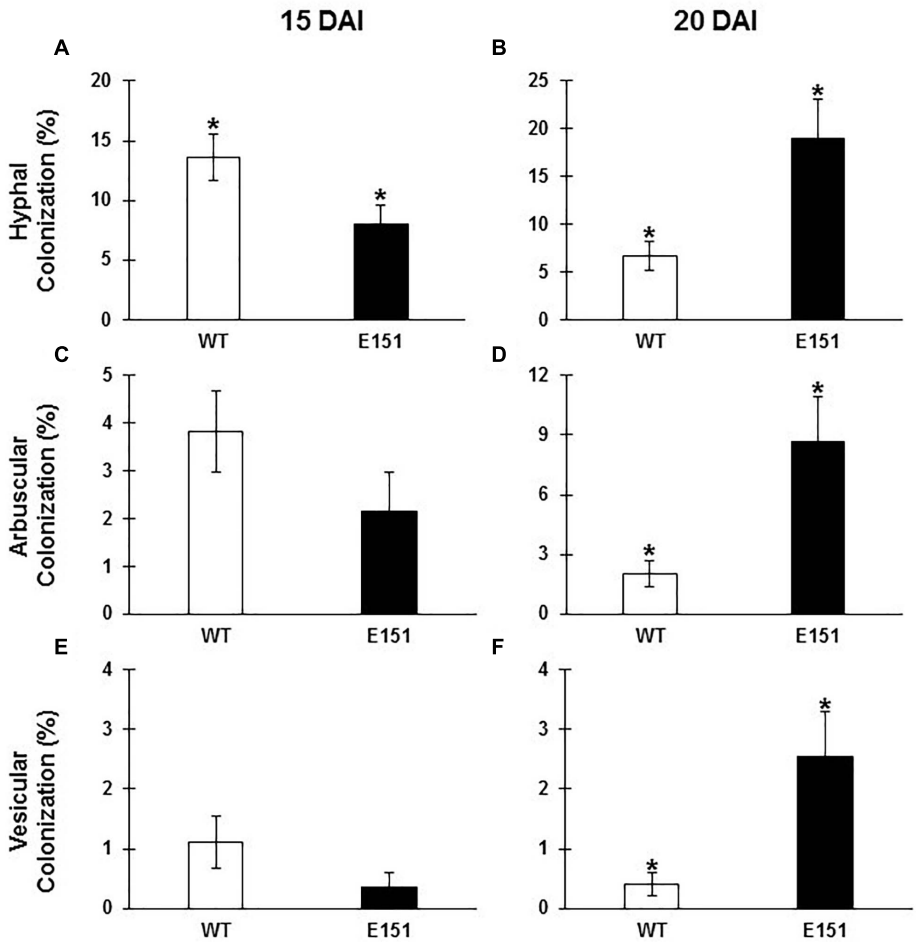

FIGURE 3 | Percent of WT (empty bars) and E151 (solid bars) roots colonized by *R. irregularis*, as determined by assessing percentages of intraradicular hyphae **(A,B)**, arbuscules **(C,D)**, and vesicles **(E,F)** observed at 15 **(A,C,E)** and 20 **(B,D,F)** DAI. These data (mean ± SE; n = 5 or 6) are the result of one replicate and are the best representative of three replicates; they were subjected to Student's t-test to determine significant differences between pea lines. An asterisk indicates significance at a 95% confidence level.

compared with that of myc$^-$ E151 roots. Overall, the colonization by the AM fungus most evidently reduced the endogenous levels of NTs, an inactive form of CKs, in WT plants but did not affect those of E151 plants.

CK Promotes the Intraradical Growth of *R. irregularis* but Not the Extraradical Growth

Levels of Endogenous CK Can Be Manipulated Pharmacologically in Pea

The effect of the synthetic CK status-modifying compounds on the total CK content of pea plants depended on the organ and the mycorrhizal status of the plant (**Table 1**). Whereas BAP and INCYDE did not have a significant effect on the total CK levels of the shoots of either myc$^-$ or myc$^+$ WT plants, the INCYDE treatment significantly reduced (Duncan's *post hoc* test; $P \leq 0.05$) the total CK levels of the roots of myc$^-$ WT plants. PI-55 treatment tended to decrease CK levels independently of plant organ or fungal presence. This compound had the strongest impact on the total CK content of myc$^+$ E151 shoots (**Table 1**) as it significantly reduced their levels (Duncan's *post hoc* test; $P \leq 0.05$). To better understand how these compounds affected the plant CK homeostasis, we compared below the changes observed in different CK fractions (NT, RB, and FB).

In the shoots and roots of myc$^-$ WT plants, NT levels (**Tables 2**, **3**, respectively; **Figure 5A**) decreased in plants treated with either BAP or INCYDE; specifically, the *cis*ZNT levels were reduced by half or more in the two organs, but the decrease was significant only in the roots (Duncan's *post hoc* test; $P \leq 0.05$). Moreover, while the levels of the RBs and FBs tended to increase in the shoots (**Table 2** and **Figure 5B**), they were not affected in the roots of myc$^-$ WT plants (**Table 3**). The NT and RB levels in the shoots of myc$^+$ WT plants were affected by the INCYDE treatment in a manner similar to those of shoots in the myc$^-$ WT plants (**Figures 5A,B** and **Table 2**), but the effect caused by BAP on the myc$^+$ plants was not as clear-cut as that of INCYDE (**Figure 5**). As for the myc$^+$ roots of INCYDE- or BAP-treated

TABLE 1 | Levels [pmol g^{-1} of fresh weight (FW)] of total CK isolated from shoots and roots of non-mycorrhizal (myc^-) and mycorrhizal (myc^+) pea plants.

Treatment	Total CK level (pmol g^{-1}FW)			
	Shoots		Roots	
	myc^-	myc^+	myc^-	myc^+
WT control	1028.31 ± 244.18[a]	915.61 ± 81.29[a]	24.40 ± 3.30[a]*	8.74 ± 1.00[a]*
WT + BAP	1074.14 ± 59.72[a]	932.95 ± 37.15[a]	14.59 ± 3.53[ab]	13.08 ± 2.60[a]
WT + INCYDE	1204.05 ± 232.30[a]	1208.59 ± 61.30[a]	11.34 ± 2.98[b]	11.06 ± 3.24[a]
E151 control	847.79 ± 50.05[ab]	1019.19 ± 190.30[a]	14.93 ± 3.20[ab]	11.26 ± 1.62[a]
E151 + PI-55	492.15 ± 52.22[b]	522.12 ± 97.58[b]	11.40 ± 2.23[b]	8.89 ± 0.80[a]

CK content was measured in wild type (WT) plants, in WT plants treated with BAP and INCYDE, in the pea mutant E151, and in E151 plants treated with PI-55. Values are means ± SE (n = 3). Different letters indicate a significant difference between treatments (one-way ANOVA followed by a Duncan's post hoc test, 95% confidence level). An asterisk indicates a significant difference between the same treatments of differing mycorrhizal status (Student's t-test, 95% confidence level).

WT plants, no significant differences were seen when compared to non-treated WT plants, and no obvious trends were seen in the specific CK fractions (**Table 3**).

Treatment of myc^- E151 plants with PI-55 resulted in a noticeable, though non-significant, increase of the shoot NT levels (**Figure 5A**) and a clear, yet non-significant, decrease of the levels of RBs (**Figure 5B**) and FBs (**Table 2**). In the roots of treated myc^- E151 plants, the results of all CK fractions tended to decrease (**Table 3**). Myc^+ E151 plants responded to the PI-55 treatment differently from myc^- E151 plants. In the presence of PI-55, NT levels (**Figure 5A**) tended to decrease in the shoots of myc^+ E151 plants compared to those of untreated plants. Moreover, the RB levels (**Figure 5B**) were significantly reduced (Duncan's *post hoc* test; $P \leq 0.05$), likely because of a significant reduction in the iPR fraction (**Table 2**). As well, the FB levels tended to decrease in the shoots of myc^+ E151 plants treated with PI-55 (**Table 2**). The levels of all CK fractions either did not change or tended to slightly decrease in the myc^+ roots of PI-55-treated E151 plants (**Table 3**).

In the shoots of both myc^- pea lines, the levels of the O-glucoside and methyl-thiol CK fractions, especially their RB conjugates, followed patterns similar to those seen in the RB and FB fractions (**Table 2**), i.e., they tended to increase in BAP- or INCYDE-treated WT plants and to decrease in PI-55-treated E151 plants. Overall, whereas the effects of BAP and INCYDE treatments on the WT plants were not strongly altered by the presence of the fungus, the effect of PI-55 on the mutant was exacerbated because E151-treated myc^+ plants exhibited a significant reduction in shoot NT levels compared to the myc^- plants (Student's *t*-test, $P \leq 0.05$).

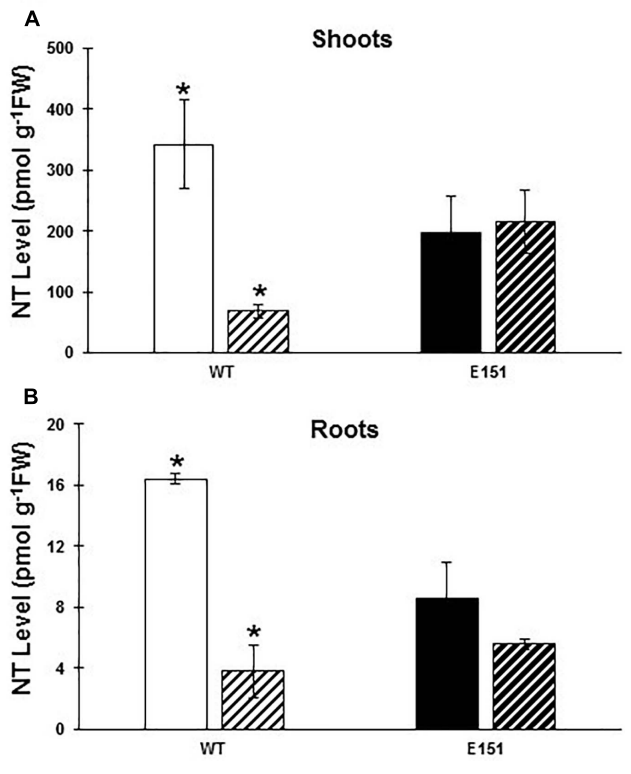

FIGURE 4 | Levels [pmol g^{-1} of fresh weight (FW)] of nucleotides (NT; *trans*ZNT, *cis*ZNT, and iPNT) in the shoots **(A)** and the roots **(B)** of WT (white bars) and E151 (black bars) plants. Plants inoculated with *R. irregularis* (bars with hatched lines) or non-inoculated (solid bars) were harvested 13 days after planting. Data (mean ± SE; $n = 3$) were subjected to a Student's *t*-test to determine significant differences between myc^- and myc^+ plants. An asterisk indicates significance at a 95% confidence level.

Endogenous CKs Affect Mycorrhizal Colonization of Plants

Altering the endogenous CK levels of the host plants via pharmacological treatments had a significant effect on the intraradicular growth of the AM fungus. When RB and FB levels tended to increase in the WT at 13 DAI, e.g., with INCYDE (**Figure 5B**), the percentages of root cortex length colonized by hyphae, arbuscules, and vesicles were significantly increased at 28 DAI (multiple comparison test; $P \leq 0.05$; **Figures 6A–C**). Moreover, decreasing the RB levels of the mutant E151 by interfering with CK perception via PI-55 treatment (**Figure 5B**) led to significant reductions (Tukey's *post hoc* test; $P \leq 0.05$) in AM fungal colonization of the roots (**Figures 6D–F**). When the E151 plants were treated with a mixture of BAP and PI-55, the percentages of root length colonized by the AM fungus were intermediate between those obtained with the application of

TABLE 2 | Levels [pmol g^{-1} of FW] of CK isolated from shoots of non-mycorrhizal (myc$^-$) and mycorrhizal (myc$^+$) pea plants.

Pea line + Treatment	Cytokinin level [pmol g^{-1}FW]							
	Free bases (FB)	Ribosides (RB)				Nucleotides (NT)		
	iP	DHZR	transZR	cisZR	iPR	transZNT	cisZNT	iPNT
				myc$^-$				
WT control	5.30 ± 0.78^{ab}	2.81 ± 0.42^{ab}	0.70 ± 0.29^{a}	172.16 ± 54.38^{ab}	211.55 ± 44.14^{ab}	1.01 ± 0.05	42.93 ± 13.67	298.47 ± 45.58^{a}*
WT+BAP	9.44 ± 0.21^{b}	3.10 ± 0.04^{ab}	1.91 ± 0.16^{b}	178.64 ± 12.08^{ab}	303.89 ± 22.34^{b}	0.82 ± 0.07	16.75 ± 1.13*	165.00 ± 18.31^{ab}
WT+INCYDE	8.07 ± 1.03^{b}	3.39 ± 0.33^{a}	1.58 ± 0.14^{bc}	215.74 ± 10.03^{a}	317.62 ± 28.39^{b}	0.80 ± 0.01	13.79 ± 3.90	129.42 ± 44.34^{b}
E151 control	5.89 ± 1.94^{ab}	2.27 ± 0.59^{ab}	1.18 ± 0.18^{abc}	122.41 ± 38.39^{ab}	201.35 ± 77.09^{ab}	1.43 ± 0.38	26.91 ± 8.84	170.14 ± 38.88^{ab}
E151+PI-55	1.68 ± 0.33^{a}	1.72 ± 0.01^{b}	1.09 ± 0.07^{ac}	60.09 ± 9.62^{b}	54.70 ± 15.28^{a}	1.22 ± 0.15	45.29 ± 11.89	241.53 ± 23.21^{ab}*
				myc$^+$				
WT control	7.05 ± 1.31^{ab}	2.64 ± 0.10	1.37 ± 0.12^{ab}	149.63 ± 19.27^{ab}	269.24 ± 25.47^{b}	0.89 ± 0.24	8.24 ± 0.32	60.04 ± 9.34^{b}*
WT+BAP	7.62 ± 1.96^{ab}	2.51 ± 0.30	1.32 ± 0.31^{ab}	147.36 ± 33.61^{ab}	238.83 ± 35.37^{b}	0.72 ± 0.06	8.43 ± 0.92*	136.77 ± 27.12^{ab}
WT+INCYDE	9.71 ± 0.37^{a}	2.06 ± 0.61	1.97 ± 0.31^{a}	176.79 ± 16.25^{a}	340.07 ± 9.29^{b}	0.70 ± 0.19	5.09 ± 1.00	45.66 ± 8.82^{b}
E151 control	6.24 ± 1.40^{ab}	2.16 ± 0.19	1.33 ± 0.18^{ab}	148.92 ± 15.16^{ab}	265.36 ± 32.44^{b}	1.01 ± 0.15	16.03 ± 5.64	198.65 ± 42.32^{a}
E151+PI-55	3.20 ± 0.80^{b}	1.46 ± 0.12	0.97 ± 0.25^{b}	80.21 ± 8.19^{b}	117.90 ± 24.79^{a}	1.27 ± 0.07	13.34 ± 2.65	129.62 ± 10.63^{ab}*

	Cytokinin level [pmol g^{-1}FW]			
	O- Glucosides (OG)		Methyl-thiols (MeS)	
	transZROG	cisZROG	MeSZ	MeSZR
		myc$^-$		
WT control	1.79 ± 0.26^{ab}	16.83 ± 3.44^{bc}	24.59 ± 7.92	250.15 ± 50.96^{ab}
WT+BAP	2.09 ± 0.27^{ab}	33.78 ± 1.23^{a}*	25.89 ± 2.17	332.82 ± 12.54^{b}
WT+INCYDE	2.28 ± 0.24^{a}	32.16 ± 5.53^{ac}	25.29 ± 1.78*	453.93 ± 50.42^{b}
E151 control	1.51 ± 0.48^{ab}	16.70 ± 5.76^{bc}	24.19 ± 6.11	273.80 ± 106.16^{ab}
E151+PI-55	0.88 ± 0.15^{b}	5.39 ± 1.64^{b}	13.29 ± 4.27	65.27 ± 8.96^{a}
		myc$^+$		
WT control	1.73 ± 0.18^{b}	23.33 ± 1.82	24.31 ± 3.32^{b}	367.13 ± 33.96^{b}
WT+BAP	1.65 ± 0.17^{ab}	22.12 ± 0.69*	24.78 ± 3.76^{b}	340.84 ± 75.54^{b}
WT+INCYDE	2.13 ± 0.23^{b}	22.33 ± 3.04	39.88 ± 3.68^{a}*	562.21 ± 2.96^{a}
E151 control	1.82 ± 0.21^{b}	21.11 ± 4.33	23.02 ± 3.65^{b}	333.54 ± 39.67^{b}
E151+PI-55	0.96 ± 0.13^{a}	13.79 ± 3.29	11.88 ± 2.19^{b}	147.51 ± 35.98^{c}

CK content was measured in wild type (WT) plants and the pea mutant E151, in WT plants treated with BAP and INCYDE, and in E151 plants treated with PI-55. For CK, Z, DHZ and iP designate zeatin, dihydrozeatin and isopentenyl adenine, respectively. Values are means ± SE (n = 3). Different letters indicate a significant difference between treatments (one-way ANOVA followed by a Duncan's post hoc test, 95% confidence level). An asterisk indicates a significant difference between the same treatments of differing mycorrhizal status (Student's t-test, 95% confidence level).

either BAP or PI-55 alone, i.e., those for the intraradical hyphae and arbuscules were significantly lower than the percentages in E151 plants treated only with BAP and significantly higher (Tukey's *post hoc* test; $P \leq 0.05$) than the percentages in E151 plants treated only with PI-55 (**Figures 6D–F**).

Finally, we tested whether a correlation occurred between AM colonization and PACK levels. We plotted in a single graph the percentages of AM fungal colonization (dependent variable) against PACK levels (independent variable) measured in non-treated WT and E151 plants as well as WT and E151 plants exposed to INCYDE and PI-55, respectively, because both of these treatments were the most effective in altering AM colonization. We did not take into consideration the pea lines or the different times of harvest but considered each treatment identity as a single data-point (**Figure 7**); as such, we subjected the data to a regression analysis. Although not significant, we observed a positive relationship between the percentages of root length colonized by AM fungal hyphae and the levels of PACK (**Figure 7**; R^2 = 0.82). Likewise, the percentage of root length colonized by the arbuscules and vesicles had an apparent positive relation with the levels of PACK, with R^2 values of 0.80 and 0.66, respectively (**Figure 7**).

Synthetic CK Status-Modifying Compounds Have No Effect on the Extraradical Hyphal Growth

To determine whether the synthetic CK status-modifying compounds could directly affect the development of AM fungus, we applied BAP, INCYDE, PI-55, or a DMSO mock solution to the HC of *in vitro* bi-compartmented Petri plates, in which the extraradical hyphae of *R. irregularis* were allowed to grow

TABLE 3 | Levels [pmol g^{-1} of FW] of CK isolated from roots of non-mycorrhizal (myc^-) and mycorrhizal (myc^+) pea plants.

Pea line +	Cytokinin level [pmol g^{-1}FW]											
Treatment	Free bases (FB)		Ribosides (RB)			Nucleotides (NT)			O-Glucosides (OG)		Methyl-thiols (MeS)	
	iP	DZR	transZR	cisZR	iPR	transZNT	cisZNT	iPNT	transZROG	cisZROG	MeSZ	MeSZR
						myc^-						
WT control	0.26 ± 0.02	0.34 ± 0.10	0.46 ± 0.12	4.57 ± 1.40^{a}	n.d.	0.61 ± 0.03^{a}	15.82 ± 1.43^{a*}	n.d.	n.d.	2.35 ± 0.19	n.d.	n.d.
WT+BAP	0.17 ± 0.00	0.22 ± 0.03	0.18 ± 0.03*	2.40 ± 0.59^{ab}	n.d.	0.41 ± 0.08^{ab}	8.84 ± 2.02^{b}	n.d.	n.d.	2.37 ± 0.21	n.d.	n.d.
WT+INCYDE	0.20 ± 0.02	0.29 ± 0.03	0.30 ± 0.05	1.67 ± 0.48^{ab}	n.d.	0.35 ± 0.03^{b*}	5.81 ± 2.21^{b}	n.d.	n.d.	2.72 ± 0.29	n.d.	n.d.
E151 control	0.24 ± 0.02	0.45 ± 0.11	0.31 ± 0.06	1.83 ± 0.41^{ab}	n.d.	0.49 ± 0.07^{ab}	8.14 ± 1.92^{b}	n.d.	n.d.	3.46 ± 0.33*	n.d.	n.d.
E151+PI-55	0.22 ± 0.05	0.52 ± 0.06	0.26 ± 0.05	1.11 ± 0.36^{b}	n.d.	0.44 ± 0.05^{ab}	5.96 ± 1.67^{b}	n.d.	n.d.	2.90 ± 0.38	n.d.	n.d.
						myc^+						
WT control	0.28 ± 0.05	0.28 ± 0.04	0.55 ± 0.15^{b}	2.28 ± 0.54	n.d.	0.54 ± 0.10	3.27 ± 0.29*	n.d.	n.d.	1.55 ± 0.18	n.d.	n.d.
WT+BAP	0.20 ± 0.06	0.32 ± 0.02	0.62 ± 0.06^{b*}	2.73 ± 0.11	0.27 ± 0.12	0.56 ± 0.10	6.54 ± 1.44	n.d.	n.d.	1.84 ± 0.05	n.d.	n.d.
WT+INCYDE	0.19 ± 0.03	0.27 ± 0.05	0.36 ± 0.05^{ab}	2.51 ± 0.70	n.d.	0.59 ± 0.03*	5.40 ± 1.47	n.d.	n.d.	1.73 ± 0.16	n.d.	n.d.
E151 control	0.16 ± 0.03	0.43 ± 0.03	0.41 ± 0.07^{ab}	2.38 ± 0.78	0.41 ± 0.34	0.72 ± 0.13	4.87 ± 1.45	n.d.	n.d.	1.88 ± 0.24*	n.d.	n.d.
E151+PI-55	0.20 ± 0.03	0.29 ± 0.04	0.21 ± 0.02^{a}	1.04 ± 0.23	n.d.	0.88 ± 0.13	4.65 ± 0.17	n.d.	n.d.	1.63 ± 0.17	n.d.	n.d.

CK content was measured in control plants of wild type (WT) and the pea mutant E151, in WT plants treated with BAP and INCYDE, and in E151 plants treated with PI-55. For CK, Z, DHZ and iP designate zeatin, dihydrozeatin and isopentenyl adenine, respectively. n.d.: not detectable. Values are means ± SE (n = 3). Different letters indicate a significant difference between treatments (one-way ANOVA followed by a Duncan's post hoc test, 95% confidence level). An asterisk indicates a significant difference between the same treatments of differing mycorrhizal status (Student's t-test, 95% confidence level).

for 35 days linked to, but separated from, the host roots. A non-significant, minor increase in hyphal length density was measured in the HC to which INCYDE or PI-55 had been added, when compared to that observed in the control HC. As for the hyphal length density in the HC supplemented with BAP, it was similar to that observed in the control HC. Thus, none of the treatments with the synthetic CK status-modifying compounds was able to affect significantly the extraradical fungal growth.

DISCUSSION

Most, and possibly all, plant hormones contribute to the fine-tuning of the development of AM symbiosis in plant roots, and as such they influence the fungal growth required for the exchange of benefits between the symbiotic partners. Amongst the many plant hormones, CKs have one of the least understood roles during AM development (e.g., Pozo et al., 2015; Bedini et al., 2018; Liao et al., 2018). Here, we provide evidence toward a stimulatory role for CKs in AM fungal colonization (**Figure 8**). On one hand, low levels of NT facilitate fungal entry into the roots; on the other hand, high levels of RBs and the most metabolically active FBs stimulate fungal proliferation within the root cortex. Our findings are strengthened by the use of a pharmacological approach whereby CK homeostasis is altered in myc^+ plants using different synthetic compounds (**Figure 8**). Increasing exogenous or endogenous CK levels leads to an increase in AM colonization whereas mimicking CK deficiency results in lower AM colonization.

Plant Endogenous CK Levels Are Affected by the Presence of the AM Fungi

It is a well-known fact that CK homeostasis is altered in response to AM fungal colonization (e.g., Allen et al., 1980; Baas and Kuiper, 1989; Danneberg et al., 1992; Drüge and Schönbeck, 1992; Goicoechea et al., 1995; van Rhijn et al., 1997; Shaul-Keinan et al., 2002). Among the many studies performed, two are of interest as the CK content was measured at different stages of AM development. While van Rhijn et al. (1997) measured CK in myc^+ alfalfa plants at 14, 16, and 18 DAI, Yurkov et al. (2017) determined CK content in *Medicago lupulina* at 1, 14, 21, 35, and 50 DAI. In both studies, CK levels were estimated by immunoassay, and thus their results are difficult to compare to ours. It is only recently that researchers have been using the HPLC-ESI MS/MS technique for a precise quantification of CKs and identification of their different forms in myc^+ plants. Schmidt et al. (2017) working on *Miscanthus* × *giganteus* and Adolfsson et al. (2017) studying *M. truncatula* used plants older than those used in our study (70 DAI and 28 DAI, respectively), and measured the leaf CK content of plants inoculated with *R. irregularis*. In both works, increases in PACK and glucosides (the latter representing CK storage forms) were reported in plants that were well colonized.

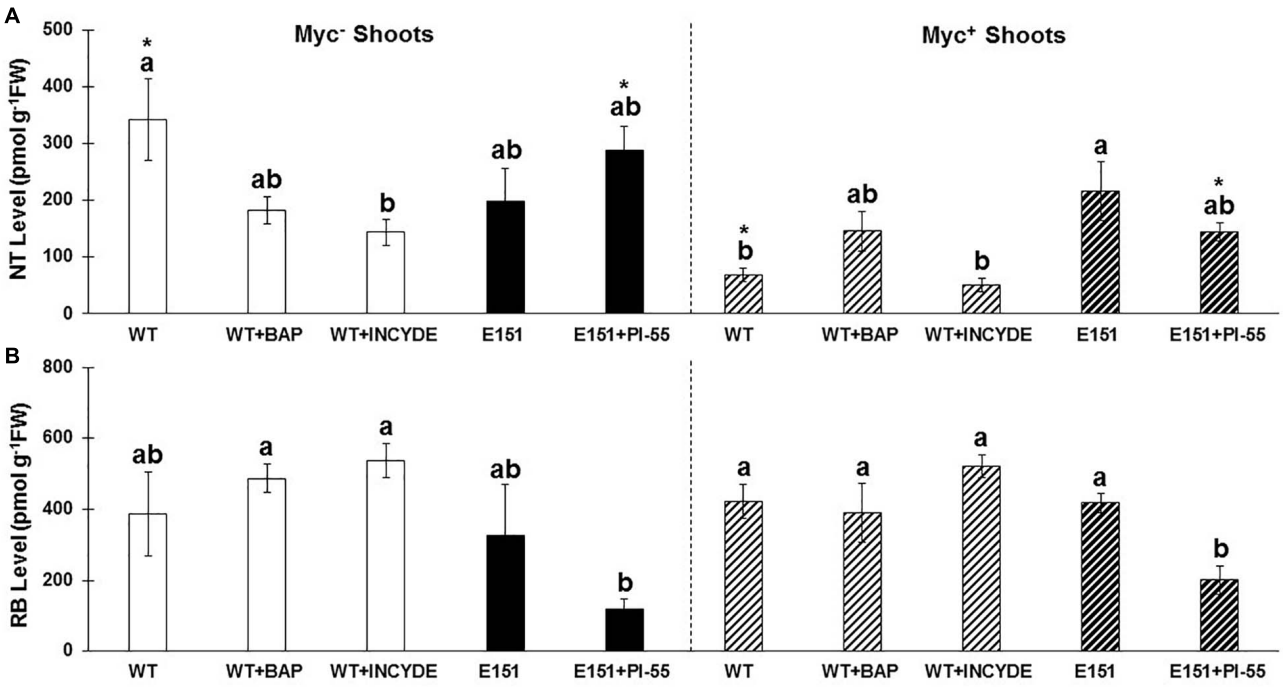

FIGURE 5 | Effects of chemical and mycorrhizal treatments on the levels (pmol g^{-1} of fresh weight) of **(A)** nucleotides (NT; *trans*ZNT, *cis*ZNT, and iPNT) and **(B)** ribosides (RB; DHZR, *trans*ZR, *cis*ZR, and iPR) in the shoots of WT (white bars) and E151 (black bars) plants, the crown of which had been treated with synthetic CK status-modifying compounds. These plants were myc^- (solid bars; on the left) or myc^+ (hatched bars; on the right). Data (mean ± SE; $n = 3$) were subjected to a one-way ANOVA followed by a Duncan's *post hoc* test (95% confidence level). Different letters indicate significant differences between different chemical treatments of a similar mycorrhizal status. Additionally, Student's *t*-tests (95% confidence level) were conducted to determine any significant differences, indicated by asterisks, between similar treatments of differing mycorrhizal status within a pea line.

To our knowledge, no study has ever reported a decrease in the NT fraction of myc^+ plants. This is not necessarily surprising since a high disparity exists among the performed studies. Differences in plants species and developmental stages, in fungal species, in growth conditions and in techniques are obvious. For example, in the two most recent studies (Adolfsson et al., 2017; Schmidt et al., 2017), the analytical methods used could not detect NT levels. Another explanation for the NT levels not being reported may be that the NT fraction is not metabolically active; however, any fluctuation in NT levels may indicate, albeit indirectly, changes occurring in the other CK fractions. Thus, high NT levels likely reflect a low turnover into active FBs or RBs, whereas low NT levels could suggest a high conversion into more metabolically active CK fractions (**Figure 1**).

In most of the previous works, CK levels were shown to be higher in myc^+ plants than in myc^- plants, and the RB fraction appeared to be the most sensitive to the fungal presence. This fraction was higher in roots (e.g., flax in Drüge and Schönbeck, 1992; tobacco in Ginzberg et al., 1998) and shoots (*M. lupulina* in Yurkov et al., 2017) of myc^+ plants. Furthermore, the changes observed depended on the infection rate (Drüge and Schönbeck, 1992) and the P levels to which the plants were exposed (*Plantago major* in Baas and Kuiper, 1989; leek in Torelli et al., 2000). RBs are considered the main form by which CKs are transported between roots and shoots (Ko et al., 2014; Zhang et al., 2014). In our study, we did not see any differences in the RB levels between myc^- and myc^+ plants and this may be because the CK profiles were analyzed early in the AM symbiosis, i.e., 13 DAI. This result is consistent with that of Dixon et al. (1988), who found that AM development increased RB transport from root to shoot in *Citrus jambhiri*, and that this effect was much weaker early in development (15-day-old) than later, with the strongest effect occurring in 90-day-old plants. It would be logical that RBs are transported in much higher quantities when nutrient exchange is well underway between the two partners of the symbiosis. An increase in CK translocation from the roots to the shoot could be part of the positive feedback thought to take place between AM functioning and shoot CKs (Cosme et al., 2016).

Pharmacological Treatments of Pea Crowns With Synthetic CK Status-Modifying Compounds Are Effective in Altering Plant CK Homeostasis

In myc^- WT plants subjected to either BAP or INCYDE, levels of the NT fraction tended to decrease and those of the PACK fraction to increase (**Figures 8A,D**). These changes were expected (Aremu et al., 2015) and likely reflect the perception by the treated plants of higher levels of CKs caused

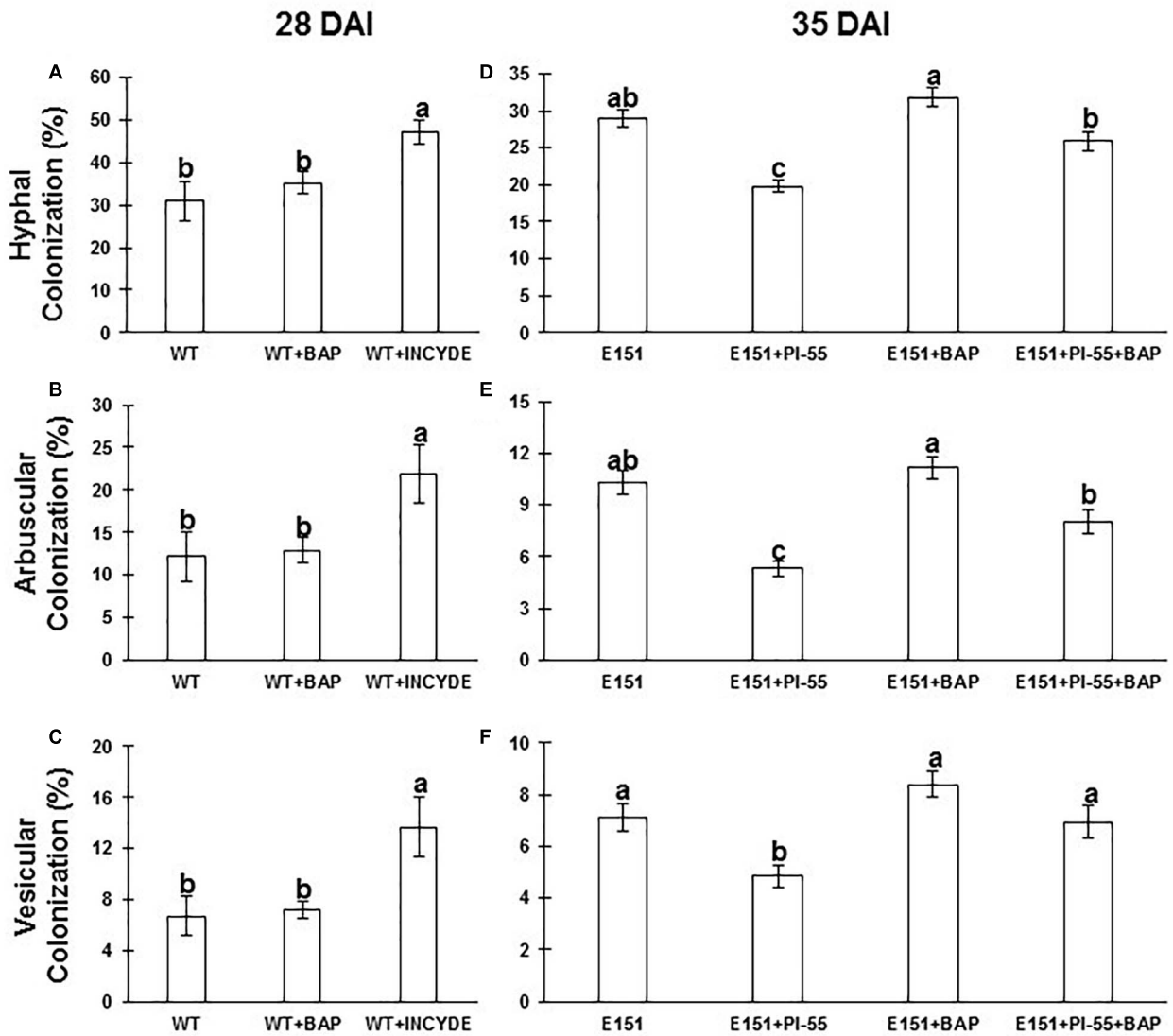

FIGURE 6 | Effect of synthetic CK status-modifying compounds on hyphal colonization **(A,D)**, arbuscular colonization **(B,E)**, and vesicular colonization **(C,F)** in the roots of WT **(A–C)** and E151 **(D–F)** plants inoculated with *R. irregularis*. Whereas WT plants were treated with BAP (0.1 μM) and INCYDE (1 μM), E151 plants were treated with PI-55 (10 μM), BAP (1 μM), and a combination of PI-55 and BAP. WT and E151 plants were harvested 28 and 35 days after inoculation (DAI), respectively. WT data (mean ± SE; n = 13, three technical replicates) and E151 data (mean ± SE; n = 15; three technical replicates) were either subjected to a one-way ANOVA followed by a Tukey's HSD *post hoc* test, or a Kruskal–Wallis followed by a multiple comparisons test; significance (95% confidence level) is indicated by different letters.

by either the exogenous application of BAP or the inhibition of cytokinin dehydrogenases (CKX). As a response to the increased endogenous PACK levels, plants likely down-regulate their CK biosynthesis, leading to a decrease of the CK precursor molecules, i.e., the NT fraction. In myc$^-$ E151 plants subjected to PI-55, a synthetic compound known to alter CK perception (Spíchal et al., 2009), the NT fraction tended to increase, whereas RB and FB fractions tended to decrease (**Figure 8C**). This suggests that, when PI-55 competes with active CK molecules for a CK receptor, a signal is conveyed to the mutant to down-regulate its CK synthesis because it perceives an abundance of CK active forms. Consequently, E151 would accumulate NTs that are not being further transformed. Interestingly, when *Eucomis autumnalis*, a species from the Asparagaceae family, was treated with 10 μM PI-55, no change in the NT levels was observed; however, when it was treated with 0.1 μM PI-55, a large increase in that fraction was noticed (Aremu et al., 2015). These differential effects highlight that responses may depend on the plant species and possibly growth conditions.

We were expecting that INCYDE and BAP would cause a similar outcome for the CK levels of the treated plants, namely that both compounds would increase the endogenous CK levels (**Supplementary Table 1**), yet there were differences. It is possible that BAP is not as biologically active as the naturally produced,

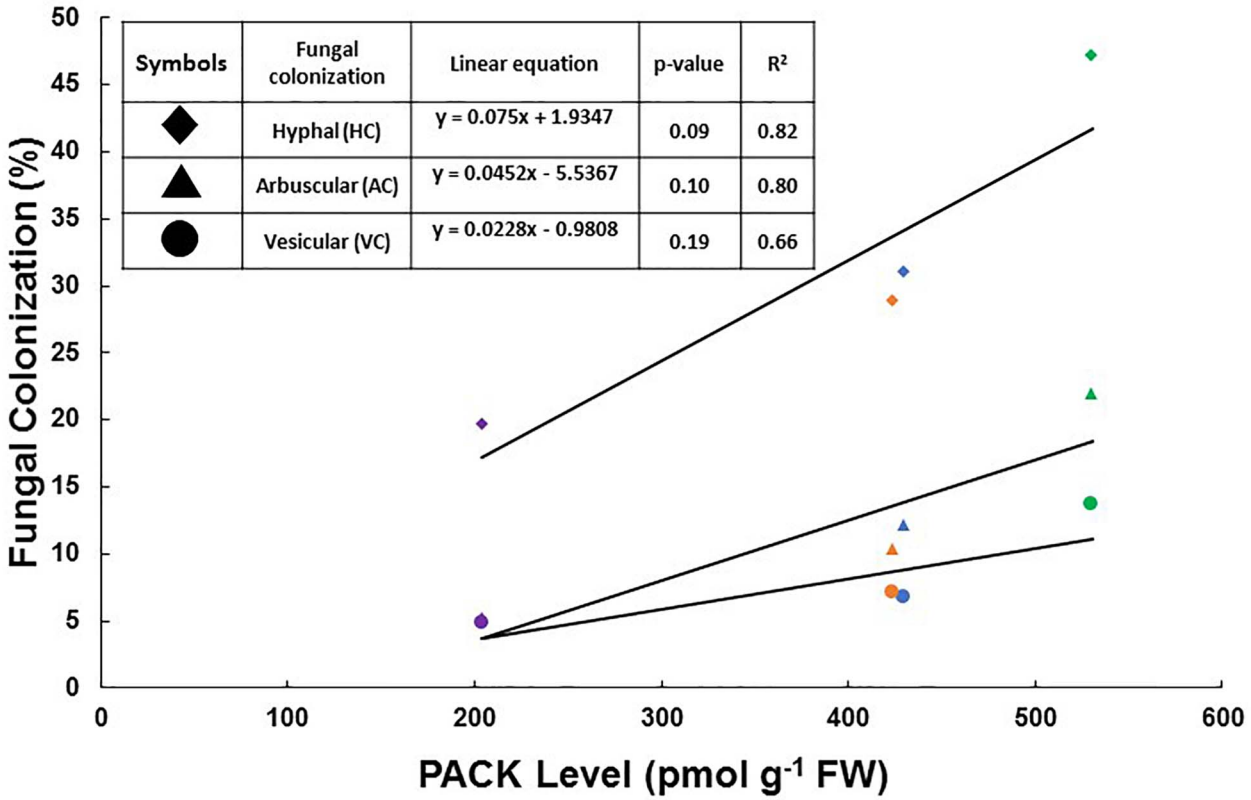

FIGURE 7 | Effect on fungal colonization (%) of the levels of putatively active CK (PACK; sum of riboside and free base fractions) measured in shoots of plants, the crowns of which had been subjected to treatments with synthetic CK status-modifying compounds. Each data-point corresponds to the mean of the fungal colonization assessed in the *R. irregularis*-inoculated plants. The symbols in purple represent the colonization seen in E151 roots treated with PI-55; those in orange represent the colonization seen in non-treated E151 roots. The symbols in blue represent the colonization assessed in non-treated WT roots, and those in green the colonization seen in WT roots treated with INCYDE. This graph is a composite graph created to decipher whether or not a relationship existed between AM fungal colonization and shoot levels of PACK. Whereas the PACK analysis was performed at 13 DAI, the assessment of fungal colonization was done at 28 DAI for WT and at 35 DAI for E151. A linear regression analysis was performed on the distribution of PACK and HC, AC, and VC; the resulting *p*-values and R^2 values are shown in a table, along with the linear equation for each fungal structure.

endogenous CKs, the levels of which increased with the INCYDE treatment. Alternately, these differences may be explained by the different fates that these two synthetic CK-related compounds have inside the plant. Whereas INCYDE would directly increase the endogenous CK pool because of the specific inhibition of its target CKX, BAP may be diverted from its site of entry to its site of action (Sakakibara, 2006) and be converted into inactive CK forms such as glucosides along the way. The action may thus be seen as "diluted" or off-target inside the plant (Sakakibara, 2006; Skalický et al., 2018).

CKs Play a Role in the Development of Mycorrhizae

High Levels of Active CKs, as Reflected by Low NT Levels, Are Required for Fungal Entry

At 13 DAI, the levels of the NT fraction in myc$^+$ WT plants, in both shoot and root, were significantly lower than those in myc$^-$ WT plants, and this drop occurred at a time of fungal entry into the roots (**Supplementary Figure 1**). In E151 myc$^+$ plants, there was no decrease in the NT fraction, and no fungal penetration in the roots was visible. However, treating the mutant with PI-55 led to reductions of both NT levels and AM colonization (**Figure 8C**). Thus, we hypothesize that, for the fungus to enter a root, it needs its host plant to have a low ratio of non-active CKs to active CKs (hereafter referred to as NT to PACK ratio). Inhibition of fungal entry in E151 is seen in the initial steps of the interaction, and also later in development as shown by Jones et al. (2015) who documented that the fungal hyphopodia were more numerous on E151 roots than on WT roots. These hyphopodia were largely abnormal and septate, which is an indication of retracted fungal cytoplasm and senescence (Glenn et al., 1985), suggesting that these hyphopodia were aborted.

If the plant accommodates fungal entry by lowering its NT to PACK ratio, especially in its roots, then fungal entry in E151 would have been impeded because that ratio did not decrease enough. At 6 DAI, Jones et al. (2015) noted a significant drop in the NT and PACK levels of E151 plants as a response to the fungal presence; yet this apparently did not

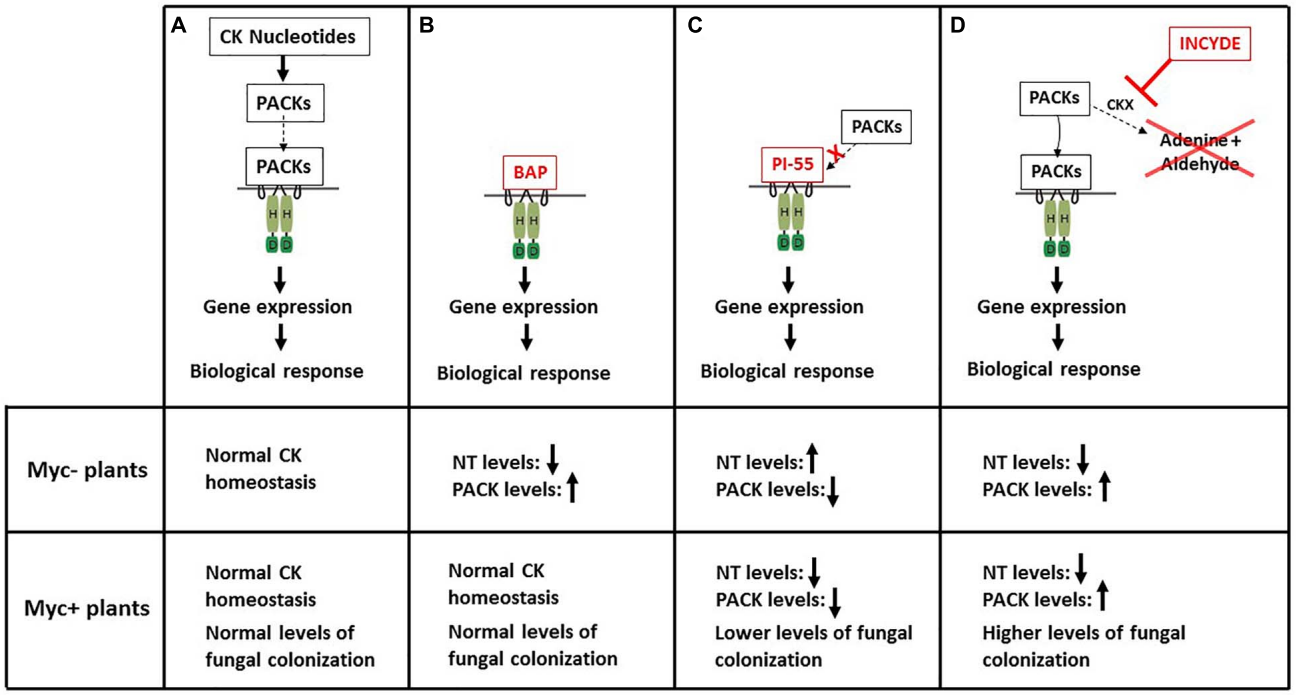

FIGURE 8 | Schematic diagram representing both the perception and the signal transduction pathway of CK in myc$^-$ and myc$^+$ plants that were either untreated **(A)**, treated with the cytokinin BAP **(B)**, the competitive inhibitor of CK action PI-55 **(C)**, or the inhibitor of CK degradation INCYDE **(D)**. Upon treatment with the synthetic compounds, levels of NTs and of putatively active CKs (PACKs, comprised of both CK ribosides and CK free bases) are altered. An arrow oriented upward corresponds to an increase in CK levels, whereas an arrow facing downward represents a decrease in CK levels. Higher PACK levels correspond to higher AM colonization whereas lower PACK levels are related to lower AM colonization.

lead to fungal entry. We propose that E151 may have overshot the levels optimal for fungal entry and take a longer time than WT to adjust its CK homeostasis. This may reflect an abnormal homeostatic control mechanism (Riefler et al., 2006) during E151 seedling establishment. Later in E151 development, when optimal CK levels are attained, i.e., when an optimal NT to PACK ratio is reached, the fungus would be allowed to enter. This adjustment in CK homeostasis may explain the delay seen in E151.

Active CKs Have a Stimulatory Effect on the Intraradicular Growth of the Fungus

Altering CK homeostasis by treating myc$^+$ pea plants with synthetic CK status-modifying compounds had a significant impact on the intraradicular growth of the fungus *R. irregularis*. When RB and FB levels increased in the shoots and the NT fraction decreased in the roots and shoots of myc$^+$ WT plants treated with INCYDE, the percentages of all fungal structures assessed in the root cortex were significantly higher (**Figure 8D**). The E151 response to PI-55 in terms of AM colonization confirmed this stimulatory effect. In the myc$^+$ mutant, interference with CK perception led to a decrease in all CK fractions, and this translated into a severe reduction of fungal growth within the root cortex (**Figure 8C**). When E151 myc$^+$ plants were treated with a mixture of BAP and PI-55 treatment, intermediate AM colonization was scored, demonstrating that PI-55 and BAP were competing for the CK receptors, and further substantiating the stimulating role of CKs in regulating AM development.

As the levels of PACKs increased (from the levels measured in PI-55-treated mutant, to levels measured in both the non-treated mutant and WT plants, to levels measured in INCYDE-treated WT), there was a simultaneous increase in the percentage of fungal colonization, and all three measured intraradicular fungal structures tended to respond positively to the PACK increase. Based on these data, we propose that active CKs have a stimulatory effect on the intraradicular growth of the fungus, and for higher growth rate of the fungus, the plant requires higher levels of PACKs in its shoots. The plant likely mediates the effects we observed on the intraradicular growth of the fungus because the extraradical fungal growth was not affected in a similar way by the synthetic CK status-modifying compounds. The promoting influence of the shoot CKs on the AM symbiosis that we uncovered fits the model of Cosme et al. (2016) which proposes that shoot CKs have a positive effect on AM colonization. In this model, CKs are thought to modulate carbon supply to the AM fungus through their influence on the plant photosynthetic ability (Cosme et al., 2016).

Our results seem also to agree with those obtained by Schmidt et al. (2017) who performed a pharmacological study of the effect of TDZ, a synthetic CK analog, on AM colonization in the perennial grass *Miscanthus* × *giganteus*. The application of TDZ was found to decrease root colonization by half. This CK analog is thought to be strongly recognized by CK receptors

and to prevent CK degradation. TDZ was found to increase the levels of conjugated CKs, but not those of FBs. Upon AM inoculation, the active CK forms were further decreased whereas the conjugated forms were further increased (Schmidt et al., 2017). The low levels of active CKs measured in the *Miscanthus* × *giganteus* grass likely prevented the AM fungi to proliferate intraradically.

An Active Role for CKs in the Establishment and Growth of AM Symbiosis Is Confirmed by the Use of the Competitive Inhibitor of CK Action PI-55

There are three known types of plant CK receptors (e.g., Spíchal, 2012; Lomin et al., 2018), represented by CRE1/AHK4, AHK2, and AHK3 in *Arabidopsis*. Each receptor differs in the CK forms it recognizes; thus, CRE1/AHK4 and AHK2 specifically bind FBs and their conjugates, while AHK3 was reported to bind active bases as well as RBs and NTs in a bacterial system (Spíchal et al., 2004). The three receptors likely differ in their functions because their expression is spatially distinct. Whereas CRE1/AHK4 is expressed predominantly in the root, AHK3 is mostly expressed in the shoot, likely sensing the RBs being translocated between roots and shoots (Spíchal, 2012).

In *Arabidopsis*, the synthetic compound PI-55 acts as a competitive inhibitor of CK action, blocking the binding of active CKs to CRE1/AHK4; however, it also interferes with AHK3 (Spíchal et al., 2009). These authors propose that the conformational change of the receptor required for the CK signal transduction pathway to be elicited cannot be triggered when PI-55 binds to it, resulting in a reduced CK status (Spíchal et al., 2009). In pea, PI-55 had been previously used to show CK-antagonizing effect (Long et al., 2012). In the present study, we further showed that PI-55 had a direct effect on CK homeostasis because treating the pea mutant E151 with PI-55 resulted in an increase in NT levels and a decrease in PACK levels, suggesting that the mutant responded to the fully occupied CK receptors by down-regulating its CK biosynthesis, and possibly triggering a feedback loop.

CRE1/AHK4, i.e., the receptor the most sensitive to PI-55 in Arabidopsis, and its orthologs are known to play a major role in controlling nodulation in legumes as was demonstrated in studies performed on the nodulation mutants of *M. truncatula* (*Mtcre1*; Gonzalez-Rizzo et al., 2006; Plet et al., 2011; Ariel et al., 2012), *Lotus japonicus* (*Ljlhk1*; Murray et al., 2007; Held et al., 2014), and *Lupinus albus* (*LaHK1*; Coba de la Peña et al., 2008). However, Laffont et al. (2015), who characterized the response of *Mtcre1* to the AM fungus *Gigaspora margarita*, concluded that CRE1/AHK4 did not play a role in AM colonization. There was no specific mycorrhizal phenotype ascribed to the mutant, and no alterations were observed in the expression of genes related to CK signaling and metabolism in response to the fungus (Laffont et al., 2015). Our results with PI-55 appear to disagree with those of Laffont et al. (2015). This may be related to the different plant and fungal species studied, as well as to the different techniques used to assess AM colonization. Alternatively, it may be because AHK3 is the receptor playing the most important role in AM symbiosis, with CRE1/AHK4 playing a secondary role. AHK3 has a genuine affinity for RBs and for *cis*Z (Romanov et al., 2006). It is likely to sense *cis*ZNT, a CK form significantly reduced in roots of WT and E151 upon AM colonization, because of a better *cis*Z recognition by AHK3 than by AHK4 (Romanov et al., 2006). The AHK3 receptor is also capable of recognizing PI-55 as a weak agonist (Spíchal et al., 2009), and in contrast to CRE1/AHK4, it recognizes free bases with side-chain modifications (Spíchal et al., 2004). Furthermore, AHK3 is expressed moderately in roots and highly in shoots (Higuchi et al., 2004). As we brought forward evidence that shoot CK levels reflect plant mycorrhizal status, the receptors expressed in the shoots could be actively involved in AM regulation.

CONCLUSION

The data presented here lead us to propose a stimulatory role for CKs in the development of the pea AM symbiosis and confirm an effect of AM inoculation on plant CK homeostasis. A low NT:PACK ratio was associated with fungal entry and the stimulation of the intraradical development of AM fungi. However, we still face an enigma: i.e., is it the observed decrease in the NT:PACK ratio that allows the extraradical fungal hyphae to enter or is it the intraradical growth of the fungus that is inducing the decrease of the NT:PACK ratio? To answer this question will require more work. Using tissue-specific transcriptome analysis, like Jardinaud et al. (2016) who studied the different roles CKs play in the epidermis and root cortex of nodulated roots, may help solve this conundrum.

DATA AVAILABILITY

All datasets generated for this study are included in the manuscript and/or the **Supplementary Files**.

AUTHOR CONTRIBUTIONS

FG designed the experiments. DG grew the plants for the cytokinin analysis, performed the developmental study of AM formation, performed all statistical analysis, and made all graphs. SM and ZS performed the pharmacological treatments of the wild type and mutant plants, respectively, and they assessed the fungal colonization of the treated plants. LS provided the synthetic CK status-modifying compounds. AK and RE measured the CK levels and analyzed the CK results. MC and SD performed the pharmacological treatment of the fungus and analyzed the results. MC, DG, and AK participated in many discussions, which led to this manuscript. MC, DG, and FG wrote the manuscript. All authors revised the manuscript.

FUNDING

FG would like to acknowledge the financial support of the Natural Sciences and Engineering Research Council (NSERC)

of Canada for a General Research Fund, and of the Faculty of Science at Wilfrid Laurier University. MC was supported by an Incoming Post-doctoral Fellowship of the Fonds Spéciaux de Recherche from the Wallonie-Bruxelles Federation, Belgium. RE would like to acknowledge NSERC for his Discovery Grant No RGPIN-2018-05436. LS acknowledges funding by an ERDF project entitled "Development of Pre-Applied Research in Nanotechnology and Biotechnology" (No. CZ.02.1.01/0.0/0.0/17_048/0007323) and the Ministry of Education, Youth and Sports of Czechia (Grant LO1204 from the National Program of Sustainability).

ACKNOWLEDGMENTS

FG would like to acknowledge Dr. Tom Larue, who generously gave her the pea mutant E151, and Drs. Moffatt and Tang for allowing the use of their freeze-dryer.

SUPPLEMENTARY MATERIAL

The Supplementary Material for this article can be found online at: https://www.frontiersin.org/articles/10.3389/fpls.2019.00262/full#supplementary-material

REFERENCES

Adolfsson, L., Nziengui, H., Abreu, I. N., Šimura, J., Beebo, A., Herdean, A., et al. (2017). Enhanced secondary- and hormone metabolism in leaves of arbuscular mycorrhizal *Medicago truncatula*. *Plant Physiol.* 175, 392–411. doi: 10.1104/pp.16.01509

Akiyama, K., Matsuzaki, K.-I., and Hayashi, H. (2005). Plant sesquiterpenes induce hyphal branching in arbuscular mycorrhizal fungi. *Nature* 435, 824–827. doi: 10.1038/nature03608

Allen, M. F., Moore, T. S. Jr., and Christensen, M. (1980). Phytohormone changes in *Bouteloua gracilis* infected by vesicular-arbuscular mycorrhizae: I. Cytokinin increases in the host plant. *Can. J. Bot.* 58, 371–374. doi: 10.1139/b80-038

Aremu, A. O., Stirk, W. A., Masondo, N. A., Plačkova, L., Novák, O., Pěnčik, A., et al. (2015). Dissecting the role of two cytokinin analogues (INCYDE and PI-55) on *in vitro* organogenesis, phytohormone accumulation, phytochemical content and antioxidant activity. *Plant Sci.* 238, 81–94. doi: 10.1016/j.plantsci.2015.05.018

Ariel, F., Brault-Hernandez, M., Laffont, C., Huault, E., Brault, M., Plet, J., et al. (2012). Two direct targets of cytokinin signaling regulate symbiotic nodulation in *Medicago truncatula*. *Plant Cell* 24, 3838–3852. doi: 10.1105/tpc.112.103267

Audet, P., and Charest, C. (2010). Identification of constraining experimental-design factors in mycorrhizal pot-growth studies. *J. Bot.* 2010:718013. doi: 10.1155/2010/718013

Baas, R., and Kuiper, D. (1989). Effects of vesicular-arbuscular mycorrhizal infection and phosphate on *Plantago* major ssp. pleiosperma in relation to internal cytokinin concentrations. *Physiol. Plant* 76, 211–215. doi: 10.1111/j.1399-3054.1989.tb05634.x

Bedini, A., Mercy, L., Schneider, C., Franken, P., and Lucic-Mercy, E. (2018). Unraveling the initial plant hormone signaling, metabolic mechanisms and plant defense triggering the endomycorrhizal symbiosis behavior. *Front. Plant Sci.* 9:1800. doi: 10.3389/fpls.2018.01800

Bompadre, M. J., Fernández Bidondo, L., Silvani, V. A., Colombo, R. P., Pérgola, M., Pardo, A. G., et al. (2015). Combined effects of arbuscular mycorrhizal fungi and exogenous cytokinins on pomegranate (*Punica granatum*) under two contrasting water availability conditions. *Symbiosis* 65, 55–63. doi: 10.1007/s13199-015-0318-2

Bravo, A., Brands, M., Wewer, V., Dörmann, P., and Harrison, M. J. (2017). Arbuscular mycorrhiza-specific enzymes FatM and RAM2 fine-tune lipid biosynthesis to promote development of arbuscular mycorrhiza. *New Phytol.* 214, 1631–1645. doi: 10.1111/nph.14533

Bucher, M., Hause, B., Krajinski, F., and Küster, H. (2014). Through the doors of perception to function in arbuscular mycorrhizal symbioses. *New Phytol.* 204, 833–840. doi: 10.1111/nph.12862

Coba de la Peña, T., Cárcamo, C. B., Almonacid, L., Zaballos, A., Lucas, M. M., Balemenos, D., et al. (2008). A cytokinin receptor homologue is induced during root nodule organogenesis and senescence in *Lupinus albus* L. *Plant Physiol. Biochem.* 46, 219–225. doi: 10.1016/j.plaphy.2007.10.021

Cosme, M., Ramireddy, E., Franken, P., Schmülling, T., and Wurst, S. (2016). Shoot and root-borne cytokinin influences arbuscular mycorrhizal symbiosis. *Mycorrhiza* 26, 709–720. doi: 10.1007/s00572-016-0706-3

Cosme, M., and Wurst, S. (2013). Interactions between arbuscular mycorrhizal fungi, rhizobacteria, soil phosphorus and plant cytokinin deficiency change the root morphology, yield and quality of tobacco. *Soil Biol. Biochem.* 57, 436–443. doi: 10.1016/j.soilbio.2012.09.024

Danneberg, G., Latus, C., Zimmer, W., Hundeshagen, B., Schneider-Poetsch, H., and Bothe, H. (1992). Influence of vesicular-arbuscular mycorrhiza on phytohormones balances in maize (*Zea mays* L.). *J. Plant Physiol.* 141, 33–39. doi: 10.1016/S0176-1617(11)80848-5

Das, D., and Gutjahr, C. (2019). "Role of phytohormones in arbuscular mycorrhiza development. Chapter 7," in *The model legume Medicago truncatula*, ed. F. de Bruijn (Hoboken, NJ: John Wiley and Sons Ltd).

Declerck, S., Strullu, D. G., and Plenchette, C. (1998). Monoxenic culture of the intraradical forms of Glomus sp. isolated from a tropical ecosystem: a proposed methodology for germplasm collection. *Mycologia* 90, 579–585. doi: 10.1080/00275514.1998.12026946

Dickson, S., Smith, F. A., and Smith, S. E. (2007). Structural differences in arbuscular mycorrhizal symbioses; more than 100 years after gallaud, where next? *Mycorrhiza* 17, 375–393. doi: 10.1007/s00572-007-0130-9

Dixon, R. K., Garrett, H. E., and Cox, G. S. (1988). Cytokinins in the root pressure exudate of *Citrus jambhiri* lush. colonized by vesicular-arbuscular mycorrhizae. *Tree Physiol.* 4, 9–18. doi: 10.1093/treephys/4.1.9

Drüge, U., and Schönbeck, F. (1992). Effect of vesicular-arbuscular mycorrhizal infection on transpiration, photosynthesis and growth of flax (*Linum usitatissimum* L.) in relation to cytokinin levels. *J. Plant Physiol.* 141, 40–48. doi: 10.1016/S0176-1617(11)80849-7

Farrow, S. C., and Emery, R. J. N. (2012). Concurrent profiling of indole-3-acetic acid, abscisic acid, and cytokinins and structurally related purines by high-performance-liquid-chromatography tandem electrospray mass spectrometry. *Plant Methods* 8:42. doi: 10.1186/1746-4811-8-42

Foo, E., Ross, J. J., Jones, W. T., and Reid, J. B. (2013). Plant hormones in arbuscular mycorrhizal symbioses: an emerging role for gibberellins. *Ann. Bot.* 111, 769–779. doi: 10.1093/aob/mct041

Franson, R. L., and Bethlenfalvay, G. J. (1989). Infection unit method of vesicular-arbuscular mycorrhizal propagules determination. *Soil Sci. Soc. Amer. J.* 53, 754–756. doi: 10.2136/sssaj1989.03615995005300030020x

Fusconi, A. (2014). Regulation of root morphogenesis in arbuscular mycorrhizae: what role do fungal exudates, phosphate, sugars and hormones play in lateral root formation? *Ann. Bot.* 113, 19–33. doi: 10.1093/aob/mct258

Gaude, N., Bortfeld, S., Duensing, N., Lohse, M., and Krajinski, F. (2012). Arbuscule-containing and non-colonized cortical cells of mycorrhizal roots undergo extensive and specific reprogramming during arbuscular mycorrhizal development. *Plant J.* 69, 510–528. doi: 10.1111/j.1365-313X.2011.04810.x

Ginzberg, I., David, R., Shaul, O., Elad, Y., Wininger, S., Ben-Dor, B., et al. (1998). *Glomus intraradices* colonization regulates gene expression in tobacco toots. *Symbiosis* 25, 145–157.

Giovannetti, M., and Mosse, B. (1980). An evaluation of techniques for measuring vesicular arbuscular mycorrhizal infection in roots. *New Phytol.* 84, 489–500. doi: 10.1111/j.1469-8137.1980.tb04556.x

Glenn, M. G., Chew, F. S., and Williams, P. H. (1985). Hyphal penetration of *Brassica* (*Cruciferae*) roots by a vesicular-arbuscular mycorrhizal fungus. *New Phytol.* 99, 463–472. doi: 10.1111/j.1469-8137.1985.tb03673.x

Goicoechea, N., Dolézal, K., Antolin, M. C., Strnad, M., and Sánchez-Diaz, M. (1995). Influence of mycorrhiza and *Rhizobium* on cytokinin content in drought-stressed alfalfa. *J. Exp. Bot.* 46, 1543–1549. doi: 10.1093/jxb/46.10.1543

Gonzalez-Rizzo, S., Crespi, M., and Frugier, F. (2006). The *Medicago truncatula* CRE1 cytokinin receptor regulates lateral root development and early symbiotic interaction with *Sinorhizobium meliloti*. *Plant Cell* 18, 2680–2693. doi: 10.1105/tpc.106.043778

Gryndler, M., Hršelová, H., Chvátalová, I., and Jansa, J. (1998). The effect of selected plant hormones on in vitro proliferation of hyphae of *Glomus fistulosum*. *Biol. Plant* 41, 255–263. doi: 10.1023/A:1001874832669

Guether, M., Neuhaüser, B., Balestrini, R., Dynowski, M., Ludewig, U., and Bonfante, P. (2009). A mycorrhizal-specific ammonium transporter from *Lotus japonicus* acquires nitrogen released by arbuscular mycorrhizal fungi. *Plant Physiol.* 150, 73–83. doi: 10.1104/pp.109.136390

Gutjahr, C. (2014). Phytohormone signaling in arbuscular mycorrhiza development. *Curr. Opin. Plant Biol.* 20, 26–34. doi: 10.1016/j.pbi.2014.04.003

Harrison, M. J., Dewbre, G. R., and Liu, J. (2002). A phosphate transporter from *Medicago truncatula* involved in the acquisition of phosphate released by arbuscular mycorrhizal fungi. *Plant Cell* 14, 2413–2429. doi: 10.1105/tpc.004861

Helber, N., Wippel, K., Sauer, N., Schaarschmidt, S., Hause, B., and Requena, N. (2011). A versatile monosaccharide transporter that operates in the arbuscular mycorrhizal fungus *Glomus* sp. is crucial for the symbiotic relationship with plants. *Plant Cell* 23, 3812–3823. doi: 10.1105/tpc.111.089813

Held, M., Hou, H., Miri, M., Huynh, C., Ross, L., Hossain, M. S., et al. (2014). *Lotus japonicus* cytokinin receptors work partially redundantly to mediate nodule formation. *Plant Cell* 26, 678–694. doi: 10.1105/tpc.113.119382

Higuchi, M., Pischke, M. S., Mähönen, A. P., Miyawaki, K., Hashimoto, Y., Seki, M., et al. (2004). In planta functions of the *Arabidopsis* cytokinin receptor family. *Proc. Natl. Acad. Sci.* 101, 8821–8826. doi: 10.1073/pnas.0402887101

Jardinaud, M.-F., Boivin, S., Rodde, N., Catrice, O., Kisiala, A., Lepage, A., et al. (2016). A laser dissection-RNAseq analysis highlights the activation of cytokinin pathways by nod factors in the *Medicago truncatula* root epidermis. *Plant Physiol.* 171, 2256–2276. doi: 10.1104/pp.16.00711

Jones, J. M. C., Clairmont, L., Macdonald, E. S., Weiner, C. A., Emery, R. J. N., and Guinel, F. C. (2015). E151 (sym15), a pleiotropic mutant of pea (*Pisum sativum* L.), displays low nodule number, enhanced mycorrhizae, delayed lateral root emergence, and high root cytokinin *levels*. *J. Exp. Bot.* 66, 4047–4059. doi: 10.1093/jxb/erv201

Kieber, J. J., and Schaller, G. E. (2010). The perception of cytokinin: a story 50 years in the making. *Plant Physiol.* 154, 487–492. doi: 10.1104/pp.110.161596

Kneen, B. E., Weeden, N. F., and LaRue, T. A. (1994). Non-nodulating mutants of *Pisum sativum* (L.) cv. *Spark*. *J. Hered.* 85, 129–133. doi: 10.1093/oxfordjournals.jhered.a111410

Knott, C. M. (1987). A key for stages of development of the pea (*Pisum sativum*). *Ann. Appl. Biol.* 111, 233–244. doi: 10.1111/j.1744-7348.1987.tb01450.x

Ko, D., Kang, J., Kiba, T., Park, J., Kojima, M., Do, J., et al. (2014). *Arabidopsis* ABCG14 is essential for the root-to-shoot translocation of cytokinin. *Proc. Natl. Acad. Sci.* 111, 7150–7155. doi: 10.1073/pnas.1321519111

Lace, B., and Ott, T. (2018). Commonalities and differences in controlling multipartite intracellular infections of legume roots by symbiotic microbes. *Plant Cell Physiol.* 59, 666–677. doi: 10.1093/pcp/pcy043

Laffont, C., Rey, T., André, O., Novero, M., Kazmierczak, T., Debellé, F., et al. (2015). The CRE1 cytokinin pathway is differentially recruited depending on *Medicago truncatula* root environments and negatively regulates resistance to a pathogen. *PLosOne* 10:e0116819. doi: 10.1371/journal.pone.0116819

Liao, D., Wang, S., Cui, M., Liu, J., Chen, A., and Xu, G. (2018). Phytohormones regulate the development of arbuscular mycorrhizal symbiosis. *Int. J. Mol. Sci.* 19:3146. doi: 10.3390/ijms19103146

Lomin, S. N., Myakushina, Y. A., Kolachevskaya, O. O., Getman, I. A., Arkhipov, D. V., Savelleva, E. M., et al. (2018). Cytokinin perception in potato: new features of canonical players. *J. Exp. Bot.* 69, 3839–3853. doi: 10.1093/jxb/ery199

Long, C., Held, M., Hayward, A., Nisler, J., Spíchal, L., Emery, R. J. N., et al. (2012). Seed development, seed germination and seedling growth in the R50 (sym16) pea mutant are not directly linked to altered cytokinin homeostasis. *Physiol. Plant.* 145, 341–359. doi: 10.1111/j.1399-3054.2012.01594.x

MacColl, K. (2017). *An Assessment of How Plant and Mycorrhizal Communities Have Been Affected Along a Mine-Impacted Watershed in the Northwest Territories*. MSc. Thesis. Waterloo ON: Wilfrid Laurier University.

McGonigle, T. P., Miller, M. H., Evans, D. G., Fairchild, G. L., and Swan, J. A. (1990). A new method which gives an objective measure of colonization of roots by vesicular-arbuscular mycorrhizal fungi. *New Phytol.* 115, 495–501. doi: 10.1111/j.1469-8137.1990.tb00476.x

Murray, J. D., Karas, B. J., Sato, S., Tabata, S., Amyot, L., and Szczyglowski, K. (2007). A cytokinin perception mutant colonized by *Rhizobium* in the absence of nodule organogenesis. *Science* 315, 101–104. doi: 10.1126/science.1132514

Plet, J., Wasson, A., Ariel, F., Le Signor, C., Baker, D., Mathesius, U., et al. (2011). MtCRE1-dependent cytokinin signaling integrates bacterial and plant cues to coordinate symbiotic nodule organogenesis in *Medicago truncatula*. *Plant J.* 65, 622–633. doi: 10.1111/j.1365-313X.2010.04447

Pozo, M. J., López-Ráez, J. A., Azcón-Aguilar, C., and García-Garrido, J. M. (2015). Phytohormones as integrators of environmental signals in the regulation of mycorrhizal symbioses. *New Phytol.* 205, 1431–1436. doi: 10.1111/nph.13252

Quesnelle, P. E., and Emery, R. J. N. (2007). Cis-cytokinins that predominate *Pisum sativum* during early embryogenesis will accelerate embryo growth *in vitro*. *Can. J. Bot.* 85, 91–103. doi: 10.1139/b06-149

R Core Team. (2017). *Integrated Development for R*. Boston, MA: RStudio, Inc.

Rausch, C., Daram, P., Brunner, S., Jansa, J., Laloi, M., Leggewie, G., et al. (2001). A phosphate transporter expressed in arbuscule-containing cells in potato. *Nature* 414, 464–470. doi: 10.1038/35106601

Resendes, C. M., Geil, R. D., and Guinel, F. C. (2001). Mycorrhizal development in a low nodulating pea mutant. *New Phytol.* 150, 563–572. doi: 10.1046/j.1469-8137.2001.00131.x

Riefler, M., Novak, O., Strnad, M., and Schmülling, T. (2006). *Arabidopsis* cytokinin receptor mutants reveal functions in shoot growth, leaf senescence, seed size, germination, root development, and cytokinin metabolism. *Plant Cell* 18, 40–54. doi: 10.1105/tpc.105.037796

Romanov, G. A., Lomin, S. N., and Schmülling, T. (2006). Biochemical characteristics and ligand-binding properties of *Arabidopsis* cytokinin receptor AHK3 compared to CRE1/AHK4 as revealed by a direct binding assay. *J. Exp. Bot.* 57, 4051–4058. doi: 10.1093/jxb/erl179

Sakakibara, H. (2006). Cytokinins: activity, biosynthesis, and translocation. *Annu. Rev. Plant Biol.* 57, 431–449. doi: 10.1146/annurev.arplant.57.032905.105231

Schmidt, C. S., Mrnka, L., Frantik, T., Motyka, V., Dobrev, P. I., and Vosátka, M. (2017). Combined effects of fungal inoculants and the cytokinin-like growth regulator thidiazuron on growth, phytohormone contents and endophytic root fungi in *Miscanthus* × *giganteus*. *Plant Physiol. Biochem.* 120, 120–131. doi: 10.1016/j.plaphy.2017.09.016

Shaul-Keinan, O., Gadkar, V., Ginzberg, I., Grünzweig, J. M., Chet, I., Elad, Y., et al. (2002). Hormone concentrations in tobacco roots change during arbuscular mycorrhizal colonization with *Glomus intraradices*. *New Phytol.* 154, 501–507. doi: 10.1046/j.1469-8137.2002.00388.x

Skalický, V., Kubeš, M., Napier, R., and Novák, O. (2018). Auxins and cytokinins–The role of subcellular organization on homeostasis. *Int. J. Mol. Sci.* 19:3115. doi: 10.3390/ijms19103115

Smith, S. E., and Read, D. J. (2008). *Mycorrhizal Symbiosis*. London: Academic Press.

Spíchal, L. (2012). Cytokinins – recent news and views of evolutionally old molecules. *Funct. Plant Biol.* 39, 267–284. doi: 10.1071/FP11276

Spíchal, L., Rakova, N. Y., Riefler, M., Mizuno, T., Romanov, G. A., Strnad, M., et al. (2004). Two cytokinin receptors of *Arabidopsis thaliana*, CRE1/AHK4 and AHK3, differ in their ligand specificity in a bacterial assay. *Plant Cell Physiol.* 45, 1299–1305. doi: 10.1093/pcp/pch132

Spíchal, L., Werner, T., Popa, I., Riefler, M., Schmülling, T., and Strnad, M. (2009). The purine derivative PI-55 blocks cytokinin action via receptor inhibition. *FEBS J.* 276, 244–253. doi: 10.1111/j.1742-4658.2008.06777.x

Torelli, A., Trotta, A., Acerbi, L., Arcidiacono, G., Berta, G., and Branca, C. (2000). IAA and ZR content in leek (*Allium porrum* L.), as influenced by P nutrition and arbuscular mycorrhizae, in relation to plant development. *Plant Soil* 226, 29–35. doi: 10.1023/A:1026430019738

van Rhijn, P., Fang, Y., Galili, S., Shaul, O., Atzmon, N., Wininger, S., et al. (1997). Expression of early nodulin genes in alfalfa mycorrhizae indicates that signal transduction pathways used in forming arbuscular mycorrhizae and *Rhizobium*-induced nodules may be conserved. *Proc. Natl. Acad. Sci.* 94, 5467–5472. doi: 10.1073/pnas.94.10.5467

Vierheilig, H., Coughlan, A. P., Wyss, U., and Piché, Y. (1998). Ink and vinegar, a simple staining technique for arbuscular-mycorrhizal fungi. *Appl. Environ. Microbiol.* 64, 5004–5007.

Werner, T., and Schmülling, Y. (2009). Cytokinin action in plant development. *Curr. Opin. Plant Biol.* 12, 527–538. doi: 10.1016/j.pbi.2009.07.002

Yurkov, A., Veselova, S., Jacobi, L., Stepanova, G., Yemelyanov, V., Kudoyarova, G., et al. (2017). The effect of inoculation with arbuscular mycorrhizal fungus *Rhizophagus irregularis* on cytokinin content in a highly mycotrophic *Medicago lupulina* line under low phosphorus level in the soil. *Plant Soil Environ.* 63, 519–524. doi: 10.17221/617/2017-PSE

Zatloukal, M., Gemrotová, M., Doležal, K., Havlíček, L., Spíchal, L., and Strnad, M. (2008). Novel potent inhibitors of *A. thaliana* cytokinin oxidase/dehydrogenase. *Bioorg. Med. Chem.* 16, 9268–9275. doi: 10.1016/j.bmc.2008.09.008

Zhang, K., Novak, O., Wei, Z., Gou, M., Zhang, X., Yu, Y., et al. (2014). *Arabidopsis* ABCG14 protein controls the acropetal translocation of root-synthesized cytokinins. *Nat. Commun.* 5:3274. doi: 10.1038/mcomms427

Conflict of Interest Statement: The authors declare that the research was conducted in the absence of any commercial or financial relationships that could be construed as a potential conflict of interest.

frontiers in Microbiology

ORIGINAL RESEARCH
published: 12 March 2019
doi: 10.3389/fmicb.2019.00380

Beneficial and Pathogenic Arabidopsis Root-Interacting Fungi Differently Affect Auxin Levels and Responsive Genes During Early Infection

*Anja K. Meents[1,2,3], Alexandra C. U. Furch[2], Marília Almeida-Trapp[1], Sedef Özyürek[2], Sandra S. Scholz[2], Alexander Kirbis[4], Teresa Lenser[4], Günter Theißen[4], Veit Grabe[5], Bill Hansson[5], Axel Mithöfer[1,3] and Ralf Oelmüller[2]**

[1] Department of Bioorganic Chemistry, Max Planck Institute for Chemical Ecology, Jena, Germany, [2] Department of Plant Physiology, Matthias Schleiden Institute of Genetics, Bioinformatics and Molecular Botany, Friedrich-Schiller-University Jena, Jena, Germany, [3] Research Group Plant Defense Physiology, Max Planck Institute for Chemical Ecology, Jena, Germany, [4] Department of Genetics, Matthias Schleiden Institute of Genetics, Bioinformatics and Molecular Botany, Friedrich-Schiller-University Jena, Jena, Germany, [5] Department of Evolutionary Neuroethology, Max Planck Institute for Chemical Ecology, Jena, Germany

Auxin (indole-3-acetic acid, IAA) is an important phytohormone involved in root growth and development. Root-interacting beneficial and pathogenic fungi utilize auxin and its target genes to manipulate the performance of their hosts for their own needs. In order to follow and visualize auxin effects in fungi-colonized Arabidopsis roots, we used the dual auxin reporter construct *DR5*::*EGFP-DR5v2*::*tdTomato* and fluorescence microscopy as well as LC-MS-based phytohormone analyses. We demonstrate that the beneficial endophytic fungi *Piriformospora indica* and *Mortierella hyalina* produce and accumulate IAA in their mycelia, in contrast to the phytopathogenic biotrophic fungus *Verticillium dahliae* and the necrotrophic fungus *Alternaria brassicicola*. Within 3 h after exposure of Arabidopsis roots to the pathogens, the signals of the auxin-responsive reporter genes disappeared. When exposed to *P. indica*, significantly higher auxin levels and stimulated expression of auxin-responsive reporter genes were detected both in lateral root primordia and the root elongation zone within 1 day. Elevated auxin levels were also present in the *M. hyalina*/Arabidopsis root interaction, but no downstream effects on auxin-responsive reporter genes were observed. However, the jasmonate level was strongly increased in the colonized roots. We propose that the lack of stimulated root growth upon infection with *M. hyalina* is not caused by the absence of auxin, but an inhibitory effect mediated by high jasmonate content.

Keywords: auxin, phytohormones, plant-fungus interaction, *Piriformospora indica*, *Mortierella hyalina*, *Alternaria brassicicola*, *Verticillium dahliae*, light sheet fluorescence microscopy

OPEN ACCESS

Edited by:
Eloise Foo,
University of Tasmania, Australia

Reviewed by:
Jason Liang Pin Ng,
Australian National University, Australia
Antonio Figueira,
University of São Paulo, Brazil
Philip B. Brewer,
University of Adelaide, Australia

***Correspondence:**
Ralf Oelmüller
b7oera@uni-jena.de

Specialty section:
This article was submitted to Plant Microbe Interactions, a section of the journal Frontiers in Microbiology

Received: *08 November 2018*
Accepted: *13 February 2019*
Published: *12 March 2019*

Citation:
Meents AK, Furch ACU, Almeida-Trapp M, Özyürek S, Scholz SS, Kirbis A, Lenser T, Theißen G, Grabe V, Hansson B, Mithöfer A and Oelmüller R (2019) Beneficial and Pathogenic Arabidopsis Root-Interacting Fungi Differently Affect Auxin Levels and Responsive Genes During Early Infection. Front. Microbiol. 10:380. doi: 10.3389/fmicb.2019.00380

INTRODUCTION

Auxin plays a central role for root growth and participates in many aspects of root development, including cell elongation, differentiation (Rahman et al., 2007), lateral root, and root hair formation (Masucci and Schiefelbein, 1994, 1996; Pitts et al., 1998; Reed et al., 1998; Casimiro et al., 2001; Bhalerao et al., 2002), and gravitropic responses (Rashotte et al., 2000; Sukumar et al., 2009). Auxin action depends on its differential distribution within plant tissues, where it forms local maxima or gradients between cells. The different auxin levels arise from auxin metabolism (biosynthesis, degradation, and conjugation), long-distance transport and directional cell-to-cell translocation (Petrášek and Friml, 2009). Auxin interacts with other phytohormones and imbalances in the phytohormone levels have severe consequences. Well-studied examples are the auxin/cytokinin balance (De Rybel et al., 2014) and the control of lateral root growth by an interplay between auxin, abscisic acid, brassinosteroids, ethylene, and jasmonates (cf. Fukaki and Tasaka, 2009; Ishimaru et al., 2018). In addition, auxin produced by plant-associated microorganisms mediates phytostimulatory effects on plants. Pathogens can manipulate auxin biosynthesis, signaling, and transport pathways to promote host susceptibility. Auxin responses are also coupled to antagonistic and synergistic interactions with salicylic acid (SA)- and jasmonic acid (JA)-mediated defenses, respectively (Hoffmann et al., 2011; Naseem et al., 2015; Huang et al., 2017). Jasmonates participate in the regulation of primary root growth and reproductive development, thereby interacting with auxins. Crosstalk can occur at multiple levels, including hormone perception, since indole-acetic acid (IAA) and JA-isoleucine (JA-Ile) are perceived by SCF E3-ligases through the interaction of IAA- and JA-related regulators of gene expression and the modulation of each other's homeostasis (Hoffmann et al., 2011; Naseem et al., 2015). Auxin induces JA biosynthesis and JA controls the expression of some of the auxin biosynthetic genes (Dombrecht et al., 2007; Sun et al., 2009; Hentrich et al., 2013). Furthermore, high JA concentrations reduce the accumulation of the PIN-FORMED1 (PIN1) and PIN2 auxin transporters (Gutjahr et al., 2005; Hoffmann et al., 2011; Sun et al., 2011). IAA binds to the receptor AUXIN SIGNALING F-BOX PROTEIN TIR1 and inhibits a family of transcriptional repressors known as AUXIN/IAAs (Dharmasiri et al., 2005; Kepinski and Leyser, 2005; Salehin et al., 2015). In the presence of IAA, the SKP1-CULLIN1-F-BOX TIR1 ubiquitin ligase complex binds to AUXIN/IAAs and triggers their degradation (Calderon-Villalobos et al., 2010).

The vast majority of roots in the ecosystems is associated with beneficial fungi. They form mycorrhizal symbiosis or interact with endophytes. Plants benefit from these associations in many ways, such as better access to water and nutrients, promotion of growth and biomass production and resistance to biotic and abiotic stress. The fungi are supplied with reduced carbon from the host photosynthesis and live in a protected shelter. The beneficial symbiosis results in alterations of the host phytohormone levels. For example, beneficial microbes synthesize auxin or auxin precursors, interfere with the plant auxin biosynthesis and metabolism or manipulate auxin signaling and responses. In many cases, the microbes utilize the plant phytohormone machinery and reprogram it to their own needs (Xu et al., 2018, and references therein).

In this study, we used the previously described auxin-responsive reporter system *DR5::EGFP-DR5v2::tdTomato* (Ulmasov et al., 1997; Liao et al., 2015) to monitor how the root-interacting microbes *Piriformospora indica*, *Mortierella hyalina*, *Verticillium dahlia,* and *Alternaria brassicicola* manipulate the root auxin metabolism during early phases of the interaction with Arabidopsis roots. *P. indica*, a member of *Sebacinales*, grows inter- and intracellularly and forms pear shaped spores, which accumulate within the roots and on the root surface (Peškan-Berghöfer et al., 2004; Oelmüller et al., 2009; Camehl et al., 2011). The fungus promotes the growth of the host plants (Peškan-Berghöfer et al., 2004), induces early flowering (Pan et al., 2017) and confers resistance against abiotic and biotic stress (Narayan et al., 2017; Zhang et al., 2017; Vahabi et al., 2018). The endophyte produces indole derivatives but they are not required for growth promotion in barley roots (Hilbert et al., 2012). *P. indica* releases cellotriose that induces root-specific $[Ca^{2+}]_{cyt}$ elevation required for the activation of a mild defense response (Vadassery et al., 2008; Johnson et al., 2018a; Oelmüller, 2018). Root-specific $[Ca^{2+}]_{cyt}$ elevation is also induced by an exuded info-chemical from *M. hyalina* (Johnson et al., 2018b), a growth promoting fungus of *Mortierellales* (Shinmen et al., 1989) which results in defense gene activation. The fungus promotes growth of the aerial parts of Arabidopsis via a fungus-released volatile, while the growth behavior of colonized roots resembles that of un-colonized controls (Johnson et al., 2018b). *V. dahliae* is hemibiotroph with an initial biotrophic life phase in the root xylem, followed by a necrotrophic phase once the hyphae reach the aerial plant tissues. While infected roots show little or no disease symptom development during the biotrophic phase, the fungus blocks xylem transport and synthesizes a cocktail of toxins during the necrotrophic phase, which results in wilting and disease symptom development in the leaves of *Brassicaceae* species (Pemberton and Salmond, 2004; Gijzen and Nürnberger, 2006; Qutob et al., 2006; van der Does and Rep, 2007; Bolton et al., 2008; de Jonge and Thomma, 2009; van Esse et al., 2009; de Jonge et al., 2010, 2011; Oliva et al., 2010; Klosterman et al., 2011; Scholz et al., 2018). The necrotrophic fungus *Alternaria* causes black leaf spot disease in crucifers and was used in this study since it infects both leaves and roots. Root infection induces rapid $[Ca^{2+}]_{cyt}$ elevations which results in host defense gene activation, jasmonate accumulation, ROS production and innate immunity. A few days after root infection, the Arabidopsis seedlings are dead (Johnson et al., 2018b).

In this study, we addressed the hypothesis that interactions of Arabidopsis roots with pathogenic and beneficial fungi are accompanied by different activation of auxin-responsive genes during very early phases of contact. Our results suggest that the activation of auxin-responsive genes and auxin-induced developmental programs in the colonized roots are controlled by the phytohormone balance, rather than by the auxin concentration alone.

MATERIAL AND METHODS

Plant Material and Growth Conditions

Seedlings of *Arabidopsis thaliana* containing the dual auxin reporter construct *DR5::EGFP-DR5v2::tdTomato* were generally described in Ulmasov et al. (1997) and Liao et al. (2015). Here, plants containing T-DNA comprising construct *pGWB601-DR5::EGFP-DR5v2::tdTomato* were used, which had been generated as described (Kirbis, 2017). The seeds were surface-sterilized and placed on petri dishes containing full Murashige-Skoog nutrient medium (MS) (Murashige and Skoog, 1962) supplemented with 40 mM sucrose, 2.6 mM 2-(N-morpholino)ethanesulfonic acid and 1% Kobe Agar (all supplies from Carl Roth, Karlsruhe, Germany). After a 48 h stratification at 4°C, plates were incubated vertically for 10 days at 22°C under long day conditions (16 h light/ 8 h dark; 80 μmol m^{-2} s^{-1}).

Fungal Material and Growth Conditions

P. indica (syn. Serindipita indica) was grown on petri dishes with modified Kaefer's medium (KM) as previously described (Verma et al., 1998; Peškan-Berghöfer et al., 2004) and kept in the dark at room temperature for 3 weeks. *A. brassicicola*, *M. hyalina*, and *V. dahliae* were cultivated for 2 weeks at 22 ± 1°C on potato dextrose agar (PDA) medium as reported in Johnson et al. (2014). *A. brassicicola*, *M. hyalina*, and *V. dahliae* were obtained from the Jena Microbial Resource Center and *P. indica* was provided by Ajit Varma (Amity Institute of Microbial Technology, India).

Spore suspensions of the fungi were prepared according to Johnson et al. (2014) by rinsing the plates containing the fungi with sterile H_2O, gently scraping the spores and hyphae off the plate followed by filtration through a sterilized nylon membrane (75 μm pore size). The spore concentration was determined using a hemocytometer and adjusted with sterile H_2O containing 0.01 % Tween-20 to 2 × 10^6 spores/ml. As control the same solution was used without spores. Viability of the spores was routinely checked via germination tests.

Co-cultivation for Fluorescence Microscopy

In order to investigate the impact of different fungi on the distribution of auxin maxima, Arabidopsis seedlings containing the reporter construct *pGWB601-DR5::EGFP-DR5v2::tdTomato* were co-cultivated with fungal plaques of *P. indica*, *A. brassicicola*, *M. hyalina*, or *V. dahliae* as described previously by Johnson et al. (2011, 2014) with modifications. For co-cultivation with subsequent fluorescence microscopy, 12 day-old plants were placed on microscope slides on top of a thin layer of full MS medium containing 1% Kobe agar and a plaque (5 mm diameter) of medium (PDA or KM, for control), or fungus agar cultures were applied (see **Figure 1A**). The seedling and fungal plug were coated with sterile tap water, covered with a cover slip and placed in a petri dish until microscopy was performed. The plates were then sealed with Parafilm (American National Can Company, Greenwich, USA) to prevent drying out of the sample and kept at 22°C under long day conditions (16 h light/8 h dark; 80 μmol m^{-2} s^{-1}) for 1 to 3 days. The fluorescence of the reporter construct was analyzed by fluorescence microscopy (see below) after 24 h of incubation. To analyze the dose-dependent induction of fluorescence, the MS agar was supplemented with 0, 5, 10, or 20 μM of IAA (Merck, Darmstadt, Germany) or 0, 1, 5, or 10 μM of JA (Sigma-Aldrich, Taufkirchen, Germany).

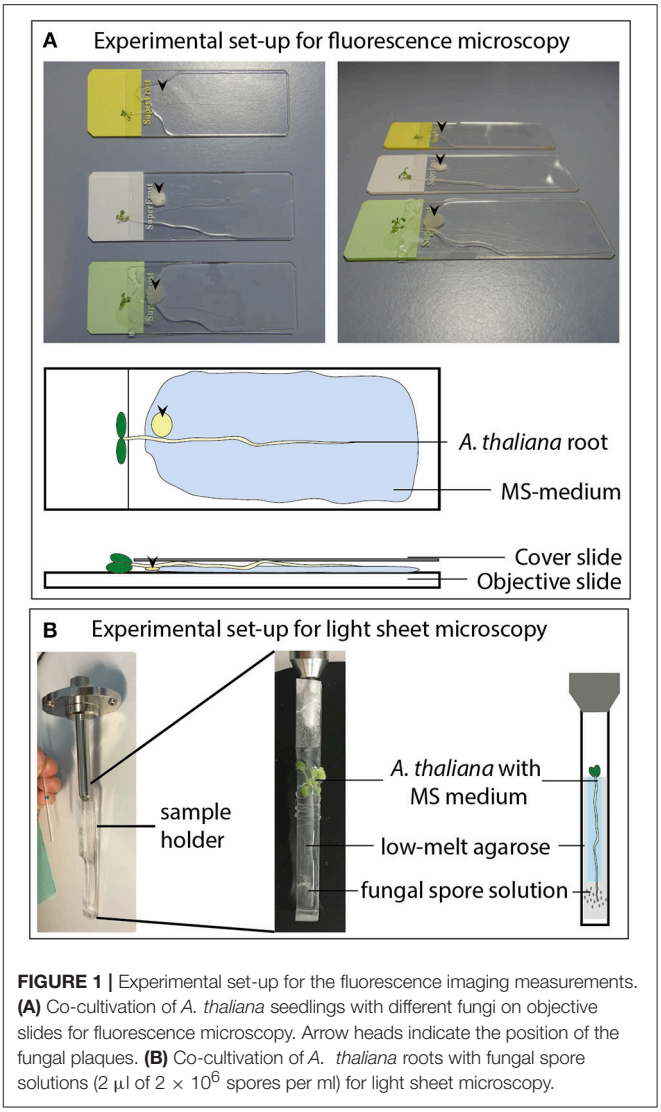

FIGURE 1 | Experimental set-up for the fluorescence imaging measurements. **(A)** Co-cultivation of *A. thaliana* seedlings with different fungi on objective slides for fluorescence microscopy. Arrow heads indicate the position of the fungal plaques. **(B)** Co-cultivation of *A. thaliana* roots with fungal spore solutions (2 μl of 2 × 10^6 spores per ml) for light sheet microscopy.

Fluorescence Microscopy

The entire Arabidopsis roots, elongation zones, root tips and primordia were imaged using an AXIO Imager.M2 (Zeiss Microscopy GmbH, Jena, Germany) equipped with a 10x objective (N-Achroplan 10x/0.3). The bright field and fluorescence images (EX 545/25 and EM 605/70) were recorded with a color camera (AXIOCAM 503 color Zeiss, Jena, Germany) by use of an EGFP (EM 525/50 nm) and DsRED filter (EM 605/70 nm). Digital images were processed with the ZEN software (Zeiss, Jena, Germany), treated with Adobe® PhotoShop to optimize brightness, contrast and coloring and to overlay the photomicrographs. The quantification of fluorescence was measured using the ZEN software by analyzing a region of interest at the root tip and/or the whole root.

Light Sheet Fluorescence Microscopy

Twelve day-old Arabidopsis seedlings (grown as described above) were mounted on a custom plastic holder (see **Figure 1B**). Afterwards the root tip was infected with 2 µl of a *P. indica, A. brassicicola, M. hyalina,* or *V. dahliae* spore suspension (2×10^6 spores/ml) or sterile water containing 0.01 % Tween-20 as a control. The whole plant was fixed using 2% low melting agarose (Carl Roth, Karlsruhe, Germany) and Parafilm to prevent unspecific movement (see **Figure 1B**). The measuring chamber was flooded with full Murashige-Skoog nutrient medium to ensure optimal nutrient supply during the whole measurement. Time series of the root response to the spore treatments were recorded on a LightSheet.Z1 (ZEISS, Oberkochen, Germany) equipped with a W Plan Apochromat 20x/1.0 UV-VIS (ZEISS, Oberkochen, Germany) and two lasers (laser lines: Argon 488 nm and Helium-Neon 561 nm). The red fluorescence was visualized using the 561 nm Helium-Neon laser at 20% transmission with a LBF 405/488/561 emission filter BP 575-615. For all recordings an exposure time of 350 ms was used at a zoom of 0.36 and a light sheet thickness of 6.68 µm. Image stacks series were acquired at 1,920·pixels, 20 µm z-thickness and 16 bit every 30 min for 24 h. Representative intensity kinetics were generated with the ZEN software (Zeiss, Jena, Germany).

Co-cultivation for Phytohormone Analyses

For phytohormone analyses, 15 Arabidopsis seedlings were positioned on a full MS square plate on a sterilized nylon membrane, stratified for 2 days at 4°C and vertically grown for 10 days at 22°C under long day conditions (16 h light/8 h dark; 80 µmol m^{-2} s^{-1}). In accordance with the previous plaque treatment, a 5 mm broad stripe of PDA medium with or without (control) fungal mycelium of *A. brassicicola, M. hyalina*, or *V. dahliae* was placed on the roots and incubated for 1 day. For co-cultivation with *P. indica,* a stripe of KM medium with or without fungus was used for treatment. The plates were co-cultured for 24 h before the entire root of each plate was collected, immediately frozen in liquid nitrogen and stored at −80°C before phytohormone extraction. Mycelium from each fungus grown alone was additionally collected from a whole plate, frozen and kept at −80°C.

Quantification of Phytohormones

Prior to phytohormone extraction, the collected fungal samples (40–200 mg fresh weight, $n = 3$) were freeze-dried in a Modulyo®D Freeze Dryer (Thermo Scientific, Waltham, USA) for 48 h. The freeze-dried fungal samples and the collected root tissue of co-cultivated seedlings (1 sample = 12–15 seedlings from the same plate; which corresponded to 30–150 mg fresh weight, $n = 8$) were weighed and homogenized using a Geno/Grinder® (Spex SamplePrep, Stanmore, UK) at 1,100 rounds per min for 1 min. As described in Almeida Trapp et al. (2014), 1 ml of methanol: water (7:3) containing 20 µg/ml of d4-SA and d5-IAA as well as 10 µg/ml d5-JA and d6-ABA was added to the powdered root and fungal material. After mixing, samples were shaken for 30 min and centrifuged at 16,000 *g* at 4°C for 5 min. Subsequently the supernatant was transferred into a new tube and concentrated for 4 h at 45°C in an Eppendorf Concentrator plus (Eppendorf AG, Hamburg, Germany). The concentrate was resuspended in 100 µl of 50% methanol with 0.05% formic acid, mixed and centrifuged at 16,000 *g* at 4°C for 10 min. Afterwards the supernatant was collected and measured on an Agilent 1100 HPLC system (Agilent Technologies, Böblingen, Germany) connected to a LTQ Orbitrap mass spectrometer (Thermo Scientific, Waltham, USA) (Almeida Trapp et al., 2014).

Statistics

Statistical analyzes of phytohormone data were performed in R studio (version 1.1.456), using one way ANOVA on log transformed data to ensure that the residues followed a normal distribution. Tukey's HSD test was used as *post-hoc* test to examine the differences between factor levels (treated plants vs. control) or multiple comparison for the amount of phytohormones present in fungi samples.

RESULTS

The Reporter Construct *DR5*::*EGFP-DR5v2*::*tdTomato* Responds to Exogenously Applied IAA in a Concentration-Dependent Manner in Arabidopsis Roots

To test the expression of the auxin reporters to exogenously applied IAA, the roots of 12 day-old Arabidopsis seedlings were incubated with increasing IAA concentrations. After 24 h, the EGFP and tdTomato fluorescence was monitored (for experimental set-up see: **Figures 1A**, **2A,B**). Without exogenously applied IAA, the fluorescence from both reporters was detectable in the quiescent center, columella, pericycle, and vascular system of the roots (**Figure 2A**, second image, EGFP; third image, tdTomato; fourth image, merged). Incubation with the lowest applied concentration of 5 µM IAA resulted in a significant increase in both fluorescence signals which were extended to the rhizodermal cell layers (**Figure 2B**). The intensity of the signals after the application of 5 µM IAA was twice as high as in the untreated controls and increased almost linear with increasing IAA concentrations (**Figures 2B,C**). Because the fluorescence signals were detectable throughout the entire root tissues (**Figure 2B**) exogenously applied IAA did not cause cell- or tissue-specific induction of the reporter genes. For these experiments and the pictures for the physiological experiments shown below, the fluorescence from both reporters was always measured; however, the overlay analysis never discovered meaningful differences (see **Figure 2B**). Since the fluorescence signal for the EGFP reporter was much lower than the one observed for the tdTomato reporter, the cell- and tissue-specific resolution was better for the latter reporter system. Therefore, for the presentation of the data, we show the results for the stronger fluorescent tdTomato reporter. Furthermore, the linear increase of the fluorescence signals with increasing exogenous applied IAA (**Figure 2B**) makes it likely that the fluorescence reports fungus-induced changes in the expression of auxin-responsive genes in the root tissues.

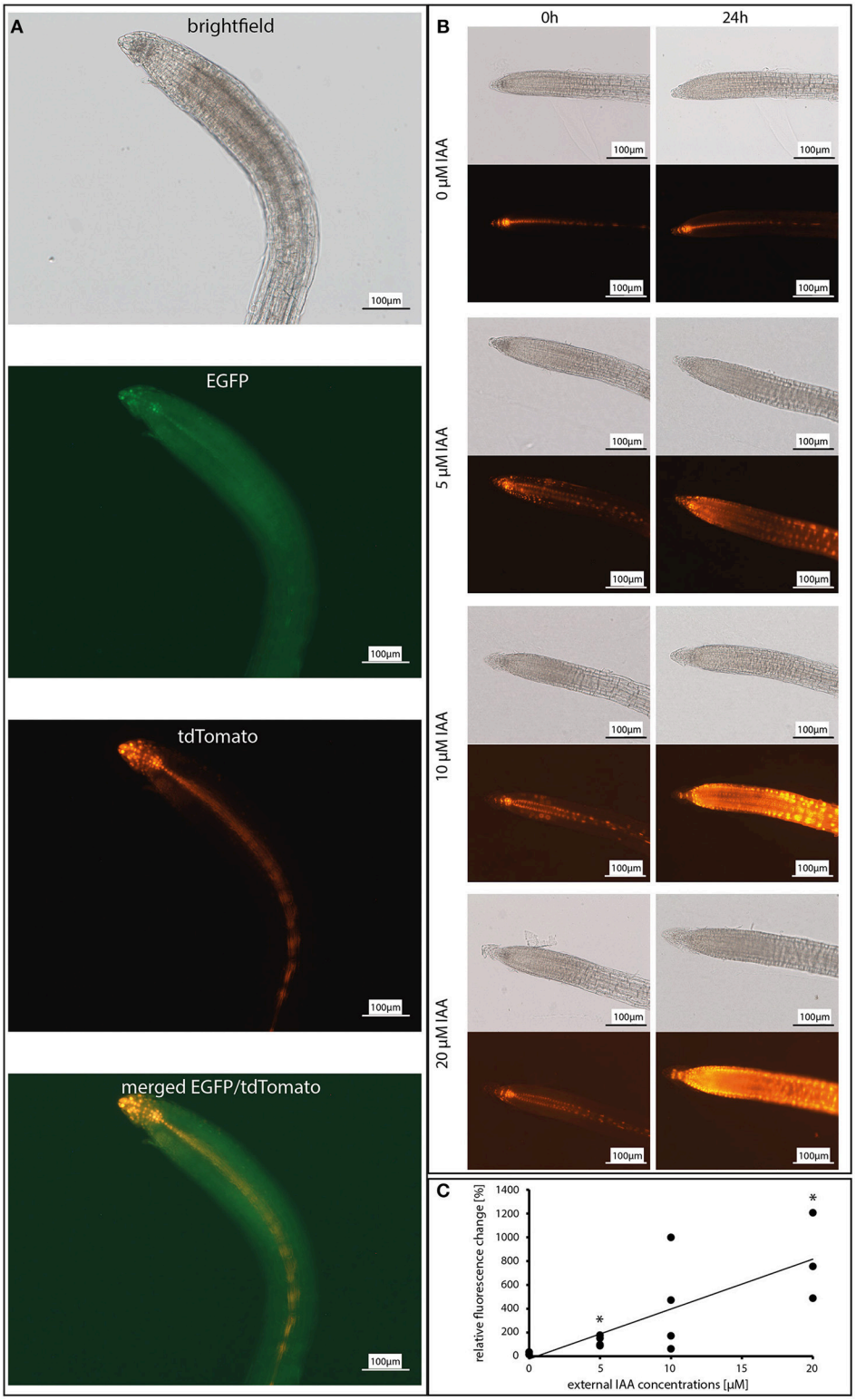

FIGURE 2 | Dose-response curve of the reporter construct *DR5::EGFP-DR5v2::tdTomato* in response to incubation with 0, 5, 10, and 20 µM IAA (indole-3-acetic acid). **(A)** Co-localization of the *EGFP* and *tdTomato* expression in 12 day-old *A. thaliana* roots. Shown are the brightfield image, GFP channel (for EGFP), DS red channel (for tdTomato), and a merged image of the GFP and the DS red channel. **(B)** Fluorescence images of the tdTomato signal after 0 and 24 h. **(C)** Graphic presentation of the relative fluorescence change in response to exogenous IAA concentrations ($n = 3$–4). Asterisks indicate significant differences to 0 µM IAA ($p < 0.05$).

Live Imaging of Root Infection Reveals Fungus-Specific Redistribution of Auxin Maxima in *A. thaliana*

The auxin response was monitored over 24 h after spore application to the roots by measuring the fluorescence emitted from the DR5v2::tdTomato reporter using light sheet fluorescence microscopy (**Figures 1B**, **3A,B**). Representative pictures from the movies (**Supplementary Videos S1**–**S5**) are shown in **Figure 3A**. **Figure 3B** shows quantified fluorescence signals of the entire roots and of the root tip separately. Without spores, the tdTomato-derived fluorescence displayed initially a stable signal in the quiescent center, columella, pericycle and vascular system (**Figure 3A**). After 10–12 h, the overall fluorescence in the entire root increased. In the root tip, we observed a continuous decrease of the fluorescence (see **Figure 3B**), while the fluorescence from cells located in the elongation zone and from rhizodermal cells increased. The measurements were stopped after 24 h because the reporter system showed the first bleaching symptoms at the root tip.

Application of spores from *P. indica* led to an almost linear increase of the fluorescence in the entire root which started after a lag phase of ∼1 h. Most of the fluorescence was emitted from cells of the basal meristem and the transition zone. Furthermore, the decrease of the fluorescence emitted from the root tip, which was observed for uncolonized roots, was stopped. This clearly indicates that signals from *P. indica* activate the auxin-responsive reporter gene in Arabidopsis roots.

A quite different scenario was observed for *M. hyalina*. The overall emission from the entire root remained almost constant over the measuring period (<20% decrease over the 24 h period), indicating that the fungus inhibits the stimulation which is observed for uncolonized and *P. indica*-colonized roots (more than 70% increase over the 24 h period). Furthermore, after initial stimulation of the fluorescence emission, the activity also declines at the root tip, similar to the decline observed for the uncolonized control. These results demonstrate that *M. hyalina* prevents the activation of the reporter gene.

The two pathogenic fungi *A. brassicicola* and *V. dahliae* showed almost identical effects on the expression of the reporter gene, although the first fungus is a necrotroph and the second a biotroph. A few hours after spore application the fluorescence in the roots and root tips completely disappeared. Thus, signals from the fungi very likely inhibit the activation of the reporter gene.

In summary, compared to uncolonized roots, *P. indica* stimulated and the pathogens inhibited the expression of the reporter gene. Besides an initial positive effect on the root tip, the reporter gene activity is not altered by *M. hyalina*.

Phytohormone Levels in Colonized *A. thaliana* Roots

The phytohormone levels in Arabidopsis roots are strongly influenced by the 24 h incubation period with the different fungi (**Figure 4**). Compared to the uncolonized control, the IAA level in *P. indica-*, *M. hyalina-*, and *A. brassicicola*-colonized roots increased, whereas *V. dahliae* colonization had no effect. Interestingly, co-cultivation with *M. hyalina* resulted in the highest stimulation of the IAA level (∼4-fold stimulation); *P. indica* and *A. brassicicola* showed a similar, but lower induction (∼3-fold stimulation). These results are not consistent with expression data of the auxin reporter gene (**Figures 2**, **3**).

However, quantification of the amounts of the defense-related phytohormones revealed that only *M. hyalina*, but not the other three fungi, stimulated the accumulation of the jasmonates JA and JA-Ile. In addition to *M. hyalina,* the JA precursor 12-oxophytodienoic acid (OPDA) showed a low, however significant increase after infection with *P. indica* and *V. dahliae*. The only other significant alteration induced by any of the fungi was a slight stimulation of the SA level in *P. indica*-infected roots. These results suggest the jasmonates play an important role during the early phase in the *M. hyalina*/Arabidopsis interaction, and that the sharp decline in the reporter gene expression in response to the two pathogens is probably not directly caused by the phytohormones but by factors influencing the cell fate in the symbiotic roots (cf. section Discussion).

Phytohormone Levels in the Fungal Mycelia

To investigate whether the observed differences in the regulation of the reporter gene in Arabidopsis roots are caused by differences in fungal auxin levels, the phytohormone concentrations were measured in the mycelia. Strikingly, the IAA contents in the four fungi varied tremendously. The highest level was found in *P. indica*, *M. hyalina* contained ∼5 times less auxin, and the levels in the two pathogens was quite low (**Figure 5**). We also measured the amounts of the stress related JA, SA and abscisic acid. None of the mycelia contained JA and JA-Ile (data not shown). The lowest SA level was found in *M. hyalina*. *P. indica* contained twice as much and the pathogens 6–7 times more SA than *M. hyalina*. No abscisic acid was found in the two beneficial fungi, while the pathogens contained comparable levels (**Figure 5**). Taken together, the auxin levels that were detectable in the mycelia were consistent with the regulation of the auxin-responsive reporter gene in Arabidopsis roots.

Jasmonate Impairs *DR5*::*EGFP-DR5v2*::*tdTomato* Fluorescence

Due to the elevated jasmonate contents found during the *M. hyalina*/Arabidopsis interaction (**Figure 4**), the question arose whether jasmonates can affect the expression of the auxin reporter gene. Therefore, roots of 12 day-old *DR5*::*EGFP-DR5v2*::*tdTomato* seedlings were incubated with increasing JA concentrations for 24 h and the fluorescence was monitored. Incubation with 1 and 5 μM JA resulted in a stable but decreased tdTomato fluorescence intensity compared to control samples (**Figures 6A,B**). Application of 10 μM JA showed the significantly highest detectable loss of fluorescence (∼20%) in the roots, supporting the hypothesis that increased JA levels during early *M. hyalina*/Arabidopsis interaction impede the activation of the IAA-responsive reporter construct.

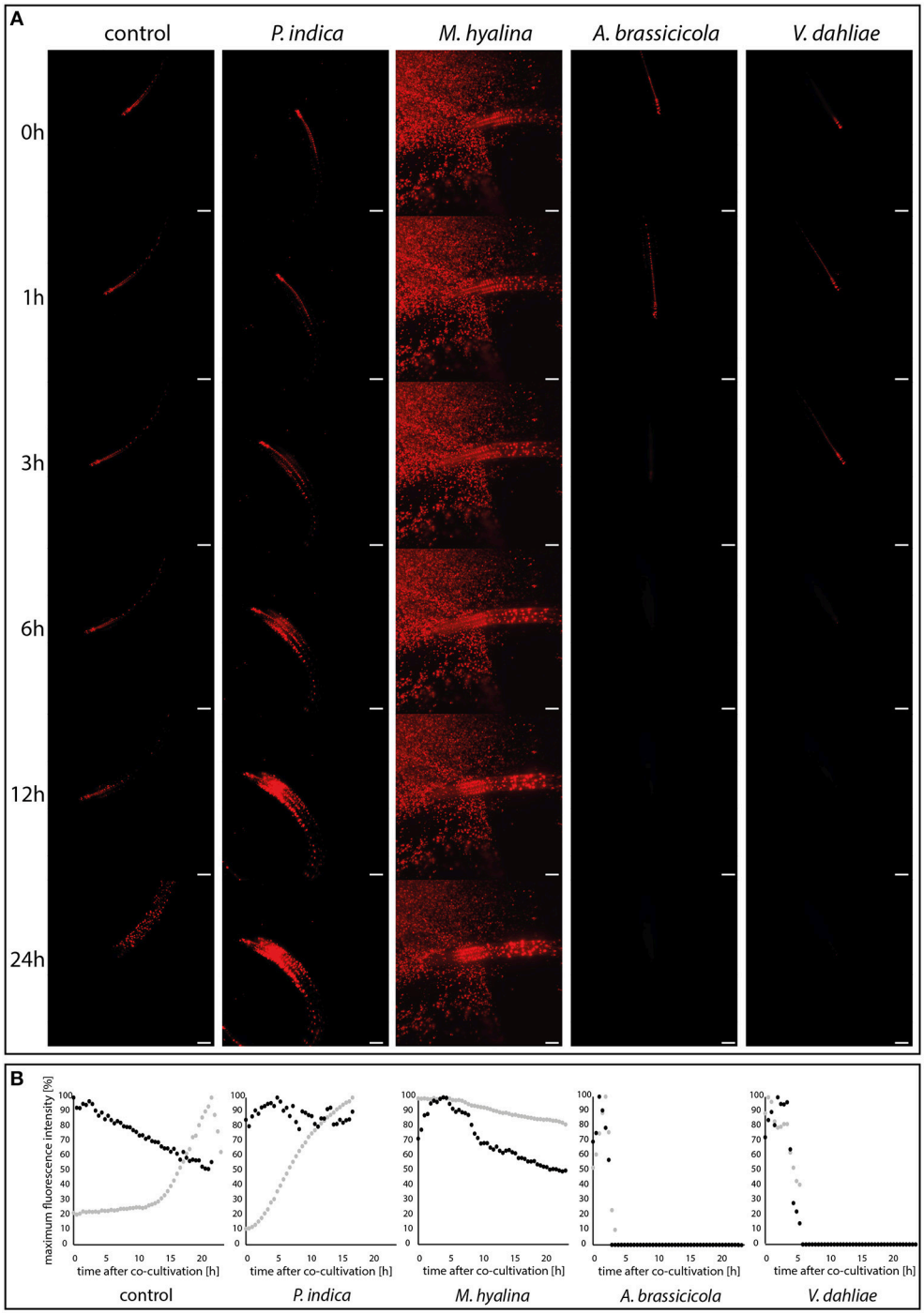

FIGURE 3 | Visualization of auxin maxima using the reporter construct *DR5::EGFP-DR5v2::tdTomato* during plant-fungus interaction. **(A)** Light sheet images of 24 h-recordings of control and co-cultivation with spore solutions of *P. indica*, *M. hyalina, A. brassicicola,* and *V. dahliae*. Scale bar = 200 μm. Background fluorescence in *M. hyalina* co-culture is due to autofluorescence of spores. **(B)** Quantification curves of fluorescence maxima of each co-culture in a time-dependent manner. Black dots, root tip; gray dots, whole root ($n = 3$).

P. indica Induces the Formation of Lateral Root Primordia

The former results suggest that only *P. indica* can initiate processes which may result in the promotion of root development within the 24 h of experimentation. In accordance with this idea, we found that the initiation of lateral root primordia was stimulated by *P. indica* but not by *M. hyalina* (**Figure 7**).

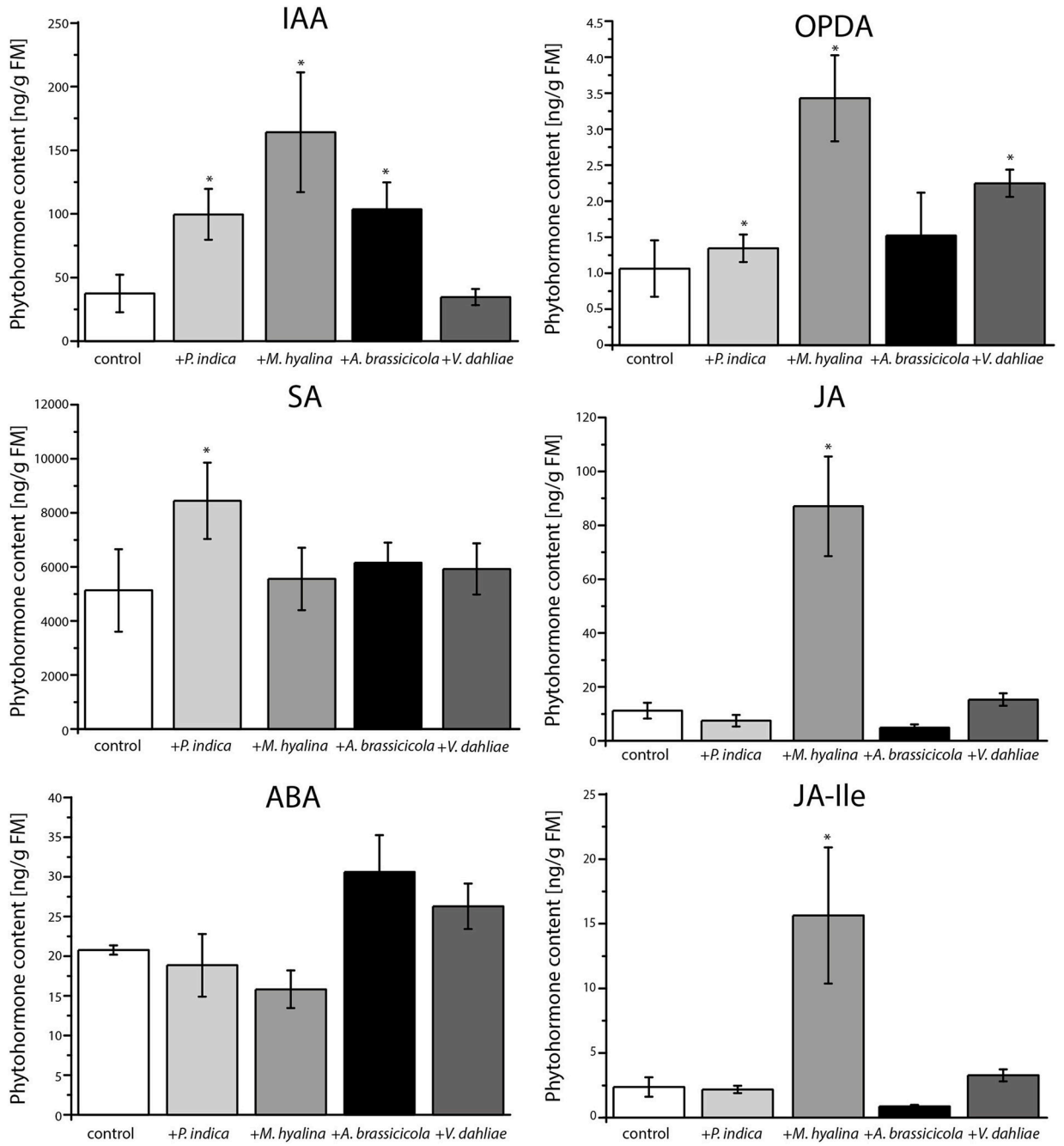

FIGURE 4 | Phytohormone measurements of *A. thaliana* roots after one day of co-cultivation with *P. indica*, *M. hyalina, A. brassicicola,* and *V. dahliae*. (IAA, indole-3-acetic acid; ABA, abscisic acid; SA, salicylic acid; JA, jasmonic acid; OPDA, 12-oxophytodienoic acid (*cis* and *trans*); JA-Ile, jasmonoyl-isoleucine conjugate). Asterisks mark statistically significant differences against control treatment ($n = 8$; $^*p < 0.05$) as determined by one–way ANOVA followed by Tukey's test.

DISCUSSION

Expression of Auxin Reporter Is Dose-Dependent in Arabidopsis Roots

Liao et al. (2015) demonstrated that the auxin reporter construct *DR5*::*EGFP-DR5v2*::*tdTomato* induced a dose- and time-dependent fluorescence development as well as IAA-induced gene expression when Arabidopsis plants are treated with 0.0001–1.0 μM IAA. The construct was used to monitor the auxin level in different tissues of transformed *A. thaliana, P. tremula* × *alba, H. vulgare,* and *N. benthamiana* plants (Hilbert et al., 2012; Chen et al., 2013; Liao et al., 2015; Kirbis, 2017). A previous study showed that the EGFP signal was relatively low compared to the tdTomato signal (Kirbis, 2017). We

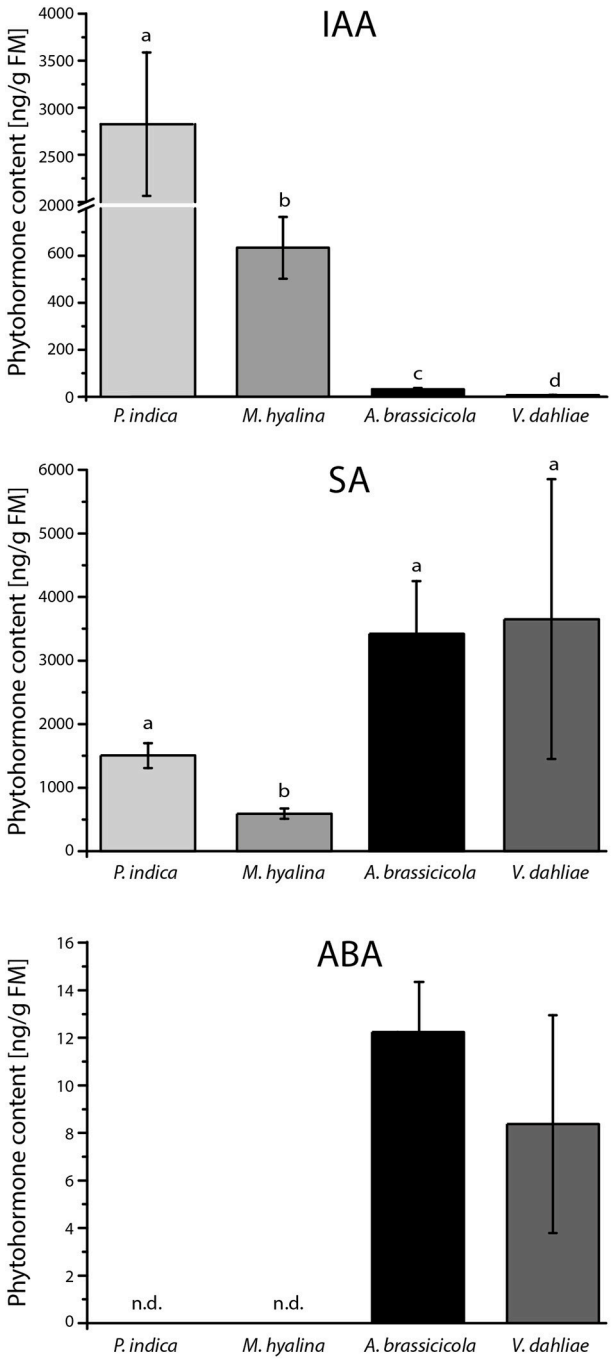

FIGURE 5 | Phytohormone content of mycelia from *P. indica* cultivated on Kaefer's medium for three weeks and *M. hyalina, A. brassicicola,* and *V. dahliae* grown for 2 weeks on potato dextrose agar medium (IAA, indole-3-acetic acid; ABA, abscisic acid; SA, salicylic acid). Statistically significant differences between all fungal species were analyzed using one–way ANOVA. Different letters indicate significant differences among groups for $p < 0.05$, determined by Tukey's test ($n = 3$).

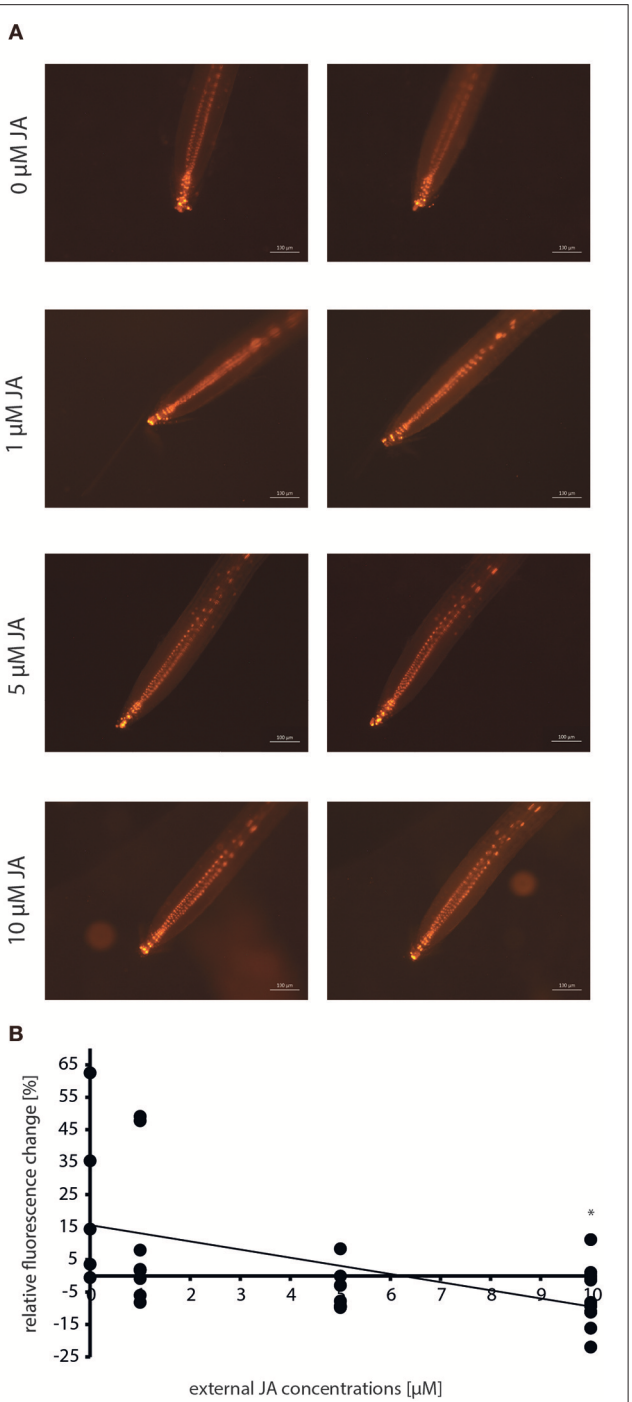

FIGURE 6 | Dose-response curve of the reporter construct *DR5::EGFP-DR5v2::tdTomato* in response to incubation with 0, 1, 5, and 10 µM JA (jasmonic acid) before and after 24 h. **(A)** Fluorescence images of the tdTomato signal after 0 and 24 h. **(B)** Graphic presentation of the relative fluorescence change in response to exogenous JA concentrations ($n = 6$–10). Asterisks indicate significant differences to 0 µM JA ($p < 0.05$).

observed the same for fungus-exposed and control Arabidopsis roots but did not observe differences in the expression for the two reporters (**Figure 2A**). Due to better resolution, we used the tdTomato fluorescence (**Figures 2A,B**) for our study and demonstrate that the expression is dose-dependent and shows expression in tissues and cells which are known to be

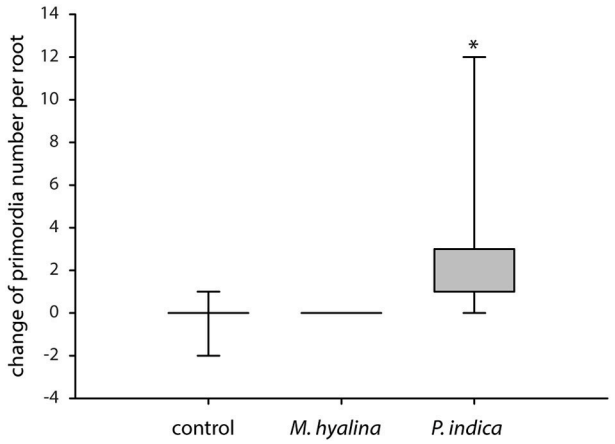

FIGURE 7 | Measurement of lateral root primordia induction in *A. thaliana* after 1 day of co-cultivation with *M. hyalina* and *P. indica.* Graphical illustration of the absolute change of primordia number. The asterisk mark statistical significant differences against control and *M. hyalina* treatment ($n = 5$–7; $^*p < 0.05$).

involved in root growth (**Figures 2B,C**). With an increase in the applied IAA concentration, the fluorescence appeared also in tissues which are located shootwards of the elongation zone in the roots. The expression pattern matches known polar auxin transport mechanisms where IAA is translocated to the root apex and toward the root–shoot junction (Bennett et al., 1998; Reed et al., 1998; Rashotte et al., 2000; Casimiro et al., 2001). Therefore, the construct was used to monitor rapid changes in the auxin distribution in Arabidopsis roots in response to different root-interacting fungi.

P. indica, but Not *M. hyalina* and the Pathogenic Fungi Activate the *DR5v2* Promoter in Arabidopsis Roots

The endophytic fungus *P. indica* promotes the growth of *A. thaliana* by enhancing both root and shoot biomass production (Peškan-Berghöfer et al., 2004; Camehl et al., 2011; Lee et al., 2011; Das et al., 2012). In Chinese cabbage it was demonstrated that colonization by *P. indica* also strongly enhances lateral root development (Lee et al., 2011; Dong et al., 2013). It is known that auxin plays a role in the beneficial interaction and that the fungus produces auxin and auxin precursors which interfere with hormones inside the plant (Sirrenberg et al., 2007; Vadassery et al., 2008; Hilbert et al., 2012; Xu et al., 2018). The auxin reporter was utilized to analyze the auxin kinetic in the early infection stages of *P. indica*-colonized roots as well as in roots colonized by *M. hyalina*, *A. brassicicola* and *V. dahliae* (**Figure 3**). Colonization with *P. indica* showed a strong, 10-fold increase in fluorescence in the entire root while the expression at the root tip stayed at a rather constant level (**Figure 3B**). Already 3 h after co-culture, the increase in the fluorescence (**Figure 3A**) indicates a higher amount of available IAA in the root tissue, which may be provided by the fungus or is produced by the plant. A similar (but only 3-fold) elevation of free IAA was observed in barley roots co-cultured with *P. indica* for 3 d (Hilbert et al., 2012). At later time points (5 and 14 days after infection) this effect was gone in barley which was also observed for Arabidopsis seedlings where the IAA level in colonized seedlings was not different from uncolonized controls 7, 10 and 14 days after infection (Vadassery et al., 2008; Hilbert et al., 2012). Our data suggests that *P. indica* induces a rapid increase in auxin levels during early recognition phases which might be crucial for reprogramming root development. Initiation of the formation of lateral root primordia can already be detected 24 h after co-cultivation with *P. indica*, but not with *M. hyalina* (**Figure 7**).

Phytohormones controlling the development of colonized roots can be of fungal or plant origin. Hilbert et al. (2012) showed that indole derivative production by *P. indica* is not required for growth promotion but for biotrophic colonization of barley roots. In other symbiotic interactions, promotion of root or plant growth was proposed to be caused by microbial phytohormones—in particular auxin (e.g., Contreras-Cornejo et al., 2009; Dudeja et al., 2012; Khan et al., 2014; Lee et al., 2015; Liao et al., 2017, and references therein). The examples demonstrate that fungal auxin or metabolites which can be converted to auxin in the plant, participate in growth regulatory effects in the host. Apparently, phytohormones that are active in the roots can be of either plant or microbial origin. Which one of the two sources might play a more important role in the symbiotic interaction and how these processes are related to circuits, which manipulate plant's phytohormone metabolism and function is probably symbiosis-specific.

M. hyalina did not induce such an auxin increase in the entire root during the first 24 h of co-culture, in fact, the level even decreased slightly about 20% (**Figure 3B**). Five h after co-cultivation, the fluorescence at the root tip increased by 30% and decreased again afterwards to half of the initial level. The initial increase in fluorescence during the recognition of the fungus by the plant could be caused by fungus-derived auxin which is later on stopped by other processes (cf. below). These results match the phenotype observed for *M. hyalina*-colonized Arabidopsis seedlings: we did not observe any significant increase in the root biomass while the aerial parts of the colonized seedlings became bigger (Johnson et al., 2018b).

In contrast, the fluorescence in the entire root decreased in response to the two pathogenic fungi *V. dahliae* and *A. brassicicola* after short periods of co-cultivation (**Figure 3A**). For *V. dahliae*, this was unexpected since it is well known that its interaction starts with a biotrophic phase associated with the stimulation of growth which is followed by a necrotrophic phase later on (Schnathorst, 1981; Reusche et al., 2014; Cho, 2015). In the *A. brassicicola* co-culture, the fluorescence was no longer detectable after 3 h while *V. dahliae*-infected plants lost the fluorescence ∼6 h after co-cultivation (**Figure 3B**). This is accompanied by visible destruction of plant tissue and the root tip (data not shown). Both pathogens colonized the roots rapidly. For *V. dahliae*, the roots were covered with conidia already 6 h after infection (Zhao et al., 2014). Downregulation of the auxin response is

likely caused by toxic effects: *V. dahliae* produces different phytotoxins and other molecules that induce the hosts' cell death associated with the degradation of host tissue (Fradin and Thomma, 2006). *A. brassicicola* produces the AB-toxin which is released by the germinating spores on host tissue (Oka et al., 2005).

M. hyalina Induces Jasmonate and *P. indica* SA Accumulation in the Host Roots

Arabidopsis plants respond to colonization by different fungi with the accumulation of different phytohormones. Beneficial fungi like *P. indica* often induce SA, while necrotrophic fungi induce jasmonates (Schäfer et al., 2009; Sun et al., 2014; Johnson et al., 2018b; Scholz et al., 2018; Vahabi et al., 2018; Xu et al., 2018). To analyze whether the observed IAA-induced fluorescence changes during root colonization (**Figure 3**) are exclusively mediated by auxin changes or whether other phytohormones might also be involved, we measured the phytohormone profiles in the roots (**Figure 4**). Compared to uncolonized control roots, both beneficial fungi showed a significant accumulation of IAA within the first 24 h of co-culture. For later time points, quite different results for IAA accumulation were reported for *P. indica*-colonized roots (Vadassery et al., 2008; Lee et al., 2011; Hilbert et al., 2012; Hua et al., 2017). *M. elongata*-colonized maize roots and *M. alpina*-colonized *Crocus sativus* L. plants also showed significantly elevated IAA contents (Wani et al., 2017; Li et al., 2018). However, expression of auxin-responsive genes has never been investigated at the early time points studied here (**Figure 3**). Apparently, although *P. indica* and *M. hyalina* colonization results in the accumulation of auxin, the outcome is quite different. While *P. indica* induces fluorescence, *M. hyalina* does not. This suggests that auxin in the *M. hyalina*-colonized roots cannot (fully) activate the downstream IAA signaling cascade. A possible explanation could be that IAA signaling is antagonistically regulated by other hormones or elicitors.

Furthermore, *V. dahliae* did not induce IAA accumulation in Arabidopsis roots which matches the observed fluorescence. However, the IAA increase was similar for *A. brassicicola* and *P. indica*, although the pathogen did not induce the fluorescence from the auxin reporter (**Figure 3**). Similar observations were made in previous studies (Qi et al., 2012; Riet et al., 2016). This might be due to the rapidly induced cell death by the fast growing pathogen and its release of toxins. The importance of auxins for resistance against different pathogens has been repeatedly demonstrated: For instance, auxin biosynthesis defective mutants are more susceptible to *A. brassicicola* infection compared to wild-type plants (Bari and Jones, 2009; Kazan and Manners, 2009; Qi et al., 2012). Furthermore, *A. brassicicola* infection leads to the degradation of AUX/ IAA proteins indicating that the fungus activates the auxin signal transduction pathway (Qi et al., 2012). Since the hormone data in previous studies were measured for entire roots or even plants, it is difficult to compare them with locally occurring infections and generation of auxin maxima.

Recent studies have demonstrated an antagonistic crosstalk between IAA and SA, which in turn regulates plants' resistance to different fungi. It has been hypothesized that downregulation of auxin signaling is part of the SA-mediated disease-resistance mechanism (Navarro et al., 2006; Chen et al., 2007; Wang et al., 2007; Kazan and Manners, 2009). Our analysis of the SA content of colonized roots is consistent with this assumption, since roots with high IAA content did not show a strong accumulation of SA upon fungal infection at least with *A. brassicicola* and *M. hyalina* (**Figure 4**). However, *P. indica*-colonized roots showed a small increase in both—IAA and SA levels; the latter was also observed in our previous studies (Sun et al., 2014; Vahabi et al., 2018). This seemingly contradiction was addressed in a previous study showing that SA does not directly affect the IAA concentration but the auxin-dependent signaling (Wang et al., 2007). Colonization by *M. hyalina* did not result in elevated SA levels as already shown by Johnson et al. (2018b). The two pathogenic fungi did not induce SA. Similar results were obtained in previous studies where SA content was not elevated and SA mutants did not show a different susceptibility (Botanga et al., 2012; Sun et al., 2014; Scholz et al., 2018). Apparently, significant amounts of SA accumulate only during early phases of the *P. indica*/Arabidopsis interaction.

The class of jasmonates is mainly induced by wounding of plant tissue and plays a major role in defense against necrotrophic fungi (Thaler et al., 2004; Kachroo and Kachroo, 2009; Acosta and Farmera, 2010). Our study revealed that after 24 h of co-culture, the JA and JA-Ile contents were not significantly up-regulated in the roots colonized by the two pathogens (**Figure 4**). A previous study with *V. dahliae* showed the same result (Scholz et al., 2018), although a precursor of JA, OPDA, was stimulated by *V. dahliae*. In this study, we could not distinguish between the active *cis*- and inactive *trans*-OPDA, so a statement about the relevance of this JA precursor would not be appropriate. Interestingly, there was a clear difference in the induction of jasmonates between the two beneficial fungi. While *P. indica*-colonized roots contained the same levels of JA and JA-Ile as the uncolonized control roots, *M. hyalina* colonization resulted in a significant increase in the OPDA (3-fold), JA and JA-Ile levels (8-fold) (**Figure 4**). This appears to be restricted to the early recognition phase of the two partners, since we did not detect an increase of jasmonates in *M. hyalina*-colonized plants during later time points (Johnson et al., 2018b). A recent study in Arabidopsis indicated that JA interferes with auxin signaling independent of the JA-receptor complex COI1. The expression of auxin-inducible genes and lateral rooting is inhibited in Arabidopsis seedlings treated with JA (Ishimaru et al., 2018). These findings are supported by our experiment showing that the incubation with increasing concentrations of JA impairs the expression of the IAA-responsive reporter construct (**Figures 6A,B**) in spite of the presence of elevated IAA levels in *M. hyalina* colonized roots (**Figure 4**). Finally, although ABA is involved in plant defense (**Figure 4**), we did not find a significant accumulation of this hormone during the early phase of interaction for any of the four fungi with Arabidopsis roots.

The crosstalk of phytohormones during recognition and early phases of plant/fungus interaction is not well understood

and most studies focus on defense-related hormones. The presented results and measuring techniques open new research fields, which will shine more light on the first steps in symbiotic interactions.

DATA AVAILABILITY

All datasets generated for this study are included in the manuscript and/or the supplementary files.

AUTHOR CONTRIBUTIONS

AKM, AF, SS, and RO designed the experiments. AKM, AF, SÖ, and MA-T performed the experiments. AKM, AF, and MA-T analyzed the data. VG and BH provided and assisted with the light sheet microscope. AK, TL, and GT generated and provided the transgenic seed material. AKM, AF, SS, AM, and RO wrote the manuscript with contributions from all authors.

ACKNOWLEDGMENTS

We thank Frank Müller and Daniel Veit for technical and Anindya Majumder for experimental support. The research was supported by the CRC1127 to SS and RO; AKM was supported by the International Max Planck Research School and MA-T by the Alexander von Humboldt Foundation.

SUPPLEMENTARY MATERIAL

The Supplementary Material for this article can be found online at: https://www.frontiersin.org/articles/10.3389/fmicb.2019.00380/full#supplementary-material

Supplementary Video S1 | Visualization of auxin maxima using the reporter construct *DR5::EGFP-DR5v2::tdTomato* during plant-fungus interaction. Light sheet videos of 17 h-recordings of control without addition of fungal spores.

Supplementary Video S2 | Visualization of auxin maxima using the reporter construct *DR5::EGFP-DR5v2::tdTomato* during plant-fungus interaction. Light sheet video of 17 h-recording of co-cultivation with *P. indica* spore solution.

Supplementary Video S3 | Visualization of auxin maxima using the reporter construct *DR5::EGFP-DR5v2::tdTomato* during plant-fungus interaction. Light sheet video of 17 h-recording of co-cultivation with *M. hyalina* spore solution. Background fluorescence in *M. hyalina* co-culture is due to autofluorescence of spores.

Supplementary Video S4 | Visualization of auxin maxima using the reporter construct *DR5::EGFP-DR5v2::tdTomato* during plant-fungus interaction. Light sheet video of 17 h-recording of co-cultivation with *A. brassicicola* spore solution.

Supplementary Video S5 | Visualization of auxin maxima using the reporter construct *DR5::EGFP-DR5v2::tdTomato* during plant-fungus interaction. Light sheet video of 17 h-recording of co-cultivation with *V. dahliae* spore solution.

REFERENCES

Acosta, I. F., and Farmer, E. E. (2010). Jasmonates. *Arabidopsis Book* 8:e0129. doi: 10.1199/tab.0129

Almeida Trapp, M., De Souza, G. D., Rodrigues-Filho, E., Boland, W., and Mithöfer, A. (2014). Validated method for phytohormone quantification in plants. *Front. Plant Sci.* 5:417. doi: 10.3389/fpls.2014.00417

Bari, R., and Jones, J. D. (2009). Role of plant hormones in plant defence responses. *Plant Mol. Biol.* 69, 473–488. doi: 10.1007/s11103-008-9435-0

Bennett, M. J., Marchant, A., May, S. T., and Swarup, R. (1998). Going the distance with auxin: unravelling the molecular basis of auxin transport. *Philos. Trans. R Soc. Lond. B Biol. Sci.* 353, 1511–1515. doi: 10.1098/rstb.1998.0306

Bhalerao, R. P., Eklöf, J., Ljung, K., Marchant, A., Bennett, M., and Sandberg, G. (2002). Shoot-derived auxin is essential for early lateral root emergence in Arabidopsis seedlings. *Plant J.* 29, 325–332. doi: 10.1046/j.0960-7412.2001.01217.x

Bolton, M. D., van Esse, H. P., Vossen, J. H., de Jonge, R., Stergiopoulos, I., Dekker, H. L., et al. (2008). The novel *Cladosporium fulvum* lysin motif effector Ecp6 is a virulence factor with orthologues in other fungal species. *Mol. Microbiol.* 69, 119–136. doi: 10.1111/j.1365-2958.2008.06270.x

Botanga, C. J., Bethke, G., Chen, Z., Gallie, D. R., Fiehn, O., and Glazebrook, J. (2012). Metabolite profiling of Arabidopsis inoculated with *Alternaria brassicicola* reveals that ascorbate reduces disease severity. *Mol. Plant Microbe Interact.* 12, 1628–1638. doi: 10.1094/MPMI-07-12-0179-R

Calderon-Villalobos, L. I., Tan, X., Zheng, N., and Estelle, M. (2010). Auxin perception—structural insights. *Cold Spring Harb. Perspect. Biol.* 2:a005546. doi: 10.1101/cshperspect.a005546

Camehl, I., Drzewiecki, C., Vadassery, J., Shahollari, B., Sherameti, I., Forzani, C., et al. (2011). The OXI1 kinase pathway mediates *Piriformospora indica*-induced growth promotion in Arabidopsis. *PLoS Pathog.* 7:e1002051. doi: 10.1371/journal.ppat.1002051

Casimiro, I., Marchant, A., Bhalerao, R. P., Beeckman, T., Dhooge, S., Swarup, R., et al. (2001). Auxin transport promotes Arabidopsis lateral root initiation. *Plant Cell* 13, 843–852. doi: 10.1105/tpc.13.4.843

Chen, Y., Yordanov, Y. S., Ma, C., Strauss, S., and Busov, V. B. (2013). DR5 as a reporter system to study auxin response in Populus. *Plant Cell Rep.* 32, 453–463. doi: 10.1007/s00299-012-1378-x

Chen, Z., Agnew, J. L., Cohen, J. D., He, P., Shan, L., Sheen, J., et al. (2007). *Pseudomonas syringae* type III effector AvrRpt2 alters *Arabidopsis thaliana* auxin physiology. *Proc. Natl. Acad. Sci. U.S.A.* 104, 20131–20136. doi: 10.1073/pnas.0704901104

Cho, Y. (2015). How the necrotrophic fungus *Alternaria brassicicola* kills plant cells remains an enigma. *Eukaryot. Cell* 14, 335–344. doi: 10.1128/EC.00226-14

Contreras-Cornejo, H. A., Macías-Rodríguez, L., Cortés-Penagos, C., and López-Bucio, J. (2009). Trichoderma virens, a plant beneficial fungus, enhances biomass production and promotes lateral root growth through an auxin-dependent mechanism in Arabidopsis. *Plant Physiol.* 149, 1579–1592. doi: 10.1104/pp.108.130369

Das, A., Kamal, S., Shakil, N. A., Sherameti, I., Oelmüller, R., Dua, M., et al. (2012). The root endophyte fungus *Piriformospora indica* leads to early flowering, higher biomass and altered secondary metabolites of the medicinal plant, *Coleus forskohlii*. *Plant Signal. Behav.* 7, 103–112. doi: 10.4161/psb.7.1.18472

de Jonge, R., Bolton, M. D., and Thomma, B. P. H. J. (2011). How filamentous pathogens co-opt plants: the ins and outs of fungal effectors. *Curr. Opin. Plant Biol.* 14, 400–406. doi: 10.1016/j.pbi.2011.03.005

de Jonge, R., and Thomma, B. P. H. J. (2009). Fungal LysM effectors: extinguishers of host immunity? *Trends Microbiol.* 17, 151–157. doi: 10.1016/j.tim.2009.01.002

de Jonge, R., van Esse, H. P., Kombrink, A., Shinya, T., Desaki, Y., Bours, R., et al. (2010). Conserved fungal LysM effector Ecp6 prevents chitin-triggered immunity in plants. *Science* 329, 953–955. doi: 10.1126/science.1190859

De Rybel, B., Adibi, M., Breda, A. S., Wendrich, J. R., Smit, M. E., Novák, O., et al. (2014). Plant development. Integration of growth and patterning during vascular tissue formation in Arabidopsis. *Science* 345:1255215. doi: 10.1126/science.1255215

Dharmasiri, N., Dharmasiri, S., and Estelle, M. (2005). The F-box protein TIR1 is an auxin receptor. *Nature* 435, 441–445. doi: 10.1038/nature03543

Dombrecht, B., Xue, G. P., Sprague, S. J., Kirkegaard, J. A., Ross, J. J., Reid, J. B., et al. (2007). MYC2 differentially modulates diverse jasmonate-dependent functions in Arabidopsis. *Plant Cell* 19, 2225–2245. doi: 10.1105/tpc.106.048017

Dong, S., Tian, Z., Chen, P. J., Senthil Kumar, R., Shen, C. H., Cai, D., et al. (2013). The maturation zone is an important target of *Piriformospora indica* in Chinese cabbage roots. *J. Exp. Bot*. 64, 4529–4540. doi: 10.1093/jxb/ert265

Dudeja, S. S., Giri, R., Saini, R., Suneja-Madan, P., and Kothe, E. (2012). Interaction of endophytic microbes with legumes. *J. Basic Microbiol.* 52, 248–260. doi: 10.1002/jobm.201100063

Fradin, E. F., and Thomma, B. P. (2006). Physiology and molecular aspects of Verticillium wilt diseases caused by *V. dahliae* and *V. albo-atrum*. *Mol. Plant Pathol.* 7, 71–86. doi: 10.1111/j.1364-3703.2006.00323.x

Fukaki, H., and Tasaka, M. (2009). Hormone interactions during lateral root formation. *Plant Mol. Biol.* 69, 437–449. doi: 10.1007/s11103-008-9417-2

Gijzen, M., and Nürnberger, T. (2006). Nep1-like proteins from plant pathogens: recruitment and diversification of the NPP1 domain across taxa. *Phytochemistry* 67, 1800–1807. doi: 10.1016/j.phytochem.2005.12.008

Gutjahr, C., Riemann, M., Müller, A., Düchting, P., Weiler, E. W., and Nick, P. (2005). Cholodny-Went revisited: a role for jasmonate in gravitropism of rice coleoptiles. *Planta* 222, 575–585. doi: 10.1007/s00425-005-0001-6

Hentrich, M., Böttcher, C., Düchting, P., Cheng, Y., Zhao, Y., Berkowitz, O., et al. (2013). The jasmonic acid signaling pathway is linked to auxin homeostasis through the modulation of YUCCA8 and YUCCA9 gene expression. *Plant J.* 74, 626–637 doi: 10.1111/tpj.12152

Hilbert, M., Voll, L. M., Ding, Y., Hofmann, J., Sharma, M., and Zuccaro, A. (2012). Indole derivative production by the root endophyte *Piriformospora indica* is not required for growth promotion but for biotrophic colonization of barley roots. *New Phytol.* 196, 520–534. doi: 10.1111/j.1469-8137.2012.04275.x

Hoffmann, M., Hentrich, M., and Pollmann, S. (2011). Auxin-oxylipin crosstalk: relationship of antagonists. *J. Integr. Plant Biol.* 53, 429–444. doi: 10.1111/j.1744-7909.2011.01053.x

Hua, M. S., Kumar, R. S., Shyur, L. F., Cheng, Y. B., Tian, Z., Oelmüller, R., et al. (2017). Metabolomic profiles delineate symbiotic functions of the root endophytic fungus *Piriformospora indica* colonizing Chinese cabbage roots. Sci. *Rep*. 7:9291. doi: 10.1038/s41598-017-08715-2

Huang, H., Liu, B., Liu, L., and Song, S. (2017). Jasmonate action in plant growth and development. *J. Exp. Bot*. 68, 1349–1359. doi: 10.1093/jxb/erw495

Ishimaru, Y., Hayashi, K., Suzuki, T., Fukaki, H., Prusinska, J., Meester, C., et al. (2018). Jasmonic acid inhibits auxin-induced lateral rooting independently of the CORONATINE INSENSITIVE1 receptor. *Plant Physiol.* 177, 1704–1716. doi: 10.1104/pp.18.00357

Johnson, J. M., Ludwig, A., Furch, A. C. U., Mithöfer, A., Scholz, S. S., Reichelt, M., et al. (2018b). The beneficial root-colonizing fungus *Mortierella hyalina* promotes the aerial growth of Arabidopsis and activates calcium-dependent responses which restrict *Alternaria brassicae*-induced disease development in roots. *Mol. Plant Microbe Interact.* doi: 10.1094/MPMI-05-18-0115-R

Johnson, J. M., Reichelt, M., Vadassery, J., Gershenzon, J., and Oelmüller, R. (2014). An Arabidopsis mutant impaired in intracellular calcium elevation is sensitive to biotic and abiotic stress. *BMC Plant Biol.* 14:162. doi: 10.1186/1471-2229-14-162

Johnson, J. M., Sherameti, I., Ludwig, A., Nongbri, P. L., Sun, C., Lou, B., et al. (2011). Protocols for *Arabidopsis thaliana* and *Piriformospora indica* co-cultivation - a model system to study plant beneficial traits. *Endocyt. Cell Res.* 21, 101–113.

Johnson, J. M., Thürich, J., Petutschnig, E. K., Altschmied, L., Meichsner, D., Sherameti, I., et al. (2018a). Poly(A) ribonuclease controls cellotriose-based interaction of *Piriformospora indica* and its host Arabidopsis. *Plant Physiol.* 176, 2496–2514. doi: 10.1104/pp.17.01423

Kachroo, A., and Kachroo, P. (2009). Fatty acid-derived signals in plant defense. *Ann. Rev. Phytopathol.* 47, 153–176. doi: 10.1146/annurev-phyto-080508-081820

Kazan, K., and Manners, J. M. (2009). Linking development to defense: auxin in plant-pathogen ineractions. *Trends Plant Sci.* 14, 373–382. doi: 10.1016/j.tplants.2009.04.005

Kepinski, S., and Leyser, O. (2005). The Arabidopsis F-box protein TIR1 is an auxin receptor. *Nature* 435, 446–451. doi: 10.1038/nature03542

Khan, A. L., Waqas, M., Kang, S. M., Al-Harrasi, A., Hussain, J., Al-Rawahi, A., et al. (2014). Bacterial endophyte *Sphingomonas* sp. LK11 produces gibberellins and IAA and promotes tomato plant growth. *J Microbiol.* 52, 689–95. doi: 10.1007/s12275-014-4002-7

Kirbis, A. (2017). *Monitoring Auxin Distribution in the Fruits of Lepidium and Aethionema Employing Transgenic Reporter Constructs*. Masterthesis, FSU, Jena.

Klosterman, S. J., Subbarao, K. V., Kang, S., Veronese, P., Gold, S. E., Thomma, B. P. H. J., et al. (2011). Comparative genomics yields insights into niche adaptation of plant vascular wilt pathogens. *PLoS Pathog.* 7:e1002137. doi: 10.1371/journal.ppat.1002137

Lee, K. E., Radhakrishnan, R., Kang, S. M., You, Y. H., Joo, G. J., Lee, I. J., et al. (2015). Enterococcus faecium LKE12 cell-free extract accelerates host plant growth via gibberellin and indole-3-acetic acid secretion. *J. Microbiol. Biotechnol.* 25, 1467–1475. doi: 10.4014/jmb.1502.02011

Lee, Y. C., Johnson, J. M., Chien, C. T., Sun, C., Cai, D., Lou, B., et al. (2011). Growth promotion of Chinese cabbage and Arabidopsis by *Piriformospora indica* is not stimulated by mycelium-synthesized auxin. *Mol. Plant Microbe Interact*. 24, 421–431. doi: 10.1094/MPMI-05-10-0110

Li, F., Chen, L., Redmile-Gordon, M., Zhang, J., Zhang, C., Ning, Q., et al. (2018). Mortierella elongata's roles in organic agriculture and crop growth promotion in a mineral soil. *Land Degrad. Dev*. 29, 1642–1651. doi: 10.1002/ldr.2965

Liao, C. Y., Smet, W., Brunoud, G., Yoshida, S., Vernoux, T., and Weijers, D. (2015). Reporters for sensitive and quantitative measurement of auxin response. *Nat. Methods* 12, 207–210. doi: 10.1038/nmeth.3279

Liao, X., Lovett, B., Fang, W., and St Leger, R. J. (2017). Metarhizium robertsii produces indole-3-acetic acid, which promotes root growth in Arabidopsis and enhances virulence to insects. *Microbiology* 163, 980–991. doi: 10.1099/mic.0.000494

Masucci, J. D., and Schiefelbein, J. W. (1994). The rhd6 mutation of *Arabidopsis thaliana* alters root-hair initiation through an auxin- and ethylene-associated process. *Plant Physiol.* 106, 1335–1346. doi: 10.1104/pp.106.4.1335

Masucci, J. D., and Schiefelbein, J. W. (1996). Hormones act downstream of TTG and GL2 to promote root hair outgrowth during epidermis development in the Arabidopsis root. *Plant Cell* 8, 1505–1517. doi: 10.1105/tpc.8.9.1505

Murashige, T., and Skoog, F. (1962). A revised medium for rapid growth and bioassay with tobacco cultures. *Physiol. Plant.* 15, 473–497. doi: 10.1111/j.1399-3054.1962.tb08052.x

Narayan, O. P., Verma, N., Singh, A. K., Oelmüller, R., Kumar, M., Prasad, D., et al. (2017). Antioxidant enzymes in chickpea colonized by *Piriformospora indica* participate in defense against the pathogen *Botrytis cinerea*. *Sci. Rep.* 7:13553. doi: 10.1038/s41598-017-12944-w

Naseem, M., Srivastava, M., Tehseen, M., and Ahmed, N. (2015). Auxin crosstalk to plant immune networks: a plant-pathogen interaction perspective. *Curr. Protein Pept. Sci.* 16, 389–394. doi: 10.2174/1389203716666150330124911

Navarro, L., Dunoyer, P., Jay, F., Arnold, B., Dharmasiri, N., Estelle, M., et al. (2006). A plant miRNA contributes to antibacterial resistance by repressing auxin signaling. *Science* 312, 436–439. doi: 10.1126/science.1126088

Oelmüller, R. (2018). Sensing environmental and developmental signals via cellooligomers. *J. Plant Physiol.* 229, 1–6. doi: 10.1016/j.jplph.2018.06.010

Oelmüller, R., Sherameti, I., Tripathi, S., and Varma, A. (2009). *Piriformospora indica*: a novel multifunctional symbiotic fungus. *Symbiosis* 49, 1–18. doi: 10.1007/s13199-009-0009-y

Oka, K., Akamatsu, H., Kodama, M., Nakajima, H., Kawada, T., and Otanib, H. (2005). Host-specific AB-toxin production by germinating spores of *Alternaria brassicicola* is induced by a host-derived oligosaccharide. *Physiol. Mol. Plant Pathol.* 66, 12–19. doi: 10.1016/j.pmpp.2005.03.005

Oliva, R., Win, J., Raffaele, S., Boutemy, L., Bozkurt, T. O., Segretin, M. E., et al. (2010). Recent developments in effector biology of filamentous plant pathogens. *Cell. Microbiol.* 12, 705–715. doi: 10.1111/j.1462-5822.2010.01471.x

Pan, R., Xu, L., Wie, Q., Wu, C., Tang, W., Oelmüller, R., et al. (2017). *Piriformospora indica* promotes early flowering in Arabidopsis through regulation of the photoperiod and gibberellin pathways. *PLoS ONE* 12:e0189791. doi: 10.1371/journal.pone.0189791

Pemberton, C. L., and Salmond, G. P. C. (2004). The Nep1-like proteins - a growing family of microbial elicitors of plant necrosis. *Mol. Plant Pathol.* 5, 353–359. doi: 10.1111/j.1364-3703.2004.00235.x

Peškan-Berghöfer, T., Shahollari, B., Giang, P. H., Hehl, S., Markert, C., Blanke, V., et al. (2004). Association of *Piriformospora indica* with *Arabidopsis thaliana* roots represents a novel system to study beneficial plant-microbe interactions and involves early plant protein modifications in the endoplasmatic reticulum and at the plasma membrane. *Physiol. Plant.* 122, 465–477. doi: 10.1111/j.1399-3054.2004.00424.x

Petrášek, J., and Friml, J. (2009). Auxin transport routes in plant development. *Development* 136, 2675–2688. doi: 10.1242/dev.030353

Pitts, R. J., Cernac, A., and Estelle, M. (1998). Auxin and ethylene promote root hair elongation in Arabidopsis. *Plant J.* 16, 553–560. doi: 10.1046/j.1365-313x.1998.00321.x

Qi, L., Yan, J., Li, Y., Jiang, H., Sun, J., Chen, Q., et al. (2012). *Arabidopsis thaliana* plants differentially modulate auxin biosynthesis and transport during defense responses to the necrotrophic pathogen *Alternaria brassicicola*. *New Phytol.* 195, 872–882. doi: 10.1111/j.1469-8137.2012.04208.x

Qutob, D., Kemmerling, B., Brunner, F., Kufner, I., Engelhardt, S., Gust, A. A., et al. (2006). Phytotoxicity and innate immune responses induced by Nep1-like proteins. *Plant Cell* 18, 3721–3744. doi: 10.1105/tpc.106.044180

Rahman, A., Bannigan, A., Sulaman, W., Pechter, P., Blancaflor, E. B., and Baskin, T. I. (2007). Auxin, actin and growth of the *Arabidopsis thaliana* primary root. *Plant J.* 50, 514–528. doi: 10.1111/j.1365-313X.2007.03068.x

Rashotte, A. M., Brady, S. R., Reed, R. C., Ante, S. J., and Muday, G. K. (2000). Basipetal auxin transport is required for gravitropism in roots of Arabidopsis. *Plant Physiol.* 122, 481–490. doi: 10.1104/pp.122.2.481

Reed, R. C., Brady, S. R., and Muday, G. K. (1998). Inhibition of auxin movement from the shoot into the root inhibits lateral root development in Arabidopsis. *Plant Physiol.* 118, 1369–1378. doi: 10.1104/pp.118.4.1369

Reusche, M., Truskina, J., Thole, K., Nagel, L., Rindfleisch, S., Tran, V. T., et al. (2014). Infections with the vascular pathogens *Verticillium longisporum* and *Verticillium dahliae* induce distinct disease symptoms and differentially affect drought stress tolerance of *Arabidopsis thaliana*. *Environ. Exp. Bot.* 108, 23–37. doi: 10.1016/j.envexpbot.2013.12.009

Riet, K. B., Ndlovu, N., Piater, L. A., and Dubery, I. A. (2016). Simultaneous analysis of defense-related phytohormones in *Arabidopsis thaliana* responding to fungal infection. *Appl. Plant Sci.* 4:1600013. doi: 10.3732/apps.1600013

Salehin, M., Bagchi, R., and Estelle, M. (2015). SCFTIR1/AFB-based auxin perception: mechanism and role in plant growth and development. *Plant Cell* 27, 9–19. doi: 10.1105/tpc.114.133744

Schäfer, P., Pfiffi, S., Voll, L. M., Zajic, D., Chandler, P. M., Waller, F., et al. (2009). Phytohormones in plant root-*Piriformospora indica* mutualism. *Plant Signal. Behav.* 4, 669–671. doi: 10.4161/psb.4.7.9038

Schnathorst, W. C. (1981). "Life cycle and epidemiology of verticillium," in *Fungal Wilt Diseases of Plants*, eds M. E. Mace, A. A. Bell, and C. H. Beckman (NewYork, NY: Academic Press Inc), 81–111.

Scholz, S. S., Schmidt-Heck, W., Guthke, R., Furch, A. C. U., Reichelt, M., Gershenzon, J., et al. (2018). *Verticillium dahliae-Arabidopsis* interaction causes changes in gene expression profiles and jasmonate levels on different time scales. *Front. Microbiol.* 9:217. doi: 10.3389/fmicb.2018.00217

Shinmen, Y., Shimizu, S., Akimoto, K., Kawashima, H., and Yamada, H. (1989). Production of arachidonic acid by *Mortierella* fungi: selection of a potent producer and optimization of culture for large-scale production. *Appl. Microbiol. Biotechnol.* 31, 11–16. doi: 10.1007/BF00252518

Sirrenberg, A., Göbel, C., Grond, S., Czempinski, N., Ratzinger, A., Karlovsky, P., et al. (2007). *Piriformospora indica* affects plant growth by auxin production. *Physiol. Plant.* 131, 581–589. doi: 10.1111/j.1399-3054.2007.00983.x

Sukumar, P., Edwards, K. S., Rahman, A., Delong, A., and Muday, G. K. (2009). PINOID kinase regulates root gravitropism through modulation of PIN2-dependent basipetal auxin transport in Arabidopsis. *Plant Physiol.* 150, 722–735. doi: 10.1104/pp.108.131607

Sun, C., Shao, Y., Vahabi, K., Lu, J., Bhattacharya, S., Dong, S., et al. (2014). The beneficial fungus *Piriformospora indica* protects Arabidopsis from *Verticillium dahliae* infection by downregulation plant defense responses. *BMC Plant Biol.* 14, 268–283. doi: 10.1186/s12870-014-0268-5

Sun, J., Chen, Q., Qi, L., Jiang, H., Li, S., Xu, Y., et al. (2011). Jasmonate modulates endocytosis and plasma membrane accumulation of the Arabidopsis PIN2 protein. *New Phytol.* 191, 360–375. doi: 10.1111/j.1469-8137.2011.03713.x

Sun, J., Xu, Y., Ye, S., Jiang, H., Chen, Q., Liu, F., et al. (2009). Arabidopsis ASA1 is important for jasmonate-mediated regulation of auxin biosynthesis and transport during lateral root information. *Plant Cell* 21, 1495–1511. doi: 10.1105/tpc.108.064303

Thaler, J. S., Owen, B., and Higgins, V. J. (2004). The role of the jasmonate response in plant susceptibility to diverse pathogens with a range of lifestyles. *Plant Physiol.* 135, 530–538. doi: 10.1104/pp.104.041566

Ulmasov, T., Murfett, J., Hagen, G., and Guilfoyle, T. J. (1997). Aux/IAA proteins repress expression of reporter genes containing natural and highly active synthetic auxin response elements. *Plant Cell* 9, 1963–1971. doi: 10.1105/tpc.9.11.1963

Vadassery, J., Ritter, C., Venus, Y., Camehl, I., Varma, A., Shahollari, B., et al. (2008). The role of auxins and cytokinins in the mutualistic interaction between Arabidopsis and *Piriformospora indica*. *Mol. Plant Microbe Interact.* 21, 1371–1383. doi: 10.1094/MPMI-21-10-1371

Vahabi, K., Reichelt, M., Scholz, S. S., Furch, A. C. U., Matsuo, M., Johnson, J. M., et al. (2018). *Alternaria Brassicae* induces systemic jasmonate responses in Arabidopsis which travel to neighboring plants via a *Piriformospora indica* hyphal network and activate abscisic acid responses. *Front. Plant Sci.* 9:626. doi: 10.3389/fpls.2018.00626

van der Does, H. C., and Rep, M. (2007). Virulence genes and the evolution of host specificity in plant-pathogenic fungi. *Mol. Plant Microbe Interac.* 20, 1175–1182 doi: 10.1094/MPMI-20-10-1175

van Esse, H. P., Fradin, E. F., de Groot, P. J., de Wit, P. J., and Thomma, B. P. (2009). Tomato transcriptional responses to a foliar and a vascular fungal pathogen are distinct. *Mol. Plant Microbe Interact.* 22, 245–258. doi: 10.1094/MPMI-22-3-0245

Verma, S., Varma, A., Rexer, K.-H., Hassel, A., Kost, G., Sarbhoy, A., et al. (1998). *Piriformospora indica*, gen. et sp. nov., a new root-colonizing fungus. *Mycologia* 90, 898–905. doi: 10.1080/00275514.1998.12026983

Wang, D., Pajerowska-Mukhtar, K., Culler, A. H., and Dong, X. (2007). Salicylic acid inhibits pathogen growth in plants through repression of the auxin signaling pathway. *Curr. Biol.* 17, 1784–1790. doi: 10.1016/j.cub.2007.09.025

Wani, Z. A., Kumar, A., Sultan, P., Bindu, K., Riyaz-Ul-Hassan, S., and Ashraf, N. (2017). *Mortierella alpina* CS10E4, an oleaginous fungal endophyte of *Crocus sativus* L. enhances apocarotenoid biosynthesis and stress tolerance in the host plant. *Sci. Rep.* 7:8598. doi: 10.1038/s41598-017-08974-z

Xu, L., Wu, C., Oelmüller, R., and Zhang, W. (2018). Role of phytohormones in *Piriformospora indica*-induced growth promotion and stress tolerance in plants: more questions than answers. *Front. Microbiol.* 9:1646. doi: 10.3389/fmicb.2018.01646

Zhang, W., Wang, J., Xu, L., Wang, A., Huang, L., Du, H., et al. (2017). Drought stress responses in maize are diminished by Piriformospora indica. *Plant Signal. Behav.* 13:e1414121. doi: 10.1080/15592324.2017.1414121

Zhao, P., Zhao, Y.-L., Jin, Y., Zhang, T., and Guo, H.-S. (2014). Colonization process of *Arabidopsis thaliana* roots by a green fluorescent protein-tagged isolate of *Verticillium dahliae*. *Protein Cell* 5, 94–98. doi: 10.1007/s13238-013-0009-9

Conflict of Interest Statement: The authors declare that the research was conducted in the absence of any commercial or financial relationships that could be construed as a potential conflict of interest.

frontiers in Plant Science

ORIGINAL RESEARCH
published: 15 March 2019
doi: 10.3389/fpls.2019.00285

Gibberellins Inhibit Nodule Senescence and Stimulate Nodule Meristem Bifurcation in Pea (*Pisum sativum* L.)

*Tatiana A. Serova[1], Anna V. Tsyganova[1], Igor A. Tikhonovich[1,2] and Viktor E. Tsyganov[1]**

[1] Laboratory of Molecular and Cellular Biology, Department of Biotechnology, All-Russia Research Institute for Agricultural Microbiology, Russian Academy of Agricultural Sciences, Saint Petersburg, Russia, [2] Department of Genetics and Biotechnology, Saint Petersburg State University, Saint Petersburg, Russia

The development of nitrogen-fixing nodules formed during *Rhizobium*–legume symbiosis is strongly controlled by phytohormones. In this study, we investigated the effect of gibberellins (GAs) on senescence of pea (*Pisum sativum*) symbiotic nodules. Pea wild-type line SGE, as well as corresponding mutant lines SGEFix$^-$-1 (*sym40*), SGEFix$^-$-2 (*sym33*), SGEFix$^-$-3 (*sym26*), and SGEFix$^-$-7 (*sym27*), blocked at different stages of nodule development, were used in the study. An increase in expression of the *GA2ox1* gene, encoding an enzyme involved in GA deactivation (GA 2-oxidase), and a decrease in the transcript abundance of the *GA20ox1* gene, encoding one of the enzymes involved in GA biosynthesis (GA 20-oxidase), were observed in analyzed genotypes during nodule aging. A reduction in the amount of bioactive GA_3 was demonstrated by immunolocalization in the early senescent mutant and wild-type lines during aging of symbiotic nodules. Down-regulated expression of senescence-associated genes encoding cysteine proteases 1 and 15a, thiol protease, bZIP transcription factor, 1-aminocyclopropane-1-carboxylate (ACC) synthase, ACC oxidase, and aldehyde oxidase was observed in the nodules of wild-type plants treated with exogenous GA_3 relative to the untreated plants. GA_3-treated plants also showed increases in nodule size and the nitrogen fixation zone, and decreases in the number of nodules and the senescence zone. Immunogold localization revealed higher levels of GA_3 in the peribacteroid spaces in symbiosomes than in the matrix of infection threads. Furthermore, a decrease in GA_3 label in mature and senescent symbiosomes in comparison with juvenile symbiosomes was observed. These results suggest a negative effect of GAs on the senescence of the pea symbiotic nodule and possible involvement of GAs in functioning of the mature nodule. Simultaneously, GA_3 treatment led to nodule meristem bifurcation, indicating a possible role of GAs in nodule meristem functioning.

Keywords: *Rhizobium*–legume symbiosis, nodule senescence, cysteine protease, ethylene, abscisic acid, gibberellins, meristem

OPEN ACCESS

Edited by:
Eloise Foo,
University of Tasmania, Australia

Reviewed by:
Frederique Catherine Guinel,
Wilfrid Laurier University, Canada
Erik Limpens,
Wageningen University & Research, Netherlands

***Correspondence:**
Viktor E. Tsyganov
tsyganov@arriam.spb.ru

Specialty section:
This article was submitted to Plant Microbe Interactions, a section of the journal Frontiers in Plant Science

Received: *26 October 2018*
Accepted: *20 February 2019*
Published: *15 March 2019*

Citation:
Serova TA, Tsyganova AV, Tikhonovich IA and Tsyganov VE (2019) Gibberellins Inhibit Nodule Senescence and Stimulate Nodule Meristem Bifurcation in Pea (Pisum sativum L.). Front. Plant Sci. 10:285. doi: 10.3389/fpls.2019.00285

INTRODUCTION

Legume–*Rhizobium* interactions culminate in the formation of nitrogen-fixing nodules. Rhizobia growing near the plant adhere to the root hair and eventually penetrate the root, initiating the formation of an infection thread (Brewin, 2004; Tsyganova and Tsyganov, 2017). When the infection thread reaches reactivated cortical root cells, which form a nodule primordium, rhizobia are released into the host cell cytoplasm from unwalled infection droplets (Brewin, 2004). After release, rhizobia differentiate into bacteroids and become surrounded by a peribacteroid membrane; these form symbiosomes, organelle-like structures in which bacteroids fix nitrogen (Tsyganova et al., 2018).

If the nodule meristem functions for a long time, nodules of an indeterminate type are formed with different histological zones, which include the meristem (zone I), the infection zone (zone II), the nitrogen fixation zone (zone III), and the senescence zone (zone IV) (Guinel, 2009).

Senescence completes symbiotic nodule development and is accompanied by the destruction of symbiotic partners, large-scale protein degradation, and remobilization of nutrients to other plant organs (Puppo et al., 2005; Serova and Tsyganov, 2014). In particular, the catabolism of leghemoglobin, which is one of the most abundant proteins in the nodule, is observed during nodule senescence resulting in a color change of aged nodules from pink to green. Senescence in the indeterminate nodule is associated with the senescence zone formed at the base of the nodule and spreads toward its apical part and periphery (Pérez Guerra et al., 2010; Dupont et al., 2012). Hormonal regulation has a major impact on symbiotic nodule development (Ferguson and Mathesius, 2014; Tsyganova and Tsyganov, 2015, 2018). Current data suggest that both ethylene and abscisic acid (ABA) contribute to the aging of the symbiotic nodule (Puppo et al., 2005; Van de Velde et al., 2006; Karmarkar, 2014; Serova et al., 2017). In contrast, based on expression analysis of the nodules of *Medicago truncatula* (Van de Velde et al., 2006) and pea (Serova et al., 2017), it has been suggested that gibberellins (GAs) may have a negative impact on nodule senescence.

Gibberellins are a large group of diterpenoid carboxylic acids in higher plants. GAs stimulate organ growth, causing the enhancement of cell elongation and cell division (Hedden and Thomas, 2012). GA biosynthesis includes several steps catalyzed by terpene cyclases (Hedden and Thomas, 2012). The first steps involve the production of GA_{12}, the common precursor of all types of GAs in plants (Hedden and Phillips, 2000). GA_{12} can be converted to another GA precursor, GA_{53}. The final stages of GA biosynthesis are catalyzed by GA 20-oxidase and GA 3-oxidase. Their activity contributes to the content of bioactive forms of GA in the plant. In pea, GA 20-oxidases encoded by *PsGA20ox* genes (*PsGA20ox1*, *PsGA20ox2*) are involved in different stages of GA biosynthesis. They mainly catalyze the conversion of GA_{12} to GA_9 and GA_{53} to GA_{20}, where GA_9 and GA_{20} are precursors of bioactive GAs (García-Martínez et al., 1997). The conversion of GA_9 and GA_{20} to bioactive forms of GAs is catalyzed by GA 3-oxidases (García-Martínez et al., 1997; Hedden and Thomas, 2012).

GA_1, GA_3, GA_4, GA_5, and GA_7 are the most common biologically active forms in higher plants (Hayashi et al., 2014). Along with bioactive forms, plants also contain inactive forms of GAs, including the precursors and metabolites of active GAs. Inactive GAs are present at higher concentrations and may perform yet unknown functions (Hedden and Thomas, 2012; Hayashi et al., 2014). There are several mechanisms of GA inactivation, the most prevalent of which is 2β-hydroxylation, catalyzed by GA 2-oxidases (GA2oxs) (Thomas et al., 1999; Hedden and Thomas, 2012). In pea, conversion of bioactive GAs, GA_1 and GA_4, and of its precursors GA_9 and GA_{20}, to inactive catabolites occurred by C_{19}-GA 2-oxidases encoded by the *PsGA2ox1* and *PsGA2ox2* genes (Lester et al., 1999; Martin et al., 1999; Hedden and Thomas, 2012). Inactivation of the precursors GA_{12} and GA_{53} is catalyzed by C_{20}-GA 2-oxidases (Hedden and Thomas, 2012).

Optimal GA levels differ during various stages of plant development and are maintained through feed-back and feed-forward regulation of GA metabolism (Weston et al., 2008; Hedden and Thomas, 2012). Bioactive GAs reduce GA biosynthesis and enhance GA deactivation (Weston et al., 2008). A GA signal transduction pathway is triggered by the binding of GAs to the soluble receptor GID1 (GIBBERELLIN-INSENSITIVE DWARF 1) (Ueguchi-Tanaka et al., 2005). Downstream signal transduction pathways involve DELLA proteins, which are key repressors of GA responses (Davière and Achard, 2013). After GA binding, the formation of a GA-GID1-DELLA complex occurs with its subsequent degradation by the 26S proteasome in the nucleus (Sun, 2011).

During nodulation, GAs are involved in the negative control of rhizobial infection and the positive regulation of nodule development (Lievens et al., 2005; Maekawa et al., 2009; Ferguson et al., 2011; Hayashi et al., 2014; McAdam et al., 2018). Up-regulation of GA biosynthetic genes, *GA20ox* and *GA3ox*, was observed in the early stages of nodulation in *Sesbania rostrata* (Lievens et al., 2005), *Glycine max* (Hayashi et al., 2012), and *Lotus japonicus* (Kouchi et al., 2004). The negative effect of GAs on rhizobial infection in *L. japonicus* and *S. rostrata* was accompanied by suppressed expression of the transcription factors NIN (Nodule Inception) and NSP (Nodulation Signaling Pathway) (Kouchi et al., 2004; Lievens et al., 2005; Maekawa et al., 2009). Analysis of the *M. truncatula* root transcriptome revealed that Nod factor perception led to spatial-temporal activation of genes involved in GA biosynthesis and catabolism (Larrainzar et al., 2015). Within the first hours of infection, an increase in the expression of GA deactivation genes was shown, which may promote the Nod factor signaling pathway (Larrainzar et al., 2015). However, up-regulation of GA biosynthesis genes was later observed, which likely causes an increase in GA content and may limit further infection (Larrainzar et al., 2015). The negative impact of GAs on rhizobial infection is mediated through destruction of DELLA proteins. It was previously shown that DELLA proteins interact with and activate a wide set of transcription factors involved in Nod factor signaling [NSP1, NSP2, IPD3 (interacting protein with DMI3), NF-YA1 (nuclear factor-YA1), and ERN1 (ERF required for nodulation 1)] (Fonouni-Farde et al., 2016; Jin et al., 2016).

Furthermore, the positive effect of DELLA proteins was confirmed by poor nodulation of *della* mutants in *M. truncatula* (Jin et al., 2016).

There is evidence to suggest that different optimal levels of bioactive GAs are required at different stages of nodulation (Ferguson et al., 2005, 2011). Moreover, optimal levels seem to be species-specific and to depend on growth conditions. Inhibition of GA biosynthesis reduced nodulation in *S. rostrata* (Lievens et al., 2005). In pea, reduced GA levels inhibited nodulation, as demonstrated using a series of GA biosynthesis mutants, including the severely GA-deficient *na-1* pea mutant (Ferguson et al., 2005). In *L. japonicus*, treatment of wild-type plants with exogenous GA_3 induced the initiation of divisions in the pericycle leading to formation of pseudo-nodules (Kawaguchi et al., 1996). However, in the *snf1* and *snf2* mutants of *L. japonicus*, application of exogenous GA_3 suppressed spontaneous nodulation by inhibiting the NSP (Maekawa et al., 2009). High concentrations of exogenous GA_3 inhibited root hair infection in *S. rostrata* (10^{-5} M) (Lievens et al., 2005) and *L. japonicus* (10^{-6}, 10^{-7} M) (Maekawa et al., 2009), and also reduced nodulation in pea (10^{-3} M) (Ferguson et al., 2005) and *M. truncatula* (10^{-7}–10^{-4} M) (Fonouni-Farde et al., 2016; Jin et al., 2016). In contrast, low concentrations (10^{-9} M) of exogenous GA_3 promoted nodulation in pea plants (Ferguson et al., 2005). Further overexpression of a GA signaling component, *SLEEPY1*, resulted in fewer nodules in transgenic roots of *L. japonicus* than in wild-type roots (Maekawa et al., 2009). However, the GA_1-overproducing *sln* mutant of pea, which is strongly blocked in GA deactivation, formed nodules only on lateral roots and had the same number of nodules as the wild-type (Ross et al., 1995; Lester et al., 1999; Ferguson et al., 2005, 2011).

An ambivalent role for GAs in nodulation was clarified in a recent study (McAdam et al., 2018). The authors confirmed the well-known negative effect of GAs on development of infection threads and demonstrated the positive effect on nodule tissue development and functioning of nitrogen-fixing nodules. The action of GAs was shown to be mediated by DELLA proteins, which, on the contrary, promote infection thread growth and inhibit the initiation of cortex cell division and nodule development (McAdam et al., 2018).

Little is known about the interactions between GAs and other hormones during nodulation. In an earlier study using the strongly GA-deficient *na-1* pea mutant, it was shown that low GA content resulted in elevated ethylene levels and decreased nodulation (Ferguson et al., 2011). This was confirmed by partial recovery of nodulation in the mutant *na-1* treated with an inhibitor of ethylene biosynthesis (Ferguson et al., 2011), while an increase in the level of GAs rescued the number and structure of mutant nodules (Ferguson et al., 2005). Recently, a detailed phenotypic characterization of the *na-1 ein2* double mutant and an analysis of epistatic interactions of the mutations revealed that, to some extent, GAs inhibit infection thread formation independently of ethylene, and that GAs facilitate the formation of nodules by partial inhibition of ethylene (McAdam et al., 2018).

Thus, a number of previous studies confirm involvement of GAs in the initial stages of *Rhizobium*–legume symbiosis. However, at present, the effect of GAs on the later stages of nodule development is not well understood. Therefore, the aim of this study was to identify a role for GAs in senescence of the symbiotic nodule of pea. It is known that in wild-type pea nodules, senescence is initiated at 4 weeks after inoculation (WAI) and actively developed in 6-week-old nodules (Kardailsky and Brewin, 1996; Serova et al., 2017, 2018). The study was carried out using pea wild-type line SGE and a number of mutant lines, SGEFix$^-$-1 (*sym40*), SGEFix$^-$-2 (*sym33*), SGEFix$^-$-3 (*sym26*), and SGEFix$^-$-7 (*sym27*), which are blocked at different stages of nodule development. Recently, we demonstrated the activation of nodule senescence in all analyzed mutants, which starts in 2-week-old nodules and is especially active in 4-week-old nodules (Serova et al., 2018). Based on data obtained from expression, immunolocalization, and pharmacological analyses, we suggest a negative effect of GAs on the senescence of the pea symbiotic nodule and possible involvement of GAs in the functioning of nodule meristem and cells from the nitrogen fixation zone.

MATERIALS AND METHODS

Plant Material, Bacterial Strain, and Plant Growth Conditions

The pea (*Pisum sativum* L.) laboratory line SGE (Kosterin and Rozov, 1993) and corresponding mutant lines SGEFix$^-$-1 (*sym40*), SGEFix$^-$-2 (*sym33*), SGEFix$^-$-3 (*sym26*), and SGEFix$^-$-7 (*sym27*) were used in this study (**Table 1**). *Rhizobium leguminosarum* bv. *viciae* strain 3841

TABLE 1 | Plant material used in the study.

Genotype	Mutant gene	Nodule phenotype	Reference
SGE		Wild type	Kosterin and Rozov, 1993; Tsyganov et al., 1998
SGEFix$^-$-1	*sym40**	Hypertrophic infection threads and infection droplets; abnormal bacteroids	Tsyganov et al., 1994, 1998
SGEFix$^-$-2	*sym33***	"Locked" infection threads, no bacterial release; in some cells and nodules infection droplets are formed and bacterial release occurs	Tsyganov et al., 1994, 1998; Voroshilova et al., 2001
SGEFix$^-$-3	*sym26****	Premature degradation of symbiotic structures	Tsyganov et al., 2000; Serova et al., 2018
SGEFix$^-$-7	*sym27****	Premature degradation of symbiotic structures	Tsyganov et al., 2013; Serova et al., 2018

**The Sym40 gene is orthologous to the Medicago truncatula EFD gene (Nemankin, 2011). **The Sym33 gene is orthologous to the M. truncatula IPD3 gene (Ovchinnikova et al., 2011). ***The gene sequence is unknown.*

(Wang et al., 1982) was used as an inoculant. Methods for sterilization of seeds, plant inoculation, and growth conditions were described previously (Serova et al., 2017). For microscopic and expression analyses and quantitative measurement of nodulation, nodules were collected at 2, 4, and 6 WAI.

Expression Analysis of Genes Associated With GA Metabolism in SGE and Mutant Lines

Primers for one GA biosynthesis gene, *PsGA20ox1*, and one GA deactivation gene, *PsGA2ox1,* were designed previously (Weston et al., 2008; Serova et al., 2017). For RNA extraction, 2, 4, and 6 WAI nodules of SGE, mutants SGEFix$^-$-1 (*sym40*), SGEFix$^-$-2 (*sym33*), SGEFix$^-$-3 (*sym26*), and SGEFix$^-$-7 (*sym27*) were ground in liquid nitrogen. Total RNA from each sample was isolated using PureZol reagent (Bio-Rad, Hercules, CA, United States) according to the manufacturer's recommendations. RNA quantity and purity were checked using a MultiNA electrophoresis system on microchips for analysis of nucleic acids (Shimadzu Corporation, Kyoto, Japan). Reverse transcription was performed on 1.5 μg total RNA treated with DNAse I (MBI Fermentas, Vilnius, Lithuania) using 200 U RevertAid Reverse Transcriptase and 0.5 μg Oligo(dT)$_{18}$ (MBI Fermentas) for cDNA synthesis under manufacturer-recommended conditions. cDNA synthesis was carried out in 20 μl of reaction mix, and the resulting cDNAs were diluted five times for following use. The reaction was carried out in an automated C1000^{TM} Thermal Cycler (Bio-Rad).

For gene expression quantification, relative real-time PCR was performed in a C1000^{TM} Thermal Cycler combined with the optical module CFX96^{TM} Real-Time System (Bio-Rad), using iQ SYBR Green Supermix (Bio-Rad) according to manufacturer's instructions. Results of reactions were processed using Bio-Rad CFX Manager software (Bio-Rad). Relative expression was calculated with the $2^{-\Delta\Delta C_T}$ method using the reference gene *PsGapC1* (accession number L07500.1). Two-WAI nodules of SGE were used as a calibrator for calculation of relative transcript abundance. For *PsGA20ox1* transcript abundance, 6-WAI nodules were used as a calibrator. Reactions were carried out in three technical replicates and averaged. Statistical treatment of experimental results was carried out with Microsoft Excel software. Statistically significant differences were calculated using one-way ANOVA at P-value ≤ 0.05. Experiments were performed in three replicates with six to eight plants per variant.

GA_3 Immunolabeling and Confocal Microscopy

Nodules of SGE and of the mutants SGEFix$^-$-1 (*sym40*), SGEFix$^-$-2 (*sym33*), SGEFix$^-$-3 (*sym26*), and SGEFix$^-$-7 (*sym27*) at 2, 4, and 6 WAI were fixed in freshly prepared 4% paraformaldehyde buffered in PBS (136 mM NaCl, 2.68 mM KCl, 10 mM Na_2HPO_4, 1.7 mM KH_2PO_4, pH 7.4) with addition of 3% *N*-ethyl-*N*′-(3-dimethylaminopropyl) carbodiimide hydrochloride and 0.1% Triton X-100 (Sigma-Aldrich, Dorset, United Kingdom). Samples were fixed under vacuum (−0.9 bar), for 7 min three times with 15 min intervals using a VacuuBrand ME 1C vacuum pump (Vacuubrand, Wertheim, Germany), and incubated overnight at 4°C. Nodules were rinsed with PBS three times, with 15 min intervals, and stained with 0.5% toluidine blue solution in PBS for 1 h. Washing of the residual dye was carried out with PBS two times, with 15 min intervals. Samples were subsequently molded in 3% agarose gel.

Sections (50 μm) were prepared at room temperature with a HM650V microtome (Microm, Walldorf, Germany). After this, GA_3 immunolabeling and nuclei and bacteria staining were carried out in accordance with Serova et al. (2018). Anti-GA_3 rat antibodies (Agrisera, Vännäs, Sweden) and goat anti-rat IgG Alexa Fluor 488 (Thermo Fisher Scientific, Waltham, MA, United States) were used as primary and secondary antibodies for GA_3 immunolabeling, respectively. Sections were mounted in ProLong Gold antifade reagent (Thermo Fisher Scientific).

Control of GA_3-specific signal was carried out using GA_3-BSA conjugate (Agrisera) (**Supplementary Figure S1**). Anti-GA_3 antibodies were incubated with GA_3-BSA conjugate in a 1:40 ratio in PBS for 24 h at 4°C in a total volume of 100 μl. Then, the mix was used as primary antibodies for immunolabeling of pea nodules (**Supplementary Figures S1A–C**). Anti-GA_3 antibodies were omitted as a control for specific binding of secondary antibodies in the absence of primary antibodies (**Supplementary Figures S1D–F**). Also, the control of specificity of GA_3-antibodies in nuclei is shown (**Supplementary Figures S1G–L**).

Sections were analyzed using the laser scanning confocal system LSM 510 META (Carl Zeiss, Oberkochen, Germany) and ZEN2009 software (Carl Zeiss).

Immunogold Labeling, Transmission Electron Microscopy, and Quantitative Analysis

Nodules of SGE and mutant SGEFix$^-$-3 (*sym26*) at 2 WAI were used. Preparation of samples for transmission electron microscopy (TEM) and immunogold labeling of GA_3 was done with ultrathin sections on gold grids as described by Tsyganova et al. (2009). A total of 15–20 nodules from at least five different plants were fixed in 2.5% glutaraldehyde in 0.06 M phosphate buffer (pH 7.2) at 4°C overnight. Samples were then rinsed in buffer and dehydrated in increasing concentrations of ethanol (30% at room temperature; 50%, 70%, 90%, and twice with 100% at 35°C) for 20 min at each step. Subsequently, specimens were gradually infiltrated with increasing concentrations of LR-White resin (Polysciences Europe, Eppelheim, Germany) at a ratio of 1:1, 1:2, and 1:3 mixed with ethanol (100%) at −20°C and finally embedded in LR-White resin and polymerized at −20°C for 48 h in small plastic containers using UV polymerization in a Leica EM AFS2 (Leica Microsystems, Wetzlar, Germany).

Ultrathin sections (90 nm) of the samples were obtained with a Leica EM UC7 ultramicrotome (Leica Microsystems) and blocked with a blocking solution (5% BSA, 0.5% goat serum, 0.05% cold water fish skin) and they were then washed in 0.1% acetylated BSA (BSA-C) in PBS. Sections were treated with the primary anti-GA_3 rat antibodies (Agrisera) diluted 1:25 in 0.1% BSA-C in PBS at 4°C overnight. After four rinses in 0.1% BSA-C in PBS, samples were incubated with a 10 nm gold-conjugated

secondary antibody goat anti-rat IgG (Amersham International, Little Chalfont, United Kingdom), diluted 1:50 in 0.1% BSA-C in PBS, for 4 h at 37°C. After short washes in PBS and distilled water, labeled grids were post-stained with uranyl acetate for 15 s.

The specificity of the immunogold labeling procedures was tested by several negative controls. Negative controls were treated either with pre-immune serum instead of the primary antibody and with non-specific secondary antibody (goat anti-mouse IgG). Negative controls for gibberellic acid revealed that no labeling occurred on the section when they were treated with pre-immune serum instead of the primary antibody (**Supplementary Figure S2A**) and with non-specific secondary antibody (**Supplementary Figure S2B**).

Nodule tissues were analyzed in a JEM–1400 EM transmission electron microscope (JEOL Ltd., Tokyo, Japan) at 80 kV. Electron micrographs were obtained by Veleta CCD camera (Olympus, Münster, Germany). Micrographs of randomly photographed immunogold-labeled sections were digitized, and gold particles were counted in visually identified cell structures. For statistical analysis, at least 10 different samples of root nodules and at least 50 sectioned symbiosomes were examined for SGE or mutant SGEFix$^-$-3 (*sym26*). The SGEFix$^-$-3 (*sym26*) mutant was chosen as an example of mutants with premature degradation of symbiotic structures (early senescence phenotype) for comparison with wild-type nodules. Previously, we demonstrated that early senescence is more pronounced in this mutant (Serova et al., 2018). Morphometrical data were obtained as described previously (Ivanova et al., 2015). Briefly, the number of gold particles per unit area was calculated. The areas and the number of gold particles were measured using software Zen 2 Core version 2.5 (Carl Zeiss). The data are presented as the number of gold particles/μm^2. Data were analyzed by one-way ANOVA using the software SigmaPlot for Windows version 12.5 (Systat Software, Inc., San Jose, CA, United States). Means were separated by the Tukey multiple range test (P-value ≤ 0.001).

Pharmacological Treatment

GA_3 treatment was carried out for evaluation of GA action on pea nodule senescence. After inoculation with rhizobia, 100 ml of a 10^{-6} M GA_3 (Sigma-Aldrich) aqueous solution was applied into substrate to SGE plants every 3 days until plants were harvested. Control plants were watered without GA_3. Nodules were harvested for expression and light microscopy analyses. Photographs of pea nodules were made with a SteREO Lumar.V12 stereomicroscope equipped with an Axiocam ICc 1 video camera (Carl Zeiss).

Quantitative Measurements of Nodulation

GA_3-treated and untreated pea plants were harvested for quantitative measurement. The shoots and roots were separated, and cotyledons were removed. Nodules on the primary and secondary roots were removed with a blade and counted. For weight measurements, separated shoots, roots, and nodules were dried at 42°C for 3 days. Experiments were performed with 9–16 plants per GA_3-treated and untreated variants. Statistically significant differences were calculated using one-way ANOVA at P-value ≤ 0.01.

The sizes of nodules and senescence zones were measured with AxioVision Rel. 4.8 software (Carl Zeiss). Pictures of separate nodules of GA_3-treated and untreated plants were taken as described above. **Supplementary Figure S3** illustrates the selection and measurement of nodule projection areas using the example of analysis for a nodule of untreated plant at 6 WAI. Projection areas were measured as average projection area of nodules from the main root of a single plant. Experiments were performed with 8–12 plants per GA_3-treated and untreated variants. Statistically significant differences were calculated using one-way ANOVA at P-value ≤ 0.01.

Light Microscopy Analysis of Nodules of GA_3-Treated and Untreated Plants

Fixation of pea nodules for light microscopy was the same as described above. Samples were subsequently dehydrated with a series of ethanol solutions in water and embedded in Steedman's wax as previously described (Serova et al., 2017). Sections of 10 μm were obtained with a HM360 microtome (Microm) and placed on slides in a few drops of water. After drying at 28°C for 30 min, slices were de-waxed in ethanol solutions and placed in PBS (Serova et al., 2017). Slices were then stained with toluidine blue (0.1% solution in PBS) for 10 min and washed in PBS (two times for 10 min). Sections were mounted in PBS.

Light microscopy analysis of nodule sections of GA_3-treated and untreated plants was carried out with Axio Imager.Z1 (Carl Zeiss). Photographs were taken with a microscope camera Axiocam 506 color (Carl Zeiss) and analyzed using ZEN 2 core SP1 software (Carl Zeiss).

Expression Analysis of Senescence-Associated Genes

Primers for selected senescence-associated marker genes encoding cysteine protease 1 and 15a (*PsCyp1*, *PsCyp15a*), thiol protease (*PsTPP*), bZIP transcription factor (*PsATB2*), enzymes of ethylene (*PsACS2*, *PsACO1*) and ABA (*PsAO3*) biosynthesis, and an enzyme of bioactive GAs deactivation (*PsGA2ox1*) were designed previously (Serova et al., 2017). In addition, primers for a GA biosynthesis gene (*PsGA20ox1*) designed by Weston et al. (2008) were used.

RNA was extracted from 2, 4, and 6 WAI nodules of GA_3-treated and untreated SGE as described above (see section "Expression Analysis of Genes Associated With GA Metabolism in SGE and Mutant Lines"). Reverse transcription and relative real-time PCR were performed in accordance with the previous description (see section "Expression Analysis of Genes Associated With GA Metabolism in SGE and Mutant Lines").

RESULTS

Expression Analysis of Genes Encoding Enzymes Involved in Biosynthesis and Deactivation of GAs

To study the involvement of GAs in senescence of pea symbiotic nodules, an expression analysis of one GA biosynthesis gene (*PsGA20ox1*) and one GA deactivation

gene (*PsGA2ox1*) was carried out in SGE and the mutant lines (**Figure 1**).

The transcript level of *PsGA20ox1* was down-regulated due to the aging of the wild-type and the mutant nodules with the exception of the mutant SGEFix$^-$-2 (*sym33*), which showed statistically insignificant differences (**Figure 1A**). In the wild-type nodules, a significant (6.8-fold) decrease in transcript abundance was observed from 2 to 6 WAI. In 2- and 4-week-old nodules of the mutant SGEFix$^-$-2 (*sym33*), the *PsGA20ox1* mRNA level was significantly reduced in comparison with the wild-type. In the mutant SGEFix$^-$-3 (*sym26*), a slight down-regulation was detected from 4 to 6 WAI only. Furthermore, in 4-week-old nodules of the mutant SGEFix$^-$-3 (*sym26*), the *PsGA20ox1* mRNA level was 3.8-fold higher than that in the wild-type. A significant (7.6-fold) down-regulation of the transcript level was observed in the mutant SGEFix$^-$-7 (*sym27*) already at 4 WAI. In addition, *PsGA20ox1* transcript abundance was 2.6-fold lower in 4-week-old nodules of the mutant SGEFix$^-$-7 (*sym27*) than in those of the wild-type. The difference in transcript levels in the nodules of the mutant SGEFix$^-$-1 (*sym40*) from the wild-type was insignificant.

During aging of wild-type nodules, *PsGA2ox1* transcript abundance was significantly (48.4-fold) up-regulated at 6 WAI only. In contrast, the mutants SGEFix$^-$-3 (*sym26*) and SGEFix$^-$-7 (*sym27*) showed 23.5- and 49.4-fold elevation of the expression level, respectively, already at 4 WAI. However, in the case of the mutant SGEFix$^-$-7 (*sym27*), a decrease in *PsGA2ox1* transcript abundance was detected at 6 WAI. In 4-week-old nodules of the mutant SGEFix$^-$-1 (*sym40*), an increase in *PsGA2ox1* mRNA was less pronounced. *PsGA2ox1* transcript abundance was significantly higher in the mutants SGEFix$^-$-1 (*sym40*), SGEFix$^-$-3 (*sym26*), and SGEFix$^-$-7 (*sym27*) than in the wild-type nodules at 4 WAI. The expression level of *PsGA2ox1* gene was slightly higher than in the wild-type in 4-week-old nodules of the mutant SGEFix$^-$-2 (*sym33*). However, changes in the transcript level of the mutant SGEFix$^-$-2 (*sym33*) were statistically insignificant.

Overall, the expression of the GA biosynthesis gene *PsGA20ox1* was decreased, while the expression of the GA deactivation gene *PsGA2ox1* was increased during aging of the pea nodules of wild-type and early senescent mutants.

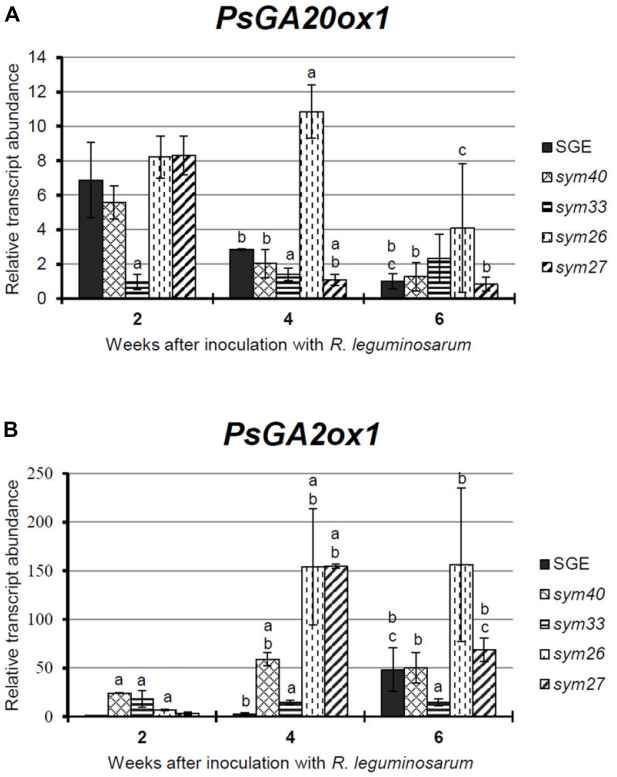

FIGURE 1 | Relative transcript levels of *PsGA20ox1* **(A)** and *PsGA2ox1* **(B)** genes in nodules of wild-type SGE and corresponding pea mutants SGEFix$^-$-1 (*sym40*), SGEFix$^-$-2 (*sym33*), SGEFix$^-$-3 (*sym26*), and SGEFix$^-$-7 (*sym27*) at 2, 4, and 6 weeks after inoculation (WAI). *Letters* indicate significant differences (one-way ANOVA, *P*-value $\leq$ 0.05) a, from wild-type SGE at one time point; b, within genotype compared with 2 WAI; c, within genotype compared with 4 WAI.

GA_3 Immunolocalization in Wild-Type and Mutant Nodules

To complement the data obtained by expression analysis of GA metabolism genes, GA_3 immunolocalization was carried out in wild-type and mutant nodules of different ages (**Figures 2–4** and **Supplementary Figures S4–S6**).

In 2- and 4-week-old wild-type nodules, GA_3 labeling was detected in cells from the meristem, and in the infection and nitrogen fixation zones (**Figures 2A–C**, **3A–C** and **Supplementary Figure S4**). The GA_3 label was observed in both infected and uninfected cells; in the latter, it was associated with cytoplasm surrounding starch granules (**Figures 4A–C**). In wild-type nodules, a high signal of GA_3 labeling was also detected in nuclei, mostly in cells from the nitrogen fixation zone (**Figures 4A–C** and **Supplementary Figures S1G–L**). The intensity of labeling was much lower in 6-week-old wild-type nodules (**Supplementary Figures S5A–C,G–I**), especially in the senescence zone (**Supplementary Figures S5D–F**). Traces of GA_3 label were detected in senescent uninfected cells (**Supplementary Figures S5J–L**). In 2-week-old nodules of the mutant SGEFix$^-$-1 (*sym40*), a high intensity of labeling was observed in nuclei and cytoplasm, but was absent in infection threads and infection droplets (**Figures 4D–F**). Whole nodule intensity of labeling was lower in the mutant SGEFix$^-$-1 (*sym40*) than in the wild-type (**Figures 2D–F**). In 4-week-old nodules of the mutant SGEFix$^-$-1 (*sym40*), the intensity of GA_3 labeling was significantly decreased (**Figures 3D–F**); traces of the GA_3 label were observed in nuclei and cytoplasm, particularly at the cell periphery (**Supplementary Figures S6A–C**). In nodules of the mutant SGEFix$^-$-2 (*sym33*), the lowest level of GA_3 was observed (**Figures 2G–I**). The GA_3 label was detected mainly in nuclei and cytoplasm, but was absent in infection threads (**Figures 4G–I**). In 4-week-old mutant nodules, a high level of fluorescence was associated with nuclei (**Figures 3G–I**

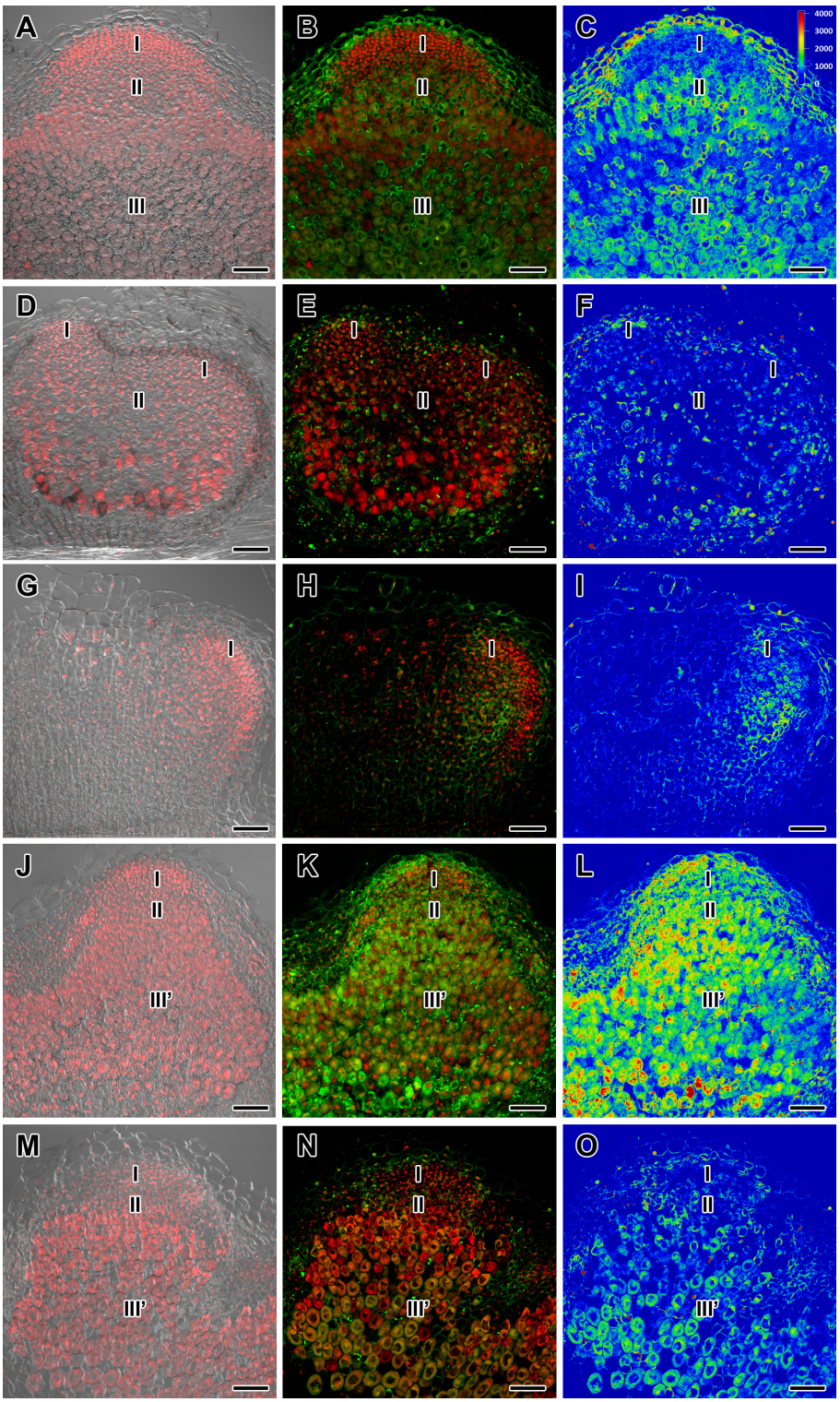

FIGURE 2 | Immunolocalization of gibberellin (GA_3) in nodules of wild-type SGE **(A–C)** and corresponding pea mutants SGEFix$^-$-1 (*sym40*) **(D–F)**, SGEFix$^-$-2 (*sym33*) **(G–I)**, SGEFix$^-$-3 (*sym26*) **(J–L)**, and SGEFix$^-$-7 (*sym27*) **(M–O)** at 2 weeks after inoculation. Zones of nodules are designated by Roman numerals: I – meristem, II – infection zone, III – fixation zone, III' – zone corresponding to nitrogen fixation zone in wild-type. A differential interference contrast microscopy image merged with laser scanning confocal microscopy image in red channel **(A,D,G,J,M)**. Merged images of laser scanning confocal microscopy in green and red channels **(B,E,H,K,N)**. Heat map provides a color code of fluorescence signal intensities **(C,F,I,L,O)**. Visualization of GA_3 by the Alexa Fluor 488 conjugated secondary antibody (green), nuclei, and bacteria stained with propidium iodide (red). Scale bar = 100 μm.

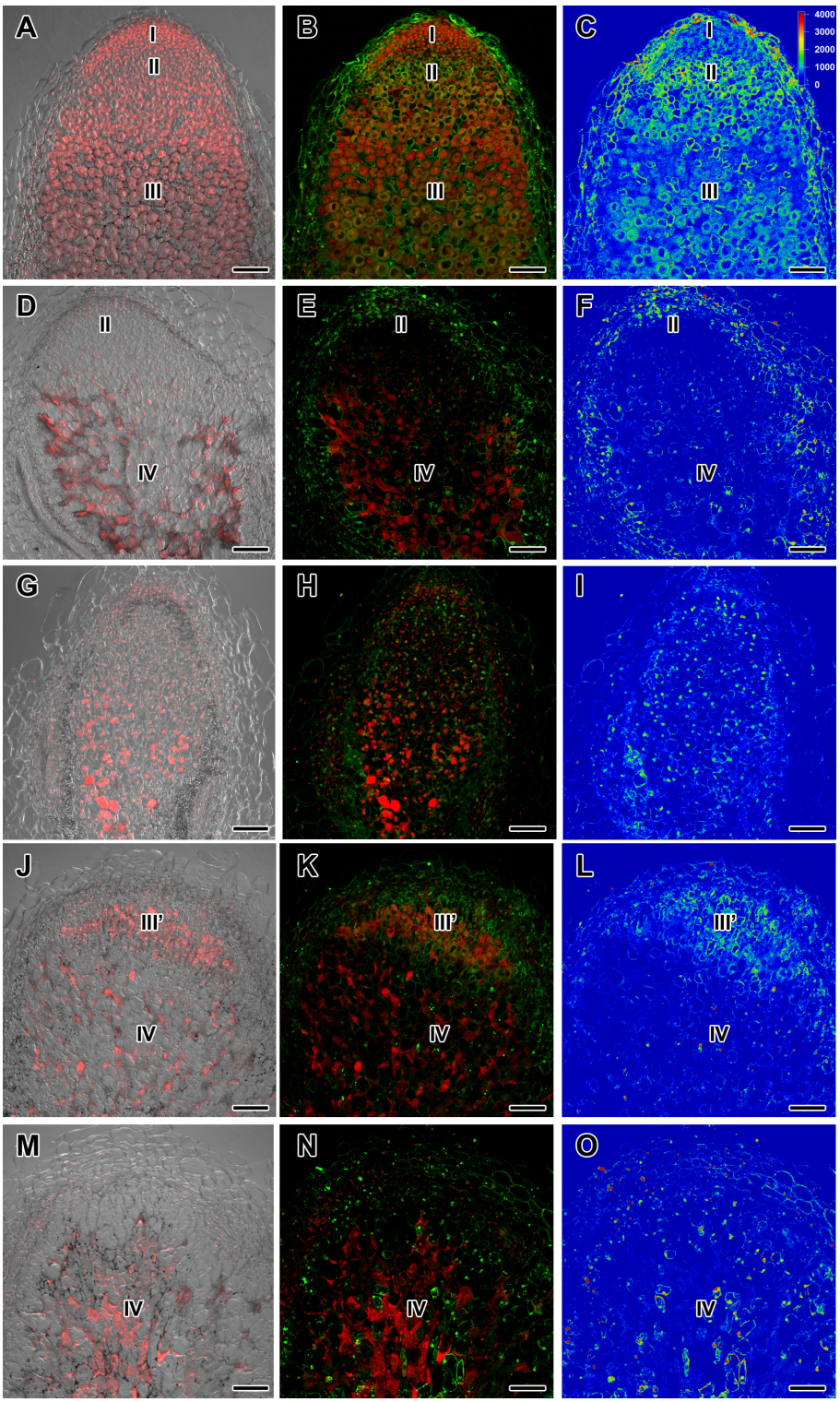

FIGURE 3 | Immunolocalization of gibberellin (GA_3) in nodules of wild-type SGE **(A–C)** and corresponding pea mutants SGEFix$^-$-1 (*sym40*) **(D–F)**, SGEFix$^-$-2 (*sym33*) **(G–I)**, SGEFix$^-$-3 (*sym26*) **(J–L),** and SGEFix$^-$-7 (*sym27*) **(M–O)** at 4 weeks after inoculation. Zones of nodule are designated by Roman numerals: I – meristem, II – infection zone, III – fixation zone, III' – zone corresponding to nitrogen fixation zone in wild-type, IV – senescence zone. A differential interference contrast microscopy image merged with laser scanning confocal microscopy image in red channel **(A,D,G,J,M)**. Merged images of laser scanning confocal microscopy in green and red channels **(B,E,H,K,N)**. Heat map provides a color code of fluorescence signal intensities **(C,F,I,L,O)**. Visualization of GA_3 by the Alexa Fluor 488 conjugated secondary antibody (green), nuclei, and bacteria stained with propidium iodide (red). Scale bar = 100 μm.

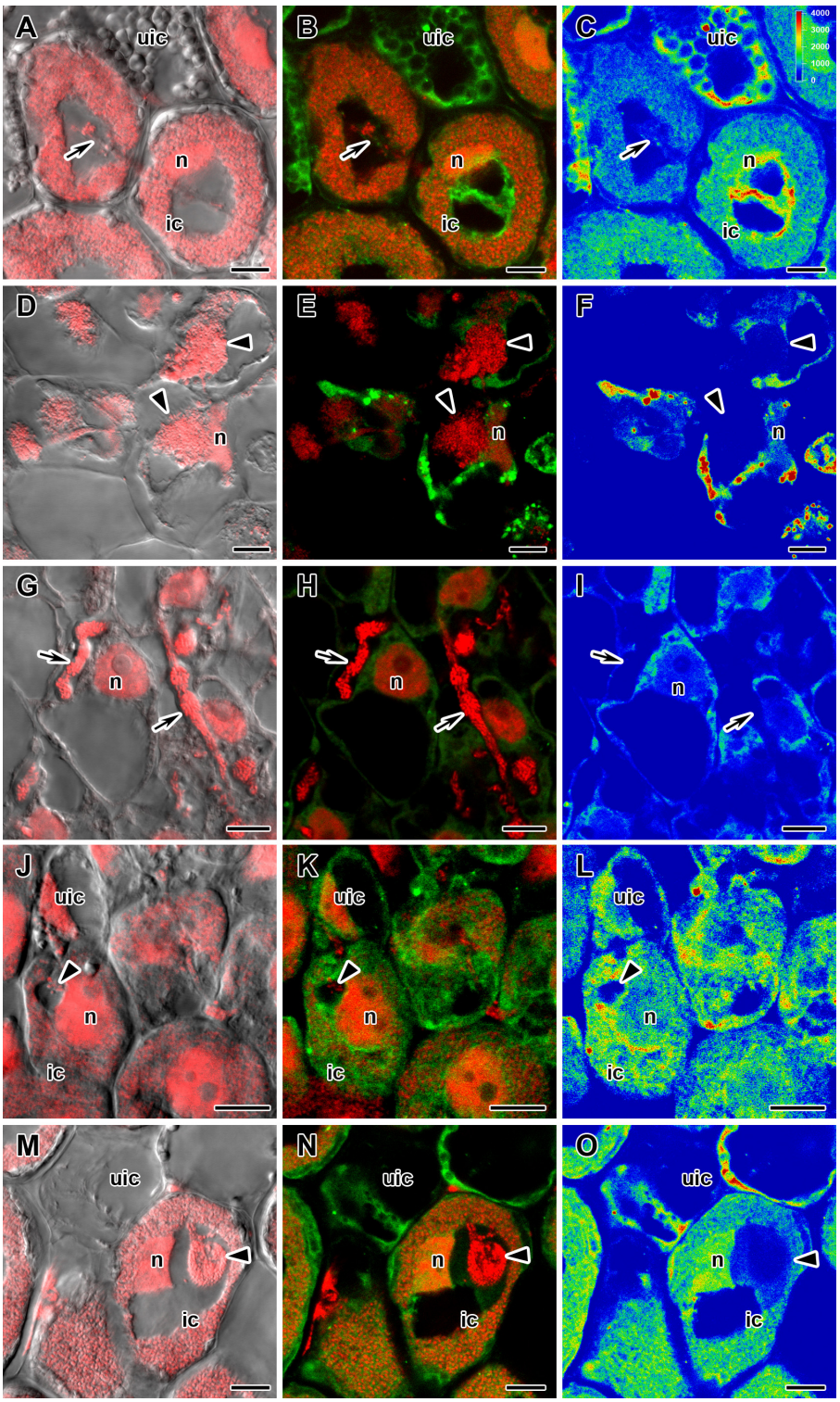

FIGURE 4 | Immunolocalization of gibberellin (GA_3) in cells in central part of nodules of wild-type SGE **(A–C)** and corresponding pea mutants SGEFix$^-$-1 (*sym40*) **(D–F)**, SGEFix$^-$-2 (*sym33*) **(G–I)**, SGEFix$^-$-3 (*sym26*) **(J–L)**, and SGEFix$^-$-7 (*sym27*) **(M–O)** at 2 weeks after inoculation. ic, infected cell; uic, uninfected cell; n, nucleus. Arrow indicates infection thread, arrowhead indicates infection droplet. A differential interference contrast microscopy image merged with laser scanning confocal microscopy image in red channel **(A,D,G,J,M)**. Merged images of laser scanning confocal microscopy in green and red channels **(B,E,H,K,N)**. Heat map provides color code of fluorescence signal intensities **(C,F,I,L,O)**. Visualization of GA_3 by the Alexa Fluor 488 conjugated secondary antibody (green), nuclei, and bacteria stained with propidium iodide (red). Scale bar = 10 μm.

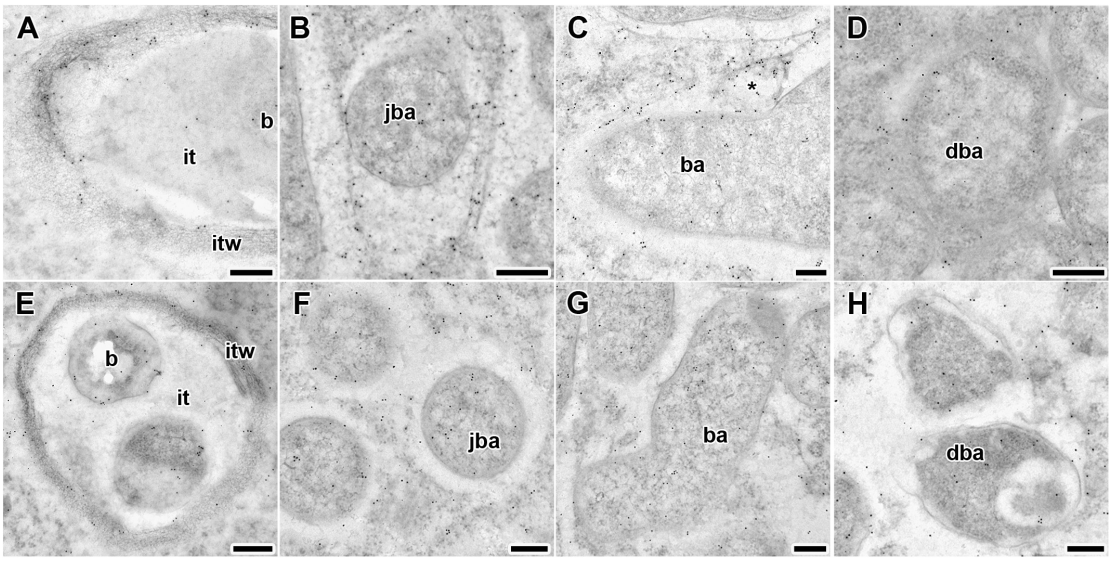

FIGURE 5 | Immunogold localization of gibberellin (GA_3) in nodules of wild-type SGE **(A–D)** and mutant SGEFix$^-$-3 (*sym26*) **(E–H)** at 2 weeks after inoculation. Secondary goat anti-rat IgG MAb conjugated to 10 nm diameter colloidal gold was used. it, infection thread; itw, infection thread wall; b, bacterium; ba, bacteroid; jba, juvenile bacteroid; dba, degrading bacteroid; asterisk indicates vesicle with GA_3 label. **(A,E)** Infection threads, **(B,F)** juvenile symbiosomes, **(C,G)** mature symbiosomes, **(D,H)** senescent symbiosomes. Scale bar **(A,E)** = 500 nm, **(B–D,F–H)** = 200 nm.

and **Supplementary Figures S6D–F**). A high intensity of fluorescence was detected in the mutants SGEFix$^-$-3 (*sym26*) (**Figures 2J–L**) and SGEFix$^-$-7 (*sym27*) (**Figures 2M–O**) in 2-week-old nodules. In SGEFix$^-$-3 (*sym26*), it was even higher than that of the wild-type nodules of the same age. In the mutants SGEFix$^-$-3 (*sym26*) and SGEFix$^-$-7 (*sym27*), the maximum GA_3 signal was observed in infected and uninfected cells of regions corresponding to the nitrogen fixation zone of wild-type nodules (**Figures 4J–O**). The amount of GA_3 was significantly decreased in the senescence zone occupying the dominant part of 4-week-old mutant nodules (**Figures 3J–O**). Trace levels of GA_3 label were observed in uninfected cells (**Supplementary Figures S6G–L**).

Thus, a decline in the amount of detectable GA_3 during aging of pea symbiotic nodules of wild-type and mutant lines and its distribution in different histological nodule zones were demonstrated.

Immunogold Localization of GA_3 in Nodules of Wild-Type SGE and Mutant SGEFix$^-$-3 (*sym26*)

To compare the localization of GA_3 in the infection structures in 2-week-old nodules, immunogold localization of GA_3 was carried out in the wild-type and SGEFix$^-$-3 (*sym26*) nodules (**Figure 5**).

Gold particles were observed in nuclei, vacuoles, and plastids, and were very abundant in cytoplasm (data not shown). Rare gold particles were observed in the matrix of infection threads in wild-type (**Figure 5A**) and SGEFix$^-$-3 (*sym26*) (**Figure 5E**) as well as in the infection droplets (**Table 2**). Gold particles were mainly found in the infection thread walls and in bacteria embedded in the infection thread matrix (**Figures 5A,E**). With respect to symbiosomes, numerous gold particles were observed mainly in bacteroids of both SGE and mutant SGEFix$^-$-3 (*sym26*) (**Figures 5B–D,F–H**), although some labeling was also found in the symbiosome membrane especially in the juvenile symbiosomes in nodules of wild-type SGE (**Figure 5B**). In nodules of SGE, some vesicles with GA_3 label were found in the peribacteroid spaces (**Figure 5C**). The highest amount of gold particles was

TABLE 2 | Distribution of gold particles in 2-week-old nodules of pea wild-type SGE and mutant SGEFix$^-$-3 (*sym26*) (immunogold localization).

Genotype	Localization	Mean value	*SE*
SGE	Juvenile symbiosomes	61.25^{ad}	2.73
	Mature symbiosomes	43.03^{bd}	2.46
	Senescent symbiosomes	19.90^{cd}	2.94
	Infection threads and infection droplets	11.15^{f}	2.78
SGEFix$^-$-3 (*sym26*)	Juvenile symbiosomes	40.95^{ae}	6.29
	Mature symbiosomes	32.28^{be}	3.38
	Senescent symbiosomes	24.85^{ce}	2.98
	Infection threads and infection droplets	15.36^{f}	2.23

Results are presented as the number of gold particles/μm^2. Mean value ± SE (n = 30–60) are shown. Letters indicate statistically significant differences by the Tukey multiple range test (P-value ≤ 0.001): a, between juvenile symbiosomes of wild type and the mutant; b, between mature symbiosomes of wild type and the mutant; c, between senescent symbiosomes of wild type and the mutant; d, between juvenile, mature, and senescent symbiosomes in wild type; e, between juvenile, mature, and senescent symbiosomes in the mutant; f, between infection threads and infection droplets in wild type and the mutant.

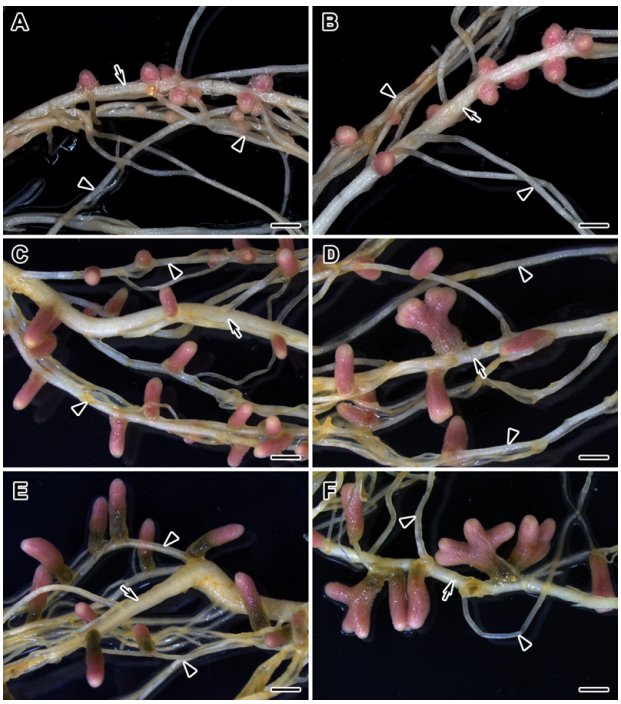

FIGURE 6 | Nodulated main and lateral roots of wild-type SGE pea plants untreated **(A**,**C**,**E)** and treated with exogenous gibberellin (GA_3) (**B**,**D**,**F)** at 2, 4, and 6 weeks after inoculation. Arrow indicates main roots; arrowheads indicate lateral roots. Scale bar = 2 mm.

observed in juvenile symbiosomes in both analyzed genotypes (**Figures 5B,F** and **Table 2**). In mature symbiosomes and especially in senescent symbiosomes in nodules of SGE and mutant SGEFix$^-$-3 (*sym26*), the amount of gold particles of the GA_3 label was lower than that in juvenile symbiosomes (**Figures 5C,D,G,H** and **Table 2**). It is necessary to note that the amount of gold particles of the GA_3 label was lower in symbiosomes of the mutant SGEFix$^-$-3 (*sym26*) than in wild-type nodules (**Table 2**).

Thus, it was shown that with an increase in the age of wild-type and mutant nodules, the amount of GA_3 decreased in symbiosomes.

Analysis of Nodules of SGE Treated With Exogenous GA_3 Relative to Untreated Plants

The involvement of bioactive GAs in senescence of pea symbiotic nodules was also measured via GA_3 treatment of wild-type plants (**Figure 6**). A quantitative analysis of 2-, 4-, and 6-week-old nodules of GA_3-treated and untreated plants was carried out (**Tables 3**, **4**). Additionally, an analysis of the effect of GA_3-treatment on the histological structure of the symbiotic nodule was performed (**Figure 7**). To identify the involvement of bioactive GAs in senescence of pea nodules at the transcriptional level, the analysis of senescence-associated genes was carried out in nodules of GA_3-treated and untreated plants at 2, 4, and 6 WAI (**Figures 8**, **9**).

TABLE 4 | Projection areas of whole nodule and senescence zone of GA_3-treated and untreated wild-type SGE pea plants at 2, 4, and 6 weeks after inoculation (WAI).

Treatment	WAI	Projection area of whole nodule, mm^2	Projection area of senescence zone, % of whole nodule projection area
SGE	2	0.91 ± 0.05	ND
	4	2.82 ± 0.12^b	ND
	6	3.56 ± 0.17^{bc}	62.4 ± 2.47
SGE + 10^{-6} M GA_3	2	1.63 ± 0.07^a	ND
	4	5.48 ± 0.35^{ab}	ND
	6	5.84 ± 0.76^{ab}	34.0 ± 3.08^a

Plants were inoculated with R. leguminosarum 3841. Results are means ± SEM (n = 8–13). Letters indicate statistically significant differences (P-value ≤ 0.01): a, from untreated plants at one time point; b, within variant (GA_3-treated or untreated) compared with 2 WAI; c, within variant (GA_3-treated or untreated) compared with 4 WAI. ND, no data.

TABLE 3 | Shoot, root, and nodule dry weight (DW), nodule number per plant, percentage of nodules with meristem bifurcation and nodules without senescence zone of GA_3-treated and untreated wild-type SGE at 2, 4, and 6 weeks after inoculation (WAI).

Treatment	WAI	Shoot DW, mg	Root DW, mg	Total nodule DW, mg	Average nodule DW, mg	Number of nodules per plant	Percentage of nodules with meristem bifurcation	Percentage of nodules without senescence zone
SGE	2	61.6 ± 5.97	30.64 ± 2.47	2.11 ± 0.26	0.1 ± 0.008	21 ± 1.81	ND	ND
	4	148.65 ± 11.39^b	48.82 ± 4.55^b	15.03 ± 1.19^b	0.27 ± 0.012^b	54.75 ± 3.52^b	9.13 ± 1.91	ND
	6	659.62 ± 45.17^{bc}	118.52 ± 14.18^{bc}	21.02 ± 2.48^b	0.28 ± 0.016^b	78.45 ± 6.68^{bc}	3.63 ± 0.74	13.92 ± 2.34
SGE + 10^{-6}M GA_3	2	77.24 ± 9.79	36.17 ± 3.28	3.24 ± 0.52	0.21 ± 0.018^a	13.45 ± 1.63^a	ND	ND
	4	244 ± 15.58^{ab}	52.38 ± 4.35^b	14.32 ± 1.34^b	0.67 ± 0.085^{ab}	22.64 ± 1.45^{ab}	32.52 ± 4.86^a	ND
	6	747.44 ± 96.54^{bc}	109.03 ± 14.35^{bc}	17.7 ± 3.03^b	0.64 ± 0.15^{ab}	36.78 ± 5.94^{ab}	23.01 ± 4.57^a	40.26 ± 3.96^a

Plants were inoculated with R. leguminosarum 3841. Results are means ± SE (n = 9–16). Letters indicate statistically significant differences (P-value ≤ 0.01): a, from untreated plants at one time point; b, within variant (GA_3-treated or untreated) compared with 2 WAI; c, within variant (GA_3-treated or untreated) compared with 4 WAI. ND, no data.

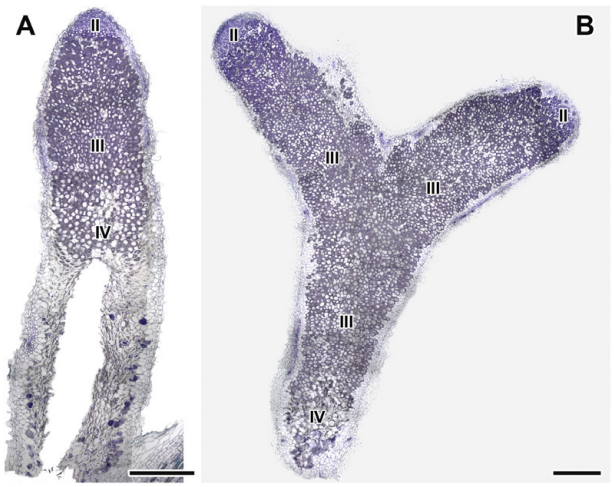

FIGURE 7 | Histological organization of nodules in wild-type SGE pea plants untreated **(A)** and treated with exogenous gibberellin (GA_3) **(B)** at 6 weeks after inoculation. Zones in nodules are designated by Roman numerals: II – infection zone, III – fixation zone, IV – senescence zone. Sections were stained with toluidine blue. Scale bar = 500 μm.

Quantitative Measurements of Nodulation of GA_3-Treated and Untreated Plants

During nodule aging, an increase in dry weight (DW) and size of nodules was observed in both GA_3-treated and untreated plants (**Tables 3**, **4**). In the untreated plants, the average nodule DW and the projection area of the whole nodule were increased 2.8 and 4 times, respectively, during aging from 2 to 6 WAI (**Figures 6A,C,E** and **Tables 3**, **4**). In 6-week-old untreated plants, 10- and 3.7-fold increases in the total nodule DW and the number of nodules, respectively, were observed relative to 2-week-old plants (**Table 3**). A low degree (9.13 and 3.63%) of meristem bifurcation was detected in 4- and 6-week-old nodules of untreated plants, respectively (**Figures 6C,E** and **Table 3**). At 6 WAI, the senescence zone dominated in the nodules of untreated plants and occupied approximately 62% of the entire nodule (**Figure 6E** and **Table 4**).

In the case of GA_3-treatment, 3- and 3.6-fold increases in the average nodule DW and projection area of the whole nodule, respectively, were observed at 6 WAI, in comparison with 2 WAI (**Figures 6B,D,F** and **Tables 3**, **4**). In GA_3-treated plants, the total nodule DW and the number of nodules were 5.4- and 2.7-times higher, respectively, during aging from 2 to 6 WAI (**Table 3**). Pronounced meristem bifurcation (32.52 and 23.01%) was observed in 4- and 6-week-old nodules of GA_3-treated plants, respectively (**Figures 6D,F** and **Table 3**). Despite the presence of the senescence zone occupying approximately 34% of the entire nodule, the biggest part of the nodules in GA_3-treated plants was represented by the nitrogen fixation zone (**Figure 6F** and **Table 4**).

The average DW and projection area of whole 2-week-old nodules of GA_3-treated plants were 2.1 and 1.8 times, respectively, larger than those of nodules of untreated plants (**Tables 3**, **4**). At 2 WAI, visual manifestation of the senescence zone (green color) was absent in nodules of GA_3-treated and untreated plants (**Figures 6A,B**). At 4 WAI, the average nodule DW and projection area of nodules of plants treated with exogenous GA_3 were 2.5 and 2 times larger, respectively, than the nodules of the untreated plants (**Tables 3**, **4**). In addition to the increase in size, the percentage of nodules exhibiting meristem bifurcation was 3.6 times greater in GA_3-treated plants than in untreated plants at 4 WAI (**Figures 6C,D** and **Table 3**). At 6 WAI, GA_3-treated plants also had a high percentage of nodules with branching due to meristem bifurcation being 6.3 times higher than that in untreated plants (**Figure 6F** and **Table 3**). At 6 WAI, nodules of plants treated with exogenous GA_3 were 2.3 and 1.6 times (average nodule DW and nodule projection area, respectively) larger than the nodules of the untreated plants (**Figure 6F** and **Tables 3**, **4**). In addition, in 6-week-old GA_3-treated plants, the number of nodules without visible signs of senescence was 2.8 times higher than that of untreated plants (**Table 3**). Also, it was noted that the number of nodules of plants treated with exogenous GA_3 was 1.5, 2.4, and 2.1 times smaller than that of the nodules of untreated plants at 2, 4, and 6 WAI, respectively (**Table 3**). In GA_3-treated plants, a 1.6-fold increase in shoot DW was observed at 4 WAI relative to the control (**Table 3**). At 2 and 6 WAI, these differences were insignificant.

Microscopic Analysis of Nodule Structure of GA_3-Treated and Untreated Plants

Longitudinal toluidine blue-stained sections of nodules of untreated and GA_3-treated plants were compared at 6 WAI. The nodules of untreated and GA_3-treated plants had the typical zonation of indeterminate nodules (**Figure 7**). In 6-week-old nodules of untreated plants, the senescence zone, which was characterized by flattened cells, loss of cell rigidity and cellular integrity, and plant cell wall breakage, occupied most of the nodule and contained a cavity due to complete decay of nodule cells (**Figure 7A**). While nodules of GA_3-treated plants had a vast nitrogen fixation zone, the senescence zone contained both infected and uninfected cells and occupied a smaller part than that in the nodules of untreated plants (**Figure 7B**).

Expression Analysis of Senescence-Associated Genes in Wild-Type Nodules Treated With Exogenous GA_3

In this study, an analysis of the expression of senescence-associated genes (Serova et al., 2017, 2018) and genes encoding enzymes of GA biosynthesis (*PsGA20ox1*) and deactivation (*PsGA2ox1*) was carried out. Changes in the mRNA levels of these genes during GA_3 treatment allowed us to evaluate the possible effect of GAs on nodule senescence at the level of transcription.

A significant increase in the expression levels of selected cysteine protease genes was observed during nodule aging of the untreated plants. However, elevation of transcript abundance in nodules of GA_3-treated plants was less pronounced (**Figures 8A–C**). In 6-week-old nodules of the untreated plants, expression levels of *PsCyp1*, *PsCyp15a*, and *PsTPP* genes were significantly increased relative to 2-week-old nodules, while in nodules of GA_3-treated plants, no statistically significant differences in *PsCyp1* and *PsTPP* transcript abundances were

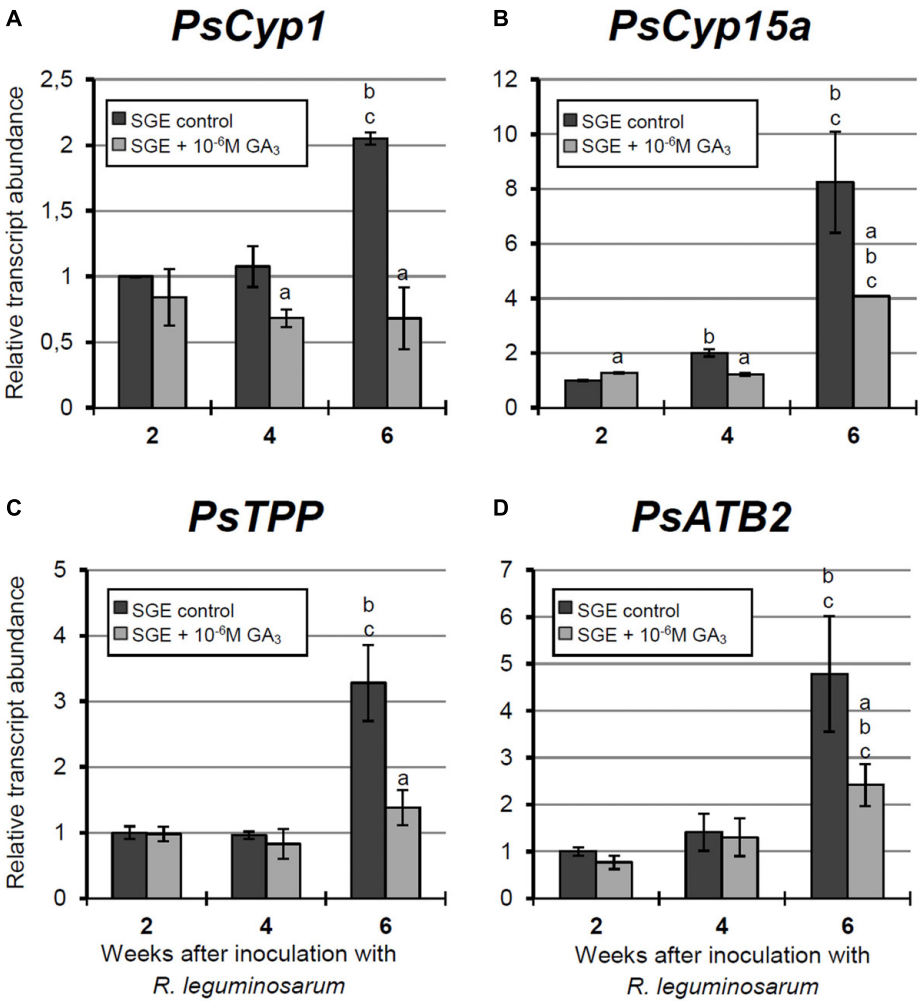

FIGURE 8 | Relative expression of **(A–D)** *PsCyp1*, *PsCyp15a*, *PsTPP*, and *PsATB2* genes in nodules of GA_3-treated and untreated wild-type SGE at 2, 4, and 6 weeks after inoculation (WAI). *Letters* indicate significant differences (one-way ANOVA, *P*-value ≤ 0.05, $n = 3$) a, from untreated plants at one time point; b, within variant (GA_3-treated or untreated) compared with 2 WAI; c, within variant (GA_3-treated or untreated) compared with 4 WAI.

detected during nodule aging (**Figures 8A,C**). At 6 WAI, an up-regulation in *PsCyp15a* mRNA was detected in nodules of GA_3-treated plants; however, the expression level was two times lower than in the untreated control (**Figure 8B**). In the case of *PsCyp1* and *PsTPP* genes, expression levels in mature nodules of GA_3-treated plants were 3- and 2.4-times lower, respectively, than in the untreated plants (**Figures 8A,C**).

A significant up-regulation of *PsATB2* transcript abundance was observed in the nodules of untreated plants from 4 to 6 WAI. A less pronounced elevation of expression was detected during aging of nodules of GA_3-treated plants, in comparison with the untreated control. Also, it was noted that at 6 WAI, *PsATB2* transcript abundance was two times lower in nodules of GA_3-treated plants than in the untreated plants (**Figure 8D**).

During nodule aging of the untreated plants, the expression levels of genes encoding key enzymes of ethylene biosynthesis, *PsACS2* and *PsACO1*, were significantly increased from 2 to 6 WAI. A less pronounced up-regulation of *PsACS2* and *PsACO1* mRNA levels was observed in 6-week-old nodules of GA_3-treated plants in comparison with 2-week-old nodules. At 6 WAI, *PsACS2* and *PsACO1* expression levels were 7.6- and 1.7-times lower, respectively, in nodules of GA_3-treated plants than in those of untreated plants (**Figures 9A,B**).

A significant decrease in the expression level of the *PsGA20ox1* gene was observed during nodule aging in both untreated and GA_3-treated plants. It is worth noting that in 6-week-old nodules of GA_3-treated plants, *PsGA20ox1* transcript abundance was 2.15-times lower than that in the nodules of untreated plants (**Figure 9C**). At 6 WAI, a significant elevation in the expression of *PsGA2ox1* was observed in the nodules of untreated and GA_3-treated plants, relative to 2 WAI. However, the difference between nodules of untreated and GA_3-treated plants at 6 WAI was not statistically significant. In 2-week-old nodules of GA_3-treated plants, however, *PsGA2ox1* transcript

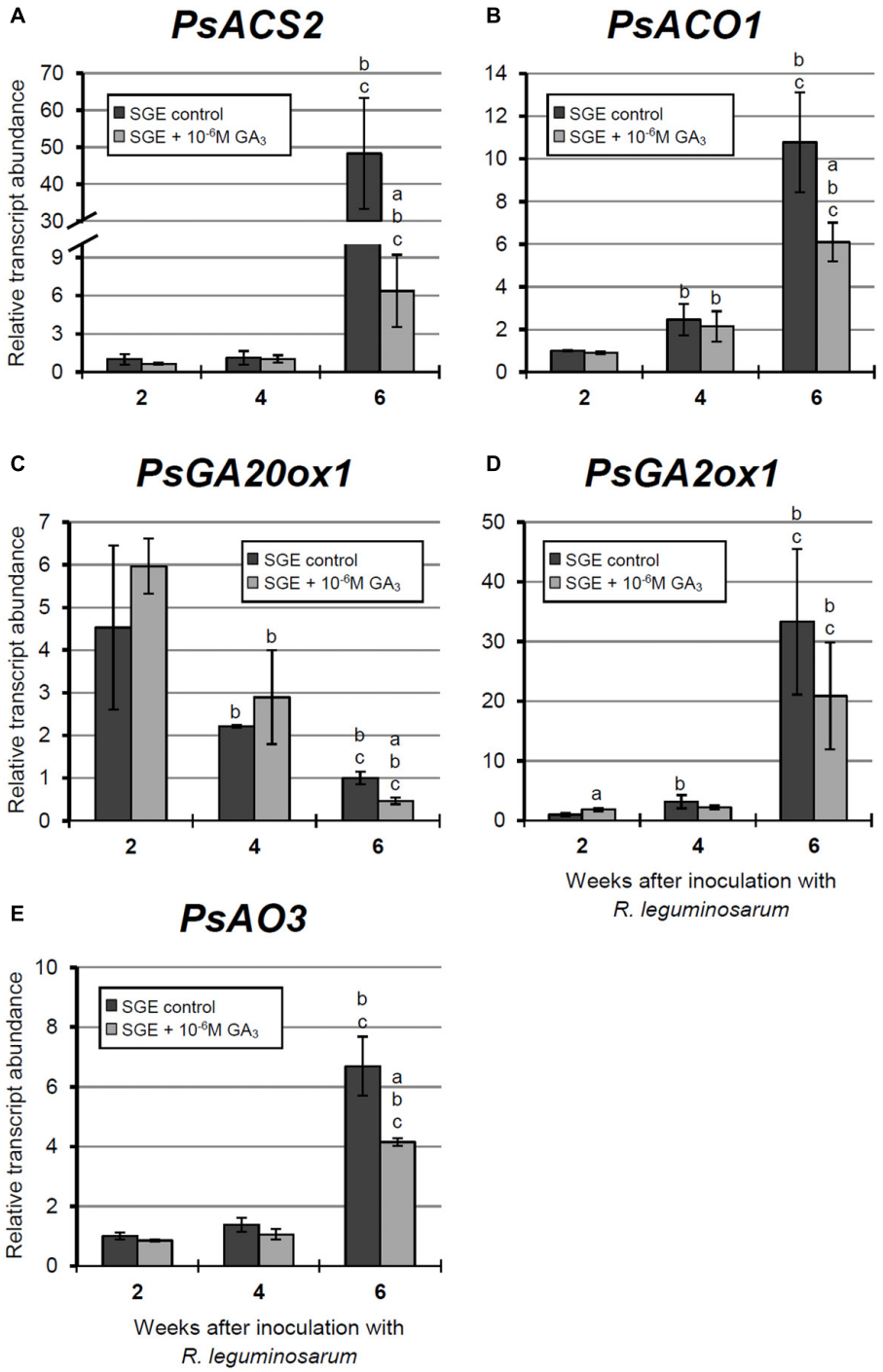

FIGURE 9 | Relative expression of **(A–E)** *PsACS2*, *PsACO1*, *PsGA20ox1*, *PsGA2ox1*, and *PsAO3* genes in nodules of GA_3-treated and untreated wild-type SGE at 2, 4, and 6 weeks after inoculation (WAI). *Letters* indicate significant differences (one-way ANOVA, *P*-value ≤ 0.05, $n = 3$) a, from untreated plants at one time point; b, within variant (GA_3-treated or untreated) compared with 2 WAI; c, within variant (GA_3-treated or untreated) compared with 4 WAI. Breaks of histogram bars indicate a change in scale.

abundance was slightly higher than in the nodules of untreated plants (**Figure 9D**).

Finally, up-regulated expression of *PsAO3*, the gene encoding an enzyme of the final stage of ABA biosynthesis, was detected in the nodules of untreated and GA_3-treated plants from 2 to 6 WAI. In 6-week-old nodules of GA_3-treated plants, *PsAO3* transcript abundance was slightly reduced relative to that in untreated plants (**Figure 9E**).

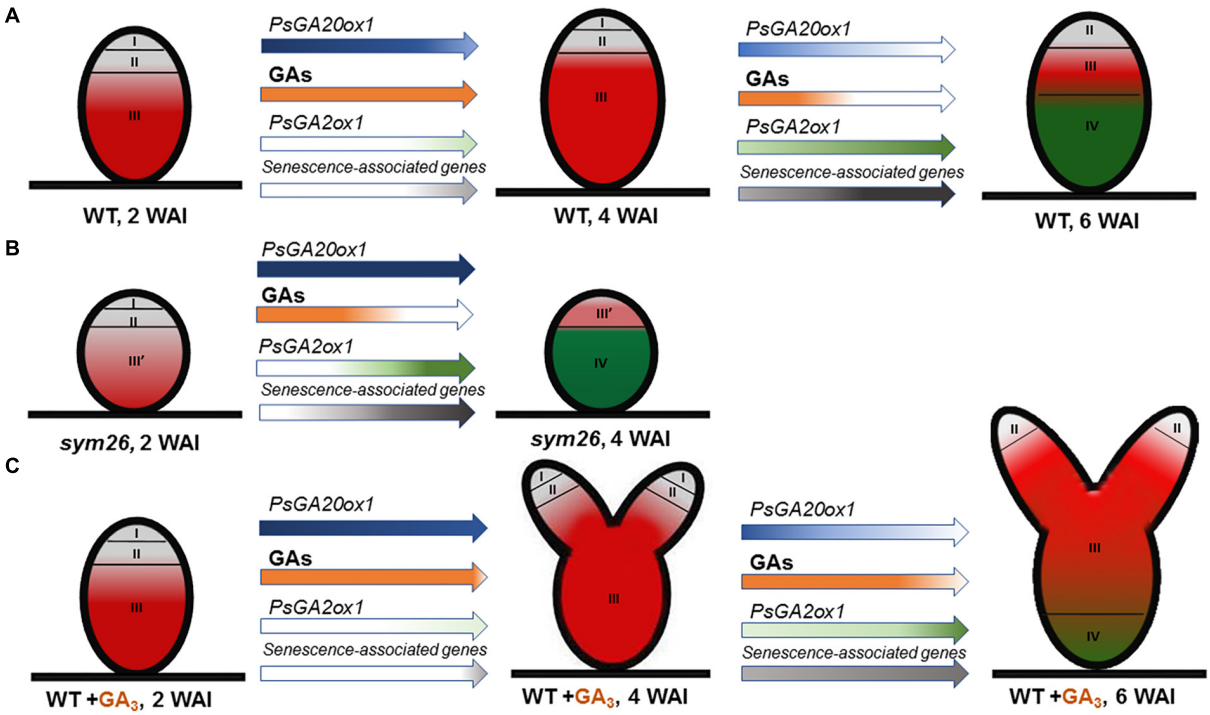

FIGURE 10 | Scheme of endogenous gibberellin influence on nodule senescence in wild-type **(A)** and mutant SGEFix$^-$-3 (*sym26*) nodules **(B)** and influence of exogenous GA_3 on nodule senescence and meristem bifurcation in wild-type **(C)**. Zones of nodule are designated by Roman numerals: I – meristem (in gray), II – infection zone (in gray), III – fixation zone, (in red) III' – zone corresponding to nitrogen fixation zone in wild-type (in red), IV – senescence zone (in green), WAI – weeks after inoculation. An increase in the color intensity of the arrows indicates elevated levels of gene expression, a decrease in color intensity indicates a reduction in expression levels. A decrease in orange intensity indicates a reduction in GA levels. The scheme is based on the results of this study and Serova et al. (2018).

Thus, a down-regulation of senescence-associated genes, a decrease of senescence zone, an extension of nitrogen-fixation zone, an increase of nodule size, and the pronounced meristem bifurcation were observed in wild-type nodules treated with exogenous GA_3 in comparison with the untreated plants.

DISCUSSION

In this study, we investigated the involvement of GAs in senescence of the symbiotic nodule using SGE and corresponding pea mutants blocked at different stages of nodule development. The mutant SGEFix$^-$-1 (*sym40*) forms numerous white nodules with hypertrophied infection threads and droplets, and abnormal bacteroids (Tsyganov et al., 1998). White nodules colonized with "locked" suberinized infection threads are typical for SGEFix$^-$-2 (*sym33*) (Tsyganov et al., 1998; Ivanova et al., 2015). SGEFix$^-$-2 carries a weak allele of the gene *sym33* and manifests a leaky phenotype. Usually, bacteria are not released from these infection threads; however, in some cells or some nodules, bacterial release occurs (Voroshilova et al., 2001). The mutants SGEFix$^-$-3 (*sym26*) and SGEFix$^-$-7 (*sym27*) are characterized by premature degradation of symbiotic structures, with degradation more pronounced in the former than in the latter (Serova et al., 2018). Recently, we demonstrated activation of nodule senescence in nodules of all analyzed mutants (Serova et al., 2018).

Previously, an increase in the expression level of GA biosynthesis genes (*GA20ox*, *GA3ox*) during early stages of the development of both determinate (Kouchi et al., 2004; Lievens et al., 2005; Maekawa et al., 2009; Hayashi et al., 2012) and indeterminate (Larrainzar et al., 2015) nodules was shown. A decrease in the transcript abundance of the GA biosynthesis genes was observed in mature nodules (Lievens et al., 2005; Hayashi et al., 2012). In our study, a significant decline in the transcript level of the *PsGA20ox1* gene was detected in wild-type nodules at 4 and 6 WAI (**Figure 10A**). One of the mechanisms to maintain optimal concentrations of bioactive GAs is 2β-hydroxylation, which leads to a decrease in content of bioactive GAs (Thomas et al., 1999; Hedden and Thomas, 2012). *GA2ox* transcript levels were found to be elevated during the aging of symbiotic nodules of *M. truncatula* (Van de Velde et al., 2006) and pea (Serova et al., 2017) plants. Furthermore, *GA2ox* transcripts were detected in maturing nodules of *L. japonicus* (Kouchi et al., 2004). In this study, the *PsGA2ox1* mRNA level was elevated at 6 WAI (**Figure 10A**). Thus, we suggest that during nodule aging, bioactive GA levels decrease; maintaining the optimal concentration of bioactive GAs appears to occur via the down-regulation of its biosynthetic genes and the up-regulation of its deactivation genes. The results of expression analysis were complemented by those

obtained from immunolocalization of bioactive GA_3. In the wild-type plants, a high intensity of GA_3 label was detected in 2-week-old nodules and was maintained in mature 4-week-old nodules, but it was significantly decreased in old 6-week-old nodules (**Figure 10A**). The high GA_3 content in meristematic cells may indicate the involvement of GAs in cell cycle activation, cell division, and persistence of the nodule meristem. Previously, it was shown that GAs modulate cell cycle activity in Arabidopsis roots (Achard et al., 2009). In addition, pea mutants impaired in GA biosynthetic genes displayed decreased nodulation and aberrant nodule meristem formation (Ferguson et al., 2005, 2011).

A high intensity of GA_3 labeling was detected in the infected cells in the nitrogen fixation zone, where it was associated mainly with cytoplasm and symbiosomes. In juvenile symbiosomes, the amount of label was higher than in mature and senescent symbiosomes. It is worth noting that McAdam et al. (2018) recently revealed that GAs promote the functioning of nitrogen-fixing nodules. However, the exact function of GAs in infected cell and symbiosome development merits elucidation. Previously, a negative impact of GAs on infection thread development was revealed (McAdam et al., 2018). In our study, we observed that the amount of GA_3 in the infection threads was lower than in symbiosomes. However, GA_3 was detected in infection thread walls. The function of GAs in infection thread development is currently unknown. It is interesting to note that GA involvement in facilitating bacterial release from the infection threads was recently suggested (Tatsukami and Ueda, 2016).

In uninfected cells, labeling of GA_3 was associated with cytoplasm around starch granules. Ferguson and Mathesius (2003) suggested involvement of GAs in the hydrolysis of nodule starch through enhancement of α-amylase production. Substrates formed during this reaction might support the energetic requirements of rhizobia. In general, GAs may benefit both symbiotic partners through involvement in cell division and elongation, and by providing energy to support plant growth. GAs may enhance photosynthetic capacity, leading to an increase in photoassimilate content for growth and functioning of the symbiotic nodule (Ferguson and Mathesius, 2003). Six-week-old wild-type nodules contained a low amount of bioactive GA_3 (**Figure 10A**). Traces of GA_3 label were detected in the uninfected cells of the senescence zone; these cells might be degraded later that the infected cells of that same zone (Pladys et al., 1991).

Expression analysis of GA metabolism genes revealed down-regulation of a GA biosynthesis gene, *PsGA20ox1*, and significant up-regulation of a GA deactivation gene, *PsGA2ox1*, during nodule aging of the early senescent mutants SGEFix$^-$-7 (*sym27*) and SGEFix$^-$-3 (*sym26*), which confirms involvement of GAs in senescence of symbiotic nodules (**Figure 10B**). However, for mutant SGEFix$^-$-3 (*sym26*), an increase in *PsGA20ox1* expression in 4-week-old nodules in comparison with 2-week-old nodules was observed. This increase is difficult to explain, but future elucidation of the gene *sym26* molecular product may be informative. Data obtained with GA_3 immunolocalization coincided with the observed transcriptional patterns. In 2-week-old nodules of the mutants SGEFix$^-$-3 (*sym26*) and SGEFix$^-$-7 (*sym27*), the maximum GA_3 signal was observed in cells of the region corresponding to the nitrogen fixation zone of the wild-type nodules (**Figure 10B**). In the vast senescence zone of 4-week-old nodules, the intensity of GA_3 label was low and predominantly found in uninfected cells. Both mutants form nodules with morphologically differentiated bacteroids, which characterized with early senescence (Serova et al., 2018). Recently, it was shown that in defective nodules of GA-deficient mutant *na-1*, bacteroids undergo premature degradation (McAdam et al., 2018). Together, these data strongly indicate that aging of symbiotic nodules is accompanied by a decrease in the level of GAs, which suggests involvement of GAs in the delay of nodule senescence (**Figures 10A,B**).

No significant differences in *PsGA20ox1* and *PsGA2ox1* transcript abundance were seen during nodule aging of the mutant SGEFix$^-$-2 (*sym33*), blocked at the earliest stage of symbiosis. In addition, a low level of GA_3 labeling in nodules of the mutant SGEFix$^-$-2 (*sym33*) was observed. Recently, we have shown early activation of senescence-associated genes in this mutant at 2 WAI (Serova et al., 2018). This activation may explain the low level of GAs in the mutant. The low level of bioactive GAs in the mutant SGEFix$^-$-2 (*sym33*) is accompanied by the absence of infected cells due to the absence of bacterial release (Tsyganov et al., 1998). These results may reflect the necessity of GAs for bacterial release (Tatsukami and Ueda, 2016) and infected cell development.

Analysis of the mutant SGEFix$^-$-1 (*sym40*), blocked at a later stage of symbiosis than mutant SGEFix$^-$-2 (*sym33*) (Tsyganov et al., 2011) and manifesting signs of premature nodule senescence (Tsyganov et al., 1998; Serova et al., 2018), demonstrated a similar transcriptional pattern of *PsGA20ox1* to that observed in wild-type nodules and a significant increase in *PsGA2ox1* mRNA as well as low GA_3 label content in 4-week-old nodules. These data are suggestive of a negative role of GAs during nodule senescence.

Aging of the symbiotic nodule is regulated by changes in gene expression. In particular, the expression levels of genes encoding cysteine proteases, transcription factors, enzymes of GA deactivation, and enzymes of ethylene and ABA biosynthesis were shown to increase during senescence of *M. truncatula* and pea nodules (Kardailsky and Brewin, 1996; Van de Velde et al., 2006; D'haeseleer et al., 2010; de Zélicourt et al., 2012; Karmarkar, 2014; Serova et al., 2017, 2018). To assess the effect of GAs on the senescence of the pea symbiotic nodules, we analyzed the mRNA levels of senescence-associated genes in 2-, 4-, and 6-week-old nodules of wild-type plants treated with exogenous GA_3 relative to untreated plants. A less pronounced increase in transcript levels of genes *PsCyp1*, *PsCyp15*, and *PsTPP* was shown during aging of the nodules of GA_3-treated plants, in contrast to the nodules of the untreated plants. In addition, the transcript abundance of all analyzed genes

was significantly higher in the nodules of untreated plants than in nodules of plants treated with GA_3 at 6 WAI, which may indicate a delay of nodule senescence upon treatment with exogenous GA_3 (**Figure 10C**). It is known that cysteine proteases carry out large-scale protein degradation during nodule senescence (Pladys et al., 1991; Granell et al., 1992; Kardailsky and Brewin, 1996; Van de Velde et al., 2006; Pérez Guerra et al., 2010). Thus, our data suggest that a decrease in GAs is required to induce the degradation processes during nodule aging. Previously, it was shown that the expression level of the *ATB2* gene was up-regulated during senescence of *M. truncatula* (D'haeseleer et al., 2010) and pea (Serova et al., 2017) nodules. The transcript level of *PsATB2* was reduced in the nodules of GA_3-treated plants in comparison with the nodules of untreated plants (**Figure 10C**). This may indicate possible regulation of nodule senescence by GAs through an effect on the bZIP transcription factor. Similar expression patterns were observed for genes encoding key enzymes of ethylene biosynthesis, ACC synthase (*PsACS2*), ACC oxidase (*PsACO1*), and aldehyde oxidase (*PsAO3*), an enzyme catalyzing the last step of ABA biosynthesis (**Figure 10C**). It is known that ethylene and ABA promote nodule senescence (Swamy and Smith, 1999; Guinel, 2015; Serova et al., 2017, 2018). In addition, elevation of ethylene levels in the *na-1* mutant was previously demonstrated (Ferguson et al., 2011). Thus, a lower expression level of *PsACS2*, *PsACO1*, and *PsAO3* genes in the nodules of GA_3-treated plants may also suggest integration of hormonal signaling during nodule senescence. During the nodule aging of both GA_3-treated and untreated plants, down-regulation of one GA biosynthetic gene, *PsGA20ox1*, and up-regulation of one GA deactivation gene, *PsGA2ox1*, were demonstrated (**Figure 10C**). However, only *PsGA2ox1* transcript abundance was significantly lower in the nodules of GA_3-treated plants than in those of untreated plants at 6 WAI. Thus, it can be assumed that regulation of bioactive GAs in the nodules of GA_3-treated plants occurred mainly by regulation of GA biosynthesis.

Two-week-old nodules of GA_3-treated plants were about two times larger than the nodules of untreated plants, probably due to involvement of GAs in cell division and cell elongation (Hedden and Thomas, 2012). The number of nodules formed by GA_3-treated plants was nearly two times smaller than that in untreated plants. Previously, a similar concentration (10^{-6} M) of GA_3 had no effect on nodule number in the wild type, but a higher concentration (10^{-3} M) inhibited nodule formation (Ferguson et al., 2005). This contradiction may be due to differences in plant genotypes and experimental conditions. However, GA_3 treatment of the severely inhibited GA mutant *na-1*, characterized as having a low number of nodules, restored nodule number, which suggests a direct role for GAs in nodule development (Ferguson et al., 2005). Most of the GA mutants were characterized by a reduced number of nodules, but increased nodule dry weight. It has been suggested by Ferguson et al. (2005) that there is a compensation mechanism to regulate the size of individual nodules, depending on the number of nodules per plant.

Pronounced meristem bifurcation was observed in 4- and especially 6-week-old nodules of GA_3-treated plants (**Figure 10C**). This may indicate the involvement of GAs in functioning of the nodule meristem. Previously, it was shown that meristem bifurcation during root branching is under phytohormonal control, including auxin, cytokinins, and ethylene (Gola, 2014). GA_3 immunolocalization in pea nodules performed in this study and previous studies carried out on Arabidopsis and pea plants (Ferguson et al., 2005, 2011; Achard et al., 2009) confirms the involvement of GAs in nodule meristem functioning. It should be noted that 6-week-old nodules of GA_3-treated plants also had a senescence zone, but it occupied a smaller part (about 34%) of the nodule than in nodules of the untreated plants (about 62%). This may be due to the meristem bifurcation observed in the nodules of GA_3-treated plants. It is known that senescence of the nodule is associated with arrested division of meristem cells and the discontinuance of rhizobial release from infection droplets (Guinel, 2015).

The main part of mature nodules of GA_3-treated plants was represented by the nitrogen fixation zone (**Figure 10C**). Also, the high content of GA_3 label in cells of the nitrogen fixation zone in young and mature pea nodules indicates a possible involvement of GAs in the functioning of nitrogen fixation nodules and, consequently, delay of nodule senescence. In *A. thaliana*, it was shown that DELLAs repress the inhibitory effect of JASMONATE ZIM-domain proteins (JAZ), which are transcriptional regulators, on the expression of jasmonate (JA) responsive genes, such as lipoxygenase and defense genes (Hou et al., 2010). On the contrary, GAs suppress the expression of JA-responsive genes via DELLA degradation. Thus, the involvement of GAs in suppressing the response to JA-induced signaling may be one of the mechanisms by which GAs contribute to the delay of nodule senescence, which is regarded as a delayed response of the plant to rhizobia as a potential pathogen (Mellor, 1989). Furthermore, an up-regulation of transcripts of JA biosynthesis genes was observed during *M. truncatula* nodule senescence (Van de Velde et al., 2006).

CONCLUSION

In this study, the involvement of bioactive GAs in nodule senescence of pea wild-type and nodule development mutants was studied by assessing transcriptional patterns of GA metabolism genes, and through GA_3 immunolocalization and pharmacological analyses. A decrease in GA content during nodule aging was demonstrated at the transcriptional level via a down-regulation of the GA biosynthesis gene, *PsGA20ox1*, and an up-regulation of the GA deactivation gene, *PsGA2ox1*, and also by the immunolocalization of bioactive GA_3 in the mutant and wild-type nodules. These results indicate a role of GAs in a delay of nodule senescence. A down-regulation of senescence-associated genes, a decrease of the senescence zone, and an increase of the nitrogen fixation zone in nodules of wild-type plants treated with exogenous GA_3 confirm a negative regulation of nodule senescence by GAs and involvement of GAs in the functioning of the mature nodule.

DATA AVAILABILITY

All datasets generated for this study are included in the manuscript and/or the **Supplementary Files**.

AUTHOR CONTRIBUTIONS

IT designed the experiments. TS and AT performed the experiments. TS and VT analyzed the data and wrote the manuscript.

FUNDING

This work was supported by Russian Science Foundation (grant 17-76-30016).

ACKNOWLEDGMENTS

The research was performed using equipment of the Core Centrum "Genomic Technologies, Proteomics and Cell Biology" in ARRIAM and the "Molecular and Cell Technologies" Research Resource Centre at Saint Petersburg State University. We thank Charlesworth Author Services for English editing of a draft of this manuscript.

SUPPLEMENTARY MATERIAL

The Supplementary Material for this article can be found online at: https://www.frontiersin.org/articles/10.3389/fpls.2019.00285/full#supplementary-material

REFERENCES

Achard, P., Gusti, A., Cheminant, S., Alioua, M., Dhondt, S., Coppens, F., et al. (2009). Gibberellin signaling controls cell proliferation rate in Arabidopsis. *Curr. Biol.* 19, 1188–1193. doi: 10.1016/j.cub.2009.05.059

Brewin, N. J. (2004). Plant cell wall remodelling in the Rhizobium–legume symbiosis. *Crit. Rev. Plant Sci.* 23, 293–316. doi: 10.1080/07352680490480734

Davière, J.-M., and Achard, P. (2013). Gibberellin signaling in plants. *Development* 140, 1147–1151. doi: 10.1242/dev.087650

de Zélicourt, A., Diet, A., Marion, J., Laffont, C., Ariel, F., Moison, M., et al. (2012). Dual involvement of a *Medicago truncatula* NAC transcription factor in root abiotic stress response and symbiotic nodule senescence. *Plant J.* 70, 220–230. doi: 10.1111/j.1365-313X.2011.04859.x

D'haeseleer, K., De Keyser, A., Goormachtig, S., and Holsters, M. (2010). Transcription factor MtATB2: about nodulation, sucrose and senescence. *Plant Cell Physiol.* 51, 1416–1424. doi: 10.1093/pcp/pcq104

Dupont, L., Alloing, G., Pierre, O., El Msehli, S., Hopkins, J., Hérouart, D., et al. (2012). "The legume root nodule: from symbiotic nitrogen fixation to senescence," in *Senescence*, ed. T. Nagata (Rijeka: IntechOpen), 137–168. doi: 10.5772/34438

Ferguson, B. J., Foo, E., Ross, J. J., and Reid, J. B. (2011). Relationship between gibberellin, ethylene and nodulation in *Pisum sativum*. *New Phytol.* 189, 829–842. doi: 10.1111/j.1469-8137.2010.03542.x

Ferguson, B. J., and Mathesius, U. (2003). Signaling interactions during nodule development. *J. Plant Growth Regul.* 22, 47–72. doi: 10.1007/s00344-003-0032-9

Ferguson, B. J., and Mathesius, U. (2014). Phytohormone regulation of legume-rhizobia interactions. *J. Chem. Ecol.* 40, 770–790. doi: 10.1007/s10886-014-0472-7

Ferguson, B. J., Ross, J. J., and Reid, J. B. (2005). Nodulation phenotypes of gibberellin and brassinosteroid mutants of pea. *Plant Physiol.* 138, 2396–2405. doi: 10.1104/pp.105.062414

Fonouni-Farde, C., Tan, S., Baudin, M., Brault, M., Wen, J., Mysore, K. S., et al. (2016). DELLA-mediated gibberellin signalling regulates Nod factor signalling and rhizobial infection. *Nat. Commun.* 7:12636. doi: 10.1038/ncomms12636

García-Martínez, J. L., López-Diaz, I., Sánchez-Beltrán, M. J., Phillips, A. L., Ward, D. A., Gaskin, P., et al. (1997). Isolation and transcript analysis of gibberellin 20-oxidase genes in pea and bean in relation to fruit development. *Plant Mol. Biol.* 33, 1073–1084. doi: 10.1023/A:1005715722193

Gola, E. M. (2014). Dichotomous branching: the plant form and integrity upon the apical meristem bifurcation. *Front. Plant Sci.* 5:263. doi: 10.3389/fpls.2014.00263

Granell, A., Harris, N., Pisabarro, A. G., and Carbonell, J. (1992). Temporal and spatial expression of a thiolprotease gene during pea ovary senescence, and its regulation by gibberellin. *Plant J.* 2, 907–915. doi: 10.1046/j.1365-313X.1992.t01-5-00999.x

Guinel, F. C. (2009). Getting around the legume nodule: I. The structure of the peripheral zone in four nodule types. *Botany* 87, 1117–1138. doi: 10.1139/B09-074

Guinel, F. C. (2015). Ethylene, a hormone at the center-stage of nodulation. *Front. Plant Sci.* 6:1121. doi: 10.3389/fpls.2015.01121

Hayashi, S., Gresshoff, P. M., and Ferguson, B. J. (2014). Mechanistic action of gibberellins in legume nodulation. *J. Integr. Plant Biol.* 56, 971–978. doi: 10.1111/jipb.12201

Hayashi, S., Reid, D. E., Lorenc, M. T., Stiller, J., Edwards, D., Gresshoff, P. M., et al. (2012). Transient Nod factor-dependent gene expression in the nodulation-competent zone of soybean (*Glycine max* [L.] Merr.) roots. *Plant Biotechnol. J.* 10, 995–1010. doi: 10.1111/j.1467-7652.2012.00729.x

Hedden, P., and Phillips, A. L. (2000). Gibberellin metabolism: new insights revealed by the genes. *Trends Plant Sci.* 5, 523–530. doi: 10.1016/S1360-1385(00)01790-8

Hedden, P., and Thomas, S. G. (2012). Gibberellin biosynthesis and its regulation. *Biochem. J.* 444, 11–25. doi: 10.1042/BJ20120245

Hou, X., Lee, L. Y. C., Xia, K., Yan, Y., and Yu, H. (2010). DELLAs modulate jasmonate signaling via competitive binding to JAZs. *Dev. Cell* 19, 884–894. doi: 10.1016/j.devcel.2010.10.024

Ivanova, K. A., Tsyganova, A. V., Brewin, N. J., Tikhonovich, I. A., and Tsyganov, V. E. (2015). Induction of host defences by *Rhizobium* during ineffective nodulation of pea (*Pisum sativum* L.) carrying symbiotically defective mutations *sym40* (*PsEFD*), *sym33* (*PsIPD3/PsCYCLOPS*) and *sym42*. *Protoplasma* 252, 1505–1517. doi: 10.1007/s00709-015-0780-y

Jin, Y., Liu, H., Luo, D., Yu, N., Dong, W., Wang, C., et al. (2016). DELLA proteins are common components of symbiotic rhizobial and mycorrhizal signalling pathways. *Nat. Commun.* 7:12433. doi: 10.1038/ncomms12433

Kardailsky, I. V., and Brewin, N. J. (1996). Expression of cysteine protease genes in pea nodule development and senescence. *Mol. Plant Microbe Interact.* 9, 689–695. doi: 10.1094/MPMI-9-0689

Karmarkar, V. M. (2014). *Transcriptional Regulation of Nodule Development and Senescence in Medicago Truncatula*. Doctoral thesis, Wageningen University, Wageningen, D.C.

Kawaguchi, M., Imaizumi-Anraku, H., Fukai, S., and Syono, K. (1996). Unusual branching in the seedlings of *Lotus japonicus*—gibberellins reveal the nitrogen-sensitive cell divisions within the pericycle on roots. *Plant Cell Physiol.* 37, 461–470. doi: 10.1093/oxfordjournals.pcp.a028968

Kosterin, O. E., and Rozov, S. M. (1993). Mapping of the new mutation *blb* and the problem of integrity of linkage group I. *Pisum Genet.* 25, 27–31.

Kouchi, H., Shimomura, K., Hata, S., Hirota, A., Wu, G.-J., Kumagai, H., et al. (2004). Large-scale analysis of gene expression profiles during early stages of root nodule formation in a model legume, *Lotus japonicus*. *DNA Res.* 11, 263–274. doi: 10.1093/dnares/11.4.263

Larrainzar, E., Riely, B. K., Kim, S. C., Carrasquilla-Garcia, N., Yu, H.-J., Hwang, H.-J., et al. (2015). Deep sequencing of the *Medicago truncatula* root

transcriptome reveals a massive and early interaction between nodulation factor and ethylene signals. *Plant Physiol.* 169, 233–265. doi: 10.1104/pp.15.00350

Lester, D. R., Ross, J. J., Smith, J. J., Elliott, R. C., and Reid, J. B. (1999). Gibberellin 2-oxidation and the *SLN* gene of *Pisum sativum*. *Plant J.* 19, 65–73. doi: 10.1046/j.1365-313X.1999.00501.x

Lievens, S., Goormachtig, S., Den Herder, J., Capoen, W., Mathis, R., Hedden, P., et al. (2005). Gibberellins are involved in nodulation of *Sesbania rostrata*. *Plant Physiol.* 139, 1366–1379. doi: 10.1104/pp.105.066944

Maekawa, T., Maekawa-Yoshikawa, M., Takeda, N., Imaizumi-Anraku, H., Murooka, Y., and Hayashi, M. (2009). Gibberellin controls the nodulation signaling pathway in *Lotus japonicus*. *Plant J.* 58, 183–194. doi: 10.1111/j.1365-313X.2008.03774.x

Martin, D. N., Proebsting, W. M., and Hedden, P. (1999). The *SLENDER* gene of pea encodes a gibberellin 2-oxidase. *Plant Physiol.* 121, 775–781. doi: 10.1104/pp.121.3.775

McAdam, E. L., Reid, J. B., and Foo, E. (2018). Gibberellins promote nodule organogenesis but inhibit the infection stages of nodulation. *J. Exp. Bot.* 69, 2117–2130. doi: 10.1093/jxb/ery046

Mellor, R. B. (1989). Bacteroids in the *Rhizobium*-legume symbiosis inhabit a plant internal lytic compartment: implications for other microbial endosymbioses. *J. Exp. Bot.* 40, 831–839. doi: 10.1093/jxb/40.8.831

Nemankin, N. (2011). *Analysis of Pea (Pisum sativum L.) Genetic System, Controlling Development of Arbuscular Mycorrhiza and Nitrogen-Fixing Symbiosis*. Ph. D thesis, Saint-Petersburg State University, Saint-Petersburg, Russia.

Ovchinnikova, E., Journet, E.-P., Chabaud, M., Cosson, V., Ratet, P., Duc, G., et al. (2011). IPD3 controls the formation of nitrogen-fixing symbiosomes in pea and *Medicago* Spp. *Mol. Plant Microbe Interact.* 24, 1333–1344. doi: 10.1094/MPMI-01-11-0013

Pérez Guerra, J. C., Coussens, G., De Keyser, A., De Rycke, R., De Bodt, S., Van De Velde, W., et al. (2010). Comparison of developmental and stress-induced nodule senescence in *Medicago truncatula*. *Plant Physiol.* 152, 1574–1584. doi: 10.1104/pp.109.151399

Pladys, D., Dimitrijevic, L., and Rigaud, J. (1991). Localization of a protease in protoplast preparations in infected cells of French bean nodules. *Plant Physiol.* 97, 1174–1180. doi: 10.1104/pp.97.3.1174

Puppo, A., Groten, K., Bastian, F., Carzaniga, R., Soussi, M., Lucas, M. M., et al. (2005). Legume nodule senescence: roles for redox and hormone signalling in the orchestration of the natural aging process. *New Phytol.* 165, 683–701. doi: 10.1111/j.1469-8137.2004.01285.x

Ross, J. J., Reid, J. B., Swain, S. M., Hasan, O., Poole, A. T., Hedden, P., et al. (1995). Genetic regulation of gibberellin deactivation in *Pisum*. *Plant J.* 7, 513–523. doi: 10.1046/j.1365-313X.1995.7030513.x

Serova, T. A., Tikhonovich, I. A., and Tsyganov, V. E. (2017). Analysis of nodule senescence in pea (*Pisum sativum* L.) using laser microdissection, real-time PCR, and ACC immunolocalization. *J. Plant Physiol.* 212, 29–44. doi: 10.1016/j.jplph.2017.01.012

Serova, T. A., and Tsyganov, V. E. (2014). Symbiotic nodule senescence in legumes: molecular-genetic and cellular aspects (review). *Agric. Biol.* 5, 3–15. doi: 10.15389/agrobiology.2014.5.3eng

Serova, T. A., Tsyganova, A. V., and Tsyganov, V. E. (2018). Early nodule senescence is activated in symbiotic mutants of pea (*Pisum sativum* L.) forming ineffective nodules blocked at different nodule developmental stages. *Protoplasma* 255, 1443–1459. doi: 10.1007/s00709-018-1246-9

Sun, T. P. (2011). The molecular mechanism and evolution of the GA–GID1–DELLA signaling module in plants. *Curr. Biol.* 21, R338–R345. doi: 10.1016/j.cub.2011.02.036

Swamy, P., and Smith, B. N. (1999). Role of abscisic acid in plant stress tolerance. *Curr. Sci.* 76, 1220–1227.

Tatsukami, Y., and Ueda, M. (2016). Rhizobial gibberellin negatively regulates host nodule number. *Sci. Rep.* 6:27998. doi: 10.1038/srep27998

Thomas, S. G., Phillips, A. L., and Hedden, P. (1999). Molecular cloning and functional expression of gibberellin 2-oxidases, multifunctional enzymes involved in gibberellin deactivation. *Proc. Natl. Acad. Sci. U.S.A.* 96, 4698–4703. doi: 10.1073/pnas.96.8.4698

Tsyganov, V. E., Borisov, A. Y., Rozov, S. M., and Tikhonovich, I. A. (1994). New symbiotic mutants of pea obtained after mutagenesis of laboratory line SGE. *Pisum Genet.* 26, 36–37.

Tsyganov, V. E., Morzhina, E. V., Stefanov, S. Y., Borisov, A. Y., Lebsky, V. K., and Tikhonovich, I. A. (1998). The pea (*Pisum sativum* L.) genes *sym33* and *sym40* control infection thread formation and root nodule function. *Mol. Gen. Genet.* 259, 491–503. doi: 10.1007/s004380050840

Tsyganov, V. E., Seliverstova, E. V., Voroshilova, V. A., Tsyganova, A. V., Pavlova, Z. B., Lebskii, V. K., et al. (2011). Double mutant analysis of sequential functioning of pea (*Pisum sativum* L.) genes *Sym13*, *Sym33*, and *Sym40* during symbiotic nodule development. *Russ. J. Genet. Appl. Res.* 1, 343–348. doi: 10.1134/S2079059711050145

Tsyganov, V. E., Voroshilova, V. A., Borisov, A. Y., Tikhonovich, I. A., and Rozov, S. M. (2000). Four more symbiotic mutants obtained using EMS mutagenesis of line SGE. *Pisum Genet.* 32:63.

Tsyganov, V. E., Voroshilova, V. A., Rozov, S. M., Borisov, A. Y., and Tikhonovich, I. A. (2013). A new series of pea symbiotic mutants induced in the line SGE. *Russ. J. Genet. Appl. Res.* 3, 156–162. doi: 10.1134/S2079059713020093

Tsyganova, A. V., Kitaeva, A. B., and Tsyganov, V. E. (2018). Cell differentiation in nitrogen-fixing nodules hosting symbiosomes. *Funct. Plant Biol.* 45, 47–57. doi: 10.1071/FP16377

Tsyganova, A. V., and Tsyganov, V. E. (2015). Negative hormonal regulation of symbiotic nodule development. I. Ethylene (review). *Agric. Biol.* 50, 267–277. doi: 10.15389/agrobiology.2015.3.267eng

Tsyganova, A. V., and Tsyganov, V. E. (2018). Negative hormonal regulation of symbiotic nodule development. II. Salicilic, jasmonic and abscisic acids (review). *Agric. Biol.* 53, 3–14. doi: 10.15389/agrobiology.2018.1.3eng

Tsyganova, A. V., and Tsyganov, V. E. (2017). "Plant genetic control over infection thread development during legume-Rhizobium symbiosis," in *Symbiosis*, ed. E. C. Rigobelo (London: IntechOpen), 23–52. doi: 10.5772/intechopen.70689

Tsyganova, A. V., Tsyganov, V. E., Findlay, K.C., Borisov, A. Y., Tikhonovich, I. A., and Brewin, N. G. (2009). Distribution of legume arabinogalactanprotein-extensin (AGPE) glycoproteins in symbiotically defective pea mutants with abnormal infection threads. *Cell Tissue Biol.* 51, 53–62. doi: 10.1134/S1990519X09010131

Ueguchi-Tanaka, M., Ashikari, M., Nakajima, M., Itoh, H., Katoh, E., Kobayashi, M., et al. (2005). GIBBERELLIN INSENSITIVE DWARF1 encodes a soluble receptor for gibberellin. *Nature* 437, 693–698. doi: 10.1038/nature04028

Van de Velde, W., Guerra, J. C. P., Keyser, A. D., De Rycke, R., Rombauts, S., Maunoury, N., et al. (2006). Aging in legume symbiosis. A molecular view on nodule senescence in *Medicago truncatula*. *Plant Physiol.* 141, 711–720. doi: 10.1104/pp.106.078691

Voroshilova, V. A., Boesten, B., Tsyganov, V. E., Borisov, A. Y., Tikhonovich, I. A., and Priefer, U. B. (2001). Effect of mutations in *Pisum sativum* L. Genes blocking different stages of nodule development on the expression of late symbiotic genes in *Rhizobium leguminosarum* bv. viciae. *Mol. Plant Microbe Interact.* 14, 471–476. doi: 10.1094/mpmi.2001.14.4.471

Wang, T. L., Wood, E. A., and Brewin, N. J. (1982). Growth regulators, Rhizobium and nodulation in peas. *Planta* 155, 345–349. doi: 10.1007/bf00429463

Weston, D. E., Elliott, R. C., Lester, D. R., Rameau, C., Reid, J. B., Murfet, I. C., et al. (2008). The pea DELLA proteins LA and CRY are important regulators of gibberellin synthesis and root growth. *Plant Physiol.* 147, 199–205. doi: 10.1104/pp.108.115808

Conflict of Interest Statement: The authors declare that the research was conducted in the absence of any commercial or financial relationships that could be construed as a potential conflict of interest.

frontiers in Plant Science

ORIGINAL RESEARCH
published: 15 March 2019
doi: 10.3389/fpls.2019.00268

Identification and Expression Analysis of GRAS Transcription Factor Genes Involved in the Control of Arbuscular Mycorrhizal Development in Tomato

*Tania Ho-Plágaro, Nuria Molinero-Rosales, David Fariña Flores, Miriam Villena Díaz and José Manuel García-Garrido**

Department of Soil Microbiology and Symbiotic Systems, Estación Experimental del Zaidín (EEZ), CSIC, Granada, Spain

OPEN ACCESS

Edited by:
Juan Antonio Lopez Raez, Experimental Station of Zaidín (EEZ), Spain

Reviewed by:
Didier Reinhardt, Université de Fribourg, Switzerland
Philipp Franken, University of Applied Sciences Erfurt, Germany

***Correspondence:**
José Manuel García-Garrido
josemanuel.garcia@eez.csic.es

Specialty section:
This article was submitted to Plant Microbe Interactions, a section of the journal Frontiers in Plant Science

Received: *09 November 2018*
Accepted: *19 February 2019*
Published: *15 March 2019*

Citation:
Ho-Plágaro T, Molinero-Rosales N, Fariña Flores D, Villena Díaz M and García-Garrido JM (2019) Identification and Expression Analysis of GRAS Transcription Factor Genes Involved in the Control of Arbuscular Mycorrhizal Development in Tomato. Front. Plant Sci. 10:268. doi: 10.3389/fpls.2019.00268

The formation and functioning of arbuscular mycorrhizal (AM) symbiosis are complex and tightly regulated processes. Transcriptional regulation mechanisms have been reported to mediate gene expression changes closely associated with arbuscule formation, where nutrients move between the plant and fungus. Numerous genes encoding transcription factors (TFs), with those belonging to the GRAS family being of particular importance, are induced upon mycorrhization. In this study, a screening for candidate transcription factor genes differentially regulated in AM tomato roots showed that more than 30% of known GRAS tomato genes are upregulated upon mycorrhization. Some AM-upregulated GRAS genes were identified as encoding for transcription factors which are putative orthologs of previously identified regulators of mycorrhization in other plant species. The symbiotic role played by other newly identified AM-upregulated GRAS genes remains unknown. Preliminary results on the involvement of tomato *SlGRAS18*, *SlGRAS38*, and *SlGRAS43* from the SCL3, SCL32, and SCR clades, respectively, in mycorrhization are presented. All three showed high transcript levels in the late stages of mycorrhization, and the analysis of promoter activity demonstrated that *SlGRAS18* and *SlGRAS43* are significantly induced in cells containing arbuscules. When *SlGRAS18* and *SlGRAS38* genes were silenced using RNA interference in hairy root composite tomato plants, a delay in mycorrhizal infection was observed, while an increase in mycorrhizal colonization was observed in *SlGRAS43* RNAi roots. The possible mode of action of these TFs during mycorrhization is discussed, with a particular emphasis on the potential involvement of the SHR/SCR/SCL3 module of GRAS TFs in the regulation of gibberellin signaling during mycorrhization, which is analogous to other plant developmental processes.

Keywords: arbuscular mycorrhiza, tomato, GRAS transcription factors, gibberellins, RNAi interference

INTRODUCTION

Arbuscular mycorrhizal (AM) symbiosis occurs between soil fungi and higher plants, including most crop species (Smith and Read, 2008). In this mutualistic association, fungi receive photosynthetically fixed carbohydrates and lipids from plants, whose nutrient acquisition, particularly of phosphates, is improved (Smith and Smith, 2011; Bravo et al., 2017; Jiang et al., 2017; Keymer et al., 2017; Luginbuehl et al., 2017). In addition to nutrient supply, AM symbiosis increases plant resistance and tolerance to biotic and abiotic stress (Augé et al., 2001; Ruiz-Lozano, 2003; Göhre and Paszkowski, 2006; Liu et al., 2007).

AM formation in plant roots is a complex and tightly regulated process requiring signal exchange between plant and AM fungi which activate the symbiosis signaling pathway in host plant roots (Akiyama et al., 2005; Maillet et al., 2011; Genre et al., 2013; Nadal and Paszkowski, 2013; Sun et al., 2015). Although very little is known about the fungal molecular mechanisms controlling the infective process, much greater progress has been made in understanding how the plant orchestrates symbiosis. Cellular reprogramming and transcriptional regulation mechanisms have been reported to accommodate plant roots to arbuscular mycorrhizal symbiosis, particularly in those root cells harboring arbuscules, where nutrient transfers between the plant and fungus occur and are therefore of crucial importance for AM symbiosis (Harrison, 2012; Luginbuehl and Oldroyd, 2017; Pimprikar and Gutjahr, 2018).

To accommodate fungal structures, the host cell undergoes drastic cytological and morphological changes that are accompanied by massive transcriptional reprogramming, which has been observed prior to and during arbuscular formation (Genre et al., 2008; Pimprikar and Gutjahr, 2018). Extensive transcriptional changes are induced during arbuscular formation, and many genes involved in nutrient transport, primary and specialized metabolism, cell wall modification, the secretion pathway, and signal transduction are upregulated in arbuscule-containing cells (Pimprikar and Gutjahr, 2018). In this context, a precise spatiotemporal regulation of gene expression is essential for proper arbuscule development, and the identification of the transcriptional factors mediating these gene expression changes is therefore crucial to understanding how arbuscule formation and function are regulated. At least two coordinated elements regulate arbuscule formation and functioning in root cells: a cell-autonomous wave of gibberellin (GA) accumulation coupled with a GRAS transcription factor network.

GRAS genes, which acronym is based on the first three members to be identified in this family, the gibberellin-acid insensitive (GAI), repressor of GA1 (RGA), and scarecrow-like (SCL) proteins (Pysh et al., 1999), play a crucial regulatory role in a diverse range of fundamental plant biology processes. GRAS protein family has been divided into different subfamilies, each with distinct conserved domains and functions (Tian et al., 2004). GRAS TFs play an important role as regulators of plant development, GA signaling, stress responses, and symbiotic processes (Tian et al., 2004). Several subfamilies of GRAS proteins act as regulators of GA signaling and root development, both of which are important processes that occur during AM formation. DELLA proteins, which share the amino acid sequence DELLA in their N-terminal region, repress gibberellin responses (Silverstone et al., 1998). The SCARECROW (SCR) and SHORT-ROOT (SHR) transcription factors are both involved in radial root organization (Cui et al., 2014), while the SCARECROW-LIKE3 (SCL3) transcription factor, which mediates GA-promoted cell elongation during root development, acts as a coordinator of the GA/DELLA and SCR/SHR pathways (Heo et al., 2011; Zhang et al., 2011).

The DELLA-gibberellin module plays a central role in regulating arbuscule formation (Floss et al., 2013; Foo et al., 2013; Martin-Rodriguez et al., 2016). In a complex with DELLA proteins, CYCLOPS regulates the expression of RAM1 (Pimprikar et al., 2016), which is a GRAS-domain transcription factor capable of interacting with several other GRAS-domain proteins, such as RAD1, and also regulates the expression of genes involved in arbuscule development and nutrient exchanges between the plant and the fungus, including several lipid-biosynthesis and export-related genes such as FatM, RAM2, and STR (Gobbato et al., 2012; Park et al., 2015; Luginbuehl et al., 2017).

Genetic evidence shows that nodulation in legumes as well as mycorrhization in most plant species share a common symbiotic signaling pathway (CSSP), in which GRAS transcription factors, among other actors, play a prominent role. In symbiosis, the first GRAS transcription factor to be characterized was Nodulation Signaling Pathway 2 (NSP2) which forms a DNA binding complex with another GRAS transcription factor, NSP1, and activates early nodulation gene expression (Hirsch et al., 2009). NSP1 and NSP2 genes are also expressed during mycorrhization (Liu et al., 2011), while interaction between NSP2 and RAM1 has also been reported (Gobbato et al., 2012). NSP1 and NSP2, which regulate gene expression related to strigolactone (SL) biosynthesis, can therefore affect the stimulation of mycorrhization mediated by this hormone or other derived compounds such as certain apocarotenoids. Double *nsp1/nsp2* mutants actually have both low SL and mycorrhization levels (Liu et al., 2011).

In recent years, the search for new inducible GRAS TFs during mycorrhization, some of whose symbiotic role has been demonstrated, has been intensified (Xue et al., 2015; Heck et al., 2016; Rich et al., 2017). Thus, the above-mentioned RAM1 is necessary for arbuscule branching and induction of maker genes associated to arbuscule development in *Medicago truncatula*, *Lotus japonicus,* and *Petunia hybrida* (Park et al., 2015; Rich et al., 2015; Xue et al., 2015; Pimprikar et al., 2016), and Required for Arbuscule Development 1 (RAD1) is essential for arbuscular maintenance and functionality (Park et al., 2015). It appears that the relative importance of RAM1 and RAD1 in supporting arbuscule development differs between *Lotus* and *Medicago* and this fact provides an evidence for a diversification in the regulatory networks between plant species (Park et al., 2015; Xue et al., 2015). DELLA Interacting Protein

Abbreviations: AM, Arbuscular Mycorrhiza; GA, Gibberellins; qPCR, Quantitative RT-PCR; SHR, SHORT-ROOT; SCR, SCARECROW; SCL, SCARECROW-LIKE.

1 (DIP1), which interacts with RAM1 and DELLA in rice, controls arbuscule formation (Yu et al., 2014), and Mycorrhiza Induced GRAS 1 (MIG1) is necessary for cortex cell shape and size remodeling to accommodate fungal arbuscules (Heck et al., 2016). Given the ability of MIG1 to interact with DELLA1, it has been proposed that a MIG1-DELLA1 complex regulates root development to accommodate fungal infection structures during AM symbiosis. MIG1 belongs to a novel clade of GRAS-domain proteins not present in non-host *Arabidopsis thaliana*, and several members of which are transcriptionally upregulated during mycorrhizal colonization in *M. truncatula*, *L. japonicus*, as well as in *Petunia*, suggesting that this clade of GRAS-domain proteins could play a role in regulating AM development (Xue et al., 2015; Heck et al., 2016; Rich et al., 2017).

As mentioned above, DELLA proteins, a subfamily of GRAS transcription factors, are necessary for the regulation of arbuscule development at different levels, but, paradoxically, are also involved in arbuscule degeneration. Floss et al. (2017) has reported the existence of a transcriptional regulatory complex composed of DELLA and NSP1 which, together with transcription factor MYB1 (a member of the MYB family), forms a regulatory module for the transcription of genes encoding proteins with hydrolytic activities such as proteases and chitinases associated with arbuscular degeneration. Thus, the same set of transcription factors (including DELLA), depending on their combination and association in different regulatory complexes, might modulate both arbuscule formation and arbuscule degeneration.

In this study, we investigated the transcriptional regulation of arbuscule development in tomato roots by screening for candidate GRAS transcription factors. We found that a large number of GRAS genes are induced in mycorrhizal roots, including those previously identified as symbiotic in other plant species. Other genes identified, especially those belonging to the SCL3, SCL32, and SCR subfamilies, had not been studied previously in relation to their possible symbiotic role. We found that AM-induced genes from the SCL3 and SCR subfamilies are expressed in cells containing arbuscules and also regulate AM development. Our results suggest that the GRAS network plays an essential role in transcriptional reprogramming in the tomato host cell during mycorrhization.

MATERIALS AND METHODS

Plant Growth and AM Inoculation

Solanum lycopersicum seeds were surface sterilized with 5 min of soaking using 2.35% w/v sodium hypochlorite, subjected to shaking at room temperature for 1 day in the dark, and germinated on a sterilized moistened filter paper for 4 days at 25°C in the dark. Germinated seeds were placed on vermiculite for hypocotyl elongation for 1 week. Each seedling was transferred to a 500-ml pot containing an autoclave-sterilized (20 min at 120°C) mixture of expanded clay, washed vermiculite, and coconut fiber (2:2:1, by volume). In the AM-inoculated (I) treatments, plants were inoculated with a piece of monoxenic culture in Gel-Gro medium produced according to Chabot et al. (1992), containing 50 spores of *R. irregularis* (DAOM 197198) and infected carrot roots. For the non-inoculated (NI) treatment, a piece of Gel-Gro medium containing only uninfected carrot roots was used. Plant growth took place in a growth chamber (day: night cycle; 16 h, 24°C: 8 h, 20°C; relative humidity 50%).

One week after planting and weekly thereafter, the pots were given 20 ml of a modified Long Ashton nutrient solution containing 25% of the standard phosphorus (P) concentration to prevent mycorrhizal inhibition as a result of excess of phosphorous. In the case of non-mycorrhizal plants, the same modified Long Ashton solution was used. Plants were harvested at different times after inoculation. The root system was washed and rinsed several times with tap water, weighed and used for the different measurements according to the nature of the experiments. In each experiment, at least five independent plants were analyzed per treatment.

Estimation of Root Colonization by AM Fungus

The non-vital trypan blue histochemical staining procedure was used according to the Phillips and Hayman (1970) method. Stained roots were observed with a light microscope, and the intensity of root cortex colonization by AM fungus was determined as described by Trouvelot (1986) using the MYCOCALC software[1]. The parameters measured were frequency of colonization (%F), intensity of colonization (%M), and arbuscular abundance (%A) in the whole root. At least five microscope slides were analyzed per biological replicate, and each slide contained 30 root pieces of 1 cm.

Plasmid Construction and Hairy Root Transformation

The RNAi fragments of *SlGRAS18* (Solyc01g008910.2.1), *SlGRAS38* (Solyc07g052960.2.1), and *SlGRAS43* (Solyc09g066450.2.1) were amplified from *S. lycopersicum* cDNA of roots infected by the AM fungus *R. irregularis*. The putative promoters of *SlGRAS27* (Solyc02g094340.1), *SlGRAS18*, and *SlGRAS43* (fragments with a size around 1,600 bp immediately upstream of the start codon of the corresponding genes) were obtained from genomic DNA of *S. lycopersicum* cv Moneymaker. Amplifications were carried out by PCR using the iProof High Fidelity DNA-polymerase (BioRad) and specific primers (**Supplementary Table 1**). PCR fragments were introduced in pENTR/D-TOPO (Invitrogen) vector and sequenced. pENTR/D-TOPO vectors containing the different RNAi or promoter fragments were subsequently recombined into pK7GWIWG2_II-RedRoot[2] or pBGWFS7::pAtUbq10::DsRed (modified from Karimi et al., 2002) vectors, respectively, using the GATEWAY technology (Invitrogen).

For hairy root transformation, *Agrobacterium rhizogenes* MSU440 cultures harboring the corresponding promoter-GUS and RNAi constructs, were used to transform *S. lycopersicum* cv Moneymaker plantlets according to Ho-Plágaro et al. (2018). Composite plants were transferred to pots and followed the

[1]http://www.dijon.inra.fr/mychintec/Mycocalc-prg/download.html
[2]http://gateway.psb.ugent.be

same plant growth conditions as explained before. Screening and selection of DsRed (transformed) roots was done by observation under a fluorescent stereomicroscope Leica M165F.

Gene Expression Localization

In order to localize the expression of *SlGRAS27, SlGRAS18*, and *SlGRAS43* genes, AM-inoculated and non-inoculated transgenic roots carrying the respective promoter-GUS fusions were used, based on a technique originally developed by Jefferson (1989). Roots transformed by a *PT4* promoter-GUS fusion were used as a control in the same manner as in Ho-Plágaro et al. (2018). Hairy roots carrying the promoter-GUS fusions were vacuum-infiltrated with a GUS staining solution composed of 0.05 M sodium phosphate buffer, 1 mM potassium ferrocyanide, 1 mM potassium ferricyanide, 0.05% Triton X-100, 10.6 mM EDTA-Na, and 5 μg mL-1 X-gluc cyclohexylammonium salt (previously dissolved in N,N-dimethylformamide) for 30 min to improve the penetration of the substrate. Then, the tissues were incubated in the dark at 37°C from 1 h to overnight or until the staining was satisfactory in the same staining solution.

In order to stain the AM fungal structures, the inoculated roots were embedded in 4% agarose blocks and 60-μm transverse sections were cut on a vibratome (Leica VT1200S). Root sections were vacuum-infiltrated with 10 μg ml^{-1} WGA-Alexa Fluor 488 conjugate (Molecular Probes, Eugene, Oreg., USA) in PBS 1X for 60 min in the dark and analyzed under an inverted transmission microscope (Leica DMI600B).

RNA Extractions and Gene Expression Quantification

For the qPCR experiments, representative root samples from each root system were collected, immediately frozen in liquid nitrogen, and stored at −80°C until RNA extraction. Total RNA was isolated from about 0.2-g samples using the RNeasy Plant Mini Kit (Qiagen, Hilden, Germany) following the manufacturer's instructions, and treated with RNase-Free DNase. 1 μg of DNAse-treated RNA was reverse-transcribed into cDNA using the iScriptTM cDNA synthesis kit (Bio-Rad, Hercules, CA, USA) following the supplier's protocol. qPCRs were prepared in a 20-μl reaction volume containing 1 μl of diluted cDNA (1:10), 10 μl 2× SYBR Green Supermix (Bio-Rad, Hercules, CA, USA), and 200 nM of each primer (**Supplementary Table 1**). A negative control with the RNA sample prior to reverse-transcription was used in order to confirm that the samples were free from DNA contaminations. PCR program consisted of a 3-min incubation at 95°C, followed by 35 cycles of 30 s at 95°C, 30 s at 58–63°C, and 30 s at 72°C. The specificity of the PCR amplification procedure was checked using a melting curve after the final PCR cycle (70 steps of 30 s, from 60 to 95°C, at a heating rate of 0.5°C). Experiments were carried out on three biological replicates, and the threshold cycle (Ct) was determined in triplicate. The relative transcription levels were calculated by using the 2-ΔΔCt method (Livak and Schmittgen, 2001). The Ct values of all genes were normalized to the Ct value of the *LeEF-1α* (accession number X14449) housekeeping gene.

The qPCR data for each gene were shown as relative expression with respect to the control treatment ("reference treatment") to which it was assigned an expression value of 1. The reference treatment generally corresponded to the non-AM-inoculated treatment. Measurements of transcript abundance of GRAS genes were carried out using the primers previously designed by Huang et al. (2015), and for the qPCR analysis of the reference *LeEF-1α* gene 5′-GGTGGCGAGCATGATTTTGA-3′ and 5′-CGAGCCAACCATGGAAAACAA-3′ primers were used.

Transcriptome Profiling

Six different root pools (each pool from two different plants) were collected for the RNA-seq analysis: three pools from non-inoculated plants (NI) and three pools from AM-inoculated plants (I). Total RNA was extracted using the Rneasy Plant Mini Kit (Qiagen, Hilden, Germany). cDNA library preparation and sequencing were performed by Sistemas Genómicos S. L. (Paterna, Valencia, Spain) using an Illumina HiSeq1000 machine. The TopHat v2.1.0 algorithm (Trapnell et al., 2009) was used to align reads from the RNA-Seq experiment to the Tomato Genome Reference Sequence SL3.0 provided by the Sol Genomics consortium,[3] using the last ITAG 3.10 annotation. Then, low-quality reads were removed from the map through Picard Tools,[4] and high-quality reads were selected for assembly and identification through Bayesian inference using the Cufflinks v2.2.1 algorithm proposed by Trapnell et al. (2010). Gene quantification process was performed by the htseq-count 0.6.1p1 tool (Anders et al., 2015). Isoform quantification and differential expression were carried out through the DESeq2 method (Anders and Huber, 2010). The RNA-seq data have been deposited in the National Center for Biotechnology Information (NCBI) Short Read Archive (SRA) with accession number PRJNA509606.

Phylogenetic Analysis

Amino acid sequences from the GRAS protein families in tomato (Huang et al., 2015) and *Arabidopsis* (Tian et al., 2004), together with proteins corresponding to AM-related GRAS genes from other plant species, were submitted for the determination of phylogenetic relationships to create a neighbor-joining tree using the Jukes-Cantor model with Geneious software.

Statistical Analysis

When two means were compared, the data were analyzed using a two-tailed Student's *t*-test. For comparisons among all means, a one-way or two-way ANOVA was performed followed by the LSD multiple comparison test. The Graphpad Prim version 6.01 (Graphpad Software, San Diego, California, USA) was used to determine statistical significance. Differences at $p < 0.05$ were considered significant. Data represent the mean ± SE.

[3]https://solgenomics.net/organism/solanumlycopersicum/genome
[4]http://picard.sourceforge.net

RESULTS

Phylogenetic Analysis of AM-Induced GRAS Transcription Factor Genes in Tomato

To investigate transcriptional regulation of arbuscular mycorrhizal development and to screen for candidate transcription factor genes in tomato, three independent biological replicates of *S. lycopersicum* cv. Moneymaker roots 8 weeks after inoculation with the AM fungus *R. irregularis* (I), exhibiting a 40.2 ± 4% of mycorrhizal colonization, and three non-inoculated (NI) tomato root samples of a similar age were subjected to in-depth messenger RNA sequencing (RNA-seq) analysis. The cutoff for differentially expressed genes (DEGs) was at least a 2-fold induction or repression ($p < 0.05$), and the DEGs coding for transcription factors (TFs) were identified according to the tomato TF list previously published by Geng et al. (2017). As a result, 246 genes encoding transcription factors or transcriptional regulators were significantly upregulated in AM-inoculated roots as compared to non-mycorrhizal roots, while only 59 genes were downregulated (**Supplementary Table 2**). The most abundant AM-induced TF genes were those encoding the MYB factor family (40 members), APETALA2 and ethylene-responsive element binding protein (AP2-EREBP) family (31 members), C2H2 zinc finger protein family (22 members), NAC protein family (21 members), basic helix–loop–helix (bHLH) protein family (20 members), and the GRAS TF family (19 members). In relative terms, the GRAS transcription factor gene family is the most induced during mycorrhization, followed by the Tify, OFP, and NAC families (**Figure 1**). Although the downregulation of TF-encoding genes during mycorrhization was not very significant, in some TF families, repression of a large percentage of gene family members, such as SBP (23.53%), GRF, HSF (15.38%), and ARR-B (10%) was observed (**Figure 1**).

We decided to focus on the GRAS TF gene family. In particular, using RNA-seq analysis, we found that 19 GRAS genes are significantly induced (fold change >2, $p < 0.05$) in AM roots out of a total of 54 tomato GRAS genes, which means that 35.19% of GRAS tomato genes are upregulated upon mycorrhization (**Figure 1**). **Table 1** shows the fold-change induction and corresponding p of these 19 AM-upregulated GRAS genes. Similarly, it was recently found that the GRAS TF family was also the most relatively induced during mycorrhization in another *Solanaceae* species, *P. hybrida* (Rich et al., 2017), and in the legume *L. japonicus* (Xue et al., 2015).

The GRAS gene family has been previously identified and characterized in tomato (Huang et al., 2015; Niu et al., 2017). We performed a phylogenetic analysis comprising tomato and *Arabidopsis* GRAS proteins, together with other tomato GRAS genes homologous to GRAS members from other species, whose involvement during mycorrhization and/or nodulation has been reported, including DELLA (Floss et al., 2013; Yu et al., 2014; Takeda et al., 2015), RAM1 (Gobbato et al., 2012; Rich et al., 2015; Xue et al., 2015), RAD1 (Xue et al., 2015), and MIG1 genes (Heck et al., 2016). In addition, GRAS genes from *Petunia*, *Lotus*, and *Medicago* previously reported to be AM-induced were also included in the analysis (Xue et al., 2015; Heck et al., 2016; Rich et al., 2017). **Figure 2** shows the resulting phylogenetic tree containing the GRAS clades with tomato protein family members corresponding to AM-induced genes, which were designated following the nomenclature described by Huang et al. (2015) and the updated clade classification of Cenci and Rouard (2017). Out of a total of 15 clades of GRAS TFs in tomato, GRAS genes from 11 clades were found to be induced during mycorrhization. Ten clades were coincident with GRAS clades previously reported to contain AM-induced genes in other species (Xue et al., 2015; Heck et al., 2016; Rich et al., 2017), but also a GRAS member from the LS group was firstly detected to be induced during mycorrhization. Among the AM-induced tomato GRAS, we found in tomato some members homologous to genes with a previously established functionality in the mycorrhization process from the following clades: NSP2, RAM1, RAD1, LISCL, and the AM-host exclusive clade SCLB, which

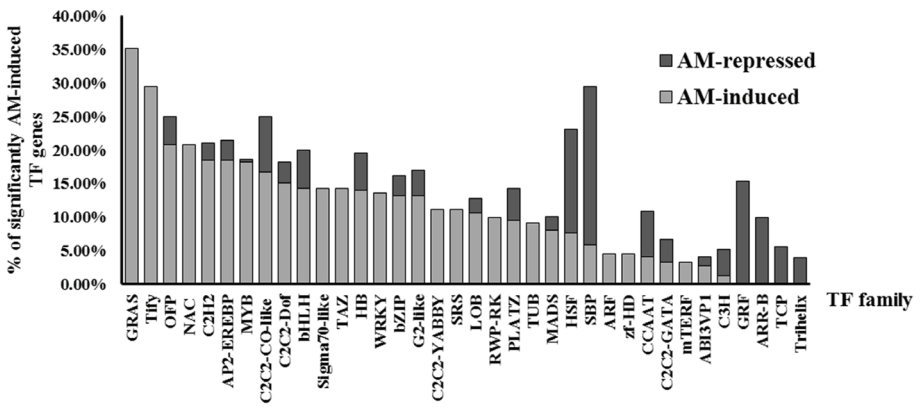

FIGURE 1 | Relative abundance of TF genes differentially regulated upon mycorrhization in tomato. Percentage of AM-repressed and AM-induced TF genes, with RNA-seq fold change <– or > 2 and $p < 0.05$, belonging to each TF gene family in tomato.

TABLE 1 | Effect of mycorrhization on the expression of GRAS family genes.

GRAS gene		I *vs* NI	
Huang et al. (2015) nomenclature	SolycDB ID	Fold change	*p*
SlGRAS36	Solyc06g082530	2.023	1.51E-06
SlGRAS46	Solyc10g086530	2.079	2.38E-04
SlGRAS26	Solyc02g092570	4.905	6.22E-10
SlGRAS38	Solyc07g052960	24.058	1.28E-15
SlGRAS39	Solyc08g014030	2.215	6.55E-03
SlGRAS5	Solyc09g018460	2.039	1.03E-02
SlGRAS18	Solyc01g008910	2.012	4.63E-02
SlGRAS47	Solyc11g005610	11.123	1.59E-09
SlGRAS48	Solyc11g013150	2.111	1.99E-04
SlLS	Solyc07g066250	4.383	3.54E-04
SlGRAS37	Solyc07g043330	2.002	2.20E-03
SlGRAS43	Solyc09g066450	49.088	2.15E-37
SlGRAS21	Solyc01g059960	4.006	1.40E-03
SlGRAS22	Solyc01g079370	3.233	2.80E-04
SlGRAS23	Solyc01g079380	2.117	4.54E-02
SlGRAS33	Solyc06g009610	14.588	8.72E-14
SlGRAS27	Solyc02g094340	12.524	6.97E-20
SlGRAS28	Solyc03g110950	35.716	–
SlGRAS49	Solyc11g017100	8.205	–

RNA-seq fold change >2 and p-values of GRAS genes upregulated in roots of mycorrhizal plants (I) with respect to non-inoculated (NI) plants.

includes the MIG1 transcription factor (Maillet et al., 2011; Gobbato et al., 2012; Takeda et al., 2013; Yu et al., 2014; Fiorilli et al., 2015; Xue et al., 2015; Heck et al., 2016; Rich et al., 2017). However, several other tomato GRAS genes induced upon mycorrhization belong to clades, such as Os19, SCL32, LS, SHR, SCR, and SCL3, whose functionality during mycorrhization has not been investigated. Although the function of proteins from the Os19 and SCL32 clades is unknown, LS members are involved in lateral shoot formation during vegetative development (Schumacher et al., 1999; Greb et al., 2003). Finally, SHR, SCR, and SCL3 are involved in a pathway that modulates DELLA/gibberellin signaling involved in root radial patterning and growth, cell division, endodermis specification, and quiescent center identity (Heo et al., 2011; Zhang et al., 2011).

Tomato Orthologs of GRAS Transcription Factors That Play a Role During Symbiosis

On the basis of the RNA-seq results, we decided to screen the expression of a set of nine tomato GRAS genes, which are putative orthologs known to be involved in mycorrhization. Using qPCR, their expression was assessed in roots in a time-course experiment with *S. lycopersicum* plants after 32, 42, 52, and 62 days post inoculation (dpi) with the AM fungus *R. irregularis* (**Figure 3**). In these plants, the percentage of mycorrhizal infection gradually increased from 12 ± 0.5% at 35 dpi to 60 ± 5% at 62 dpi. The qPCR data confirmed the mycorrhizal upregulation of *SlGRAS23* and *SlGRAS33* (*MtMIG1* homologs), *SlGRAS47* and *SlGRAS48* genes (close to *LjNSP2*), *SlGRAS28* (*LjRAD1* homolog), and *SlGRAS27* (*MtRAM1* homolog).

The transcripts of *SlGRAS50* and *SlGRAS16*, which are putative orthologs of *NSP1*, did not significantly increase upon mycorrhization (**Table 1**). However, we hypothesize that the *SlGRAS16* gene might be orthologous to *NSP1*, as the RNA-seq data, with a fold change of 1.96 and $p < 0.05$ (**Supplementary Table 2**), and the time-course experiment for this gene (**Figure 3**), indicates a tendency toward gene induction in AM roots.

The AM-induced genes *SlGRAS21*, *SlGRAS22*, *SlGRAS23*, and *SlGRAS33* are putative homologs to the *MtMIG1* gene, which has been reported to be induced in arbuscule-containing cells and to encode a transcription factor suggested as playing a role in cell remodeling during AM fungal accommodation (Heck et al., 2016). In the HAM subfamily, we found that *SlGRAS47, SlGRAS48*, and *SlGRAS5,* according to RNA-seq analysis, are AM-activated genes. *MtNSP2* and the pea gene *PsSYM7,* whose mutation causes a decrease in AM fungal colonization, also belong to this clade (Maillet et al., 2011; Shtark et al., 2016). *SlGRAS28,* whose gene expression has been reported to increase under mycorrhizal conditions, is homologous to *LjRAD1* from *L. japonicus*, whose mutation triggers an acceleration in arbuscule degeneration and a sharp reduction in the number of arbuscules (Xue et al., 2015).

SlGRAS27, which is also induced upon mycorrhization, is the putative homolog of *MtRAM1* and *PhATA/RAM1* from *Medicago* and *Petunia*, respectively. The localization of the *SlGRAS27* gene's promoter activity was analyzed. Composite tomato plants with transgenic roots containing the p*SlGRAS27*-GUS fusion were generated, and the promoter of the tomato phosphate transporter (*PT4*), previously reported to be specifically expressed in arbuscule-containing cells (Nagy et al., 2005), was used as a positive control for GUS staining in these cells (**Supplementary Figure 1**). In non-mycorrhizal roots transformed by the p*SlGRAS27*-GUS fusion, we eventually observed some promoter activity associated with endodermis and pericycle cells (**Figure 4A**), although, as described by Gobbato et al. (2013) and Park et al. (2015), no staining was detected in most roots. By contrast, under mycorrhizal conditions, promoter activity was observed in AM-colonized cortex zones (**Figures 4B–D**); this activity appeared to be specifically located in arbuscule-containing cells, as demonstrated by counterstaining with the WGA-alexa488 which enables fluorescent staining of fungal structures (**Figures 4E–J**).

Novel AM-Related GRAS Genes From SCL3, SCR, and SCL32 Families

Transcripts of the SCARECROW-LIKE3 (SCL3; *SlGRAS18*), SCARECROW-LIKE32 (SCL32; *SlGRAS38*), and SCARECROW (SCR; *SlGRAS43*) families were also induced upon mycorrhization (**Figure 2**). Their expression increased at the late stages (52–62 dpi) of the interaction (**Figure 5**) when the roots reached a colonization ratio of 45 ± 3.5% and 60 ± 5%, respectively. Although their putative symbiotic role has not been studied, some members of the SCR, SCL3, and SHR families are known to form a regulatory module that interacts with GA-DELLA signaling in certain root development processes (Heo et al., 2011; Zhang et al., 2011).

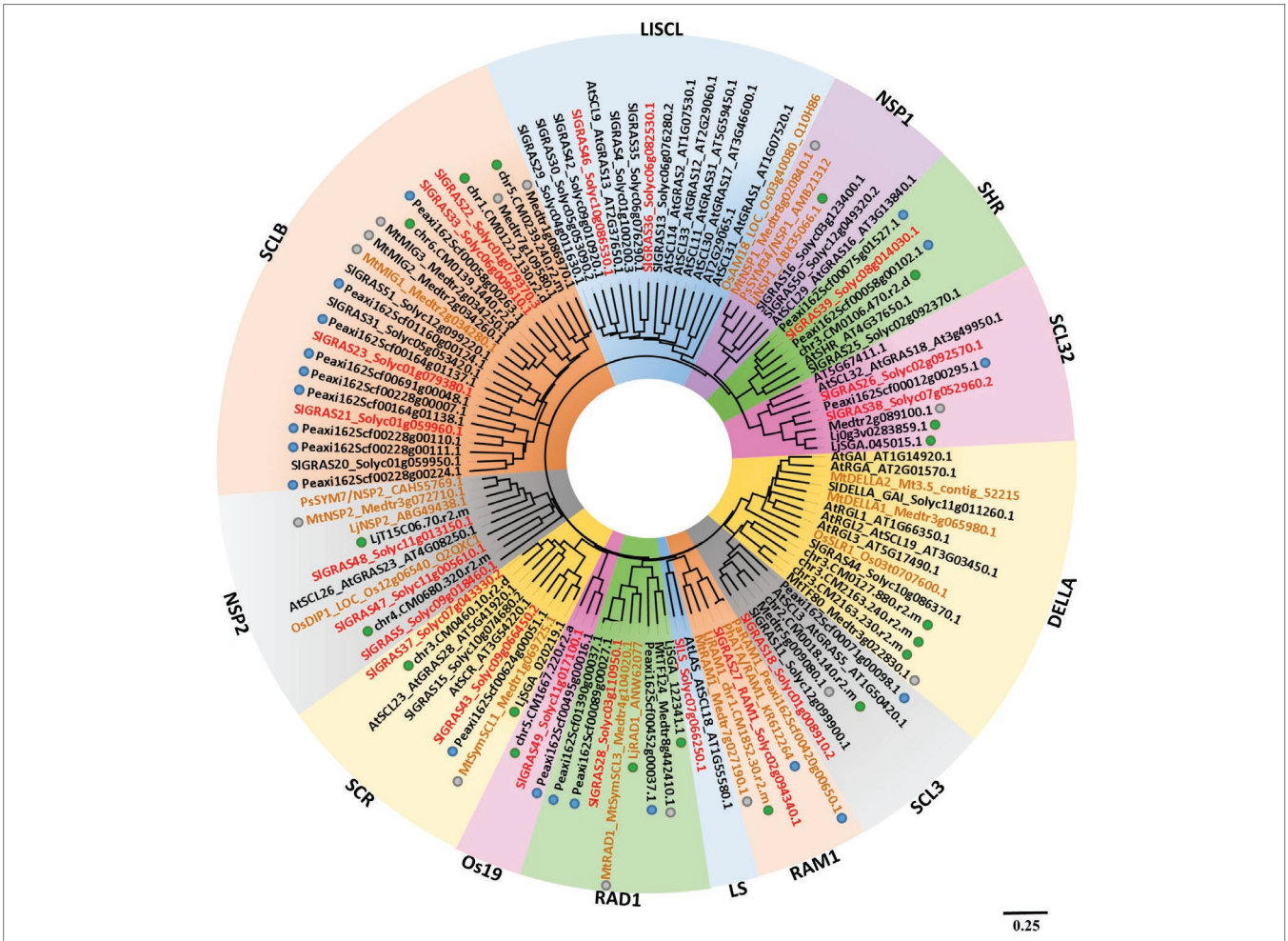

FIGURE 2 | Phylogenetic analysis of AM-related GRAS protein family members in *S. lycopersicum*. An unrooted phylogenetic tree was generated according to amino acid alignment of GRAS proteins from tomato and *Arabidopsis* (Tian et al., 2004), together with AM-induced GRAS members from *P. hybrida* (blue dots), *L. japonicus* (green dots), and *M. truncatula* (gray dots), as well as proteins previously reported to be involved in AM symbiosis (typed in brown) from *L. japonicus* (LjRAD1, LjNSP1, and LjNSP2), *P. hybrida* (PhATA/RAM1), *M. truncatula* (MtDELLA1, MtDELLA2, MtMIG1, MtRAM1, MtNSP1, and MtNSP2), *Oryza sativa* (OsDIP1, OsAM18), and *Pisum sativum* (PsSYM7, PsSYM34). Tomato GRAS proteins, whose corresponding coding genes were induced upon mycorrhization during RNA-seq analysis, are typed in red. Common protein names assigned by Huang et al. (2015) are indicated. The SolDB accessions (http://solgenomics.net/) for tomato proteins and the PlantGDB IDs (http://www.plantgdb.org) for *Arabidopsis* and *Medicago* proteins are also shown. GenBank/RefSeq accession numbers are used for proteins from other species. Background colors correspond to each clade from the GRAS protein family. The scale bar represents the number of substitutions per site.

The promoter activity of AM-induced genes *SlGRAS18* and *SlGRAS43* was analyzed. A 1600-bp region upstream of each gene was fused to a GUS reporter construct, composite tomato plants were generated and transgenic roots were checked for the presence of the blue dye corresponding to GUS activity. In non-mycorrhizal hairy roots, the promoter activity of the *SlGRAS18* and *SlGRAS43* genes was restricted to cells surrounding the central cylinder and to the apical meristem (**Supplementary Figure 2**). Although more in-depth analysis is required to determine the specific cell types involved, the expression pattern might be similar to the *Arabidopsis* homologs *SCL3* and *SCR*, described to be induced in the endodermis and the quiescent center (Pysh et al., 1999; Cui et al., 2007; Heo et al., 2011). Mycorrhizal roots examined 8 weeks after inoculation also showed GUS activity in the cortex zones affected by AM fungal root colonization, mainly in arbuscule-containing cells (**Figures 6A–D**). The GUS-stained roots, which were longitudinally sectioned and counterstained with WGA-Alexa 488 to visualize fungal structures, showed that colonization by *R. irregularis* clearly activated *SlGRAS18* and *SlGRAS43* gene expression in arbusculated cells (**Figures 6E–H**), although some additional green autofluorescence was also observed around the central stele and in the epidermal root cells.

RNAi Interference of *SlGRAS18*, *SlGRAS38*, and *SlGRAS43* Genes Affects Mycorrhization

To carry out a functional analysis of *SlGRAS18*, *SlGRAS38*, and *SlGRAS43* genes, RNAi experiments were performed. Composite

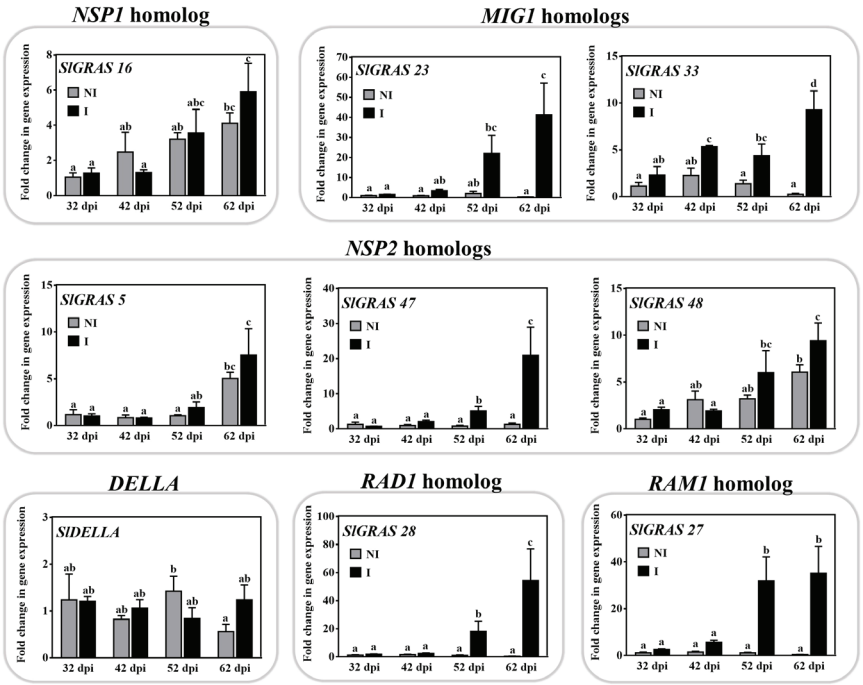

FIGURE 3 | Characterization of expression of mycorrhiza-related GRAS genes in tomato roots. The expression of several putative GRAS genes was analyzed by qPCR in tomato roots after 32, 42, 52, and 62 dpi (days post inoculation) with the AM fungus *R. irregularis*. The qPCR data show relative gene expression in the roots of AM-inoculated plants (I) with respect to their expression in non-inoculated (NI) plants at 32 dpi, with a gene expression of 1. Values correspond to mean ± SE (n = 3). Bars with the same letter do not significantly differ ($p > 0.05$) according to the LSD multiple comparison test.

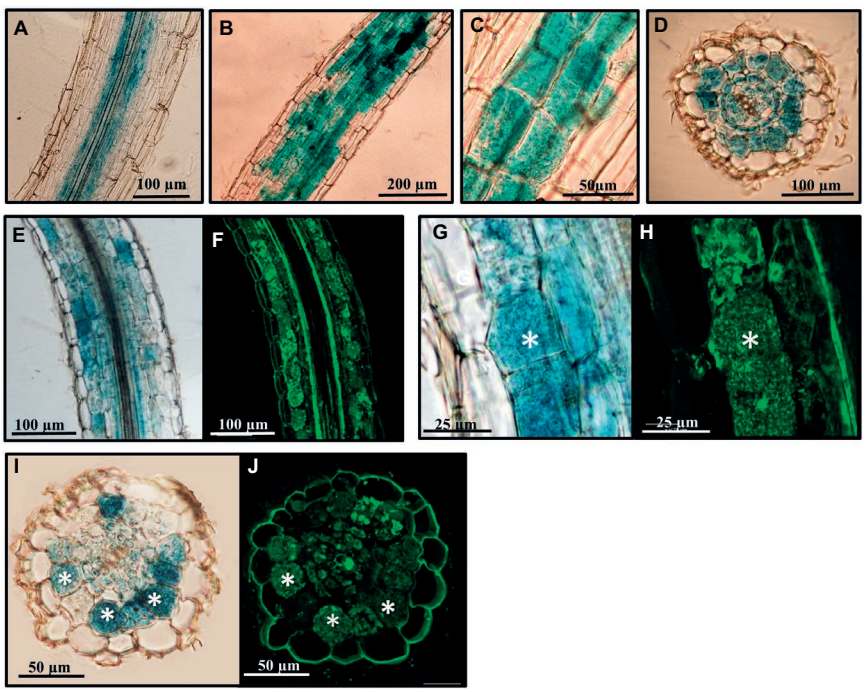

FIGURE 4 | Analysis of the *SlGRAS27* promoter activity in transgenic *S. lycopersicum* roots after GUS staining. GUS activity in sections of *A. rhizogenes*-transformed roots expressing the p*SlGRAS27*:GUS fusion. **(A)** Non-inoculated root. **(B–J)** Transformed roots 8 weeks after inoculation with *R. irregularis*. **(F,H,J)** Images corresponding to root sections from **(E)**, **(G)**, and **(J)**, respectively, co-stained with WGA-Alexa Fluor 488, which labels the AM fungus and fluoresces green. White asterisks indicate arbuscules in the host cortical cells.

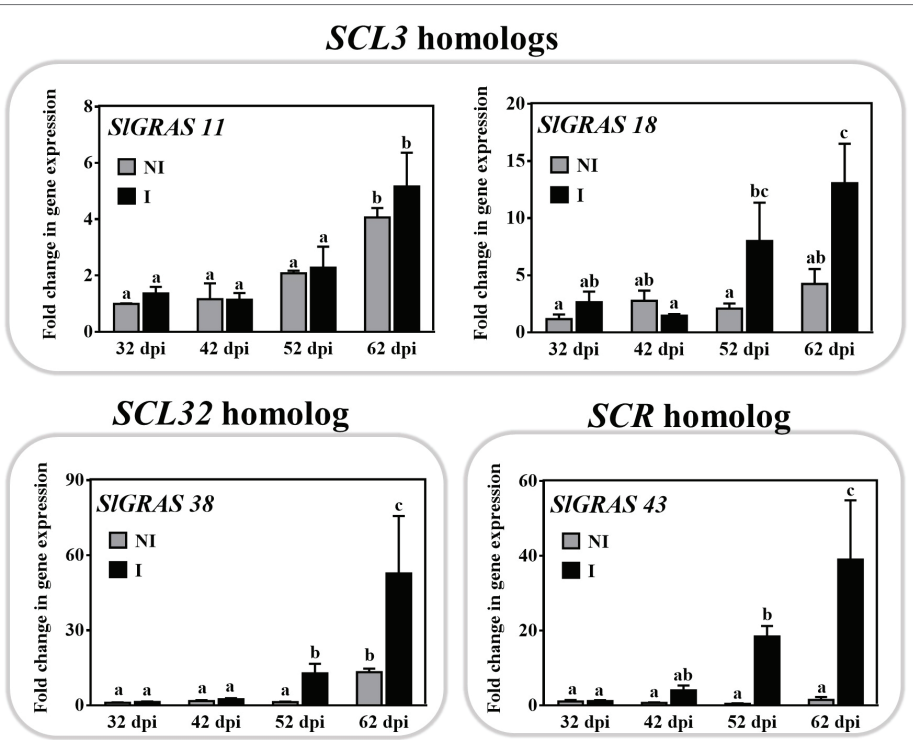

FIGURE 5 | Time-course expression of *GRAS11*, *SlGRAS18*, *SlGRAS38*, and *SlGRAS43* genes during mycorrhization in tomato roots. The expression of putative GRAS genes from SCL3, SCL32, and SCR families, thus far not reported to be related to mycorrhizal symbiosis, was analyzed by qPCR in roots after 32, 42, 52, and 62 dpi (days post inoculation) with the AM fungus *R. irregularis*. The qPCR data represent relative gene expression in the roots of AM-inoculated plants (I) with respect to their expression in non-inoculated (NI) plants at 32 dpi with a designated gene expression of 1. Values correspond to mean ± SE (n = 3). Bars with the same letter are not significantly different ($p > 0.05$) according to the LSD multiple comparison test.

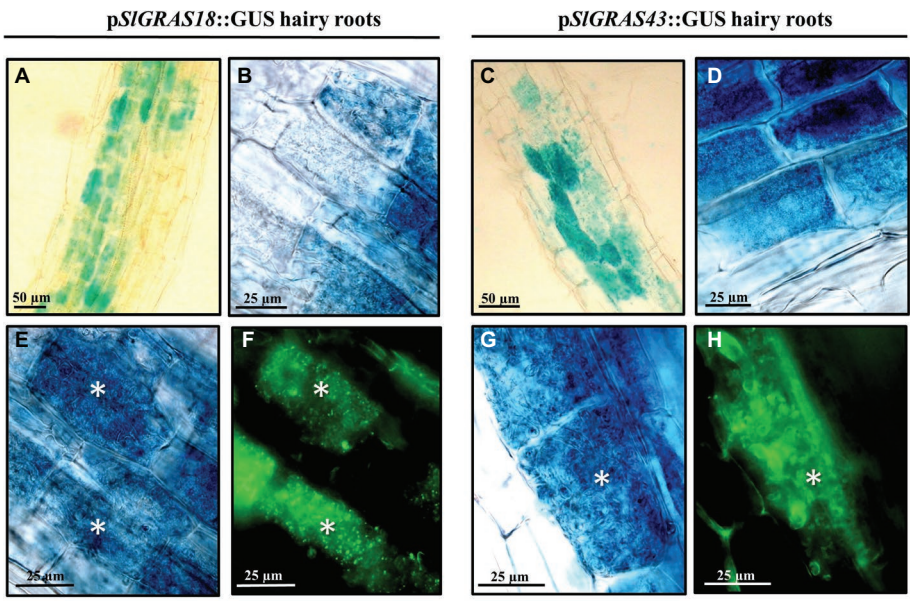

FIGURE 6 | Analysis of the *SlGRAS18* and *SlGRAS43* promoter activity in transgenic *S. lycopersicum* roots after GUS staining. GUS activity in *A. rhizogenes*-transformed roots expressing the p*SlGRAS18*:GUS fusion (images on left) and the p*SlGRAS43*::GUS fusion (images on right) was assessed after 8 weeks of inoculation with *R. irregularis*. **(A–D)** GUS-stained whole roots. **(E,G)** GUS-stained and vibratome-sectioned roots. **(F,H)** Images corresponding to root sections from **(E)** and **(G)**, respectively, co-stained with WGA-Alexa Fluor 488, which labels the AM fungus and fluoresces green. White asterisks indicate arbuscules in the host cortical cells.

plants with hairy roots transformed with the control empty vector (pK7GWIWG2_II-RedRoot) and the corresponding RNAi constructs were used. We tested the expression levels of the corresponding silenced GRAS genes at 63 and/or 84 days post inoculation (dpi) and obtained a successful repression of the respective GRAS genes (**Supplementary Figure 3**), with the exception of the SlGRAS38 RNAi AM-inoculated roots at 84 dpi.

Analysis of the percentage of mycorrhization in the different *GRAS* RNAi roots revealed important changes. Compared to the control, *SlGRAS18* RNAi roots showed a delay in the colonization process, with a significant decrease in the percentage of root length colonized by the AM fungus observed at both harvesting times (63 and 84 dpi) (**Figure 7A**). A significant decrease in all the mycorrhizal parameters measured was observed at 63 dpi, but not at 84 dpi (**Figure 7A**), indicating that *SlGRAS18* gene silencing negatively affects relative mycorrhizal intensity (M%), as well as arbuscule abundance (A%), and that these differences disappear at late stages of mycorrhization.

Similar results were obtained for the *SlGRAS38* RNAi roots. A significant reduction in mycorrhizal colonization was also observed and, again, F, M, and A% were negatively affected in *SlGRAS38*-silenced roots at 63 dpi, although only arbuscular intensity remained significantly reduced at 84 dpi (**Figure 7B**).

SlGRAS43 RNAi composite plants presented a significant increase in the percentage of root length colonized by the AM fungus, but no significant differences in the mycorrhizal parameters were observed (**Figure 7C**).

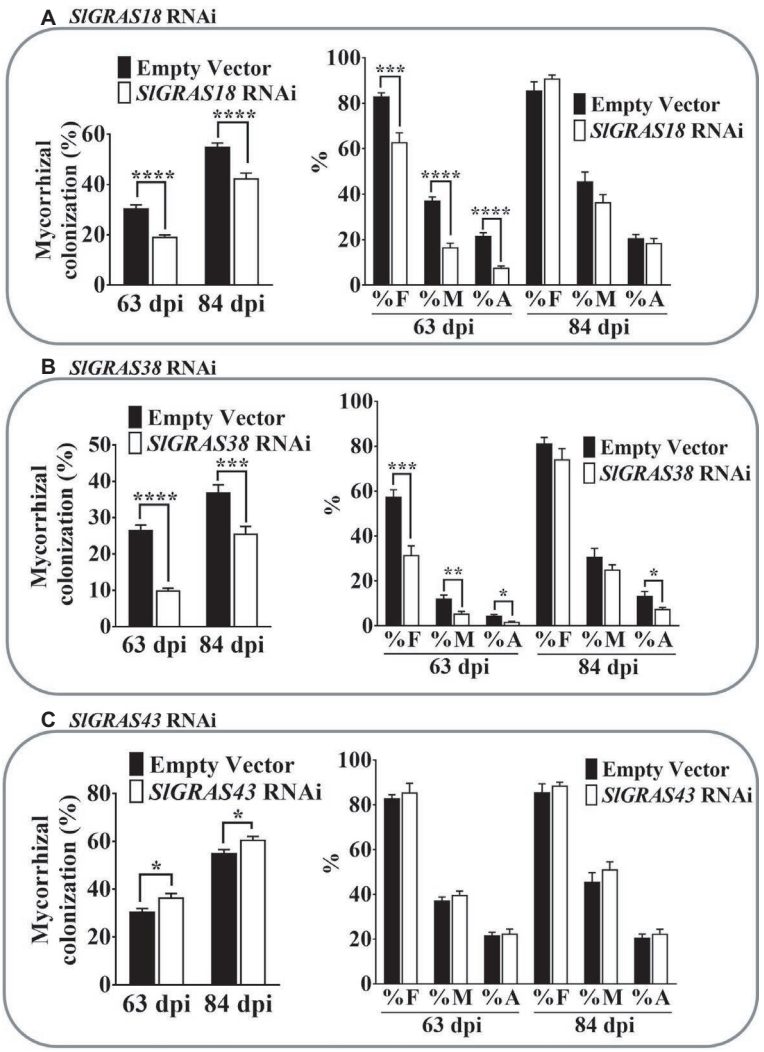

FIGURE 7 | Mycorrhizal colonization parameters in roots of *SlGRAS18*, *SlGRAS38*, and *SlGRAS43* RNAi AM-inoculated composite tomato plants. Percentage of colonized root length (graphs on left) and mycorrhization parameters (graphs on right) were analyzed after 63 and 84 dpi (days post inoculation) with the AM-fungus *R. irregularis* in hairy roots silenced for different GRAS genes. **(A)** *SlGRAS18* RNAi hairy roots. **(B)** *SlGRAS38* RNAi hairy roots. **(C)** *SlGRAS43* RNAi roots. Values correspond to mean ± SE ($n = 5$). Bars with the same letter do not significantly differ. Significant differences (Student's t test) between the mutant and the control are indicated with asterisks (*$p < 0.05$; **$p < 0.01$; ***$p < 0.001$; ****$p < 0.0001$).

DISCUSSION

Transcriptional reprograming of root cellular development in AM symbiosis is being intensely studied. However, although our understanding of the molecular mechanisms involved has increased considerably in recent years (Pimprikar and Gutjahr, 2018), only some components of the transcriptional machinery and certain cis-regulatory elements essential for AM-specific gene expression in arbuscule-containing cells have been described (Rubio et al., 2001; Karandashov et al., 2004; Chen et al., 2011). In this study, RNA-seq analysis revealed a more than two-fold induction ($p < 0.05$) of 246 putative transcription factors during tomato mycorrhization (**Supplementary Table 2**), with the GRAS family showing the highest relative abundance level of AM-induced TF genes. A total of 19 GRAS genes were identified as upregulated upon mycorrhization. As for *Petunia* (Rich et al., 2017) and *Lotus* (Xue et al., 2015), the GRAS genes were prominent among the AM-inducible TF genes in tomato. In addition, some of the AM-induced GRAS genes, particularly those belonging to the SCLB, RAD1, RAM1 clades, did not cluster with any of the genes in the non-mycorrhizal plant *Arabidopsis*. These facts reinforce the idea that GRAS TFs are conserved core components involved in transcriptional reprogramming in plant roots required for AM formation.

Although the functionality of most GRAS gene family members remains undetermined, several have been functionally characterized and found to have diverse functions and to play an important role in many plant growth and development processes (Bolle, 2015), probably due, to a great extent, to their ability to regulate gibberellic acid (GA) responses (Sun, 2010; Zhang et al., 2011; Gong et al., 2016).

Several GRAS gene family members, including DELLA (Floss et al., 2013; Foo et al., 2013; Yu et al., 2014; Takeda et al., 2015), RAM1 (Gobbato et al., 2012; Rich et al., 2015; Xue et al., 2015), RAD1 (Xue et al., 2015), and MIG1 (Heck et al., 2016), have been reported to play a major role during mycorrhization and nodulation. The RNA-seq analysis found an overall alteration in the expression of genes encoding GRAS transcription factors, thus suggesting that the GRAS network plays an essential role in transcriptional reprogramming in the tomato host cell during mycorrhization, as reported for other species (Gobbato et al., 2012; Rich et al., 2015; Xue et al., 2015). In this study, we identified the symbiotic *RAM1, NSP2, RAD1, MIG1*, and *DIP1* GRAS genes, whose expression patterns corroborate their AM inducibility. In our experiments, although *SlGRAS16*, a putative ortholog of NSP1, did not increase significantly upon mycorrhization, a tendency toward gene induction in AM roots was observed in the RNA-seq and qPCR data. Thus, as with its homologs MtNSP1, OsNSP1, LjNSP1, and PsSYM34/NSP1 in other species, SlGRAS16 could be expected to have a mycorrhizal-related function. The mutation or silencing of *NSP1* gives rise to an impaired response to Myc-LCOs at the pre-symbiotic stage and reduced frequency of mycorrhizal colonization in *Medicago* (Delaux et al., 2013; Hohnjec et al., 2015), delayed AM development in pea (Shtark et al., 2016), and a decrease in the frequency of *L. japonicus* plant colonization by AM fungi (Takeda et al., 2013).

We found that *SlGRAS27* is the putative homolog of *PhATA/RAM1* and that *SlGRAS27* promoter expression appeared to be specifically located in arbuscule-containing cells. Likewise, Park et al. (2015) showed that the promoter expression of *MtRAM1*, the homolog of *SlGRAS27* in *M. truncatula*, appears to be associated with arbuscule-containing cells. This finding differs from that of Gobbato et al. (2013), who reported that the *MtRAM1* promoter presents homogenous activity in all AM-colonized root tissues, rather than specifically in cortical cells harboring arbuscules. These divergent observations suggest that the specific localization of *RAM1* expression during mycorrhization may depend on the plant species and mycorrhizal stage.

In this study, several tomato GRAS genes from the SCL32, SHR, SCR, and SCL3 clades were found to be induced in mycorrhizal roots. Although putative orthologs of these members have been functionally analyzed in the non-host *Arabidopsis*, their putative symbiotic role has not yet been studied in AM-host species or nodulating plants. Finely tuned hormonal signaling, in which the gibberellin/DELLA module plays an essential role, is well known to occur during mycorrhization (Floss et al., 2013; Takeda et al., 2015). SCL3 and the upstream transcription factors SHR and SCR are involved in gibberellin response regulation. SCL3, in particular, which acts as a positive regulator of gibberellin signaling, antagonistically interacts with DELLA, and is transcriptionally activated *via* SHR-SCR in certain root development processes (Heo et al., 2011; Zhang et al., 2011). In this respect, we hypothesized that the SHR/SCR/SCL3 module of GRAS TFs may act as a regulator during mycorrhization by modulating GA signaling.

In order to investigate the possible role played by SHR, SCR, and SCL3 GRAS transcription factors during mycorrhization, we focused on tomato putative orthologs which exhibit higher expression transcript levels under mycorrhizal conditions and selected the *SlGRAS18*, *SlGRAS43*, and *SlGRAS38* genes for further analysis. *SlGRAS18* was the only GRAS member from the SCL3 clade to show some gene induction upon mycorrhization. Of the three tomato GRAS proteins belonging to the SHR clade, *SlGRAS43* was undoubtedly the most AM-upregulated gene, which showed a 49-fold induction in our RNA-seq analysis. Finally, although *SlGRAS39* is the putative AM-induced ortholog gene of *AtSHR* (**Figure 2**), instead, we decided to analyze *SlGRAS38*, belonging to the closely related SCL32 clade, which showed a 24-fold induction in AM-roots as compared to a two-fold induction for *SlGRAS39*. We functionally characterized these three tomato GRAS genes during mycorrhization using RNA interference. All the experiments were performed with transformed composite tomato plants, which is a useful technique as a first screening and a less time-consuming approach than the whole plant transformation (Ho-Plágaro et al., 2018) which will be required to test the exact role of the genes in mycorrhizal functioning. The observed effects on the mycorrhizal parameters due to RNA interference were more evident for *SlGRAS18* and *SlGRAS38* at the first harvest, where roots showed

a lower level of all the measured parameters, indicating that the transgenic RNAi effect was probably not effective enough at late stages with higher levels of mycorrhization in roots.

Our phylogenetic analysis suggests that SlGRAS18 could be a tomato ortholog of AtSCL3. AtSCL3 and DELLA are reported to interact and antagonize each other in regulating GA biosynthetic genes and GA responses. AtSCL3 thus attenuates DELLA in the root endodermis, acts as a positive regulator of GA signaling, and integrates GA/DELLA signaling and the SHR/SCR pathway into root elongation (Zhang et al., 2011). In this study, we show that the putative tomato homolog *SlGRAS18,* whose gene expression is higher in the late stages of mycorrhization when arbuscules are abundant in the root and whose silencing triggers a delay in mycorrhizal colonization and a decrease in mycorrhizal parameters, is expressed in arbuscule-containing cells. Given these results, we hypothesize that the *SlGRAS18* gene, which, like AtSCL3, is able to positively regulate GA signaling antagonizing DELLA (Li et al., 2011), could be involved in controlling the action of GAs in arbuscular mycorrhiza development. Gibberellin signaling exerts positive and negative effects on arbuscular mycorrhiza development by interfering with symbiotic signaling and gene expression (Takeda et al., 2015). Thus, the decrease observed in arbuscule content, colonization frequency, and intensity of mycorrhization in *SlGRAS18* RNAi roots may occur by an increase in arbuscule degradation mediated by DELLA in mature arbuscules (Floss et al., 2017) or by a reduced hyphal branching and development in root mediated by low GA conditions (Takeda et al., 2015).

SlGRAS38 RNAi was found to have a similar effect on mycorrhizal colonization patterns as *SlGRAS18* silencing, thus suggesting the possibility of a signaling pathway *via SlGRAS38(SHR)—SlGRAS18(SCL3)* which controls arbuscular mycorrhiza development through the induction of GA signaling and is analogous to the action of the SHR-SCR-SCL3 module for GA signaling induction in *Arabidopsis* (Heo et al., 2011; Zhang et al., 2011). SlGRAS38 belongs to the functionally uncharacterized SCL32 clade (Cenci and Rouard, 2017), which is phylogenetically close to the SHR and NSP1 proteins. In previous studies, all the SCL32, SHR, and NSP1 proteins were considered to belong to the SHR clade (Huang et al., 2015). In addition, given the close phylogenetic proximity of SlGRAS38 to NSP1, its direct role in arbuscule degeneration through the formation of a complex composed of DELLA and MYB1, as reported by Floss et al. (2017) for NSP1 in *M. truncatula,* cannot be ruled out.

Finally, our study shows that *SlGRAS43,* which is strongly induced in the arbusculated cortex cells of AM roots, belongs to the SCR clade. Its *Arabidopsis* homologs, AtSCR and AtSCL23, interact with each other and are needed to specify endodermal cell fate in the root meristem (Long et al., 2015) and bundle sheath cell fate in leaves (Cui et al., 2014). Although their role in symbiotic root interactions is poorly studied, curiously, *MtSymSCL1* (Medtr1g069725.1), the closest *SlGRAS43* homolog in *M. truncatula,* is induced in both mycorrhizal and nodulated roots (GEA database) and its silencing triggers a decrease in the number of nodules (Kim and Nam, 2013). An opposite result was observed in *SlGRAS43* RNAi hairy roots, which showed a slight increase in mycorrhizal colonization. After analyzing mycorrhizal parameters, no significant differences were observed. The alterations in mycorrhizal patterns upon *SlGRAS43* silencing need to be studied in more depth in order to obtain a clearer picture of the possible regulating role of *SlGRAS43* during mycorrhization.

In light of the above-mentioned hypothesis, the *SlGRAS18* and *SlGRAS38* genes could be involved as members of the hypothetical SHR-SCR-SCL3 module in a coordinated regulation of arbuscule formation/degeneration during mycorrhization by regulating DELLA repressor of GA signaling. However, our preliminary results indicate that *SlGRAS15* or the AM-induced *SlGRAS37,* rather than *SlGRAS43,* may be potential candidate orthologs of *SCR* in tomato.

In conclusion, our results indicate that, in addition to some classic GRAS transcription factors involved in AM symbiosis, other members of the GRAS family, such as SCL3, SCR, and SCL32, are involved in regulating the mycorrhizal process in tomato. The data provided in this study, together with previous functional analyses of the respective genes, suggest that gibberellin signaling during mycorrhizal symbiosis could be regulated by these other transcription factors from the GRAS family in conjunction with members of the well-known DELLA gene subfamily.

AUTHOR CONTRIBUTIONS

JG-G and TH-P designed the experiments. NM-R, DF, and MD performed the experiments. NM-R, TH-P, and JG-G analyzed the data. TH-P and JG-G edited the manuscript.

FUNDING

This study was supported by grants from the Comisión Interministerial de Ciencia y Tecnología (CICYT) and Fondos Europeos de Desarrollo Regional (FEDER) through the Ministerio de Economía y Competitividad in Spain (AGL2014-52298-P, AGL2017-83871-P).

ACKNOWLEDGMENTS

We wish to thank Michael O'Shea for proof-reading the document. Tania Ho-Plágaro was supported by a research fellowship from the FPI-MINECO program. We acknowledge support of the publication fee by the CSIC Open Access Publication Support Initiative through its Unit of Information Resources for Research (URICI).

SUPPLEMENTARY MATERIAL

The Supplementary Material for this article can be found online at: https://www.frontiersin.org/articles/10.3389/fpls.2019.00268/full#supplementary-material

REFERENCES

Akiyama, K., Matsuzaki, K., and Hayashi, H. (2005). Plant sesquiterpenes induce hyphal branching in arbuscular mycorrhizal fungi. *Nature* 435, 824–827. doi: 10.1038/nature03608

Anders, S., and Huber, W. (2010). Differential expression analysis for sequence count data. *Genome Biol.* 11:R106. doi: 10.1186/gb-2010-11-10-r106

Anders, S., Pyl, P. T., and Huber, W. (2015). HTSeq—a Python framework to work with high-throughput sequencing data. *Bioinformatics* 31, 166–169. doi: 10.1093/bioinformatics/btu638

Augé, R. M., Stodola, A. J., Tims, J. E., and Saxton, A. M. (2001). Moisture retention properties of a mycorrhizal soil. *Plant Soil* 230, 87–97. doi: 10.1023/A:1004891210871

Bolle, C. (2015). "Functional aspects of GRAS family proteins" in *Plant transcription factors, evolutionary, structural, and functional aspects*. ed. D. H. Gonzalez (Cambridge: Elsevier), 295–311.

Bravo, A., Brands, M., Wewer, V., Dörmann, P., and Harrison, M. J. (2017). Arbuscular mycorrhiza-specific enzymes FatM and RAM2 fine-tune lipid biosynthesis to promote development of arbuscular mycorrhiza. *New Phytol.* 214, 1631–1645. doi: 10.1111/nph.14533

Cenci, A., and Rouard, M. (2017). Evolutionary analyses of GRAS transcription factors in angiosperms. *Front. Plant Sci.* 8:273. doi: 10.3389/fpls.2017.00273

Chabot, S., Bécard, G., and Piché, Y. (1992). Life cycle of *Glomus intraradix* in root organ culture. *Mycologia* 84, 315–321. doi: 10.2307/3760183

Chen, A., Gu, M., Sun, S., Zhu, L., Hong, S., and Xu, G. (2011). Identification of two conserved cis-acting elements, MYCS and P1BS, involved in the regulation of mycorrhiza-activated phosphate transporters in eudicot species. *New Phytol.* 189, 1157–1169. doi: 10.1111/j.1469-8137.2010.03556.x

Cui, H., Kong, D., Liu, X., and Hao, Y. (2014). SCARECROW, SCR-LIKE 23 and SHORT-ROOT control bundle sheath cell fate and function in *Arabidopsis thaliana*. *Plant J.* 78, 319–327. doi: 10.1111/tpj.12470

Cui, H., Levesque, M. P., Vernoux, T., Jung, J. W., Paquette, A. J., Gallagher, K. L., et al. (2007). An evolutionarily conserved mechanism delimiting SHR movement defines a single layer of endodermis in plants. *Science* 316, 421–425. doi: 10.1126/science.1139531

Delaux, P. M., Bécard, G., and Combier, J. P. (2013). NSP1 is a component of the Myc signaling pathway. *New Phytol.* 199, 59–65. doi: 10.1111/nph.12340

Fiorilli, V., Volpe, V., Zanini, S., Vallino, M., Abbà, S., and Bonfante, P. (2015). A rice GRAS gene has an impact on the success of Arbuscular mycorrhizal colonization. *Am. J. Plant Sci.* 6, 1905–1915. doi: 10.4236/ajps.2015.612191

Floss, D. S., Gomez, S. K., Park, H.-J., Maclean, A. M., Müller, L. M., Bhattarai, K. K., et al. (2017). A transcriptional program for arbuscule degeneration during AM symbiosis is regulated by MYB1. *Curr. Biol.* 27, 1206–1212. doi: 10.1016/j.cub.2017.03.003

Floss, D. S., Levy, J. G., Lévesque-Tremblay, V., Pumplin, N., and Harrison, M. J. (2013). DELLA proteins regulate arbuscule formation in arbuscular mycorrhizal symbiosis. *Proc. Natl. Acad. Sci. USA* 110, E5025–E5034. doi: 10.1073/pnas.1308973110

Foo, E., Ross, J. J., Jones, W. T., and Reid, J. B. (2013). Plant hormones in arbuscular mycorrhizal symbioses: an emerging role for gibberellins. *Ann. Bot.* 111, 769–779. doi: 10.1093/aob/mct041

Geng, R., Ke, X., Wang, C., He, Y., Wang, H., and Zhu, Z. (2017). Genome-wide identification and expression analysis of transcription factors in *Solanum lycopersicum*. *Agri Gene* 6, 14–23. doi: 10.1016/j.aggene.2017.08.002

Genre, A., Chabaud, M., Balzergue, C., Puech-Pagès, V., Novero, M., Rey, T., et al. (2013). Short-chain chitin oligomers from arbuscular mycorrhizal fungi trigger nuclear Ca2+ spiking in *Medicago truncatula* roots and their production is enhanced by strigolactone. *New Phytol.* 198, 190–202. doi: 10.1111/nph.12146

Genre, A., Chabaud, M., Faccio, A., Barker, D. G., and Bonfante, P. (2008). Prepenetration apparatus assembly precedes and predicts the colonization patterns of arbuscular mycorrhizal fungi within the root cortex of both *Medicago truncatula* and *Daucus carota*. *Plant Cell* 20, 1407–1420. doi: 10.1105/tpc.108.059014

Gobbato, E., Marsh, J. F., Vernié, T., Wang, E., Maillet, F., Kim, J., et al. (2012). A GRAS-type transcription factor with a specific function in mycorrhizal signaling. *Curr. Biol.* 22, 2236–2241. doi: 10.1016/j.cub.2012.09.044

Gobbato, E., Wang, E., Higgins, G., Bano, S. A., Henry, C., Schultze, M., et al. (2013). RAM1 and RAM2 function and expression during arbuscular mycorrhizal symbiosis and *Aphanomyces euteiches* colonization. *Plant Signal. Behav.* 8:e26049. doi: 10.4161/psb.26049

Göhre, V., and Paszkowski, U. (2006). Contribution of the arbuscular mycorrhizal symbiosis to heavy metal phytoremediation. *Planta* 223, 1115–1122. doi: 10.1007/s00425-006-0225-0

Gong, X., Flores-Vergara, M. A., Hong, J. H., Chu, H., Lim, J., Franks, R. G., et al. (2016). SEUSS integrates gibberellin signaling with transcriptional inputs from the SHR-SCR-SCL3 module to regulate middle cortex formation in the *Arabidopsis* root. *Plant Physiol.* 170, 1675–1683. doi: 10.1104/pp.15.01501

Greb, T., Clarenz, O., Schäfer, E., Müller, D., Herrero, R., Schmitz, G., et al. (2003). Molecular analysis of the LATERAL SUPPRESSOR gene in *Arabidopsis* reveals a conserved control mechanism for axillary meristem formation. *Genes Dev.* 17, 1175–1187. doi: 10.1101/gad.260703

Harrison, M. J. (2012). Cellular programs for arbuscular mycorrhizal symbiosis. *Curr. Opin. Plant Biol.* 15, 691–698. doi: 10.1016/j.pbi.2012.08.010

Heck, C., Kuhn, H., Heidt, S., Walter, S., Rieger, N., and Requena, N. (2016). Symbiotic fungi control plant root cortex development through the novel GRAS transcription factor MIG1. *Curr. Biol.* 26, 2770–2778. doi: 10.1016/j.cub.2016.07.059

Heo, J. O., Chang, K. S., Kim, I. A., Lee, M. H., Lee, S. A., Song, S. K., et al. (2011). Funneling of gibberellin signaling by the GRAS transcription regulator scarecrow-like 3 in the *Arabidopsis* root. *Proc. Natl. Acad. Sci. USA* 108, 2166–2171. doi: 10.1073/pnas.1012215108

Hirsch, S., Kim, J., Munoz, A., Heckmann, A. B., Downie, J. A., and Oldroyd, G. E. (2009). GRAS proteins form a DNA binding complex to induce gene expression during nodulation signaling in *Medicago truncatula*. *Plant Cell* 21, 545–557. doi: 10.1105/tpc.108.064501

Hohnjec, N., Czaja-Hasse, L. F., Hogekamp, C., and Küster, H. (2015). Pre-announcement of symbiotic guests: transcriptional reprogramming by mycorrhizal lipochitooligosaccharides shows a strict co-dependency on the GRAS transcription factors NSP1 and RAM1. *BMC Genomics* 16:994. doi: 10.1186/s12864-015-2224-7

Ho-Plágaro, T., Huertas, R., Tamayo-Navarrete, M. I., Ocampo, J. A., and García-Garrido, J. M. (2018). An improved method for *Agrobacterium rhizogenes*-mediated transformation of tomato suitable for the study of arbuscular mycorrhizal symbiosis. *Plant Methods* 14:34. doi: 10.1186/s13007-018-0304-9

Huang, W., Xian, Z., Kang, X., Tang, N., and Li, Z. (2015). Genome-wide identification, phylogeny and expression analysis of GRAS gene family in tomato. *BMC Plant Biol.* 15:209. doi: 10.1186/s12870-015-0590-6

Jefferson, R. (1989). The GUS reporter gene system. *Nature* 342, 837–838. doi: 10.1038/342837a0

Jiang, Y., Wang, W., Xie, Q., Liu, N., Liu, L., Wang, D., et al. (2017). Plants transfer lipids to sustain colonization by mutualistic mycorrhizal and parasitic fungi. *Science* 356, 1172–1175. doi: 10.1126/science.aam9970

Karandashov, V., Nagy, R., Wegmüller, S., Amrhein, N., and Bucher, M. (2004). Evolutionary conservation of a phosphate transporter in the arbuscular mycorrhizal symbiosis. *Proc. Natl. Acad. Sci. USA* 101, 6285–6290. doi: 10.1073/pnas.0306074101

Karimi, M., Inze, D., and Depicker, A. (2002). GATEWAY vectors for *Agrobacterium*-mediated plant transformation. *Trends Plant Sci.* 7, 193–195. doi: 10.1016/S1360-1385(02)02251-3

Keymer, A., Pimprikar, P., Wewer, V., Huber, C., Brands, M., Bucerius, S. L., et al. (2017). Lipid transfer from plants to arbuscular mycorrhiza fungi. *elife* 6:e29107. doi: 10.7554/eLife.29107

Kim, G.-B., and Nam, Y.-W. (2013). A novel GRAS protein gene *MtSymSCL1* plays a role in regulating nodule number in *Medicago truncatula*. *Plant Growth Regul.* 71, 77–92. doi: 10.1007/s10725-013-9843-7

Li, J., Wang, X., Qin, T., Zhang, Y., Liu, X., Sun, J., et al. (2011). MDP25, a novel calcium regulatory protein, mediates hypocotyl cell elongation by destabilizing cortical microtubules in *Arabidopsis*. *Plant Cell* 23, 4411–4427. doi: 10.1105/tpc.111.092684

Liu, W., Kohlen, W., Lillo, A., Op Den Camp, R., Ivanov, S., Hartog, M., et al. (2011). Strigolactone biosynthesis in *Medicago truncatula* and rice requires the symbiotic GRAS-type transcription factors *NSP1* and *NSP2*. *Plant Cell* 23, 3853–3865. doi: 10.1105/tpc.111.089771

Liu, J., Maldonado-Mendoza, I., Lopez-Meyer, M., Cheung, F., Town, C. D., and Harrison, M. J. (2007). Arbuscular mycorrhizal symbiosis is accompanied by

local and systemic alterations in gene expression and an increase in disease resistance in the shoots. *Plant J.* 50, 529–544. doi: 10.1111/j.1365-313X.2007.03069.x

Livak, K. J., and Schmittgen, T. D. (2001). Analysis of relative gene expression data using real-time quantitative PCR and the 2− ΔΔCT method. *Methods* 25, 402–408. doi: 10.1006/meth.2001.1262

Long, Y., Goedhart, J., Schneijderberg, M., Terpstra, I., Shimotohno, A., Bouchet, B. P., et al. (2015). SCARECROW-LIKE23 and SCARECROW jointly specify endodermal cell fate but distinctly control SHORT-ROOT movement. *Plant J.* 84, 773–784. doi: 10.1111/tpj.13038

Luginbuehl, L. H., Menard, G. N., Kurup, S., Van Erp, H., Radhakrishnan, G. V., Breakspear, A., et al. (2017). Fatty acids in arbuscular mycorrhizal fungi are synthesized by the host plant. *Science* 356, 1175–1178. doi: 10.1126/science.aan0081

Luginbuehl, L. H., and Oldroyd, G. E. (2017). Understanding the arbuscule at the heart of endomycorrhizal symbioses in plants. *Curr. Biol.* 27, R952–R963. doi: 10.1016/j.cub.2017.06.042

Maillet, F., Poinsot, V., André, O., Puech-Pagès, V., Haouy, A., Gueunier, M., et al. (2011). Fungal lipochitooligosaccharide symbiotic signals in arbuscular mycorrhiza. *Nature* 469, 58–63. doi: 10.1038/nature09622

Martin-Rodriguez, J. A., Huertas, R., Ho-Plagaro, T., Ocampo, J. A., Tureckova, V., Tarkowska, D., et al. (2016). Gibberellin-abscisic acid balances during arbuscular mycorrhiza formation in tomato. *Front. Plant Sci.* 7:1273. doi: 10.3389/fpls.2016.01273

Nadal, M., and Paszkowski, U. (2013). Polyphony in the rhizosphere: presymbiotic communication in arbuscular mycorrhizal symbiosis. *Curr. Opin. Plant Biol.* 16, 473–479. doi: 10.1016/j.pbi.2013.06.005

Nagy, R., Karandashov, V., Chague, V., Kalinkevich, K., Tamasloukht, M. B., Xu, G., et al. (2005). The characterization of novel mycorrhiza-specific phosphate transporters from *Lycopersicon esculentum* and *Solanum tuberosum* uncovers functional redundancy in symbiotic phosphate transport in solanaceous species. *Plant J.* 42, 236–250. doi: 10.1111/j.1365-313X.2005.02364.x

Niu, Y., Zhao, T., Xu, X., and Li, J. (2017). Genome-wide identification and characterization of GRAS transcription factors in tomato (*Solanum lycopersicum*). *PeerJ* 5:e3955. doi: 10.7717/peerj.3955

Park, H.-J., Floss, D. S., Levesque-Tremblay, V., Bravo, A., and Harrison, M. J. (2015). Hyphal branching during arbuscule development requires *RAM1*. *Plant Physiol.* 169, 2774–2788. doi: 10.1104/pp.15.01155

Phillips, J. M., and Hayman, D. (1970). Improved procedures for clearing roots and staining parasitic and vesicular-arbuscular mycorrhizal fungi for rapid assessment of infection. *Trans. Br. Mycol. Soc.* 55, 158IN116–161IN118. doi: 10.1016/S0007-1536(70)80110-3

Pimprikar, P., Carbonnel, S., Paries, M., Katzer, K., Klingl, V., Bohmer, M. J., et al. (2016). A CCaMK-CYCLOPS-DELLA complex activates transcription of *RAM1* to regulate arbuscule branching. *Curr. Biol.* 26, 987–998. doi: 10.1016/j.cub.2016.04.021

Pimprikar, P., and Gutjahr, C. (2018). Transcriptional regulation of arbuscular mycorrhiza development. *Plant Cell Physiol.* 59, 673–690. doi: 10.1093/pcp/pcy024

Pysh, L. D., Wysocka-Diller, J. W., Camilleri, C., Bouchez, D., and Benfey, P. N. (1999). The GRAS gene family in *Arabidopsis*: sequence characterization and basic expression analysis of the SCARECROW-LIKE genes. *Plant J.* 18, 111–119. doi: 10.1046/j.1365-313X.1999.00431.x

Rich, M. K., Courty, P. E., Roux, C., and Reinhardt, D. (2017). Role of the GRAS transcription factor ATA/RAM1 in the transcriptional reprogramming of arbuscular mycorrhiza in *Petunia hybrida*. *BMC Genomics* 18:589. doi: 10.1186/s12864-017-3988-8

Rich, M. K., Schorderet, M., Bapaume, L., Falquet, L., Morel, P., Vandenbussche, M., et al. (2015). The petunia GRAS transcription factor *ATA/RAM1* regulates symbiotic gene expression and fungal morphogenesis in arbuscular mycorrhiza. *Plant Physiol.* 168, 788–797. doi: 10.1104/pp.15.00310

Rubio, V., Linhares, F., Solano, R., Martín, A. C., Iglesias, J., Leyva, A., et al. (2001). A conserved MYB transcription factor involved in phosphate starvation signaling both in vascular plants and in unicellular algae. *Genes Dev.* 15, 2122–2133. doi: 10.1101/gad.204401

Ruiz-Lozano, J. M. (2003). Arbuscular mycorrhizal symbiosis and alleviation of osmotic stress. New perspectives for molecular studies. *Mycorrhiza* 13, 309–317. doi: 10.1007/s00572-003-0237-6

Schumacher, K., Schmitt, T., Rossberg, M., Schmitz, G., and Theres, K. (1999). The Lateral suppressor (Ls) gene of tomato encodes a new member of the VHIID protein family. *Proc. Natl. Acad. Sci. USA* 96, 290–295. doi: 10.1073/pnas.96.1.290

Shtark, O. Y., Sulima, A. S., Zhernakov, A. I., Kliukova, M. S., Fedorina, J. V., Pinaev, A. G., et al. (2016). Arbuscular mycorrhiza development in pea (*Pisum sativum* L.) mutants impaired in five early nodulation genes including putative orthologs of *NSP1* and *NSP2*. *Symbiosis* 68, 129–144. doi: 10.1007/s13199-016-0382-2

Silverstone, A. L., Ciampaglio, C. N., and Sun, T.-P. (1998). The *Arabidopsis* RGA gene encodes a transcriptional regulator repressing the gibberellin signal transduction pathway. *Plant Cell* 10, 155–169. doi: 10.2307/3870695

Smith, S., and Read, D. (2008). *Mycorrhizal symbiosis*. 3rd edn. London: Academic Press.

Smith, S. E., and Smith, F. A. (2011). Roles of arbuscular mycorrhizas in plant nutrition and growth: new paradigms from cellular to ecosystem scales. *Annu. Rev. Plant Biol.* 62, 227–250. doi: 10.1146/annurev-arplant-042110-103846

Sun, T.-P. (2010). Gibberellin-GID1-DELLA: a pivotal regulatory module for plant growth and development. *Plant Physiol.* 154, 567–570. doi: 10.1104/pp.110.161554

Sun, J., Miller, J. B., Granqvist, E., Wiley-Kalil, A., Gobbato, E., Maillet, F., et al. (2015). Activation of symbiosis signaling by arbuscular mycorrhizal fungi in legumes and rice. *Plant Cell* 27, 823–838. doi: 10.1105/tpc.114.131326

Takeda, N., Handa, Y., Tsuzuki, S., Kojima, M., Sakakibara, H., and Kawaguchi, M. (2015). Gibberellins interfere with symbiosis signaling and gene expression and alter colonization by arbuscular mycorrhizal fungi in *Lotus japonicus*. *Plant Physiol.* 167, 545–557. doi: 10.1104/pp.114.247700

Takeda, N., Tsuzuki, S., Suzaki, T., Parniske, M., and Kawaguchi, M. (2013). *CERBERUS* and *NSP1* of *Lotus japonicus* are common symbiosis genes that modulate arbuscular mycorrhiza development. *Plant Cell Physiol.* 54, 1711–1723. doi: 10.1093/pcp/pct114

Tian, C., Wan, P., Sun, S., Li, J., and Chen, M. (2004). Genome-wide analysis of the GRAS gene family in rice and *Arabidopsis*. *Plant Mol. Biol.* 54, 519–532. doi: 10.1023/B:PLAN.0000038256.89809.57

Trapnell, C., Pachter, L., and Salzberg, S. L. (2009). TopHat: discovering splice junctions with RNA-Seq. *Bioinformatics* 25, 1105–1111. doi: 10.1093/bioinformatics/btp120

Trapnell, C., Williams, B. A., Pertea, G., Mortazavi, A., Kwan, G., Van Baren, M. J., et al. (2010). Transcript assembly and quantification by RNA-Seq reveals unannotated transcripts and isoform switching during cell differentiation. *Nat. Biotechnol.* 28, 511–515. doi: 10.1038/nbt.1621

Trouvelot, A. (1986). "Mesure du taux de mycorhization VA d'un systeme radiculaire. Recherche de methodes d'estimation ayant une significantion fonctionnelle" in *Mycorrhizae: physiology and genetics*. eds. V. Gianinazzi-Pearson and S. Gianinazzi (Paris: INRA), 217–221.

Xue, L., Cui, H., Buer, B., Vijayakumar, V., Delaux, P.-M., Junkermann, S., et al. (2015). Network of GRAS transcription factors involved in the control of arbuscule development in *Lotus japonicus*. *Plant Physiol.* 167, 854–871. doi: 10.1104/pp.114.255430

Yu, N., Luo, D., Zhang, X., Liu, J., Wang, W., Jin, Y., et al. (2014). A DELLA protein complex controls the arbuscular mycorrhizal symbiosis in plants. *Cell Res.* 24, 130–133. doi: 10.1038/cr.2013.167

Zhang, Z. L., Ogawa, M., Fleet, C. M., Zentella, R., Hu, J., Heo, J. O., et al. (2011). Scarecrow-like 3 promotes gibberellin signaling by antagonizing master growth repressor DELLA in *Arabidopsis*. *Proc. Natl. Acad. Sci. USA* 108, 2160–2165. doi: 10.1073/pnas.1012232108

Conflict of Interest Statement: The authors declare that the research was conducted in the absence of any commercial or financial relationships that could be construed as a potential conflict of interest.

The handling editor declared a shared affiliation, though no other collaboration, with the authors at time of review.

frontiers in Plant Science

MINI REVIEW
published: 15 March 2019
doi: 10.3389/fpls.2019.00269

The Role of Gibberellins and Brassinosteroids in Nodulation and Arbuscular Mycorrhizal Associations

*Peter N. McGuiness, James B. Reid and Eloise Foo**

School of Natural Sciences, University of Tasmania, Hobart, TAS, Australia

Plant hormones play key roles in nodulation and arbuscular mycorrhizal (AM) associations. These two agriculturally and ecologically important symbioses enable plants to gain access to nutrients, in particular, nitrogen in the case of nodulation and phosphorous in the case of AM. Work over the past few decades has revealed how symbioses with nitrogen-fixing rhizobia, restricted almost exclusively to legumes, evolved in part from ancient AM symbioses formed by more than 80% of land plants. Although overlapping, these symbiotic programs also have important differences, including the *de novo* development of a new organ found only in nodulation. One emerging area of research is the role of two plant hormone groups, the gibberellins (GAs) and brassinosteroids (BRs), in the development and maintenance of these symbioses. In this review, we compare and contrast the roles of these hormones in the two symbioses, including potential interactions with other hormones. This not only focuses on legumes, most of which can host both symbionts, but also examines the role of these in AM development in non-legumes. GA acts by suppressing DELLA, and this regulatory module acts to negatively influence both rhizobial and mycorrhizal infection but appears to promote nodule organogenesis. While an overall positive role for BRs in nodulation and AM has been suggested by studies using mutants disrupted in BR biosynthesis or response, application studies indicate that BR may play a more complex role in nodulation. Given the nature of these symbioses, with events regulated both spatially and temporally, future studies should examine in more detail how GAs and BRs may influence precise events during these symbioses, including interactions with other hormone groups.

Keywords: nodulation, arbuscular mycorrhizae, plant hormone, gibberellin, brassinosteroid, DELLA, symbioses

OPEN ACCESS

Edited by:
Sergio Rasmann,
University of Neuchâtel, Switzerland

Reviewed by:
Marta Bjornson,
University of Zurich, Switzerland
Jose Manuel García-Garrido,
Spanish National Research Council (CSIC), Spain

****Correspondence:***
Eloise Foo
eloise.foo@utas.edu.au

Specialty section:
This article was submitted to Plant Microbe Interactions, a section of the journal Frontiers in Plant Science

Received: *18 December 2018*
Accepted: *19 February 2019*
Published: *15 March 2019*

Citation:
McGuiness PN, Reid JB and Foo E (2019) The Role of Gibberellins and Brassinosteroids in Nodulation and Arbuscular Mycorrhizal Associations. Front. Plant Sci. 10:269. doi: 10.3389/fpls.2019.00269

INTRODUCTION

While the application of fertilizer to crop plants may compensate for poor nutrient availability in the soil, there may be negative impacts such as the use of non-renewable resources (e.g., phosphate), cost, enhancing the growth of weeds, or runoff into waterways which may cause eutrophication. An alternative way to enhance growth under low nutrient conditions is by increasing plant nutrient uptake *via* plant-microbe symbioses with arbuscular mycorrhizal fungi or rhizobial bacteria. Arbuscular mycorrhizal symbioses are ancient and widespread, occurring in over 80% of land plant taxa (Smith and Smith, 2011). In these symbioses,

the fungi act as an extension of the plant's root system, increasing the surface area for nutrient uptake (Yang et al., 2015). In return, the plants provide the fungi with energy in the form of fatty acids and sugars (e.g., Smith and Smith, 2011; Yang et al., 2015; Jiang et al., 2017). Arbuscular mycorrhizal symbioses can increase plant growth and yield in soils poor in essential nutrients, particularly phosphorus (Baum et al., 2015; Yang et al., 2015). Another important plant microbe symbiosis almost completely restricted to legumes is nodulation (Mus et al., 2016), where nitrogen-fixing rhizobial bacteria are housed in nodules in the root system. The nitrogen-fixing bacteria convert atmospheric nitrogen into ammonia, which the plant can use as a nitrogen source (Mus et al., 2016). Nodulation is thought to have evolved in part from the ancient arbuscular mycorrhizal program (Delaux et al., 2013; Martin et al., 2017).

Both nodulation and arbuscular mycorrhizal symbioses are regulated by a variety of plant signals, including many of the plant hormones (Ferguson and Mathesius, 2014; Gutjahr, 2014; Bedini et al., 2018; Liao et al., 2018). This review focuses on how two families of plant growth hormones, the gibberellins (GAs) and brassinosteroids (BR), influence the development of rhizobial and AM symbioses. It is timely to synthesize an overview across species and to examine any parallels between the two symbioses. In particular, we examine the stage of the symbiosis at which the hormones operate, as these are complex processes with distinct infection and development phases that can occur across different spatial and temporal scales. Although interactions between GA and BR has been suggested to occur at the level of signaling (for review see Ross and Quittendon, 2016), this has not yet been explored during symbioses. Although there is evidence that some rhizobial bacteria may produce GA (Tatsukami et al., 2016; Nett et al., 2017), it is not yet clear if mycorrhizal fungi produce GA, as this has yet to be tested using modern quantitative techniques (e.g., Barea and Azcón-Aguilar, 1982). As the GAs and BRs also have powerful effects on many other aspects of plant development, for example, stem elongation (Ross et al., 2011), in this synthesis, we take care to examine the evidence to determine whether the effect of the hormones on a symbiosis is direct or may result from indirect effects of these hormones on other aspects of the plant's phenotype.

GIBBERELLINS

GAs are a group of diterpenoid growth hormones strongly associated with promoting growth, including stem elongation and germination (e.g., Ross and Reid, 2010). The bioactive GAs signal by binding to intracellular receptors from the GID protein family, which then complex with DELLA transcription factors and an E3 ubiquitin ligase. The E3 ubiquitin ligase polyubiquitinates the DELLA proteins, tagging them for degradation (Daviere and Achard, 2013). DELLA proteins can act as represses of transcription; thus, the loss of the DELLA transcription factors in the presence of GA derepresses gene expression inducing GA response (Daviere and Achard, 2013).

Gibberellins Regulate Arbuscular Mycorrhizae

There is good evidence that arbuscular mycorrhizal colonization is inhibited by GA signaling (**Figure 1A**). Several studies have shown that the application of GAs inhibits the formation of arbuscular mycorrhizae, including studies in pea (El Ghachtouli et al., 1996), *Lotus japonicus* (Takeda et al., 2015), and tomato (Martín-Rodríguez et al., 2015). A negative role for GAs in arbuscular mycorrhizal development was confirmed by mutant and transgenic studies in pea, *Medicago truncatula,* rice, and wheat (Floss et al., 2013; Foo et al., 2013; Yu et al., 2014). The severely GA-deficient pea mutant *na*, which has a non-functional *ent*-kaurenoic acid oxidase enzyme (Davidson et al., 2003), has more arbuscular mycorrhizae than wild-type plants (Foo et al., 2013). This influence of low gibberellins on mycorrhizal colonization appears to be independent of ethylene (Foo et al., 2016). However, it acts through the DELLA proteins since a *DELLA*-deficient double mutant of pea, *la cry-s,* which results in permanently high GA signaling, and the *na la cry-s* triple mutant display reduced levels of arbuscular mycorrhizal colonization compared with wild-type plants (Foo et al., 2013). The formation of arbuscular mycorrhizal symbiosis occurs in several stages, including spore germination and hyphal branching, hyphopodium formation, and penetration into the root, followed by the development of hyphae and branched arbuscules (**Figure 1**; Genre et al., 2005). GA signaling through DELLA appears to be particularly involved in arbuscule initiation, rather than arbuscule branching or hyphal colonization, as loss-of-function *della1 della2* double mutants in pea and *Medicago truncatula* and the *della* mutant *slr1* in rice display a more dramatic reduction in arbuscules than wild-type plants compared to other fungal structures (Floss et al., 2013; Foo et al., 2013; Yu et al., 2014). Consistent with this, a rice *SLR-YFP* overexpression line and a wheat *Rht1/Rht2* gain-of-function *DELLA* line displayed increased arbuscule formation (Floss et al., 2013; Yu et al., 2014). Although they are altered in number, the arbuscules that do form in plants with altered GA or DELLA status appear relatively normal (Floss et al., 2013; Foo et al., 2013).

The establishment of a symbiosis requires the recognition, uptake, and accommodation of the microbe. For both nodulation and arbuscular mycorrhizal associations, this is initiated by the plant's perception of unique microbial-derived lipochitooligosaccharides or chitin oligomers, known as Nod and Myc factors, respectively (Martin et al., 2017). Genetic studies in legumes have begun to define the parts of this pathway that the two symbioses share, known as the common symbiotic signaling cascade, and the outputs unique to each symbiosis. One key output of the perception of the Nod and Myc factors is the induction of calcium spiking that is perceived by the CCaMK protein. In the formation of mycorrhizal symbioses, CCaMK phosphorylates the transcription factor CYCLOPS/IPD3, which activates a variety of symbiosis genes that facilitate fungal infection and arbuscule formation (Zipfel and Oldroyd, 2017). An important downstream target of this pathway is RAM1. RAM1 is a GRAS transcription factor required for arbuscule initiation and branching (Pimprikar et al., 2016). Several studies have examined how DELLA may

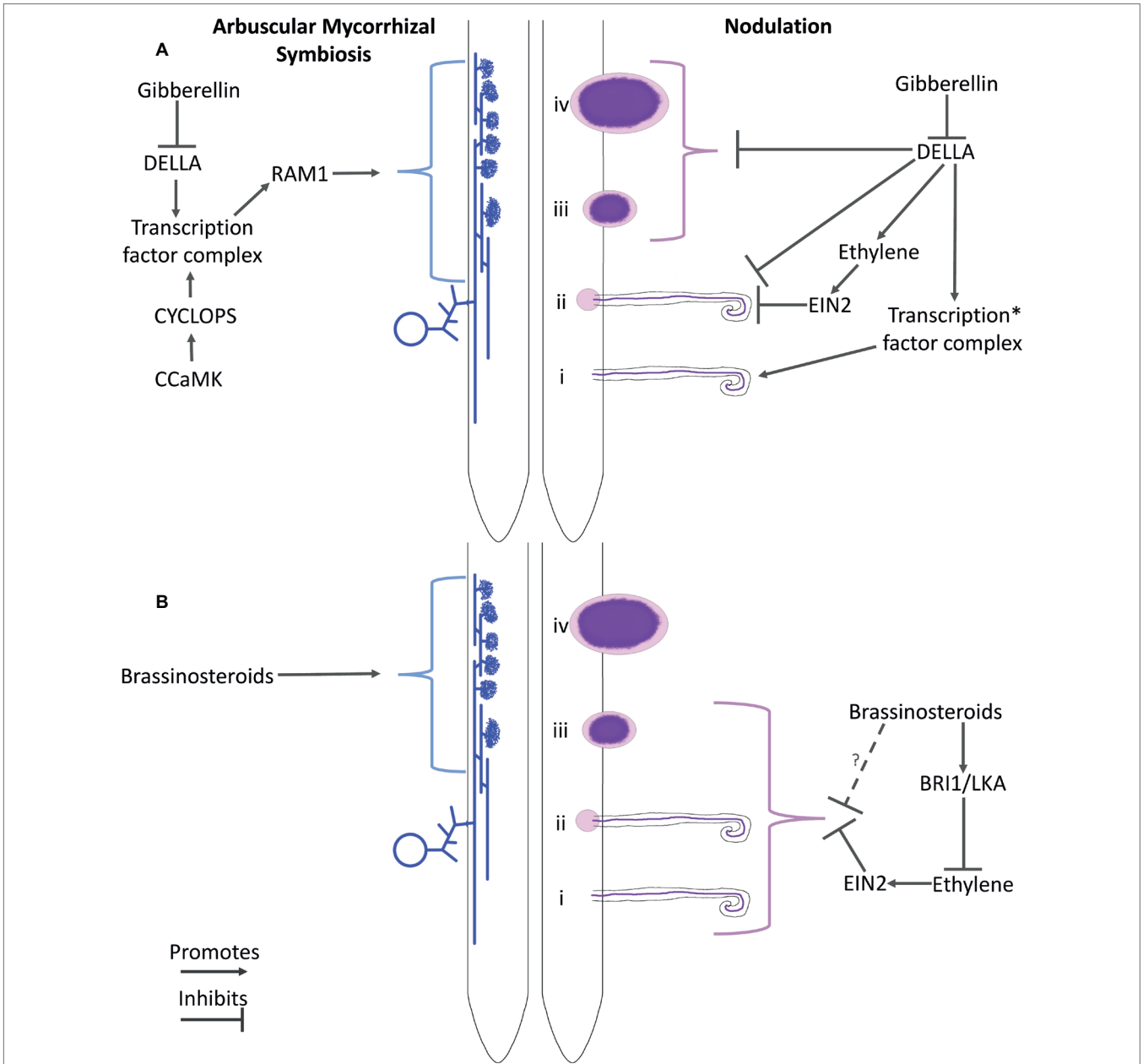

FIGURE 1 | Schematic of the proposed roles of gibberellin **(A)** and brassinosteroids **(B)** and their interaction with ethylene in arbuscular mycorrhizal colonization (LHS) and nodulation (RHS). Key players in hormone perception and potential downstream elements are indicated. For arbuscular mycorrhizal colonization, a spore, hyphae, and arbuscules are represented. For nodulation, numerals indicate the stages of development: (i) Infection thread formation, (ii) initial cortical cell divisions, (iii) nodule organogenesis, and (iv) development of the nodule into a nitrogen-fixing organ. *Proteins that have been proposed to influence this transcription factor complex include CCaMK, IPD3, NSP2, and NF-YA1 (See the text for references).

influence elements of this mycorrhizal signaling cascade. Transactivation studies, yeast two hybrid studies, bimolecular fluorescence complementation and co-immunoprecipitation studies have revealed that DELLA proteins may participate in a complex with CYCLOPS (Jin et al., 2016) and CCaMK to control RAM1 expression (Pimprikar et al., 2016). Genetic evidence for such interactions during AM development are complex and are complicated by the fact that aspects may rely on AM activation of the cortical program by CCaMK (Floss et al., 2013). Overall, studies with mutants, transgenic lines, and application of GA or GA biosynthesis inhibitors are consistent with DELLA acting with CCaMK and CYCLOPS to promote arbuscule formation *via* RAM1 (Floss et al., 2013; Pimprikar et al., 2016). However, it is important to note that gain-of-function DELLA overexpression or GA biosynthesis inhibitors can restore arbuscule formation in *cyclops* mutants; this indicates the potential for other DELLA interacting partners (Pimprikar et al., 2016).

Another approach to examine the dynamics of GA during arbuscular mycorrhizal colonization was undertaken in a study in *Lotus japonicus*, in which transgenic plants expressing the *GUS* reporter gene under the control of promoters of the GA biosynthesis genes *GA20ox1* and *GA20ox2* were generated (Takeda et al., 2015). Co-staining for GUS and arbuscular mycorrhizae revealed cells expressing these GA biosynthesis genes corresponded to cells hosting the AM fungus (Takeda et al., 2015). Bioactive GA_1 levels in whole infected roots were also somewhat elevated compared to uninoculated roots. Plants forming an arbuscular mycorrhizal symbiosis accumulate GAs in their roots, potentially due to increased activity in the 13-hydroxylation GA biosynthesis pathway (Martín-Rodríguez et al., 2015). In addition, the study by Takeda et al. (2015) proposed that exogenous GA influences fungal entry into the plant and hyphal branching of the mycorrhizal fungi, although as these studies were necessarily conducted *in planta*, it is difficult to distinguish direct effects on the fungi from indirect effects due to altered plant growth.

Gibberellins Regulate Nodulation

GA can have both positive and negative effects of the number of nodules formed. Application of bioactive GAs and/or GA biosynthesis inhibitors can both promote and inhibit nodulation, depending on the species, dose, and application method (e.g., Thurber et al., 1958; Mes, 1959; Ferguson et al., 2005; Lievens et al., 2005; Fonouni-Farde et al., 2016). This is consistent with genetic studies, where low nodule numbers are observed in pea, *Medicago*, and *Lotus* mutants with high GA signaling, due to *della* mutations, and also in pea mutants with low GA signaling, due to disruption of GA biosynthesis (Ferguson et al., 2005; Fonouni-Farde et al., 2016; Jin et al., 2016; McAdam et al., 2018).

While this apparent paradox may be explained by stating that there is an optimal level of GA for nodulation overall, this may disguise the fact that GA exerts different effects on specific stages of nodulation (**Figure 1B**; Ferguson et al., 2005; Ferguson et al., 2011; McAdam et al., 2018). As outlined above, nodulation is induced by Nod factor signaling *via* the common symbiotic pathway. This signaling not only facilitates infection at the epidermis but also induces concomitant induction of nodule organogenesis in the root cortex. These initially spatially separated events can occur independently, as demonstrated by the development of spontaneous nodules in the absence of rhizobia in gain-of-function CCaMK or cytokinin receptor mutants (e.g., Marsh et al., 2007; Tirichine et al., 2007). GA appears to have a strong negative effect on the infection stage of nodulation since loss-of-function *della* mutants or transgenic lines in *Medicago* and pea display a reduced number of infection threads compared with wild-type plants (Fonouni-Farde et al., 2016; Jin et al., 2016; McAdam et al., 2018). Consistent with this, infection thread formation is also suppressed by exogenous GA in a range of species (Maekawa et al., 2009; Fonouni-Farde et al., 2016; Jin et al., 2016; McAdam et al., 2018). Similarly, GA-deficient mutants of pea display elevated infection thread formation (McAdam et al., 2018). Yeast three hybrid and co-immunoprecipitation studies in *Medicago* suggest that this negative influence of GA signaling on infection may be mediated through physical interaction of the DELLA proteins with key components of the Nod factor signaling pathway including NF-YA1, NSP1, NSP2, and IPD3/CYCLOPS (Fonouni-Farde et al., 2016; Jin et al., 2016). DELLAs have also been reported to increase the phosphorylation state of IPD3/CYCLOPS *in vitro* (Fonouni-Farde et al., 2016). Consistent with this, Nod factor-activated gene expression was suppressed by GA treatment in wild-type *Lotus* and *Medicago* and, in the absence of GA treatment, in *Medicago della* mutant lines (Maekawa et al., 2009; Fonouni-Farde et al., 2016; Jin et al., 2016).

Several different approaches have been used to examine the role of GA during nodule initiation, organogenesis, and ultimate function. In addition to displaying reduced infection, lines with loss of DELLA function also display a reduced number of nodules (Ferguson et al., 2011; Fonouni-Farde et al., 2016; Jin et al., 2016; McAdam et al., 2018). However, the nodules that do form on *della* mutants appear similar to wild type and in pea appear to fix nitrogen at a similar rate to wild-type nodules (McAdam et al., 2018). This suppression of nodule initiation in *della* mutants, but not nodule development or function, may be due to a reduction in infection events or a more direct role for DELLAs in nodule initiation. The latter hypothesis is supported by the fact that *della* mutants of *Medicago* do not form nodule-like structures in transgenic roots overexpressing mutant gain of function versions of CCaMK or the cytokinin receptor *cre1* (Jin et al., 2016; Fonouni-Farde et al., 2017). Nodule-like structures were also observed in wild-type lines expressing della1-Δ18 dominant-active protein (Fonouni-Farde et al., 2017). However, several lines of evidence suggest a positive role for GA in nodule initiation and development. Firstly, an increased number of infection threads but not nodule numbers were observed in wild-type lines expressing a dominant version of *MtDELLA1* resistant to degradation by GA (Fonouni-Farde et al., 2016), suggesting a negative role for GA during infection but not necessarily nodule organogenesis. Secondly, GA-deficient *na* mutants of pea display strongly elevated numbers of infection threads, but a reduced number of nodules, and often no nodules at all (McAdam et al., 2018). Indeed, the few nodules that do form in severely GA-deficient lines are small, contain undifferentiated bacteria, and appear to fix less nitrogen than wild-type nodules (McAdam et al., 2018). This suggests an important role for GA in promoting the initiation and development of nodules into nitrogen fixing organs. This is consistent with the expression of GA biosynthesis genes within the nodule during formation and maturation in several species (Kouchi et al., 2004; Lievens et al., 2005; Hayashi et al., 2012).

Several studies have examined if this influence of GA on nodulation may be *via* interaction with other hormones with prominent roles in nodulation. In particular, studies have examined a link with ethylene, a gaseous hormone that has an overall negative influence on infection and nodule initiation and also influences the spatial arrangement of nodules (for review see Guinel, 2015). In pea, severely GA-deficient lines evolve more ethylene (Ferguson et al., 2011). To explore the interaction between GA and ethylene, double mutant lines

were generated that combine the severely GA-deficient *na* mutant with *ein2*, a mutant lacking an essential element of the ethylene perception pathway (Weller et al., 2015; Foo et al., 2016). Infection, nodule initiation, and nodule function were assessed in these double mutants and compared to the respective single mutants and wild-type plants. Ethylene and GA appear to influence infection relatively independently, but GA suppression of ethylene biosynthesis may be an important mechanism to promote nodule initiation, as *na ein2* mutants develop many nodules. However, the nodules that do develop on *na ein2* plants have the characteristic arrested development of *na* (GA-deficient) single mutant plants and appear to fix little nitrogen, suggesting that GA is important for nodule development (McAdam et al., 2018). It is important to note that these *na ein2* plants still display severely reduced shoot size, suggesting that it is not shoot size *per se* that restricts nodule initiation in GA-deficient lines (Foo et al., 2016). More recently, a potential crossover between the GA and cytokinin pathways has been suggested in *Medicago* roots (Fonouni-Farde et al., 2017), although future studies are required to determine if this occurs during nodulation.

Future studies could explore the spatial and temporal regulation of GA signaling during infection and nodule development to resolve the role of GA during various stages of nodulation. This will complement ongoing studies that also indicate a role for bacterial-derived GA in some, but not all, legume-rhizobial partnerships (Tatsukami et al., 2016; Nett et al., 2017).

BRASSINOSTEROIDS

Brassinosteroids Promote Arbuscular Mycorrhizal Symbioses

Brassinosteroids are a family of growth promoting steroid hormones. They have been implicated in a range of developmental processes, such as shoot elongation and vascular development by promoting cell elongation and division (Singh and Sigal, 2015). Only a handful of studies have investigated the role of brassinosteroids in arbuscular mycorrhizae. Overall, they appear to have a positive influence. Mutations in brassinosteroid biosynthesis genes resulting in severe BR-deficiency result in reduced arbuscular mycorrhizal colonization in tomato, rice, and pea mutants compared to wild-type plants (Bitterlich et al., 2014a,b; Foo et al., 2016) and foliar application of synthetic brassinosteroids to wheat resulted in increased in AM colonization (Tofighi et al., 2017). How BRs influences AM development is not known. As observed in the severely GA-deficient lines outlined above, severely BR-deficient lines also evolve more ethylene (Ross and Reid, 1986). Double mutant studies with ethylene insensitive plants deficient in BRs (*lk ein2*) suggest that the influence of BRs on AM is independent of ethylene (Foo et al., 2016). Other studies suggest that BRs may influence sucrose transport, potentially increasing the amount of sugar available to the fungus (Bitterlich et al., 2014a,b). Future studies are required to delineate the precise role of BRs during fungal infection, accommodation, and nutrient exchange, including any interaction with other plant hormones.

Brassinosteroids Influence Nodulation

Most of the early studies into the role of brassinosteroids in nodulation were based on applying synthetic brassinosteroids and brassinosteroid biosynthesis inhibitors and produced mixed results, including both positive and negative effects of BR on nodulation across a range of legumes (Vardhini and Rao, 1999; Hunter, 2001; Terakado et al., 2005; Yusuf et al., 2012). This is similar to studies with GAs outlined above, where both positive and negative effects of exogenous GAs were observed on nodule number. Genetic studies using BR biosynthesis and receptor mutants in pea and a BR receptor mutant in *Medicago truncatula* suggest that BRs act as promoters of nodule number, as all the mutants form less nodules than wild type (Ferguson et al., 2005; Foo et al., 2014, 2016; Cheng et al., 2017). BRs appear to influence nodulation in part through ethylene. The elevated ethylene of severely BR-deficient pea *lk* mutant appears to explain at least in part the low nodulation phenotype of *lk* mutants, as *lk ein2* double mutants display an elevated nodulation phenotype, similar to *ein2* single mutants (Foo et al., 2016). Cheng et al. (2017) noted that the nodules that formed on the *Medicago* BR receptor mutant, *Mtbri1,* were white, suggesting that they were non-functional. However, this phenotype has not been observed in pea BR mutants (Ferguson et al., 2005). A more direct measurement of nitrogen fixation is required to determine if BR influences nodule function in addition to nodule number. It will also be interesting to examine the various stages of nodulation in BR mutants to determine if the inconsistent application results outlined above may be due to BR influencing different stages of nodule development.

It is also important to note that grafting studies in pea suggest that BR may act through a shoot-derived signal(s) to influence nodulation. Plants with reduced BR biosynthesis in the shoot system produce less nodules than those with a wild-type shoot system, irrespective of BR production in the root system (Ferguson et al., 2005). As previous grafting studies have shown that BRs are not mobile in the plant (Symons and Reid, 2004; Symons et al., 2008), BRs must be acting through a mobile signal(s). Analysis of auxin and GA levels in these grafts suggest that BR does not act *via* auxin or GA (Ferguson et al., 2005). As double mutant studies ruled out a role for BR acting upstream of the systemic autoregulation of nodulation (AON) pathway (Foo et al., 2014), future studies are required to clarify this systemic effect.

GENERAL CONCLUSION

Two of the major plant growth hormone families, the GAs and BRs, influence both nodulation and arbuscular mycorrhizal symbioses. The GAs, acting through DELLAs, appear to inhibit arbuscular mycorrhizal symbioses and rhizobial infection-thread formation at least in part *via* elements of the common symbiotic pathway. GAs also appear to have a second role in nodulation, promoting nodule initiation and organogenesis. Genetic studies

have to date indicated overall that BRs promote both nodulation and arbuscular mycorrhizal symbioses. However, application studies have also indicated a potentially complex role for BRs in nodulation, with both positive and negative effects. Future studies could examine how GAs and BRs influence the spatial and temporal stages of hosting symbiotic microbes, including any intersection with the common symbiotic pathway and other hormones, including those with well-defined roles in nodulation such as auxin and cytokinin.

AUTHOR CONTRIBUTIONS

EF conceived the project. PM, JR, and EF wrote the manuscript.

FUNDING

We thank the Australian Research Council for financial support to EF and JR (FF140100770 and DP140101709).

REFERENCES

Barea, J. M., and Azcón-Aguilar, C. (1982). Production of plant growth-regulating substances by the vesicular-arbuscular mycorrhizal fungus *Glomus mosseae*. *Appl. Environ. Microbiol.* 43, 810–813.

Baum, C., El-Tohamy, W., and Gruda, N. (2015). Increasing the productivity and product quality of vegetable crops using arbuscular mycorrhizal fungi: a review. *Sci. Hortic.* 187, 131–141. doi: 10.1016/j.scienta.2015.03.002

Bedini, A., Mercy, L., Schneider, C., Franken, P., and Lucic-Mercy, E. (2018). Unraveling the initial plant hormone signaling, metabolic mechanisms and plant defense triggering the endomycorrhizal symbiosis behavior. *Front. Plant Sci.* 9:1800. doi: 10.3389/fpls.2018.01800

Bitterlich, M., Krügel, U., Boldt-Burisch, K., Franken, P., and Kühn, C. (2014a). Interaction of brassinosteroid functions and sucrose transporter SlSUT2 regulate the formation of arbuscular mycorrhiza. *Plant Signal. Behav.* 9:e970426. doi: 10.4161/15592316.2014.970426

Bitterlich, M., Krügel, U., Boldt-Burisch, K., Franken, P., and Kühn, C. (2014b). The sucrose transporter SlSUT2 from tomato interacts with brassinosteroid functioning and affects arbuscular mycorrhiza formation. *Plant J.* 78, 887–899. doi: 10.1111/tpj.12515

Cheng, X., Gou, X., Yin, H., Mysore, K. S., Li, J., and Wen, J. (2017). Functional characterisation of brassinosteroid receptor MtBRI1 *in Medicago truncatula*. *Sci. Rep.* 7:9327. doi: 10.1038/s41598-017-09297-9

Davidson, S. E., Elliott, R. C., Helliwell, C. A., Poole, A. T., and Reid, J. B. (2003). The pea gene *NA* encodes ent-kaurenoic acid oxidase 1. *Plant Physiol.* 131, 335–344. doi: 10.1104/pp.012963

Daviere, J. M., and Achard, P. (2013). Gibberellin signaling in plants. *Development* 140, 1147–1151. doi: 10.1242/dev.087650

Delaux, P. M., Séjalon-Delmas, N., Bécard, G., and Ané, J. M. (2013). Evolution of the plant-microbe symbiotic "toolkit". *Trends Plant Sci.* 18, 298–304. doi: 10.1016/j.tplants.2013.01.008

El Ghachtouli, N., Martin-Tanguy, J., Paynot, M., and Gianinazzi, S. (1996). First-report of the inhibition of arbuscular mycorrhizal infection of *Pisum sativum* by specific and irreversible inhibition of polyamine biosynthesis or by gibberellic acid treatment. *FEBS Lett.* 385, 189–192. doi: 10.1016/0014-5793(96)00379-1

Ferguson, B. J., Foo, E., Ross, J. J., and Reid, J. B. (2011). Relationship between gibberellin, ethylene and nodulation in *Pisum sativum*. *New Phytol.* 189, 829–842. doi: 10.1111/j.1469-8137.2010.03542.x

Ferguson, B. J., and Mathesius, U. (2014). Phytohormone regulation of legume-rhizobia interactions. *J. Chem. Ecol.* 40, 770–790. doi: 10.1007/s10886-014-0472-7

Ferguson, B. J., Ross, J. J., and Reid, J. B. (2005). Nodulation phenotypes of gibberellin and brassinosteroid mutants of pea. *Plant Physiol.* 138, 2396–2405. doi: 10.1104/pp.105.062414

Floss, D. S., Levy, J. G., Levesque-Tremblay, V., Pumplin, N., and Harrison, M. J. (2013). DELLA proteins regulate arbuscule formation in arbuscular mycorrhizal symbiosis. *Proc. Natl. Acad. Sci. USA* 110, E5025–E5034. doi: 10.1073/pnas.1308973110

Fonouni-Farde, C., Kisiala, A., Brault, M., Emery, R. J. N., Diet, A., and Frugier, F. (2017). DELLA1-mediated gibberellin signaling regulates cytokinin-dependent symbiotic nodulation. *Plant Physiol.* 175, 1795–1806. doi: 10.1104/pp.17.00919

Fonouni-Farde, C., Tan, S., Baudin, M., Brault, M., Wen, J., Mysore, K. S., et al. (2016). DELLA-mediated gibberellin signalling regulates Nod factor signalling and rhizobial infection. *Nat. Commun.* 7:12636. doi: 10.1038/ncomms12636

Foo, E., Ferguson, B. J., and Reid, J. B. (2014). The potential roles of strigolactones and brassinosteroids in the autoregulation of nodulation pathway. *Ann. Bot.* 113, 1037–1045. doi: 10.1093/aob/mcu030

Foo, E., McAdam, E. L., Weller, J. L., and Reid, J. B. (2016). Interactions between ethylene, gibberellins, and brassinosteroids in the development of rhizobial and mycorrhizal symbioses of pea. *J. Exp. Bot.* 67, 2413–2424. doi: 10.1093/jxb/erw047

Foo, E., Ross, J. J., Jones, W. T., and Reid, J. B. (2013). Plant hormones in arbuscular mycorrhizal symbioses: an emerging role for gibberellins. *Ann. Bot.* 111, 769–779. doi: 10.1093/aob/mct041

Genre, A., Chabaud, M., Timmers, T., Bonfante, P., and Barker, D. G. (2005). Arbuscular mycorrhizal fungi elicit a novel intracellular apparatus in *Medicago truncatula* root epidermal cells before infection. *Plant Cell* 17, 3489–3499. doi: 10.1105/tpc.105.035410

Guinel, F. C. (2015). Ethylene, a hormone at the center-stage of nodulation. *Front. Plant Sci.* 6:1121. doi: 10.3389/fpls.2015.01121

Gutjahr, C. (2014). Phytohormone signaling in arbuscular mycorhiza development. *Curr. Opin. Plant Biol.* 20, 26–34. doi: 10.1016/j.pbi.2014.04.003

Hayashi, S., Reid, D. E., Lorenc, M. T., Stiller, J., Edwards, D., Gresshoff, P. M., et al. (2012). Transient Nod factor-dependent gene expression in the nodulation-competent zone of soybean (*Glycine max* [L.] Merr.) roots. *Plant Biotechnol. J.* 10, 995–1010. doi: 10.1111/j.1467-7652.2012.00729.x

Hunter, W. J. (2001). Influence of root-applied epibrassinolide and carbenoxolone on thenodulation and growth of soybean (*Glycine max* L.) seedlings. *J. Agron. Crop Sci.* 186, 217–221. doi: 10.1046/j.1439-037x.2001.00466.x

Jiang, Y., Wang, W., Xie, Q., Liu, N., Liu, L., Wang, D., et al. (2017). Plants transfer lipids to sustain colonization by mutualistic mycorrhizal and parasitic fungi. *Science* 356, 1172–1173. doi: 10.1126/science.aam9970

Jin, Y., Liu, H., Luo, D., Yu, N., Dong, W., Wang, C., et al. (2016). DELLA proteins are common components of symbiotic rhizobial and mycorrhizal signalling pathways. *Nat. Commun.* 7:12433. doi: 10.1038/ncomms12433

Kouchi, H., Shimomura, K., Hata, S., Hirota, A., Wu, G. J., Kumagai, H., et al. (2004). Large-scale analysis of gene expression profiles during early stages of root nodule formation in a model legume, *Lotus japonicus*. *DNA Res.* 11, 263–274. doi: 10.1093/dnares/11.4.263

Liao, D., Wang, S., Cui, M., Liu, J., Chen, A. and Xu, G. (2018). Phytohormones regulate the development of arbuscular mycorrhizal symbiosis. *Int. J. Mol. Sci.* 19:3146. doi: 10.3390/ijms19103146

Lievens, S., Goormachtig, S., Den Herder, J., Capoen, W., Mathis, R., Hedden, P., et al. (2005). Gibberellins are involved in nodulation of *Sesbania rostrata*. *Plant Physiol.* 139, 1366–1379. doi: 10.1104/pp.105.066944

Maekawa, T., Maekawa-Yoshikawa, M., Takeda, N., Imaizumi-Anraku, H., Murooka, Y., and Hayashi, M. (2009). Gibberellin controls the nodulation signaling pathway in *Lotus japonicus*. *Plant J.* 58, 183–194. doi: 10.1111/j.1365-313X.2008.03774.x

Marsh, J. F., Rakocevic, A., Mitra, R. M., Brocard, L., Sun, J., Eschstruth, A., et al. (2007). *Medicago truncatula* NIN is essential for rhizobial-independent nodule organogenesis induced by autoactive calcium/calmodulin-dependent protein kinase 1. *Plant Physiol.* 144, 324–335. doi: 10.1104/pp.106.093021

Martin, F. M., Uroz, S., and Barker, D. G. (2017). Ancestral alliances: plant mutualistic symbioses with fungi and bacteria. *Science* 356:eaad4501. doi: 10.1126/science.aad4501

Martín-Rodríguez, J. Á., Ocampo, J. A., Molinero-Rosales, N., Tarkowská, D., Ruíz-Rivero, O., and García-Garrido, J. M. (2015). Role of gibberellins during arbuscular mycorrhizal formation in tomato: new insights revealed by endogenous quantification and genetic analysis of their metabolism in mycorrhizal roots. *Physiol. Plant.* 154, 66–81. doi: 10.1111/ppl.12274

McAdam, E. L., Reid, J. B., and Foo, E. (2018). Gibberellins promote nodule organogenesis but inhibit the infection stages of nodulation. *J. Exp. Bot.* 69, 2117–2130. doi: 10.1093/jxb/ery046

Mes, M. G. (1959). Influence of gibberellic acid and photoperiod on the growth, flowering, nodulation and nitrogen assimilation of *Vicia villosa*. *Nature* 184, 2035–2036. doi: 10.1038/1842035a0

Mus, F., Crook, B. M., Garcia, K., Costas, A. G., Geddes, B. A., Kouri, E. G., et al. (2016). Symbiotic nitrogen fixation and the challenges to its extension to nonlegumes. *Appl. Environ. Microbiol.* 82, 3698–3710. doi: 10.1128/AEM.01055-16

Nett, R. S., Contreras, T., and Peters, R. J. (2017). Characterization of CYP115 as a gibberellin 3-oxidase indicates that certain rhizobia can produce bioactive gibberellin A_4. *ACS Chem. Biol.* 12, 912–917. doi: 10.1021/acschembio.6b01038

Pimprikar, P., Carbonnel, S., Paries, M., Katzer, K., Klingl, V., Bohmer, M. J., et al. (2016). A CCaMK-CYCLOPS-DELLA complex activates transcription of RAM1 to regulate arbuscule branching. *Curr. Biol.* 26, 987–998. doi: 10.1016/j.cub.2016.01.069

Ross, J. J., and Quittendon, L. J. (2016). Interactions between brassinosteroids and gibberellins: Synthesis or Signaling?. *The Plant Cell* 28, 829–832. doi: 10.1105/tpc.15.00917

Ross, J. J., and Reid, J. B. (1986). Internode length in *Pisum*. The involvement of ethylene with the gibberellin-insensitive erectoides phenotype. *Physiol. Plant.* 67, 673–679. doi: 10.1111/j.1399-3054.1986.tb05076.x

Ross, J. J., and Reid, J. B. (2010). Evolution of growth-promoting plant hormones. *Funct. Plant Biol.* 37, 795–805. doi: 10.1071/FP10063

Ross, J. J., Weston, D. E., Davidson, S. E., and Reid, J. B. (2011). Plant hormone interactions: how complex are they? *Physiol. Plant.* 141, 299–309. doi: 10.1111/j.1399-3054.2011.01444.x

Singh, A. P., and Sigal, S. (2015). Growth control: brassinosteroid activity gets context. *J. Exp. Bot.* 66, 1123–1132. doi: 10.1093/jxb/erv026

Smith, S. E., and Smith, F. A. (2011). Roles of arbuscular mycorrhizas in plant nutrition and growth: new paradigms from cellular to ecosystem scales. *Annu. Rev. Plant Biol.* 62, 227–250. doi: 10.1146/annurev-arplant-042110-103846

Symons, G. M., and Reid, J. B. (2004). Brassinosteroids do not undergo long-distance transport in pea. Implications for the regulation of endogenous brassinosteroid levels. *Plant Physiol.* 135, 2196–2206. doi: 10.1104/pp.104.043034

Symons, G. M., Ross, J. J., Jager, C. E., and Reid, J. B. (2008). Brassinosteroid transport. *J. Exp. Bot.* 59, 17–24. doi: 10.1093/jxb/erm098

Takeda, N., Handa, Y., Tsuzuki, S., Kojima, M., Sakakibara, H., and Kawaguchi, M. (2015). Gibberellins interfere with symbiosis signaling and gene expression and alter colonization by arbuscular mycorrhizal fungi in *Lotus japonicus*. *Plant Physiol.* 167, 545–557. doi: 10.1104/pp.114.247700

Tatsukami, Y., Ueda, M., and Ueda, M. (2016). Rhizobial gibberellin negatively regulates host nodule number. *Sci. Rep.* 6:27998. doi: 10.1038/srep27998

Terakado, J., Fujihara, S., Terakado, J., Goto, S., Kuratani, R., Suzuki, Y., et al. (2005). Systemic effect of a brassinosteroid on root nodule formation in soybean as revealed by the application of brassinolide and brassinazole. *Soil Sci. Plant Nutr.* 51, 389–395. doi: 10.1111/j.1747-0765.2005.tb00044.x

Thurber, G. A., Douglas, J. R., and Galston, A. W. (1958). Inhibitory effect of gibberellins on nodulization in dwarf beans, *Phaseolus vulgaris*. *Nature* 181, 1082–1083. doi: 10.1038/1811082a0

Tirichine, L., Sandal, N., Madsen, L. H., Radutoiu, S., Albrektsen, A. S., Sato, S., et al. (2007). A gain-of-function mutation in a cytokinin receptor triggers root nodule organogenesis. *Science* 315, 104–107. doi: 10.1126/science.1132397

Tofighi, C., Khavari-Nejad, R. A., Najafi, F., Razavi, K., and Rejali, F. (2017). Brassinosteroid (BR) and arbuscular mycorrhizal (AM) fungi alleviate salinity in wheat. *J. Plant Nutr.* 40, 1091–1098. doi: 10.1080/01904167.2016.1263332

Vardhini, B. V., and Rao, S. S. R. (1999). Effect of brassinosteroids on nodulation and nitrogenase activity in groundnut (*Arachis hypogaea* L.). *Plant Growth Regul.* 28, 165–167.

Weller, J. L., Foo, E. M., Hecht, V., Ridge, S., Vander Schoor, J. K., and Reid, J. B. (2015). Ethylene signaling influences light-regulated development in pea. *Plant Physiol.* 169, 115–124. doi: 10.1104/pp.15.00164

Yang, H., Zhang, Q., Dai, Y., Liu, Q., Tang, J., Bian, X., et al. (2015). Effects of arbuscular mycorrhizal fungi on plant growth depend on root system: a meta-analysis. *Plant Soil* 389, 361–374. doi: 10.1007/s11104-014-2370-8

Yu, N., Luo, D., Zhang, X., Liu, J. J., Wang, W., Jin, Y., et al. (2014). A della protein complex controls the arbuscular mycorrhizal symbiosis in plants. *Cell Res.* 24, 130–133. doi: 10.1038/cr.2013.167

Yusuf, M., Fariduddin, Q., and Ahmad, A. (2012). 24-Epibrassinolide modulates growth, nodulation, antioxidant system, and osmolyte in tolerant and sensitive varieties of *Vigna radiata* under different levels of nickel: a shotgun approach. *Plant Physiol. Biochem.* 57, 143–153. doi: 10.1016/j.plaphy.2012.05.004

Zipfel, C., and Oldroyd, G. E. (2017). Plant signalling in symbiosis and immunity. *Nature* 543, 328–336. doi: 10.1038/nature22009

Conflict of Interest Statement: The authors declare that the research was conducted in the absence of any commercial or financial relationships that could be construed as a potential conflict of interest.

frontiers in Plant Science

ORIGINAL RESEARCH
published: 09 April 2019
doi: 10.3389/fpls.2019.00432

The DELLA Proteins Influence the Expression of Cytokinin Biosynthesis and Response Genes During Nodulation

*Alexandra V. Dolgikh[1], Anna N. Kirienko[1], Igor A. Tikhonovich[1], Eloise Foo[2] and Elena A. Dolgikh[1]**

[1] All-Russia Research Institute for Agricultural Microbiology, St. Petersburg, Russia, [2] School of Natural Sciences, University of Tasmania, Hobart, TAS, Australia

The key event that initiates nodule organogenesis is the perception of bacterial signal molecules, the Nod factors, triggering a complex of responses in epidermal and cortical cells of the root. The Nod factor signaling pathway interacts with plant hormones, including cytokinins and gibberellins. Activation of cytokinin signaling through the homeodomain-containing transcription factors KNOX is essential for nodule formation. The main regulators of gibberellin signaling, the DELLA proteins are also involved in regulation of nodule formation. However, the interaction between the cytokinin and gibberellin signaling pathways is not fully understood. Here, we show in *Pisum sativum* L. that the DELLA proteins can activate the expression of KNOX and BELL transcription factors involved in regulation of cytokinin metabolic and response genes. Consistently, pea *la cry-s* (*della1 della2*) mutant showed reduced ability to upregulate expression of some cytokinin metabolic genes during nodulation. Our results suggest that DELLA proteins may regulate cytokinin metabolism upon nodulation.

Keywords: legume-rhizobium symbiosis, root nodule development, mutants, cytokinins, gibberelllins, crosstalk

OPEN ACCESS

Edited by:
Raul Antonio Sperotto, University of Taquari Valley, Brazil

Reviewed by:
R. J. Neil Emery, Trent University, Canada
Concepción Gómez-Mena, Instituto de Biología Molecular y Celular de Plantas (IBMCP), Spain

****Correspondence:***
Elena A. Dolgikh
dol2helen@yahoo.com

Specialty section:
This article was submitted to Plant Microbe Interactions, a section of the journal Frontiers in Plant Science

Received: *04 December 2018*
Accepted: *21 March 2019*
Published: *09 April 2019*

Citation:
Dolgikh AV, Kirienko AN, Tikhonovich IA, Foo E and Dolgikh EA (2019) The DELLA Proteins Influence the Expression of Cytokinin Biosynthesis and Response Genes During Nodulation. Front. Plant Sci. 10:432. doi: 10.3389/fpls.2019.00432

INTRODUCTION

Most legume plants are able to form symbiosis with nitrogen-fixing bacteria that results in a new organ formation, the nodule. Multiple studies have shown that root nodule formation is regulated by several plant hormones (reviewed by Ferguson and Mathesius, 2014; Gamas et al., 2017). However, the mechanisms of this regulatory network remain poorly understood. The essential role of cytokinins (CKs) in symbiosis development and their interplay with Nod factor-activated symbiotic signaling pathway has been shown. Indeed, in loss-of-function *Ljlhk1* and *Mtcre1* mutants defective in the receptors to CKs, a significant decrease in the number of nodules was found (Gonzalez-Rizzo et al., 2006; Murray et al., 2006; Plet et al., 2011). It was also shown that gain-of-function mutants in genes encoding receptors to CKs have an ability to form spontaneous nodule structures in the absence of compatible bacteria and exogenous application of CKs mimics the effect of Nod factor treatment in root cortex (Cooper and Long, 1994; Tirichine et al., 2007; Heckmann et al., 2011; Ovchinnikova et al., 2011). At the same time it has been found that CKs can play both positive and negative

Abbreviations: *IPT*, isopentenyl transferase; *LOG*, lonely guy; qRT-PCR, quantitative reverse transcription PCR; *RR*, response regulator; Y2H, yeast two hybrid system.

role in symbiosis depending on place, time and surrounding phytohormonal network (Gamas et al., 2017). This means that CK-activated signaling must be tightly regulated during nodulation and may interact with other phytohormonal signaling pathways during nodulation.

The gibberellins (GAs) are well-known phytohormones control many aspects of plant growth and development (Brian, 1959; Harberd et al., 1998). GAs have also been shown to play an important role during nodulation. Indeed, application and genetic studies indicate GAs can have both positive and negative effects of the number of nodules formed (e.g., Ferguson, 2005, Ferguson et al., 2011; Maekawa et al., 2009; Fonouni-Farde et al., 2016; Jin et al., 2016; McAdam et al., 2018). Like CKs, GAs appear to act at various stages of infection and nodule development (McAdam et al., 2018). Considering the functions of GAs and CKs it is possible these hormones interact to influence nodule initiation and development.

The active forms of GAs are perceived by the GID1 (GA insensitive dwarf1) receptor that in turn binds to and activates the degradation of DELLA proteins, via 26S proteasome (Alvey and Harberd, 2005; Achard et al., 2006, 2007; Navarro et al., 2008). The DELLAs are transcriptional regulators that repress GA responses and thus the DELLA may be considered as negative regulators of GA-signaling (Sun, 2010; Hedden and Thomas, 2012). As a consequence, the level of DELLA proteins can be changed depending on different external and internal factors (Davière and Achard, 2013; Park et al., 2013). Indeed, DELLA proteins may mediate crosstalk with other hormonal signaling pathways, coordinating the plants growth with responses to various stimuli (Floss et al., 2016; Fonouni-Farde et al., 2017).

It is known that DELLA proteins do not have DNA-binding domain and their regulatory ability is based on the interaction with different transcription factors, whose activity can be stimulated or inhibited in such interactions (Sun and Gubler, 2004; Fleet and Sun, 2005). Previous studies in legume plants have shown that DELLA proteins may interact with some transcriptional regulators in Nod factor-activated signaling pathway and modulate their function (Floss et al., 2016; Fonouni-Farde et al., 2016; Jin et al., 2016). Indeed, an important role for DELLA proteins in nodulation is supported by low infection and nodule number observed in *della* mutants or loss-of-function transgenics across legume species (Fonouni-Farde et al., 2016; Jin et al., 2016; McAdam et al., 2018). This may be mediated by physical interaction of the DELLA proteins with key components of the Nod factor signaling pathway including IPD3/CYCLOPS, NSP2 and NF-YA1 (Fonouni-Farde et al., 2016; Jin et al., 2016). However, it is important to note that a positive role for GA in nodule organogenesis has also been reported, as severley GA-deficient mutants of pea form many infections but few nodules that are poorly developed (McAdam et al., 2018). In contrast, the few nodules that form on *della* mutants of pea and Medicago appear to be normal size and at least in pea have been shown to have similar function to wild type (McAdam et al., 2018).

In order to find possible mechanisms of interplay between GA- and CK-signaling pathways, we have examined how the main regulators of the GA-signaling, the DELLA proteins, may influence KNOTTED1-LIKE HOMEOBOX (KNOX) and BEL1-LIKE HOMEODOMAIN (BELL) transcription factors involved in control of CKs and GAs levels in plants. Plant KNOX and BELL proteins are transcription factors that belong to the three-amino-acid-loop-extension (TALE) superfamily (Byrne et al., 2003; Smith and Hake, 2003; Bao et al., 2004; Sharma et al., 2014). These transcription factors interact as heterodimeric complexes to regulate transcription of target genes (Bellaoui et al., 2001; Chen et al., 2004; Hake et al., 2004; Lin et al., 2013). It is known that KNOX transcription factors may control the levels of CKs and GAs via direct regulating of CK biosynthesis *IPT* gene (Yanai et al., 2005) as well as GA metabolic genes, such as *GA 20-OXIDASE* (*GA20ox*) and *GA 2-OXIDASE* (*GA2ox*) in shoot apical meristem (Jasinski et al., 2005). Moreover, we have recently reported that KNOX3 transcription factor may promote the expression of some *IPT* and *LOG* genes during symbiosis development in legume plants *M. truncatula* and pea *Pisum sativum* L. (Azarakhsh et al., 2015). Recent study has also revealed that GA signaling mediated by *Mt*DELLA1 decreases the amount of the free base CK content in roots of *M. truncatula* (Fonouni-Farde et al., 2017). However, the interaction between CKs and GAs during nodulation is still not known and the mechanisms of DELLAs' impact on CKs status remain poorly understood.

Here we used the pea *La cry-s* (*DELLA1 della2*) and *la cry-s (della1 della2*) mutants to examine the effects of DELLA proteins on KNOX and BELL transcription factors. We have found that the up-regulation of expression of some *PsKNOX* and *PsBELL* genes seen in wild type was reduced in double *la cry-s* (*della1 della2*) mutant during initial and later stages of nodulation. Pea *la cry-s* (*della1 della2*) mutants also showed reduced capacity to elevate expression of the CK metabolic and signaling genes during nodulation compared to wild type. Therefore, *Ps*DELLA proteins may be involved in regulation of the CK metabolism during nodulation. To test if this action of DELLA was via KNOX and BELL transcription factors, the Y2H studies were undertaken but did not reveal a strong direct interaction between *Ps*DELLA1 and *Ps*KNOX3 or *Ps*BELL1. Therefore, *Ps*DELLA1 may promote the expression *PsKNOX3* and *PsBELL1* and their target CK metabolic and signaling genes indirectly through other known transcription factors and we begin to examine the role of *Ps*IPD3/CYCLOPS.

MATERIALS AND METHODS

Bacterial Strains and Inoculation

Inoculation of the pea plants was conducted with the *Rhizobium leguminosarum* biovar *viciae* wild type strain 3841. Bacterial liquid culture was grown in B^- medium (van Brussel et al., 1977), diluted upto the optical density at 600 nm (OD_{600}) 0.5 and applied to plants at 2 day after planting.

Plant Material and Growth Conditions

The pea *Pisum sativum* L. *La cry* mutant lines and line segregating *la cry* carrying the mutations in *della1* and *della2* genes were generated as described by Weston et al. (2008) and wild type line is cv. Torsdag. Wild type SGE line and two derived mutants SGEFix$^-$−2 and SGEFix$^-$−5 [*ipd3*/*cyclops* (*sym33*)] were also used in this study. Gene expression experiments were carried out with seeds sterilized with sulphuric acid for 5 min, washed 3 times with water, transferred on 1% water agar plates and germinated at room temperature in the dark. 4–5 days-old plant seedlings were transferred into pots with vermiculite saturated with Jensen medium (van Brussel et al., 1982), grown in a growth chamber at 21°C at 16 h light/8 h dark cycles, 60% humidity. Fragments of main roots (responsive zone starting from 5 to 6 mm from the root tip) or fragments of main roots with primordia/nodules were collected at 2, 9, and 14 days after inoculation (2, 9, and 14 dai). Fragments of non-inoculated main roots were collected at the same developmental stages. Plant material for gene expression studies was immediately immersed in liquid nitrogen and stored in −80°C freezer.

RNA Extraction, cDNA Synthesis, and Quantitative PCR

Plant material was ground with a mortar and pestle to a fine powder in liquid nitrogen. Approximately 50–100 mg of ground tissue was used for RNA extraction, as previously described (Dolgikh et al., 2017). 1–2.5 μg of total RNA was used to synthesize cDNA with the RevertAid Reverse Transcriptase (Thermo Fisher Scientific, United States). cDNA samples were diluted to a total volume of 200 μl. For gene expression quantification, the following primer pairs were used (**Supplementary Table S1**). All primers were acquired from Evrogen company[1]. 2 μl of cDNA was used for quantitative real-time PCR using Bio-Rad iQ Sybr master mix (Bio-Rad Laboratories, United States) following the manufacturer's recommendations and run on a CFX-96 real-time PCR detection system with C1000 thermal cycler (Bio-Rad Laboratories). All reactions were done in triplicate and averaged. Cycle threshold (Ct) values were obtained using the accompanying software and data were analyzed according to the $2^{-\Delta\Delta Ct}$ method (Livak and Schmittgen, 2001). All primer pairs (**Supplementary Table S2**) were designed using the Vector NTI program and produced by Evrogen[2]. The gene expression was normalized against the constitutively expressed ubiquitin gene in pea.The gene expression in experiments with wild type and mutants was determined with several biological samples (n = 4–8 plants). For temporal *BELL1* gene expression, each replicate contained tissue of 3–4 plants and experiment was repeated three times.

Cloning of *PsDELLA1*, *PsKNOX3*, and *PsBELL1* for Yeast Transformation

Full-length *PsDELLA1*, *PsKNOX3*, and *PsBELL1* coding sequences were obtained by amplification of cDNA cv. Finale or cv. Sparkle using specific PCR primer pairs flanking with attB1 and attB2 sequences or CACC in forward primer (**Supplementary Table S2**) for subsequent cloning in pDONR221 or pENTRY-TOPO vectors (Thermo Fisher scientific, United States) according to manufacturer's protocol.

[1]www.evrogen.com

[2]http://www.evrogen.com

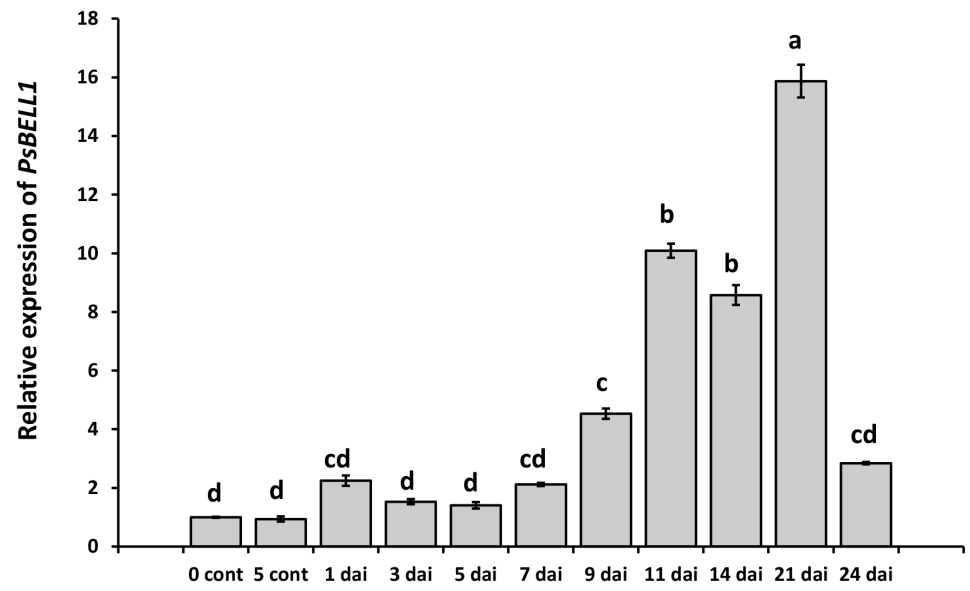

FIGURE 1 | Analysis of *PsBELL1* expression at the various stages of symbiosis development in cv. Torsdag. The roots of non-inoculated plants (NI) have been used as a control. The relative expression was normalized against the constitutively expressed ubiquitin and actin genes. Data are averages ± SEM of three technical repeats. The graphs show the results of one biological experiment, representative for three independent experiments. Values with different letters are significantly different ($P < 0.05$) as analyzed by one-way ANOVA and the Tukey's test as *post-hoc* analysis.

At the next stage they were finally subcloned into the destination vectors pDEST22 (PREY) or pDEST32 (BAIT) vectors using the LR clonase enzyme (Thermo Fisher scientific). All verified constructs were transferred into MaV203 yeast strain (Thermo Fisher scientific).

Full-length *PsNSP2* and *PsIPD3*/*CYCLOPS* coding sequences or partial coding sequences upto stop-codon corresponding to those in RisNod14, E69 *nsp2* (*sym7*) or SGEFix$^-$−5 [*ipd3/cyclops* (*sym33*)] mutants were obtained by amplification of cDNA cv. Finale or Sparkle using specific PCR primer pairs flanking with attB1 and attB2 sequences followed by cloning into pDEST22 (PREY) or pDEST32 (BAIT) vectors.

Yeast Two-Hybrid Assay (GAL4 Transcription Factor-Based Assay)

The *S. cerevisiae* strain MaV203 (Thermo Fisher scientific) was transformed simultaneously with pDEST22 and pDEST32 vectors for GAL4 based selection. To transform the *S. cerevisiae* MaV203, the protocol for preparation of chemically competent cells was used (Thermo Fisher scientific). A few pairs of vectors (pEXP32/Krev1 and pEXP22/RalGDS-wild type, pEXP22/RalGDS-m1 and pEXP22/RalGDS-m2) suggested by the manufacturer as controls were used for strong, weak and not detectable interactions. Analysis of interaction was conducted on selective media like SC –LT (without leucine and tryptophan), SC –LTH + 3AT (without leucine, tryptophan and histidine plus 3-amino-1,2,4-triazole, SC –LTU (without leucine, tryptophan and uracil).

Statistical Methods and Computer Software

Multiple alignment of nucleotide sequences was performed using Clustal W (Thompson et al., 1994) using Vector NTI Advance 10 (InforMax[3]). MEGA6 was used to generate graphic output of phylogenetic tree (Hall, 2013). One-way ANOVA and Tukey's test were used to compare gene expression levels.

RESULTS

Transcription Levels of *PsKNOX* and *PsBELL* Genes in Pea *La cry-s* (*DELLA1 della2*) and *la cry-s* (*della1 della2*) Mutants

Previously nine *PsKNOX* genes were identified in pea *P. sativum* L. (Hofer et al., 2001; Zhou et al., 2014; Azarakhsh et al., 2015). Their expression pattern was estimated during nodulation and showed stimulation of *PsKNOX3*, *PsKNOX5*, *PsKNOX9*, and *PsKNOX10* genes upon nodule development starting from 7 to 9 days after inoculation (7–9 dai) (Azarakhsh et al., 2015).

The screening of Mt4.0v1 database for model legume *M. truncatula* allowed identifying eleven *MtBELL* genes and eleven homologous genes have been found in pea database[4] (**Supplementary Table S1** and **Figure S1**). Expression atlas showed that at least one gene PsCam048179 (*PsBELL1*, the closest homologue of Medtr8g078480) is significantly induced in the nodules compared to roots. Indeed, in our experiments the enhanced level of *PsBELL1* has been revealed during nodulation in wild type pea plants of cv. Torsdag (**Figure 1**). In addition, analysis of transcriptome data for model legume *M. truncatula* showed the activation of some *MtKNOX* and *MtBELL* genes in roots in response to Nod factor treatment (van Zeijl et al., 2015; Jardinaud et al., 2016). It suggests that KNOX and BELL transcription factors may be also involved in regulation of early stages of symbiosis development in legumes.

To investigate whether the *Ps*DELLA proteins are involved in regulation of *Ps*KNOX3, *Ps*KNOX5, *Ps*KNOX9, *Ps*KNOX10, and *Ps*BELL1 transcription factors, the transcription levels of corresponding genes have been analyzed in *LA cry-s* (*DELLA1 della2*) and *la cry-s* (*della1 della2*) mutants in response to inoculation using real-time PCR. The *La cry-s* (*DELLA1 della2*) single mutant after inoculation with *R. leguminosarum* bv. *viciae* showed a nodulation phenotype that did not differ from that of the wild-type, however, the *la cry-s* (*della1 della2*) double mutant formed fewer nodules relative to the wild-type but the nodules that formed on mutant plants appeared be functional and to fix similar amount of nitrogen per gram nodule weight (Ferguson et al., 2011; McAdam et al., 2018).

At the early stages of symbiosis development the stimulation of two pea *PsKNOX* and *PsBELL* genes, the *PsKNOX9* and *PsBELL1*, was revealed in wild type and *LA cry-s* (*DELLA1 della2*) mutant roots in response to inoculation (2 dai) (**Figure 2**). In contrast, analysis of mutants showed the *PsKNOX9* and *PsBELL1* expression was not significantly elevated in inoculated *la cry-s* (*della1 della2*) mutant (**Figure 2**). This suggests that *PsKNOX9* and *PsBELL1* may be involved in the control of early steps of symbiosis in pea and the *Ps*DELLA1 and *Ps*DELLA2 proteins may directly or indirectly influence their activation. Since the effect was more pronounced, when both *della1 della2* genes were impaired, it may indicate that the PsDELLA1 could play a more significant role in symbiosis regulation. At the same time it also could be connected with the functional redundancy of *Ps*DELLA1 and *Ps*DELLA2 proteins in pea.

To verify the impact of DELLA proteins on later stages of nodulation, which includes infection thread formation and growth, nodule primordia initiation and development, we have performed the analysis with wild type and mutants in 9 and 14 dai (**Figures 3**, **4**). As previously reported (Azarakhsh et al., 2015), it was also found that *PsKNOX3*, *PsKNOX5*, *PsKNOX9*, and *PsKNOX10* expression was upregulated in wild type pea plants in the process of nodulation. In contrast to wild type, there was only little increase in *PsKNOX3* and *PsKNOX9* expression in *la cry-s* (*della1 della2*) mutant in 9 and 14 dai, while the *PsKNOX5* showed a moderate up-regulation in double *la cry-s* (*della1 della2*) mutant in 14 dai (**Figures 3**, **4**). At the same time, the up-regulation of *PsKNOX10* expression seen in wild type plants 14 dai was also observed in *la cry-s* (*della1 della2*) mutants (**Figure 4**). Therefore, our study identified *PsKNOX3* and *PsKNOX9* transcription as potentially regulated by *Ps*DELLA1 and *Ps*DELLA2 proteins

[3]http://www.informaxinc.com

[4]http://bios.dijon.inra.fr

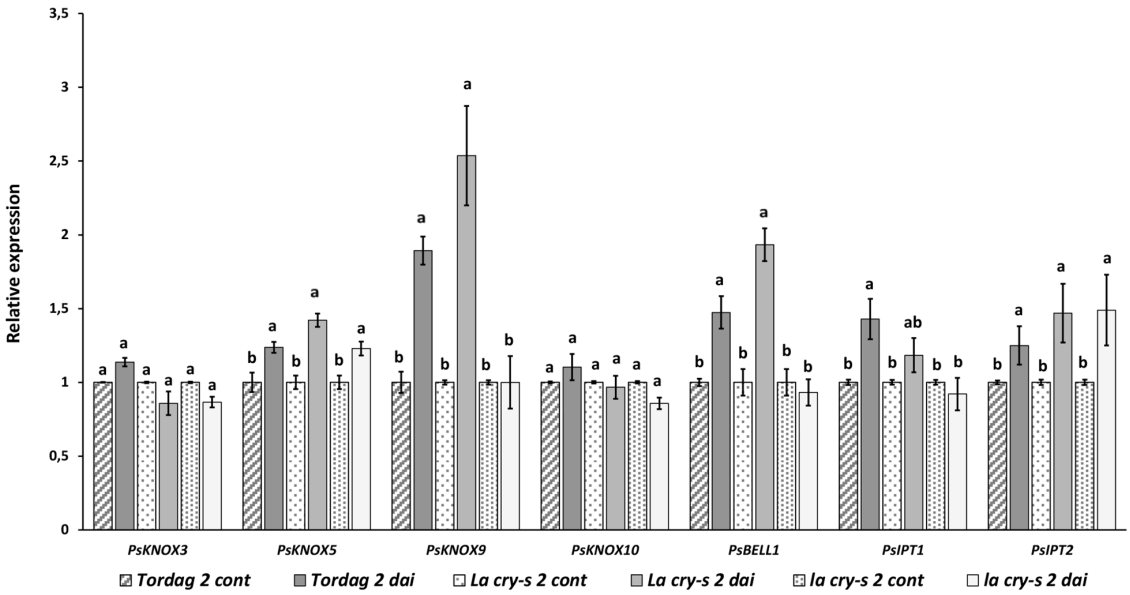

FIGURE 2 | Expression levels of *PsKNOX* and *PsBELL* genes and cytokinin metabolic genes in pea wild type cv. Torsdag and *LA cry-s* (*DELLA1 della2*), *la cry-s* (*della1 della2*) mutants in 2 days after inoculation (2 dai). The expression was normalized against the constitutively expressed ubiquitin gene. For each gene, the transcript level in non-inoculated roots of wild type or mutants was set to 1 (control), and the level in inoculated wild type or mutants was calculated relative to the control values. Data are averages ± SEM (n = 5–6 plants of wild type or mutant combined from two independent experiments). Values with different letters are significantly different ($P < 0.05$) as analyzed by one-way ANOVA and the Tukey's test as *post-hoc* analysis.

in pea *P. sativum* L. during nodulation. The *Ps*DELLA1 and *Ps*DELLA2 proteins may also be involved in an additional stimulation of the *PsKNOX5* expression in pea plants. Similarly, the significant upregulation in the expression of *PsBELL1* seen 9 and 14 dai in wild type was not significantly elevated in *la cry-s* (*della1 della2*) mutant in response to inoculation (**Figures 3**, **4**). It suggests that *Ps*DELLA1 and *Ps*DELLA2 proteins may also promote the expression of *PsBELL1* gene in pea.

Regulation of *PsLOG* and *PsIPT* Genes in Pea *LA cry* and *la cry* Mutants

It was shown that expression of some *PsLOG* and *PsIPT* genes may depend on the *Ps*KNOX3 transcription factor in pea (Azarakhsh et al., 2015). To investigate a possible link between regulation of transcription factors by DELLA and possible targets of KNOX transcription factors, we have examined the *PsLOG1*, *PsLOG2*, *PsIPT1*, *PsIPT2*, *PsIPT3*, and *PsIPT4* (all of them encode enzymes that belong to adenosine phosphate-IPTs) expression in *LA cry* and *la cry* mutants during nodulation (2, 9, and 14 dai) (**Figures 3**, **4**), because their up-regulation was shown upon nodulation in pea (Azarakhsh et al., 2015; Dolgikh et al., 2017). However, as the level of *IPT3* was very low in cv. Torsdag and both mutants it was not included in the analysis. In addition, we have also analyzed the transcription levels of the cytokinin-responsive *PsRR11* gene, which is most significantly activated in pea root in response to inoculation in comparison with other *PsRRs* like *PsRR4*, *PsRR5*, *PsRR8*, and *PsRR9* (Dolgikh et al., 2017).

Early stages of symbiosis development may be connected with stimulation of *PsIPT1* (the closest homolog of Medtr4g117330) and *PsIPT2* (the closest homolog of Medtr2g022140) genes in pea (Dolgikh et al., 2017). However, we did not find essential differences in expression of these genes between wild type cv. Torsdag and *LA cry* and *la cry* mutants in 2 dai (**Figure 2**). As it was shown previously, up-regulation of the *PsLOG1*, *PsLOG2* and *PsIPT1*, *PsIPT3* and *PsIPT4* genes involved in CK biosynthesis may take place at later stages of symbiosis development (Azarakhsh et al., 2015; Dolgikh et al., 2017). Our experiments showed that in contrast to stimulation in cv. Tosdag (wild type), the upregulation in expression of the *PsLOG1*, *PsLOG2* genes and cytokinin-responsive *PsRR11* genes observed in wild type plants was not observed in the double mutant *la cry* at 9 and 14 dai, suggesting that *Ps*DELLA1 and *Ps*DELLA2 proteins might be required for this upregulation. The pattern expression of *PsIPT1* and *PsIPT4* (the closest homolog of Medtr1g110590) expression in response to inoculation was similar in wild type, *LA cry* and *la cry* mutants in 9 and 14 dai (**Figure 4**), suggesting *Ps*DELLA is not essential for the regulation of these genes. A lack of correlation between the change in expression of *PsKNOX3* gene and the *PsIPT4* gene was previously shown in our experiments (Azarakhsh et al., 2015).

DELLA Proteins Are Able to Regulate GA Metabolic Genes

It was previously suggested that *Ps*DELLA1 and *Ps*DELLA2 proteins may regulate GA metabolism modulating the expression of corresponding genes in pea (Weston et al., 2008). Indeed,

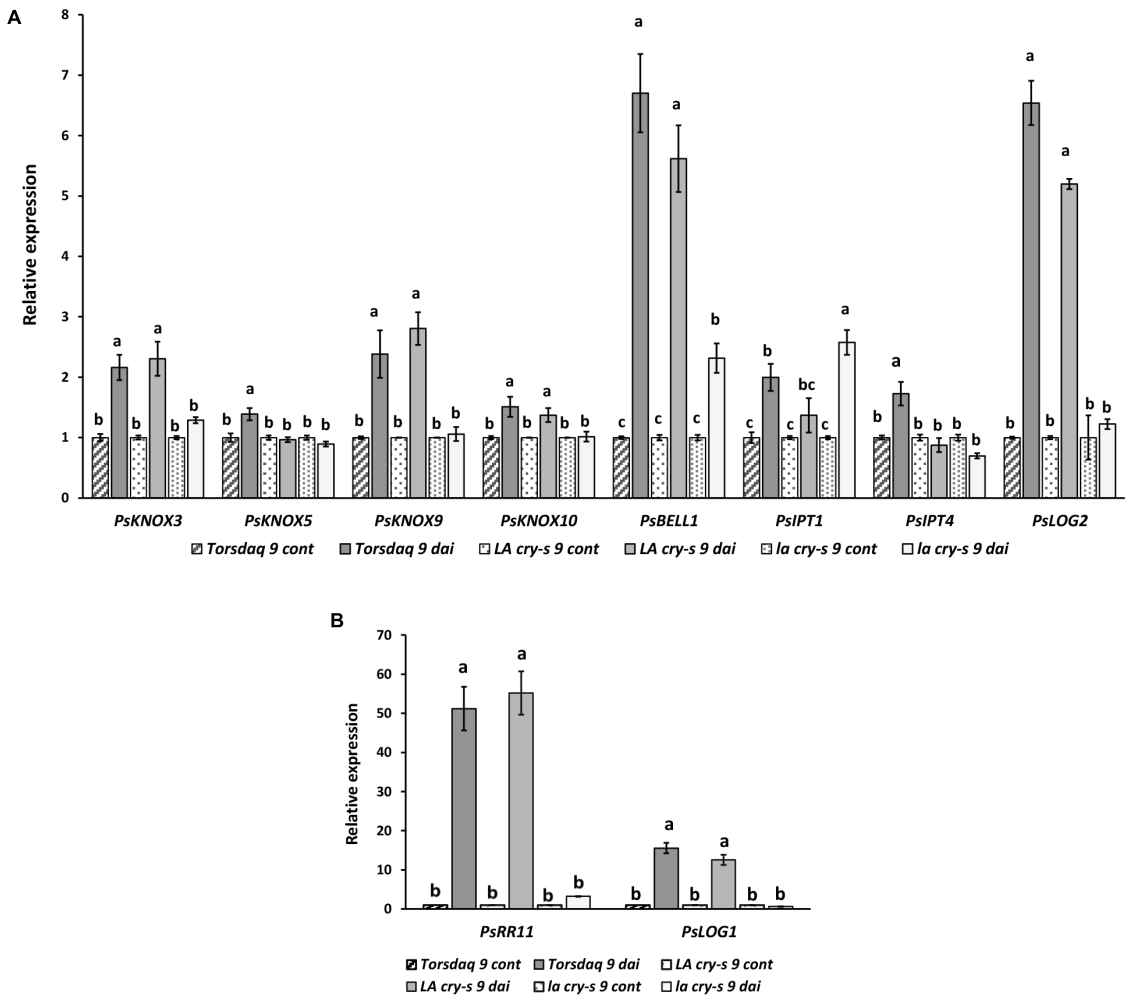

FIGURE 3 | Expression levels of *PsKNOX* and *PsBELL* genes and cytokinin metabolic and response genes in pea wild type cv. Torsdag and *LA cry-s* (*DELLA1 della2*), *la cry-s* (*della1 della2*) mutants in comparison with inoculated wild type in 9 days after inoculation (9 dai). The expression was normalized against the constitutively expressed ubiquitin gene. Panels **A** and **B** represent genes with various level of expression. For each gene, the transcript level in non-inoculated roots of wild type or mutants was set to 1 (control), and the level in inoculated wild type or mutants was calculated relative to the control values. Data are averages ± SEM (n = 6–8 plants of wild type or mutant combined from three independent experiments). Values with different letters are significantly different ($P < 0.05$) as analyzed by one-way ANOVA and the Tukey's test as *post-hoc* analysis.

a significant reduction of expression of GA biosynthesis (*PsGA20ox1*) gene, but stimulation of GA deactivation (*PsGA2ox1*) gene were found in non-inoculated roots of 6 days-old seedlings of *la cry-s* mutant compared with wild type (Weston et al., 2008). To estimate the expression dynamics of GA metabolic genes during nodulation, the transcription levels of the *PsGA20ox1* and *PsGA2ox1* genes have been measured in wild type and *la cry-s* mutant in 2, 9, and 14 dai using real-time PCR (**Figure 5**). We found a strong reduction in expression of the GA biosynthesis gene *PsGA20ox1* at all stages in *la cry-s* mutant compared to wild type, but the most significant differences were found at early stages (2 and 9 dai). At the same time in *la cry-s* a strong stimulation of the GA deactivation gene *PsGA2ox1* was found starting from 2 dai and reaching the highest level at 9 dai. This suggests that significant changes in GA metabolism may take place at initial stages of symbiosis development. It could not be excluded that the DELLA proteins are involved in this regulation, since previous studies have shown an important role of DELLA proteins in establishment of GA homeostasis (Zentella et al., 2007).

Analysis of *Ps*DELLA1 Protein Interaction With *Ps*KNOX3, *Ps*BELL1 in Yeast Two-Hybrid System (Y2H)

To determine a possible interaction between pea DELLA1 protein and the KNOX and BELL transcription factors, we performed a yeast two-hybrid (Y2H) assay with the fusion proteins. Since the most significant role may play *Ps*KNOX3 and *Ps*BELL1 transcription factors, the analysis was performed with *Ps*DELLA1-GAL4-DNA-binding domain (*Ps*DELLA1-GAL4-DBD) and *Ps*KNOX3-GAL4 activation

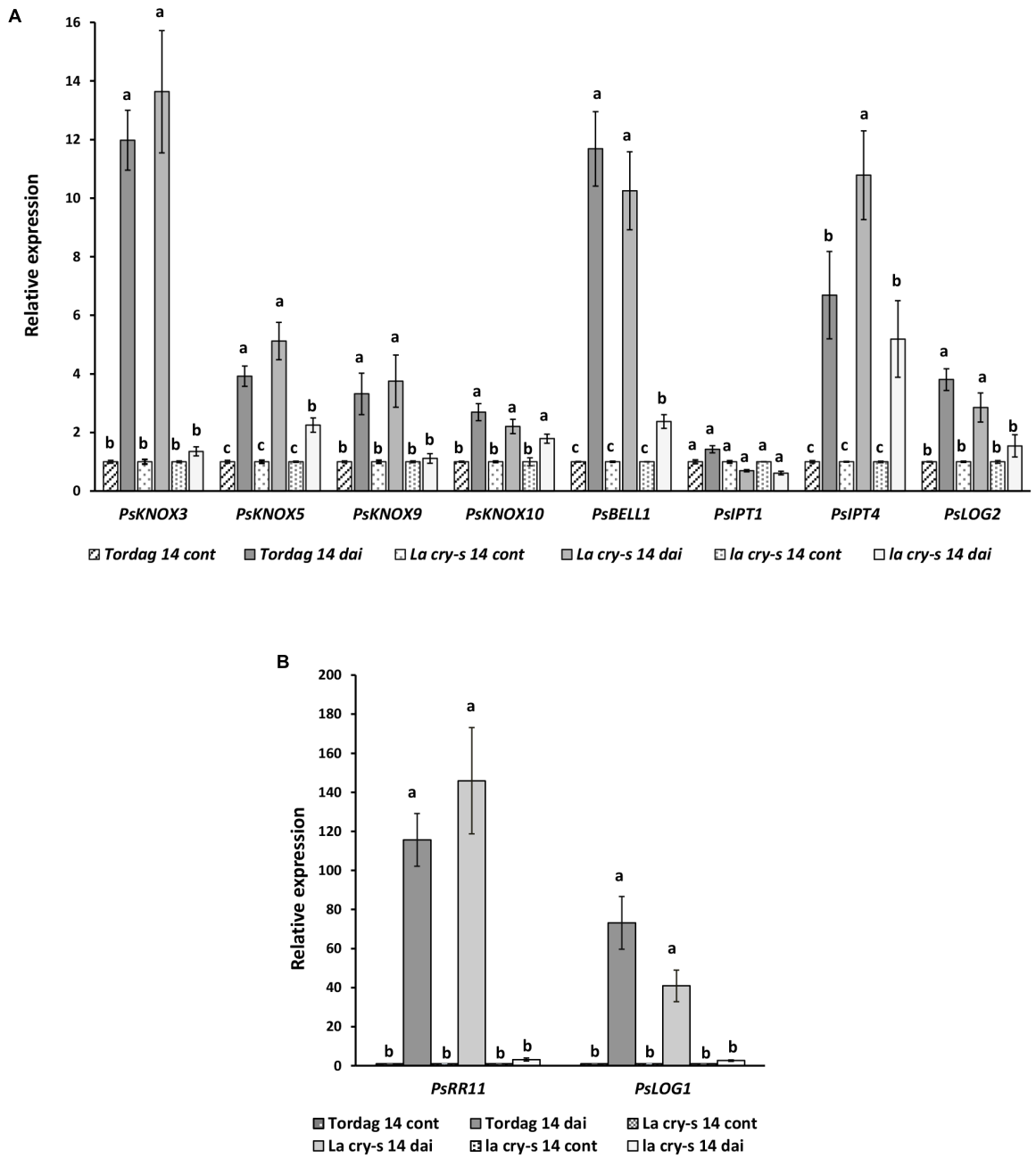

FIGURE 4 | Expression levels of *PsKNOX* and *PsBELL* genes and cytokinin metabolic genes in pea wild type cv. Torsdag and *LA cry-s* (*DELLA1 della2*), *la cry-s* (*della1 della2*) mutants in comparison with inoculated wild type in 14 days after inoculation (14 dai). Panels **A** and **B** represent genes with various level of expression. For each gene, the transcript level in non-inoculated roots of wild type or mutants was set to 1 (control), and the level in inoculated wild type or mutants was calculated relative to the control values. Data are averages ± SEM (n = 4–6 plants of wild type or mutant combined from two independent experiments). Values with different letters are significantly different ($P < 0.05$) as analyzed by one-way ANOVA and the Tukey's test as *post-hoc* analysis.

domain (*Ps*KNOX3-GAL4-AD) as well as *Ps*BELL1-GAL4 activation domain (*Ps*BELL1-GAL4-AD).

Previously the capacity of DELLA proteins to promote CCaMK–IPD3/CYCLOPS and NSP2–NSP1 complexes formation was shown for model legumes *Lotus japonicus* and *M. truncatula* (Fonouni-Farde et al., 2016; Jin et al., 2016). To verify our results, we have also performed the analysis for *Ps*DELLA1-GAL4-DNA-binding domain (*Ps*DELLA1-GAL4-DBD) and *Ps*NSP2-GAL4 activation domain (*Ps*NSP2-GAL4-AD), *Ps*IPD3/CYCLOPS-GAL4 activation domain (*Ps*IPD3/CYCLOPS-GAL4-AD). Indeed, the analysis of yeast growth on selection media showed that *Ps*DELLA1 was able to form complex with *Ps*NSP2 (SYM7) as well as *Ps*IPD3/CYCLOPS (SYM33) in Y2H (**Figures 6**, **7**). These

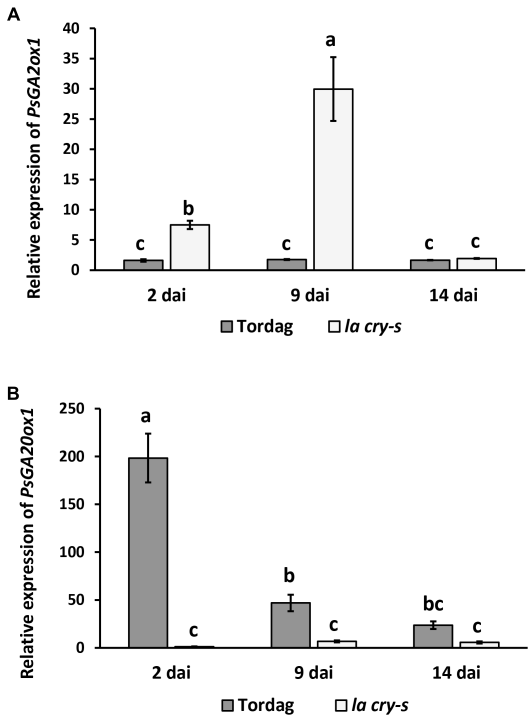

FIGURE 5 | *PsGA2ox1* **(A)** and *PsGA20ox1* **(B)** gene expression in roots of wild-type cv. Torsdag and *la cry-s* (*della1 della 2*) mutant plants inoculated by *R. leguminosarum bv. viciae* 3841 in 14 dai. For each gene, the transcript level in non-inoculated roots of wild type or mutants was set to 1 (control), and the level in inoculated wild type or mutants was calculated relative to the control values. Finally, the expression in wild type was presented relative to the level in mutant. Data are averages ± SEM (n = 4–8 plants of wild type or mutant combined from two-three independent experiments). Values with different letters are significantly different ($P < 0.05$) as analyzed by one-way ANOVA and the Tukey's test as *post-hoc* analysis.

results were in accordance with results for *L. japonicus* and *M. truncatula*.

At the same time we did not reveal a strong interaction between *Ps*DELLA1 and *Ps*KNOX3, *Ps*DELLA1 and *Ps*BELL1 in this system (**Figure 6**). This conclusion can be made on the basis of the growth of MaV203 yeast cells producing both *Ps*DELLA1-GAL4-DBD and *Ps*KNOX3-GAL4-AD, as well as *Ps*DELLA1-GAL4-DBD and *Ps*BELL1-GAL4-AD on SC –LTH + 50 mM 3 AT, but not on SC – LTU. Therefore, we have not received the evidences of a strong direct interaction between *Ps*DELLA1 and *Ps*KNOX3 or *Ps*BELL1 proteins.

The Interplay Between DELLA, KNOX3, and IPD3/CYCLOPS Regulators

Since DELLA appeared to be important in the regulation of *PsKNOX3* and *PsBELL1* expression in our experiments, we suggested that other transcription factors may be involved in transactivation of *PsKNOX3* and *PsBELL1* in pea. Among of them, the *Ps*NSP2 and *Ps*IPD3/CYCLOPS transcription factors are the most probable candidates for indirect activation of *PsKNOX* and *PsBELL* genes. Moreover, the interaction between *Ps*DELLA1 and *Ps*NSP2, *Ps*IPD3/CYCLOPS was shown in our experiments using Y2H system.

Previously a similar effect was found for *Mt*ERN1 transcription factor, which is activated by *Mt*DELLA1 through *Mt*NSP2/*Mt*NSP1 complex formation and binding with promoter of *MtERN1* (Fonouni-Farde et al., 2016). The binding with promoter induced the expression of *MtERN1* and its target the *MtENOD11* gene in *M. truncatula*.

Several pea mutants impaired in *nsp2* (*sym7*) and *ipd3/cyclops* (*sym33*) genes are available. The pea mutants E69 and RisNod14 are impaired in *nsp2* (*sym7*) gene and demonstrates the Nod$^-$ phenotype (Engvild, 1987; Kneen et al., 1994; Walker and Downie, 2000; Tsyganov et al., 2002; Kalo et al., 2005). The pea mutants SGEFix$^-$−2 and SGEFix$^-$−5 are impaired in *ipd3/cyclops* (*sym33*) gene (Fix$^-$ phenotype) and able to form rare nodules which remained uninfected (Tsyganov et al., 1998; Voroshilova et al., 2009).

To check the interaction between *Ps*DELLA1 protein and truncated *Ps*NSP2 proteins corresponding to those in E69 and RisNod14 mutants as well as truncated *Ps*IPD3/CYCLOPS protein corresponding to that in SGEFix$^-$−5 we performed analysis using Y2H system. This revealed that both truncated *Ps*NSP2 proteins were still able to interact with *Ps*DELLA1, but truncated *Ps*IPD3/CYCLOPS failed to interact with *Ps*DELLA1 (**Figure 7**). This demonstrates that interruption of mutual recognition between *Ps*DELLA1 and *Ps*IPD3/CYCLOPS may result in signal transduction failure in *ipd3/cyclops* pea mutant. In case of two *nsp2* (*sym7*) mutants the recognition between *Ps*DELLA1 and *Ps*NSP2 still takes place, but seems like the both truncated *Ps*NSP2 are not able to interact with *Ps*NSP1 or other transcription factors and subsequent signal transduction is blocked.

Similarly, with *la cry-s* (*della1 della2*) mutant, a reduced number of nodules was found in *ipd3/cyclops* (*sym33*) mutants, although the nodules of *ipd3/cyclops* (*sym33*) were not effective (Tsyganov et al., 1998; Ovchinnikova et al., 2011). Taking this into account, we might expect that in *ipd3/cyclops* (*sym33*) mutants the expression of *PsKNOX3* and *PsKNOX9* genes may be misregulated during infection as observed in *la cry-s* (*della1 della2*) mutant. To check this, we analyzed the expression of *PsKNOX3*, *PsKNOX5*, *PsKNOX9*, *PsKNOX10*, and *PsBELL1* in roots bearing nodules (14 dai) from pea mutants SGEFix$^-$−5 and SGEFix$^-$−2 [*ipd3/cyclops* (*sym33*)]. Indeed, the SGEFix$^-$−5 and SGEFix$^-$−2 [*ipd3/cyclops* (*sym33*)] did not upregulated the expression of these genes as significantly as found in wild type plants (**Figure 8**). Our results suggest that the induction of *PsKNOX3*, *PsKNOX9*, and *PsBELL1* expression may require DELLA-dependent activation and analysis of *ipd3/cyclops* (*sym33*) mutants suggests this may be via interaction with *Ps*IPD3/CYCLOPS transcription factor. In addition, a reduced transcription level of the GA biosynthesis gene *PsGA20ox1* was found in *ipd3/cyclops* (*sym33*) mutants compared to wild type in 14 dai using real-time PCR. Decreased level of *PsGA20ox1* expression in *della1 della2* and *ipd3/cyclops* (*sym33*) mutants may reflect the importance of GA for nodule development in pea. Upregulation of GA metabolic genes may be also connected with activation of *Ps*KNOX and *Ps*BELL transcription factors.

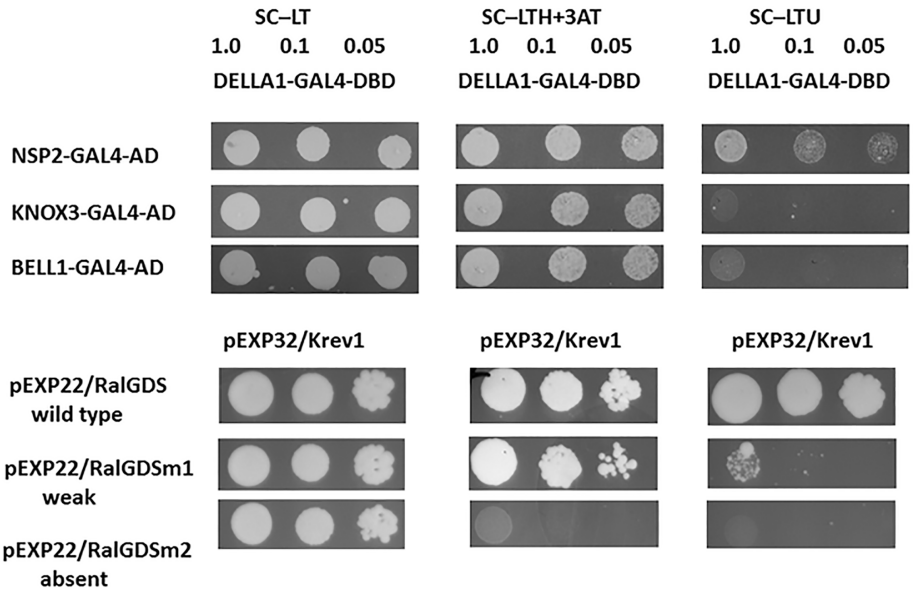

FIGURE 6 | Yeast two-hybrid assay (GAL4 transcription factor-based) for DELLA1 protein and KNOX3 and BELL1 transcription factors. The *S. cerevisiae* strain MaV203 was transformed simultaneously with pDEST22 and pDEST32 vectors for GAL4 activation domain (AD) or GAL4 DNA binding domain (DBD). The pairs of vectors pEXP32/Krev1 and pEXP22/RalGDS-wild type, pEXP22/RalGDS-m1 and pEXP22/RalGDS-m2 were used for strong, weak and not detectable interactions. Yeast growth was tested on SC medium without leucine, tryptophan and histidine with 3-amino-triazole (SC –LTH + 50 mM 3 AT) and SC without leucine, tryptophan and uracil (SC – LTU).

DISCUSSION

Multiple studies have shown an important role of CKs in regulation of infection process and nodule organogenesis during legume-rhizobial symbiosis. In addition to CKs, the GAs also have a strong impact on symbiosis development. Indeed, transcriptome analyses revealed the substantial alterations in the expression of genes encoding enzymes of CK and GA biosynthesis and degradation during symbiosis initiation and development in legume plants (Breakspear et al., 2014; van Zeijl et al., 2015; Jardinaud et al., 2016). The antagonistic relationships between CKs and GAs were shown in many developmental processes and were also described in nodulation in *M. truncatula* and *L. japonicus* (Maekawa et al., 2009; Jin et al., 2016). It was shown that the number of spontaneous nodules induced by overexpression of *LjLHK1*/*MtCRE1* genes encoding the receptor to CKs was decreased upon the addition of GAs (Maekawa et al., 2009; Jin et al., 2016). This effect was depended on DELLA proteins, suggesting that DELLAs were required for spontaneous nodule formation induced by CKs, but GAs inhibited this process.

Recent study has also revealed that GA pretreatment reduced the Nod factor-induced CK primary response in the epidermis and in the outer cortex in *M. truncatula* as well as CK response gene expression, the *MtRRA8*, *MtRRA9*, *MtRRA11* (Fonouni-Farde et al., 2017). It has been also shown that pretreatment with GAs may decrease the amount of some pools of bioactive CKs in roots in *M. truncatula* (Fonouni-Farde et al., 2017).

Indeed, exogenous GAs has a negative effect on the number of nodules in *M. truncatula* and *L. japonicus* and this was also seen at high concentrations of GA in pea (Ferguson, 2005; Maekawa et al., 2009; Fonouni-Farde et al., 2016; Jin et al., 2016). However, at lower concetrations GA actually enhanced nodule number in pea and Sesbania (Ferguson, 2005; Lievens et al., 2005). This indicates a more complicated role for GAs during nodulation. While this apparent paradox may be explained by stating that there is an optimal level of GAs for nodulation overall, this may in fact be due to GAs exerting different effects on specific stages of nodulation, inhibiting infection but promoting nodule organogenesis (Ferguson, 2005; Ferguson et al., 2011; McAdam et al., 2018). This is similar to the dual role proposed for CKs during nodulation (Gamas et al., 2017).

This regulation could be achieved by interaction between DELLA proteins and plant regulators controlling the content of CKs and GAs in plants. Since the participation of KNOX and BELL transcription factors in regulation of CK and GA metabolic genes is well-known for plants, the pea *la cry-s* (*della1 della2*) mutants have been used to examine the effect of these proteins on the expression of *PsKNOX* and *PsBELL* genes during nodulation. Indeed, we showed failure to upregulate the expression of *PsKNOX9* and *PsBELL1* genes at early stages of symbiosis development in inoculated roots of pea *la cry-s* (*della1 della2*) mutant. Although we did not find a definite correlation between *Ps*DELLAs function and regulation of some *PsIPT* genes at early stages, but influence on other CK metabolic genes could not be excluded. Recently the involvement of GAs in stimulation of CKs degradation via cytokinin oxidase *Mt*CKX3 has been revealed in *M. truncatula* (Fonouni-Farde et al., 2017). An alternative explanation might

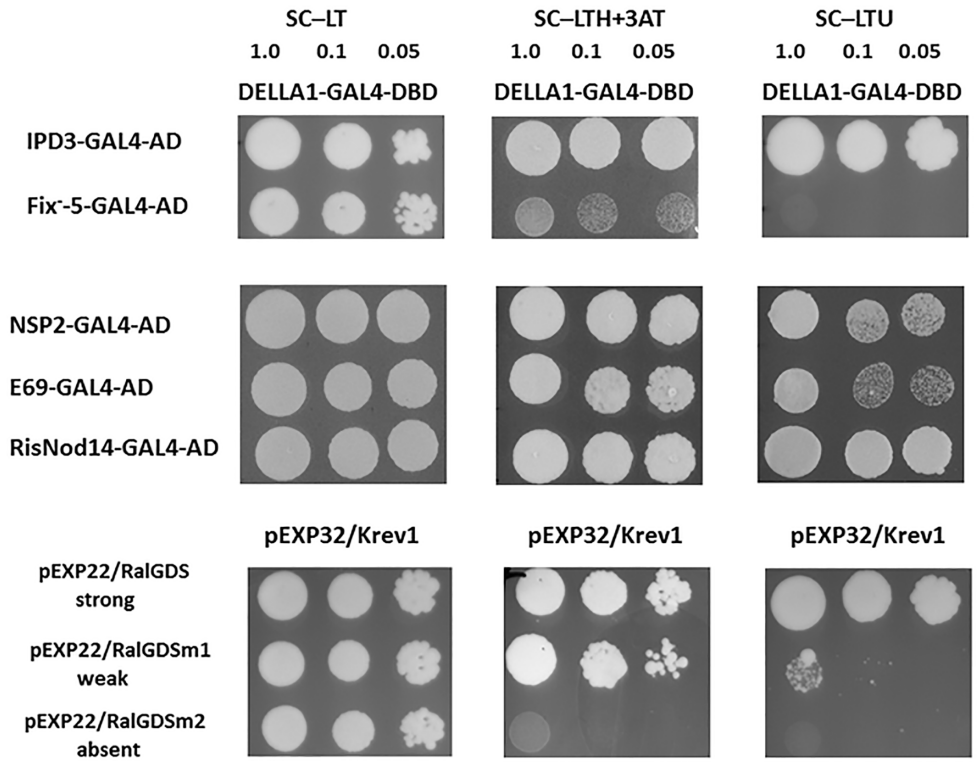

FIGURE 7 | Yeast two-hybrid assay (GAL4 transcription factor-based) for DELLA1 protein and NSP2 and IPD3/CYCLOPS transcription factors and their truncated variants corresponding to those in E69 (*nsp2/sym7-1*), RisNOD14 (*nsp2/sym7-2*) and SGEFix^{-}–5 (*ipd3/cyclops/sym33-2*). AD – activation domain of GAL4, DBD – DNA binding domain of GAL4. The pairs of vectors pEXP32/Krev1 and pEXP22/RalGDS-wild type, pEXP22/RalGDS-m1 and pEXP22/RalGDS-m2 were used for strong, weak and not detectable interactions. Yeast growth was tested on SC medium –LTH + 50 mM 3 AT and SC – LTU.

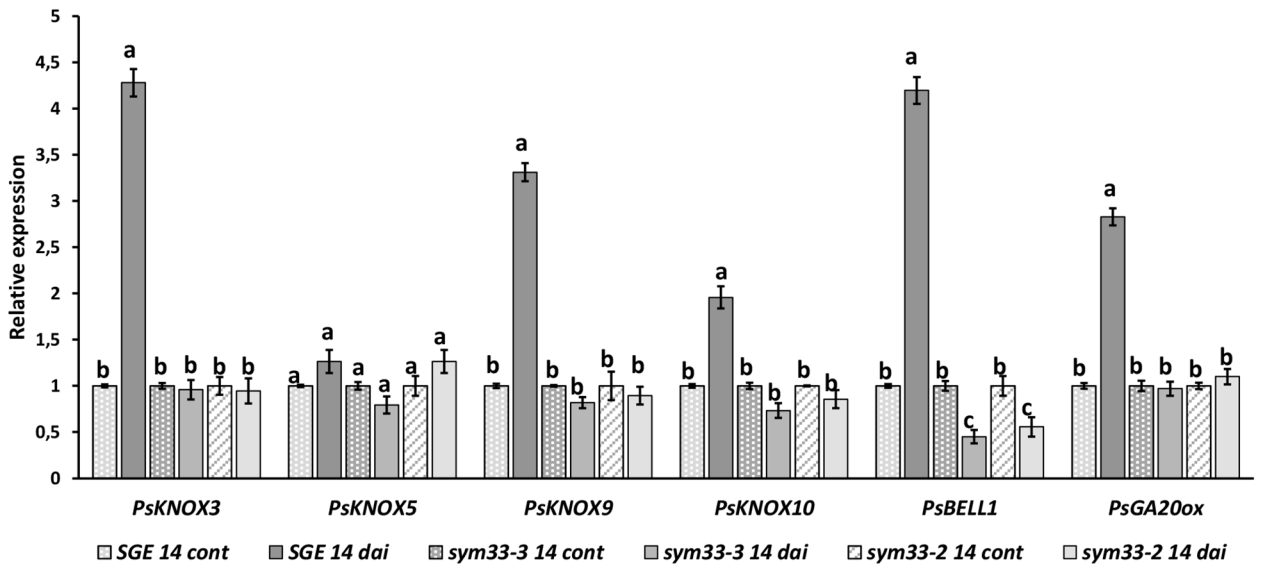

FIGURE 8 | Expression analysis of *PsGA20ox*, *PsKNOX*, and *PsBELL* genes in wild type cv. SGE and SGEFix^{-}–2 (*sym33–3*), SGEFix^{-}–5 (*sym33–2*) mutants 2 weeks after inoculation. Transcript levels of genes were normalized against ubiquitin gene. For each gene, the transcript level in non-inoculated roots of wild type or mutants was set to 1 (control), and the level in nodules of wild type or mutants was calculated relative to the control values. Data are averages ± SEM (n = 6–8 plants of wild type or mutant combined from two independent experiments). Values with different letters are significantly different ($P < 0.05$) as analyzed by one-way ANOVA and the Tukey's test as *post-hoc* analysis.

be that *PsKNOX9* and *PsBELL1* influence GA metabolic genes at early stages of symbiosis, as revealed significant changes in GA metabolism may take place at initial stages of symbiosis development and *Ps*DELLA proteins are involved in this regulation.

At later stages of symbiosis development the up regulation of expression of *PsKNOX3*, *PsKNOX9*, and *PsBELL1* was shown to be attenuated in pea *della1 della2* mutant. However, up regulation in the expression of other *PsKNOX* genes, the *PsKNOX5* and *PsKNOX10*, was only slightly reduced or similar in *della* mutant compared to wild type. Consistently, pea *la cry-s* (*della1 della2*) mutant showed reduced upregulation in the expression of the CK synthesis (*PsLOG1*, *PsLOG2*) and signaling (*PsRR11*) genes during nodulation compared to wild type. One interpretation is that *Ps*DELLA proteins can regulate the CK metabolism via *Ps*KNOX and *Ps*BELL transcription factors during nodule development. Upregulation of CK metabolic genes has previously been shown to be due to activation of KNOX and BELL transcription factors (Yanai et al., 2005; Azarakhsh et al., 2015).

As has been shown in analysis of model legumes, the DELLA proteins may regulate a number of transcription factors during nodulation. In some cases the DELLA proteins interact with individual transcription factors including NSP2, IPD3/CYCLOPS and NF-YA1 (direct activation), in other cases their effect may be indirect. Since DELLAs don't have a DNA-binding motif, they may induce binding of activated transcription factors with promoter of genes encoding other transcription factors like ERN1 (Fonouni-Farde et al., 2016).

To verify the effect of *Ps*DELLA proteins on *Ps*KNOX3 and *Ps*BELL1 transcription factors, the possibility of their interaction has been investigated using Y2H system. However, our studies did not reveal a strong direct interaction between *Ps*DELLA1 and *Ps*KNOX3 or *Ps*BELL1 in this heterologous system. We suggested that *Ps*DELLA1 may promote the expression *PsKNOX3* and *PsBELL1*, probably through other known transcription factors. This function may be related to IPD3/CYCLOPS and NSP2 transcription factors, because DELLA proteins can activate them during nodulation (Floss et al., 2016; Fonouni-Farde et al., 2016; Jin et al., 2016). We tested the interaction between *Ps*DELLA1 and truncated proteins corresponding to those in pea *ipd3/cyclops* (*sym33*) and *nsp2* (*sym7*) mutants. Surprisingly, only *Ps*IPD3/CYCLOPS truncated protein failed to interact with *Ps*DELLA1, but *Ps*DELLA1 still interacted with both *Ps*NSP2 truncated proteins. It suggests that in both *ipd3/cyclops* (*sym33*) mutants the interaction between *Ps*DELLA1 and *Ps*IPD3/CYCLOPS may be critical for subsequent signal transduction. Since similar trends for reduced ability to up regulate the expression of *PsKNOX3* and *PsKNOX9* transcription levels were found in the nodules of *ipd3/cyclops* (*sym33*) mutants as seen in *della* mutants compared with wild type, the *Ps*DELLA proteins may promote the expression of *PsKNOX3* and *PsBELL1* genes via the *Ps*IPD3/CYCLOPS transcription factor. Additional experiments that could explore this further include analyzing the binding capacity of *Ps*IPD3/CYCLOPS with promoters of the *PsKNOX3* and *PsKNOX9* genes in pea plants and the subsequent effect on target genes.

As previously reported (Ferguson et al., 2011), *la cry-s* mutant had significantly fewer nodules than wild-type plants. Similarly, *ipd3/cyclops* (*sym33*) mutants had a considerably reduced number of nodules (Tsyganov et al., 1998; Ovchinnikova et al., 2011). Therefore, it may suggest the involvement of *Ps*DELLA proteins and *Ps*IPD3/CYCLOPS transcription factor in initiation of nodule organogenesis and regulation of nodule number in pea plants. As it was shown for model legume plants *M. truncatula* and *L. japonicus*, the DELLA proteins are involved in activation of IPD3/CYCLOPS transcription factor. Our findings revealed that DELLA proteins and IPD3/CYCLOPS also influence the expression of pea *KNOX* and *BELL* genes encoding transcription factors.

The infection thread formation was significantly reduced in DELLA-deficient pea *la cry-s* double mutants compared with wild-type plants (McAdam et al., 2018). Similar to *la cry-s*, pea *ipd3/cyclops* (*sym33*) also showed impaired invasion of the nodule primordia at early stages (Voroshilova et al., 2009). The most probable explanation that impaired infection may influence the signal exchange between epidermis and cortical cells resulting in decreased number of nodule primordia in both type of mutants. Indeed, the experiments in which the expression of GA-insensitive *Mt*DELLA1 was restricted by epidermis showed that it was able to trigger the spontaneous nodule formation in spatially distant cortical cells in absence of rhizobia (Fonouni-Farde et al., 2017). It suggests that some diffusive factors may be involved in signal transduction in this case. Since the KNOX and BELL transcription factors may act in non-cell autonomous manner, additional experiments should explore a possible role of KNOX and BELL as such diffusive factors.

AUTHOR CONTRIBUTIONS

AD and ED conceived the study and designed the experiments. AD and AK performed the experiments and analyzed the data. IT supervised. AD, EF, and ED wrote the manuscript.

FUNDING

This work was financially supported by the Russian Science Foundation (Grant 17-76-30016). The research was performed using equipment of the Core Centrum "Genomic Technologies, Proteomics and Cell Biology" in ARRIAM.

SUPPLEMENTARY MATERIAL

The Supplementary Material for this article can be found online at: https://www.frontiersin.org/articles/10.3389/fpls.2019.00432/full#supplementary-material

REFERENCES

Achard, P., Baghour, M., Chapple, A., Hedden, P., Van Der Straeten, D., Genschik, P., et al. (2007). The plant stress hormone ethylene controls floral transition via DELLA-dependent regulation of floral meristem-identity genes. *Proc. Natl. Acad. Sci. U.S.A.* 104, 6484–6489. doi: 10.1073/pnas.0610717104

Achard, P., Cheng, H., De Grauwe, L., Decat, J., Schoutteten, H., Moritz, T., et al. (2006). Integration of plant responses to environmentally activated phytohormonal signals. *Science* 311, 91–94. doi: 10.1126/science.1118642

Alvey, L., and Harberd, N. P. (2005). DELLA proteins: integrators of multiple plant growth regulatory inputs? *Physiol. Plant.* 123, 153–160. doi: 10.1111/j.1399-3054.2004.00412.x

Azarakhsh, M., Kirienko, A. N., Zhukov, V. A., Lebedeva, M. A., Dolgikh, E. A., and Lutova, L. A. (2015). KNOTTED1-LIKE HOMEOBOX 3: a new regulator of symbiotic nodule development. *J. Exp. Bot.* 66, 7181–7195. doi: 10.1093/jxb/erv414

Bao, X., Franks, R. G., Levin, J. Z., Liu, Z., The, S., Cell, P., et al. (2004). Repression of AGAMOUS by BELLRINGER in floral and inflorescence meristems. *Plant Cell* 16, 1478–1489. doi: 10.1105/tpc.021147

Bellaoui, M., Pidkowich, M. S., Samach, A., Kushalappa, K., Kohalmi, S. E., Modrusan, Z., et al. (2001). The *Arabidopsis* BELL1 and KNOX TALE homeodomain proteins interact through a domain conserved between plants and animals. *Plant Cell* 13, 2455–2470. doi: 10.1105/tpc.010161

Breakspear, A., Liu, C., Roy, S., Stacey, N., Rogers, C., Trick, M., et al. (2014). The root hair "Infectome" of *Medicago truncatula* uncovers changes in cell cycle genes and reveals a requirement for auxin signaling in rhizobial infection. *Plant Cell* 26, 4680–4701. doi: 10.1105/tpc.114.133496

Brian, P. W. (1959). Effects of gibberellins on plant growth and development. *Biol. Rev.* 34, 37–77. doi: 10.1111/j.1469-185X.1959.tb01301.x

Byrne, M. E., Kidner, C. A., and Martienssen, R. A. (2003). Plant stem cells: divergent pathways and common themes in shoots and roots. *Curr. Opin. Genet. Dev.* 13, 551–557. doi: 10.1016/j.gde.2003.08.008

Chen, H., Banerjee, A. K., and Hannapel, D. J. (2004). The tandem complex of BEL and KNOX partners is required for transcriptional repression of ga20ox1. *Plant J.* 38, 276–284. doi: 10.1111/j.1365-313X.2004.02048.x

Cooper, J. B., and Long, S. R. (1994). Morphogenetic rescue of rhizobium meliloti nodulation mutants by trans-zeatin secretion. *Plant Cell* 6, 215–225. doi: 10.1105/tpc.6.2.215

Davière, J. M., and Achard, P. (2013). Gibberellin signaling in plants. *Development* 140, 1147–1151. doi: 10.1242/dev.087650

Dolgikh, E. A., Shaposhnikov, A. I., Dolgikh, A. V., Gribchenko, E. S., Bodyagina, K. B., Yuzhikhin, O. S., et al. (2017). Identification of *Pisum sativum* L. cytokinin and auxin metabolic and signaling genes, and an analysis of their role in symbiotic nodule development. *Int. J. Plant Physiol. Biochem.* 9, 22–35. doi: 10.5897/IJPPB2017.0266

Engvild, K. C. (1987). Nodulation and nitrogen fixation mutants of pea, *Pisum sativum*. *Theor. Appl. Genet.* 74, 711–713. doi: 10.1007/BF00247546

Ferguson, B. J. (2005). Nodulation phenotypes of gibberellin and brassinosteroid mutants of pea. *Plant Physiol.* 138, 2396–2405. doi: 10.1104/pp.105.062414

Ferguson, B. J., Foo, E., Ross, J. J., and Reid, J. B. (2011). Relationship between gibberellin, ethylene and nodulation in *Pisum sativum*. *New Phytol.* 189, 829–842. doi: 10.1111/j.1469-8137.2010.03542.x

Ferguson, B. J., and Mathesius, U. (2014). Phytohormone regulation of legume-rhizobia interactions. *J. Chem. Ecol.* 40, 770–790. doi: 10.1007/s10886-014-0472-7

Fleet, C. M., and Sun, T. P. (2005). A DELLAcate balance: the role of gibberellin in plant morphogenesis. *Curr. Opin. Plant Biol.* 8, 77–85. doi: 10.1016/j.pbi.2004.11.015

Floss, D. S., Lévesque-Tremblay, V., Park, H. J., and Harrison, M. J. (2016). DELLA proteins regulate expression of a subset of AM symbiosis-induced genes in medicago truncatula. *Plant Signal. Behav.* 11:e1162369. doi: 10.1080/15592324.2016.1162369

Fonouni-Farde, C., Kisiala, A., Brault, M., Emery, R. J. N., Diet, A., and Frugier, F. (2017). DELLA1-mediated gibberellin signaling regulates cytokinin-dependent symbiotic nodulation. *Plant Physiol.* 175, 1795–1806. doi: 10.1104/pp.17.00919

Fonouni-Farde, C., Tan, S., Baudin, M., Brault, M., Wen, J., Mysore, K. S., et al. (2016). DELLA-mediated gibberellin signalling regulates Nod factor signalling and rhizobial infection. *Nat. Commun.* 7:12636. doi: 10.1038/ncomms12636

Gamas, P., Brault, M., Jardinaud, M. F., and Frugier, F. (2017). Cytokinins in symbiotic nodulation: when, where, what for? *Trends Plant Sci.* 22, 792–802. doi: 10.1016/j.tplants.2017.06.012

Gonzalez-Rizzo, S., Crespi, M., and Frugier, F. (2006). The *Medicago truncatula* CRE1 cytokinin receptor regulates lateral root development and early symbiotic interaction with *Sinorhizobium meliloti*. *Plant Cell* 18, 2680–2693. doi: 10.1105/tpc.106.043778

Hake, S., Smith, H. M. S., Holtan, H., Magnani, E., Mele, G., and Ramirez, J. (2004). The role of KNOX genes in plant development. *Annu. Rev. Cell Dev. Biol.* 20, 125–151. doi: 10.1146/annurev.cellbio.20.031803.093824

Hall, B. G. (2013). Building phylogenetic trees from molecular data with MEGA. *Mol. Biol. Evol.* 30, 1229–1235. doi: 10.1093/molbev/mst012

Harberd, N. P., King, K. E., Carol, P., Cowling, R. J., Peng, J., and Richards, D. E. (1998). Gibberellin: inhibitor of an inhibitor of.?. *BioEssays* 20, 1001–1008. doi: 10.1002/(SICI)1521-1878(199812)20:12<1001::AID-BIES6>3.0.CO;2-O

Heckmann, A. B., Sandal, N., Bek, A. S., Madsen, L. H., Jurkiewicz, A., Nielsen, M. W., et al. (2011). Is regulated by a mechanism operating in the root cortex. *Mol. Plant-Microbe Interact.* 24, 1385–1395. doi: 10.1094/MPMI-05-11-0142

Hedden, P., and Thomas, S. G. (2012). Gibberellin biosynthesis and its regulation. *Biochem. J.* 444, 11–25. doi: 10.1042/BJ20120245

Hofer, J., Gourlay, C., Michael, A., and Ellis, T. H. N. (2001). Expression of a class 1 knotted1-like homeobox gene is down-regulated in pea compound leaf primordia. *Plant Mol. Biol.* 45, 387–398. doi: 10.1023/A:1010739812836

Jardinaud, M.-F., Boivin, S., Rodde, N., Catrice, O., Kisiala, A., Lepage, A., et al. (2016). A laser dissection-RNAseq analysis highlights the activation of cytokinin pathways by nod factors in the *Medicago truncatula* root epidermis. *Plant Physiol.* 171, 2256–2276. doi: 10.1104/pp.16.00711

Jasinski, S., Piazza, P., Craft, J., Hay, A., Woolley, L., Rieu, I., et al. (2005). KNOX action in *Arabidopsis* is mediated by coordinate regulation of cytokinin and gibberellin activities. *Curr. Biol.* 15, 1560–1565. doi: 10.1016/j.cub.2005.07.023

Jin, Y., Liu, H., Luo, D., Yu, N., Dong, W., Wang, C., et al. (2016). DELLA proteins are common components of symbiotic rhizobial and mycorrhizal signalling pathways. *Nat. Commun.* 7, 1–14. doi: 10.1038/ncomms12433

Kalo, P., Gleason, C., Edwards, A., Marsh, J., Mitra, R. M., and Hirsch, S. (2005). Nodulation signaling in legumes requires NSP2, a member of the GRAS family of transcriptional regulators. *Science* 308, 1786–1789. doi: 10.1126/science.1110951

Kneen, B. E., Weeden, N. F., and Larue, T. A. (1994). Non-nodulating mutants of *Pisum Sativum* (L.) cv. sparkle. *J. Hered.* 85, 129–133. doi: 10.1093/oxfordjournals.jhered.a111410 doi: 10.1093/oxfordjournals.jhered.a111410

Lievens, S., Goormachtig, S., Den Herder, J., Capoen, W., Mathis, R., and Hedden, P. (2005). Gibberellins are involved in nodulation of *Sesbania rostrata*. *Plant Physiol.* 139, 1366–1379. doi: 10.1104/pp.105.066944

Lin, T., Sharma, P., Gonzalez, D. H., Viola, I. L., and Hannapel, D. J. (2013). The impact of the long-distance transport of a BEL1-like messenger RNA on development. *Plant Physiol.* 161, 760–772. doi: 10.1104/pp.112.209429

Livak, K. J., and Schmittgen, T. D. (2001). Analysis of relative gene expression data using real-time quantitative PCR and the $2^{-\Delta\Delta Ct}$ method. *Methods* 25, 402–408. doi: 10.1006/meth.2001.1262

Maekawa, T., Maekawa-Yoshikawa, M., Takeda, N., Imaizumi-Anraku, H., Murooka, Y., and Hayashi, M. (2009). Gibberellin controls the nodulation signaling pathway in *Lotus japonicus*. *Plant J.* 58, 183–194. doi: 10.1111/j.1365-313X.2008.03774.x

McAdam, E. L., Reid, J. B., and Foo, E. (2018). Gibberellins promote nodule organogenesis but inhibit the infection stages of nodulation. *J. Exp. Bot.* 69, 2117–2130. doi: 10.1093/jxb/ery046

Murray, J., Karas, B., Ross, L., Brachmann, A., Wagg, C., Geil, R., et al. (2006). Genetic suppressors of the *Lotus japonicus har1-1* hypernodulation phenotype. *Mol Plant-Microbe Interact.* 19, 1082–1091. doi: 10.1094/MPMI-19-1082

Navarro, L., Bari, R., Achard, P., Lisón, P., Nemri, A., Harberd, N. P., et al. (2008). DELLAs control plant immune responses by modulating the balance of jasmonic acid and salicylic acid signaling. *Curr. Biol.* 18, 650–655. doi: 10.1016/j.cub.2008.03.060

Ovchinnikova, E., Journet, E.-P., Chabaud, M., Cosson, V., Ratet, P., Duc, G., et al. (2011). IPD3 controls the formation of nitrogen-fixing symbiosomes in pea and *Medicago* Spp. *Mol. Plant-Microbe Interact.* 24, 1333–1344. doi: 10.1094/MPMI-01-11-0013

Park, J., Nguyen, K. T., Park, E., Jeon, J.-S., and Choi, G. (2013). DELLA proteins and their interacting RING finger proteins repress gibberellin responses by binding to the promoters of a subset of gibberellin-responsive genes in *Arabidopsis*. *Plant Cell* 25, 927–943. doi: 10.1105/tpc.112.108951

Plet, J., Wasson, A., Ariel, F., Le Signor, C., Baker, D., Mathesius, U., et al. (2011). MtCRE1-dependent cytokinin signaling integrates bacterial and plant cues to coordinate symbiotic nodule organogenesis in *Medicago truncatula*. *Plant J.* 65, 622–633. doi: 10.1111/j.1365-313X.2010.04447.x

Sharma, P., Lin, T., Grandellis, C., Yu, M., and Hannapel, D. J. (2014). The BEL1-like family of transcription factors in potato. *J. Exp. Bot.* 65, 709–723. doi: 10.1093/jxb/ert432

Smith, H. M. S., and Hake, S. (2003). The interaction of two homeobox genes. *Plant Cell* 15, 1717–1727. doi: 10.1105/tpc.012856.stems

Sun, T., and Gubler, F. (2004). Molecular mechanism of gibberellin signaling in plants. *Annu. Rev. Plant Biol.* 55, 197–223. doi: 10.1146/annurev.arplant.55.031903.141753

Sun, T. P. (2010). Gibberellin-GID1-DELLA: a pivotal regulatory module for plant growth and development. *Plant Physiol.* 154, 567–570. doi: 10.1104/pp.110.161554

Thompson, J. D., Higgins, D. G., and Gibson, T. J. (1994). CLUSTAL W: improving the sensitivity of progressive multiple sequence alignment through sequence weighting, position-specific gap penalties and weight matrix choice. *Nucleic Acids Res.* 22, 4673–4680. doi: 10.1093/nar/22.22.4673

Tirichine, L., Sandal, N., Madsen, L. H., Radutoiu, S., Albrektsen, A. S., Sato, S., et al. (2007). A gain-of-function mutation in a root nodule organogenesis. *Science* 2680, 104–107. doi: 10.1126/science.1132397

Tsyganov, V. E., Morzhina, E. V., Stefanov, S. Y., Borisov, A. Y., Lebsky, V. K., and Tikhonovich, I. A. (1998). The pea (*Pisum sativum* L.) genes sym33 and sym40 control infection thread formation and root nodule function. *Mol. Gen. Genet.* 259, 491–503. doi: 10.1007/s004380050840

Tsyganov, V. E., Voroshilova, V. A., Priefer, U. B., Borisov, A. Y., and Tikhonovich, I. A. (2002). Genetic dissection of the initiation of the infection process and nodule tissue development in the *Rhizobium*-pea (*Pisum sativum* L.) symbiosis. *Ann. Bot.* 89, 357–366. doi: 10.1093/aob/mcf051

van Brussel, A. A., Tak, T., Wetselaar, A., Pees, E., and Wijffelman, C. (1982). Small leguminosae as test plants for nodulation of *Rhizobium leguminosarum* and other rhizobia and agrobacteria harbouring a leguminosarum sym-plasmid. *Plant Sci. Lett.* 27, 317–325. doi: 10.1016/0304-4211(82)90134-1

van Brussel, A. A. N., Planque, K., and Quispel, A. (1977). The wall of *Rhizobium leguminosarum* in bacteroid and free-living forms. *J. Gen. Microbiol.* 101, 51–56. doi: 10.1099/00221287-101-1-51

van Zeijl, A., Liu, W., Xiao, T. T., Kohlen, W., Yang, W. C., Bisseling, T., et al. (2015). The strigolactone biosynthesis gene DWARF27 is co-opted in rhizobium symbiosis. *BMC Plant Biol.* 15:260. doi: 10.1186/s12870-015-0651-x

Voroshilova, V. A., Demchenko, K. N., Brewin, N. J., Borisov, A. Y., and Tikhonovich, I. A. (2009). Initiation of a legume nodule with an indeterminate meristem involves proliferating host cells that harbour infection threads. *New Phytol.* 181, 913–923. doi: 10.1111/j.1469-8137.2008.02723.x

Walker, S. A., and Downie, J. A. (2000). Entry of *Rhizobium leguminosarum* bv. viciae into root hairs requires minimal nod factor specificity, but subsequent infection thread growth requires nodo or node. *Mol. Plant-Microbe Interact.* 13, 754–762. doi: 10.1094/MPMI.2000.13.7.754

Weston, D. E., Elliott, R. C., Lester, D. R., Rameau, C., Reid, J. B., Murfet, I. C., et al. (2008). The pea DELLA proteins LA and CRY are important regulators of gibberellin synthesis and root growth. *Plant Physiol.* 147, 199–205. doi: 10.1104/pp.108.115808

Yanai, O., Shani, E., Dolezal, K., Tarkowski, P., Sablowski, R., Sandberg, G., et al. (2005). Arabidopsis KNOXI proteins activate cytokinin biosynthesis. *Curr. Biol.* 15, 1566–1571. doi: 10.1016/j.cub.2005.07.060

Zentella, R., Zhang, Z.-L., Park, M., Thomas, S. G., Endo, A., Murase, K., et al. (2007). Global analysis of DELLA direct targets in early gibberellin signaling in *Arabidopsis*. *Plant Cell* 19, 3037–3057. doi: 10.1105/tpc.107.054999

Zhou, C., Han, L., Li, G., Chai, M., Fu, C., Cheng, X., et al. (2014). STM/BP-Like KNOXI is uncoupled from ARP in the regulation of compound leaf development in *Medicago truncatula*. *Plant Cell* 26, 1464–1479. doi: 10.1105/tpc.114.123885

Conflict of Interest Statement: The authors declare that the research was conducted in the absence of any commercial or financial relationships that could be construed as a potential conflict of interest.

frontiers in Plant Science

ORIGINAL RESEARCH
published: 02 August 2019
doi: 10.3389/fpls.2019.01000

A Toolkit for High Resolution Imaging of Cell Division and Phytohormone Signaling in Legume Roots and Root Nodules

*Marcin Nadzieja, Jens Stougaard and Dugald Reid**

Department of Molecular Biology and Genetics, Aarhus University, Aarhus, Denmark

OPEN ACCESS

Edited by:
Benjamin Gourion, UMR2594 Laboratoire Interactions Plantes-Microorganismes (LIPM), France

Reviewed by:
Ulrike Mathesius, Australian National University, Australia
Erik Limpens, Wageningen University & Research, Netherlands
Florian Frugier, Centre National de la Recherche Scientifique (CNRS), France
Jeremy Dale Murray, Shanghai Institutes for Biological Sciences (CAS), China

****Correspondence:***
Dugald Reid
dugald@mbg.au.dk

Specialty section:
This article was submitted to Plant Microbe Interactions, a section of the journal Frontiers in Plant Science

Received: *02 May 2019*
Accepted: *17 July 2019*
Published: *02 August 2019*

Citation:
Nadzieja M, Stougaard J and Reid D (2019) A Toolkit for High Resolution Imaging of Cell Division and Phytohormone Signaling in Legume Roots and Root Nodules. Front. Plant Sci. 10:1000. doi: 10.3389/fpls.2019.01000

Legume plants benefit from a nitrogen-fixing symbiosis in association with rhizobia hosted in specialized root nodules. Formation of root nodules is initiated by *de novo* organogenesis and coordinated infection of these developing lateral root organs by rhizobia. Both bacterial infection and nodule organogenesis involve cell cycle activation and regulation by auxin and cytokinin is tightly integrated in the process. To characterize the hormone dynamics and cell division patterns with cellular resolution during nodulation, sensitive and specific sensors suited for imaging of multicellular tissues are required. Here we report a modular toolkit, optimized in the model legume *Lotus japonicus,* for use in legume roots and root nodules. This toolkit includes synthetic transcriptional reporters for auxin and cytokinin, auxin accumulation sensors and cell cycle progression markers optimized for fluorescent and bright field microscopy. The developed vectors allow for efficient one-step assembly of multiple units using the GoldenGate cloning system. Applied together with a fluorescence-compatible clearing approach, these reporters improve imaging depth and facilitate fluorescence examination in legume roots. We additionally evaluate the utility of the dynamic gravitropic root response in altering the timing and location of auxin accumulation and nodule emergence. We show that alteration of auxin distribution in roots allows for preferential nodule emergence at the outer side of the bend corresponding to a region of high auxin signaling capacity. The presented tools and procedures open new possibilities for comparative mutant studies and for developing a more comprehensive understanding of legume-rhizobia interactions.

Keywords: auxin, cytokinin, nodulation and N fixation 2, lotus japonicus, symbiosis

INTRODUCTION

Plant hormones control all aspects of plant development. In legume plants, which enter into symbiotic relationship with soil bacteria called rhizobia, *de novo* formation of lateral organs called nodules must be coordinated with rhizobial infection for successful development of nitrogen fixing root nodules. These two separate, yet interdependent processes are regulated by plant hormones. Organ initiation and formation is restricted to a specific root zone and thus the spatiotemporal regulation of plant hormones is critical.

Studying plant hormone dynamics in this context requires high resolution sensors in order to discriminate signaling that regulate nodule organogenesis and infection processes. Several challenges have prevented the widespread use of hormone sensors in legume nodulation studies. Differences in promoter activity can for example impair the use of sensors developed in other model systems. Signal to noise ratios is also an issue and therefore nuclear localized variants of yellow and red fluorescent proteins are commonly employed in promoter studies instead of GFP (Suzaki et al., 2012; Reid et al., 2016). The "thick" multilayered anatomy of legume roots also pose challenges for deep imaging. However, recent advent of fluorescent compatible clearing methods which rely on fixation of fluorescent proteins prior to chemical clearing of tissue has facilitated the application of fluorescent markers in intact tissue (Warner et al., 2014).

The major plant hormones auxin and cytokinin have important roles in both nodule organogenesis and infection (Tirichine et al., 2006, 2007; Murray et al., 2007; Suzaki et al., 2012; Breakspear et al., 2014; Reid et al., 2017; Liu et al., 2018; Nadzieja et al., 2018) and we therefore focused our tool-box development on these two hormones. Transcriptional (promoter based) markers have traditionally been used, however present problems associated with gene silencing (Zürcher et al., 2013). Where available, translational markers including sensors based on ubiquitin-dependent degradation (DII, CycB) can significantly improve resolution and sensitivity (Colón-Carmona et al., 1999; Brunoud et al., 2012). Auxin and cytokinin are major regulators of the cell cycle that is activated during nodule organogenesis and we therefore aimed to characterize reporters for assessing cell cycle progression.

Here, we present a suite of tools for the study of auxin, cytokinin and cell cycle progression in legumes and demonstrate their use in the model legume *L. japonicus*. The toolbox consists of GoldenGate compatible parts (Patron et al., 2015) for rapid cloning and application. Additionally, we show that the fluorescent compatible clearing methodology provides a great improvement in imaging depth in multicellular tissues and enables comprehensive imaging of anatomical features and cell division during root and nodule development.

RESULTS

Fluorescent Compatible Clearing and Cell Type Identification

Visualization of cortical cells in intact tissue is important for nodule developmental studies. Compared to *Arabidopsis thaliana*, *L. japonicus* roots display a multilayered, complex architecture. This impairs detection of fluorescence, making it difficult to image deeper cell layers at high resolution without physical sectioning. To assess the utility of the fluorescent compatible clearing method previously developed for pea nodules (Warner et al., 2014), we expressed nuclear localized triple venus YFP (tYFPnls) under a strong constitutive promoter (*Lj*Ubiquitin). Harvested roots were fixed using 4% *p*-formaldehyde followed by 10-day clearing in 6M urea. The fluorescent compatible clearing procedure offered a great improvement in imaging depth relative to uncleared roots (**Figure S1**). Cleared roots allowed identification of all cell files within the closed-type root apex of *L. japonicus* (Potocka et al., 2011) including (i) columella, (ii) lateral root cap, (iii) stele, (iv) epidermis, (v) cortex, (vi) endodermis, and (vii) pericycle (**Figure 1**). Cell types of different identity were recolored for ease of visualization (**Figure 1B**). This imaging also enabled identification of the quiescent center (QC) and initials forming pericycle, endodermis and cortical cells and cells giving rise to additional cortical cell layers (**Figure 1B**, box).

Fluorescent compatible clearing also improves imaging depth outside the area of the root apical meristem, but the application may be limited for lowly expressed fluorescent proteins. We cleared LjDII (see below) transgenic root (**Supplemental Video 1**) and were able to identify nuclei in all cortical layers. Intensity of the fluorescent signal deeper in the tissue is however greatly reduced. In young, infected nodules (6 dpi, **Supplemental Video 2**) it is possible to visualize large networks of infection threads with clarity enabling the pinpointing of infection thread branching points within a nodule.

Application of Cytokinin Response Reporter TCSn in Nodule Development

Cytokinin signal transduction results in activation of transcription via phosphorylation of B-type response regulators (RRs). DNA binding domains of B-type Arabidopsis RRs (ARRs) are highly conserved and bind a common DNA motif (A/G)GAT(T/C) (Sakai et al., 2001; Hosoda et al., 2002; Imamura et al., 2003). This motif was used to create the synthetic cytokinin response reporter called TCS (Two Component Signaling) (Müller and Sheen, 2008), while optimization of the number, sequence and spacing between ARR-binding motifs was termed TCSn (TCS *new*; Zürcher et al., 2013). TCSn shows reduced sequence conservation to reflect a broader spectrum of naturally occurring ARR binding sites, resulting in higher sensitivity of the promoter. Reduced sequence repetition also lowers silencing of the reporter.

We previously described TCSn activity upon rhizobial inoculation over initial steps of symbiosis (Reid et al., 2017), showing a broad early activation of cytokinin signaling in the root cortex of the plant. Here, in subsequent stages of nodule development, we observed strong TCSn:YFPnls activation during establishment of nodule primordium and its subsequent proliferation, with its maxima in dividing cortical cells (**Figures 2A,B**). Nuclei directly below the infection thread appear enlarged, possibly due to endoreduplication (Suzaki et al., 2014) We also observed that epidermal, root hair activation of cytokinin signaling occurs in cells which do not contain infection threads (**Figure 2C**). In nodules at the stage of bacteria release into symbiosomes, TCSn is not active in infected cells, but remains active in interstitial uninfected cells (**Figure 2D**). Similarly, in fully developed nodules TCSn activity is not detectable in cells containing rhizobia, but in the outer nodule parenchyma (**Figure 2E**) and nodule cortex (**Figure 2F**). We did not observe TCSn activation in infected root hairs.

Auxin Accumulation Reporters

Non-transcriptional auxin reporters have been developed based on breakdown of the auxin - Aux/IAA complex (Brunoud

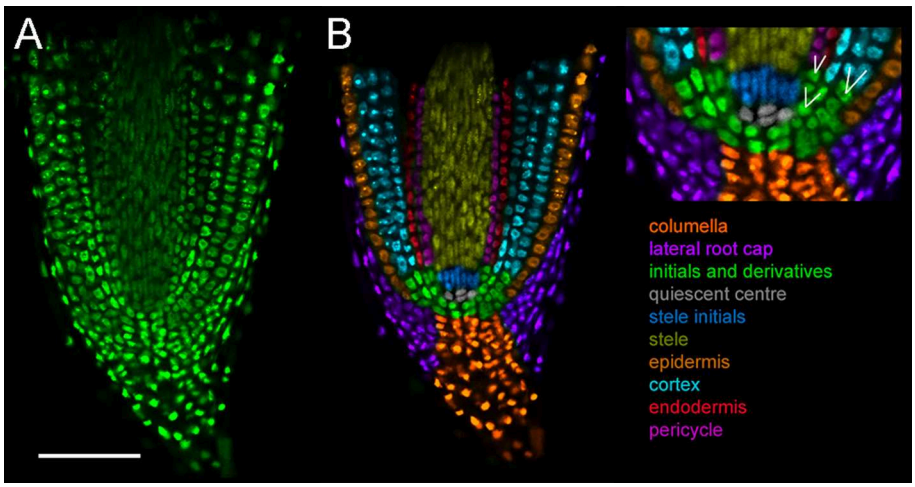

FIGURE 1 | Cell types in *L. japonicus* root tip. Hairy roots transformed with *Lj*Ubi:tYFPnls and cleared for 10 days. Whole mount roots. **(A)** Original confocal section of median longitudinal section of the root tip **(B)** recoloured showing cell types. White lines indicate cell division sites generating new cell layers. Scale bar 100 μm.

et al., 2012). This reporter, termed DII, includes the Aux/IAA degron from IAA28 cloned in frame with fast maturing yellow fluorescent protein (VENUS). Auxin mediated degradation of the DII-VENUS sensor results in a rapid decline of fluorescence. A mutated DII domain abolishing auxin binding (mDII) (Tan et al., 2007) allows for ratiometric imaging of auxin accumulation (R2D2; Liao et al., 2015).

We previously described a sensitive auxin accumulation reporter, *Lj*DII, for use in *L. japonicus* roots (Nadzieja et al., 2018). Compared to the sensor developed in Arabidopsis, we substituted the *L. japonicus* ubiquitin promoter, which shows enhanced expression in legume root tissue relative to the 35S promoter and used a triple repeat of the venus reporter (tYFPnls). To determine if a ratiometric DII was suitable for imaging in *L. japonicus*, we coupled *Lj*DII with an auxin insensitive *Lj*mDII (Liao et al., 2015) fused to NLS-DsRed to create LjR2D2. Both expression units contained *LjUbi* promoter. In transgenic hairy roots both LjR2D2 sensors localized in the nucleus (**Figure 3A**). Root hair cells of untreated control roots, appeared to have lower tYFP/DsRed fluorescence intensity ratio compared to epidermal non root hair cells (atrichoblasts) suggesting that auxin level in root hairs is elevated compared to other epidermal cells. We extracted tYFP and DsRed fluorescence intensities from 30 root hair and atrichoblasts and calculated the tYFP/DsRed ratio (**Figure 3C**). Root hair cells showed relatively lower tYFP fluorescence suggesting higher auxin levels compared to atrichoblasts. When treated with IAA, we observed quickly declining YFP fluorescence (**Figures 3A,B,D**). DsRed fluorescence declined at a much slower rate (**Figure 3D**).

Auxin Signaling Reporter

Auxin binds to the nuclear localized receptor TIR1/AFB in SKP1-CUL1-F-box (SCF) ubiquitin ligase complexes (Dharmasiri et al., 2005; Kepinski and Leyser, 2005). The binding results in recruiting auxin/indole acetic acid proteins (Aux/IAAs) into this complex (Gray et al., 2001) and subsequent ubiquitin-mediated degradation of Aux/IAAs. De-repressed auxin response factors (ARFs), may then bind auxin response elements (AuxREs) in gene regulatory elements. Tandem repeats of AuxRE together with a minimal 35S cauliflower mosaic virus (CaMV) promoter constitute the synthetic auxin response promoter DR5 (Liu et al., 1994; Ulmasov et al., 1997).

In legumes, the DR5 auxin response reporter aided identification of auxin signaling in developing lateral roots (Herrbach et al., 2014) and nodules (Suzaki et al., 2012). The DR5 activity signature displays subtle differences in *L. japonicus* and *M. truncatula,* being expressed in a wider region surrounding individual ITs in *M. truncatula* (Breakspear et al., 2014; Nadzieja et al., 2018). Here, we show that DR5:tYFPnls activity in the *L. japonicus* root apical meristem (RAM) most intensely marks the area of initials, QC, columella and outer root cap cells (**Figures 4A,B**), which is consistent with patterns described in *A. thaliana* (Blilou et al., 2005). We detected auxin signaling at stage Ib/II of LR formation (first anticlinal cell divisions, **Figure 4C**), that later organized into a pattern resembling a fully formed RAM (**Figure 4D**). At the stage of breaching the epidermis (**Figure 4F**) the auxin signaling zone extends to a subset of epidermal cells with its maxima in the delaminating cells. Activation of DR5 was also observed at the base of elongated lateral roots (**Figure 4E**).

Consistent with previous observations (Suzaki et al., 2012), in rhizobia inoculated roots, most nodule primordia and nodules showed strong DR5 activation in the root cortex (**Figure 4G**). Additionally, auxin signaling in cells adjacent to vasculature under sites of infection, was identified. Occasionally, we recorded infected nodules with no DR5 activity within the cortex, but still showing auxin signaling below the infection (**Figure 4H**), This is consistent with previous reports of DR5 activity being reduced in an autoregulation-dependent manner (Suzaki et al., 2012). We observed DR5 activation

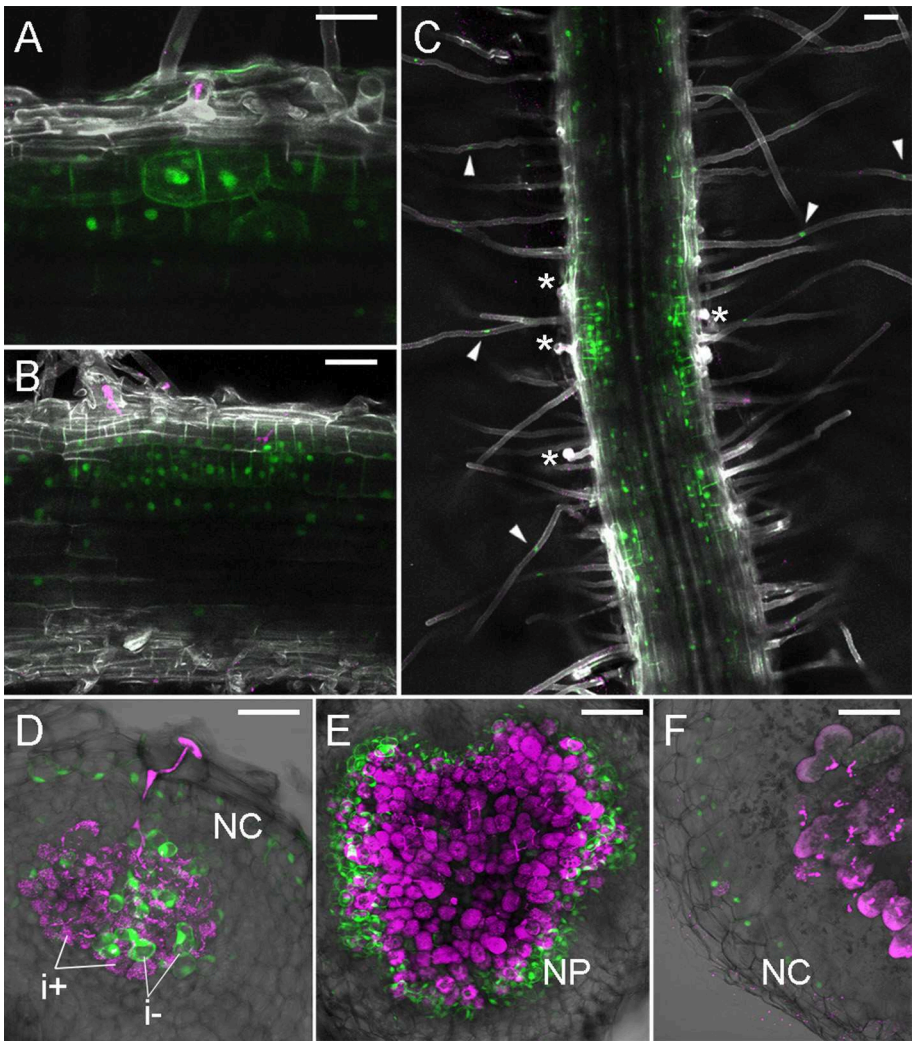

FIGURE 2 | TCSn:YFPnls activation in nodule development. Plants were inoculated with *M. loti* MAFF303099 DsRed (magenta). **(A,B)** 4 dpi nodule primordia, **(C)** roots at 5 dpi **(D)** 7 dpi nodule, **(E)** 10 dpi nodule, **(F)** 14 dpi nodule. **(A–C)** Whole mounts, cleared roots, **(D–F)** 80 μm vibratome sections. Arrowheads—epidermal TCSn activation, asterisks—epidermal infection threads. NC, nodule cortex; NP, nodule parenchyma; i+/i-, infected/uninfected nodule cells. Scale bars 50 μm.

in cells containing symbiosomes in sectioned nodules at 14 dpi (**Figure 4I**).

Simultaneous Imaging of Auxin and Cytokinin Responses

Combining hormonal reporters in the same root might improve understanding of auxin/cytokinin interplay (Fisher et al., 2018). We therefore cloned DR5:mCherry-NLS and TCSn:YFP-NLS into the same expression vector. We observed, that both DR5 and TCSn mark area of cell divisions, but their relative intensities differ (**Figure 5**). DR5 activity appears higher in cells close to the infection thread (**Figure 5**, arrowhead) and some neighboring epidermal, atrichoblasts. TCSn maximum intensity is observed in cortical cells below infection sites. Cells situated close to the vasculature show relatively higher DR5 activity.

Cell Division Reporters

Both auxin and cytokinin regulate the cell cycle and transitions between the phases of the cell cycle are controlled by cyclin-dependent protein kinases (CDKs), whose activity depends on regulatory subunits called cyclins. Transition to mitosis is dependent on B-type cyclins and a cyclin B1;1 (CYCB1;1) marker is commonly used to follow cell cycle progression (Colón-Carmona et al., 1999). The promoter of CycB1;1 is exclusively active in late G2 and early M phase of the cell cycle and translational fusions including the destruction box motif ensure rapid turnover of CYCB1;1 (Colón-Carmona et al., 1999). A *L. japonicus* CycB1;1 promoter and CycB1;1 fragment was used for identification of dividing cells in root meristems and nodule primordia (Soyano et al., 2013).

In order to visualize cell cycle progression in *L. japonicus* roots, we used an *A. thaliana* cyclin B1;1-based marker

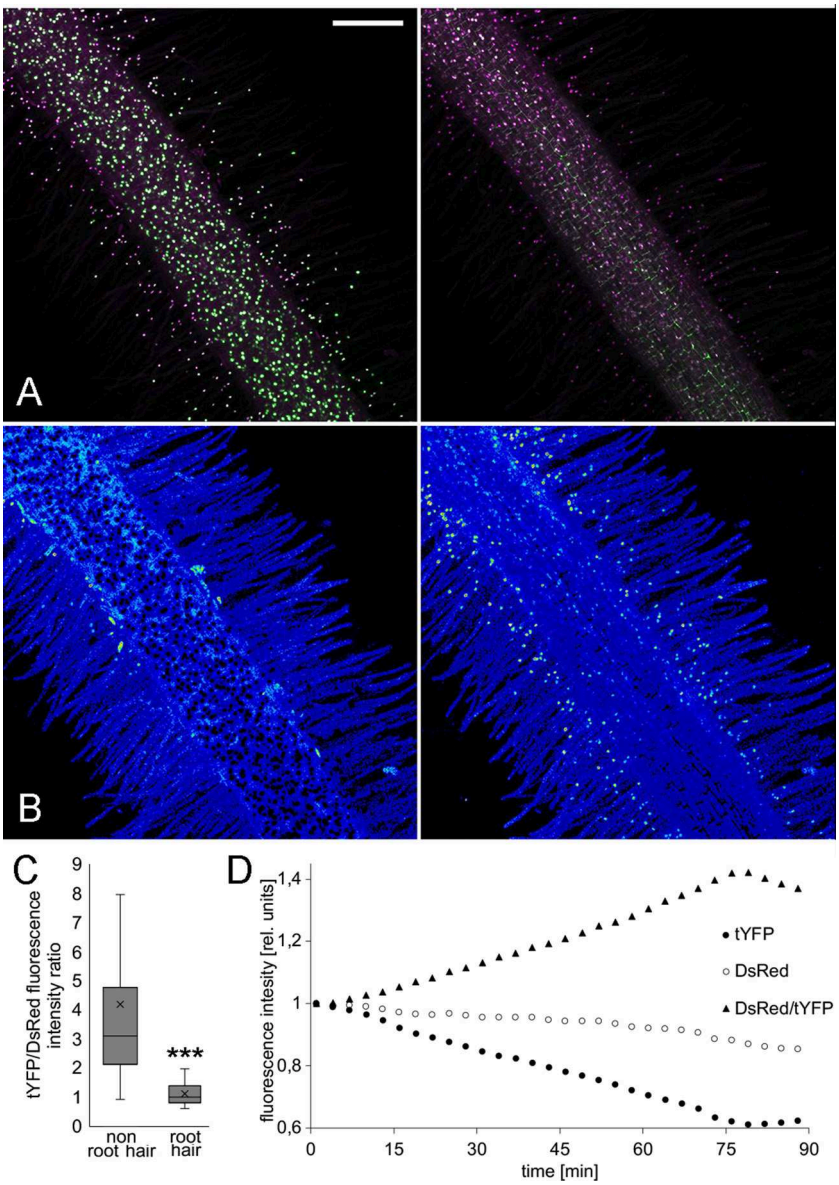

FIGURE 3 | LjR2D2 response to exogenous IAA application. **(A)** tYFP (DII) and DsRed (mDII) fluorescence, original channels, **(B)** DsRed/tYFP fluorescence ratio, 18-colors LUT. **(A,B)** Left $t = 1$ min, **(A,B)** right $t = 89$ min. Scale bar 100 μm. **(C)** tYFP/DsRed fluorescence ratio in 30 root hair and 30 non root hair epidermal cells at the beginning of the treatment, **(D)** Graph representing change of tYFP and DsRed fluorescence intensities upon 10^{-6}M IAA treatment. Whole mount live images are shown. $^{***}p < 0.001$.

(Colón-Carmona et al., 1999). The marker consisted of a cycB1;1 promoter (pCYCB1;1) driving expression of a CYCB1;1-destruction box (CYCB1;1*) fused to a reporter protein. For this reporter we created a module containing pCYCB1;1 together with the initial CYCB1;1* coding sequence in order to ease swapping reporter proteins in the modular toolkit. Both the tYFPnls- (**Figure 6A**) and GUS-based (**Figure S2A**) reporters showed the characteristic dotted pattern in the RAM as has been observed in Arabidopsis (Colón-Carmona et al., 1999) and *L. japonicus* (Soyano et al., 2013). The cell division zone identified with the construct was clearly confined to the meristem. We also observed cell cycle activation occurring in the stele (**Figure 6B**, arrowhead, lower frame). We identified a few cells with a strong fluorescence from oblong shaped nuclei (**Figure 6A**, arrowhead, frame) which is a characteristic of cyclin B1 localization at metaphase (Chen et al., 2008; Yin et al., 2014). A large number of nuclei in the cortical and epidermal layers of the RAM, as well as the stele, showed foci of very strong fluorescence (**Figure 6B**, arrowhead, top frame). No activity was observed in columella and lateral root cap (**Figures 6A,B**, **Figures S2A,B**. We observed variation in intensity of the blue GUS staining in different cells within the cell division zone (**Figure S2B**), probably due to different cell

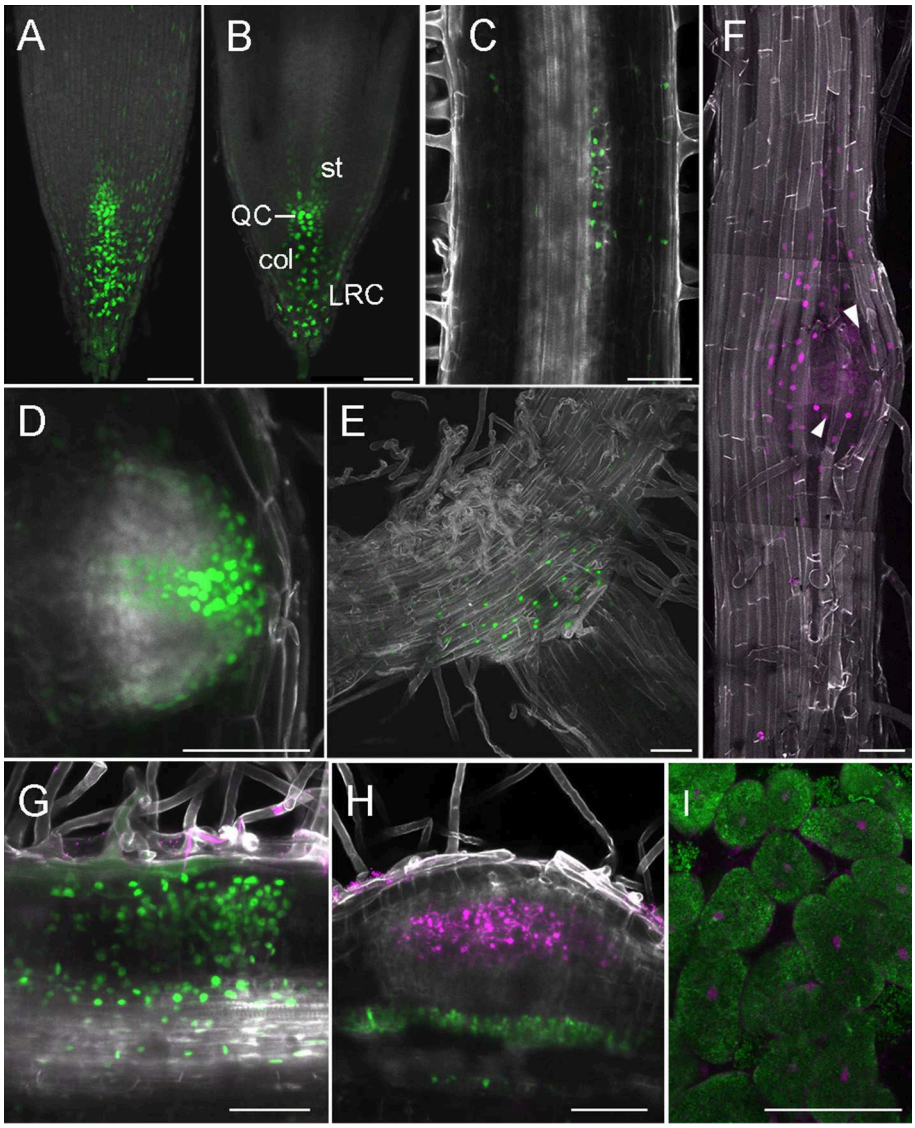

FIGURE 4 | DR5 activity in root and nodule development. **(A–H)** Whole mounts, cleared; **(I)** vibratome section. **(A)** Projection of RAM, **(B)** Confocal section dissecting middle of the root, **(C)** LR at stage Ib/II, **(D)** Emerging LR, **(E)** Base of LR, **(F)** Tile scan of LR breaching epidermis, arrowheads—delaminating epidermal cells, **(G)** Nodule primordium at 6 dpi, **(H)** Nodule with no cortical DR5 activation, **(I)** Section through 14 dpi nodule, inner cells containing symbiosomes. **(A–E,G,H)** DR5-tYFPnls, **(F,I)** DR5-mCherry. **(G,H)** DsRed labeled *M. loti* MAFF303099, **(I)** GFP labeled *M. loti* R7A. Scale bars 50 μm. col, columella; st, stele; LRC, lateral root cap; QC, quiescent center.

cycle stages and/or incomplete post-mitotic degradation of the GUS fusion.

During LR organogenesis, the marker was active at stage Ib/II (first anticlinal cell divisions, Herrbach et al., 2014) (**Figure S2C**). In the enlarging LR meristem, the marker was activated mainly in its central region (**Figure S2D**). At later stages in emerging lateral roots, activity was localized at the lateral root cap and in the central area proximal to the LR tip (**Figure 6C**, **Figure S2E**).

After inoculation with rhizobia we recorded single YFP positive nuclei in the outermost layers of cortex under elongated infection threads (**Figures 6D,E**). We detected cell divisions within the same layer of cortex (the outermost layer) in a 12-cell, early nodule primordium under an epidermal IT (**Figure 6F**, IT not shown). In these cells, formation of cell plates could be seen. At later stages of nodule organogenesis we observed cell divisions in additional cortical cell layers (**Figures 6G,H**). In large nodules, cells divisions occurred around the infected zone and among cortical ITs (**Figure 6I**).

Alteration of Auxin Distribution Affects Nodule Emergence Pattern

Given the importance of auxin signaling for rhizobial infection (Breakspear et al., 2014; Nadzieja et al., 2018) and nodule organogenesis (Suzaki et al., 2012) we developed methods to

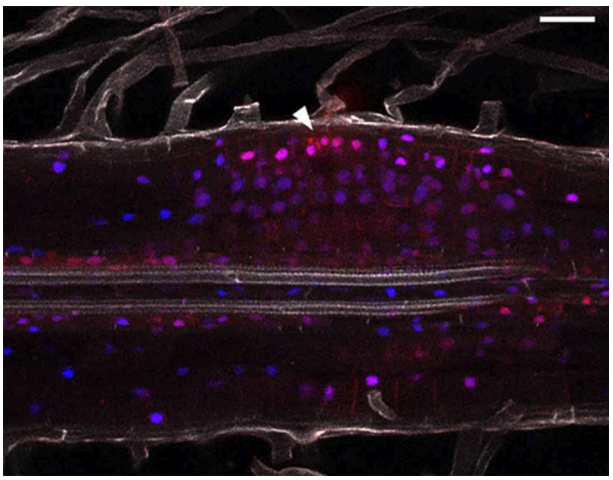

FIGURE 5 | Combined auxin and cytokinin response imaging in *L. japonicus* 5 dpi nodule primordium. Cleared whole mount root. Arrowhead depicts site of epidermal infection. Blue—TCSn:tYFP; red—DR5:mCherry and DsRed labeled rhizobia; gray—autofluorescence. Scale bar 50 μm.

disrupt auxin homeostasis in roots without chemical agonists or antagonists. Gravitropism is well-known to alter root auxin distribution and stimulate lateral root formation (Voß et al., 2015). To observe how gravitropism alters auxin response in *L. japonicus* roots, we grew DR5:GUS stable transgenic plants on agar plates for 7 days. Plates were turned 90° to induce a gravitropic bend before GUS staining of roots attached to the paper (**Figure 7**, **Figure S3**). Four hours after inducing gravitropism, an asymmetric auxin response was observed in the root tip, with stronger staining visible on the lower part of the root (**Figure S3A**). The staining in the epidermis on the lower part of the root extended further from the root tip, compared to the upper side of the root. This was observed for all examined time points (**Figure S3**). Within 8 h of the stimulus being applied, DR5 was activated near the vasculature on the outer side of the bend (**Figure S3**, **Figure 7A**, white arrowhead). This response was localized to the pericycle, as identified by vibratome sectioning (**Figure 7B**). GUS activity in the pericycle continued to be observed at later time points (**Figures S3C–E**).

Similar to observations in *A. thaliana* (Voß et al., 2015), lateral root organogenesis predominantly started in the zone of altered auxin distribution on the outside of the bend (**Figure S3F**). To determine if a gravitropic stimulus is applicable to nodulation studies, we inoculated plants 5 h after gravitropic stimulation and counted the nodules that emerged 5 mm above and below the apex of the bend. Nodules were classified as emerging either inside (lower pericycle auxin) or outside (higher pericycle auxin) of the bend. A higher frequency of nodule emergence on the outside of the bend (**Figure 7F**) was observed with 19/21 nodules positioned outside the bend ($n = 30$ plants, $p = 0.0068$ in Fisher's exact test with expected 50/50 distribution). To aid in identification of early nodule primordia at the gravitropic bend we replicated the experiment using the DR5:GUS stable line. We carried out staining at 6 dpi of gravitropism stimulated plants (**Figures 7D,E**) and observed that at this time 10 out of 12 primordia formed on the outside of the bend (n = 10 plants).

DISCUSSION

Here we present a series of modular tools for visualization of auxin, cytokinin and cell cycle responses in legume roots and nodules and demonstrate their use in *L. japonicus*. Each module is available as a GoldenGate part using standard overhangs. We also identify the fluorescent compatible clearing protocol as a suitable mean for improving imaging depth during studies of root and nodule development in *L. japonicus*. The combination of bright nuclear-localized fluorescent proteins with fixation and clearing helps overcome many of the obstacles to microscopic observations of nodule initiation and development. In our experience, tYFPnls maintains strong fluorescence intensity after fixation and clearing up to several weeks and we recommend it for application in promoter/reporter studies. We found TCSn, DR5, LjDII, and AtCycB1;1 to be robust reporters using this system. The modular nature of our toolkit will allow new components to be added in the future to create new ratiometric or two-color imaging tools such as a 2-color cell cycle progression marker (Yin et al., 2014) or endoreduplication reporters. While GUS detection of cell division is very sensitive, readily observable and can be used for discrete observations of organogenesis, the fluorescent variant of the reporter opens opportunity of prolonged live imaging of cell divisions in developing nodules with 2-photon or light sheet microscopy. Monitoring the shape of the fluorescent signal using the CycB1;1 marker for example presents an interesting future possibility as this may represent distinct phases of the cell cycle.

It was shown that auxin transport is altered upon early stages of the symbiosis (Mathesius et al., 1998; Boot et al., 1999; Pacios-Bras et al., 2003), and that expression patterns of some PIN-encoding genes are distinct in nodule primordia (Huo et al., 2006; Sanko-Sawczenko et al., 2019). Application of gravitropic stimulation alters auxin response localization and has commonly been used in studies of lateral root emergence. Here we show that this technique is also relevant for studies of symbiotic organ formation as nodules preferentially emerge on the outside of a gravitropic bend. This likely results from auxin signaling activation in pericycle and endodermis, which occurs under infection sites in a similar manner to which is observed in gravitropically stimulated roots. The preferential formation of both lateral roots and nodules on the outside of a gravitropic bend illustrates the importance of a localized auxin maxima in both these developmental processes and suggests that these two organogenesis processes share overlapping regulatory mechanisms. Additionally, we noticed that in *L. japonicus* strong activation of DR5 accompanies both developing lateral roots and nodules. In soybean, which also forms determinate type of nodules, DR5 activation appears much more prominent in lateral roots compared to nodules (Turner et al., 2013). This difference might be caused by different naturally occurring AuxREs being employed in nodule and lateral root formation processes in these two species and further analysis is required to determine if this

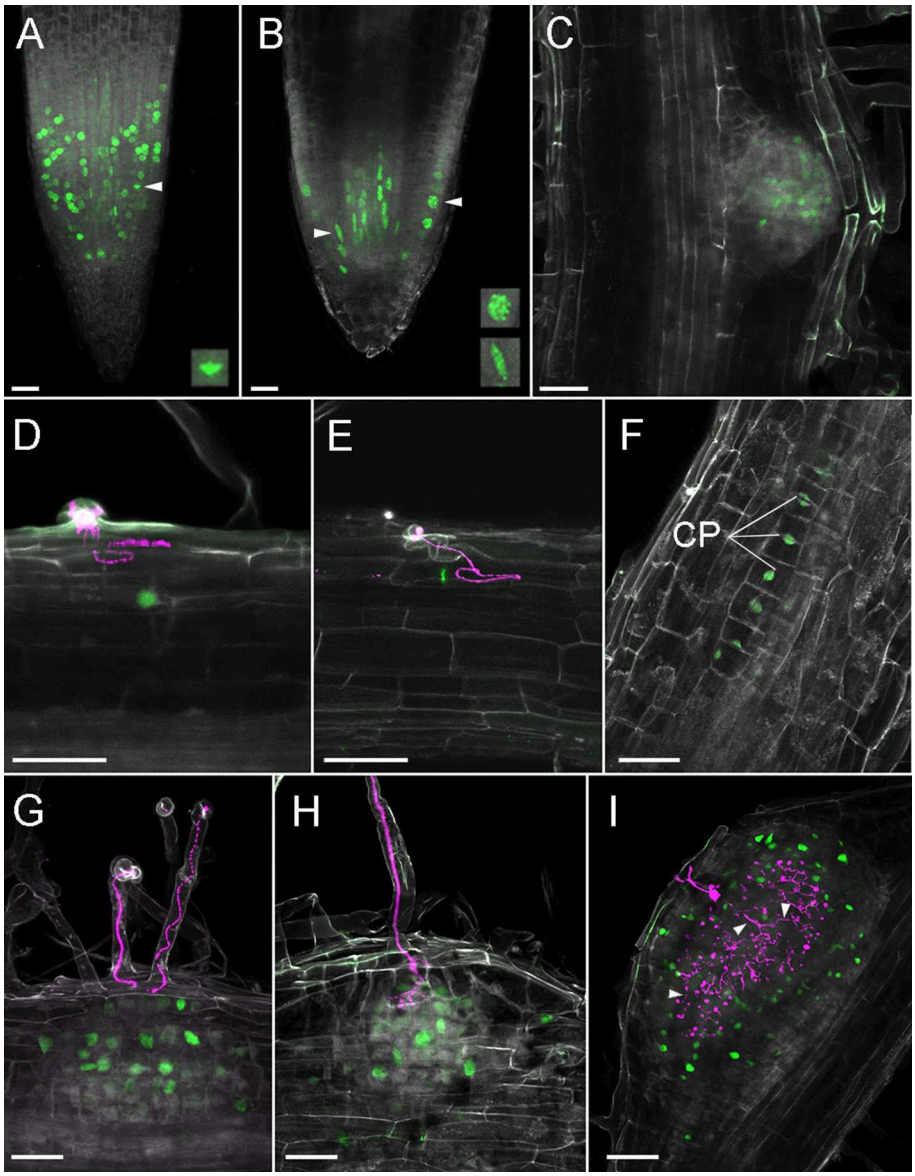

FIGURE 6 | Cell divisions in *L. japonicus* detected using pCYCB1;1::CYCB1*-tYFP and confocal microscopy in *L. japonicus* hairy roots. All panels are cleared whole mount roots. **(A)** RAM, intensity projection, arrowhead and box show metaphase nucleus; **(B)** RAM, maximal intensity projection of substack through the middle of the root tip, arrowheads and frames show prophase epidermal (top) and stele (lower) nuclei; **(C)** emerging LR; **(D)** YFP positive nucleus under IT; **(E)** metaphase nucleus under IT; **(F)** 12 cell stage of nodule primordium; **(G)** nodule primordium, ITs do not reach cortex; **(H)** nodule primordium, IT penetrate root cortex; **(I)** nodule with a large network of cortical infection threads, some marked with arrowheads. CP, cell plate; Gray, autofluorescence; green, tYFP fluorescence; magenta, DsRed labeled *M. loti*. Scale bars 50 μm.

represents a quantitative difference in auxin signaling in the two processes.

Analysis of cytokinin and auxin responses at cellular resolution during later nodule development stages also demonstrated that auxin signaling is activated in the cells containing symbiosomes in mature nodules, while cytokinin signaling appears to be exclusive to infection in the epidermis, cortex and nodules. The DR5 activation in symbiosomes may originate from auxin produced by both the plant as well as the bacteria, as auxin content in nodules can depend on microbial ability to produce IAA (Spaepen et al., 2007).

TCSn activation in nodule development resembles promoter activity of *Log4*, which was identified as the most strongly upregulated cytokinin biosynthesis gene in *L. japonicus* nodulation (Reid et al., 2017). Comparison of TCSn and promoters of individual cytokinin biosynthesis genes or other cytokinin signaling components in a multi-fluorescent reporter construct could be an interesting application of our toolkit.

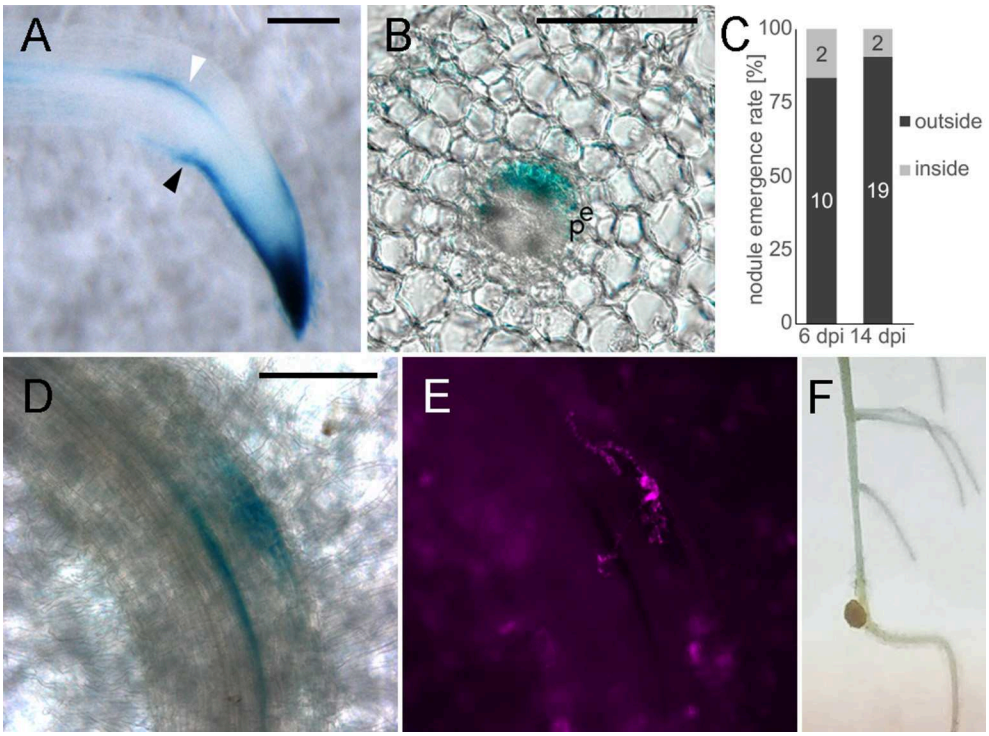

FIGURE 7 | Altered auxin distribution causes biased nodule emergence pattern. Whole mounts **(A,D,E,F)**, transverse vibratome section **(B)**. **(A)** DR5:GUS, 4 h gravitropism stimulation **(B)** 100 μm section of stained root at the gravitropic bend. **(C)** Nodule emergence ratio in gravitropic stimulated roots. $n = 10$ plants for 6 dpi, $n = 30$ for 14 dpi. **(D)** 6 dpi nodule primordium at the gravitropic bend, **(E)** DsRed labeled bacteria, corresponds to D, **(F)** 14 dpi nodule. White arrowhead—DR5 activation in vasculature adjacent cells outside the bend. Black arrowhead—asymmetric DR5 activation in the root tip. e- endodermis, p- pericycle. Scale bars 100 μm.

Our observations support that auxin signaling is associated with both cell division events and infection, whereas cytokinin signaling is inhibitory for infection but required for cell division. Auxin and cytokinin are both involved in the plant cell cycle activation and progression. Expression of a number of cell cycle genes was shown to be upregulated in root hairs during symbiosis (Breakspear et al., 2014) whereas no B-type cyclins, associated with mitosis, were found to be induced. This is consistent with our analysis of the CYCB1-based cell cycle progression marker which marks cell divisions occurring in the cortex during nodule primordia initiation, but was not detected in root hairs. The partial cell cycle activation associated with infection may then result from auxin signaling in the absence of cytokinin.

In conclusion, our modular toolkit for study of auxin, cytokinin and cell cycle progression should enhance our ability to understand root and nodule development in legumes.

MATERIALS AND METHODS

Biological Material and Growth Conditions

Lotus japonicus ecotype Gifu was used in all presented experiments. *Mesorhizobium loti* MAFF303099 labeled with DsRed and *M. loti* R7A labeled with GFP were used as a compatible symbionts. Transformed hairy root plants for imaging were grown in large plastic Microboxes (SacO2, Deinze, Belgium) in 4:1 LECA:Vermiculite substrate supplemented with 1/4 strength B&D nutrients (Broughton and Dilworth, 1971). Growth conditions were set to 16/8 h light/dark cycle with 20°C/15°C temperature.

Cloning and Available Toolkit Components

The GoldenGate modular cloning system using type IIs restriction enzymes was used for cloning and assembly of desired vectors (Weber et al., 2011). In order to ensure compatibility and exchange of genetic parts, we based our modular toolkit on GoldenGate modules using standardized overhangs (Patron et al., 2015). Module assembly schematic and available modules are shown (**Table 1**, **Figure 8**) together with accession numbers for requesting constructs from Lotus Base (lotus.au.dk; Mun et al., 2016). Level 1 constructs were created by combining level 0 modules into expression units containing the promoter (PU) coding sequence (SC) and terminator (T) modules. Level 1 constructs were obtained in reactions of 20 μl containing 100 ng of each level 0 module required for creation of desired construct, 100 ng of target vector, 5 U T4 ligase (Thermo), 2,5 U BsaI (New England BioLabs), 2 μl 10x T4 ligase buffer, 2 μl 10x BSA and water. Goldengate reactions were cycled between 37°C (3 min) and 16°C (4 min) 25 times to favor digestion-ligations reactions respectively.

TABLE 1 | GoldenGate cloning modules available in the toolkit.

Functional units	Name	Module type	5′/3′ overhangs	References	Accession
Transformation vectors	pIV10-L1	L1 acceptor	GGAG/CGCT		PMC-01391
	pIV10-L2	L2 acceptor	TGCC/GGGA		PMC-01270
Promoters	LjUbi	P	GGAG/TACT		PMC-03530
	LjUbi	PU	GGAG/AATG		PMC-01500
	TCSn			Zürcher et al., 2013	PMC-01331
	DR5			Ulmasov et al., 1997	PMC-01243
	AtCycB1;1*			Colón-Carmona et al., 1999	PMC-01241
Coding sequences	DII	U	TACT/AATG	Brunoud et al., 2012	PMC-01269
	mDII			Liao et al., 2015	PMC-03531
	NLS	S	AATG/AGGT		PMC-01303
	GUS	SC	AATG/GCTT		PMC-01722
	tYFP-NLS			Reid et al., 2016	PMC-01484
	mCherry	C	AGGT/GCTT		PMC-01302
	DsRed				PMC-01232
Terminators	35s	T	GCTT/CGCT		PMC-01118
	OCS				PMC-01319

*Full sequences of all modules are provided in **Supplemental File 1**.*
**AtCycB1;1 PU module contains promoter and cyclin B1;1 destruction box.*

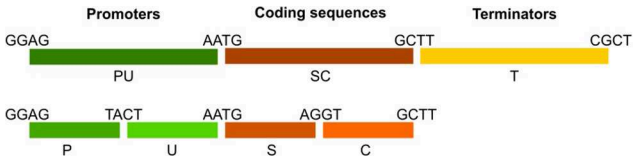

FIGURE 8 | Transcriptional unit assembly and module naming standards. Promoters are available as "PU" or separate "P" and "U" parts. Coding sequences are represented by "SC" modules or separate "S" and "C" parts to enable tagging at N- or C-terminal locations. Terminator modules are termed "T." Overhangs connecting each part are indicated. Note the PU-SC connection contains the ATG start codon.

Hairy Root Transformation

Prior to hairy root transformation, pIV10-based genetic constructions were transferred from donor *E. coli* to *A. rhizogenes* AR1193 as previously described (Stougaard et al., 1987). Hairy roots were induced according to Hansen et al. (1989).

Fluorescence Compatible Clearing

The procedure of clearing optimized for *Pisum sativum* nodule was used essentially as previously described (Warner et al., 2014) with the following modifications for *L. japonicus* roots. Fluorescence positive samples were harvested and fixed overnight in 4% p-formaldehyde, 80mM PIPES pH7 solution. Then, rinsed 3 times for 5 min in 80 mM PIPES pH7. Prior to imaging, samples were incubated for 10 days in clearing solution containing 6M urea, 30% v/v glycerol, 0,01% Triton X-100, 40 mM PIPES pH 7.

Physical Sectioning of Roots and Nodules

Roots and nodules were mounted in molten 3% agarose. To conserve fluorescence, agarose was precooled to 50°C. Solidified blocks were then excised and cut using Leica VT1000S vibratome. Sections of 60–100 μm were cut and mounted onto microscopic slides.

GUS Staining

Plant material was submerged in GUS staining solution (0,5 mg/ml 5-bromo-4-chloro-3-indolyl-beta-D-glucuronic acid, 100 mM $NaPO_4$, 10 mM EDTA, 1 mM Potassium Ferricyanide, 1 mM Potassium Ferrocyanide, 0,1% Triton X-100, pH 7). Vacuum infiltration was applied for 10 min. Samples were stained in darkness at 21°C for several hours or overnight. Staining was stopped by removing the staining solution and rinsing the samples with 70% ethanol.

Gravitropic Stimulation

Prior to 90° turn in root growth direction, plants were grown for 7 days on upright agar plates supplemented with 1/4 strength B&D nutrients. For monitoring of DR5 response upon gravitropic stimulation, plants were harvested and examined for β-glucuronidase activity at 4, 8, 16, 24, and 42 h after applying the stimulus. The roots were not detached from filter paper in order to maintain the shape of gravitropic bends during staining. For nodulation assays, plants were inoculated after 7 days growth on ¼ B&D medium and root growth direction was changed 5 h after inoculation. Nodules emerging outside and inside the gravitropic bend were distinguished. Statistical significance of the bias in nodule position was determined by Fisher's exact test, where expected distribution of nodule emergence inside/outside the bend equaled 50/50.

Microscopy and Image Processing

Confocal microscopy was performed with Zeiss LSM510 and Zeiss LSM780 microscopes. For LSM780, following excitation/emission [nm] settings were used: (i) autofluorescence of cell components 405/420–505, (ii) GFP 488/490–550, (iii) YFP 514/517–560, (iv) mCherry 561/570–700, (v) DsRed 561/580–660. For LSM510: (i) YFP 514/530–600, (ii) DsRed 543/560–615. Images of larger size samples were constructed by acquisition of smaller images and stitching them together (tile scans). For LjR2D2, 18-colors look up table (LUT) was applied to ease identification of fluorescence gradients. GUS and non-confocal DsRed fluorescence images were obtained using Zeiss Axioplan 2. Zeiss ZEN and Fiji ImageJ (Schindelin et al., 2012) were used for image processing and extraction of fluorescence intensities values.

DATA AVAILABILITY

All datasets generated for this study are included in the manuscript and/or the **Supplementary Files**.

AUTHOR CONTRIBUTIONS

MN, JS, and DR conceived the research plan. MN conducted experiments and microscopy. MN prepared the figures and wrote the manuscript together with JS and DR.

FUNDING

This work was funded by the Engineering Nitrogen Symbiosis for Africa (ENSA) project.

ACKNOWLEDGMENTS

We thank Krzysztof Szczyglowski for the DR5:GUS stable line and Bruno Müller for the original TCSn plasmid.

SUPPLEMENTARY MATERIAL

The Supplementary Material for this article can be found online at: https://www.frontiersin.org/articles/10.3389/fpls.2019.01000/full#supplementary-material

Figure S1 | Impact of fluorescence compatible clearing on imaging depth in *L. japonicus* root. Roots expressing *Lj*Ubi:tYFPnls, confocal image of median longitudinal section **(A)** uncleared root **(B)** Root cleared for 10 days. Scale bars 100 μm. Resolution obtained in XY, and YZ axes are shown.

Figure S2 | GUS-dependent identification of cell divisions in *L. japonicus* roots. pCYCB1;1::CYCB1*-GUS construct was expressed in *L. japonicus* hairy roots. **(A,B)** RAM, staining confined to the cell division zone **(C)** LR emergence from the pericycle **(D)** stage Ib/II LR, **(D)** staining in the central region of the LR, **(E)** more uniform staining in the LR; **(F–I)** nodule primordia, cell divisions localized in the cortex **(J,K)** mature nodule, marker activity observed inside the nodule. **(A,E,J)** dark field; **(B,F)** phase contrast; **(C,D,H)** bright field; **(G,I,K)** DsRed fluorescence corresponding to **(F,H,J)**. Scale bars indicate 50 μm.

Figure S3 | DR5:GUS activity upon gravitropic stimulation in *L. japonicus* roots. GUS staining at **(A)** 4 h, **(B)** 8 h (shown in **Figure 7A**), **(C)** 16 h, **(D)** 24 h, **(E,F)** 48 h after application of the stimulus. White arrowhead—asymmetric, vasculature adjacent DR5 activation outside the bend, black arrowheads—asymmetric DR5 activity in the root tip. Box in F showing emerging LR at the bending site. Scale bars 200 μm.

Video S1 | Fluorescent compatible clearing in the root outside root apical meristem Lj DII transgenic root. Green—tYFP.

Video S2 | Application of fluorescent compatible clearing for improving visualization of cortical infection threads. 6 dpi nodule primordium. Gray—autofluorescence of root cell walls, magenta—DsRed labeled *M. loti*.

File S1 | ImageJ macro and sequences of GoldenGate modules.

REFERENCES

Blilou, I., Xu, J., Wildwater, M., Willemsen, V., Paponov, I., Friml, J., et al. (2005). The PIN auxin efflux facilitator network controls growth and patterning in Arabidopsis roots. *Nature* 433, 39–44. doi: 10.1038/nature03184

Boot, K. J. M., van Brussel, A. A. N., Tak, T., Spaink, H. P., and Kijne, J. W. (1999). Lipochitin Oligosaccharides from Rhizobium leguminosarum bv. viciae Reduce Auxin Transport Capacity in Vicia sativa subsp.nigra Roots. *Mol. Plant Microbe Interactions* 12, 839–844. doi: 10.1094/MPMI.1999.12.10.839

Breakspear, A., Liu, C., Roy, S., Stacey, N., Rogers, C., Trick, M., et al. (2014). The root hair "infectome" of Medicago truncatula uncovers changes in cell cycle genes and reveals a requirement for Auxin signaling in rhizobial infection. *Plant Cell* 26, 4680–4701. doi: 10.1105/tpc.114.133496

Broughton, W. J., and Dilworth, M. J. (1971). Control of leghaemoglobin synthesis in snake beans. *Biochem. J.* 125, 1075–1080. doi: 10.1042/bj1251075

Brunoud, G., Wells, D. M., Oliva, M., Larrieu, A., Mirabet, V., Burrow, A. H., et al. (2012). A novel sensor to map auxin response and distribution at high spatio-temporal resolution. *Nature* 482, 103–106. doi: 10.1038/nature10791

Chen, Q., Zhang, X., Jiang, Q., Clarke, P. R., and Zhang, C. (2008). Cyclin B1 is localized to unattached kinetochores and contributes to efficient microtubule attachment and proper chromosome alignment during mitosis. *Cell Res.* 18, 268–280. doi: 10.1038/cr.2008.11

Colón-Carmona, A., You, R., Haimovitch-Gal, T., and Doerner, P. (1999). Technical advance: spatio-temporal analysis of mitotic activity with a labile cyclin-GUS fusion protein. *Plant J.* 20, 503–508. doi: 10.1046/j.1365-313x.1999.00620.x

Dharmasiri, N., Dharmasiri, S., and Estelle, M. (2005). The F-box protein TIR1 is an auxin receptor. *Nature* 435, 441–445. doi: 10.1038/nature03543

Fisher, J., Gaillard, P., Fellbaum, C. R., Subramanian, S., and Smith, S. (2018). Quantitative 3D Imaging of cell level auxin and cytokinin response ratios in soybean roots and nodules. *Plant Cell Environ.* 41, 2080–2092. doi: 10.1111/pce.13169

Gray, W. M., Kepinski, S., Rouse, D., Leyser, O., and Estelle, M. (2001). Auxin regulates SC FTIR1-dependent degradation of AUX/IAA proteins. *Nature* 414, 271–276. doi: 10.1038/35104500

Hansen, J., Jørgensen, J.-E., Stougaard, J., and Marcker, K. A. (1989). Hairy roots—a short cut to transgenic root nodules. *Plant Cell. Rep.* 8, 12–15. doi: 10.1007/BF00735768

Herrbach, V., Remblière, C., Gough, C., and Bensmihen, S. (2014). Lateral root formation and patterning in Medicago truncatula. *J. Plant Physiol.* 171, 301–310. doi: 10.1016/j.jplph.2013.09.006

Hosoda, K., Imamura, A., Katoh, E., Hatta, T., Tachiki, M., Yamada, H., et al. (2002). Molecular structure of the GARP family of plant Myb-related DNA binding motifs of the Arabidopsis response regulators. *Plant Cell* 14, 2015–2029. doi: 10.1105/tpc.002733

Huo, X., Schnabel, E., Hughes, K., and Frugoli, J. (2006). RNAi phenotypes and the localization of a protein::GUS fusion imply a role for *Medicago truncatula* PIN genes in nodulation. *J. Plant Growth Regul.* 25, 156–165. doi: 10.1007/s00344-005-0106-y

Imamura, A., Kiba, T., Tajima, Y., Yamashino, T., and Mizuno, T. (2003). *In vivo* and *in vitro* characterization of the ARR11 response regulator implicated in

the His-to-Asp phosphorelay signal transduction in Arabidopsis thaliana. *Plant Cell Physiol.* 44, 122–131. doi: 10.1093/pcp/pcg014

Kepinski, S., and Leyser, O. (2005). The Arabidopsis F-box protein TIR1 is an auxin receptor. *Nature* 435, 446–451. doi: 10.1038/nature03542

Liao, C.-Y., Smet, W., Brunoud, G., Yoshida, S., Vernoux, T., and Weijers, D. (2015). Reporters for sensitive and quantitative measurement of auxin response. *Nat Methods* 12, 207–10, 2 p following 210. doi: 10.1038/nmeth.3279

Liu, H., Sandal, N., Andersen, K. R., James, E. K., Stougaard, J., Kelly, S., et al. (2018). A genetic screen for plant mutants with altered nodulation phenotypes in response to rhizobial glycan mutants. *New Phytol.* 220, 526–538. doi: 10.1111/nph.15293

Liu, Z. B., Ulmasov, T., Shi, X., Hagen, G., and Guilfoyle, T. J. (1994). Soybean GH3 promoter contains multiple auxin-inducible elements. *Plant Cell* 6, 645–657. doi: 10.1105/tpc.6.5.645

Mathesius, U., Schlaman, H. R., Spaink, H. P., Of Sautter, C., Rolfe, B. G., and Djordjevic, M., a. (1998). Auxin transport inhibition precedes root nodule formation in white clover roots and is regulated by flavonoids and derivatives of chitin oligosaccharides. *Plant J.* 14, 23–34. doi: 10.1046/j.1365-313X.1998.00090.x

Müller, B., and Sheen, J. (2008). Cytokinin and auxin interaction in root stem-cell specification during early embryogenesis. *Nature* 453, 1094–1097. doi: 10.1038/nature06943

Mun, T., Bachmann, A., Gupta, V., Stougaard, J., and Andersen, S. U. (2016). Lotus base: an integrated information portal for the model legume Lotus japonicus. *Sci. Rep.* 6:39447. doi: 10.1038/srep39447

Murray, J. D., Karas, B. J., Sato, S., Tabata, S., Amyot, L., and Szczyglowski, K. (2007). A cytokinin perception mutant colonized by Rhizobium in the absence of nodule organogenesis. *Science* 315, 101–104. doi: 10.1126/science.1132514

Nadzieja, M., Kelly, S., Stougaard, J., and Reid, D. (2018). Epidermal auxin biosynthesis facilitates rhizobial infection in Lotus japonicus. *Plant J.* 95, 101–111. doi: 10.1111/tpj.13934

Pacios-Bras, C., Schlaman, H. R. M., Boot, K., Admiraal, P., Langerak, J. M., Stougaard, J., et al. (2003). Auxin distribution in Lotus japonicus during root nodule development. *Plant Mol. Biol.* 52, 1169–1180. doi: 10.1023/B:PLAN.0000004308.78057.f5

Patron, N. J., Orzaez, D., Marillonnet, S., Warzecha, H., Matthewman, C., Youles, M., et al. (2015). Standards for plant synthetic biology: a common syntax for exchange of DNA parts. *N. Phytol.* 208, 13–19. doi: 10.1111/nph.13532

Potocka, I., Szymanowska-Pułka, J., Karczewski, J., and Nakielski, J. (2011). Effect of mechanical stress on Zea root apex. I. Mechanical stress leads to the switch from closed to open meristem organization. *J. Exp. Bot.* 62, 4583–4593. doi: 10.1093/jxb/err169

Reid, D., Nadzieja, M., Novák, O., Heckmann, A. B., Sandal, N., and Stougaard, J. (2017). Cytokinin biosynthesis promotes cortical cell responses during nodule development. *Plant Physiol.* 175, 361–375. doi: 10.1104/pp.17.00832

Reid, D. E., Heckmann, A. B., Novák, O., Kelly, S., and Stougaard, J. (2016). CYTOKININ OXIDASE/DEHYDROGENASE3 maintains cytokinin homeostasis during root and nodule development in lotus japonicus. *Plant Physiol.* 170, 1060–1074. doi: 10.1104/pp.15.00650

Sakai, H., Honma, T., Aoyama, T., Sato, S., Kato, T., Tabata, S., et al. (2001). ARR1, a transcription factor for genes immediately responsive to cytokinins. *Science* 294, 1519–1521. doi: 10.1126/science.1065201

Sanko-Sawczenko, I., Dmitruk, D., Łotocka, B., and Rózanska E, Czarnocka, W. (2019). Expression analysis of PIN genes in root tips and nodules of Lotus japonicus. *Int. J. Mol. Sci.* 20:235. doi: 10.3390/ijms20020235

Schindelin, J., Arganda-Carreras, I., Frise, E., Kaynig, V., Longair, M., Pietzsch, T., et al. (2012). Fiji: an open-source platform for biological-image analysis. *Nat. Methods* 9, 676–682. doi: 10.1038/nmeth.2019

Soyano, T., Kouchi, H., Hirota, A., and Hayashi, M. (2013). Nodule inception directly targets NF-Y subunit genes to regulate essential processes of root nodule development in Lotus japonicus. *PLoS Genet.* 9:e1003352. doi: 10.1371/journal.pgen.1003352

Spaepen, S., Vanderleyden, J., and Remans, R. (2007). Indole-3-acetic acid in microbial and microorganism-plant signaling. *FEMS Microbiol. Rev.* 31, 425–448. doi: 10.1111/j.1574-6976.2007.00072.x

Stougaard, J., Abildsten, D., and Marcker, K. A. (1987). The Agrobacterium rhizogenes pRi TL-DNA segment as a gene vector system for transformation of plants. *Mol. Gen. Genet.* 207, 251–255. doi: 10.1007/BF00331586

Suzaki, T., Ito, M., Yoro, E., Sato, S., Hirakawa, H., Takeda, N., et al. (2014). Endoreduplication-mediated initiation of symbiotic organ development in Lotus japonicus. *Development* 141, 2441–2445. doi: 10.1242/dev.107946

Suzaki, T., Yano, K., Ito, M., Umehara, Y., Suganuma, N., and Kawaguchi, M. (2012). Positive and negative regulation of cortical cell division during root nodule development in Lotus japonicus is accompanied by auxin response. *Development* 139, 3997–4006. doi: 10.1242/dev.084079

Tan, X., Calderon-Villalobos, L. I. A., Sharon, M., Zheng, C., Robinson, C. V., Estelle, M., et al. (2007). Mechanism of auxin perception by the TIR1 ubiquitin ligase. *Nature* 446, 640–645. doi: 10.1038/nature05731

Tirichine, L., James, E. K., Sandal, N., and Stougaard, J. (2006). Spontaneous root-nodule formation in the model legume *Lotus japonicus* : a novel class of mutants nodulates in the absence of rhizobia. *Mol. Plant Microbe Interact.* 19, 373–382. doi: 10.1094/MPMI-19-0373

Tirichine, L., Sandal, N., Madsen, L. H., Radutoiu, S., Albrektsen, A. S., Sato, S., et al. (2007). A gain-of-function mutation in a cytokinin receptor triggers spontaneous root nodule organogenesis. *Science* 315, 104–107. doi: 10.1126/science.1132397

Turner, M., Nizampatnam, N. R., Baron, M., Coppin, S., Damodaran, S., Adhikari, S., et al. (2013). Ectopic expression of miR160 results in auxin hypersensitivity, cytokinin hyposensitivity, and inhibition of symbiotic nodule development in Soybean. *Plant Physiol.* 162, 2042–2055. doi: 10.1104/pp.113.220699

Ulmasov, T., Murfett, J., Hagen, G., and Guilfoyle, T. J. (1997). Aux/IAA proteins repress expression of reporter genes containing natural and highly active synthetic auxin response elements. *Plant Cell* 9, 1963–1971. doi: 10.1105/tpc.9.11.1963

Voß, U., Wilson, M. H., Kenobi, K., Gould, P. D., Robertson, F. C., Peer, W. A., et al. (2015). The circadian clock rephases during lateral root organ initiation in Arabidopsis thaliana. *Nat. Commun.* 6:7641. doi: 10.1038/ncomms8641

Warner, C. A., Biedrzycki, M. L., Jacobs, S. S., Wisser, R. J., Caplan, J. L., and Sherrier, D. J. (2014). An optical clearing technique for plant tissues allowing deep imaging and compatible with fluorescence microscopy. *Plant Physiol.* 166, 1684–1687. doi: 10.1104/pp.114.244673

Weber, E., Engler, C., Gruetzner, R., Werner, S., and Marillonnet, S. (2011). A modular cloning system for standardized assembly of multigene constructs. *PLoS ONE* 6:e16765. doi: 10.1371/journal.pone.0016765

Yin, K., Ueda, M., Takagi, H., Kajihara, T., Sugamata Aki, S., Nobusawa, T., et al. (2014). A dual-color marker system for *in vivo* visualization of cell cycle progression in Arabidopsis. *Plant J.* 80, 541–552. doi: 10.1111/tpj.12652

Zürcher, E., Tavor-Deslex, D., Lituiev, D., Enkerli, K., Tarr, P. T., and Müller, B. (2013). A robust and sensitive synthetic sensor to monitor the transcriptional output of the cytokinin signaling network in planta. *Plant Physiol.* 161, 1066–1075. doi: 10.1104/pp.112.211763

Conflict of Interest Statement: The authors declare that the research was conducted in the absence of any commercial or financial relationships that could be construed as a potential conflict of interest.

Advantages of publishing in Frontiers

OPEN ACCESS
Articles are free to read for greatest visibility and readership

FAST PUBLICATION
Around 90 days from submission to decision

HIGH QUALITY PEER-REVIEW
Rigorous, collaborative, and constructive peer-review

TRANSPARENT PEER-REVIEW
Editors and reviewers acknowledged by name on published articles

Frontiers
Avenue du Tribunal-Fédéral 34
1005 Lausanne | Switzerland

Visit us: www.frontiersin.org
Contact us: info@frontiersin.org | +41 21 510 17 00

REPRODUCIBILITY OF RESEARCH
Support open data and methods to enhance research reproducibility

DIGITAL PUBLISHING
Articles designed for optimal readership across devices

FOLLOW US
@frontiersin

IMPACT METRICS
Advanced article metrics track visibility across digital media

EXTENSIVE PROMOTION
Marketing and promotion of impactful research

LOOP RESEARCH NETWORK
Our network increases your article's readership